AN INVESTIGATION OF THE ENZYMATIC KINETIC RESOLUTION OF MORITA-BAYLIS-HILLMAN ADDUCTS AND THEIR FURTHER FUNCTIONALISATION

By

WANYAMA PETER JUMA

A thesis submitted to the Faculty of Science

University of the Witwatersrand

Johannesburg

A thesis submitted in fulfilment of the requirements for the degree of Doctor of Philosophy

30TH JULY 2019

DECLARATION

I declare that this thesis is an original report of my research, has been written by me and has never been presented for a degree in any university. The experimental work is entirely my own work under the supervision of **Professor Moira L. Bode** and **Professor Dean Brady**. The thesis is being submitted for the degree of Doctor of Philosophy at the University of Witwatersrand, Johannesburg.

……

WANYAMA PETER JUMA

30th JULY 2019

.

DEDICATION

This thesis is dedicated to my beloved mother, ***Florah Khakasa*** *and my brothers:* ***Tisa***, ***Shivachi***, ***James*** *and my sisters:* ***Irene*** *and* ***Robai****. They encouraged me to soldier on until I succeed.*

ABSTRACT

The Morita-Baylis-Hillman reaction (MBHR) is a carbon-carbon bond forming reaction that affords multifunctional Morita-Baylis-Hillman adducts (MBHA) with various synthetic applications. Unfortunately, many of the synthetic applications of these adducts cannot be realised because these adducts are formed in racemic form. This thesis has investigated functionalisation of enantiopure MBHA obtained using biocatalytic methods.

The first part of the thesis describes the use of enantiopure aldehydes *N*-Boc-L-phenylalaninal and *N*-Boc-D-phenylalaninal to synthesize several Morita-Baylis-Hillman adducts in order to obtain diastereomers that would be separable by chromatographic methods. Unfortunately, this approach proved unsuccessful due to racemization of the aldehydes or MBHA under the reaction conditions applied.

The second approach described is the resolution of racemic MBH acetates and esters using different enzymes. This exercise led to the identification of several lipases that were able to resolve racemic MBH acetates with excellent enantiomeric excess (ee) values and enantiomeric ratios (E). Racemic MBH adducts derived from the reaction of acrylonitrile with benzaldehyde, cinnamaldehyde and hydrocinnamaldehyde were successfully resolved. In each case the (+)-alcohol products were isolated in 94 - 97% ee after lipase-mediated enzymatic kinetic resolution of the corresponding acetates. Mosher's ester derivatisation protocol was used to determine the absolute configuration of the resolved adducts, which was found to be (*S*). A lipase from *Pseudomonas fluorescens,* and *Candida antarctica* type B were found to be the best-performing enzymes.

The last part of the thesis investigated the use of nitrogen nucleophiles for Michael addition to MBH adducts. The process confirmed that the use of nitrogen nucleophiles on TBS protected MBH adducts afforded nucleophilic addition products of high diastereoselectivity. The use of one of the enantiopure isolated MBH adducts in a diastereoselective Michael addition reaction with benzylamine led to a significantly enantio-enriched final product.

ACKNOWLEDGEMENTS

I would like to thank **Prof. Moira Bode** for giving me an opportunity to be her PhD candidate. I am very grateful for her prompt guidance, support and inspiration throughout my PhD work. This opportunity has widened my research skills and research ideas. It is because of your outstanding character that this project has been a success as you have supported me in so many ways. May God bless you, your family as you continue to help others that will come after me. Special thanks to my Co-supervisor **Prof. Dean**, who used all means to ensure I succeed. Your advice on research ideas, life experiences is highly appreciated. May God bless you in all your endeavours.

Special thanks to **Dr V. Chhiba** for supplying enzymes, HPLC columns and your assistance on carrying out enzymatic work. I am also very grateful to **Prof. Charles de Koning**, **Prof. Jo Michael** and **Dr Maya Makatini** for their encouragement and suggestions during the organic group meetings. It is because of these ideas that enabled me to grow in terms of research. **Dr Amanda L. Rosseau** always ensured I am comfortable throughout my stay at Wits, thank you very much.

Special appreciation to **Dr Izak Kotze**, **Dr Myron Johnson** and **Dr Hendrik Henning** for your support on the use of NMR instruments. Similar appreciation is extended to **Dr Maya Makatini**, **Eric Morifi**, **Thapelo** and **Refilwe** for the support I received when performing MS experiments. I also thank **Dineo**, who was attached to this research for her honours project.

A big thanks to **Dr Jimmy Sumani**, **Dr Kennedy Ngwira**, **Dr Charles Changunda**, **Dr Donald Seanego**, **Memory Zimuwandeyi** for your encouragement and creating a good environment for research.

I would like to thank the **Tebogo, Gcininwe**, **Jean**, **Thabo**, **Pious**, **Phathu**, **Mudzuli**, **Khanani, Ntobi**, **Songz**, **Fatima**, **Kamogelo**, **Amy**, **Adelaide**, **Nompumelelo**, **Fatema**, **Edward**, **Dennis** and **Robin** for the company I received when I was in the laboratory.

I am extremely grateful to the **University of the Witwatersrand** for providing enabling environment that helped me carry out this research. I thank **DST biocatalysis** for funding the project.

My parents, brothers, sisters, friends and colleagues are sincerely thanked for their endless support and encouragement. Finally, I wish to thank the **Almighty God** for giving me life, strength and protection during the entire study period. To Him, I give all the Honour and Glory, Amen.

LIST OF ABBREVIATIONS

EWG	Electron Withdrawing group	DKR	Dynamic kinetic resolution
MBH	Morita-Baylis-Hillman	CALB	Lipase B from *Candida antarctica*
DABCO	1,4-diazabicyclo[2.2.2]octane	WT	Wild type
DMSO	Dimethylsulfoxide	SDS-PAGE	Sodium dodecyl sulphate polyacrylamide Gel electrophoresis
EVK	Ethyl vinyl ketone	HPLC	High Performance liquid chromatography
MVK	Methyl vinyl ketone	XRD	X-ray diffraction
IPA	Isopropanol	HIV	Human immunodeficiency virus
DMF	Dimethylformamide	TNF	Tumour necrosis factor
MTPA	α-methoxy-α-(trifluoromethyl)phenylacetic acid	TLC	Thin layer chromatography
DMAP	4-Dimethylaminopyridine	IR	Infra-red
BF_3OEt_2	Boron trifluoro diethyl etherate	NMR	Nuclear magnetic resonance
TBS	*Tert*-butyldimethylsilyl	MHz	Megahertz
TBSOTf	*Tert*-butyldimethylsilyl trifluoromethanesulfonate	δ	Chemical shifts in delta values
TEA	Trethylamine	COSY	Correlation spectroscopy
m-CPBA	*Meta*-chloroperoxybenzoic acid	HSQC	Heteronuclear multiple quantum coherence
TBAF	Tetra-*n*-butylammonium fluoride	HMBC	Heteronulcear multiple bond correlation
THF	Tetrahydrofuran	DEPT	Distortionless enhancement by polarisation transfer
TQO	4-(3-ethyl-4-oxa-1-azatricyclo[4.4.0.0]dec-5-yl)quinolin-6-ol	HRMS	High resolution mass spectrometry
BOC	Tert-butyloxycarbonyl	Hz	Hertz
ee	Enantiomeric excess	*J*	Coupling constant
ee_s	Enantiomeric excess of the substrate	d	doublet
ee_p	Enantiomeric excess of the product	dd	Doublet of doublets
E	Enantiomeric ratio	ddd	Doublet of doublet of doublets
dr	Diastereomeric ratio	s	singlet
OYE	Old yellow enzyme	t	Triplet
PLAP	Pig liver acetone powder	Ax	Axial
PCL	*Pseudomonas cepacia* lipase	Eq	Equatorial

Table of Contents

CHAPTER ONE

1 INTRODUCTION

1.1MORITA-BAYLIS-HILLMAN REACTION

1.1.1 The origin and development of the Morita-Baylis-Hillman reaction

One of the most important and unique carbon-carbon bond forming reactions known to the scientific community is the Morita-Baylis-Hillman (MBH) reaction.[1] This reaction, involves coupling of electrophiles **1** with alkenes containing an electron withdrawing group (EWG) **2** and is catalysed by nucleophilic amines or phosphines (**Figure 1**) to generate Morita-Baylis-Hillman adducts (MBHA) **3** (**Scheme 1**). In the event that imines participate in this reaction then the process is called the aza-Morita-Baylis-Hillman (aza-MBH) reaction generating aza-Morita-Baylis-Hillman adducts (aza-MBHA).[2] The most widely used amine catalyst is 1,4-diazabicyclo[2.2.2]octane (DABCO) **4** with fewer reports on the use of triphenylphosphine **5** as an accelerator of this reaction. The reaction dates back to 1968,[3] when Ken-ichi Morita explained unusual adducts arising from the reaction between various aldehydes and acrylic compounds catalysed by a tertiary phosphine **5**. A similar reaction, in which the catalytic potential of tertiary amines such as DABCO **4**, quinuclidine **6** and indolizine **7** were investigated, was reported by Baylis and Hillman in 1972.[4]

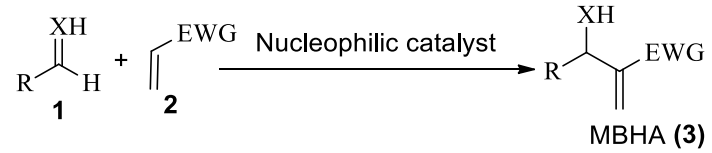

R = alkyl, aryl, heteroaryl
X = O, NCO_2R, NTs, NSO_2Ph
EWG = Electron withdrawing group

Scheme 1: Morita-Baylis-Hillman reaction

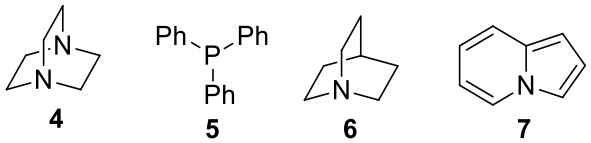

Figure 1: Examples of reported catalysts used in the Morita-Baylis-Hillman reaction

The MBH reaction is one of the most significant, creative, and intellectually inspiring reactions as it generates multifunctional adducts with many synthetic applications.[5] Furthermore, the reaction is simple to perform, requires mild reaction conditions to take place and is atom economical.[6] This advantageous reaction has gained an overwhelming synthetic popularity as shown by the many reviews and publications.[7-10] A steady increase in the number of reviews and publications over the past twenty years is supported by data from the Web of Science database shown in **Figure 2**.

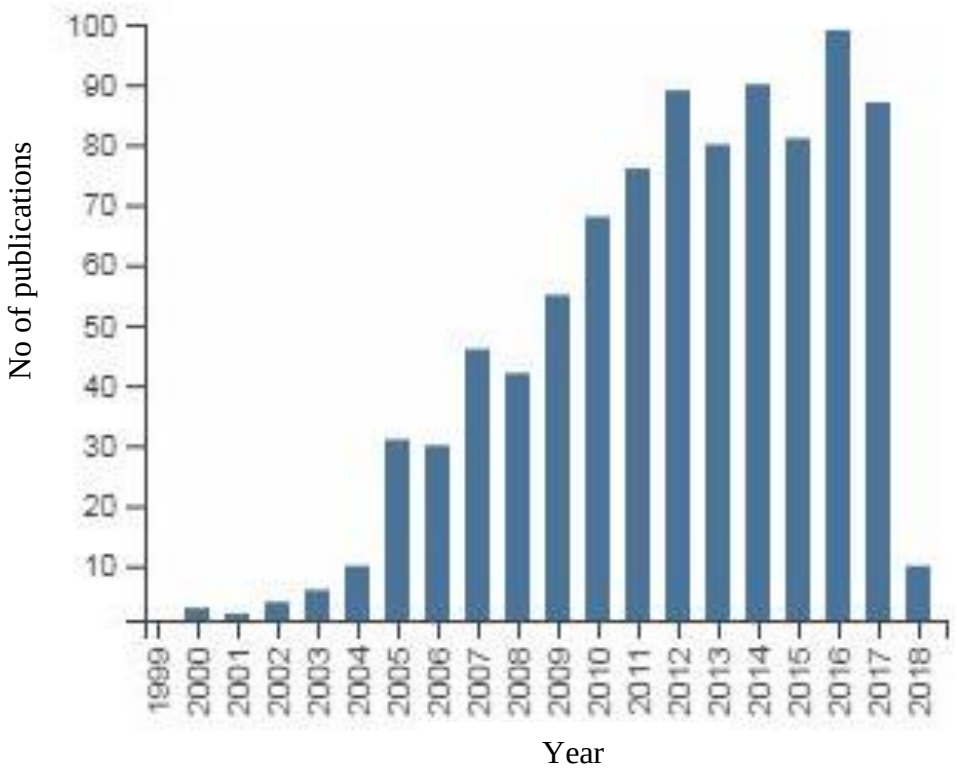

Figure 2: A graph showing the number of articles published on the MBH reaction for the past 20 years via the Web of Science database (accessed on February 5, 2019)

Unfortunately, the synthetic use of this reaction is hindered by low yields and long reaction times. For example, there are reactions that have been reported to take more than 65 days with poor yields of less than 50%.[8] Due to the synthetic potential of these adducts, several protocols have been developed to overcome the aforementioned shortcomings. These newer protocols that have accelerated the reaction and improved the yields include the use of microwaves,[11] ultrasound,[12] high pressure,[13, 14] aqueous media,[15, 16] and ionic liquids.[17, 18] Interestingly, the mechanism of this reaction has been the subject of major debate globally. In other words, it is not clear why some reaction conditions accelerate the reaction or

increase the yield. This has resulted in more research designed to logically explain the mechanisms by using either experimental observation or by use of computational methods.

1.1.2 The mechanistic aspects of the Morita-Baylis-Hillman reaction

Hillman and Isaacs were the first researchers to use the rate, pressure dependence and kinetic isotope effect (KIE) data to propose a mechanism for the MBH reaction.[19] They discovered that the mechanism involved three major steps; namely 1,4-Michael addition, aldol reaction and elimination, which take place sequentially (**Scheme 2**). Michael addition of the nucleophile catalyst **8** onto the α,β-unsaturated carbonyl **9** generates the zwitterion **10** (step **1**). Aldol reaction between zwitterion **10** and aldehyde **11** leads to alkoxide **12** (step **2**) which undergoes proton transfer, affording enolate **13**. The catalyst attached to intermediate **13** is eliminated by either an E2 or E1Cb elimination mechanism to produce the intended MBHA **14** (step **4**)**.**

The absence of a primary kinetic isotope effect convinced Hillman and Isaacs to conclude that step **2** is the rate limiting step (RLS). This mechanism was supported by Bode[20] and refined by Beutner,[21] Hundley[22] and Pfaltz.[23]

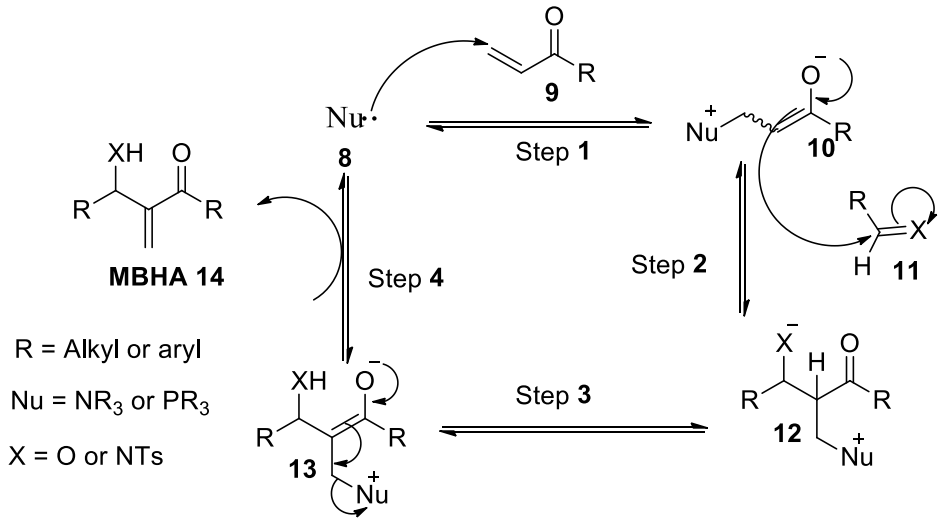

Scheme 2: The generally accepted MBH mechanism as proposed by Hillman and Isaacs

Unfortunately, the above proposal could not explain some of the reported observations. For instance, the accepted mechanism could not explain why the reaction rate was slow,[8] what led to the formation of dioxanone,[24, 25] autocatalysis[26] as well as rate acceleration under the influence of protic solvents.[27] Later, more detailed reports were available to account for the

unexplained observations and other proposed mechanisms were put forward by different research groups in an attempt to clarify the unexplained observations.

The McQuade group,[28, 29] clearly explained the key stages in the MBH mechanism based on kinetic and theoretical data. According to McQuade, the intermediate **12** undergoes several steps to generate MBH adduct **14** in the absence of protic species as shown in **Scheme 3**. The first step involves nucleophilic addition of the alkoxy oxygen of **12** to a second molecule of electrophile **11** affording a hemiacetal anion **15**. The hemiacetal reorganises itself to form a six membered transition state **16** (step **2**); this process promotes intramolecular proton transfer leading to the formation of **17** and elimination of the catalyst (step **3**). This step of eliminating the catalyst is the rate determining step (RDS). Consequently, the unstable hemiacetal **17** decomposes to generate the final MBHA **14** with the formation of dioxane **18** as a by-product. This was the first report to propose a mechanism to explain the formation of dioxane that had previously been observed by other researchers.

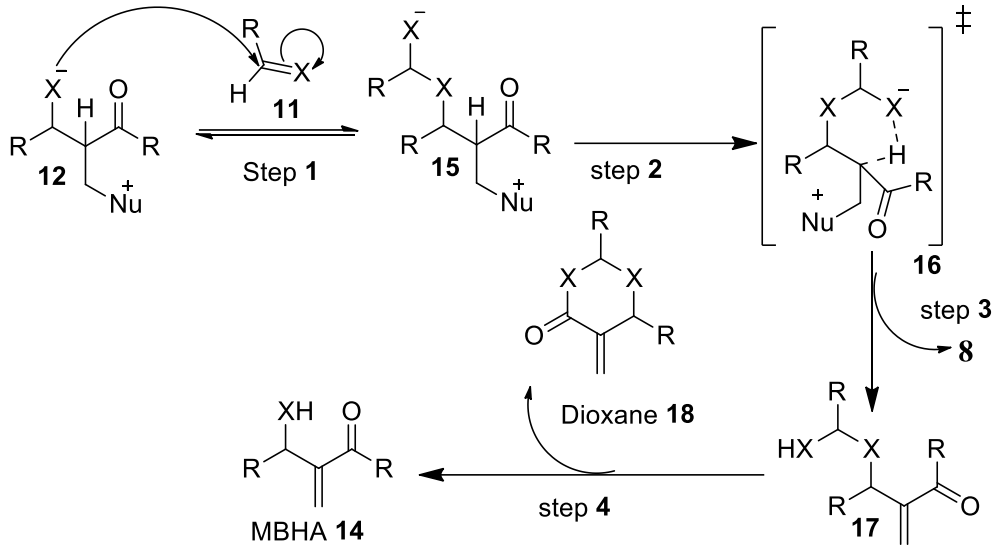

Scheme 3: The proposed mechanism of the MBH reaction by the McQuade group in the absence of protic species

McQuade's report did not explain the rate enhancing effect of polar species that readily form hydrogen bonds on the MBH reaction. This gap attracted Aggarwal,[26, 30] and Singleton,[31] to explore the mechanism further. Their research findings are summarized in **Scheme 4**. According to Singleton, the alkoxy oxygen of **12** associates with polar species and the process facilitates the acid base reaction affording adduct **14** by eliminating the catalyst. This proposal is in contrast to the earlier proposal by Aggarwal where it was suggested that

the formation of **14** and elimination of the catalyst is achieved by a proton transfer step via a six membered transition state **18.** The findings of Aggarwal and McQuade were supported by computational methods,[30, 32] and intermediate fragments that were characterized by mass spectrometry with electrospray ionisation (ESI-MS) during the MBH reaction.[33] It is important to note that the mechanistic proposals by Singleton and Aggarwal are still the subject of discussion.

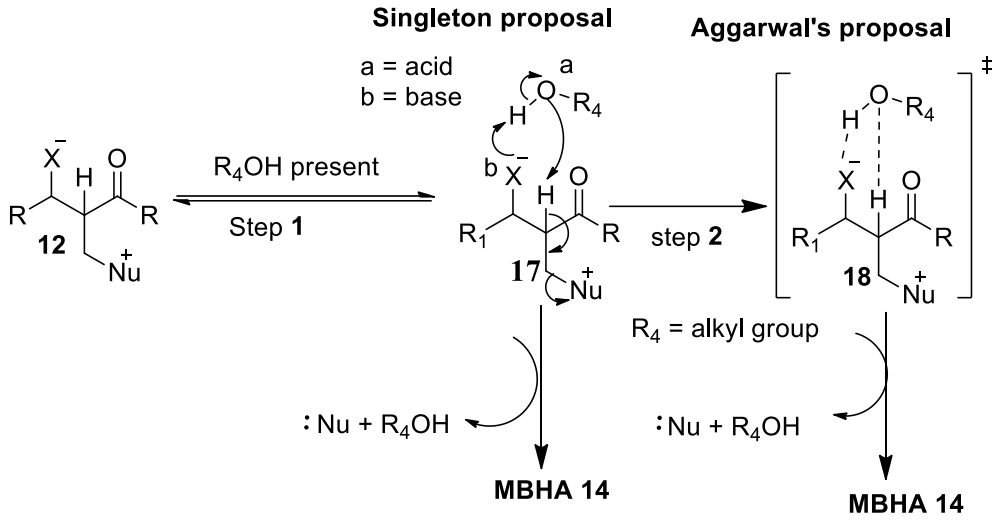

Scheme 4: The proposed mechanism of the MBH reaction as explained by Singleton and Aggarwal

A number of reviews discussing the various proposed mechanisms of the MBH reaction have been published.[34, 35]

1.1.3 Methods of carrying out the Morita-Baylis-Hillman reaction

Morita-Baylis-Hillman reactions can be carried out by either the use of chemicals or enzymes. The means of obtaining MBH adducts through chemical means has been researched extensively and there exist numerous reports as mentioned earlier.

1.1.3.1 Conventional MBH reaction

In principle, chemical methods involve coupling of the α-position of activated alkenes or alkynes with electrophiles in the presence of a catalyst. The reported acyclic activated alkenes famously used in the MBH reaction are acrylonitrile,[36] alkyl (aryl) acrylates, alkyl vinyl ketones, acrylamides,[37] vinyl sulfonates and vinyl phosphonates. Coupling of the

activated alkenes with various electrophiles in the presence of a catalyst affords MBH adducts as shown in **Scheme 5**.

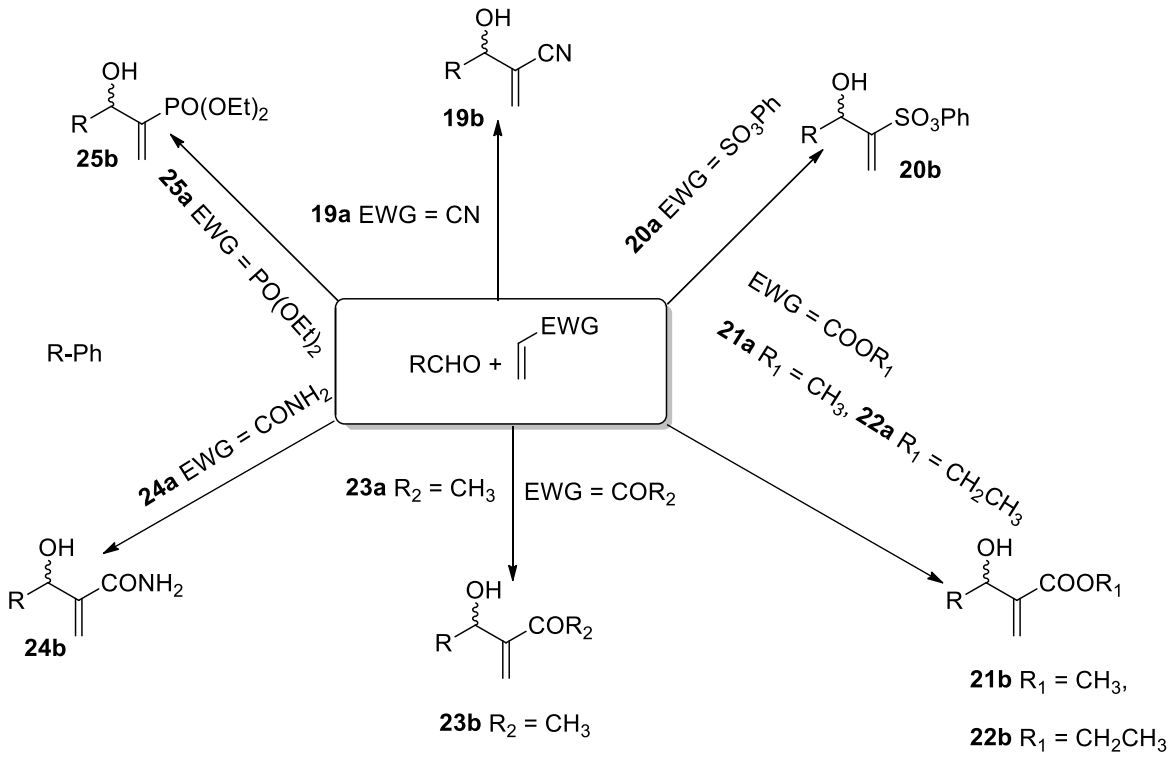

Scheme 5: Reactions of benzaldehyde with different activated alkenes to form various MBH adducts

This section provides a selection of the numerous MBH reactions that have been reported in the literature, and other examples can be found in comprehensive review articles.[38, 39]

In addition to the electrophiles discussed in the previous sections, chiral α-amino aldehydes also have the potential to be used in MBH reactions. There is scanty information available on the use of α-amino aldehydes as electrophiles in performing MBH reaction as evidenced by the limited number of publications that are available. The use of enantiopure amino aldehydes is significant as it produces multifunctional α-methylene-β-hydroxy-γ-amino acid compounds having the potential to be applied in synthetic chemistry. This has been illustrated by a few reports in which diastereomers have been synthesized by reacting α-amino aldehydes and methyl acrylate.[40, 41] These reports, where protected or unprotected α-amino aldehydes were reacted with methyl acrylate in the presence of DABCO gave an average yield of 63% with poor diastereocontrol (**Scheme 6**).

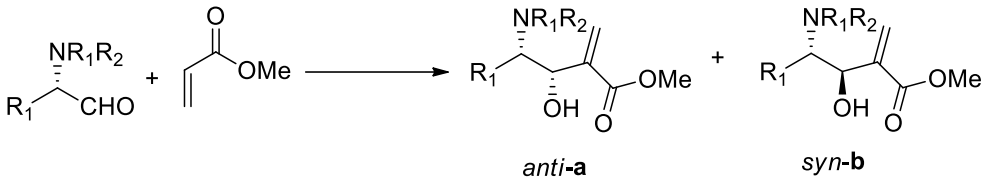

anti-**a** *syn*-**b**

	R_1	R_2	R_3		R_1	R_2	R_3		R_1	R_2	R_3	*anti* : *syn*
26	Me	Bn	Bn	**26a**	Me	Bn	Bn	**26b**	Me	Bn	Bn	72 : 28
27	Bn	Bn	Bn	**27a**	Bn	Bn	Bn	**27b**	Bn	Bn	Bn	67: 33
28	Me	Boc	H	**28a**	Me	Boc	H	**28b**	Me	Boc	H	26: 74

Scheme 6: Morita-Baylis-Hillman reaction of protected α-amino aldehydes with methyl acrylate in the presence of DABCO giving *anti*-**a** and *syn*-**b** diastereomers of indicated ratio

The dearth of literature material on the use of enantiopure amino aldehydes in MBH reactions creates space for research covering this topic to generate additional knowledge in synthetic chemistry.

1.1.3.2 Enzymes as catalysts in the MBH reaction

Unfortunately, the use of organic catalysts like DABCO in performing MBH reaction are disadvantageous because of toxicity, are costly and sometimes they are non-biodegradable. This has more recently encouraged researchers to search for other methods of performing the Morita-Baylis-Hillman reaction. An example of this involves the use of enzymes, which in many different applications have been proven to be highly advantageous. The use of enzymes as catalysts in the MBH reaction has been demonstrated by the use of computationally bioengineered enone binding enzymes to catalyse the reaction between cyclohexenone **29** and *p*-nitrobenzaldehyde **30a** affording MBHA **31a** in very low yield as documented by Bjelic *et al*., (**Table 1, entry 1**).[42] Although it is tedious to obtain bioengineered enone binding enzyme, it can be efficient if enone binding enzymes that are highly promiscuous and have best enzymatic activity are formulated to accommodate various substrate and improve the yield.

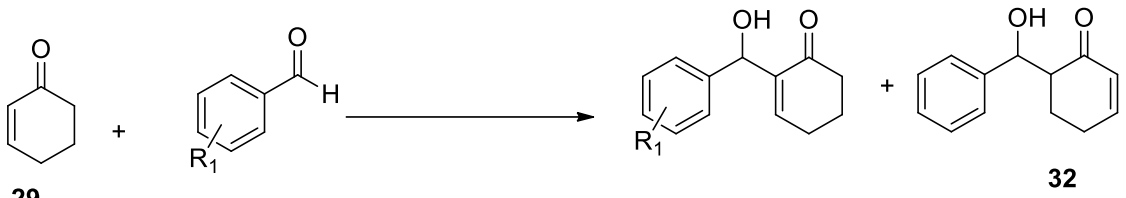

29

32

30a R_1 = 4-NO_2 **30b** R_1 = 3-NO_2

30c R_1 = 2-NO_2 **30d** R_1 = 2,4-dinitro

30e R_1 = H **30f** R_1 = 4-F

30g R_1 = 4-Cl, **30h** R_1 = 4-Br

30l R_1 = 4-CH_3O

31a R_1 = 4-NO_2 **31b** R_1 = 3-NO_2

31c R_1 = 2-NO_2 **31d** R_1 = 2,4-dinitro

31e R_1 = H **31f** R_1 = 4-F

31g R_1 = 4-Cl, **31h** R_1 = 4-Br

31l R_1 = 4-CH_3O

Scheme 7: Biocatalytic MBH reaction between cyclohexenone and benzaldehyde derivatives

Table 1: Comparison of yield and enantiomeric excesses when different enzymes are used to couple cyclohexenone and benzaldehyde derivative

Entry	Aldehyde	Products	yield	ee_p
1	30a	31a	ND	ND
2	30a	31a	ND	63
		32	ND	79
3	30a	31a	64	32
4	30b	31b	67	18
5	30f	31f	76	26
6	30g	31g	77	32
7	30h	31h	75	38
8	30a	31a	21.4	ND
9	30b	31b	16.1	ND
10	30f	31f	16.2	ND
11	30a	31a	43.4	ND

ND- Not determined

A similar reaction was also investigated by Kapoor *et al*., using different lipases in various solvent systems.[43] During screening, they discovered that an aldol product **32** was formed in addition to the MBH adduct **31a**. Their detailed proposed mechanism explained how the aldol product was formed. They were able to get the best results when lipase from *Mucor javanicus* was used in 50% (v/v) DMSO; as this condition gave an enantioselectivity of 63% for the MBH adduct and 79% for the aldol product (**Table 1**, **entry 2**). The use of serum albumin from different sources and lipases have also demonstrated the ability to couple cyclohexenone and *p*-nitrobenzaldehyde leading to adduct **31a** with low conversion of

below 25% and enantiomeric excess below 20%.[44] The use of pepsin and DABCO in a solvent mixture of cyclohexane and phosphate buffer at pH 6.5 has been reported to afford encouraging results (**Table 1**, **entries 3-7**).[45] This comprehensive report was able to confirm that under suitable conditions the substitutions on the phenyl ring of the electrophiles could be varied and coupling with cyclohexenone to obtain adducts in reasonable yields and enantiomeric excess. The results obtained by Tian *et al*., were also very interesting. They were able to confirm that cyclohexenone and *p*-nitrobenzaldehyde could be coupled using Novozym 435 in the presence of isonicotinamide as a co-catalyst (**Table 1**, **entries 8-11**).[46] The report concluded that the best yield of adduct **31a** could be obtained when β-cyclodextrin was added to the mixture of Novozym 435 and isonicotinamide (**Table 1**, **entry 11**). It is likely that the poor yields could probably be improved if better conditions are further researched.

Bjelic *at al*., proposed a lipase catalysed MBH reaction mechanism based on the reaction between cyclohexenone and *p*-nitrobenzaldehyde (**Scheme 8**).

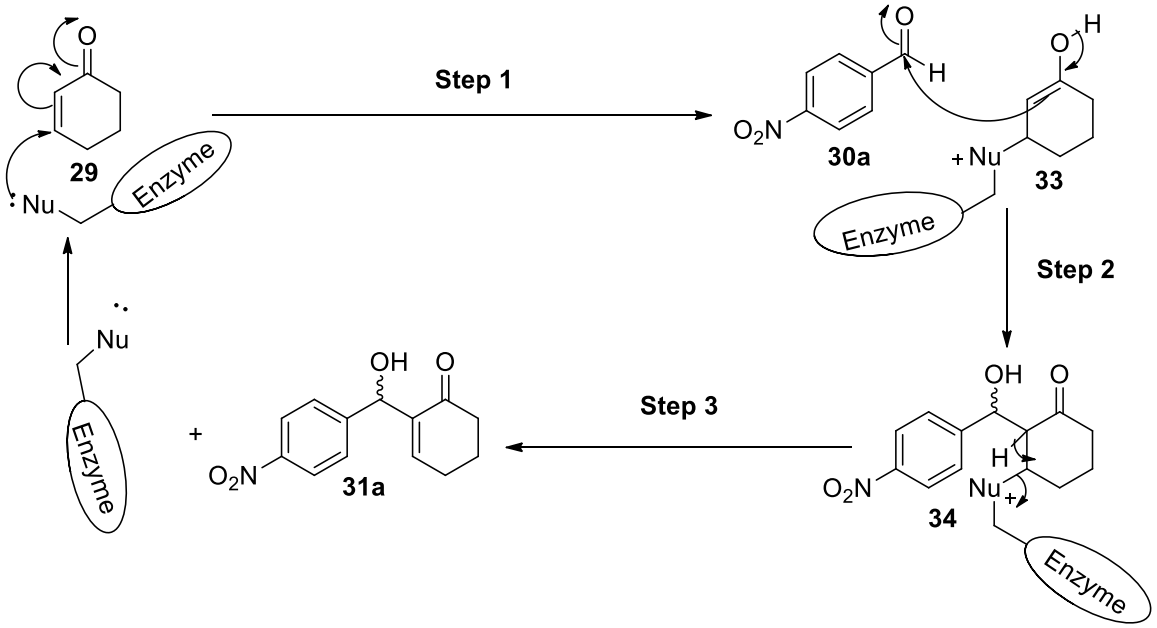

Scheme 8: Lipase catalysed MBH reaction mechanism proposed by Bjelic *et al*.

The proposal suggests that the nucleophilic enzyme attacks the electrophilic carbon of cyclohexenone **29** leading to the formation of enolate (**Scheme 8**, **step 1**). The *p*-

nitrobenzaldehyde **30** is later attacked by enolate **33** to form intermediate **34** which loses the acidic proton to form the MBH adduct **31a** and regenerate the enzyme.

The use of an esterase (BioH) from *Escherichia coli* for facilitating the MBH reaction of various benzaldehydes and activated alkenes has also been documented.[47] This enzyme successfully catalysed the reaction between various nitrobenzaldehydes and activated methyl and ethyl acrylates using acetonitrile as solvent (**Scheme 9**) affording adducts shown in **Figure 3**. Disappointingly, BioH only afforded adducts in yields below 50%. The same report also described the use of different lipases to couple *p*-nitrobenzaldehyde and methyl vinyl ketone in acetonitrile leading to the formation of adduct **40** (**Figure 3**). The lipases investigated included lipase AK, lipase AS, lipase from *C. rugosa* and *R. miehei*, with none of them giving a yield above 10%. These poor yields can be a starting point for any researcher interested in using enzymes to perform the MBH reaction.

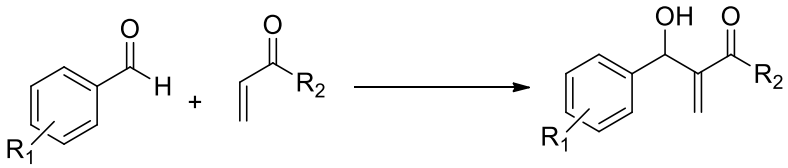

Scheme 9: MBH reaction promoted both by an esterase (BioH) from *E. coli* and various lipases affording adducts shown in **Figure 3**

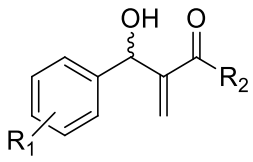

35 R_1 = 4-NO_2 R_2 = Me
36 R_1 = 3-NO_2 R_2 = Me
37 R_1 = 2-NO_2 R_2 = Me
38 R_1 = 4-CN R_2 = Me
39 R_1 = 4-NO_2 R_2 = OMe
40 R_1 = 3-NO_2 R_2 = OMe
41 R_1 = 2-NO_2 R_2 = OMe
42 R_1 = 4-NO_2 R_2 = OEt
43 R_1 = 3-NO_2 R_2 = OEt

Figure 3: MBH adducts that have been synthesized using **Scheme 8**

The use of enzymes in performing the MBH reaction is a generally unexplored area as there are many reactions that needs to be investigated.

1.1.4 Asymmetric synthesis of Morita-Baylis-Hillman adducts

Research aimed at obtaining enantiopure MBH adducts is currently being given the highest priority, as evidenced from the recent literature.[23] This is because monochiral MBH adducts have various synthetic applications; including their use as building blocks in pharmaceuticals. The demand for these homochiral adducts has attracted many research groups to dedicate their efforts towards obtaining enantiopure MBH adducts. Enantiopure adducts can only be obtained by either using organocatalysts that promote enantioselectivity during the MBH reaction or the use of biocatalysts to resolve the already synthesised racemic MBH adduct. The efficiency of any asymmetric method can be determined by measurable parameters that will be explained in the following section.

1.1.4.1 Important measurable parameters used in asymmetric synthesis

It is very important for any research to understand the fundamental terminologies that measure the degree of selectivity in asymmetric synthesis. It is during stereoselective synthesis that products with either one or more stereogenic centers are produced, thus affording either enantiomers or diastereomers. Enantiomers which are non-superimposable on their mirror images have the same physical and chemical properties whereas diastereomers have different physical and chemical properties.

The practical application of enantiomers and diastereomers in organic synthesis is subject to purity measured by specific parameters. For instance, if an enantiomer is produced then it is important to measure the enantiomeric excess (ee), conversion and enantiomeric ratio (E). Percentage enantiomeric excess is the percent of one enantiomer over the total of both enantiomers and it can either be for the substrate (ee_s) or for the product (ee_p). If diastereomers are obtained, then the percent of one diastereomer over the total of both diastereomers is called diastereomeric excess (de). Sometimes the quantities of the diastereomers produced are compared to give a diastereomeric ratio (dr). The most critical parameter in asymmetric synthesis is the selectivity factor or enantiomeric ratio (E) which relates the enantiomeric excess of the product (ee_p), enantiomeric excess of the substrates (ee_s) and conversion (C). Reactions having enantiomeric ratio values less than 15 are not

practically viable. The importance and mathematical expressions of equations **1** – **4** showing the relationship of the parameters are discussed in literature.[48, 49]

$$ee = \%\ Major\ enantiomer - \%\ Minor\ enantiomer \quad \ldots\ldots\ldots\ldots\ldots\ldots\ldots\ldots\ldots\ldots\ldots\ldots (\mathbf{1})$$

$$de = \%\ Major\ diastereomer - \%\ Minor\ diastereomer \quad \ldots\ldots\ldots\ldots\ldots\ldots\ldots\ldots\ldots\ldots\ldots\ldots (\mathbf{2})$$

$$\%\ \text{Conversion} = \frac{\text{ee}_s}{\left(ee_s + ee_p\right)} \times 100 \qquad \ldots\ldots\ldots\ldots\ldots\ldots\ldots\ldots\ldots\ldots\ldots\ldots\ldots\ldots\ldots\ldots\ldots (\mathbf{3})$$

$$\text{E} = \frac{\text{Ln}\left[1 - \text{c}\left(1 + ee_p\right)\right]}{\text{Ln}\left[1 - \text{c}\left(1 - ee_p\right)\right]};\ \text{ or E} = \frac{\text{Ln}[(1 - \text{c})(1 + ee_s)]}{\text{Ln}[(1 - \text{c})(1 + ee_s)]} \ldots\ldots\ldots\ldots\ldots\ldots\ldots\ldots\ldots\ldots\ldots\ldots (\mathbf{4})$$

Using unhindered tertiary amines like DABCO or trialkylphosphine to catalyse the MBH reaction results in racemic adducts, where each enantiomer is formed in equal proportions. By analysing the MBH reaction mechanism, it becomes possible to design organocatalysts that are hindered such that their orientation during the transition state will influence stereoselectivity.[50] These chiral organocatalysts that have an influence on the stereoselectivity can be divided into three major groups. These groups are nucleophilic chiral tertiary amines, chiral acids and chiral tertiary phosphines. The use of chiral tertiary phosphines in promoting stereoselective aza-MBH reaction has not been discussed as this work involves only the use of electrophilic aldehydes for MBH reaction.

1.1.4.2 Chiral tertiary amines as catalysts

The use of chiral tertiary amines for asymmetric synthesis has been known for many years.[51] Using the properties of these stystems has enabled researchers to develop powerful chiral organocatalysts that promote enantioselective transformations. Examples of chiral tertiary amines that have been used to promote enantioselectivity are shown in **Figure 4**.

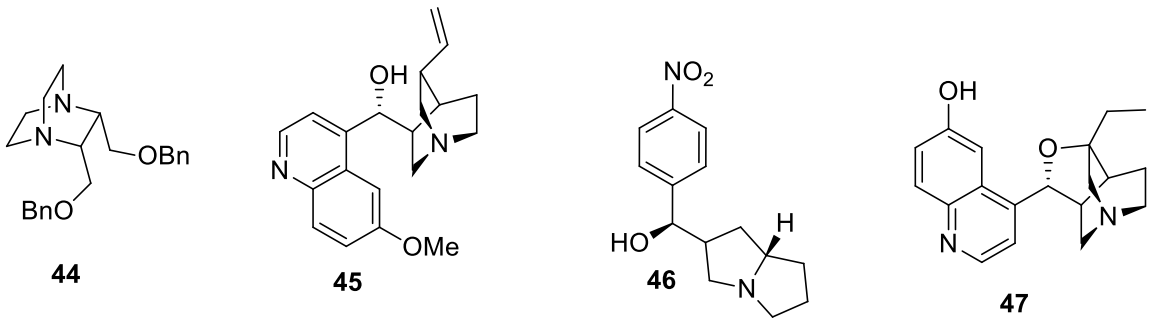

Figure 4: Examples of chiral tertiary amines that have been reported to promote enantioselectivity during MBH reaction

The use of enantiopure DABCO derivative **44** allowed Hirama to couple methyl acrylate with benzaldehyde at elevated pressure resulting in adduct **48** in a yield of 93%, with a low ee value of 47% (**Scheme 10**, reaction 1).[14] The other chiral amines such as cinchona alkaloid derivative quinidine **45,** having a free hydroxyl group, promoted an enantioselective reaction between cyclohexane carbaldehyde and methyl vinyl ketone in dichloromethane at 25 °C (**Scheme 10**, reaction 2).[22] The resultant adduct that was confirmed to be of *S*-configuration was obtained in a yield of 50% with an ee of 45%. The chiral bicyclic pyrrolizidine derivative **46** was demonstrated by Barret *et al.*, to catalyse the reaction between ethyl vinyl ketone (EVK) and benzaldehyde in the presence of a Lewis acid catalyst, affording adduct of *R*- configuration with a reasonable enantiomeric excess of 72% (**Scheme 10**, reaction 3).[52]

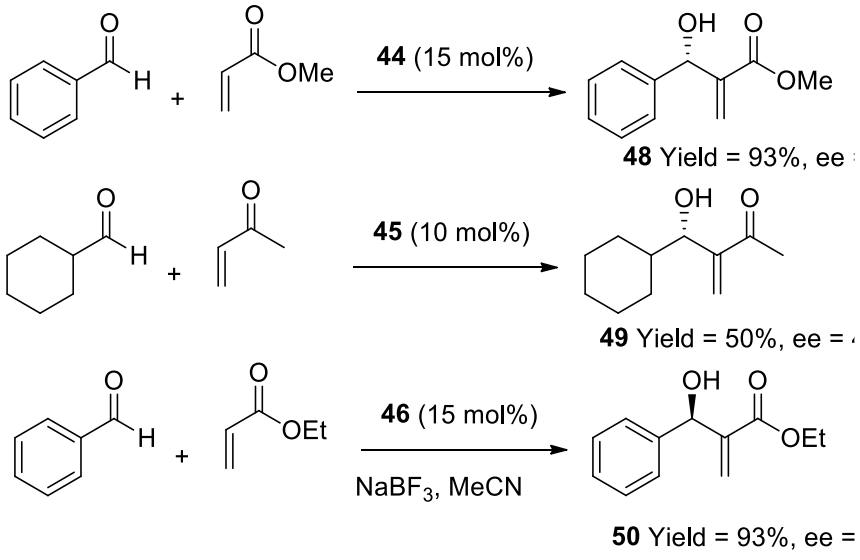

Scheme 10: The use of chiral tertiary amines in promoting enantioselective reactions

A detailed mechanism on the use of catalyst **45** and **46** leading to the observed configuration of **49** and **50** was also proposed by the authors (**Scheme 11**). According to their proposal, the transition state forms a *Z*-enolate that is stabilised by electrostatic interactions. The Z-enolate **a** adds to the *Re*-face of the aldehyde resulting in adduct **49** of *S*- configuration (**Route 1**). On the other hand, the enolate **b** attacks the *Si*-face of the aldehyde affording adduct **50** of *R*- configuration (**Route 2**). Logically this proposal can only make sense in the presence of supporting kinetic data.

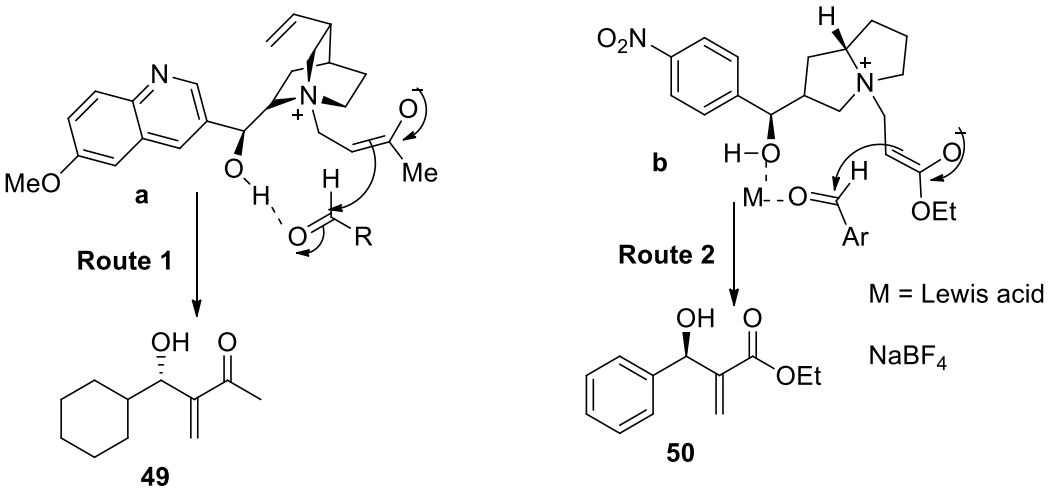

Scheme 11: Proposed mechanism for the transition state of the chiral amine used in reaction 2 and 3 of Scheme **10**

The successful use of catalyst **45** enticed other researchers to improve this compound so that catalytic and enantioselective properties could be improved. The improvement of **45** led to β-isocupreidine **47** that has been used to catalyse the reaction between isatin derivatives **51** and maleimide **52**.[53] These reactions that were done in chloroform as a solvent, led to the corresponding chiral 3-substituted 3-hydroxyindole derivatives **53** with the best performing compounds giving yields ranging from 75 – 96% and enantioselectivities ranging from 77% to greater than 98% (**Scheme 12**). Such excellent enantioselectivities are encouraging as they make the reaction practically viable. However, this will only be possible if catalyst **47** can be obtained at a cheaper price or if it can be synthesized easily without using the complex methodologies currently reported in literature. The proposed, convincing mechanism to explain the enantioselectivity was same as the one shown in **Scheme 11**.

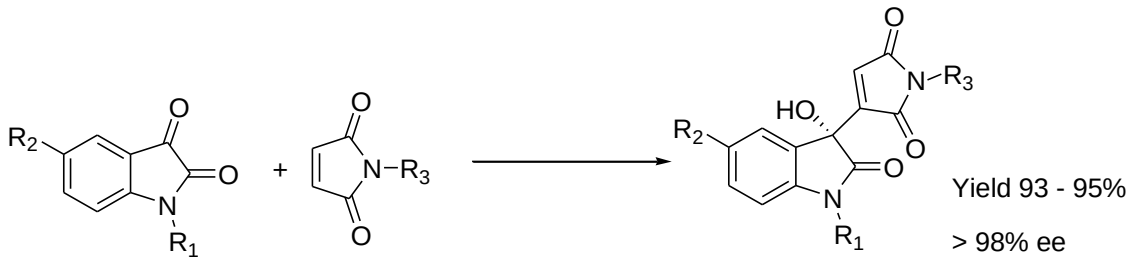

51 **52** **53**

51a R_1 = Bn R_2 = H

51b R_1 = Allyl R_2 = H

51c R_1 = MOM R_2 = H

51d R_1 = Bn R_2 = F

51e R_1 = Bn R_2 = H

52a R_3 = Ph

52b R_3 = Ph

52c R_3 = Ph

52d R_3 = Ph

52e R_3 = 4-Cl-C_6H_4

53a R_1 = Bn R_2 = H R_3 = Ph

53b R_1 = Allyl R_2 = H R_3 = Ph

53c R_1 = MOM R_2 = H R_3 = Ph

53d R_1 = Bn R_2 = F R_3 = Ph

53e R_1 = Bn R_2 = H R_3 = 4-Cl-C_6H_4

Scheme 12: Use of β-isocupreidine in enantioselective catalysis of MBH reaction. Reagents and conditions: 20% mol of catalyst **47**, $CHCl_3$, room temperature.

1.1.4.3 Use of chiral acids

Using chiral acids promotes the reaction by coordination with the electrophiles and this enables the catalyst to orient in space on one side of the plane, thus activating the electrophiles and at the same time promoting enantioselectivity. The chiral acid can either be a Lewis acid or a Brønsted acid. A report by Chen *et al*, used diimine ligand **54** complexed with $La(OTf)_3$ to catalyse the reactions between aldehydes **55** and activated alkenes **56** affording adducts **57**, with the best performing reaction giving an enantiomeric excess greater than 93% (**Scheme 13**).[54] Although the mechanism is unclear, the adducts were obtained in very low yields with reasonable enantioselectivity.

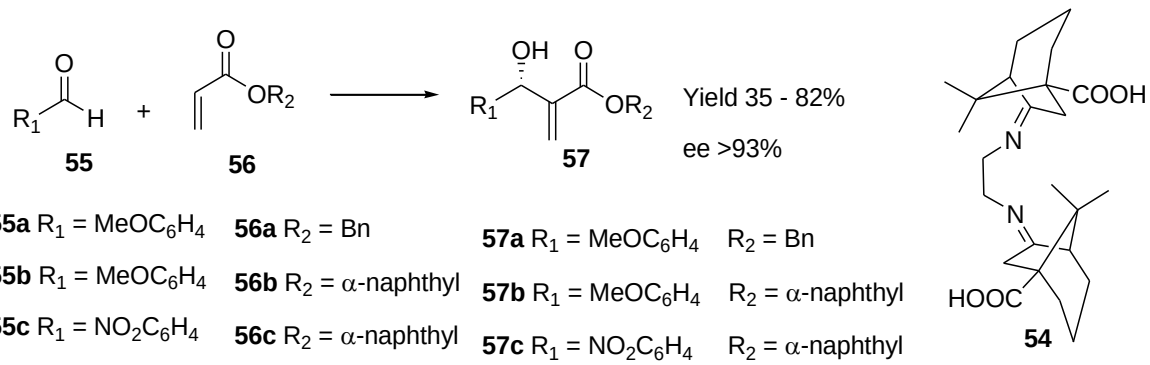

Scheme 13: Reactions of acrylates with aldehydes. Reagents and conditions: a complex of Ligand **55** with $La(OTf)_3$, DABCO, in MeCN at RT

The use of a Brønsted acid activates the electrophilic carbon by forming hydrogen bonds as documented in literature.[55, 56] This concept was extended to the activation and enantioselective investigation of MBH reactions by Nagasawa *et al*.[57] In his investigation, different aldehydes were reacted with cyclohexenone in the presence of urea **58**, and thiourea **59** and **60** using various amines without solvent. The use of thiourea **60** and DMAP was found to be the best combination for giving adducts in a yield range between 40 - 99% and enantiomeric excess range of 33 to 90%. The use of cyclohexane carbaldehyde and cyclohexenone gave the best enantiomeric excess of 90%.

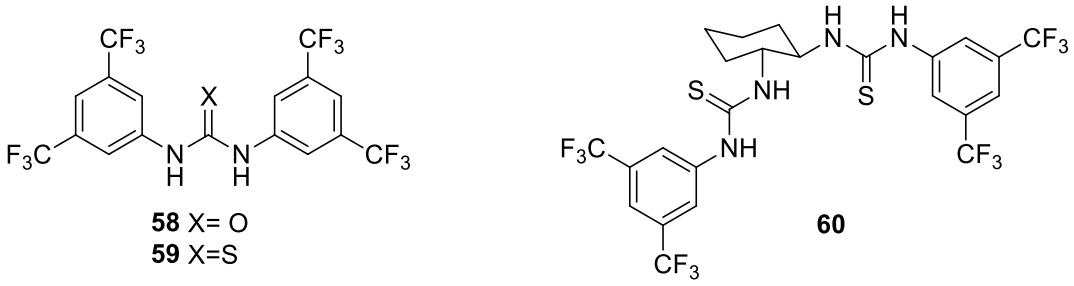

Figure 5: Structures of Brønsted acid thiourea and bis-thiourea compounds

The authors proposed a mechanism to explain why adducts formed were of the *R*-configuration (**Scheme 14**). According to the mechanism, the aldehyde and enone are positioned on the opposite side of thiourea through hydrogen bonding. This enables the enolate formed to attack the electrophile from the less sterically hindered side resulting in an *R*- alcohol.

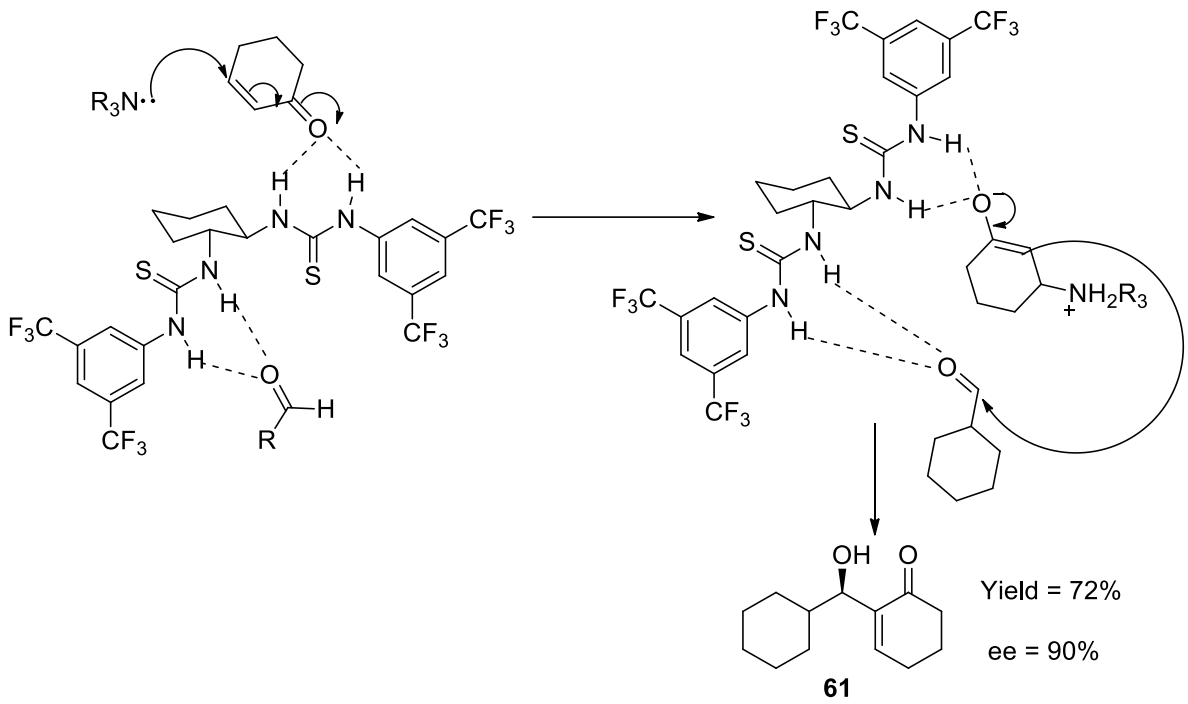

Scheme 14: The proposed mechanism that leads to enantioselection when bis-thiourea is used in the MBH reaction

More detailed information on the use of organo catalysts that promote enantioselectivity during MBH reactions can be found in the latest available review.[58]

In reality, almost none of the reported organocatalysts promote the formation of enantiopure adducts, although enantioselectivities are generally improving. Furthermore, synthetic procedures for preparation of the organocatalyst are complex and involve several steps. It is with these challenges in mind that development of simple single-step protocols are sought for the preparation of enantiopure MBHA. This has led to a resurgence in the popularity of alternatives that utilise enzymes to resolve the MBH racemates. This method is called enzymatic kinetic resolution (EKR) or enzymatic dynamic kinetic resolution (EDKR).

1.1.5 Enzymatic kinetic resolution of Morita-Baylis Hillman adducts

Biocatalysts have played an important role in resolution of MBH adducts. Enzymes such as enoate reductase (ER), alcohol dehydrogenase, nitrilase, nitrile hydratase, amidase, esterase

and lipases have been applied widely in resolving MBH adducts. The use of any of these enzymes relies heavily on the functional group one is targeting to achieve resolution. Reduction of activated alkenes has been reported to be achieved by enoate reductase (ER) while enantioselective reduction of the carbonyl group can be achieved by alcohol dehydrogenase (ADH) enzyme.[59] Both of these two enzymes originate from yeast strains. The use of nitrile hydrolyzing enzymes such as nitrilase, nitrile hydratase and amidase has been reported.[60] The lipases and esterases which have been widely applied in resolution target either an alcohol or ester functional group of the racemate.[61]

1.1.5.1 Use of yeast enzymes

The use of yeast in reducing MBH adducts was first reported by Takeda and co-workers.[62] In their pioneering work, they used Baker's yeast famously known to have enoate reductase (ER) enzymes to reduce *β*-hydroxy-*α*-methylene ketones (**Scheme 15**). This significant work resulted in *syn*- products of general configurations 3*R* and 4*S*; and *anti*- products of general configurations of 3*R* and 4*R* (**Table 2**). The specific optical rotations of the reduced adducts were found to have positive values. Their results showed that the reaction time and enantiomeric excess of *anti*- products increased when there was an increase in the size of the alkyl group of the aldehydes.

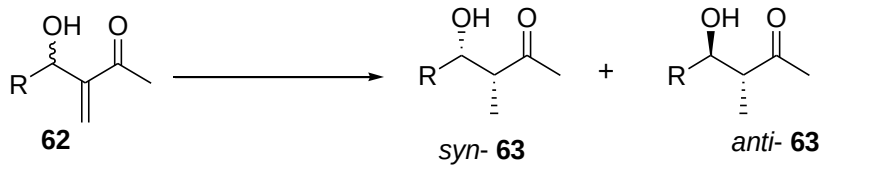

62a R = C_2H_5
62b R = C_3H_7
62C R = C_4H_9
62d R = C_5H_{11}

63a R = C_2H_5
63b R = C_3H_7
63C R = C_4H_9
63d R = C_5H_{11}

63a R = C_2H_5
63b R = C_3H_7
63C R = C_4H_9
63d R = C_5H_{11}

Scheme 15: Reduction of MBH adducts using baker's fermenters yeast. *Reagents and conditions*: glucose, baker's yeast immobilised on sodium alginate, water, 30 °C.

Table 2: Enantiomeric excess of the *syn*- and *anti*- products originating from the reduction of MBH adducts using baker's yeast

Entry	Adduct	Time (h)	Yield (%)	*syn*- 63, ee_p (%)	*anti*- 63, ee_p (%)	Specific optical rotation
1	**62a**	24	61	>98	>98	*syn*- **63a** (+44.0), *anti*- **63a** (+27.2)
2	**62b**	27	64	>98	72	*syn*- **63b** (+37.6), *anti*- **63b** (+26.5)
3	**62c**	69	56	>98	67	*syn*- **63c** (+31.5), *anti*- **63c** (+22.5)
4	**62d**	114	72	>98	69	*syn*- **63d** (+26.7), *anti*- **63d** (+17.8)

The report clearly explained how the optical rotation measurements and, where necessary, derivatisation were applied and compared with authentic samples to determine the configurations as indicated in **Table 2**. This pioneering work was not comprehensive as it did not investigate a variety of substrates and did not use different yeast strains and different reaction conditions. However, this formed a basis for other researchers to further investigate the enzymatic reduction reactions of other MBH adducts to address the shortcomings of the original study.

The second report in which Old Yellow Enzyme (OYE) homologue OYE 2.6 from *Pichia stiptis* and mutants of OYE from *Saccharomyces pastorianus* were used to reduce MBH adducts was by Steward and co-workers (**Scheme 16**).[63] OYE 2.6 from *P. stiptis* was applied to substrate **64** and the mutated OYE 2.6 was applied to adducts **65** and **66**. This process afforded products **67**, **68** and **69** all having *S*- configurations. The enantiomeric excess of **67** and **68** was greater than 98% while the enantiomeric excess of **69** was 76%.

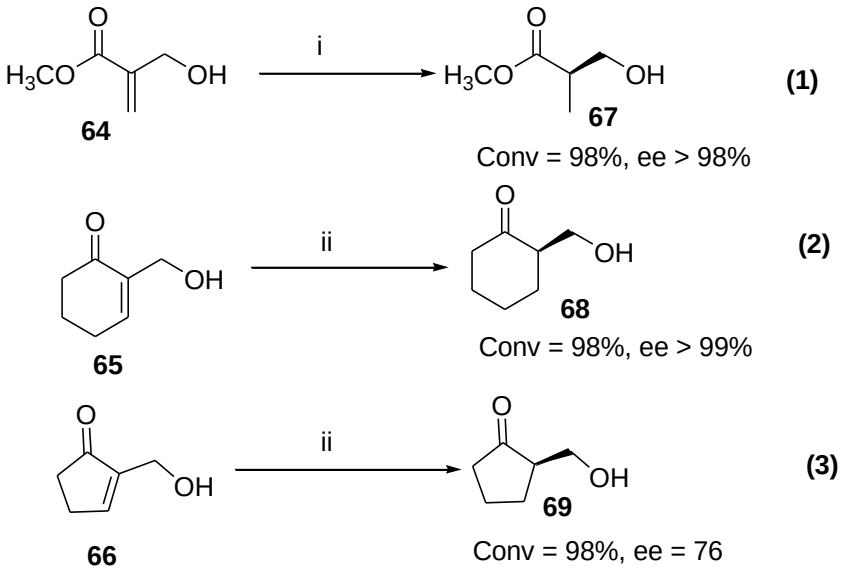

Scheme 16: Reduction of the double bonds of MBH adducts. *Reagents and conditions*: (i) OYE 2.6 from *P. stiptis* (ii) Mutant OYE 2.6 both done in phosphate buffer at pH 7.5, glucose, 37 °C.

The last report involved screening of *S. cerevisiae*, *R. glutinis*, *P. stipities* and *P. kluyveri* yeast strains on the reduction of α-methylene-β-ketoesters (**Scheme 17**).[64] This led to the identification of *S. cerevisiae* as the best performing strain on the tested substrates. The enzymatic activity of this strain was tested when the substrate was in water, Amberlite XAD7HP and on filter paper. The best enzymatic activities were observed when the substrates were in an Amberlite XAD7HP reservoir and on filter paper (**Table 3**). Excellent results were observed when the substrates were adsorbed onto filter paper as an efficient method to transfer the substrate to the biocatalytic reaction, with yields above 70% being obtained and an enantiomeric excess of 99%. The ratio of between *syn* and *anti*- products was found to be 9:1.

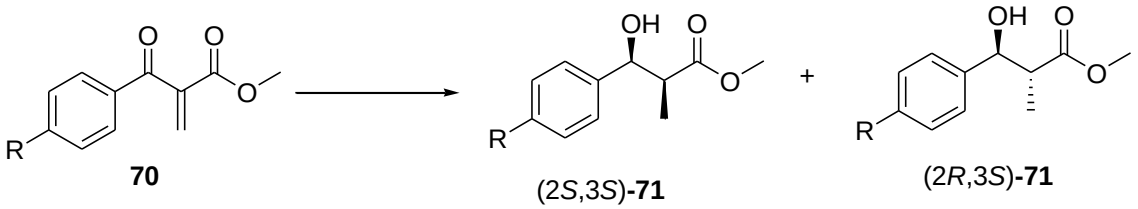

70

70a R = H

70b R = Cl

70c R = Br

(2*S*,3*S*)**-71**

71a R = H

71b R = Cl

71c R = Br

(2*R*,3*S*)**-71**

71a R = H

71b R = Cl

71c R = Br

Scheme 17: Reduction of *α*-methylene–*β*-ketoesters. *Reagents and conditions*: *S. cerevisiae*, ethanol, glucose, 42 °C.

Table 3: Use of *S. cerevisiae* in reducing *α*-methylene-*β*-ketoesters in two different reaction conditions

Compound	**Filter paper**			**XAD7 HP**		
	Yield (%)	**71** (2*S*,3*S*) (% ee)	**71** (2*R*,3S) (% ee)	Yield (%)	**71** (2*S*,3*S*) (% ee)	**71** (2*R*,3*S*) (% ee)
70a	75	99	99	75	98	98
70b	70	99	99	69	99	99
70c	73	99	99	61	99	99

The main drawback of using the enzymatic activity of the yeast strains for obtaining enantiopure adducts is that the double bond is not retained for further reactions. Therefore, the use of enzymes that target another functional group, for example the nitrile group, is likely to be a better alternative.

1.1.5.2 Use of nitrile hydrolysing enzymes

Research has shown that nitrile bio-transformation can be achieved using nitrilase, nitrile hydratase (NHases) and amidase.[65] Nitrile hydratase transforms a nitrile group **72** to an amide **73** which can be converted to the corresponding carboxylic acid **74** using an amidase, while nitrilase transforms a nitrile group directly to a carboxylic acid (**Scheme 18**).

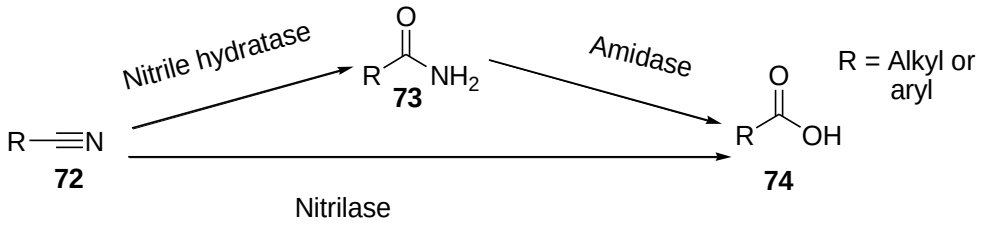

Scheme 18: Routes for converting the nitriles functional group using enzymes

An investigation by Wu and Wang demonstrated the use of *Rhodococcus sp.* AJ270 containing nitrile hydratase/amidase to hydrolyse the nitrile group of several MBH adducts into an amide and an acid (**Scheme 19**).[66] Among the 14 compounds investigated, only four MBH adducts afforded reasonable yields and enantiomeric excesses (**Table 4**, **entry 1-4**). The yields of the amides **76** obtained were in the range of 29 - 50%, with enantiomeric excesses ranging from 78 - 80%. The corresponding acids **77** were obtained in yields ranging from 44 - 63% with enantiomeric excesses in the range of 31 - 80%. The use of substrates **75b** and **75d** led to amides and acids with acceptable enantiomeric ratio (E) values of above 15. The use of protected hydroxyl **75e** decreased the reaction rate but increased the enantiomeric ratio (E) from 4.2 to 12 (**Table 4, entry 5**). Further increasing the reaction time for the methyl protected alcohol **75e** led to an increase in enantiomeric excess and enantiomeric ratio (E) (**Table 4 entry 6**). The results obtained for the protected hydroxyl group compound suggested that it is the steric effect and not hydrogen bonding that determined the enantioselectivity of the nitrile hydratase/amidase reaction for *Rhodococcus sp.* AJ270.

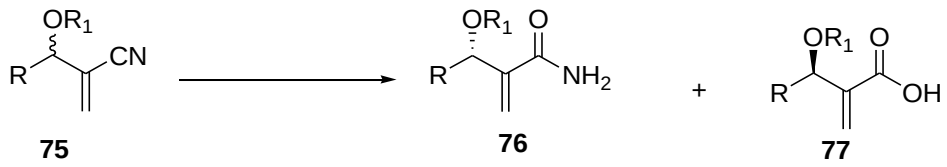

75a R = C_6H_5 R_1 = H	**76a** R = C_6H_5 R_1 = H	**77a** R = C_6H_5 R_1 = H
75b R = 3-MeO-C_6H_5 R_1 = H	**76b** R = 3-MeO-C_6H_5 R_1 = H	**77b** R = 3-MeO-C_6H_5 R_1 = H
75c R = 2-MeO-C_6H_5 R_1 = H	**76c** R = 2-MeO-C_6H_5 R_1 = H	**77c** R = 2-MeO-C_6H_5 R_1 = H
75d R = 2-Cl-C_6H_5 R_1 = H	**76d** R = 2-Cl-C_6H_5 R_1 = H	**77d** R = 2-Cl-C_6H_5 R_1 = H
75e R = C_6H_5 R_1 = Me	**76e** R = C_6H_5 R_1 = Me	**77e** R = C_6H_5 R_1 = Me

Scheme 19: Biotransformation of MBH adducts affording amides and carboxylic acids. *Reagents and conditions*: *Rhodococus sp*. AJ270 in phosphate buffer at pH 7.00 at 30 °C.

Table 4: Bioconversion of nitriles to amides and carboxylic acids

Entry	**Substrate**	**Time (h)**	**76**		**77**		**E**
			Yield (%)	**ee$_p$** (%)	**Yield** (%)	**ee$_p$** (%)	
1	**75a**	48	29	80	63	31	4.2
2	**75b**	48	48	81	45	75	17
3	**75c**	72	50	79	44	70	13
4	**75d**	50	50	78	48	80	21
5	**75e**	72	47	53	43	77	12
6	**75e**	168	57	38	34	82	14

A similar *Rhodococcus sp.* AJ270 whole cell catalyst was applied to modified MBH adducts (**Scheme 20**).[67] The use of substrate **78a - 78c** gave amides **79** of *S*- configurations and lactones **80** of *R*- configuration. Apart from substrate **78b**, all the other substrates afforded amide and lactone in very low yields and enantioselectivity. The use of **78b** led to an amide **79b** in a yield of 51% and enantiomeric excess of 82%; with the corresponding lactone **80b** being obtained in 33% yield and an ee of 77%. The use of **78c** led to a lactone **80c** in a yield of 30% with an ee of 70%.

Applying the same enzyme to protected substrates **78d** – **78f** afforded amides **79d - 79f** of *R*-configuration and corresponding acids **81d** – **81f** of *S*-configuration without the formation of any lactone. Although the yield and enantioselectivity were not encouraging; only substrate **78e** performed better as compared to the rest in this group. The use of **78e** resulted

to an amide in 59% yield and an ee of 40%; the corresponding acid was obtained in 40% yield with an ee of 69%.

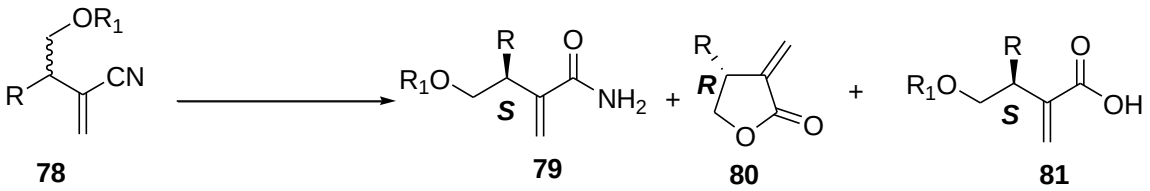

78 **79** **80** **81**

78a R = C_2H_5 R_1 = H
78b R = $CHMe_2$ R_1 = H
78c R = C_5H_{11} R_1 = H
78d R = C_2H_5 R_1 = Me
78e R = $CHMe_2$ R_1 = Me
78f R = C_5H_{11} R_1 = Me

79a R = C_2H_5 R_1 = H
79b R = $CHMe_2$ R_1 = H
79c R = C_5H_{11} R_1 = H
79d R = C_2H_5 R_1 = Me
79e R = $CHMe_2$ R_1 = Me
79f R = C_5H_{11} R_1 = Me

80a R = C_2H_5 R_1 = H **81d** R = C_2H_5 R_1 = Me
80b R = $CHMe_2$ R_1 = H **81e** R = $CHMe_2$ R_1 = Me
80c R = C_5H_{11} R_1 = H **81f** R = C_5H_{11} R_1 = Me

Scheme 20: Hydrolysis of MBH nitriles affording amides, carboxylic acids and lactones. *Reagents and conditions*: *Rhodococcus sp*. AJ270 whole cell in phosphate buffer at pH 7.00 at 30 °C.

A summary on the use of enzymes from *Rhodococcus sp.* AJ270 on MBH nitriles can also be obtained from a short review.[68] The use of adducts in **Scheme 20** for synthetic application is limited especially when the oxygen atom next to the stereogenic carbon is required for further functionalization.

The use of nitrilase from *Rhodococcus erythropolis* SET 1 on MBH adducts was reported to afford insignificant results.[69] This is because among the 14 nitriles originating from aliphatic and aromatic aldehydes that were tested, only adduct **82** gave reasonable results (**Scheme 21**).

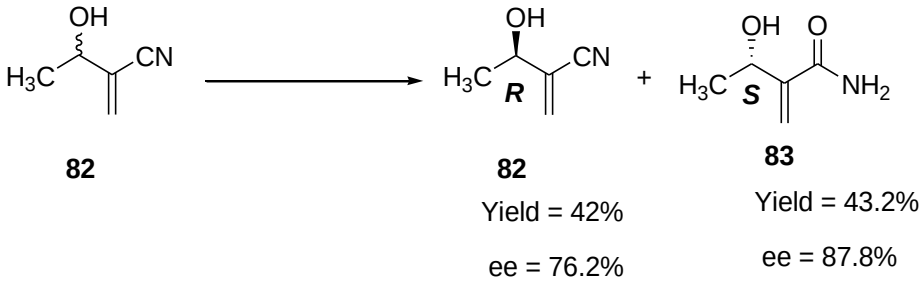

Scheme 21: Biotransformation of MBH adduct. *Reagent and conditions*: Nitrilase from *R. eryhthropolis* SET 1, phosphate buffer at pH 7.00 at 20 °C.

Further information explaining the mechanism by which nitrilase,[70] nitrile hydratase[71] and amidase[72] hydrolyse the nitrile group is also available in literature. Apparently, this mode of resolution is restricted to nitriles and it seems that the chances of getting products in high yields and enantiomeric excess above 90% are minimal.

1.1.5.3 Use of lipases and esterases

Another option for resolving MBH adducts is the use of lipases and esterases, which has many advantages such as that the identity of the molecule is retained. Lipases and esterases belong to the α/β-hydrolases fold family and are able to resolve a racemic alcohol by either hydrolysis or esterification.[73] Generally, lipases and esterases are very similar with the major difference being that lipases are activated by the oil phase which induces the opening of the lid or flap that covers the catalytic site.[74] Both lipases and esterases have a catalytic triad consisting of serine **84**, histidine and aspartic acid or glutamic acid and therefore they resolve alcohols or acetates with a similar mechanism as shown in **Schemes 22** and **23**.[75, 76]

The esterification process starts with a nucleophilic attack on the carbonyl ester bond of acylating agent **85** by the serine hydroxyl functional group generating a tetrahedral intermediate **86** (**Scheme 22**, **step 1**). Intermediate **86** then loses alcohol **87** to give an acyl-enzyme intermediate **88**. The acyl-enzyme complex is attacked by the hydroxyl group of a racemic alcohol **88** affording intermediate **90**. Step 3 takes place in such a way that only one enantiomer will be able to attack intermediate **88** hence controlling stereoselectivity. The last step involves the loss of stereoselectively acylated compound **91a** or **91b** and regeneration of the active enzyme.

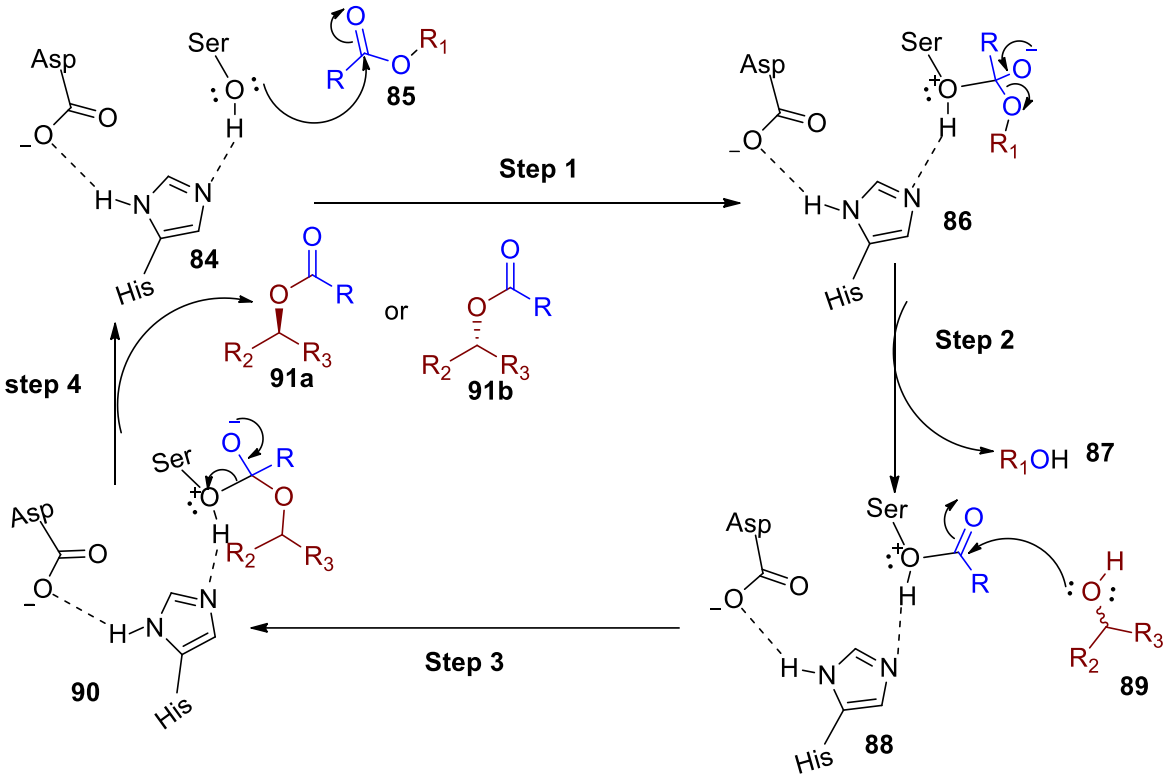

Scheme 22: Esterification reaction mechanism mediated by esterase or lipase enzymes

Stereoselective hydrolysis involves nucleophilic attack on the carbonyl ester **91** by the nucleophilic serine hydroxyl **84**, this leads to a tetrahedral intermediate **90** that loses alcohol **89a** or **89b** of specific configuration to give an acyl-enzyme intermediate **88** (**Scheme 23**). Histidine, which is stabilized by the aspartyl carboxyl group, increases the nucleophilicity of the hydroxyl group through hydrogen bonding. The acyl-enzyme complex is attacked by a water molecule to give a second intermediate **92** which finally loses a carboxylic acid **93** to regenerate the enzyme in its active state.

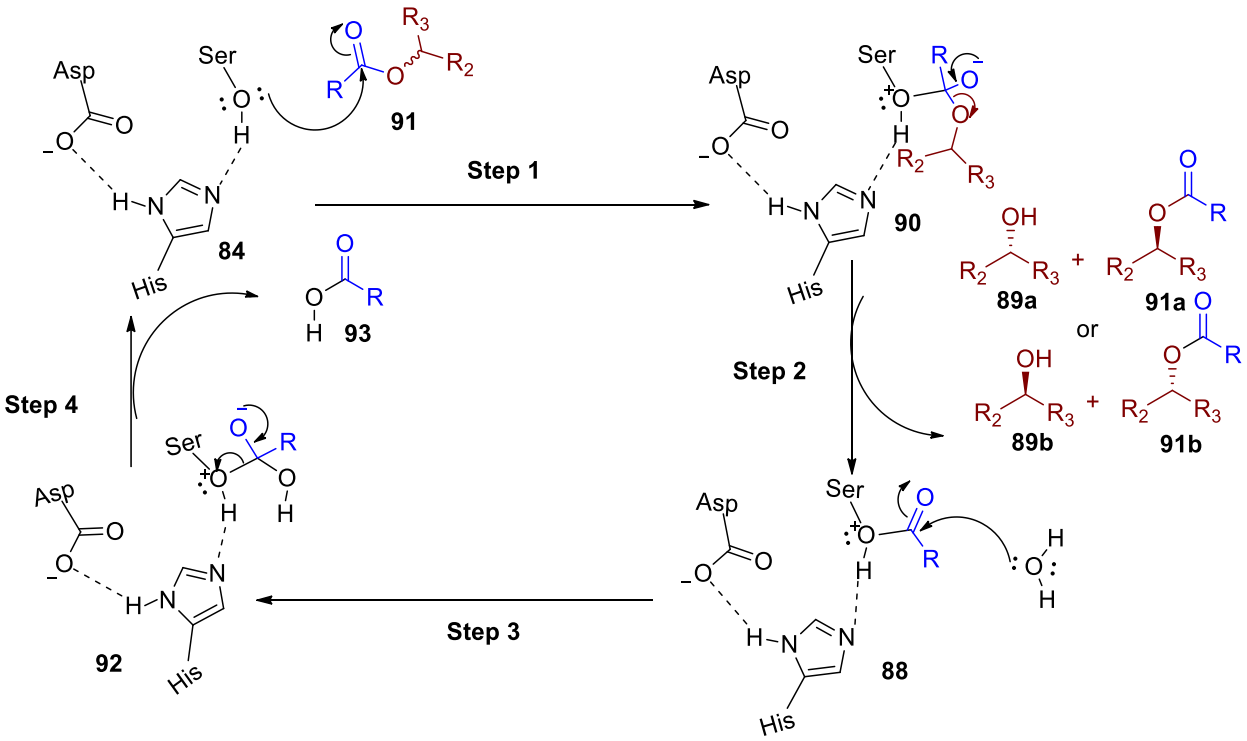

Scheme 23: Reaction mechanism of esterase or lipase mediated hydrolysis of esters

The numerous uses of lipases and esterases for resolving structurally diverse alcohols also attracted many researchers to apply the same enzymes for resolving Morita-Baylis-Hillman adducts. Burgess and Jennings are the pioneers in resolving Morita-Baylis-Hillman adducts by acetylation.[77] In the process of resolving other alcohols, they were able to resolve MBHA **94a** (**Figure 6**). This enantiopure *S*- alcohol and *R*- acetate were obtained after using crude lipase AK from *Pseudomonas* species in the presence of vinyl acetate and hexane as solvent. Convincingly, they were able to determine the stereochemistry using Mosher's ester derivatization protocol. Their encouraging result of enantiomeric excess of both substrate and product of greater than 95% and enantiomeric ratio (E) greater than 20 after resolving **94a** enticed them to investigate 10 additional adducts (**Figure 6**, **94b** – **94k**). In their extension of this work, which was published, they used similar reagents and conditions shown in **Scheme 24** to resolve the additional adducts (**Table 5**).[78]

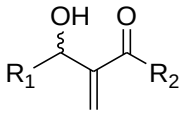

94

94a $R_1 = CH_3$ R_2 = Phe **94b** $R_1 = CH_3$ R_2 = OBu **94c** $R_1 = CH_3$ $R_2 = OCH_2CHCH_2$

94d $R_1 = CH_3$ $R_2 = OCH_2CCH$ **94e** $R_1 = CH_3$ $R_2 = OCH_3$ **94f** $R_1 = CH_3$ R_2 = Bu

94g $R_1 = CH_3$ $R_2 = (CH_2)_2Ph$ **94h** $R_1 = CH_3$ $R_2 = O(CH_2)_2SPh$

94i $R_1 = (CH_2)_2CH_3$ R_2 = OBu **94j** $R_1 = (CH_2)_2CH_3$ $R_2 = OCH_3$ **94k** $R_1 = (CH_2)_2CH_3$ $R_2 = CH_3$

Figure 6: *α*-Methylene-*β*-hydroxy carbonyl compounds resolved by Burgess and Jennings

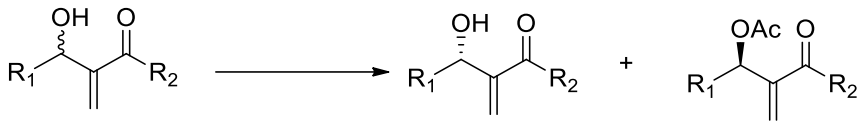

(±)–**94** (*S*)-**94** (*R*)-**95**

Scheme 24: Esterification of α-methylene-β-hydroxy carbonyl compounds. *Reagents and conditions*: *Pseudomonas* AK, vinyl acetate in hexane at 25 °C.

Table 5: Resolution of MBH alcohols in **Figure 6** using **Scheme 24**

Entry	**Substrate**	**Time (h)**	**Conv (%)**	**Alcohol**			**E**
				Adduct	Yield (%)	ee_s (%)	
1	(±)-**94a**	70	52	(*S*)-**94a**	32	>95	>20
2	(±)-**94b**	48	50	(*S*)-**94b**	41	>95	>56
3	(±)-**94c**	12	53	(*S*)-**94c**	43	>95	>43
4	(±)-**94d**	17	54	(*S*)-**94d**	43	>95	>34
5	(±)-**94e**	12	64	(*S*)-**94e**	22	87	8
6	(±)-**94f**	12	52	(*S*)-**94f**	23	>95	>56
7	(±)-**94g**	12	56	(*S*)-**94g**	41	>95	>24
8	(±)-**94h**	12	55	(*S*)-**94h**	39	>95	>29
9	(±)-**94i**	60	50	(*S*)-**94i**	23	>95	>56
10	(±)-**94j**	240	46	(*S*)-**94j**	32	52	7
11	(±)-**94k**	24	67	(*S*)-**94k**	21	72	4

The additional adducts gave encouraging results as shown in **Table 5** (**entries 2-11**). Seven adducts afforded enantiomeric ratio (E) values greater than 20 with excellent ee_s and ee_p of 95% and above (**entries 2-4**, **6-9**). A lower E value below 10 and ee_s of less than 87% was observed when R_2 was a methoxy group, suggesting that the presence of this group reduced the enantio-discrimination of the enzyme investigated (**entry 5**, **10-11**). This observation suggests that *Pseudomonas* AK prefers a longer chain substituent at R_2 for better enantioselectivity. It is also clear that adducts with a longer chain as the R_1 group experienced longer reaction times relative to those with shorter alkyl chain. The stereochemistry of the resulting enantiopure adducts were determined accurately by use of Eu $(hfc)_3$ shift experiments. The use of phenyl as R_1 made the reaction so slow that the resolution was not possible.

Following on from this work of Burgess and Jennings, Hayashi and co-workers used lipases from *Pseudomonas* species to investigate the resolution of adducts as shown in **Scheme 25**.[79] Varying the acylating agent and using lipase PS, in acetonitrile at 35 °C led to the results shown in **Table 6**.

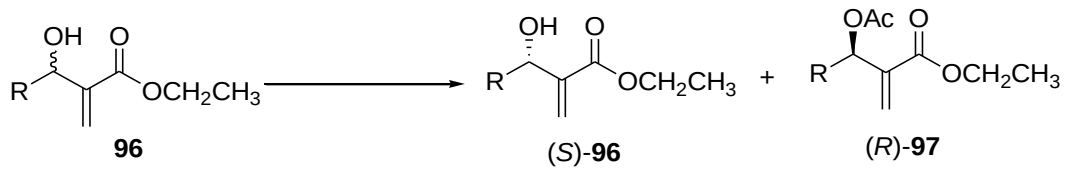

96a R = CH_3 **96b** R = CH_2CH_3

96c R = n-C_5H_{11} **96d** R = CCl_3,

97a R = CH_3 **97b** R = CH_2CH_3

Scheme 25: Transesterification of MBH ethyl esters. *Reagents and conditions*: Lipase PS, acetonitrile and different acylating agents

Table 6: Resolution of MBH alcohols by acetylation

Entry	**Substrate**	**Time (d)**	**Acylating agent**	**Alcohol**		**Acetate**		**E**
				Yield (%)	ee_s (%),	Yield (%)	ee_p (%),	
1	(±)-**96a**	6	Isopropenyl acetate	(*S*)-**96a**; 42	>99	(*R*)-**97a**, 43	97	>349
2	(±)-**96b**	7	Isopropenyl acetate	**96b**; 53	44	(*R*)-**97b**, 34	90	29
3	(±)-**96b**	7	Vinyl acetate	(*S*)-**96b**; 50	70	(*R*)-**97b**, 37	>99	>424
4	(±)-**96b**	7	Vinyl trifluoro acetate	(*S*)-**96b**; 62	13	(*R*)-**97b**		

The use of isopropenyl acetate as acylating agent on racemic **96a** afforded enantiopure alcohol *S*- **96a** and enantiopure acetate **97a** with ee_s greater than 99% and ee_p of 97% respectively in 6 days (**Table 6**, **entry 1**). Using isopropenyl acetate on racemic **96b** afforded a scalemic alcohol **96b** with an ee_s of 44% and an enantiopure acetate (*R*)- **97b** of 90% enantiomeric excess with an E value of 29. By applying vinyl acetate on **96b**, both the ee_p and ee_s increased to greater than 99% and 70% respectively. There was no reaction when vinyl trifluoroacetate was used to acetylate **96b**. The use of adducts **96c** and **96d** with any of the acylating agents led to no reaction. The authors demonstrated how the enzymatic activity of lipase from *Pseudomonas* was affected by different acylating agents. It is worth noting that no MBH adducts derived from benzaldehyde were included in the study, and only aliphatic adducts were successfully resolved.

In addition to resolution by esterification, the same report by Hayashi investigated resolution by hydrolysis of acetates as shown in **Scheme 26** where the ester bond was hydrolysed using *Pseudomonas* lipase PS and lipase AK.

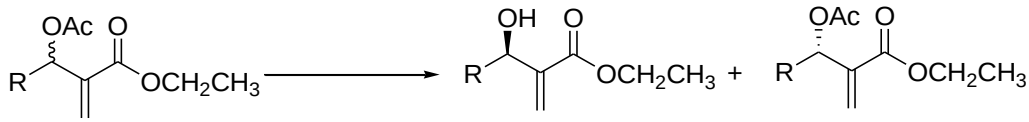

97b R = CH_2CH_3 (*R*)-**96b** (*S*)-**97b** **97b** R = CH_2CH_3

98a R = n-C_7H_{15} (*R*)-**99a** (*S*)-**98a** **98a** R = n-C_7H_{15}

Scheme 26: Hydrolysis of MBH acetates. *Reagents and conditions*: *Pseudomonas* Lipase PS or AK, phosphate buffer at 30 °C

Table 7: Resolution of MBH acetates by hydrolysis

Entry	**Substrate**	**Lipase**	**Time (d)**	**Alcohol**		**Acetate**		**E**
				Yield (%)	ee_s (%),	Yield (%)	ee_p (%),	
1	(±)-**97b**	PS	5	(*R*)-**96b**, 20	75	(*S*)-**97b**, 49	12	8
2	(±)-**97b**	AK	13	(*R*)-**96b**, 17	>99	(*S*)-**97b**, 33	46	>321
3	(±)-**98a**	PS	11	(*R*)-**99a**, 17	85	(*S*)-**98a**, 61	27	16
4	(±)-**98a**	AK	14	(*R*)-**99a**, 14	92	(*S*)-**98a**, 76	1	26
5	(±)-**98a**	AK	11	(*R*)-**99a**, 20	93	(*S*)-**98a**, 58	41	41

It can be observed from **Table 7** that the yields are very low, and the authors noted a slow reaction rate. It was only the use of lipase AK on racemic **97b** and **98a** (**entry 2 and 5**) that gave a reasonable enantiomeric ratio of greater than 321 and 41 respectively. The ee_s values of the corresponding enantiopure alcohols were observed to be greater than 99% and 93% respecively. Once again, only MBH adducts originating from aliphatic aldehydes were investigated while other adducts with structural diversity were not mentioned in this investigation. The authors did not independently determine the absolute stereochemistry of the products, but instead assigned the stereochemistry of the products by comparing the optical rotation values with thos reported in the literature.

It was Basavaiah and co-workers who were the first to enzymatically resolve MBH methyl ester adducts derived from aromatic aldehydes using pig liver acetone powders (PLAP) (**Scheme 27**).[80] Their search led to alcohols **101** in yields ranging from 19 - 37% with a very variable enantiomeric excess range of 46 – 86%. The observed enantiomeric excesses were too poor for the practical production of the enantiopure products required for asymmetric transformations.

100a R = H

100b R = 4-CH_3

100c R = 4-Cl

100d R = 2-OCH_3

101a R = H

101b R = 4-CH_3

101c R = 4-Cl

101d R = 2-OCH_3

Scheme 27: Resolution of MBH methyl esters. *Reagents and conditions*: Pig liver acetone powders in phosphate buffer at pH 7.00 at room temperature.

The poor enantiomeric excesses recorded by Basavaiah were a motivating factor that attracted Bhuniya *et al*. to investigate an alternative resolution strategy of MBH ethyl esters originating from aromatic aldehydes (**Scheme 28**).[81] It was hoped that the enzymes used would hydrolyse the ethyl ester bond stereoselectively to give the corresponding carboxylic acids. Indeed, they were able to confirm that by shifting the hydrolysis target from an acetate to an ethyl ester bond they were able to obtain some enantioselectivity. Their observed enantiomeric excesses of the remaining substrate of greater than 99% for all the tested compound with a reaction time range of 16 to 28 hours was very encouraging. However, the enantiomeric excesses they obtained had unacceptable enantiomeric ratio (E) values of below 10 (**Table 8**). Their use of optical rotation values for determining the stereochemistry by comparing their recorded values and literature values was also not convincing.

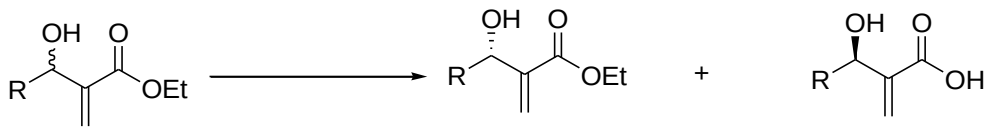

102

102a R = 4-NO_2-Ph

102b R = 3-NO_2-Ph

102c R = 4-F-Ph

102d R = 3-OH-Ph

102e R = PhCHCH

S-**102**

102a R = 4-NO_2-Ph

102b R = 3-NO_2-Ph

102c R = 4-F-Ph

102d R = 3-OH-Ph

102e R = PhCHCH

R-**103**

103a R = 4-NO_2-Ph

103b R = 3-NO_2-Ph

103c R = 4-F-Ph

103d R = 3-OH-Ph

103e R = PhCHCH

Scheme 28: Resolution of MBH ethyl esters. *Reagents and conditions*: Porcine liver esterase in phosphate buffer at pH 7.00 using DMSO as a co-solvent.

Table 8: Resolution of MBH ethyl esters

Entry	Substrate	Time (h)	*S*-**102**		*R*-**103**		E
			Yield (%)	ee_s (%)	Yield (%)	ee_p (%)	
1	**102a**	24	30	>99	65	35	9.5
2	**102b**	16	35	>99	60	15	5.2
3	**102c**	16	30	>99	65	17	5.4
4	**102d**	24	30	99	65	10	4.3
5	**102e**	28	25	99	56	26	7.1

By analysing the resolution results discussed so far, it is clear that resolution of MBH adducts has been achieved by hydrolysing a nitrile to the corresponding amide or carboxylic acid, or by creating or breaking an ester bond of methyl and ethyl derivatives. It was with this view that it was an intellectually inspiring idea for others to target resolution of MBH adducts prepared from acrylonitrile derivatives. This idea was first investigated by Bornscheuer and co-workers.[82] They used *Pseudomonas cepacia* lipase (PCL) in the presence of cyclohexyl acetate as an acyl donor to resolve adducts **75a, 82** and **104a** – **104c** by esterification. By using the reaction shown in **Scheme 29**, they were able to obtain enantiopure acetates **105a - 105e** with the enantiomeric excesses ranging from 63 – 98% (**Table 9**, **entries 1 – 2** and **5**– **7**). It is worth noting that for the MBH adduct **75a**, derived from benzaldehyde, only 9% conversion was achieved and a poor product ee of 76% was

obtained. This report also recorded poor enantiomeric excesses for all the substrates and absolute stereochemistry was not assigned, with the sign of optical rotation being the only parameter reported.

The use of vinyl acetate and different enzymes in a transesterification reaction of **82** was later investigated by Strub and co-workers.[83] Their investigation led to enantiopure alcohol **82** of *R*- configuration and an enantiopure acetate **105b** of *S*- configuration. The absolute configuration of the enantiopure alcohol was convincingly confirmed using Mosher's derivatisation protocol. The enantiomeric excess of the acetate was found to be 96% and 94% when lipase Novozyme 435 and PS amano from *Pseudomonas cepacia* were used, respectively (**Table 9**, **entries 3 - 4**). The same enzymes resolved the racemic acetate **105b** by hydrolysis, generating enantiopure acetate with an enantiomeric excess of greater than 99%.

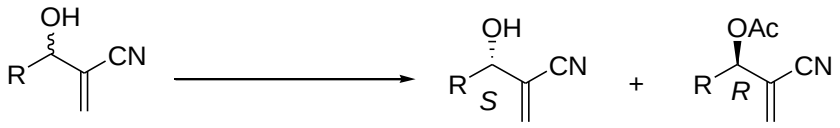

75a R = Ph **82** R = CH_3

104a R = Et **104b** R = n-Pr

104c R = Cyh

105a R = Ph **105b** R = CH_3

105c R = Et **105d** R = n-Pr

105e R = Cyh

Scheme 29: Transesterification of MBH nitriles using different lipases and acyl donors. *Reagents and conditions*: (a) Bornscheuer and co-workers- Lipase from *P. cepacia*, cyclohexyl acetate, 30 °C (b) Strub and co-workers-vinyl acetate, isopropyl ether at room temperature. Note: *n – Pr* = n-propyl; Cyh = Cyclohexyl

Table 9: Resolution of MBH nitriles by esterification as described by Uwe *et al*., and Strub *et al*.

Entry	Substrate	Time days/h	Conv (%)	ee_s (%)	ee_p (%)	E
1	**75a**	35d	9	8	76	NC
2	**82**	20d	27	11	98	NC
3	**82**	48h	33	48	96	79
4	**82**	48h	46	81	94	81
5	**104a**	9 d	42	5	63	NC
6	**104a**	35d	22	21	75	NC
7	**104a**	14d	56	9	NME	

NC = Not calculated, NME = Not measured experimentally

The use of CALB for resolution of acetates **106a** and **106b** has been reported to lead to enantiopure alcohols **107a** and **107b** with enantiomeric excesses greater than 99% (**Scheme 30)**.[84] Hydrolysis of the enantiopure acetates **106a** and **106b** using chemical means afforded enantiopure alcohols having opposite stereochemistry to that of **107a** and **107b**. The enantiomeric excesses of these alcohols with opposite stereochemistry was found to be greater than 87%. The four alcohols *R*- **107a**, *R*- **107b**, *S*- **107a** and *S*- **107b** whose stereochemistry was determined using Mosher's protocol displayed antileishmanial activity.

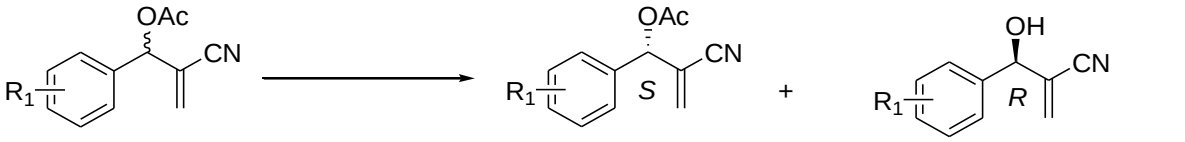

106a R_1 = 3-NO_2 **106b** R_1 = 4-NO_2

107a R_1 = 3-NO_2 **107b** R_1 = 4-NO_2

Scheme 30: Resolution of MBH nitriles. *Reagents and conditions*: water, CALB, 30 °C.

The latest report for resolving MBH adducts applied the dynamic kinetic resolution (DKR) principle. Unlike normal enzymatic kinetic resolution which affords 50% conversion of starting material, DKR leads to 100% conversion of the starting material to products that can either be of *R* or *S*- configuration.[85] The essential components required for DKR are the

racemic mixture, a solvent, an enzyme, acyl donor and a racemizing agent.[86] For DKR to be successful then the reation rate of converting one enantiomer to an enantiopure product has to be faster than the reaction rate of the opposite enantiomer. In addition, the rate of racemizing must be equal to or greater than the rate at which the faster reacting enantiomer is converted to product (**Scheme 31**).

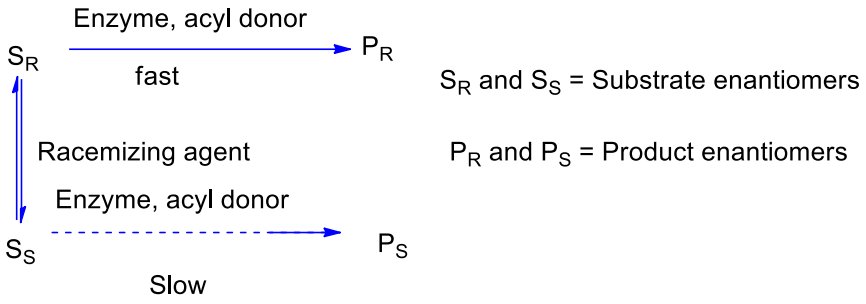

Scheme 31: Concept of dynamic kinetic resolution for resolving racemic mixtures

This last outstanding report discusses the use of the wild type (WT) and bioengineered CALB to dynamically and kinetically resolve acetates **106b**, and **108a** – **108b** in the presence of triethylamine as a racemisation agent (**Scheme 32**).[87] Nucleophilic addition of triethylamine to the *S*- acetate generates intermediate **109** which is transformed to *R*- acetate when the nucleophilic acetate is added back to eliminate the triethylamine. Using *S*- selective WT CALB afforded enantiopure alcohols **107b**, and **110a** – **110b** of *S*- configuration in yields greater than 90% and enantiomeric excesses greater than 72%. The use of *R*- selective CALB mutant WB13 led to the alcohols of *R*- configuration with enantiomeric excesses greater than 77% and yields range between 71% to 95%.

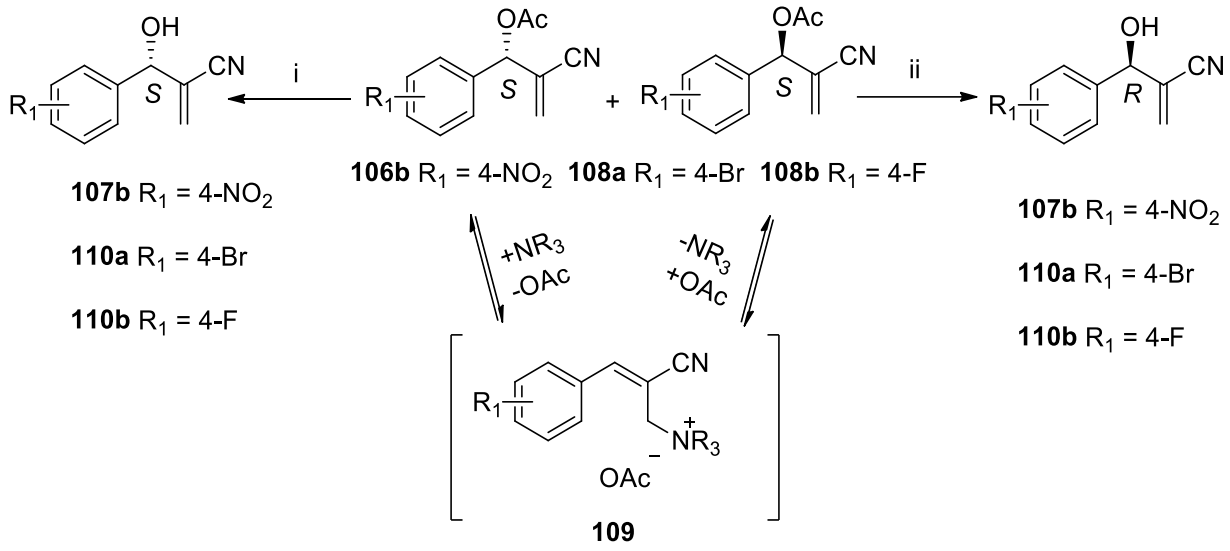

Scheme 32: Triethylamine-lipase co-catalysed dynamic kinetic resolution of MBH nitrile acetate. *Reagents and conditions*: (i) *S*- selective WT CALB, triethylamine, toluene, 40 °C; (ii) *R*- selective CALB mutant WB13, triethylamine, toluene, 20 °C.

1.1.6 Synthetic applications of Morita-Baylis-Hillman adducts (MBHA)

Almost all the reactions that can be performed on the MBH adducts can be classified into three major categories based on the mechanism involved (**Scheme 33**).[88] The first is 1,4-addition of a nucleophile to the electrophilic α,β-unsaturated system of adducts such as **111**. These reactions proceed by a Michael addiction mechanism to generate **112** (**Step 3**). Converting the hydroxyl group into a better leaving group, such as an acetoxy group, increases the likelihood of an allylic substitution by an S_N2' mechanism (**Step 2**) to give **114**. Sequential S_N2' reactions, going via intermediate **116** can give rise to compound **115** (**Step 1**).

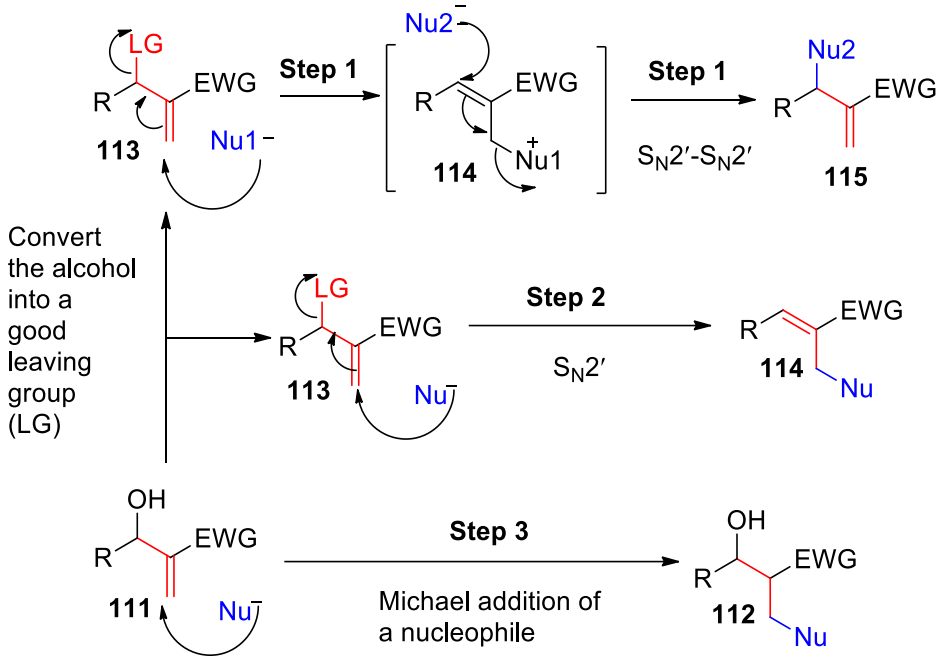

Scheme 33: Nucleophilic addition and allylic substitution in the Morita-Baylis-Hillman alcohols and acetates

The reactions shown in **Scheme 33** have been applied in the synthesis of biologically active compounds, natural products and intermediates for various synthetic applications. Therefore, the focus of this discussion is on the reported use of each mechanism starting from **step 1**.

1.1.6.1 Sequential use of S_N2'-S_N2' reactions

The application of successive S_N2'-S_N2' reactions using different nucleophiles on MBH adducts has not been extensively explored. This is evidenced by limited literature illustrating the use of nitrogen, phosphorus and carbanion nucleophiles for allylic nucleophilic substitution. Du and co-workers were able to use DABCO and TQO **116** for catalysing allylic substitution using nitrogen, oxygen and carbanion nucleophiles (**Scheme 34**).[89]

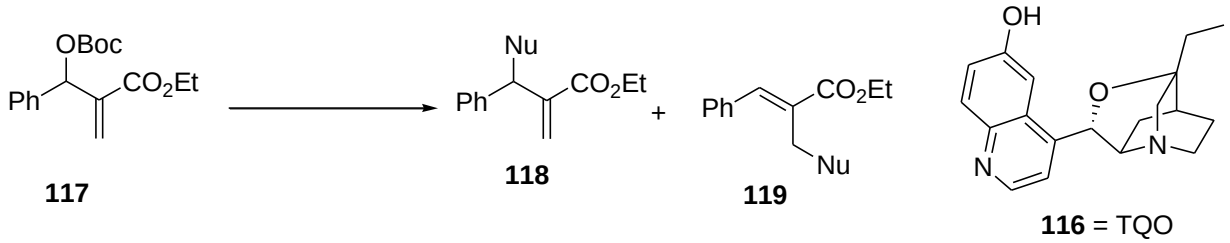

Scheme 34: Catalysis of allylic nucleophilic substitution of BOC protected MBH adducts. *Reagents and conditions*: Nucleophile, DABCO or TQO, toluene at room temperature.

The use of different nucleophiles led to the major product of scaffold **118** and minor product of scaffold **119**. The major adducts consisted of compound **120 - 123** in **Figure 7**. The use of DABCO afforded adducts with very low stereoselectivity that improved when TQO was used.

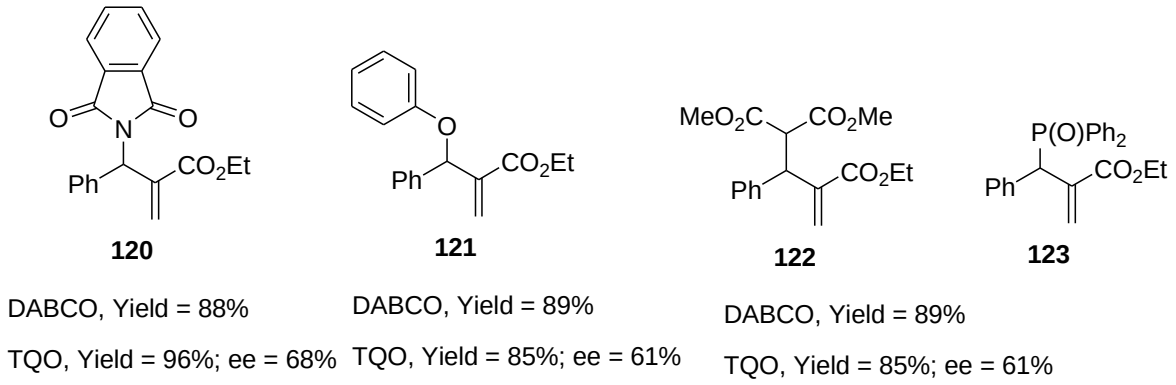

Figure 7: Nucleophilic allylic substitution of MBH adducts

The importance of scaffold **123** as a lead compound for different biological activities attracted others to search for an alternative way of synthesising it.[90] As reported, the use of MBH bromides **124a** – **124c** generated DABCO salts of scaffold **125**, that were reacted with phosphite derivatives to generate adducts **126a** – **126c** in yields ranging from 60% - 80% (**Scheme 34**). Kim and co-workers synthesised more allylic substituted phospha-Morita-Baylis-Hillman products of scaffold **126** via Michaelis-Arbuzov reaction.[91]

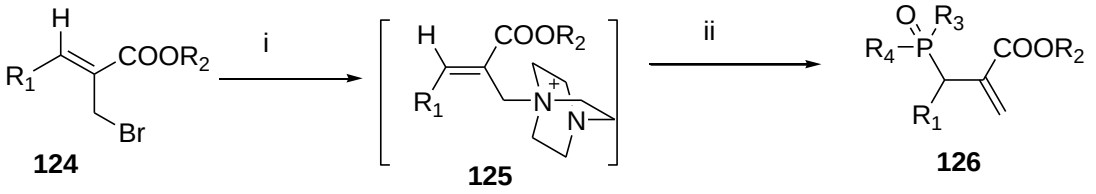

124 **125** **126**

124a R_1 = Phe,R_2 = Me

124b R_1 = 4-Cl-Phe R_2 = Et

124c R_1 = 4-NO_2Phe R_2 = Et

126a R_1 = Phe, R_2 = Me, R_3 = R4 = Phe

126b R_1 = 4-Cl-Phe R_2 = Et, R_3 = R_4 = $PhCh_2$-

126c R_1 = 4-NO_2Phe , R_2 = Et, R_3 = R_4 = EtO

Scheme 35: Synthesis of phosphorylalkanoates from alkene MBH bromides. *Reagents and conditions*: (i) DABCO in acetonitrile at room temperature (ii) Triphenyl Phosphite at 80 °C.

The reaction between cyclic acetates and triethyl phosphite has been reported to afford regioselective γ-keto allylphosphonates **129a** – **129c** in a yield of 70 – 93% (**Scheme 36**).[92]

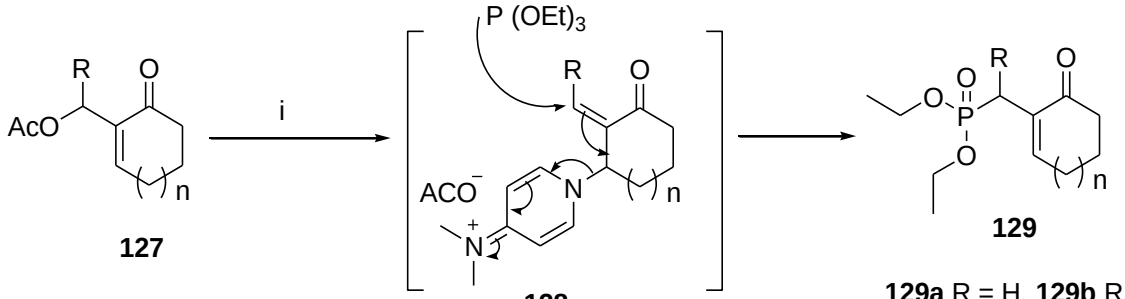

127 **128** **129**

127a R = H, **127b** R = alkyl

127c R = aryl, n = 0, 1

129a R = H, **129b** R = alkyl

129c R = aryl n = 0, 1

Scheme 36: Substitution of cyclic allyl ketones. *Reagents and conditions* (i) DMAP and triethyl phosphite at 80 °C in solvent free conditions

1.1.6.2 Nucleophilic allylic substitution (S_N2') reaction

The allylic nucleophilic substitution reactions by purely the S_N2' mechanism have been widely used on MBH protected alcohols. This is partly because this reaction is straightforward, and the presence of a good leaving group such as an acetate enhances the electrophilicity of the unsaturated Sp^2 carbon. The total synthesis of enantiomerically pure furanone derivative **132** of *S* and *R*- configuration has been reported to be achieved starting from MBH acetate **130a** (**Scheme 37**).[93] The steps involved allylic substitution on **130a**

using lithium diethyl copper in ether affording cinnamate derivative **131** that was converted to an anti-inflammatory agent **132** in 5 steps. More examples illustrating the use of acetylated MBH adducts for the synthesis of different natural product can also be found in a recent mini review.[94]

The synthesis of β^2-amino acid derivatives with the potential of being the key intermediates for the synthesis of antifungal agents was reported to start from several MBH acetates **100a** and **130b** – **130d** (**Scheme 37**).[95] The reaction of these acetates with benzylhydroxylamine, led to the formation of intermediate amino acrylates **133a** – **133d** which were hydrogenated to form products **134a** – **134d** in yields ranging from 42 – 99% with enantiomeric excesses in the range of 83 – 99%.

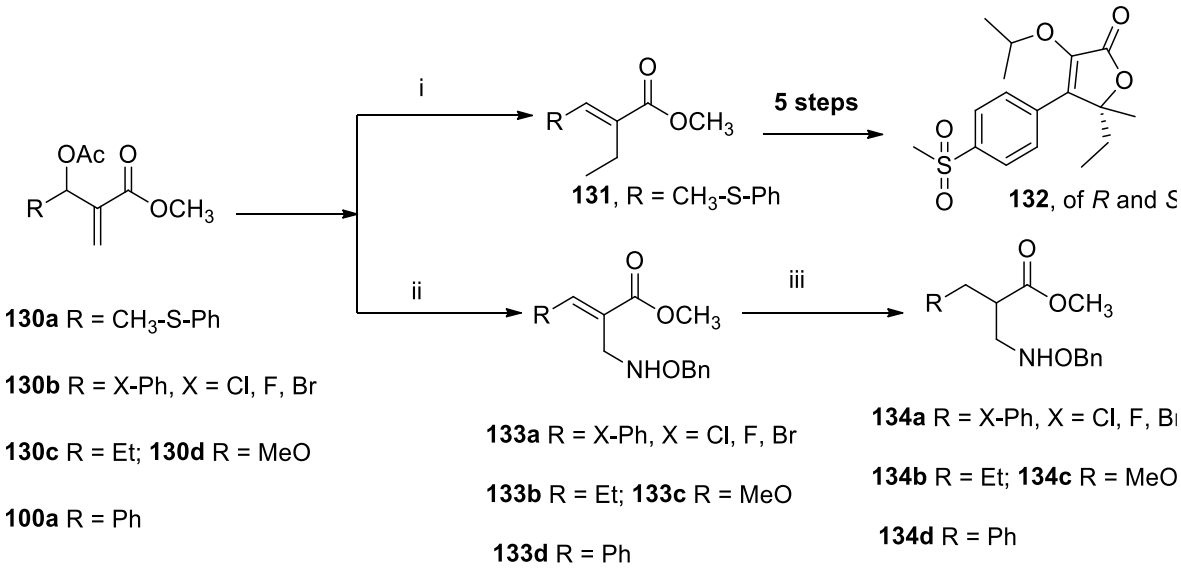

Scheme 37: Synthesis of furanone derivative and an anti-inflammatory agent and β^2-amino acids. *Reagents and conditions*: (i) Lithium diethyl copper in ether at -20 to -40 °C (ii) Benzylhydroxylamine hydrochloride in THF at room temperature (iii) [Rh(Et-DUPHOS)(COD)BF_4)], hydrogen gas.

The synthesis of other derivatives starting from acetates has also been reported (**Scheme 38**). The use of a multicomponent reaction of Baylis-Hillman acetates **135** with trimethyl silane azide, and aryl nitrile **136** led to a 1,5-disubstituted tetrazoles **137a** and **137b** that are reported to be TNF-α inhibitors.[96] The use of nitrogen nucleophiles for allylic nucleophilic substitution on acetates **135** has been reported to generate geometrical isomers that are

potentially synthetic intermediates in organic synthesis. By using *N*-substituted hydroxylamines as a nucleophile and reacting them with **138** in DMF afforded products **139a** – **139b** of *E*-configuration.[97] The use of methanolic ammonia on acetates **135** has been reported to afford several allylic products including compounds **140a** and **140b** in yields above 80%.[98] In addition to the use of nitrogen as a nucleophile, cyanide can be used instead to generate scaffolds **141a** and **141b**.[99]

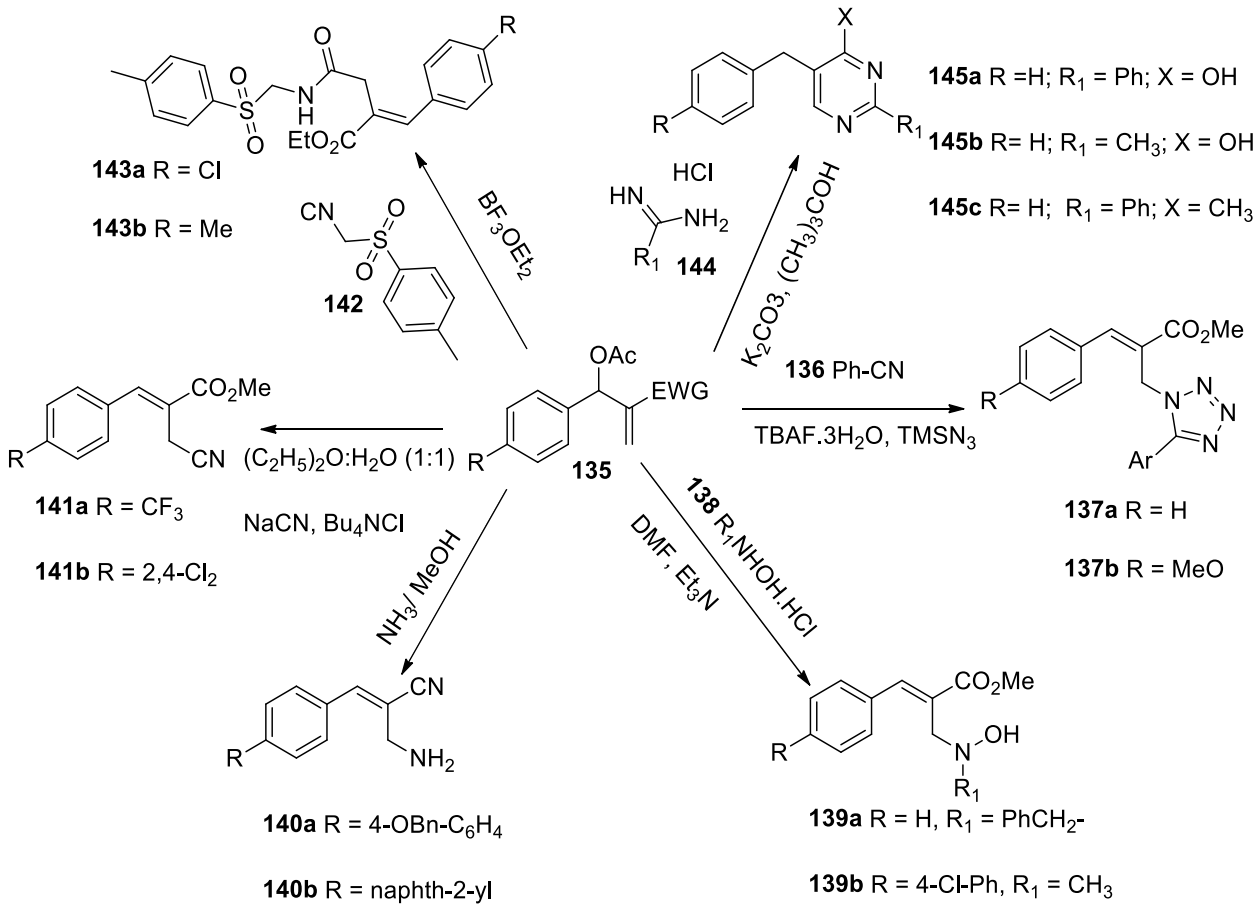

Scheme 38: Products originating from allylic substitution of MBH acetates using different nucleophiles.

A unique allylic nucleophilic substitution reaction on MBH acetates was reported by Yadav and co-workers.[100] In their work, they were able to react tosylmethyl isocyanide **142** with the corresponding MBH acetates in the presence of a Lewis acid boron trifluoride diethyl etherate (BF_3OEt_2) to afford trisubstituted olefin derivatives **143a** and **143b**. The synthesis

of the pyrimidine moiety, an important heterocycle commonly found in drugs and biologically active compounds, can be a very challenging task especially where unique substitution patterns are required. An example of a unique 2,4,5-trisubstituted pyrimidine moiety that can now be synthesised in good yields by reacting acetates **135** with benzamidine hydrochloride **144** in *tert*-butanol to afford compounds **145a** – **145c**[101] is also shown in **Scheme 38**.

The synthesis of indenoquinoline derivatives confirmed to display anti-inflammatory and antimalarial activities has previously been reported to be achieved by disadvantageous methods such as aza-Bergman cyclization.[102] Reacting acetates **146a** and **146b** with different derivatives of aniline under reflux conditions, led to intermediates **147** that were converted to indenoquinolone derivatives **148** and **149** in yields ranging from 55% to 80% (**Scheme 39**).[103]

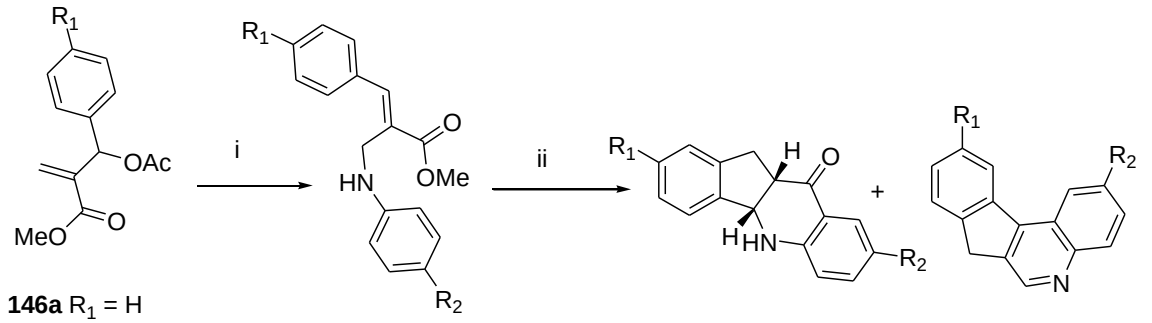

146a R_1 = H

146b R_1 = Me

147a R_1 = Me; R_2 = CH_3

147b R_1 = Me; R_2 = H

148a R_1 = H, R_2 = Me

148b R_1 = Me, R_2 = H

149a R_1 = H, R_2 = Me

149b R_1 = Me, R_2 = H

Scheme 39: Synthesis of indenoquinolines derivatives starting from MBH acetates. *Reagents and conditions* (i) THF, aniline derivatives, reflux (ii) Phosphoric acid, 120 °C.

Unfortunately, the use of any of the discussed methodology on protected MBH adducts cannot be applied in situations where it is desirable for the stereogenic centre to be maintained. It is with this limitation in mind that other interested parties demonstrated the synthesis of other important compounds by performing Michael addition reactions on racemic MBH alcohols.

1.1.6.3 Use of 1,4-Michael addition

So far it is only nitrogen and sulfur nucleophiles that have been reported to participate in Michael addition reactions on MBH adducts. In the search for synthetic routes towards 2-amino-1,4,5,6-tetrahydro-pyrimidines that are heterocyclic frameworks widely found in drugs, Batra and co-workers were able to synthesise intermediate amino derivatives **151a** and **151b** by performing Michael addition reactions of different primary amines with MBH adducts **75a** and **150** in methanol (**Scheme 40**).[104] The available amino intermediates were then converted to the tetrahydro-pyrimidine derivatives **152a** and **152b** in yields of 40 – 87%.

75a R = C_6H_5 **151a** R = C_6H_5 R_1 = $C_6H_5CH_2$ **152a** R = C_6H_5 R_1 = $C_6H_5CH_2$

150 R = 4-Cl-C_6H_4 **151b** R = 4-Cl-C_6H_4 R_1 = 4-F-$C_6H_4CH_2$ **152b** R = 4-Cl-C_6H_4 R_1 = 4-F-$C_6H_4CH_2$

Scheme 40: Synthesis of tetrahydro-pyrimidine derivatives from MBH adducts. *Reagents and conditions*: (i) Amine, MeOH at room temperature.

Another example illustrating the use of nitrogen nucleophiles for nucleophilic addition was during the synthesis of antithrombotic agents. Synthesis of MBH adducts by reacting various isoxazole aldehydes with different activated alkenes gave rise to adducts **153a** – **153c** that were reported to be synthetic intermediates of antithrombotic agents.[105] The antithrombotic agents that displayed protection activity above 20% were obtained when these adducts underwent Michael addition with *N*-methyl piperazine **154** to form racemic compounds **155a** – **155c** (**Scheme 41)**.

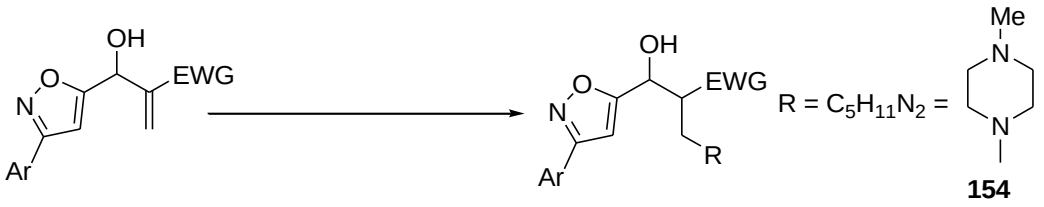

153a Ar = C_6H_5, EWG = CO_2Et

153b Ar = 2-Cl-C_6H_5, EWG = CO_2Et

153c Ar = C_6H_5, EWG = CN

155a Ar = C_6H_5, EWG = CO_2Et, R = $C_5H_{11}N_2$

155b Ar = 2-Cl-C_6H_5, EWG = CO_2Et, R = $C_5H_{11}N_2$

155c Ar = C_6H_5, EWG = CN, R = $C_5H_{11}N_2$

Scheme 41: Synthesis of antithrombotic agents by performing nucleophilic additions on MBH adducts. *Reagents and conditions*: Amine, MeOH at room temperature.

The racemic *N*,*N*′-disubstituted piperazine derivatives that have the potential of being developed into HIV-1 protease and integrase inhibitors **157a** – **157d** were obtained when adducts **41**, **156a** – **156c** underwent nucleophilic conjugate addition with piperazine (**Scheme 42**).[106]

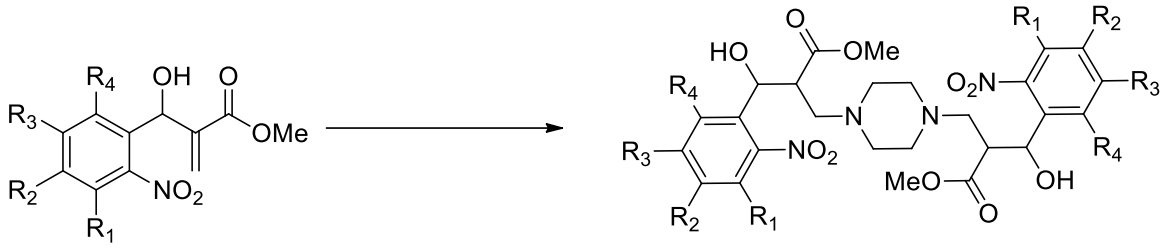

41 R_1 = H, R_2 = H, R_3 = H R_4 = H

156a R_1 = OMe, R_2 = H, R_3 = H R_4 = H

156b R_1 = H, R_2 = H, R_3 = H R_4 = Cl

156c R_1 = H, R_2 = OCH_2OH, R_3 = H R_4 = H

157a R_1 = H, R_2 = H, R_3 = H R_4 = H

157b R_1 = OMe, R_2 = H, R_3 = H R_4 = H

157c R_1 = H, R_2 = H, R_3 = H R_4 = Cl

157d R_1 = H, R_2 = OCH_2OH, R_3 = H R_4 = H

Scheme 42: Synthesis of racemic *N*, *N*′-disubstituted piperazine derivatives. *Reagents and conditions*: Piperazine in THF.

From these reports, it appears that reactions used are non-stereoselective nucleophilic addition reactions. Therefore, it means that multiple compounds are obtained from each reaction, making their use and application very complex.

Apart from nitrogen nucleophiles participating in Michael addition reactions, sulphur has also been documented to undergo a similar reaction. The inspiration of using xanthates (dithiocarbonates) in the synthesis of complex molecules attracted Miranda and co-workers to research methods for their synthesis.[107] Their research specifically addressed how xanthate derivatives can be obtained from MBH adducts. Their reaction of potassium *O*-ethyl dithiocarbonate **158** with adducts **41**, and **160a** – **160c** in the presence of a Lewis acid 9-borabicyclo[3.3.1]nonane (9-BBN) **159** afforded MBH xanthates **161a** – **161d** (**Scheme 43**). The yields of the xanthates were in the range of 57 – 95% with diastereomeric excess in the range of 32 – 70%. The use of 9-BBN was confirmed to promote the reaction by interacting with the hydroxyl group and the carbonyl group hence making the alkene electrophilic enough for nucleophilic attack. The use of MBH xanthate derivatives is yet to be applied in further synthesis as there are no current reports illustrating their application

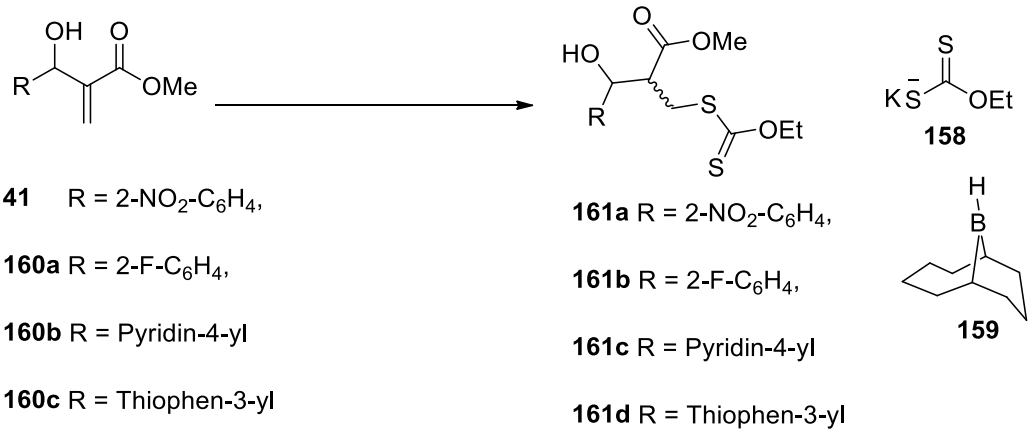

Scheme 43: Nucleophilic addition of xanthate salt on MBH esters. *Reagents and conditions*: potassium *O*-ethyl dithiocarbonate, 9-borabicyclo[3.3.1]nonane (9-BBN), acetic acid in acetonitrile as a solvent.

In addition to xanthates, thiols have also been reported to participate in nucleophilic addition reactions on racemic MBH alcohols.[108] In one report, the use of unprotected MBH alcohol

94e for nucleophilic addition with ethanethiol afforded **164a** with low *syn* and *anti*-product ratio of 7:3. The use of thiophenol with MBH acetate **95e** in the presence of triethylamine led to nucleophilic substitution product **163a**. The change of protecting group from acetate to *tert*-butyldimethylsilyl (TBS) on compound **162a** – **162c** afforded adducts **164b** – **164d** in a yield range of 60% to 95% with *syn* and *anti*-product ratio in the range of 90 to 10. The use of unprotected MBH alcohols for nucleophilic addition led to a product whose diastereoselectivity reduced drastically, confirming that the use of the bulky TBS group was responsible for the observed stereoselectivity.

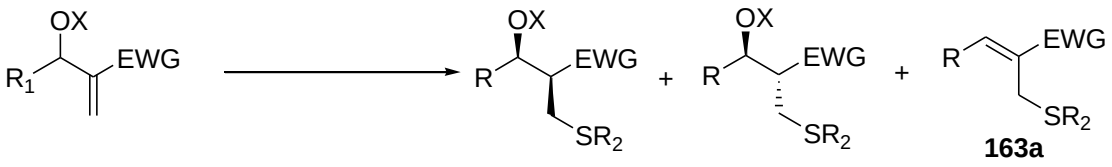

163a

94e R_1 = Me EWG = CO_2Me X = H

95e R_1 = Me EWG = CO_2Me X = Ac

162a R_1 = Me EWG = CO_2Me X = TBS

162b R_1 = Me EWG = CO_2Bu-*t* X = TBS

162c R_1 = Me EWG = CN X = TBS

164a R_1 = Me EWG = CO_2Me X = H R_2 = Et

163a R_1 = Me EWG = CO_2Me R_2 = Ph

164b R_1 = Me EWG = CO_2Me X = TBS R_2 = Et

164c R_1 = Me EWG = CO_2Bu-*t* X = TBS R_2 =Et

164d R_1 = Me EWG = CN X = TBS R_2 = Et

Scheme 44: Michael addition of thiols on MBH adducts affording racemic products. *Reagents and conditions*: thiophenol/ethanethiol in THF at -50 °C.

The promotion of the formation of the major *syn* diastereomer during addition was explained by the convincing proposed mechanism shown (**Scheme 45**). The nucleophilic addition forms an enolate intermediate that forms two conformers **A** and **B**. Conformer **A** is favoured because there is no unfavourable steric interaction between the enolate residue R_3 and R_1, unlike in conformer **B**. Favoured conformer **A** allows the incoming proton to approach from the bottom as the top side is blocked by the bulky TBS group, thus favouring the formation of the *syn*-product. In the absence of a bulky group, the proton can approach from either the top or the bottom, thus leading to low diastereoselectivity.

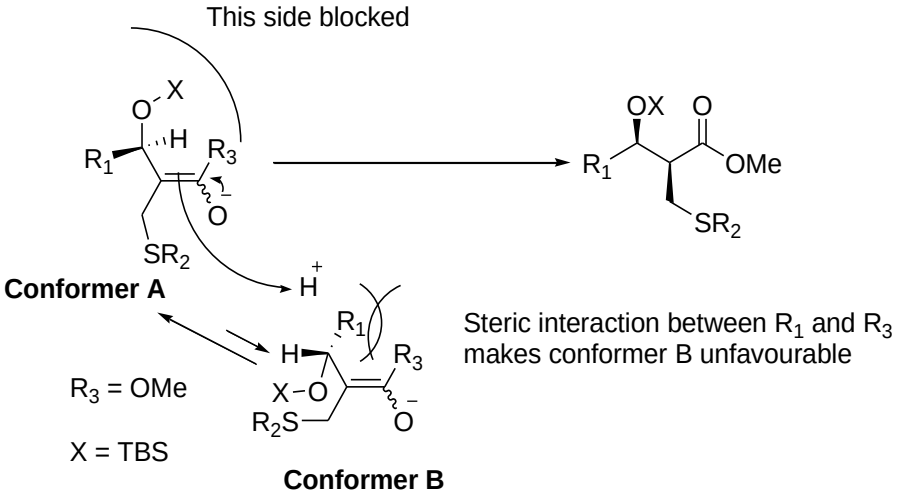

Scheme 45: Proposed mechanism leading to the major *syn*-product on protected MBH alcohols.

Unfortunately, all of the nucleophilic addition reactions on protected and unprotected MBH alcohols reported in the literature form racemic products, although diastereoselectivity has been demonstrated in some cases. Furthermore, none of these reports have demonstrated the use of enantiopure MBH adducts for nucleophilic addition reactions. Therefore, the use of enantiopure MBH adducts for investigation of nucleophilic addition is of significant contribution to the scientific community.

CHAPTER TWO

2 PROJECT RATIONALE

It is clear that the formation Morita-Baylis-Hillman adducts has been researched extensively as confirmed by the numerous publications available. The use of these adducts in the synthesis of different compounds is also commonly described, especially using the nucleophilic allylic substitution mechanism. To date, there are only a few examples in the literature illustrating the use of nitrogen and sulphur for nucleophilic addition reactions, and these have all been performed on racemic MBH alcohols. However, compounds resulting from Michael addition reactions are most useful if they are obtained in diastereopure or enantiopure form.

2.1Aims and objectives

The overall aim of this project was to develop methodologies for the production of enantiopure functionalised MBH adducts with multiple stereogenic centres.

Two approaches were considered to achieve this aim.

Approach one: This first approach was to perform the MBH reaction starting with enantiopure aldehydes and attempting to control the diastereoselectivity of the MBH reaction (**Scheme A**). Once this was achieved, a diastereoselective Michael addition reaction could be performed to obtain enantiopure products.

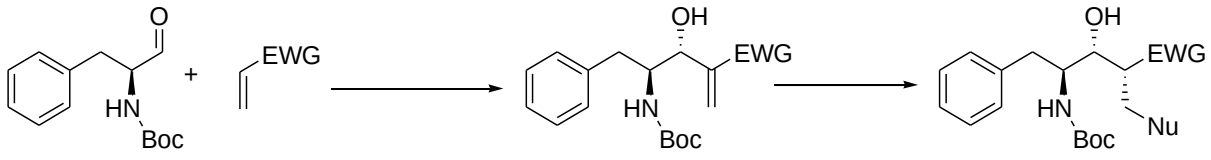

EWG = CN

EWG = CO_2CH_3

EWG = $CO_2CH_2CH_3$

EWG = $COCH_3$

Scheme A. Approach one

Approach two: In this second approach, we planned to obtain enantiopure MBH adducts by enzymatic kinetic resolution of racemic MBH adducts (**Scheme B**). Once an enantiopure product was obtained, a diastereoselective (or enantioselective) reaction would give rise to enantiopure functionalised adducts (**Scheme C**).

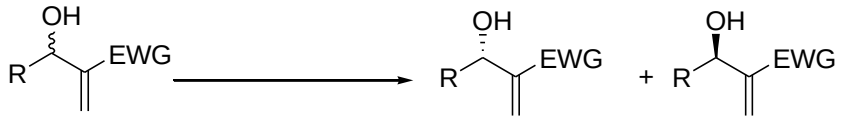

R = Ph, EWG = CN; R = PhCh = CH, EWG = CN

R = $PhCH_2CH_2$, EWG = CN; R = Phe, EWG = CO_2Et

R = PhCH=CH, EWG = CO_2Et; R = $PhCH_2CH_2$, EWG = CO_2Et

Scheme B. EKR of MBH adducts

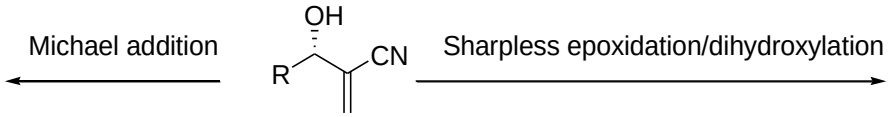

R = $PhCH_2CH_2$

Scheme C. Diastereoselective or enantioselective reaction on enantiopure MBH adduct

2.1.1 Specific project objectives

a) Synthesise MBH adducts diastereoselectively, starting with enantiopure amino-acid derived aldehydes.
b) Perform diastereoselective Michael addition reactions on amino-acid derived MBH adducts using nitrogen or sulphur nucleophiles.
c) Test enzymatic kinetic resolution of MBH acetates, using a variety of lipases.
d) Perform enantioselective or diastereoselective reactions on enantiopure MBH adducts.

CHAPTER THREE

3 RESULTS AND DISCUSSION

3.1 Use of α-amino acid derived aldehydes in the Morita-Baylis-Hillman reaction

3.1.1 Background information

Proteases are well known for their critical role in many biological processes. They aid a biological process mainly by hydrolysing a peptide bond of a specific amino acids sequence in a unique way.[109] The unique way in which proteases catalyse the hydrolysis of a peptide bond has enabled mankind to design therapeutic agents that mimic their action. An example of these therapeutic agents include the known HIV protease inhibitors **165** – **170** shown in **Figure 8.**[110, 111] The generation of the core structure of most HIV-1 protease inhibitors already on the market involves several steps that are complex and time consuming.[112, 113] In this project, we were interested in synthesizing new core structures **171** and **172** that could be substituted for the reported core structures shown in red of known anti-HIV protease inhibitors (**Figure 8)**. The generation of new core structures with the potential of being transformed into compounds with anti-HIV activity is highly encouraged because of the reported high rate of mutations of HIV-1 virus.[114, 115]

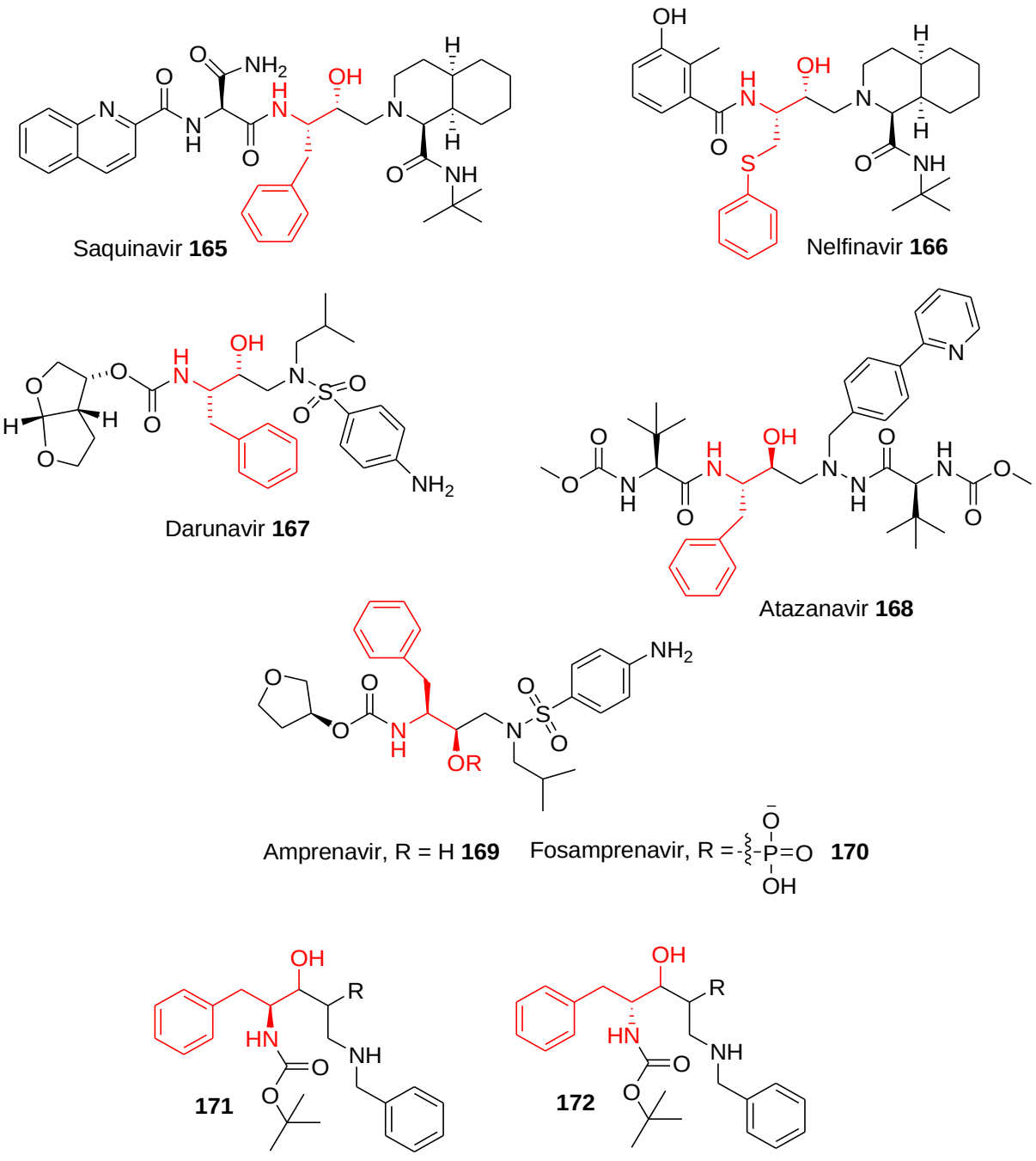

Figure 8: Comparison of proposed core structures **171** and **172** with known core structures of HIV-1 protease inhibitors.

Although most of the drugs on the market are modelled before synthesis, the proposed core structures **171** and **172** were a trial and error way of investigating the use of functionalised Morita-Baylis-Hillman adducts in drug discovery. Furthermore, it is hoped that a successful synthesis of the core structures containing three contiguous stereogenic centres would attract other researchers to investigate their possible biological applications, particularly if the stereochemistry at all the centres could be controlled. It is expected that the proposed core

structure **171** could be obtained starting with Morita-Baylis-Hillman reaction of amino acid-derived *N*-Boc-L-phenylalaninal **173** followed by nucleophilic addition to the adduct using nitrogen nucleophiles. Similarly, compound **172** could be obtained starting with reaction of *N*-Boc-D-phenylalaninal **174**, followed by nucleophilic addition. Morita-Baylis-Hillman adducts of general structure **175** and **176** would be the targeted intermediates (**Figure 9**). It was hoped that the separation of these diastereomers would lead to diastereopure compounds that could be subjected to the subsequent nucleophilic addition reactions.

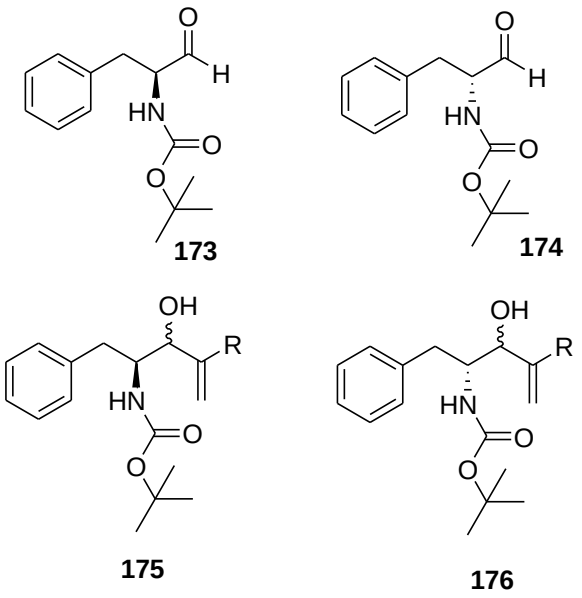

Figure 9: Amino acid-derived aldehydes, and the proposed MBH adducts

The potential of the MBH diastereomers as possible HIV-1 protease inhibitor precursors is attributed to the fact that they could be separated to give diastereopure compounds **A** and upon further functionalization could generate a central core, containing the 1,2-amino alcohol moiety, a key element in HIV-1 protease inhibitors (**Figure 8**). This detailed reasoning and the method of achieving it is shown in **Scheme 46.**

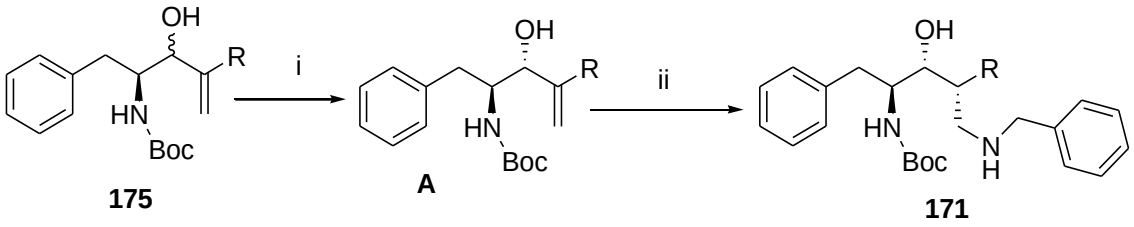

175 **A** **171**

Scheme 46: Proposed route for generation of core structure **171**. (i) Separation of major and minor diastereomers (ii) Diastereoselective Michael addition using nitrogen nucleophiles.

3.1.2 Synthesis of N-Boc-L-phenylalaninal 173 and N-Boc-D-phenylalaninal 174

The first task at hand was to synthesise the required aldehydes for MBH reaction by converting L- and D-phenylalanine into L- and D-phenylalaninal, respectively. Synthesis of *N*-Boc-L-phenylalaninal **173** was achieved in two steps (**Scheme 47**). The first step involved dissolving *N*-Boc-L-phenylalanine **177** in dichloromethane followed by portionwise addition of carbonyldiimidazole (CDI). Stirring of the reaction mixture was continued until there was no more release of carbon dioxide. The absence of carbon dioxide generation in the reaction mixture confirmed that the acid had been activated for nucleophilic substitution.[116] This was followed by the addition of solid *N*,*O*-dimethylhydroxylamine hydrochloride with a resumption of stirring until all the starting material was consumed as indicated by TLC. Work up was done and the crude product was purified by column chromatography using 20% ethyl acetate in hexane to afford (*S*)-*tert*-butyl (1-(methoxy(methyl)amino)-1-oxo-3-phenylpropan-2-yl)carbamate **178** as a viscous colourless oil in good yield of 97%.

The formation of the Weinreb amide **178** was confirmed by ^{1}H NMR spectroscopy. The presence of a characteristic singlet at δ 3.65 for O-CH_3 and the second singlet at δ 3.16 for N-CH_3 each integrating for three protons confirmed the presence of the Weinreb amide. The multiplet at δ 7.32 – 7.13 represented the five aromatic protons while the doublet at δ 5.20 with a coupling constant of 7.2 Hz was attributed to the NH proton. The characteristic stereogenic centre proton H-2 showed a multiplet at δ 5.08 – 4.81 integrating for one proton. The first diastereotopic benzylic proton H-3a showed a multiplet at δ 3.11 – 2.98 while the second diastereotopic proton H-3b showed a doublet of doublets with coupling constants of 13 Hz and 7 Hz, representing vicinal coupling with H-2 and geminal coupling with H-3a respectively. The singlet at δ 1.39 integrating for 9 protons was a characteristic peak for the

tert-butyl protons of the Boc group. The formation of the Weinreb amide was further supported by ^{13}C NMR spectroscopy. This was indicated by the presence of two carbonyl carbon atoms at δ 172.4 for C-1 and δ 155.2 for C-8. The remaining characteristic peaks for the Weinreb amide appeared at δ 61.5 for C-11 and δ 32.1 for C-12. The presence of one carbon signal at δ 79.6 and the three chemically equivalent carbon atoms giving rise to a signal at δ 28.3 represented the quaternary carbon atom and the three methyl groups of the Boc group, respectively. The appearance of a peak at 1650 cm^{-1} in the IR spectrum clearly confirmed the presence of the carbonyl group of the amide functional group. The formation of the Weinreb amide was further supported by the absence of an OH stretch in the IR spectrum. The spectral data obtained were identical to those previously reported. [117]

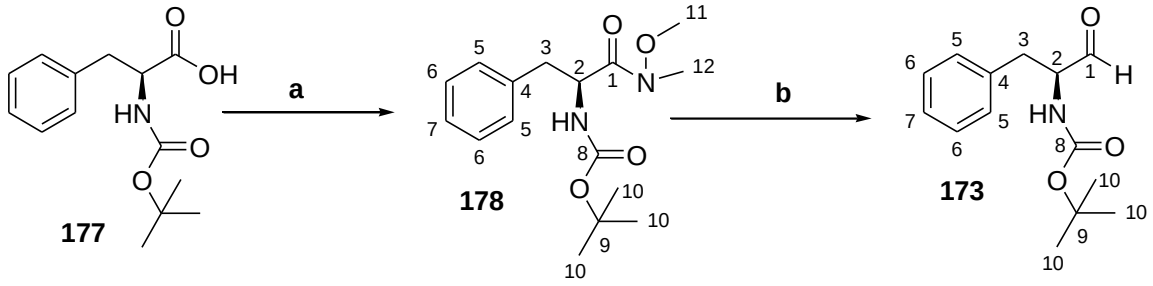

Scheme 47: Synthesis of *N*-Boc-L-phenylalaninal. *Reagents and conditions*: (a) (i) Carbonyldiimidazole (CDI), (ii) *N,O*-dimethylhydroxylamine hydrochloride, CH_2Cl_2, RT (b) $LiAlH_4$, THF at 0 °C, 4 hours

The second step involved the conversion of the Weinreb amide into an aldehyde (**Scheme 47, conditions b**). This was achieved by adding (*S*)-*tert*-butyl (1-(methoxy(methyl)amino)-1-oxo-3-phenylpropan-2-yl)carbamate **178** into a two-necked flame dried round bottom flask containing THF under the circulation of nitrogen. The mixture was cooled to 0 °C followed by addition of $LiAlH_4$ with a continuation of stirring for four hours under nitrogen. The addition of $LiAlH_4$ led to the formation of a stable tetrahedral metal chelated intermediate that only collapses after mild acidic work up.[118] The tetrahedral intermediate formed ensures that there is no complete reduction of the Weinreb amide to an alcohol, but instead stops at the aldehyde stage.[119] After this, work up was applied to the reaction mixture affording **(***S*)-*tert*-butyl (1-oxo-3-phenylpropan-2-yl)carbamate **173** as a white solid in an excellent yield of 92%.

The formation of **173** was confirmed by ^{1}H NMR spectroscopy. The characteristic most deshielded singlet H-1 peak at δ 9.62 with an integration of one proton confirmed the presence of an aldehyde peak. The presence of aromatic protons was evidenced by a multiplet at δ 7.35 – 7.23 integrating for three protons and another multiplet at δ 7.20 – 7.14 integrating for two protons. The other proton peaks were assigned as in **178**. The presence of a carbon signal at δ 199.2 in the ^{13}C NMR spectrum confirmed the presence of the carbonyl of the aldehyde functional group. The IR peak at 1687 cm^{-1} further supported the formation of the aldehyde peak. The melting point of the synthesized aldehyde was found to be 84 – 85 °C while the measured optical rotation of the aldehyde was found to be $[\alpha]_D$ = -45.500 (c = 0.5, MeOH). The optical rotation was very important as its value confirmed that there was no racemisation during the reaction. The measured melting point and the optical rotation value of **173** was in agreement with reported data in the literature.[120]

It was then the turn to investigate the use of *N*-Boc-D-phenylalaninal **174** in the MBH reaction. The use of **174** would make it easy to compare the reactivity of the two enantiomeric aldehydes. The synthesis of **174** was accomplished starting from *N*-Boc-D-phenylalanine **179**, then converting it into a Weinreb amide **180** and finally converting the Weinreb amide to an aldehyde (**Scheme 48 conditions a and b**).

All the characteristics peaks observed in the synthesis of *N*-Boc-L-phenylalaninal **173** were also observed during the synthesis of *N*-Boc-D-phenylalaninal **174**. For example, the Weinreb amide **180** showed a singlet at δ 3.65 for N-OCH_3 and another singlet at δ 3.16 for N-CH_3 in the ^{1}H NMR spectrum. The chemical shift at δ 79.7 for N-OCH_3 and another chemical shift at δ 32.0 for N-CH_3 in the ^{13}C NMR spectrum clearly supported these observations. The formation of *N*-Boc-D-phenylalaninal **174** was confirmed by the presence of a singlet at δ 9.62 in the ^{1}H NMR spectrum for the aldehyde peak and a carbon signal at δ 199.4 in the ^{13}C NMR spectrum. All the NMR data obtained were in agreement with the data for **173**, as expected.

The melting point of **174** was found to be 84 – 85 °C while the measured optical rotation was found to be $[\alpha]_D$ = +43.400 (c = 0.5, MeOH). All the physical and spectroscopic data was in agreement with literature data.[120]

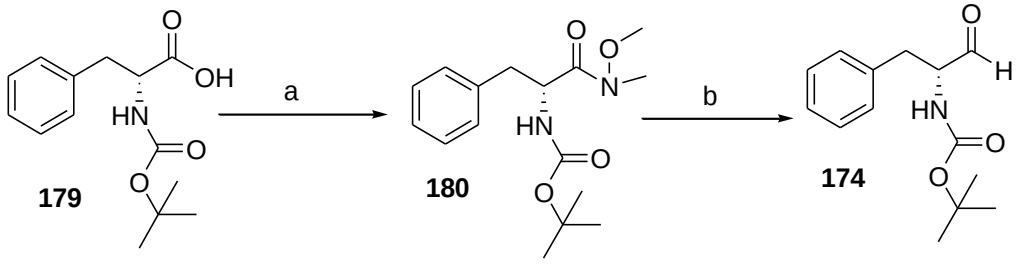

Scheme 48: Synthesis of *N*-Boc-D-phenylalaninal **174**. *Reagents and conditions*: (a) (i) Carbonyldiimidazole (CDI), (ii) *N,O*-dimethylhydroxylamine hydrochloride, CH_2Cl_2, RT (b) $LiAlH_4$, THF at 0 °C, 2 hours.

Enantiopure *N*-Boc-L-phenylalaninal **173** and *N*-Boc-D-phenylalaninal 1**74** were thus successfully obtained and were ready for use as electrophiles in the Morita-Baylis-Hillman reaction (MBHR). These aldehydes were used immediately to avoid racemisation that had been previously reported.[121]

3.1.3 Synthesis of Morita-Baylis-Hillman adducts (MBHA)

3.1.3.1 Synthesis of MBHA by reacting acrylonitrile with N-Boc-L-phenylalaninal (173) and N-Boc-D-phenylalaninal (174)

The electrophilic enantiopure *N*-Boc-L-phenylalaninal **173** was reacted with acrylonitrile at room temperature in the presence of DABCO as catalyst to generate the MBHA in 12 days (**Scheme 49**). This reaction afforded *ter*t-butyl ((2*S*)-4-cyano-3-hydroxy-1-phenylpent-4-en-2-yl)carbamate as diastereomeric mixtures of **181a** as white solid and **181b** as a colourless oil. The white solid **181a** was isolated in a yield of 14% while the colourless oil **181b** was isolated in a yield of 32%.

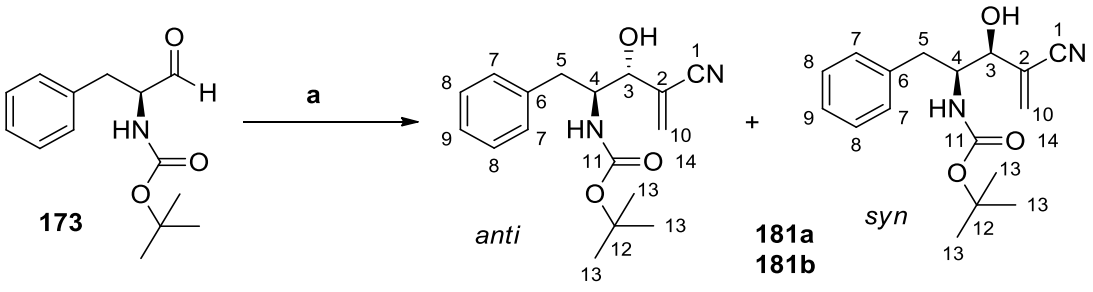

Scheme 49: Preparation of Morita Baylis Hillman adducts from *N*-Boc-L-phenylalaninal. *Reagents and conditions*: (a) DABCO, acrylonitrile, RT or 0 °C or -15 °C.

^{1}H NMR spectroscopy was used to confirm the identity of white solid **181a**. The two multiplets at δ 6.13 – 6.05 and δ 6.03 – 5.98 each integrating for one proton are characteristic peaks for vinylic protons H-10a and H-10b. The appearance of a multiplet at δ 4.46 – 4.16 integrating for one proton confirmed the presence of the OH group. The stereogenic centre proton H-3 at δ 5.00 appeared as a doublet with a coupling constant of 6.5 Hz. The disappearance of the aldehyde peak of the electrophile and the appearance of H-10, H-3 and OH confirmed that the electrophile and the activated alkene had reacted to form the product. The multiplet at δ 7.34 – 7.15 was assigned to the five aromatic protons while the doublet at δ 5.12 with a coupling constant of 8.5 Hz was assigned to the NH proton. The multiplet at δ 4.18 – 3.78 was assigned to the stereogenic centre proton H-4. The two benzylic protons at H-5 also showed a multiplet at δ 3.05 – 2.75 while the multiplet at δ 1.42 – 1.30 with an integration of 9 protons was assigned to the three chemically equivalent methyl groups of the Boc group. The presence of the Boc group creates rotamers as a result of restricted rotation about the N-C bond of the carbamate. This means that the methyl groups of the Boc group do not give one averaged NMR signal, but the existence of different conformations leads to the observed muliplet for these methyl groups in the ^{1}H NMR spectrum. This is observed for all similar compounds that are discussed later in this thesis.

The structure of **181a** was further supported by ^{13}C NMR spectroscopic data. The disappearance of the carbon signal at 199.4 ppm for the aldehyde and the appearance of a carbon signal at δ 117.3 for C-1, δ 124.9 for C-2, δ 130.9 for C-10 and δ 72.0 for C-3 clearly confirmed that the electrophile had reacted with the activated alkene. The carbon chemical shift at δ 156.7 was assigned to the carbonyl functional group of the Boc group while the chemical shift at δ 55.9 was assigned to the stereogenic centre carbon C-4 and that at δ 37.3 for the benzylic carbon C-5. The chemical shift of C-5, C-4, C-3, C-10 and C-13 were assigned precisely using a DEPT experiment.

The presence of IR stretches at 3651 cm^{-1}, 3376 cm^{-1}, 2225 cm^{-1} and 1689 cm^{-1} for NH, OH, C≡N and C=O stretches, respectively, indeed confirmed that the intended product was formed. The mass spectrum also corresponded well with the expected mass of the product (calculated for $C_{17}H_{22}N_2O_3Na$: 325.1523, found: [M+Na^{+}] 325.1524).

After successfully using all the spectroscopic data to confirm the structure of the white solid **181a**, the next diastereomer to characterize was compound **181b**. Analysis of the ^{1}H NMR, ^{13}C NMR spectrum and IR data clearly indicated that the two compounds were

diastereomers. The characteristic stereogenic centre proton H-3 for the diastereomer **181a** appeared as a downfield doublet while a similar proton of **181b** appeared as an upfield multiplet (**Table 10**). It seems the protons in **181a** are being deshielded by the anisotropic effect of the benzene ring and this might explan why the protons are appearing downfield as compared to **181b**. This possibility can only be confirmed if each diastereomer is obtained in pure form for further analysis.

Table 10: Comparison of ^{1}H NMR signals of **181a** and **181b**

	181a	**181b**
Aromatic protons (ppm)	7. 34 – 7.15 (m)	7.36 – 7.16 (m)
H-10 (ppm)	6.13 – 6.05 (m, H-10a) 6.03 – 5.98 (m, H-10b)	6.12 (brs)
NH (ppm)	5.12 (d, *J* = 8.6 Hz)	5.07 – 4.94 (m)
H-3 (ppm)	**5.00 (d, *J* = 6.5 Hz)**	**4.88 – 4.74 (m)**
OH (ppm)	4.46 – 4.16 (m)	4.39 (s)
H-4 (ppm)	4.18 – 3.78 (m)	4.12 – 3.94 (m)
H-5 (ppm)	3.05 – 2.75 (m)	2.95 – 2.80 (m)
H-13 (ppm)	1.42 – 1.30 (m)	1.43 – 1.34 (m)

The ^{13}C NMR signals for the two diastereomers were also compared and tabulated in **Table 11**. As can be seen in the Table, most of the chemical shift values were very similar between the two diastereomers, with the biggest difference being seen for the stereogenic centres. Stereogenic centre carbon C-3 of diastereomer **181a** was the more shielded as compared to the similar carbon signal of **181b**. The difference in chemical shifts of the stereogenic centre carbon might be due to the shielding effect of the benzene ring. The anisotropic effect is more pronounced on the two stereogenic centres as the four different groups attached cause different conformations. This possible explanation can only be confirmed by doing further analysis on a diastereopure compound.

Table 11: Comparison of ^{13}C NMR signals of **181a** and **181b**

	181a	**181b**
Aromatic carbons	129.2 (C-7 or C-8), 128.6 (C-7 or C-8), 126.7 (C-9)	129.2 (C-7 or C-9), 128.7 (C-7 0r C-8), 126.9 (C-9)
C-11 and C-6	156.7 and 137.8	157. 3 and 137.1
C-10 and C-2	130.9 and 124.9	132.3 and 123.5
C-1 and C-12	117. 3 and 80.3	117.5 and 80.8
C-3 and C-4	**72.0** and 55.9	**74.5** and 57.0
C-5 and C-13	37.3 and 28.2	35.5 and 28.2

The key IR signals and the HRMS data for the two diastereomers were found to be similar (**Table 12**).

Table 12: Comparison of Key IR signals and MS data of **181a** and **181b**

	181a	**181b**
NH (cm^{-1})	3651	3440
OH (cm^{-1})	3376	3373
C≡N (cm^{-1})	2225	2225
C=O (cm^{-1})	1698	1679
Molecular mass	Calculated for $C_{17}H_{22}N_2O_3Na$: 325.1523, found: $[M+Na^+]$ 325.1524	Calculated for $C_{17}H_{22}N_2O_3Na$: 325.1523, found: $[M+Na^+]$ 325.1528.

When **181a** was subjected to reverse phase C18 HPLC column chromatography using acetonitrile and water as a mobile phase at a flow rate of 1 mL/min, two peaks at retention times of 15.11 minutes and 18.14 minutes were observed (**Figure 10).** It was clear from the chromatogram that **181a** was contaminated with **181b**. The diastereomeric ratio between **181a** and **181b** in the sample (90 mg) was found to be 3:1.

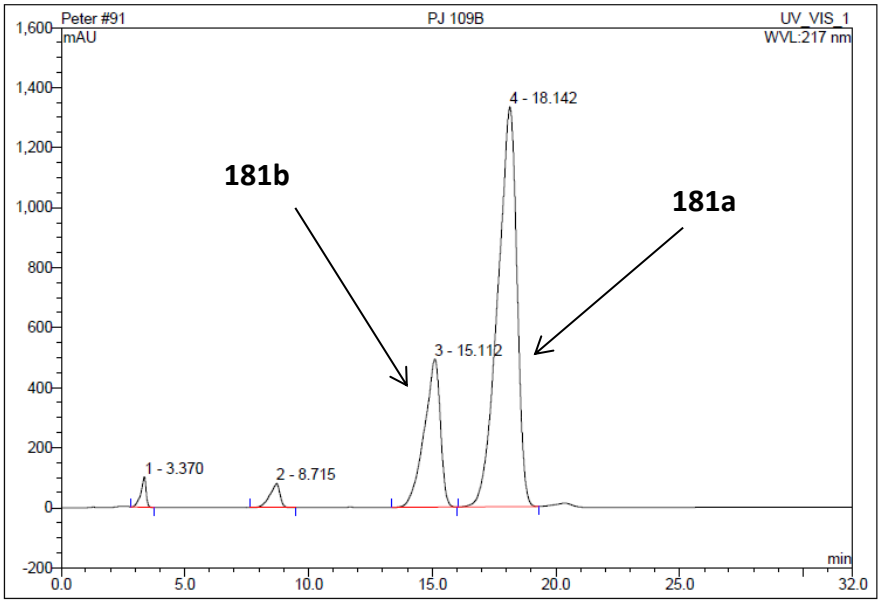

No.	Ret.Time min	Peak Name	Height mAU	Area mAU*min	Rel.Area %	Amount	Type
1	3.37	n.a.	101.638	24.965	1.52	n.a.	BMB
2	8.72	n.a.	79.746	37.805	2.31	n.a.	BMB
3	15.11	n.a.	493.506	372.825	22.74	n.a.	BMB
4	18.14	n.a.	1332.001	1204.005	73.43	n.a.	BMB
Total:			2006.890	1639.601	100.00	0.000	

Figure 10: HPLC chromatogram of the white solid diastereomer **181a** contaminated with colourless diastereomer **181b** when the reaction was done at room temperature.

When the colourless oil tert-butyl ((2*S*)-4-cyano-3-hydroxy-1-phenylpent-4-en-2-yl)carbamate **181b** was subjected to reverse phase C18 HPLC column chromatography using acetonitrile and water as a mobile phase at a flow rate of 1 mL/min, it also gave two peaks at retention times of 15.13 minutes and 18.24 minutes (**Figure 11).** The diastereomer **181b** was found to be contaminated with **181a** and the diastereomeric ratio for the sample (200 mg) was found to be 7:1.

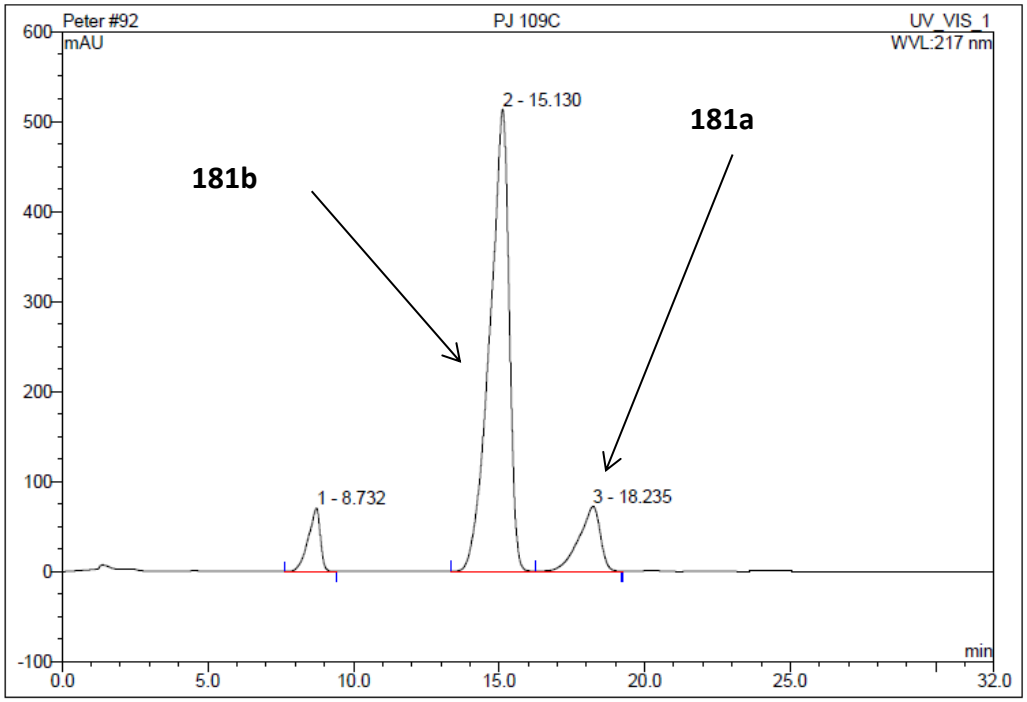

No.	Ret.Time min	Peak Name	Height mAU	Area mAU*min	Rel.Area %	Amount	Type
1	8.73	n.a.	70.290	33.620	6.84	n.a.	BMB
2	15.13	n.a.	512.968	396.853	80.74	n.a.	BMB
3	18.24	n.a.	71.998	61.032	12.42	n.a.	Rd
Total:			655.257	491.505	100.00	0.000	

Figure 11: HPLC chromatogram of the colourless oil diastereomer **181b** contaminated with the white solid diastereomer **181a** when the reaction was done at room temperature.

In order to confirm the identity of the peaks, samples **181a** and **181b** were mixed and this mixture was subjected to similar chromatographic conditions (**Figure 12**). It was confirmed from the HPLC chromatograms that the two peaks having a retention time of 14.91 and 17.94 minutes were for the diastereomer **181b** and **181a**, respectively.

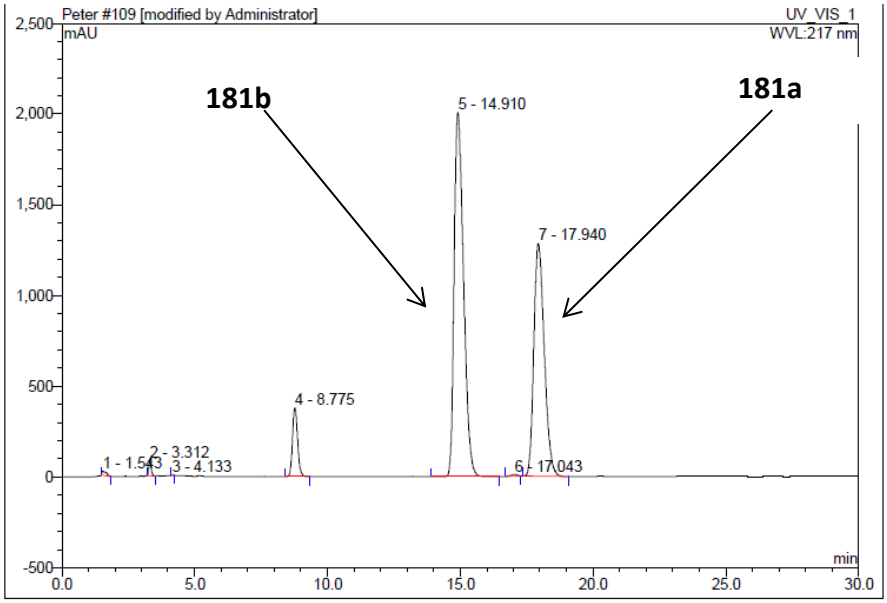

No.	Ret.Time min	Peak Name	Height mAU	Area mAU*min	Rel.Area %	Amount	Type
1	1.54	n.a.	26.123	4.529	0.30	n.a.	BMB*
2	3.31	n.a.	84.550	8.715	0.58	n.a.	BMB
3	4.13	n.a.	0.694	0.051	0.00	n.a.	BMB*
4	8.78	n.a.	378.852	84.036	5.56	n.a.	BMB
5	14.91	n.a.	2006.707	826.253	54.69	n.a.	BMB
6	17.04	n.a.	7.824	2.359	0.16	n.a.	BMB*
7	17.94	n.a.	1283.839	584.900	38.71	n.a.	BMB
Total:			3788.589	1510.844	100.00	0.000	

Figure 12: HPLC chromatogram of the diastereomeric mixture **181a** and **181b**.

It was clear that complete separation of diastereomers **181a** and **181b** had not occurred when using column chromatography, but HPLC column chromatography was used to calculate the overall diastereomeric ratio for the MBH reaction performed at room temperature. From the HPLC chromatograms **(Figures 10** and **11**) it was possible to calculate the final mass of **181a** obtained from the reaction as 92.5 mg, and that of **181b** as 197.5 mg. Thus, the diastereomeric ratio of products **181b**:**181a** at room temperature was 2.1:1.

The change of the reaction conditions by coupling aldehyde **173** with acrylonitrile at zero degrees was meant to determine if this would improve the reaction diastereoselectivity. Surprisingly, this procedure led to the isolation of diastereomer **181a** in 20% yield and diastereomer **181b** in 14% yield after 16 days. In this instance, diastereomer **181a** was isolated together with only traces of **181b** as observed from the HPLC chromatogram (**Figure 13**). A similar observation of **181b** being contaminated with only traces of **181a** was also observed (**Figure 14**). This amounted to a diastereomeric ratio of **181b**:**181a** at zero degrees of 1: 1.5.

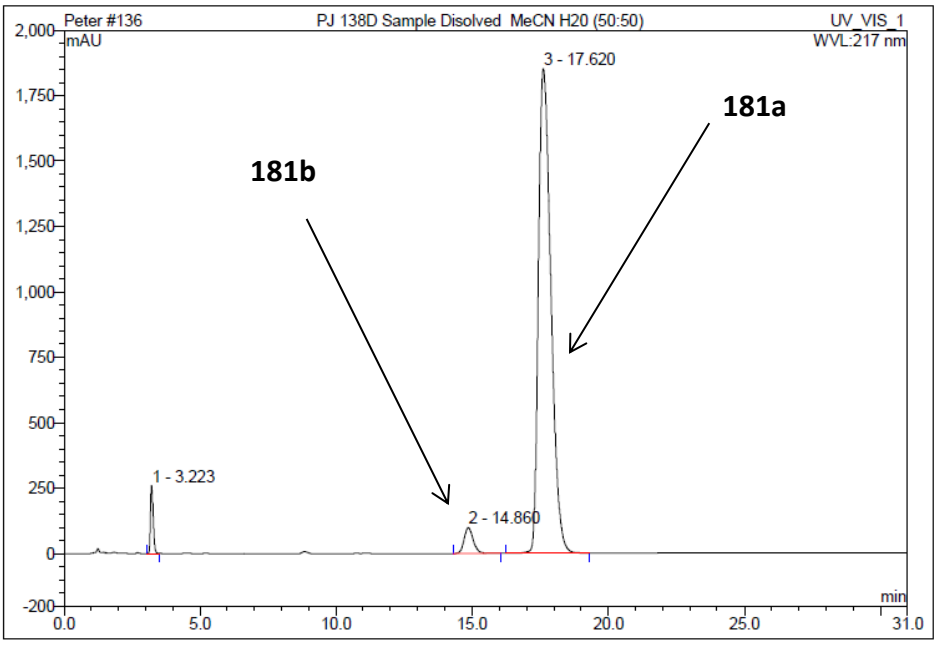

No.	Ret.Time min	Peak Name	Height mAU	Area mAU*min	Rel.Area %	Amount	Type
1	3.22	n.a.	258.346	29.882	2.85	n.a.	BMB
2	14.86	n.a.	98.943	37.998	3.62	n.a.	BMB
3	17.62	n.a.	1849.529	981.783	93.53	n.a.	BMB
Total:			2206.819	1049.663	100.00	0.000	

Figure 13: HPLC chromatogram of the white solid diastereomer **181a** with traces of **181b** when the reaction was done at 0 °C.

From HPLC chromatogram **13** and **14**, low temperature promotes the formation of the major diastereomers.

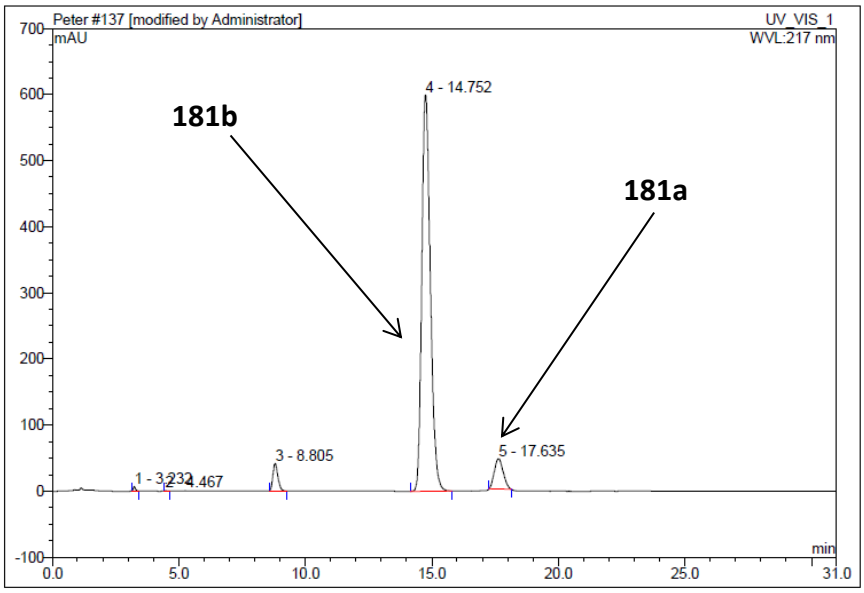

No.	Ret.Time min	Peak Name	Height mAU	Area mAU*min	Rel.Area %	Amount	Type
1	3.23	n.a.	6.684	0.710	0.27	n.a.	BMB*
2	4.47	n.a.	0.161	0.019	0.01	n.a.	BMB*
3	8.81	n.a.	41.297	9.367	3.55	n.a.	BMB*
4	14.75	n.a.	599.354	235.003	89.18	n.a.	BMB
5	17.64	n.a.	45.493	18.419	6.99	n.a.	BMB*
Total:			692.988	263.517	100.00	0.000	

Figure 14: HPLC chromatogram of the colourless oil diastereomer **181b** with traces of **181a** when the reaction was done at 0 °C.

Out of curiosity, the same reaction was performed at -18 °C. This reaction that took 13 days led, again surprisingly, to **181a** in a yield of 20% with only traces of **181b** being present (**Figure 15**). The use of the low temperature of -18 °C presumably reduces the kinetic energy of reacting molecules and thereore the less sterically hindered site of the aldehydes is likely to be attacked by the nucleophile, thus leading to the observed major diastereomer **181a**.

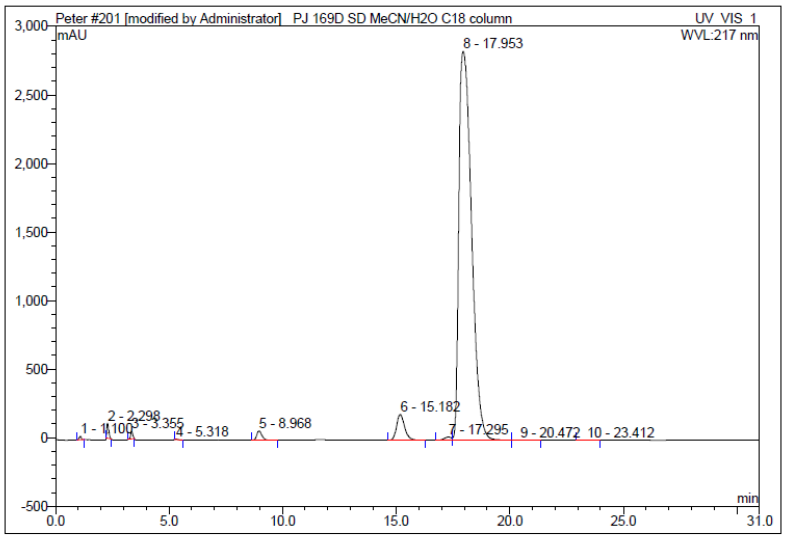

No.	Ret.Time min	Peak Name	Height mAU	Area mAU*min	Rel.Area %	Amount	Type
1	1.10	n.a.	26.153	2.685	0.14	n.a.	BMB*
2	2.30	n.a.	108.956	10.553	0.54	n.a.	BMB*
3	3.36	n.a.	56.537	6.342	0.33	n.a.	BMB*
4	5.32	n.a.	2.483	0.250	0.01	n.a.	BMB*
5	8.97	n.a.	67.397	17.103	0.88	n.a.	BMB
6	15.18	n.a.	186.164	75.770	3.89	n.a.	BMB*
7	17.30	n.a.	22.252	7.565	0.39	n.a.	BM
8	17.95	n.a.	2835.434	1825.069	93.75	n.a.	M
9	20.47	n.a.	1.930	1.270	0.07	n.a.	MB
10	23.41	n.a.	0.297	0.174	0.01	n.a.	BMB
Total:			3307.603	1946.781	100.00	0.000	

Figure 15: HPLC chromatogram of the product **181a** when the reaction was done at -18 °C.

It was clear that the synthesis of the MBH adducts using *N*-Boc-L-phenylalaninal **173** was a success; but explaining the unusual diastereoselectivity results using stereochemical principles was not easy. It is with this in mind that the synthesis of MBH adducts using *N*-Boc-D-phenylalaninal **174** was necessary for the purpose of comparison. This specific reaction was done at zero degrees in the presence of DABCO as a catalyst (**Scheme 50**).

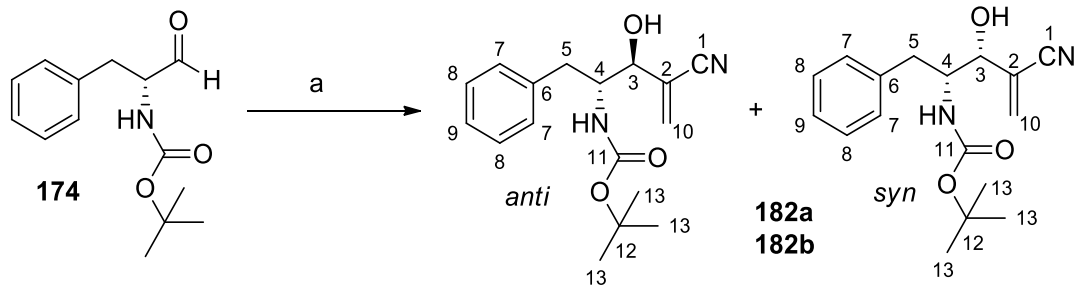

Scheme 50: Preparation of Morita-Baylis-Hillman adducts from *N*-Boc-D-phenylalaninal. *Reagents and conditions*: (a) DABCO, acrylonitrile, 0 °C.

Carrying out the reaction shown in **Scheme 50** led to the formation of two diastereomers, one of which was compound **182a**, isolated as a white solid in 13% yield, while the other diastereomer **182b** was isolated as a colourless oil in 18% yield after 13 days.

The formation of **182a** was confirmed by ^{1}H NMR spectroscopic data. The characteristic alkene peaks were seen as two multiplets at δ 6.13 – 6.07 and 6.05 – 5.99 each integrating for one proton for H-10a and H-10b. The other characteristic proton peaks were evident as two singlets at δ 4.97 and 4.26 each integrating for one proton corresponding to H-3 and OH, respectively. The appearance of the hydroxyl peak and the stereogenic centre proton H-3 was a clear indication that the aldehyde had reacted. The five aromatic protons appeared as a multiplet at δ 7.35 – 7.18 while the doublet at δ 5.06 with a coupling constant of 8 Hz was assigned to NH. The two multiplets at δ 3.97 – 3.74 and 3.10 – 2.81 integrating for one proton and two protons, respectively, were for the stereogenic centre proton H-4 and benzylic proton H-5, respectively. The multiplet at δ 1.44 – 1.31 integrating for nine protons was for the three chemically equivalent methyl groups of the Boc group. The multiplet of the Boc group is due to the presence of the carbamate bond that creates rotamers.

The formation of **182a** was further supported by ^{13}C NMR spectroscopy. The carbon signals observed at δ 130.9 for C-10, 124.8 for C-2 and 72.3 for C-3 were characteristic peaks. The disappearance of the aldehyde peak and the appearance of the peak at δ 72.3 was a clear indication that the aldehyde of the electrophile had reacted to form a stereogenic cenre carbon C-3. The carbonyl peak of the Boc group was observed at δ 156.9, while the nitrile carbon atom was evident at δ 117.3. The presence of the second stereogenic centre carbon C-4 was confirmed at δ 56.2 and the benzylic carbon signal was observed at δ 37.0. The three methyl carbon atoms of the Boc group were observed at δ 28.2.
The presence of the peaks at 3372 cm^{-1}, 3358 cm^{-1}, 2224 cm^{-1} and 1680 cm^{-1} in the IR spectrum supported the presence of NH, OH, C≡N and C=O functional groups. The mass spectrum obtained corresponded well with the expected mass of the product (calculated for $C_{17}H_{22}N_2O_3Na$: 325.1528, found: [M+Na^{+}] 325.1528).

After managing to logically use all the spectroscopic data to confirm the structure of the white solid **182a**, the second diastereomer to confirm was **182b**. Analysis of the ^{1}H NMR and ^{13}C NMR spectra, and the IR and MS data clearly indicated that the two compounds were diastereomers. The comparison of the ^{1}H NMR data of the two diastereomers is shown

in **Table 13**. From the Table, it is clear that stereogenic centre proton H-3 of the diastereomer **182a** appeared as a downfield doublet as compared to a similar proton for **182b**, which appeared as an upfield multiplet on the ^{1}H NMR spectrum.

Table 13: Comparison of ^{1}H NMR chemical shift of **182a** and **182b**

	182a	**182b**
Aromatic protons (ppm)	7.35 – 7.18 (m)	7.38 – 7.15 (m)
H-10a (ppm)	6.13 – 6.07 (m)	6.13 (brs) for both H-10a and H-10b
H-10b (ppm)	6.05 – 5.99 (m)	
NH (ppm)	5.06 (d, *J* = 8.0 Hz)	5.05 – 4.90 (m)
H-3 (ppm)	**4.97 (d, *J*= 6.1 Hz)**	**4.85 – 4.70 (m)**
OH (ppm)	4.26 (s)	4.40 (brs)
H-4 (ppm)	3.97 – 3.74 (m)	4.13 – 3.93 (m)
H-5 (ppm)	3.10 – 2.81 (m)	2.95 – 2.80 (m)
H-9	1.44 – 1.31 (m)	1.46 – 1.30 (m)

The carbon chemical shift values of **182a** and **182b** are shown in **Table 14**. It is clear that the stereogenic centre carbon signal for the diastereomer **182a** was shielded as compared to the same carbon signal of the diastereomer **182b**.

Table 14: Comparison of carbon chemical shift of **182a** and **182b**

	182a	**182b**
C-11, C-6 and C-10	156.9, 137.7 and 130.9	157.5, 137.0 and 132.3
C-7 or 8, C-7 or 8	129.2, 128.6	129.2 128.8
C-9, C-2 and C-1	126.7, 124.8 and 117.3	126.9, 123.4 and 117.5
C-12, **C-3** and C-4	80.4, **72.3** and 56.2	80.9, **74.6** and 57.2
C-5 and C-13	37.0 and 28.2	35.4 and 28.2

The IR characteristic peaks and HRMS data of **182a** and **182b** were similar (T**able 15**).

Table 15: IR and HRMS data of **182a** and **182b**

	182a	**182b**
NH (cm^{-1})	3372	3370
OH (cm^{-1})	3358	3356
C≡N (cm^{-1})	2224	2224
C=O (cm^{-1})	1680	1680
HRMS data	calculated for $C_{17}H_{22}N_2O_3Na$: 325.1523, found: [M+Na^+] 325.1528)	calculated for $C_{17}H_{22}N_2O_3Na$: 325.1523, found: [M+Na^+] 325.1529

The structures of **182a** and **182b** were thus successfully confirmed using all the spectroscopic information, as discussed. It was clear from the spectroscopic information that the data for compound **182a** matched that for compound **181a**, as expected for enantiomers. Similarly, data for compound **182b** matched that for compound **181b**.

The next step was to separate each diastereomer on a C-18 column to determine the diastereomeric ratio for the reaction. Subjecting **182a** to a reverse phase C18 HPLC column chromatography using acetonitrile and water as a mobile phase at a flow rate of 1 mL/min gave two peaks at retention times of 15.08 minutes and 17.83 minutes (**Figure 16**). Compound **182a** was found to be relatively pure, with only a small amount of contamination by the second diastereomer. The diastereomeric ratio for this sample (128 mg) was 52:1.

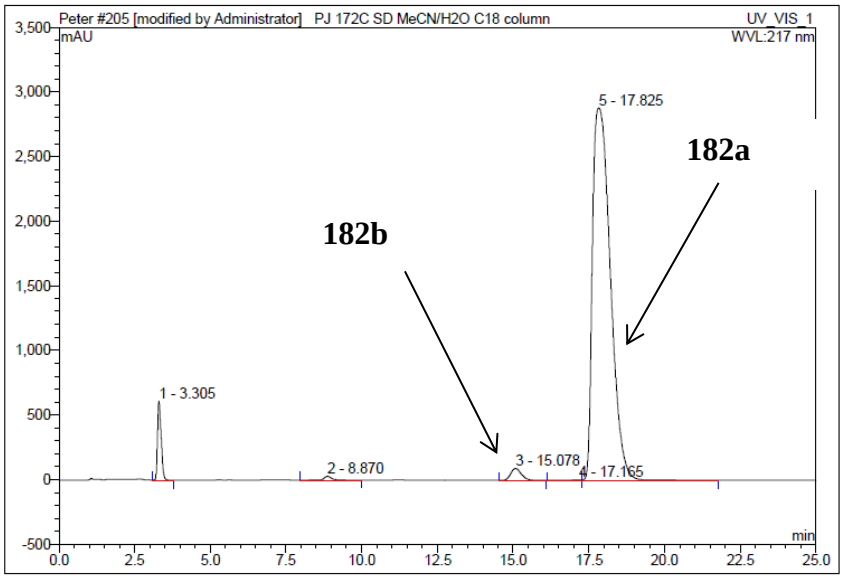

No.	Ret.Time min	Peak Name	Height mAU	Area mAU*min	Rel.Area %	Amount	Type
1	3.31	n.a.	609.977	87.134	4.13	n.a.	BMB
2	8.87	n.a.	29.615	8.870	0.42	n.a.	BMB*
3	15.08	n.a.	92.622	37.865	1.80	n.a.	BMB*
4	17.17	n.a.	4.836	1.845	0.09	n.a.	BM *
5	17.83	n.a.	2883.699	1972.665	93.56	n.a.	MB*
Total:			3620.750	2108.379	100.00	0.000	

Figure 16: HPLC chromatogram of the white solid diastereomer **182a** when the reaction was done at zero degrees.

The second diastereomer **182b** was then subjected to reverse phase C-18 HPLC column chromatography. This afforded two peaks at retention times of 14.94 minutes and 18.06 minutes with a diastereomeric ratio of 1:7 for this sample (170 mg) (**Figure 17**).

Using the HPLC results (**Figures 16** and **17**) to calculate the diastereoselectivity of this reaction showed that the ratio of the two diastereomers obtained was almost 1:1. This result again was a surprised, as it did not match the results of the equivalent reaction carried out on the enantiomeric aldehyde.

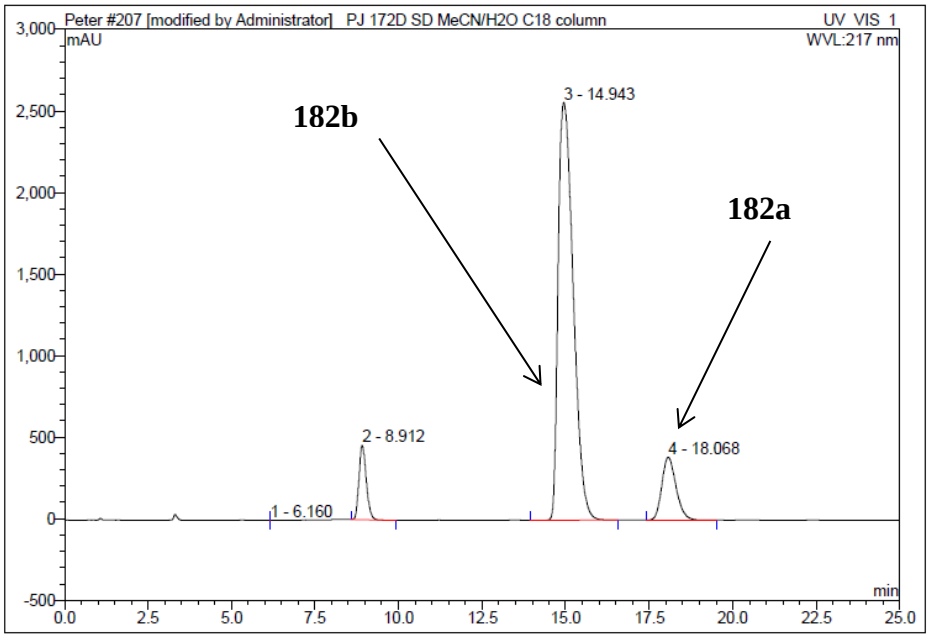

No.	Ret.Time min	Peak Name	Height mAU	Area mAU*min	Rel.Area %	Amount	Type
1	6.16	n.a.	0.001	0.000	0.00	n.a.	BMB*
2	8.91	n.a.	456.565	116.165	7.06	n.a.	BMB*
3	14.94	n.a.	2560.626	1338.622	81.41	n.a.	BMB*
4	18.07	n.a.	384.767	189.605	11.53	n.a.	BMB*
Total:			3401.959	1644.393	100.00	0.000	

Figure 17: HPLC chromatogram of diastereomer **182b** when the reaction was done at zero degrees.

After successfully synthesizing the acrylonitrile derivatives, we turned to the use of methyl and ethyl acrylate derivatives so as to increase the number of MBH adducts for investigation.

3.1.3.2 Synthesis of MBHA esters by reacting methyl and ethyl acrylate with N-Boc-L-phenylalaninal 181 and N-Boc-D-phenylalaninal 182

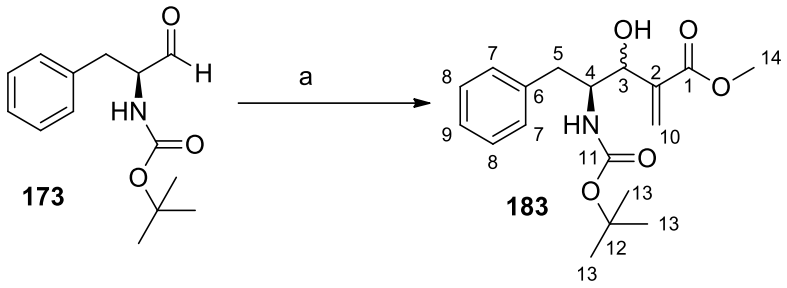

Scheme 51: Preparation of Morita-Baylis-Hillman Adducts from *N*-Boc-L-phenylalaninal. *Reactions and conditions*: (a) DABCO, methyl acrylate at RT and 0 °C.

The reaction between (*S*)-*tert*-butyl (1-oxo-3-phenylpropan-2-yl)carbamate **173** and methyl acrylate in the presence of DABCO at room temperature afforded (4*S*)-methyl 4-((*tert*-butoxycarbonyl)amino)-3-hydroxy-2-methylene-5-phenylpentanoate **183** as a colourless oil that was a mixture of diastereomers in a poor yield of 31% (**Scheme 51**). The identity of the product was confirmed by ^{1}H NMR spectroscopy. The diastereomers were not separable by gravity column chromatography and distinct signals for each of the two diastereomers were not visible in the proton NMR spectrum. The presence of a singlet at δ 6.32 and a multiplet at δ 5.95 – 5.88 each integrating for one proton were assigned to the vinylic protons H-10a and H-10b. The doublet at δ 4.52 with a coupling constant of 5.7 Hz was assigned to stereogenic centre proton H-3. The doublet at δ 3.62 with a coupling constant of 5.8 Hz was assigned to the OH proton. These characteristic protons H-10a, H-10b, H-3 and OH showed that the methyl acrylate had reacted with the aldehyde. The presence of the five aromatic protons was confirmed by the presence of a multiplet at δ 7.34 – 7.15 while the doublet at δ 4.83 with a coupling constant of 8.7 Hz was assigned to the NH proton. The stereogenic centre proton H-4 appeared as a multiplet at δ 4.11 – 3.92 and integrated for one proton. The methoxy group was confirmed by the multiplet at δ 3.81 – 3.69 integrating for three protons. The appearance of a multiplet for the methoxy protons suggests that the two diastereomeric compounds exist in multiple conformations as a result of restricted rotation about the C-N bond of the carbamate. The benzylic protons H-5 gave rise to a multiplet at δ 3.14 – 2.80 which integrated for two protons while the three methyl groups of the Boc moiety were evident by the presence of a multiplet at δ 1.43 – 1.24.

The proposed structure was supported by the ^{13}C NMR spectrum. Most signals were distinct for each of the two diastereomers, and values reported here are for the major diastereomer. The presence of carbon signals at δ 140.6 for C-2, 125.9 for C-10 and δ 70.8 for C-3 confirmed that the reaction had indeed taken place. The carbon signal at δ 166.6 for C-1 and δ 156.3 for C-11 were for the carbonyl carbon of the ester group and the carbonyl of the Boc group, respectively. The quaternary carbon atom of the Boc group (C-12) appeared at δ 79.6 while the stereogenic centre carbon C-4 was found at δ 54.9. The methoxy carbon signal was found at δ 51.8 while the benzylic carbon C-5 gave rise to the signal at δ 38.1. The three methyl groups of the Boc group gave rise to a signal at δ 28.2.

The ^{13}C NMR spectrum of **183** showed duplication of the carbon signals indicating the presence of the major and a minor diastereomer. The major diastereomer showed all the 14 carbon signals while the minor diastereomer showed the signals of only specific carbon atoms. The precise assignment of the stereogenic centre carbon signal for C-3 of the major and minor diastereomer was achieved using DEPT 135 experiment.

The IR spectrum showed a peak at 3385 cm^{-1} for the NH and OH group and other two peaks at 1697 cm^{-1} and 1690 cm^{-1} for the two carbonyl groups. The molecular ion of **183** was confirmed by HRMS to be $[M+Na^+]$ 358.1640 which was consistent with the mass calculated for $C_{18}H_{25}NO_5Na$ of 358.1625.

Separation of **183** on reverse phase C18 HPLC gave two peaks at retention times of 17.90 minutes and 20.03 minutes (**Figure 18**). The diastereomeric ratio of the reaction yielding **183** was found to be 1:4.

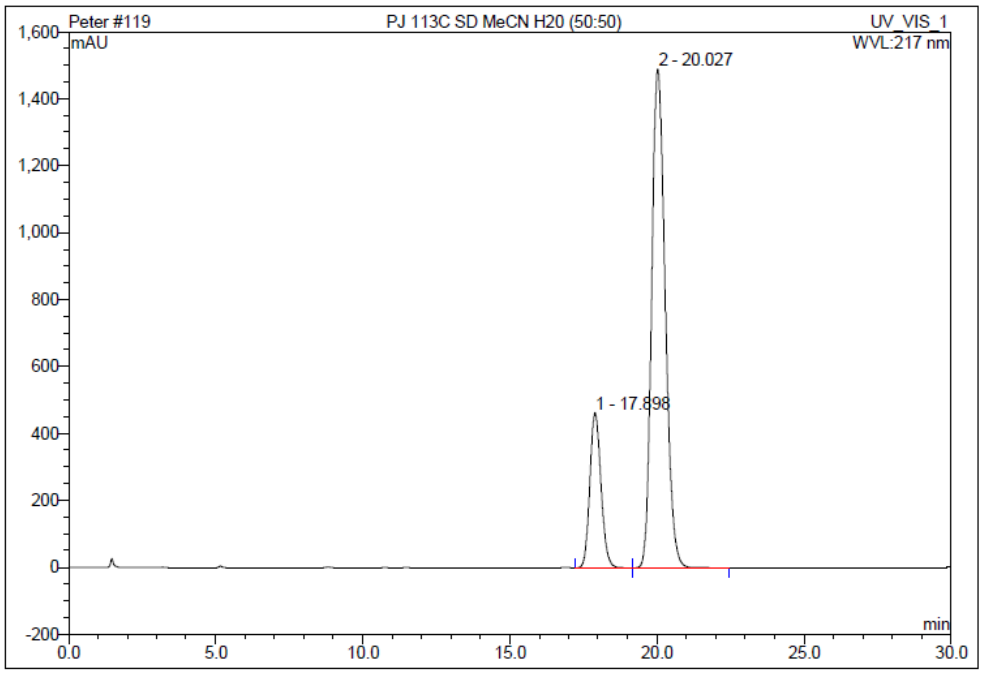

No.	Ret.Time min	Peak Name	Height mAU	Area mAU*min	Rel.Area %	Amount	Type
1	17.90	n.a.	463.432	204.071	20.40	n.a.	BM
2	20.03	n.a.	1489.955	796.377	79.60	n.a.	MB
Total:			1953.387	1000.448	100.00	0.000	

Figure 18: HPLC chromatogram of **183** showing a mixture of diastereomers when the reaction was done at room temperature.

The sound scientic question one would ask is whether it is possible that repeating the reaction at 0 °C would have a significant effect on the diastereomeric ratio of the product. This question can only be answered by repeating the reaction between methyl acrylate and *N*-Boc-L-phenylalaninal at 0 °C to afford **183**.

Separation of **183** on reverse phase C18 HPLC gave two peaks at retention times of 18.02 minutes and 20.04 minutes (**Figure 19**). The diastereomeric ratio of **183** was found to be 1:3, with the same major diastereomer being found as before, but in a decreased ratio.

Sample Name:	**PJ 137D repeat 1 Sample Disolved MeCN H20 (50:50)**	*Injection Volume:*	**20.0**
Vial Number:	**161**	*Channel:*	**UV_VIS_1**
Sample Type:	**unknown**	*Wavelength:*	**217**
Control Program:	**Peter chiral**	*Bandwidth:*	**4**
Quantif. Method:	**Peter**	*Dilution Factor:*	**1.0000**
Recording Time:	**2014/9/11 13:52**	*Sample Weight:*	**1.0000**
Run Time (min):	**35.00**	*Sample Amount:*	**1.0000**

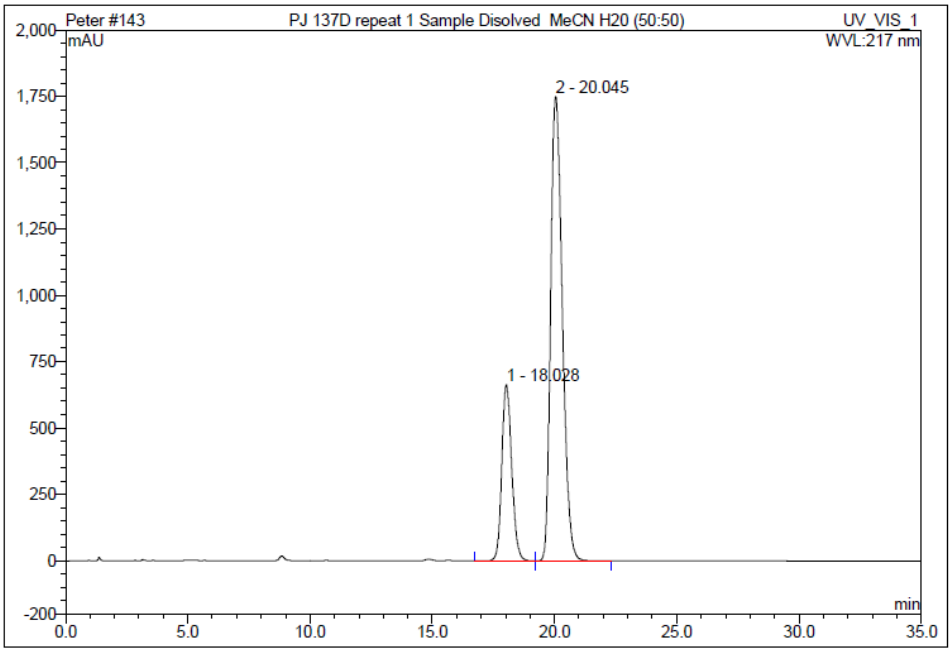

No.	Ret.Time min	Peak Name	Height mAU	Area mAU*min	Rel.Area %	Amount	Type
1	18.03	n.a.	663.660	311.555	24.36	n.a.	BM
2	20.05	n.a.	1748.296	967.590	75.64	n.a.	MB
Total:			2411.956	1279.145	100.00	0.000	

Figure 19: HPLC chromatogram of the two diastereomers of **183** when the reaction was done at 0 °C.

The diastereomeric ratios of the products from the two different reactions were similar, in other words performing the reaction at 0 °C did not change the diastereoselectivity by a significant value. The next reaction was to use the enantiomeric aldehyde, *N*-Boc-D-phenylalaninal **174** in performing the MBH reaction so that we could compare the results with those obtained for **183** (**Scheme 51**).

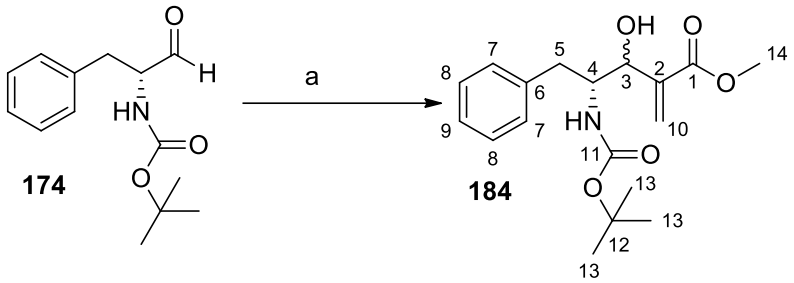

Scheme 52: Preparation of Morita-Baylis-Hillman adducts from *N*-Boc-D-phenylalaninal. *Reactions and conditions*: (a) DABCO, methyl acrylate 0 °C.

The reaction between *N*-Boc-D-phenylalaninal **174** and methyl acrylate under the influence of DABCO afforded **184** as a colourless oil that was a mixture of diastereomers in a yield of 32%. The identity of the product was confirmed by ^{1}H NMR spectroscopy.

The ^{1}H NMR spectroscopic data of **184** showed a multiplet at δ 6.34 – 6.24 integrating for one proton for H-10a and a singlet at δ 5.92 integrating for one proton for H-10b. There were a further two multiplets; one at δ 4.54 – 4.43 and another multiplet at δ 4.12 – 3.95 each integrating for one proton for H-3 and OH respectively. The presence of these protons in the ^{1}H NMR spectrum clearly indicated that the activated alkene had reacted with the electrophile to form the MBHA. The aromatic protons were evident as a multiplet at δ 7.32 – 7.14 integrating for five protons. The multiplet at δ 5.12 – 4.93 integrating for one proton was assigned to the NH proton while the multiplet at δ 4.12 – 3.95 also integrating for one proton was assigned to the OH proton. It was also very clear that the multiplet at δ 3.78 – 3.64 integrating for three protons was the methoxy group of the activated alkene. The multiplet of the methoxy and the OH group suggests that the diastereomers **184** exist in multiple conformations as a result of restricted rotation. The benzylic protons H-5 were seen as a multiplet at δ 3.08 – 2.83 with an integration of two protons while the multiplet at δ 1.42 – 1.19 integrating for nine protons was for the three methyl group protons of the Boc group. The presence of the carbamate C-N bond creates rotamers that result in the observed multiplets for the NH and Boc group.

^{13}C NMR spectroscopy supported the ^{1}H NMR data. As for compound **183**, diastereomers were not separated, and the signals reported here are for the major diastereomer of **184**. The presence of carbon signals at δ 125.8 for C-10, 140.7 for C-2, and 70.3 for C-3 was clear evidence that the intended product had been formed. The characteristic carbonyl carbon

signal at δ 166.5 for C-1 and 156.3 for C-11 supported this observation. The methoxy carbon atom of the ester gave a signal at a chemical shift of δ 51.8. The stereogenic carbon atom for C-4 was found at 54.6 ppm, while the benzylic carbon (C-5) signal was observed at δ 38.2. The quaternary carbon signal at δ 79.4 and the saturated carbon signal at δ 28.2 were for C-12 and C-13, respectively.

Duplication of carbon signals in the ^{13}C NMR spectrum was observed, indicating the presence of a major and a minor diastereomer. A comparison of the ^{13}C chemical shifts between the major diastereomers of **183** and **184** is shown in shown in **Table 16**. The major diastereomers of **183** and **184** had the same chemical shifts for the carbon signals, as expected for enantiomers. The observation was similar for the minor diastereomers in which the stereogenic centre carbon signal C-3 was observed at δ 74.5 for **183** and δ 73.9 for **184**, downfield of the chemical shift observed for this carbon signal in the major diastereomers (70.8 and 70.2 ppm).

Table 16: Comparison of ^{13}C chemical shift of the major diastereomer of **183** and **184**

Carbon number	**183**	**184**
C-1, C-11 and C-2	166.6, 156.3 and 140.6	166.5, 156.3 and 140.7
C-6, C-7 or 8, C-7 or 8	138.4, 129.3, 128.4	138.5, 129.3 128.4
C-9, C-10 and C-12	126.4, 125.9 and 79.6	126.3, 125.8 and 79.4
C-3 and C-4	**70.8** and 54.9	**70.2** and 55.6
C-14, C-5 and C-13	51.8 and 38.2 and 28.2	51.8, 38.2 and 28.2

The IR spectrum was used to identify the characteristic functional groups of **184**. The presence of a peak at 3376 cm^{-1} confirmed the presence of the NH and OH groups while the peaks at 1700 cm^{-1} and 1685 cm^{-1} were characteristic peaks for the two carbonyl groups. The molecular ion of **184** was confirmed by HRMS to be $[M+Na^+]$ 358.1640 which was consistent with the mass calculated for $C_{18}H_{25}NO_5Na$ of 358.1625.

The next step was to separate the diastereomers using reverse phase C-18 HPLC after successfully confirming the structure of **184**. This led to two peaks at retention times of 18.84 and 20.95 minutes. The diastereomeric ratio of **184** was found to be 1:3 (**Figure 20**).

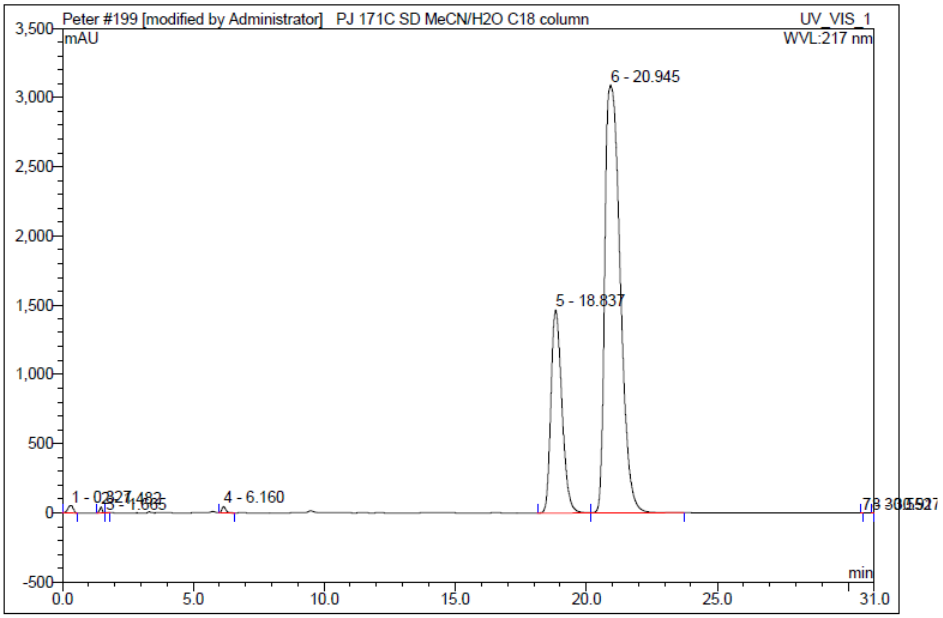

No.	Ret.Time min	Peak Name	Height mAU	Area mAU*min	Rel.Area %	Amount	Type
1	0.33	n.a.	53.762	12.541	0.44	n.a.	BMB
2	1.48	n.a.	42.555	4.685	0.16	n.a.	BM *
3	1.67	n.a.	1.882	0.198	0.01	n.a.	MB*
4	6.16	n.a.	43.758	7.460	0.26	n.a.	BMB*
5	18.84	n.a.	1467.102	713.146	25.05	n.a.	BM *
6	20.95	n.a.	3090.091	2108.886	74.08	n.a.	MB*
7	30.55	n.a.	0.019	0.001	0.00	n.a.	BMB
8	30.92	n.a.	0.029	0.002	0.00	n.a.	BMB
Total:			4699.198	2846.917	100.00	0.000	

Figure 20: HPLC chromatogram of **184** when the reaction was done at 0 °C.

The next compound to synthesize was the MBH ethyl acrylate ester. This ester was obtained after reacting (*S*)-*tert*-butyl (1-oxo-3-phenylpropan-2-yl)carbamate **173** with **e**thyl acrylate using DABCO as a catalyst at 0 °C for 12 days (**Scheme 53**). The reaction afforded (4*S*)-ethyl 4-((*tert*-butoxycarbonyl)amino)-3-hydroxy-2-methylene-5-phenylpentanoate **185** as a colourless oil that was a mixture of diastereomers in a yield of 28%.

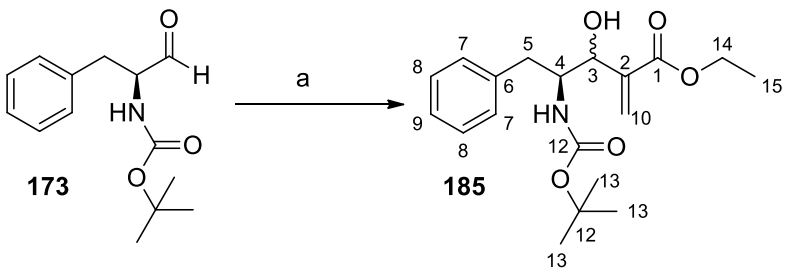

Scheme 53: Preparation of Morita Baylis Hillman Adducts from *N*-Boc-L-phenylalaninal. *Reactions and conditions*: (a) DABCO, ethyl acrylate at 0 °C.

The formation of **185** was confirmed by ^{1}H NMR spectroscopy. The singlet at δ 6.32 integrating for one proton was assigned to H-10a while the multiplet at δ 5.92 – 5.86 integrating for one proton was assigned to H-10b. The stereogenic centre proton H-3 gave rise to a multiplet at δ 4.55 – 4.49 while the hydroxyl group was evidenced by the presence of a multiplet at δ 3.75 – 3.60 integrating for one proton. The presence of vinylic protons H-10 from the activated ethyl acrylate and the formation of the stereogenic centre H-3 accompanied by the presence of the hydroxyl group confirmed that the reaction had indeed taken place. The other expected proton signals were also observed. The presence of the five aromatic protons was evident by the presence of the multiplet at δ 7.34 – 7.14 while the NH peak was confirmed by a doublet with a coupling constant of 9.3 Hz at δ 4.88. The presence of a multiplet at δ 4.31 – 4.11 integrating for two protons was evidence of H-14. The stereogenic centre proton H-4 was seen as a multiplet at δ 4.10 – 3.99 integrating for one proton while the benzylic protons H-5 were seen as a multiplet at δ 3.14 – 2.82 integrating for two protons. The last multiplet integrating for four methyl group protons was evident at δ 1.50 – 1.17 for H-13 and H-15. The existence of the multiple conformers for the diastereomers of **185** explains why H-15, H-13 and the hydroxyl group are observed as multiplets.

The ^{1}H NMR spectrum was supported by the ^{13}C NMR spectrum. Signals reported here are for the major diastereomer. The presence of carbon signals at δ 125.6 for C-10, 140.8 for C-2 and 70.6 for C-3 indicated that that the aldehyde had reacted with ethyl acrylate. The presence of two carbonyl signals was evident at δ 166.1 for C-1 and 156.3 for C-11 while the signals at δ 79.4 and 60.8 were for C-12 and C-14, respectively. The C-4 stereogenic centre was evident at δ 54.9 while the benzylic carbon C-5 was seen at δ 38.2. The remaining signals at δ 28.3 and 14.1 were for C-13 and C-15 respectively.

The duplication of the carbon signals in the ^{13}C NMR spectrum was a clear confirmation that **185** was present as two diastereomers. The presence of the C-3 stereogenic centre carbon evidenced at δ 70.6 for the major diastereomer and δ 74.4 for the minor diastereomer was very clear from a DEPT experiment.

The presence of an IR peak at 3320 cm^{-1} was characteristic for the NH and OH groups while the peaks at 1690 cm^{-1} and 1697 cm^{-1} were characteristic for the two carbonyl groups. The

formation of **185** was further confirmed by HRMS to be [M+H$^+$] 350.1955 which was consistent with the mass calculated for $C_{19}H_{28}NO_5$ of 350.1955.

The next step was to separate the diastereomers of **185** on reverse phase C-18 HPLC. Separation of **185** on reverse phase C-18 HPLC afforded two peaks at retention times of 120.20 and 128.77 minutes. The diastereomeric ratio of **185** was found to be 1:2 (**Figure 21**).

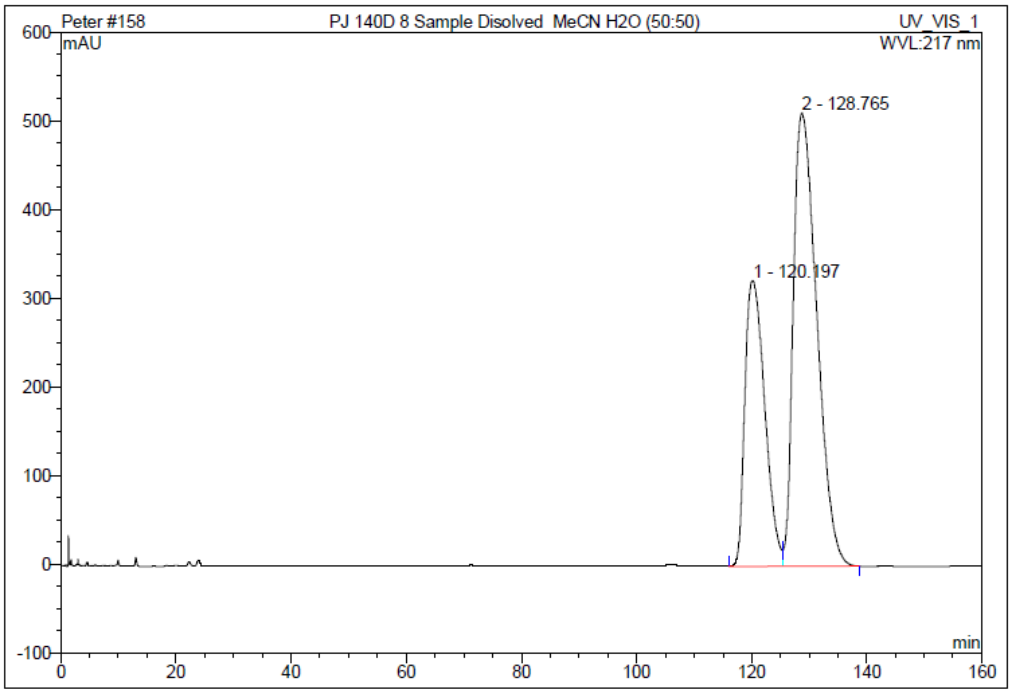

No.	Ret.Time min	Peak Name	Height mAU	Area mAU*min	Rel.Area %	Amount	Type
1	120.20	n.a.	322.040	1288.144	34.78	n.a.	BM
2	128.77	n.a.	511.151	2415.959	65.22	n.a.	MB
Total:			833.191	3704.103	100.00	0.000	

Figure 21: HPLC chromatogram of **185** when the reaction was done at 0 °C.

The last compound to be synthesized was the MBH adducts arising from methyl vinyl ketone.

3.1.3.3 Synthesis of MBHA by reacting methyl vinyl ketone with N-Boc-L-phenylalaninal

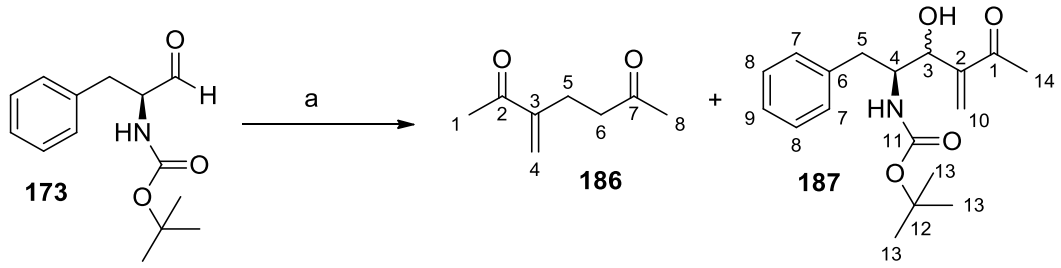

Scheme 54: Preparation of Morita Baylis Hillman Adducts from *N*-Boc-L-phenylalaninal. *Reagents and conditions*: (a) DABCO, methyl vinyl ketone, DCM at RT.

The MBHA was obtained by reacting (*S*)-tert-butyl (1-oxo-3-phenylpropan-2-yl)carbamate **173** with methyl vinyl ketone (MVK) in dichloromethane in the presence of DABCO at room temperature (**Scheme 54**). The reaction took 12 days affording 3-methyleneheptane-2,6-dione **186** as a colourless oil with a yield of 47% and *tert*-butyl ((2S)-3-hydroxy-4-methylene-5-oxo-1-phenylhexan-2-yl)carbamate **187** as a colourless oil that was a mixture of diastereomers in a yield of 35%. In addition, a second fraction that had the same R_f value on TLC as **187** was also obtained. There was no reaction when aldehyde **173** was reacted with methyl vinyl ketone at 0 °C.

The first compound **186** was an unexpected product. The compound was characterised by ^{1}H NMR spectroscopy. The two singlets at δ 6.04 and δ 5.84 each integrating for one proton were assigned to H-4a and H-4b. The multiplet at δ 2.64 – 2.49 integrating for four protons was assigned to H-5 and H-6. The two singlets at δ 2.34 and δ 2.13 each integrating for three protons were assigned to the two methyl groups H-1 and H-8. The ^{13}C NMR spectrum supported the proposed structure of **186**. The presence of carbon signals at δ 207.8 and δ 199.5 indeed confirmed that there were two carbonyl groups which were assigned to C-7 and C-2, respectively. Using a DEPT experiment, we were able to assign signals at δ 147.7 for C-3, δ 126.2 for C-4, δ 42.4 for C-6 and δ 25.3 for C-5. The methyl carbon signals that were observed at δ 29.8 and δ 25.8 were assigned either for C-1 or C-8. The IR spectrum was clear as the peaks at 1675 cm^{-1} and 1671 cm^{-1} confirmed the presence of the two carbonyl functional groups.

The formation of **186** has never been reported when methyl vinyl ketone reacts with any of the α-amino aldehydes but has been reported by Idahosa when 3-methoxy-2-nitrobenzaldehyde was reacted with MVK.[122] In this report, the convincing mechanism was explained how **186** was formed and why it was a major product. The spectroscopic data of **186** was in agreement with the same product that was reported by Idahosa.

The next compound to confirm was the MBH adduct **187**. The ^{1}H NMR spectrum was used to assign all the protons. The singlets at δ 6.12 and δ 6.08 each integrating for one proton were assigned to H-10a and H-10b. The proton shift at δ 4.59 integrating for one proton with a coupling constant of 5.1 Hz was assigned to the stereogenic centre proton H-3. The hydroxyl proton appeared as a multiplet at δ 3.06 – 2.80. The presence of H-10, H-3 and the OH group clearly indicated that the electrophile had reacted with MVK. The multiplet at δ 7.34 – 7.15 integrating for five protons was assigned to the aromatic protons. The NH proton peak appeared as a doublet at δ 4.78 with a coupling constant of 8.9 Hz. The other stereogenic centre proton H-4 appeared as a multiplet at δ 4.02 – 3.89, while the benzylic proton H-5 also appeared as a multiplet at δ 3.57 – 3.49. The methyl group of MVK appeared as a singlet at δ 2.32 integrating for three protons. The proton peak which appeared as a multiplet at δ 1.40 - 1.32 integrating for nine protons was assigned to the three methyl groups of the Boc moiety. Compound **187**, in addition to being a mixture of two diastereomers, also has different conformations as a result of restricted rotation, and that is why a number of signals that would normally appear as singlets, appeared as multiplets.

The ^{13}C NMR data also supported the identity of **187**. The disappearance of the aldehyde peak of the electrophile and the appearance of carbon signals at δ 125.6 for C-10, 148.7 for C-2 and 70.6 for C-3 confirmed to us that the activated MVK had reacted with the aldehyde. The three carbon atoms C-10, C-2 and C-3 were precisely assigned using a DEPT experiment. The characteristic carbonyl carbon signals at δ 200.2 and 156.3 were assigned to C-1 and C-11, respectively. The stereogenic centre carbon C-4 was assigned to the signal at δ 54.7 while the benzylic carbon C-5 was assigned to the signal that appeared at δ 38.1. The three methyl carbon atoms of the Boc group appeared at δ 28.3 while the methyl group of the MVK was assigned to the signal at δ 26.3.

The IR spectrum confirmed the presence of two carbonyl groups and one NH functional group. The peak at 3334 cm^{-1} represented both the NH and OH functional groups while the

peaks at 1671 cm^{-1} and 1664 cm^{-1} represented the two carbonyl groups. The molecular ion was confirmed by HRMS to be [M+Na^+] 342.1676 which was consistent with the mass calculated for $C_{18}H_{25}NO_4Na$ of 342.1676.

Separation of **187** using reverse phase C-18 HPLC column chromatography using a mobile phase of acetonitrile and water with flow rate of 1 mL/min gave two peaks, one major and one minor, at retention times of 16.91 (minor) and 18.41 minutes (major) (**Figure 22**). The HPLC chromatogram of **187** showed that it was contaminated with only small amounts of another diastereomer.

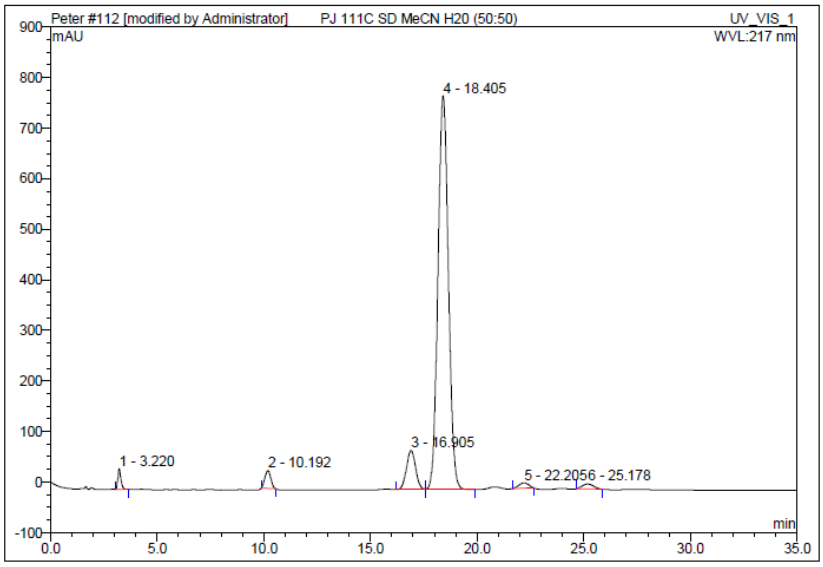

No.	Ret.Time min	Peak Name	Height mAU	Area mAU*min	Rel.Area %	Amount	Type
1	3.22	n.a.	40.585	6.751	1.33	n.a.	BMB*
2	10.19	n.a.	35.500	11.382	2.24	n.a.	BMB*
3	16.91	n.a.	77.689	38.845	7.63	n.a.	BM
4	18.41	n.a.	779.086	440.677	86.56	n.a.	MB
5	22.21	n.a.	10.510	5.586	1.10	n.a.	BMB*
6	25.18	n.a.	9.671	5.885	1.16	n.a.	BMB*
Total:			953.041	509.126	100.00	0.000	

Figure 22: HPLC chromatogram of diastereomer **187** contaminated with a small amount of another diastereomer when the reaction was done at room temperature

Separation of the second fraction of **187** on reverse phase C-18 HPLC column chromatography afforded two peaks of equal relative areas at retention times of 16.98 and 18.52 minutes (**Figure 23**).

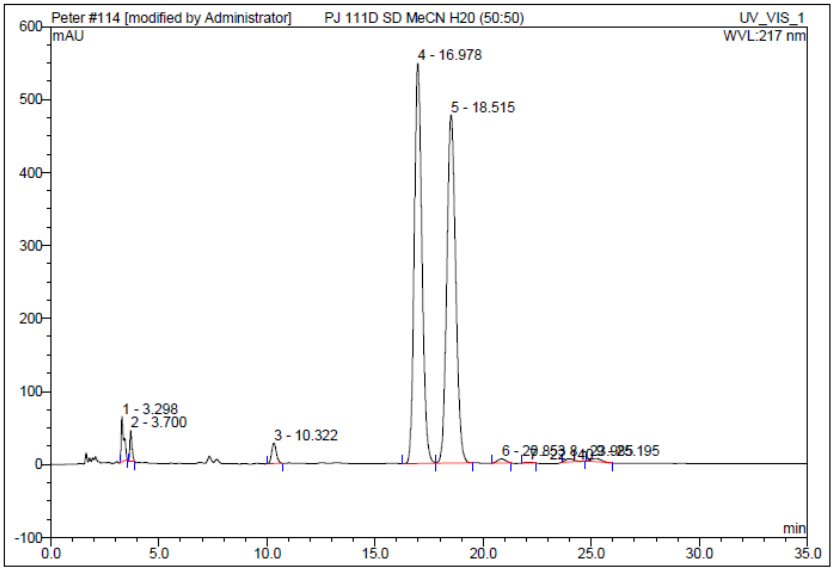

No.	Ret.Time min	Peak Name	Height mAU	Area mAU*min	Rel.Area %	Amount	Type
1	3.30	n.a.	62.302	9.335	1.94	n.a.	BMB*
2	3.70	n.a.	42.083	4.866	1.01	n.a.	BMB*
3	10.32	n.a.	27.873	7.062	1.47	n.a.	BMB*
4	16.98	n.a.	547.925	226.935	47.17	n.a.	BM
5	18.52	n.a.	477.220	225.636	46.90	n.a.	MB
6	20.85	n.a.	5.600	2.499	0.52	n.a.	BMB*
7	22.14	n.a.	0.920	0.389	0.08	n.a.	BMB*
8	23.99	n.a.	4.423	1.947	0.40	n.a.	BMB*
9	25.20	n.a.	4.560	2.398	0.50	n.a.	BMB*
Total:			1172.907	481.068	100.00	0.000	

Figure 23: HPLC chromatogram of the second fraction of **187** containing the two diastereomers in equal proportions when the reaction was done at room temperature.

At this particular juncture, a total of seven MBH adducts having a new stereogenic centre bearing a hydroxyl group had been successfully synthesized. The chemical shifts of the newly generated stereogenic centres of all the synthesized adducts was compared and tabulated in **Table 17**.

Table 17: Comparison of the ^{13}C NMR chemical shift values of the stereogenic centre attached to a hydroxyl group (C-3) of the adducts synthesized.

Compound	**181a**	**181b**	**182a**	**182b**	**183**	**184**	**185**	**187**
Chemical shift (δ)	72.0	74.5	72.3	74.6	70.8 74.5	70.2 73.9	70.6 74.4	70.6

It was confirmed from **Table 17** that compounds that are mirror images of each other had the same chemical shift for the stereogenic centre carbon. For example, compound **181a** and

compound **182a**. For compounds **183 - 185** and **187**, it is clear that the major product in each case is that with the more upfield C-3 chemical shift. For two diastereomers, the biggest differences in chemical shifts are expected to be those centres where the stereochemistry differs between the diastereomers, such as C-3.

A repeat of the MVK reaction at room temperature afforded a solid that we were able to crystallise in 30% ethyl acetate in hexane. Spectroscopic analysis of this crystal confirmed that the compound was **187**. The use of X-ray crystallography revealed that the crystal structure was composed of a mixture of four stereoisomers, but only two are shown in **Figure 24**. The presence of a mixture of *R*,*R* and *S*,*S* enantiomers was extremely disappointing, as the only explanation for this observation was that the original stereogenic centre of the aldehyde had racemized during the course of the reaction. This was an opportunity to re-examine previous adducts in order to find out if they were also racemic adducts.

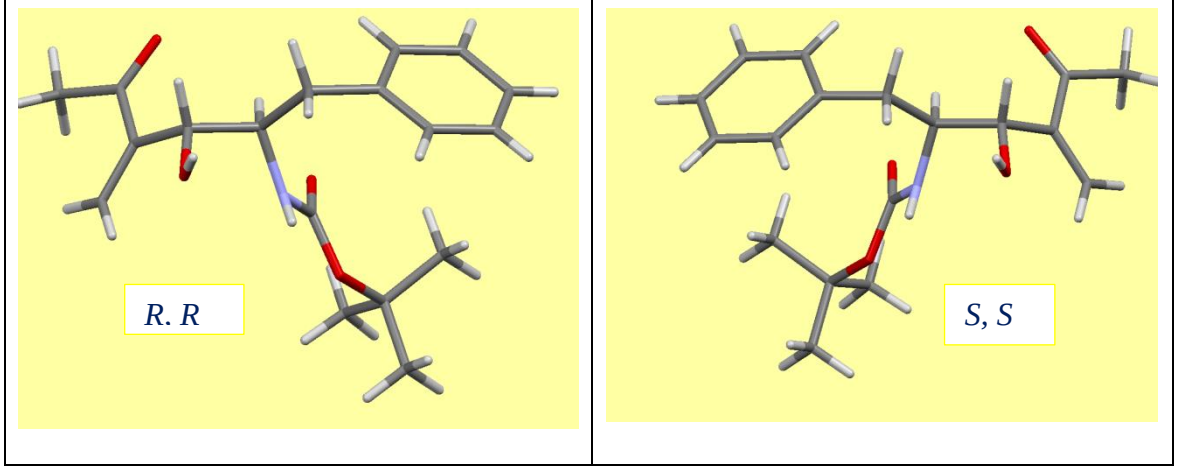

Figure 24: Crystal structure of **187** clearly showing the presence of enantiomers.

The fastest way to confirm if racemisation had taken place was to subject the available diastereomers to chiral HPLC chromatography. The use of chiral HPLC on diastereomer **181a** led to four poorly resolved peaks which was an indication that racemisation had indeed taken place (**Figure 25**).

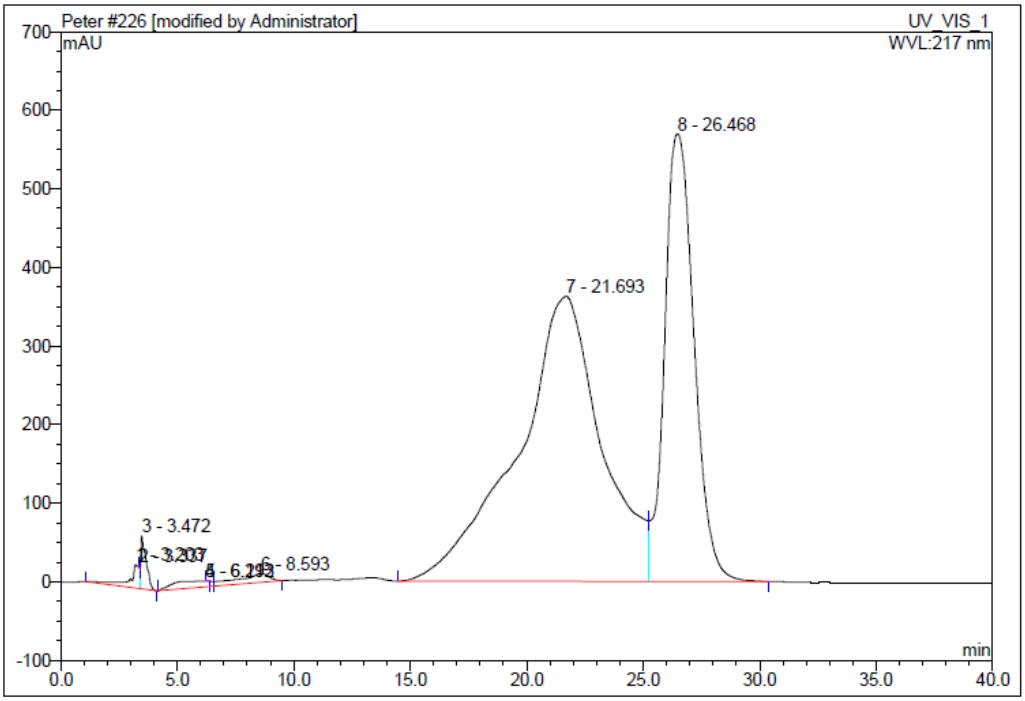

No.	Ret.Time min	Peak Name	Height mAU	Area mAU*min	Rel.Area %	Amount	Type
1	3.20	n.a.	29.553	15.614	0.65	n.a.	BM *
2	3.34	n.a.	0.614	0.053	0.00	n.a.	Rd
3	3.47	n.a.	67.516	17.844	0.74	n.a.	MB
4	6.19	n.a.	7.271	16.431	0.68	n.a.	BM *
5	6.21	n.a.	0.010	0.004	0.00	n.a.	Rd
6	8.59	n.a.	11.353	18.055	0.75	n.a.	MB*
7	21.69	n.a.	362.832	1508.250	62.49	n.a.	BM
8	26.47	n.a.	569.418	837.290	34.69	n.a.	MB
Total:			1048.566	2413.541	100.00	0.000	

Figure 25: Chiral HPLC chromatogram of the **181a** when the reaction was done at 0 °C.

The second diastereomer to investigate was **184**. Using the Chiralcel OJ column with a mobile phase of hexane and isopropanol at a flow rate of 1 mL/min afforded peaks of almost equal area at retention times 4.41, 12.95, 16.46 and 19.16 minutes (**Figure 26**). This observation therefore confirmed to us that racemisation had taken place when the MBHR was done under the reaction conditions used. The fact that racemisation of the compounds was occurring might also explain the strange results obtained when investigating the diastereoselectivity of the reactions.

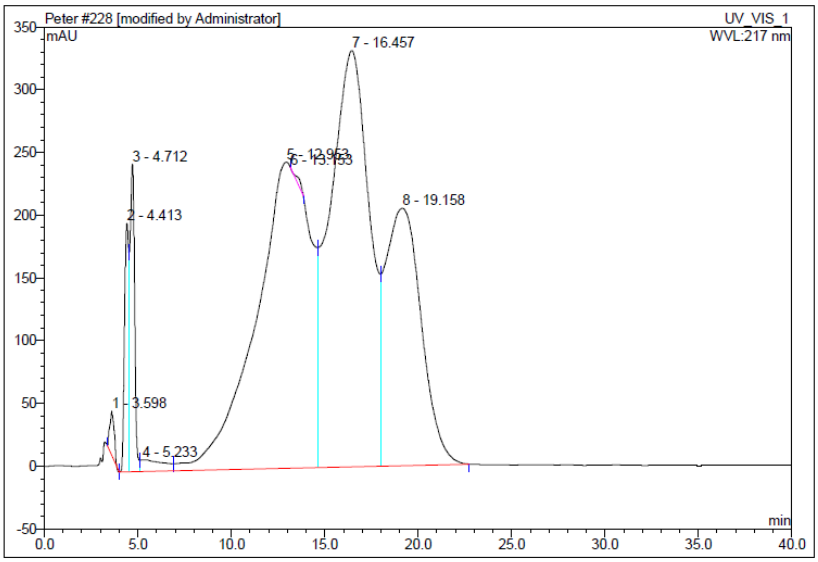

No.	Ret.Time min	Peak Name	Height mAU	Area mAU*min	Rel.Area %	Amount	Type
1	3.60	n.a.	35.151	9.557	0.43	n.a.	BMB*
2	4.41	n.a.	198.019	51.669	2.31	n.a.	BM *
3	4.71	n.a.	245.211	70.698	3.16	n.a.	M *
4	5.23	n.a.	9.100	13.170	0.59	n.a.	M *
5	12.95	n.a.	243.866	820.597	36.68	n.a.	M *
6	13.15	n.a.	-0.006	1.975	0.09	n.a.	Rd*
7	16.46	n.a.	331.611	811.434	36.27	n.a.	M *
8	19.16	n.a.	204.990	458.253	20.48	n.a.	MB*
Total:			1267.942	2237.353	100.00	0.000	

Figure 26: Chiral HPLC of **184** confirming that racemisation had taken place when the reaction was done at 0 °C.

The problem of racemisation that was confirmed by the crystal structures and the chiral HPLC chromatograms necessitated a literature search just to check if similar observations had been reported by other researchers. Apparently, reports exist in which methyl acrylate has been reacted with α-amino aldehydes in the presence of DABCO affording diastereomers without racemisation of the stereogenic center. In this first report by Manickum and Roos,[40] different electrophiles were reacted with methyl acrylate to generate diastereomeric MBH adducts. There was no reported racemisation when the *N*-dibenzyl (**188a - 188b**) and *N*-Boc aldehydes (**188c**) were used (**Scheme 55**). Interestingly, the reaction of *N*-Boc-L-alaninal **188c** with methyl acrylate that generated the *anti* and *syn* products **189c** and **190c**, respectively is similar to the reactions investigated in this thesis. These adducts relate well with adducts **183** and **184** as they are all derivatives of *N*-Boc protected aldehydes.

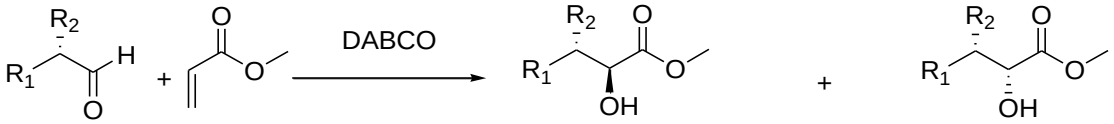

188 **189** **190**

a. R_1 = Me R_2 = $N(CH_2Ph)_2$

b. R_1 = CH_2Ph R_2 = $N(CH_2Ph)_2$

c. R_1 = Me R_2 = NH^tBoc

Scheme 55: Reported reaction of α-aminoaldehydes with methyl acrylate at room temperature. *Reagents and conditions*: DABCO as a catalyst at room temperature.

One would expect that electrophiles **188a** and **188b** have a proton attached to the stereogenic centre that is not as acidic as that of electrophile **188c**; therefore, it is more likely that **188c** could racemise under the applied conditions. In the second report by the same author,[41] (S)-tert-butyl (1-oxopropan-2-yl)carbamate **188c** reacted with methyl acrylate to generate diastereomers with an overall yield of 80% and diastereomeric excess of 48% in 7 days when 10 equivalents of DABCO was used. It is further reported that it took one day for the formation of diastereomers with an overall yield of 76% with diastereomeric excess of 42% when 100 equivalents of DABCO were used.

The only worry with these two reports is that chiral HPLC was never performed to confirm that indeed there was no racemisation. It would have also been more convincing to the scientific community if the author had obtained a crystal structures as all the doubts would have been cleared. It is with these facts that it is fully suspected there was racemisation, only that the author was unable to detect it.

The only convincing report where there was no racemization of aldehydes bearing acidic hydrogens is by Coelho.[123] This report clearly illustrated several α-amino aldehydes reacted under the influence of ultrasound to generate adducts without racemisation of the stereogenic centre. The author was able to demonstrate this using chiral HPLC, and a derivatisation method that indeed no racemisation took place for any of the electrophiles used including the adduct arising from the reaction between *N*-Boc-L-phenylalaninal **173** and methyl acrylate (**Scheme 56**). They reported that the *anti*-product was the major product, but unfortunately, they did not report their NMR data for this product, so it was impossible to use this for comparing with the data of **183** and **184** in this thesis. The use of compound **173** has also been reported as a starting material for the synthesis of 2-oxazolidine derivatives.[124]

The two reports have emphasized the use of an ultrasonic bath which was never applied in this thesis to confirm their findings.

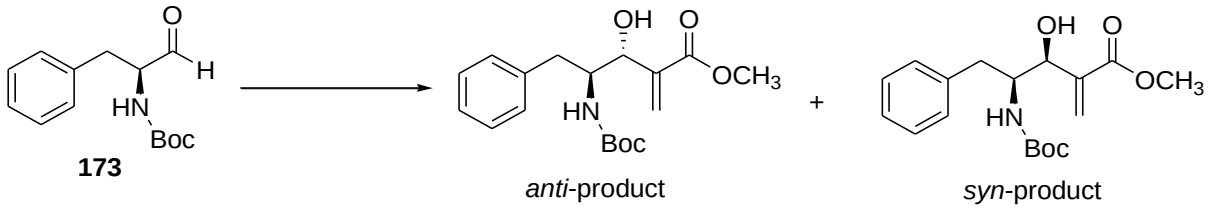

Scheme 56: Synthesis of diastereopure compound reported. *Reagents and conditions*: methyl acrylate, DABCO using ultra-sound apparatus.

3.1.4 Conclusion

The MBH reaction has been used to generate adducts **181 - 185** and **187** (**Figure 27**) from phenylalaninal in poor yields with the reactions taking many days. Unfortunately, it is impossible to use these adducts in further reactions because of the racemisation of the stereogenic centre of phenylalaninal. The racemisation might have occurred partly due to the methodology that was applied in the synthesis of these adducts. The use of an ultrasound radiation[123] instrument was not available and the use of *β*-isocupreidine to facilitate stereoselective reaction as reported in the literature was not convincing.[125]

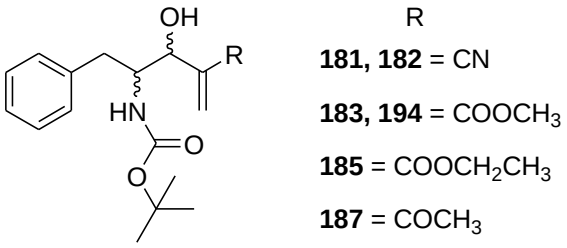

Figure 27: MBH adducts synthesized from phenylalaninal.

The only way to overcome the racemisation challenge was to adopt a completely different approach. For this second approach, we hypothesized that enzymes could be used to resolve MBH adduct **191** and then transform this enantiopure adduct to the compounds of interest (**Figure 28**). The crucial step in this transformation is the use of enzymes for resolving compound **191**. The investigation on the enzymatic resolution of **191** and other related MBH adducts is discussed in the next section.

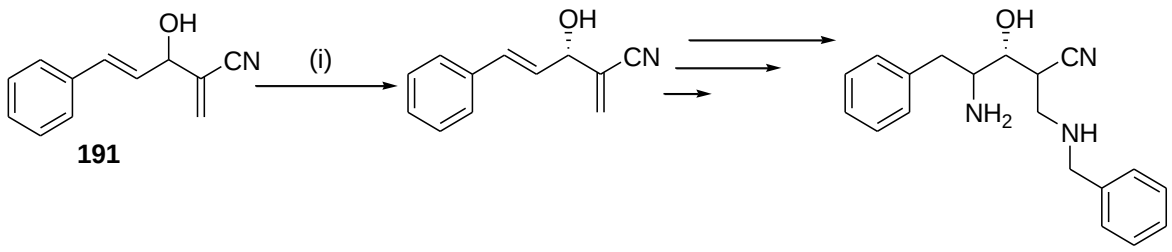

Figure 28: Proposed alternative route for the synthesis of the intended adducts. *Reagents and conditions*: (i) Enzymes, buffer at pH 7.00

3.2ENZYMATIC KINETIC RESOLUTION OF MORITA-BAYLIS HILLMAN ADDUCTS

3.2.1 Background information

As shown in the previous section, we proposed a new synthetic route that would make use of (±)-(*E*)-3-hydroxy-2-methylene-5-phenyl-4-pentenenitrile **191** as the starting material. In this proposed route, compound **191** would be resolved enzymatically to obtain an enantiopure alcohol which could then be subjected to several reactions. It was wise not just to resolve **191**, but to include other compounds as well, as there is other important information which can be obtained in cases where more substrates are included in the process of resolution. This information includes the effect of varying the chain length between the phenyl ring and the hydroxyl group, as well as increasing the flexibility between the phenyl ring and the hydroxyl group. The use of scaffolds similar to **191** was also wise so that this could create other avenues for our synthesis in the event that resolution of **191** proved difficult or impossible. For example, in addition to investigating the resolution of nitrile derivatives such as **191**, ester derivatives could be included as well. The rationale of the proposed approach is shown in **Scheme 57**.

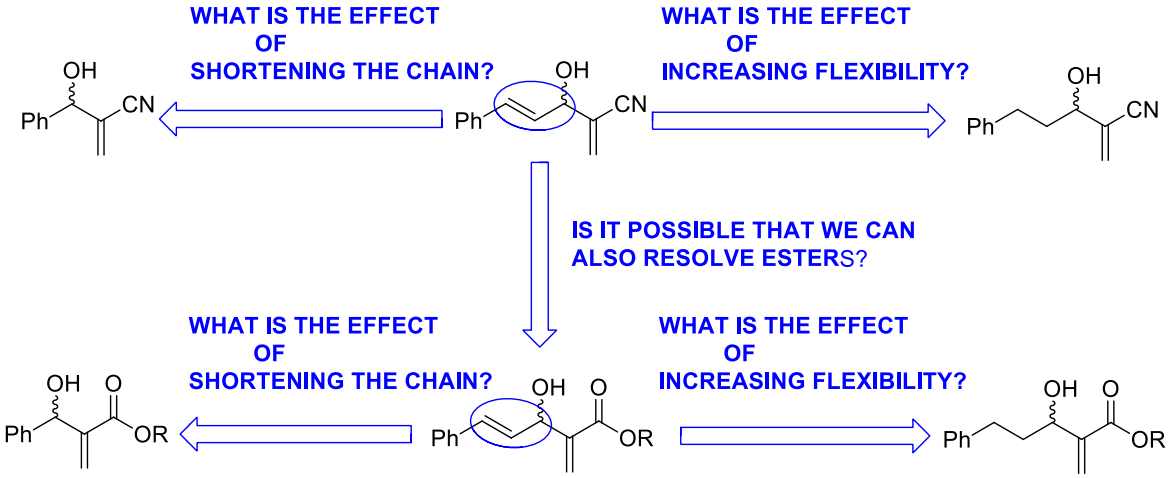

Scheme 57: The rationale for the choice of substrates in resolution experiments

It was therefore scientifically convincing to include other substrates in the resolution experiments. The substrates that were included were **75a**, **101a**, **102e** and **191 - 198** (**Figure 29**).

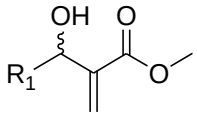

101a R_1 = Ph,

192 R_1 = 4-NO_2Ph

193 R_1 = PhCH=CH-

194 R_1 = $PhCH_2CH_2$-

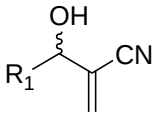

75a R_1 = Ph,

191 R_1 = PhCH=CH-

195 R_1= $PhCH_2CH_2$-

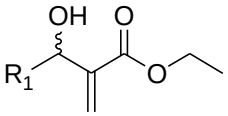

196 R_1 = Ph,

102e R_1 = PhCH=CH-,

197 R_1 = $PhCH_2CH_2$-

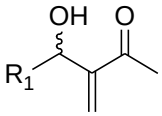

198 R_1 = PhCH=CH-

Figure 29: Proposed Morita-Baylis-Hillman alcohols to be resolved

It is very clear that scientific principles had been used to select a few compounds for use in enzymatic resolution. The next task was to think deeply about the way resolution would be achieved. In simple terms it was necessary to fully understand what enzymatic resolution means and how the process can be achieved in the laboratory.

3.2.2 Concept of enzymatic kinetic resolution

Resolution is the process of obtaining an enantiopure compounds from a racemate. In the event that this process involves the use of enzymes then it is referred to as enzymatic kinetic resolution. Use of enzymes for resolution is highly preferred as compared to other methods of resolution as enzymes are chemoselective, regioselective, and highly enantioselective.[126] In addition, they have high substrate specificity, high substrate tolerance and require mild conditions for a reaction to take place.[61, 127] There exist many types of enzymes, but resolution has mostly been reported to be achieved by lipases.[128, 129] The wide-spread use of lipases for resolution has been attributed to the fact that they are excellent biocatalysts, have wide substrate specificity with high regio- and enantioselectivity.[130] Furthermore, they catalyse a reaction without co-factors which makes it easier for use in organic synthesis.[131] Lipases are able to achieve resolution by selectively hydrolysing an ester bond or by forming an ester bond.[132, 133] The selective formation of an ester bond can be achieved by either esterification, transesterification or by reversible and irreversible acyl transfer.[134]

The most widely used method of resolution is by use of hydrolysis and esterification. These two methods that have been reported for resolving mandelic acid are shown in **Scheme 58**.[135]

Resolution by esterification is more challenging as compared to resolution by hydrolysis. This is because there are many variables to be investigated during esterification as compared to hydrolysis. These variables include the use of different solvents, acyl donor, temperature, enzyme and substrate loading. Hydrolysis is a straightforward method as you only need a buffer solution, and co-solvent. Regardless of the method you apply, you need to evaluate the performance of the enzyme.

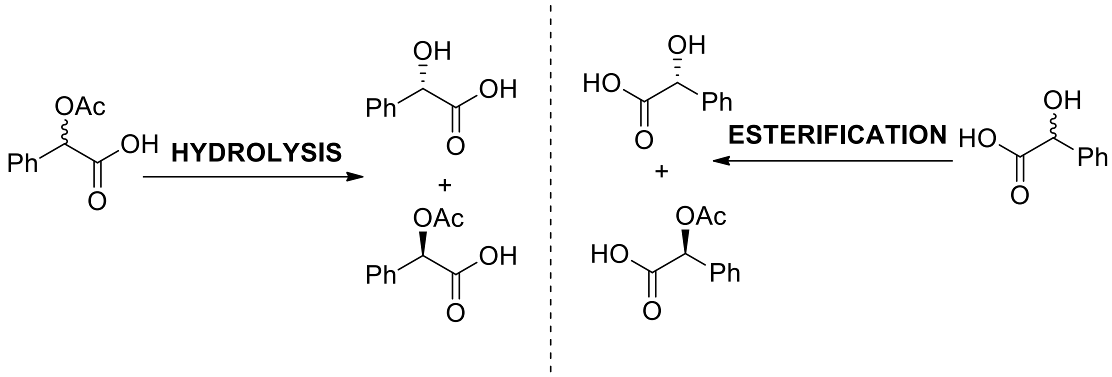

Scheme 58: Resolution of enantiomers by hydrolysis and esterification

The measure of an enzyme's performance during resolution is determined by mathematical parameters that have been documented.[136, 137] The parameters used during evaluation of an enzyme are enantiomeric excess of the product (ee_p), enantiomeric excess of the substrate (ee_s), percentage conversion (% conv) and enantiomeric ratio or selectivity factor (E). The enantiomeric ratio is a very important factor as it informs the researcher the overall selectivity of an enzyme. The fraction of conversion (C) is incorporated in the selectivity formula. All these parameters are mathematically expressed in equations **1**, **3** and **4**. As mentioned earlier, resolution reactions where the enatiomeric ratio is equal to or greater than 15 are practically viable.

$$ee = \%\,Major\ enantiomer - \%\,Minor\ enantiomer \ldots\ldots\ldots\ldots\ldots\ldots\ldots\ldots\ldots\ldots\ldots\ldots\ldots\ldots.\,(\mathbf{1})$$

$$\%\ \text{Conversion} = \frac{\text{ee}_s}{(ee_s + ee_p)} \times 100 \qquad \ldots\ldots\ldots\ldots\ldots\ldots\ldots\ldots\ldots\ldots\ldots\ldots\ldots\ldots\ldots\ldots\ldots\ldots\ldots\,(\mathbf{3})$$

$$\text{E} = \frac{\text{Ln}[1 - \text{c}(1 + ee_p)]}{\text{Ln}[1 - \text{c}(1 - ee_p)]};\ \ \text{or E} = \frac{\text{Ln}[(1 - \text{c})(1 + ee_s)]}{\text{Ln}[(1 - \text{c})(1 + ee_s)]} \ldots\ldots\ldots\ldots\ldots\ldots\ldots\ldots\ldots\ldots\ldots\ \ldots.\,(\mathbf{4})$$

Having thoroughly analysed the different methods of enzymatic resolution, it was now clear which of the resolution techniques could be investigated on different MBH adducts. It was obvious that MBH alcohols, MBH acetates and MBH esters were required for investigating resolution by hydrolysis, and esterification. The MBH adduct derivatives **105a** and **199** - **204** that were required for investigation are shown in **Figure 30**, while the carboxylic acids **103e**, **205** – **206** to be prepared as standards to assist in reaction monitoring are shown in **Figure 31**.

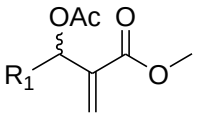

199 R_1 = 4-NO_2Ph

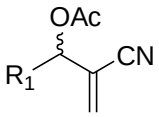

105a R_1 = Ph,

200 R_1 = PhCH=CH-

201 R_1 = $PhCH_2CH_2$-

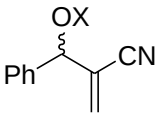

202 X = $COCH_2Cl$

203 X = $COCH_2CH_2CH_3$

204 X = $COCH_2CH(CH_3)_2$

Figure 30: MBH derivatives planned for synthesis for the enzymatic resolution investigation.

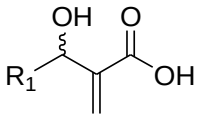

205 R_1 = Ph,

103e R_1= PhCH=CH-

206 R_1= $PhCH_2CH_2$-

Figure 31: Planned MBH carboxylic acid derivatives required as standards.

It was now time to start the synthesis of the proposed compounds from **Figures 29**, **30** and **31**. These investigations began with the synthesis of MBH alcohols for investigating enzymatic resolution by esterification.

3.2.3 Synthesis of Morita-Baylis Hillman (MBHA) alcohols

The Morita-Baylis Hillman alcohols shown in **Table 18** were synthesized by reacting an aldehyde with the corresponding activated alkene in the presence of 1,4-diazabicyclo [2.2.2] octane (DABCO) (**Scheme 59**). In situations where *trans*-cinnamaldehyde was used, phenol was added to accelerate the reaction.[138]

Scheme 59: Preparation of Morita-Baylis-Hillman alcohols. *Reagents and conditions*: DABCO, 0 °C - RT:

Table 18 shows the different electrophiles (RCHO), activated alkenes with different electron withdrawing groups (EWG), time taken for the reaction to take place and the isolated yield of each compound. The activated alkenes used were methyl acrylate, acrylonitrile, methyl vinyl ketone, and ethyl acrylate. The reaction times varied from hours to days affording colourless oils in yields ranging from 30% to 95%.

Table 18: The Morita-Baylis-Hillman reactions of various aldehydes and activated alkenes

Entry	R	EWG	Time in hours (h)	Yield (%)
1	Ph	CO_2CH_3	72	**101a**, 74
2	4-NO_2Ph	CO_2CH_3	4	**192**, 84
3	PhCH=CH	CO_2CH_3	48	**193**, 72
4	$PhCH_2CH_2$	CO_2CH_3	192	**194**, 64
5	Ph	CN	19	**75a**, 95
6	PhCH=CH	CN	24	**191**, 80
7	$PhCH_2CH_2$	CN	144	**195**, 65
8	Ph	$CO_2CH_2CH_3$	144	**196**, 77
9	PhCH=CH	$CO_2CH_2CH_3$	48	**102e**, 72
10	$PhCH_2CH_2$	$CO_2CH_2CH_3$	144	**197**, 77
11	PhCH=CH	$COCH_3$	216	**198**, 31

The synthesized adducts were characterized using IR, ^{1}H NMR, and ^{13}C NMR spectroscopy. The diagnostic peaks of methyl acrylate derivatives **101a** and **192 - 194** are shown **Table 19**. The characteristic hydroxyl group and carbonyl functional group of the methyl acrylate derivatives were observed in the IR spectra. It is evident from the table that all the four compounds had the aromatic protons which were the most deshielded signals. The formation of these adducts was confirmed by the appearance of key signals in ^{1}H and ^{13}C NMR spectra. The appearance of ^{1}H signals for H-3, H-8 and OH for **101a** and **192**; H-3, H-10 and OH for **193** and **194** supported these observations (**Figure 32**). The vinylic protons of **101a**, **192** and **194** appeared as singlets confirming that there was no observed geminal coupling in ^{1}H NMR spectrum. The vinylic protons of **193** appeared as two multiplets confirming that there

was observed long range coupling of these protons with H-3 in addition to the geminal coupling. Furthermore, the presence of ^{13}C signals for C-2, C-3 and C-8 for **101a** and **192**; C-2, C-3 and C-10 for **193** and **194** endorsed the formation of these adducts. The key signals are shown in bold in **Table 19**. The accurate assignment of the vinyl carbon signal **C-8** for **101a** and **192**; C-10 for **193** and **194** were observed as negative signals in the sp^2 region in the spectrum of the DEPT experiment. The synthesis of **101a**, **193**, **194** has been reported to be achived using chemical means whereas synthesis of **192** has been reported to be achieved using greener means.[139]

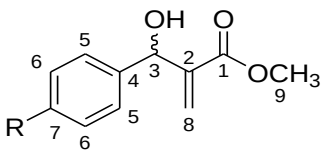

101a R = H

192 R = NO_2

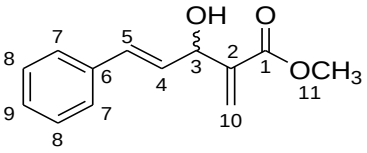

193

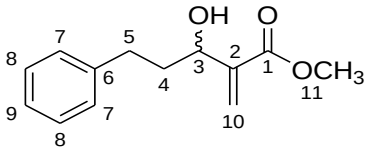

194

Figure 32: Methyl acrylate derivatives of MBH alcohols

Table 19: IR, ^1H and ^{13}C NMR data of methyl acrylate derivative of MBH alcohols

Compound	**IR (cm^{-1}); functional group**	**^1H (δ) and ^{13}C(δ)**	**Reference**
101a	3338 (OH), 1708 (C=O).	7.29 – 7.23 (m, Ar-2H), 7.22 – 7.08 (m, Ar-3H), **6.20 (1H, s, H-8a), 5.85 (s, H-8b), 5.45 (d, *J* = 4.8 Hz, H-3), 4.23 (1H, d, *J* = 5.0 Hz, OH)**, 3.41 (s, H-9). 166.5 (C-1), 142.7 (C-4), **141.8 (C-2)**, 128.3 (C-5 or C-6), 127.6 (C-7), 126.9 (C-5 or C-6), **125.1 (C-8), 72.3 (C-3),** 51.6 (C-9).	140
192	3508 (OH), 1695 (C=O).	8.20 (d, *J* = 8.6 Hz, H-6), 7.57 (d, *J* = 8.9 Hz, H-5), **6.40 (s, H-8a), 5.88 (s, H-**	141

Compound	IR (cm^{-1}); functional group	^{1}H (δ) and ^{13}C(δ)	Reference
		8b), 5.63 (d, *J* = 6.2 Hz, H-3), 3.75 (s, H-9), **3.35 (d, *J* = 6.2 Hz, OH)**. 166.4 (C-1), 148.6 (C-7), 147.5 (C-4), **141.0 (C-2)**, 127.4 (C-6), **127.2 (C-8),** 123.6 (C-5), **72.8 (C-3),** 52.2 (C-9).	
193	3256 (OH), 1715 (C=O).	7.37 (d, *J* = 7.6 Hz, H-7), 7.29 (t, *J* = 7.5 Hz, H-8), 7.22 (t, *J* = 7.2 Hz, H-9), 6.65 (d, *J* = 15 Hz, H-5), **6.32-6.24 (m, H-4 and H-10a), 5.91 (s, H-10b), 5.15 – 5.10 (m, H-3),** 3.77 (s, H-11), **3.16 (d, *J* = 5.8 Hz, OH).** 166.7 (C-1), 141.3 (C-6), **136.5 (C-2),** 131.4 (C-5), 129.3 (C-9), 128.5 (C-7 or C-8), 127.8 (C-4), 127.0 (C-7 or C-8), **125.8 (C-10), 71.9 (C-3)**, 52.0 (C-11).	18, 142
194	3434 (OH), 1711 (C=O).	7.30 – 7.22 (m, Ar-2H), 7.21 – 7.12 (m, Ar-3H), **6.22 (s, H-10a), 5.80 (s, H-10b), 4.47 – 4.37 (m, H-3)**, 3.73 (s, H-1), **2.95 (d, *J* = 6.5 Hz, OH),** 2.86 – 2.61 (m, H-5), 2.03 – 1.82 (m, H-4). 167.0 (C-1), 142.3 (C-6), **141.6 (C-2),** 128.5 (C-9), 128.4 (C-7 or C-8), 125.9 (C-7 or C-8), **125.2 (C-10), 70.8 (C-3)**, 51.9 (C-11), 37.7 (C-4), 32.0 (C-5).	142

The next group of compounds to characterize were the acrylonitrile derivatives of MBH alcohols shown in **Figure 33**. The IR characteristic peaks, ^{1}H, and ^{13}C NMR signals of **75a**, **191** and **195** are shown in **Table 20**. The characteristic hydroxyl group and nitrile functional group of the acrylonitrile derivatives were observed in the IR spectrum. It is evident from the table that all three compounds had the aromatic protons as the most deshielded signals.

The appearance of ^{1}H signals for H-3, H-8 and OH for **75a**; H-3, H-10 and OH for **191** and **195** supported the formation of these adducts. The appearance of a doublet for H-8a with a coupling constant of 1.5 Hz and the second doublet for H-8b with a coupling constant of 1.2 Hz for adduct **75a** confirmed geminal coupling between the two protons. The vinylic protons for **191** and **195** appeared as mutliplets indicating that there was geminal coupling between H-10a and H-10b and long range coupling with H-3. The presence of ^{13}C NMR signals for C-2, C-3 and C-8 for **75a**; C-2, C-3 and C-10 for **191** and **195** confirmed the formation of these adducts. These key signals are shown in bold in **Table 20**. The appearance of negative carbon signal in the sp^2 region of a DEPT 135 spectrum confirmed the presence of vinyl carbon C-8 for **75a**; and C-10 for **191** and **195**.

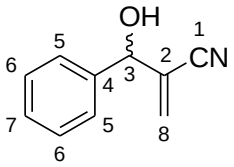

75a

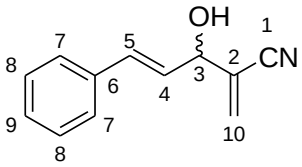

191

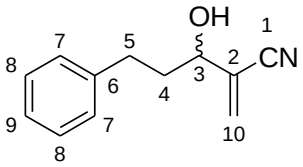

195

Figure 33: Acrylonitrile derivatives of MBH alcohols

Table 20: IR, ^{1}H and ^{13}C NMR data of acrylonitrile derivatives of MBH alcohols

Compound	**IR (cm^{-1}); functional group**	**^{1}H (δ) and ^{13}C(δ)**	**Reference**
75a	3421 (OH), 2229 (C≡N).	7.41 – 7.34 (m, Ar-H), **6.09 (d, *J* = 1.5 Hz, H-8a), 6.01 (d, *J* = 1.2 Hz, H-8b), 5.28 – 5.26 (m, H-3), 2.69 (br s, OH).** 139.2 (C-4), **130.3 (C-8),** 128.7 (C-5 or C-6), 128.6 (C-7), 126.5 (C-5 or C-6), **126.0 (C-2),** 117.0 (C-1), **73.7 (C-3).**	143
191	3421 (OH), 2228 (C≡N),	7.43 – 7.23 (m, Ar-H), 6.73 (d, *J* = 15.8 Hz, H-5), 6.19 (dd, *J* = 15.9, 6.9 Hz, H-4), **6.11 – 6.07 (m, H-10a), 6.04 – 5.99 (m, H-10b), 4.90 (d, *J* = 6.7 Hz, H-3), 2.52 (br s, OH)**.	144

		135.6 (C-6), 133.8 (C-5), **130.1 (C-10),** 128.7 (C-7 or C-8), 128.5 (C-9), 126.9 (C-7 or C-8), 126.6 (C-4), **125.5 (C-2),** 117.0 (C-1), **72.9 (C-3).**	
195	3420 (OH), 2227 (C≡N).	7.30 – 7.22 (m, Ar-H), 7.20 – 7.13 (m, Ar-H), **5.95 – 5.89 (m, H-10a and H-10b), 4.21 – 4.12 (m, H-3), 3.21 (d, *J* = 4.4 Hz, OH),** 2.79 – 2.59 (m, H-5), 2.06 – 1.85 (m, H-4). 140.8 (C-6), **130.4 (C-10),** 128.5 (C-7 or C-8), 128.4 (C-7 or C-8), **126.6 (C-2),** 126.1 (C-9), 117.1 (C-1), **71.3 (C-3),** 37.0 (C-4), 31.2 (C-5).	[145]

The next group of MBH alcohols to characterize were the ethyl acrylate derivatives (**Figure 34)**. The IR characteristic peaks, ^{1}H, and ^{13}C NMR signals of the three adducts are shown in **Table 21**. The characteristic hydroxyl group and carbonyl functional group of the ethyl acrylate derivatives were observed in the IR spectrum. The aromatic protons of the three ethyl acrylate derivatives were the most deshielded protons as observed in **Table 21**. The appearance of ^{1}H signals for H-3, H-8 and OH for **196**; H-3, H-10 and OH for **102e** and **197** supported the formation of these adducts. The presence of two singlets for H-8a and H-8b in adduct **196** confirmed that there was no geminal coupling observed between these protons. The observed mutliplets for H-10a and H-10b in adducts **102e** and **197** confirmed that the two protons experienced geminal coupling with each other and long range coupling with H-3. The presence of C-8 for **196**; and C-10 for **102e** and **197** was confirmed by the presence of negative carbon signals in the alkene region of the DEPT 135 spectrum. The presence of ^{13}C signals for C-2, C-3 and C-8 for **196**; C-2, C-3 and C-10 for **102e** and **197** supported the formation of these adducts.

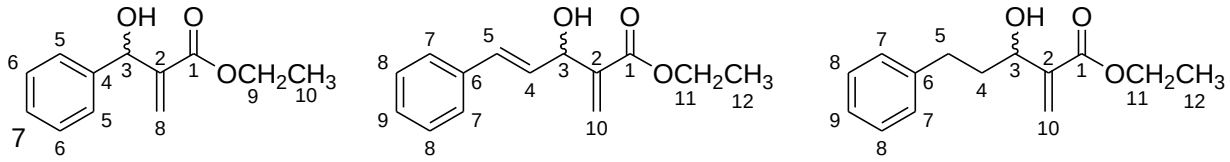

196 **102e** **197**

Figure 34: Ethyl acrylate derivatives of MBH alcohols

Table 21: IR, ^{1}H and ^{13}C NMR data of ethyl acrylate derivative of MBH alcohols

Compound	**IR (cm^{-1}); functional group**	**^{1}H (δ) and ^{13}C(δ)**	**Reference**
196	3432 (OH), 1702 (C=O)	7.35 - 7.18 (Ar-H), **6.28 (s, H-8a), 5.82 (s, H-8b), 5.48 (d, *J* = 5.2 Hz, H-3)**, 4.07 (q, *J* = 6.5 Hz, H-9), **3.68 – 3.48 (m, OH),** 1.16 (t, *J* = 7.1 Hz, H-10). 166.2 (C-1), 142.5 (C-4), **141.6 (C-2),** 128.3 (C-5 or C-6), 127.7 (C-5 or C-6), 126.7 (C-7), **125.4 (C-8), 72.8 (C-3),** 60.81 (C-9), 14.0 (C-10).	146
102e	3422 (OH), 1701 (C=O).	7.42 – 7.18 (m, Ar-H), 6.66 (d, *J* = 16.0 Hz, H-5), **6.34 – 6.24 (m, H-4 and H-10a), 5.90 (s, H-10b)**, **5.17 – 5.09 (m, H-3),** 4.24 (q, *J* = 7.1 Hz, H-11), **3.09 (d, *J* = 5.2 Hz, OH)**, 1.31 (t, *J* = 7.1 Hz, H-12). 166.4 (C-1), 141.6 (C-6), **136.5 (C-2)** 131.41 (C-5), 129.4 (C-9), 128.6 (C-7 or C-8), 127.8 (C-4), 126.6 (C-7 or C-8**), 125.6 (C-10), 72.12 (C-3)**, 61.0 (C-11), 14.2 (C-12).	147

Compound	**IR (cm^{-1}); functional group**	**^{1}H (δ) and ^{13}C(δ)**	**Reference**
197	3398 (OH), 1701 (C=O)	δ 7.30 – 7.10 (m, Ar-H), **6.25 – 6.19 (m, H-10a), 5.84 – 5.75 (m, H-10b)**, **4.50 – 4.38 (m, H-3),** 4.17 (q, *J* = 7.1 Hz, H-11**), 3.32 – 3.18 (m, OH),** 2.90 – 2.58 (m, H-5), 2.06 – 1.80 (m, H-4), 1.24 (t, *J* = 7.1 Hz, H-12). 166.5 (C-1), 143.0 (C-6), **141.8 (C-2),** 128.4 (C-9), 128.3 (C-7 or C-8), 125.8 (C-7 or C-8), **124.7 (C-10), 70.5 (C-3),** 60.8 (C-11), 37.9 (C-4), 32.0 (C-5), 14.1 (C-12)	[148]

The last compound to characterize was the methyl vinyl ketone derivative **198**. The IR peaks observed at 3471 and 1709 cm^{-1} were for the hydroxyl group and carbonyl functional group, respectively. The five aromatic protons were evident from the presence of the most deshielded multiplet at δ 7.38 – 7.16 while the key characteristic ^{1}H signals were represented by the three multiplets at δ 6.13 – 6.08 for the two H-11 protons, 5.22 – 5.12 ppm for stereogenic centre proton H-4 and 3.56 – 3.36 ppm for the OH group. The observed splitting pattern shows that both H-1l protons experience geminal coupling and long range coupling with H-4. Similarly, H-4 also experiences long range coupling with the H-11 protons and vicinal coupling with H-5.

The ^{13}C NMR spectrum supported the structure by showing a total of 11 carbon signals with the characteristic carbon C-3, C-11 and C-4 appearing at a chemical shift value of 136.6, 130.9 and 71.2 ppm, respectively. The accurate assignment of carbon signal C-4 was confirmed by the presence of negative carbon signals in the alkene range on the DEPT experiment spectrum. The spectroscopic data of **198** was in agreement with the reported data in literature.[149] Unfortunately, **198** was very unstable and therefore it was only subjected to a few reactions.

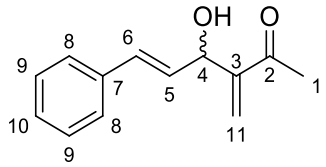

198

3.2.4 Synthesis of Morita-Baylis Hillman adduct (MBHA) acetates

The next group of compounds to be synthesized were the acetates as they were required for investigating enzymatic resolution by hydrolysis. The synthesis of acetates was achieved by the reaction of the corresponding alcohol with acetic anhydride or acyl chloride in the presence of a base (**Scheme 60**). At this particular point, only four compounds were acetylated to enable the investigations to start.

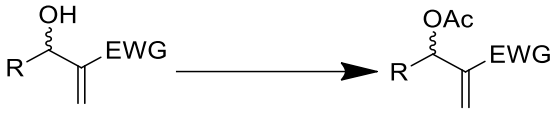

Scheme 60: Preparation of Morita-Baylis-Hillman acetates. *Reagents and conditions*: Et_3N, Ac_2O, DMAP, CH_2Cl_2, 0°C or Et_3N, AcCl, THF, 0 °C.

The first reaction to attempt was the acetylation of **192**. This reaction led to an unexpected colourless oil **207** in 96% yield when the reaction was left for two hours. The ^{1}H NMR spectrum of the unexpected product contained a total of 13 protons that were in 6 different chemical environments. The *ortho*-coupled benzene protons H-5 and H-6 were observed at δ 8.28 and δ 7.55 while the methoxy protons appeared at δ 3.88. The expected stereogenic centre proton H-3 and vinyl proton signals were absent from the ^{1}H NMR spectrum but instead three signals were observed. The three signals appeared as three singlets, two signals integrating for one proton and one signal integrating for three protons. The first alkene singlet appeared at δ 7.97, the second signal for methylene protons attached to oxygenated carbon appeared at δ 4.91 and the last signal for three protons appearing at δ 2.10.

The ^{13}C NMR spectrum showed a total of 11 signals that represented 11 carbons in different chemical environments. The observed three positive CH signals in the alkene region of the DEPT 135 spectrum confirmed the presence of two aromatic carbons and one alkene carbon bearing one proton as observed in the ^{1}H NMR spectrum. The absence of an alkene carbon bearing two protons ruled out the presence of the usual CH_2 vinyl protons. Furthermore, the

presence of one negative CH_2 signal for oxygenated carbon in the DEPT 135 spectrum suggested there was no stereogenic carbon bearing one proton. The last positive signals in the DEPT 135 spectrum for oxygenated CH_3 and and saturated CH_3 for the methoxyl and methyl group was supported by the three methoxy and three methyl protons observed in the ^{1}H NMR spectrum.

The presence of two carbonyl functional groups was evidenced by the peaks appearing at 1739 and 1715 cm^{-1} in the IR spectrum. By combining information from ^{1}H NMR, ^{13}C NMR data, DEPT 135 experimental data and IR information led to the proposed structure **207** whose molecular formula was confirmed to be $C_{13}H_{13}NO_6$. The unexpected product is formed when the oxygen atom of the acetoxy group participates in an allylic substitution reaction on **199**.

A repeat of the reaction with a short reaction time of thirty minutes afforded acylated adduct **199** as a yellow solid with a melting point range between 88 – 89 °C.

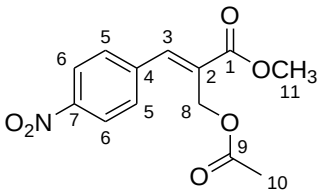

207

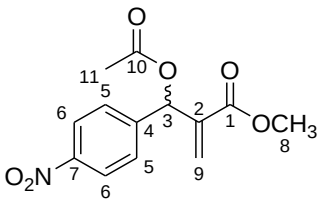

199

The ^{1}H NMR spectrum of **199** showed a total of thirteen protons of which four were aromatic protons that were *ortho* coupled to each other with a coupling constant of 8.8 Hertz. The two vinyl protons appeared as two singlets at δ 6.72 and δ 6.47. The appearance pf the two singlets indicates that geminal coupling was not observed in the ^{1}H NMR spectrum. The stereogenic centre proton H-3 and the methoxy protons were observed as singlets at δ 5.98 δ 3.72 respectively. The new methyl protons that were most shielded appeared at δ 2.14.

The ^{13}C NMR spectrum showed a total of eleven carbon signals of which two of them emerged after performing the acetylation reaction. The two new carbon signals appeared at δ 169.1 for C-10 and 21.0 ppm for C-11 confirming that acetylation had taken place. The IR data supported this by showing two carbonyl functional groups at 1736 cm^{-1} and 1713 cm^{-1}.

The obtained spectroscopic data obtained for **199** was in agreement with reported literature data.[95]

The second sets of acetates to be synthesized were the three acrylonitrile derivatives shown in **Figure 35**.

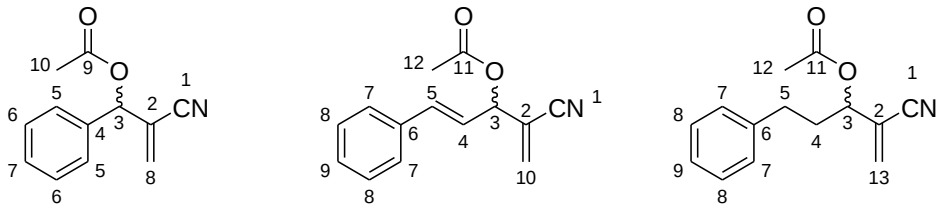

Figure 35: Acetates of acrylonitrile derivatives of MBH alcohols

All the acetates in **Figure 35** were isolated as colourless oils with a yield ranging from 82 to 91%. The structures of the acetates were confirmed using IR, ^{1}H, ^{13}C NMR spectroscopy and mass spectrometer data (**Table 22**). The IR spectrum of each acetate confirmed the presence of a nitrile and a carbonyl functional group. The ^{1}H and ^{13}C NMR spectra confirmed the number of protons and carbon atoms in different chemical environments, as expected. The acetate group was confirmed by the presence of the most shielded methyl protons and carbon signal and the most deshielded carbonyl group for each compound. These are highlighted in the table. The vinyl proton of all the three acetates in **Table 22** appeared as a multiplet because of geminal coupling with the other vinyl proton and and long range coupling with the stereogenic centre proton. The calculated mass of each compound corresponded well with the found mass. The supporting data obtained for **105a** was similar to the literature reported data.[101, 150]

Table 22: IR, ^{1}H, ^{13}C and MS data of acrylonitrile acetate derivatives

Compound	**IR (cm^{-1}); functional group**	**^{1}H (δ) and ^{13}C(δ)**	**HRMS**
105a	2229 (C≡N), 1745 (C=O).	7.41 – 7.32 (m, Ar-5H), 6.33 – 6.31 (m, H-3), 6.03 – 6.00 (m, H-8a), 5.98 – 5.96 (m, H-8b), **2.13 (s, H-10).**	Calculated for $C_{12}H_{11}NO_2Na$: 224.0687,

		169.2 (C-9), 135.7 (C-4), 132.0 (C-8), 129.2 (C-7), 128.9 (C-5 or C-6), 126.9 (C-5 or C-6), 123.2 (C-2), 116.2 (C-1), 74.3 (C-3), **20.8 (C-10).**	found: $[M+Na^+]$, 224.0681.
201	2227 (C≡N), 1742 (C=O).	7.31 – 7.12 (m, Ar-5H), 6.01 – 5.99 (m, H-10a), 5.94 – 5.92 (m, H-10b), 5.30 – 5.21 (m, H-3), 2.65 (t, *J* = 7.8 Hz, H-5), 2.23 – 1.96 (m, H-4) overlapping **2.06 (3H, s, H-12).** **169.7 (C-11),** 140.1 (C-6), 132.9 (C-10), 128.6 (C-7 or C-8), 128.3 (C-7 or C-8), 126.3, (C-9) 122.5 (C-2), 116.1 (C-1), 72.6 (C-3), 34.4 (C-4), 31.1 (C-5), **20.8 (C-12).**	Calculated for $C_{14}H_{15}NO_2Na$: 252.1000, found: $[M+Na^+]$, 252.0985.
200	2228 (C≡N), 1741 (C=O).	7.43 – 7.24 (m, Ar-H), 6.76 (d, *J* = 15.9 Hz, H-5), 6.17 (dd, *J* = 15.9, 7.3 Hz, H-4), 6.08 – 6.04 (m, H-10a and H-10b), 5.96 – 5.91 (m, H-3), **2.14 (s, H-12).** **169.3 (C-11),** 135.7 (C-5), 135.3 (C-6), 132.2 (C-10), 128.8 (C-9), 128.7 (C-7 or C-8), 126.9 (C-7 or C-8), 122.5 (C-4), 122.3 (C-2), 116.2 (C-1), 73.4 (C-3), **21.0 (C-12).**	Calculated for $C_{14}H_{13}NO_2Na$: 250.0844, found: $[M+Na^+]$, 250.0824.

3.2.5 Synthesis of Morita-Baylis Hillman adducts (MBHA) nitrile containing esters

Apart from investigating resolution of the acetates of nitrile derivatives, one could also resolve compounds with ester groups originating from other carboxylic acids of varying chain lengths. This set of compounds would help in understanding the enzyme activity when the acetate is substituted with a group with a longer chain. For the purpose of this investigation, only the simplest MBH alcohol 2-[(hydroxyphenyl)methyl)]acrylonitrile **75a** was used for the synthesis of the longer chain esters.

The synthesis of these esters was achieved by coupling the different acids with **75a** in dichloromethane using *N*′,*N*-dicyclohexylcarbodiimide (DCC) and DMAP (**Scheme 61**). The synthesised compound **202 - 204** whose protons and carbons are numbered are shown in **Figure 36**.

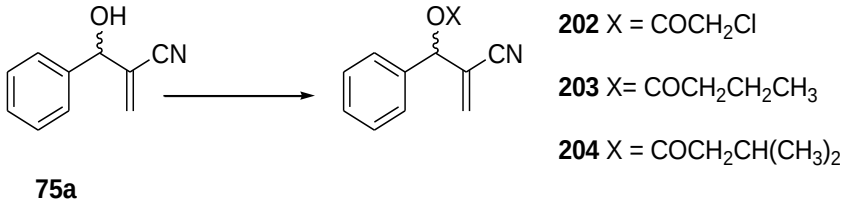

75a

Scheme 61: Coupling of **75a** with different carboxylic acids. *Reagents and conditions*: DCC, $ClCH_2COOH$ or $CH_3CH_2CH_2COOH$ or $(CH_3)_2CHCH_2COOH$, DMAP in CH_2Cl_2 at room temperature.

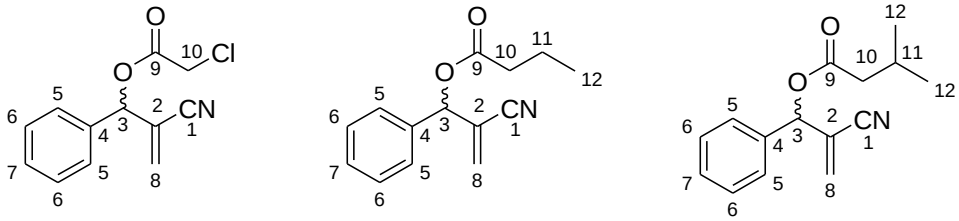

Figure 36: Longer chain esters of acrylonitrile derivatives

The first compound to be synthesized in this group was **202**, which was isolated as a colourless oil in a yield of 41%. The ^{1}H NMR spectrum of this compound showed five sets of protons that were in different chemical environments. The most deshielded were the aromatic protons which appeared as a multiplet at δ 7.43 – 7.37 followed by the stereogenic centre proton H-3 which also appeared as a multiplet at δ 6.38 – 6.36. The long range coupling of H-3 with the two vinylic protons H-8 led to the observed multiplet for H-3. The vinyl proton H-8a appeared as a doublet at δ 6.09 with a geminal coupling constant of 0.9 Hz with H-8b while proton H-8b also appeared as a doublet at δ 6.05 with geminal coupling constant of 1.3 Hz with H-8a. The remaining protons H-10 appeared as doublet at δ 4.1 with a coupling constant of 2.2 Hz. This implies that H-10a and H-10b protons are in different chemical environments and hence couple with each other.

The proposed structure of **202** was supported by the ^{13}C NMR spectrum. This spectrum showed a total of ten chemically non-equivalent carbon atoms of which two originated from the chloroacetate. These two carbons of the chloroacetate chain appeared at δ 165.8 for C-9 and 40.7 for C-10. The disappearance of four signals in the aromatic region and nitrile region on DEPT 135 spectrum led to the assignment of C-1, C-2, C-4 and C-9. In addition, C-3 appeared as a positive CH attached to oxygen carbon while C-8 appeared as a negative alkene CH_2 in the spectrum of the DEPT experiment. The peaks at 2230 and 1747 cm^{-1} in the IR spectrum supported the presence of the nitrile and carbonyl group functional groups of **202**. The HRMS showed the presence of an $[M+Na^+]$ ion peak at 258.0282 which corresponded well with the molecular formula $C_{12}H_{10}ClNO_2Na$.

The second compound to be synthesized was **203**, which was isolated as a colourless oil in a yield of 48%. The ^1H NMR spectrum showed a total of seven chemically non-equivalent protons, as expected. The presence of butanoate protons indeed confirmed to us that the reaction had taken place. This was confirmed by the presence of H-10 which appeared as a triplet of a doublets at δ 2.41 with a coupling constant of 7.4 and 1.9 Hz. This explained to us that two H-10 protons were chemically non-equivalent and therefore they are coupling with each other and coupling with H-11. The appearance of a sextet at δ 1.70 with a coupling constant of 7.4 Hz corresponded well with H-11 and the most shielded protons H-12 appeared at δ 0.95 as a triplet with a coupling constant of 7.4 Hz.

The ^1H NMR information was supported by the ^{13}C NMR spectrum. A total of twelve chemically non-equivalent carbon signals were observed, four of which were from the butanoate chain. The butanoate carbon signals appeared at δ 171.2 for C-9, 36.1 for C-10, 18.3 for C-11 and 13.6 for C-12. The presence of the peaks at 2229 and 1744 cm^{-1} in the IR spectrum supported the presence of C≡N and C=O functional groups. A peak at *m/z* 230.1112 attributed to the $[M+H^+]$ ion corresponded well with the observed molecular formula $C_{14}H_{16}NO_2$, of **203**.

The last compound to be synthesized in this series was **204** which was isolated as a colourless oil in 72% yield. The expected seven sets of chemically non-equivalent protons were observed with three sets representing the isovalerate ester chain. The isovalerate ester was confirmed by the presence of a multiplet at δ 2.40 – 2.24 for H-10, nonet at δ 2.15 with

a coupling constant of 6.9 Hz for H-11 and a doublet at δ 0.96 with a coupling constant of 6.6 Hz for H-12.

The ^{13}C NMR spectrum showed a total of twelve carbons that were chemically non-equivalent. The isovalerate ester carbon signals were observed at δ 171.3, 43.2, 25.7 and 22.4 for C-9, C-10, C-11 and C-12, respectively. The appearance of peaks at 2214 cm^{-1} and 1704 cm^{-1} in the IR spectrum confirmed the presence of nitrile and carbonyl functional groups. The mass spectrum corresponded well with the expected mass of **204** (calculated for $C_{15}H_{17}NO_2Na$: 266.1151, found: $[M+Na^+]$ 266.1144). The synthesis of **204** reported in literature was achieved using lithium selenolates as a nucleophile.[151]

3.2.6 Synthesis of Morita-Baylis Hillman adduct (MBHA) acids

There were several options for resolving compounds **102e**, **196** and **197 (Figure 29**). The first method is applying resolution by transesterification. This is where the enzyme would selectively acetylate one enantiomer as it leaves the other enantiomer untouched. This method of resolution is demanding, especially identifying the right conditions for enzymatic activity to be realised. The method that was convenient to apply was resolution by hydrolysing the ester bond of these compounds (**Scheme 62**). In this kind of investigation, it is expected that the enzyme will selectively hydrolyse the ester of one enantiomer to form an enantiopure acid as it leaves the other enantiomer untouched.

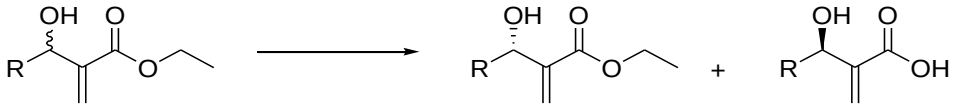

196 R = Ph

102e R = PhCH=CH-

197 R = $PhCH_2CH_2$-

Scheme 62: Possible outcome when resolving the ethyl acrylate derivative of MBH alcohols

To investigate resolution by hydrolysis of this ethyl ester bond of MBH alcohols, the corresponding acids **205**, **103e** and **206** as standards were required so that the progress of the reaction would be monitored easily. Consequently, these corresponding acids were synthesized starting from the already synthesized methyl acrylate alcohols **101a**, **193** and **194** (**Figure 32**).

The hydrolysis of the esters was achieved by refluxing the ester with potassium hydroxide in a mixture of water and ethanol at 70 °C (**Scheme 63**). This led to the Morita-Baylis-Hillman acids shown in **Figure 37**.

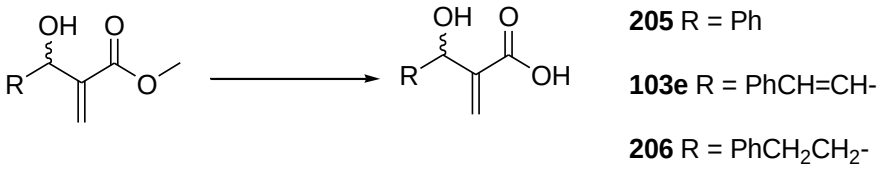

Scheme 63: Synthesis of MBH acids. *Reagents and conditions*: KOH, reflux at 70 °C.

The synthesized acid **205** and **206** were isolated as white solids, with a melting point range of 81 - 82°C and 70 - 72°C respectively. The yield of **205** was 91% while the yield of **206** was 82%. The acid **103e** was isolated as a colourless oil in a yield of 95%.

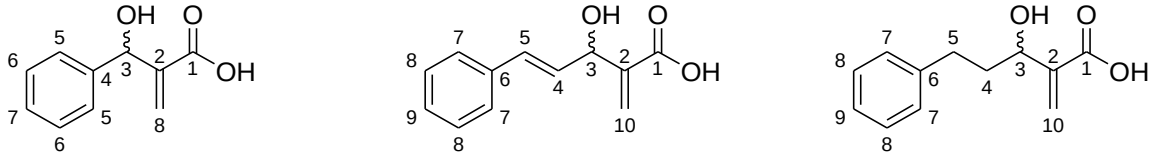

205 **103e** **206**

Figure 37: Synthesized Morita-Baylis-Hillman acids

The synthesized acids were characterized using IR, ^{1}H, and ^{13}C NMR data. This information is presented in **Table 23**. There was no observed geminal coupling between the vinylic protons as all the protons appeared as singlets in ^{1}H NMR spectrum. The data obtained for all the three acids were identical to the ones reported in literature.

Table 23: IR, ^{1}H, ^{13}C NMR data of MBH acids

Compound	**IR (cm^{-1}); functional group**	**^{1}H (δ) and ^{13}C(δ)**	**Reference**
205	3556 (OH), 1681 (C=O).	7.35 – 7.21 (m, Ar-5H), 6.82 (br s, 2 x OH), 6.43 (s, H-8a), 5.89 (s, H-8b), 5.52 (s, H-3).	[152]

		171.0 (C-1), 141.4 (C-4), 140.9 (C-2), 128.5 (C-5 or C-6), 128.4 (C-8), 128.0 (C-7), 126.7 (C-6 or C-5), 72.8 (C-3).	
103e	3368 (OH), 1685 (C=O).	7.93 (br s, 2 x OH), 7.38 – 7.14 (Ar-5H), 6.62 (d, *J* = 15.9 Hz, H-5), 6.39 (s, H-10a), 6.25 (dd, *J* = 15.9, 6.4 Hz, H-4), 5.97 (s, H-10b), 5.14 (d, *J* = 6.3 Hz, H-3). 170.8 (C-1), 140.8 (C-6), 136.4 (C-2), 131.9 (C-5), 128.8 (C-9), 128.6 (C-7 or C-8), 128.1 (C-10), 128.0 (C-4), 126.7 (C-7 or C-8), 71.6 (C-3).	[81]
206	3341 (OH), 1692 (C=O).	8.01-6.67 (m, Ar-5H and 2 x OH), 6.40 (s, H-10a), 5.92 (s, H-10b), 4.45 (t, *J* = 6.3 Hz, H-3), 2.88 – 2.62 (m, H-4), 2.08 – 1.92 (m, H-5). 171.0 (C-1), 141.7 (C-6), 141.4 (C-2), 128.5 (C-7 or C-8), 128.4 (C-7 or C-8), 127.5 (C-10), 125.9 (C-9), 70.7 (C-3), 37.5 (C-4), 32.0 (C-5).	[153]

3.2.7 Lipase catalyzed kinetic resolution

3.2.7.1 Identification of active enzymes in the biocatalysis store

This investigation was done by screening the activities of different enzymes that were available in our biocatalysis store. This was done by carrying out a test reaction using the lipases and esterases, benzyl alcohol and acyl donor in acetonitrile as described in literature (**Scheme 64, condition a**).[154, 155] Lipases that led to the formation of benzyl acetate **208** confirmed that these enzymes were active. A hydrolysis reaction on benzyl acetate was also performed (**Scheme 64, condition b**). This exercise led to the identification of 101 active enzymes that had the ability to acetylate benzyl alcohol and hydrolyse the benzyl acetate **208**.

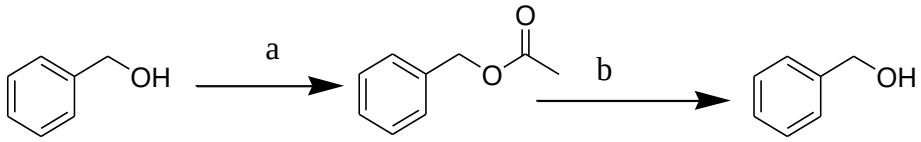

208

Scheme 64: Screening of enzymes activity. *Reagents and conditions*: (a) Lipase, vinyl acetate in acetonitrile at RT, (b) Lipase, Phosphate buffer at pH 7.00 at RT.

3.2.7.2 Method development for enzymatic kinetic resolution

The method development began by subjecting adducts **101a** and **192** to resolution by transesterification to obtain stereochemical products shown in **Scheme 65**. A total of 61 enzymes including lipases and esterases were used in this screening exercise. Unfortunately, this reaction did not work despite varying the solvent and acylating agent. The reaction also did not work when **75a** was used in this investigation. An attempt to use synthesized acylating agent, 4-Chlorophenyl acetate (PCPA) **209** in **Scheme 65** was also fruitless.

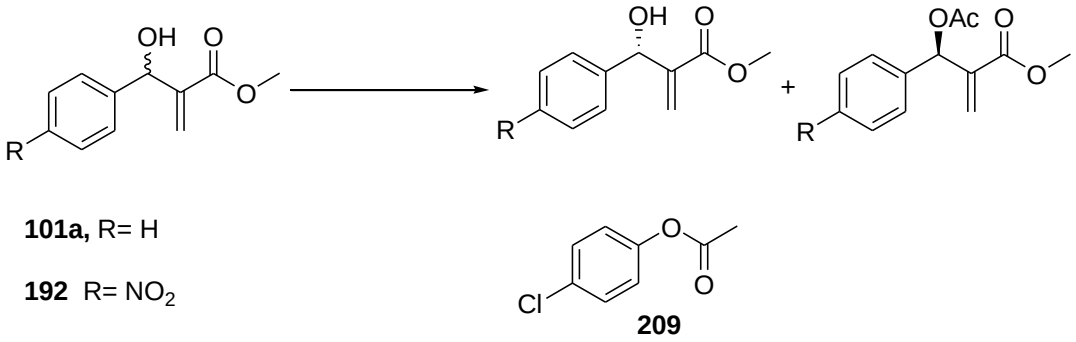

101a, R= H

192 R= NO_2

209

Scheme 65: Failed reaction on resolution of MBH adducts by transesterification. *Reagents and conditions*: Lipase, vinyl acetate or isopropenyl acetate or 4-chlorophenyl acetate **209** in acetonitrile at RT. Adduct **75a** was also used in the investigation.

It was very difficult to explain why the reaction in **Scheme 65** could not work. The only possible explanation among the many is that maybe the substrates chosen are not compatible with the tested enzyme or the organic solvent tested might be making the enzyme lose activity as reported in literature.[156] In addition to that, there might be a possibility that the chosen acylating agent is not compatible with the lipases investigated. It was impossible to specifically point out what led the reaction not to work. There were examples in literature where MBH adducts had been enzymatically resolved by transesterification as reviewed by Basavaiah (**Figure 38**).[8] However, it is interesting to note that none of the Morita-Baylis-

Hillman adducts successfully resolved by transesterification were those derived from benzaldehyde.

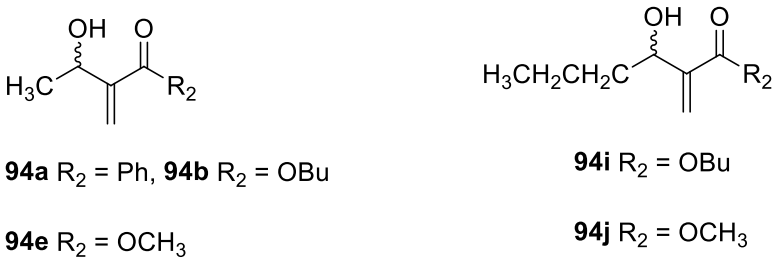

94a R_2 = Ph, **94b** R_2 = OBu

94e R_2 = OCH_3

94i R_2 = OBu

94j R_2 = OCH_3

Figure 38: Examples of MBH alcohols that have been resolved by transesterification

The next attempt was to investigate resolution of **199** by hydrolysis, expecting to obtain products of shown stereochemistry in **Scheme 66**.

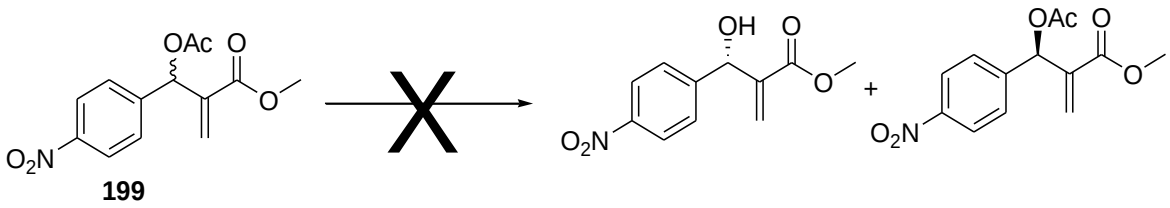

199

Scheme 66: Failed reaction for resolving **199** by hydrolysis. *Reagent and conditions*: Lipase, Phosphate buffer at pH 7.00 at RT.

The few lipases that were investigated using the reaction shown in **Scheme 66** did not yield fruit and only the starting material was observed by TLC. These were disappointing moments as the reactions attempted were not working. It was clear from the attempted reaction that investigating resolution by hydrolysis can be done with ease as compared to investigating resolution by transesterification. The latter requires varying many parameters to establish suitable conditions for the reaction to take place. Consequently, resolution by hydrolysis was investigated as it had the potential to succeed as only few parameters needed to be varied for the reaction to take place.

Different substrates were chosen for investigation as the reaction did not take place when methyl acrylate derivatives were used. Acetate **201** that had the nitrile functional group and was flexible between the phenyl ring and the acetate group was chosen to start the reaction.

Acetate **201** was dissolved in acetone and subjected to three different enzymes in a phosphate buffer while monitoring the ratio of the product and the starting material using a C-18 column. The control reaction in which **201** was dissolved in acetone and added to a phosphate buffer without enzyme was also set. The monitoring was done at the intervals of 3, 24 and 48 hours. The hydrolysis is shown in **Scheme 67**.

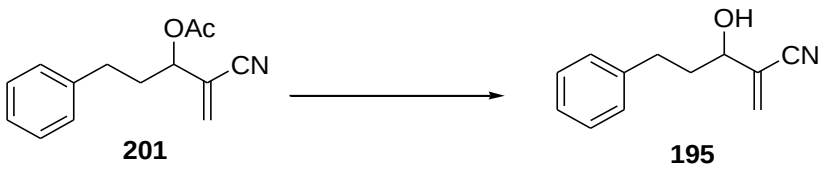

201 **195**

Scheme 67: Investigation of hydrolysis of the acetate **201** in the presence and absence of an enzyme. *Reagents and conditions*: esterases and lipases, Phosphate buffer at pH 7.00.

The enzymes investigated for this reaction were two esterases of different preparations (from Recombinant Biocatalyis Inc.) and lipoprotein lipase from *Burkholderia* sp. The HPLC chromatogram of **195** and **201** on C-18 column for the purposes of monitoring the reactions are shown in **Figure 39**. Their retention times are 3.30 minutes for **195** and 3.82 for **201**. It was a surprise that all the three enzymes hydrolysed **201** to almost completion after three hours. A similar observation of almost complete hydrolysis of **201** was also observed in the control reaction. These chromatograms are shown in in **Figure 40**. The observed hydrolysis of **201** in the control was shocking as this was not expected. This observation led to an investigationof exactly what was going on in these reactions.

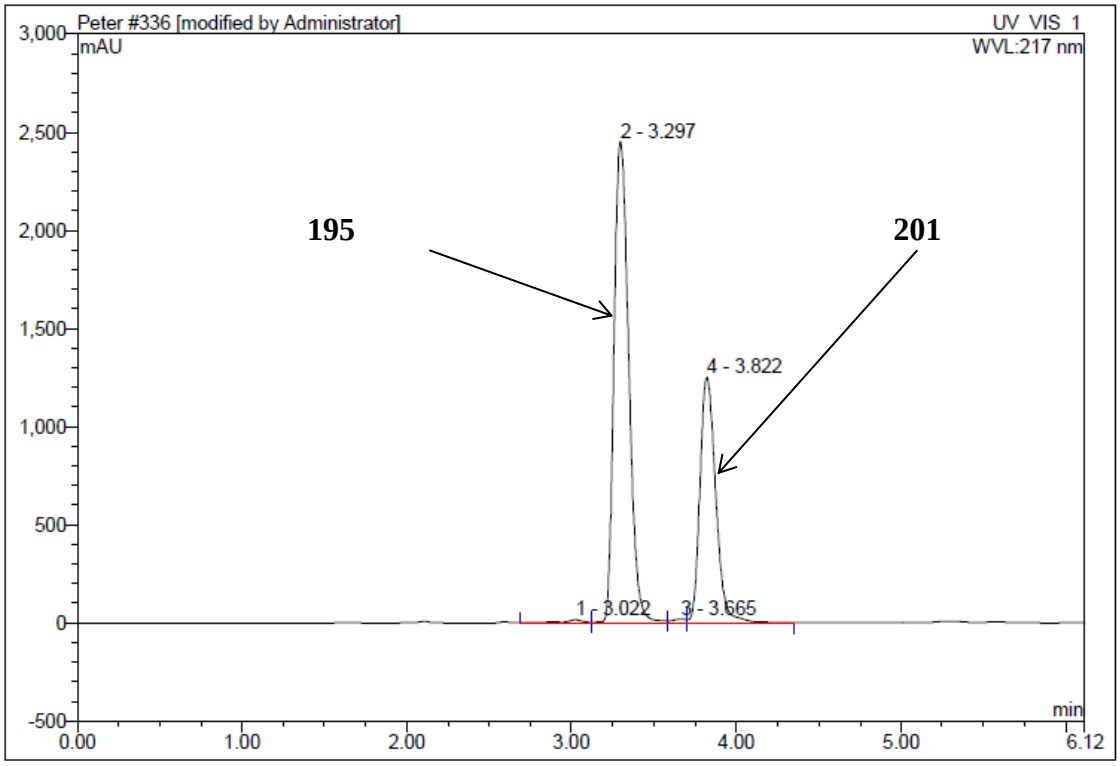

No.	Ret.Time min	Peak Name	Height mAU	Area mAU*min	Rel.Area %	Amount	Type
1	3.02	n.a.	14.848	1.726	0.44	n.a.	BM *
2	3.30	n.a.	2452.015	254.427	64.17	n.a.	M *
3	3.67	n.a.	19.163	1.721	0.43	n.a.	M *
4	3.82	n.a.	1251.058	138.641	34.96	n.a.	MB*
Total:			3737.084	396.515	100.00	0.000	

Figure 39: HPLC chromatogram of **195** and **201** using C-18 column to be used for monitoring the process of enzymatic reaction

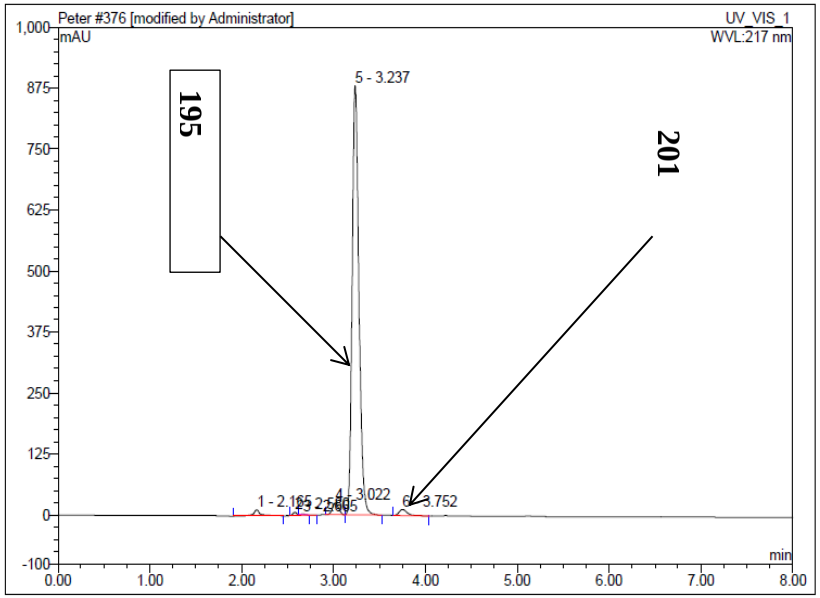

No.	Ret.Time min	Peak Name	Height mAU	Area mAU*min	Rel.Area %	Amount	Type
1	2.17	n.a.	12.276	1.221	1.52	n.a.	BMB
2	2.58	n.a.	6.412	0.481	0.60	n.a.	BMB*
3	2.67	n.a.	0.927	0.051	0.06	n.a.	Rd
4	3.02	n.a.	24.406	1.946	2.43	n.a.	BM *
5	3.24	n.a.	879.285	75.253	93.79	n.a.	MB*
6	3.75	n.a.	12.721	1.286	1.60	n.a.	BMB
Total:			936.028	80.238	100.00	0.000	

Figure 40a: HPLC chromatogram of **195** after 3 hours of esterase activity

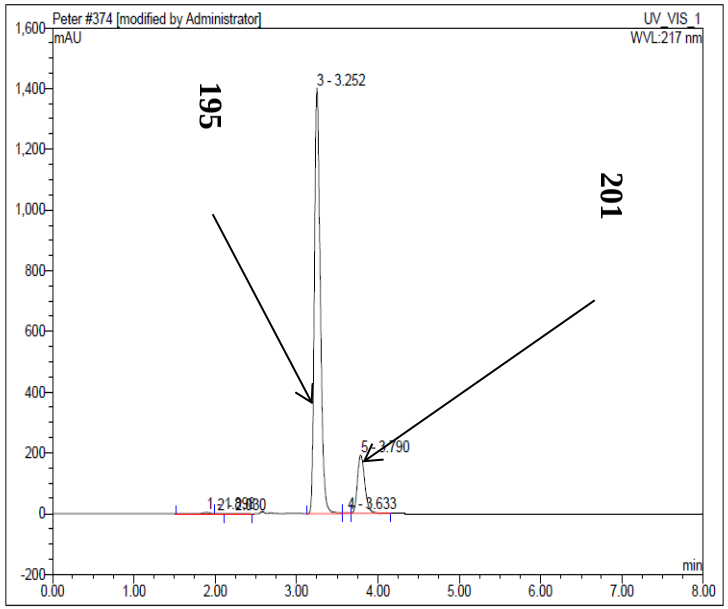

No.	Ret.Time min	Peak Name	Height mAU	Area mAU*min	Rel.Area %	Amount	Type
1	1.90	n.a.	4.825	1.076	0.77	n.a.	BMB*
2	2.03	n.a.	0.215	0.017	0.01	n.a.	Rd
3	3.25	n.a.	1401.682	118.578	84.49	n.a.	BM *
4	3.63	n.a.	3.658	0.348	0.25	n.a.	M *
5	3.79	n.a.	192.844	20.328	14.48	n.a.	MB*
Total:			1603.224	140.347	100.00	0.000	

Figure 40b: HPLC chromatogram of **195** after hydrolysis of **201** in the absence of enzymes after 48 hours

At this point, it was not possible to point out if the buffer used was the one promoting hydrolysis or the use of co-solvent. Therefore, freshly prepared phosphate buffer and Tris buffer were used in different co-solvents. Acetate **201** was dissolved in acetone, DMSO and introduced in phosphate and Tris buffer at pH 7.00. The controls were also set up and the relative areas of **195** and **201** were determined using C-18 column chromatography at different times. These investigations were to determine whether acetate **201** was hydrolysing in the absence of the enzyme.

The use of 5% acetone in Tris buffer, 10% acetone in Tris buffer, 5% DMSO in phosphate buffer, 10% DMSO in phosphate buffer, 5% DMSO in Tris buffer and 10% DMSO in Tris buffer led to the appearance of Tris and DMSO peaks in the C-18 column chromatogram. These two peaks interfered with the peak of the analyte. Based on this observation, we could not apply any of these combinations for the resolution investigation of the acetate.

On the other hand, use of phosphate buffer only, 5% acetone in phosphate buffer and 10% acetone in phosphate buffer afforded very clear HPLC spectra where identities and peak areas of the starting material and the product could be accurately determined. Furthermore, the use of both 5% acetone in phosphate buffer and 10% acetone in phosphate buffer indicated no observable hydrolysis of **201.** The use of 5% acetone in phosphate buffer at different times is shown in chromatograms in **Figure 41a** and **41b**.

The earlier observed acetate hydrolysis was due to the inaccurate way of preparing the phosphate buffer, which did not have the correct pH 7.00. The use of 5% acetone in phosphate buffer at pH 7.00 was used for the next set of investigations just to confirm the repeatability of the results.

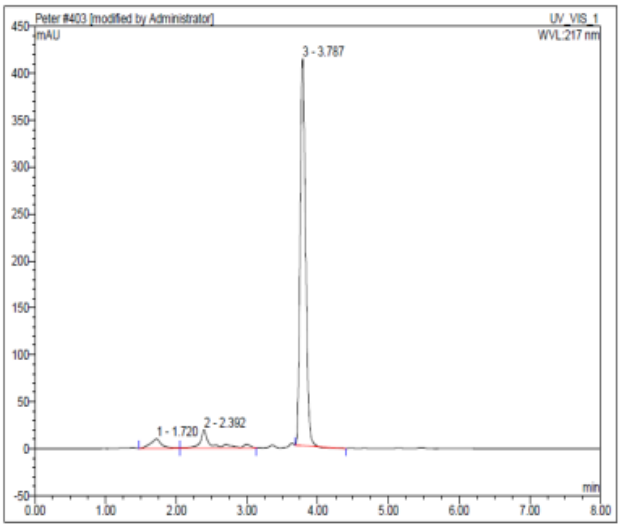

No.	Ret.Time min	Peak Name	Height mAU	Area mAU*min	Rel.Area %	Amount n.a.	Type
1	1.72	n.a.	9.885	1.779	4.24	n.a.	BM *
2	2.39	n.a.	19.461	3.424	8.16	n.a.	MB*
3	3.79	n.a.	412.652	36.764	87.60	n.a.	BMB*
Total:			441.998	41.967	100.00	0.000	

Figure 41a: Chromatogram of **201** in 5% acetone in phosphate buffer after 7 hours

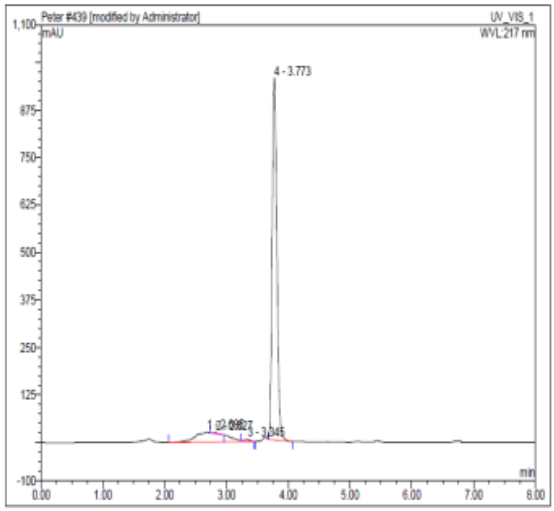

No.	Ret.Time min	Peak Name	Height mAU	Area mAU*min	Rel.Area %	Amount n.a.	Type
1	2.69	n.a.	25.245	14.641	14.74	n.a.	BMB*
2	2.83	n.a.	2.415	0.249	0.25	n.a.	Rd
3	3.35	n.a.	4.609	0.380	0.38	n.a.	Rd
4	3.77	n.a.	951.432	84.037	84.62	n.a.	BMB*
Total:			983.702	99.306	100.00	0.000	

Figure 41b: Chromatogram of **201** in 5% acetone in phosphate buffer after 48 hours

The use of 5% acetone in phosphate in the presence of an enzyme as a way of confirming that indeed any hydrolysis is due to the biocatalyst was investigated. This was done by dissolving **201** in acetone and introducing this to a buffer containing an enzyme; and a phosphate buffer without an enzyme as a control. The enzymes used for the investigations were esterase, lipase from *Candida antarctica* type B, and Lipase AK "amano". The time was varied from 30 minutes, 24 hours and 48 hours.

The results were encouraging as there was no hydrolysis of **201** in the absence of the enzyme after 48 hours. On the other hand, there was hydrolysis of the acetate in the presence of the enzyme at different times after 24 hours. The HPLC chromatogram for the two enzymes investigated confirmed to us 50% of **201** had hydrolysed to **195.**

Although method development was tedious and time consuming, it was a break through as a suitable method for the resolution investigation had been identified. The only worry was whether other enzymes that were active and enantioselective on the intended substrates

could be identified. The next discussion is on the investigation of the resolution of of (±)-2-cyano-phenyl acetate **105a**.

3.2.7.3 Resolution of (±)-2-cyano-phenyl acetate (105a)

The first compound to explore was the acetate (±)-2-cyano-phenyl acetate **105a**. The process of exploration entailed screening the substrate against lipases and esterases of different preparations. The first step of the screening reaction involved dissolving 7 mg of **105a** in acetone and introducing the solution in a phosphate buffer at pH 7.00 containing 7 mg of the enzyme in a 1 mL Eppendorf tube. The second step was to put the reaction mixture on an orbital shaker at a specific temperature and monitor the reaction using TLC and C-18 HPLC column chromatography. This screening exercise tested a total of 101 enzymes.

The enzymatic reaction mixtures that showed activity were further subjected to chiral HPLC analysis to determine if indeed they were also enantioselective (**Scheme 68**). The determination of enantioselectivity was only possible after establishing the chromatographic conditions for separating the racemic acetate **105a** and racemic alcohol (±)-2-[(hydroxyphenyl)methyl]acrylonitrile **75a**. The racemic acetate and the racemic alcohol separated on two different chiral columns; racemic acetate **105a** separated on a Chiralpak AD-H while the racemic alcohol **75a** separated on a Lux 3 μM cellulose-2. In separating the two, the same mobile flow rate of 1 mL/min was applied with the same mobile flow composition of hexane and isopropanol (IPA) in a ratio of 96:4. The HPLC chromatograms of **105a** and **75a** are shown in **Figures 42** and **43** respectively.

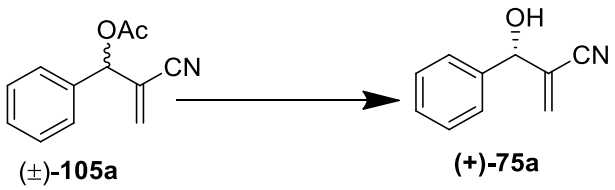

Scheme 68: Hydrolysis of **105a** using different lipases and esterases in phosphate buffer at pH 7.00 at different temperatures

The reaction shown in **Scheme 68** was used to monitor the enzymatic activities of different lipases and esterases and their results are shown in **Table 24**.

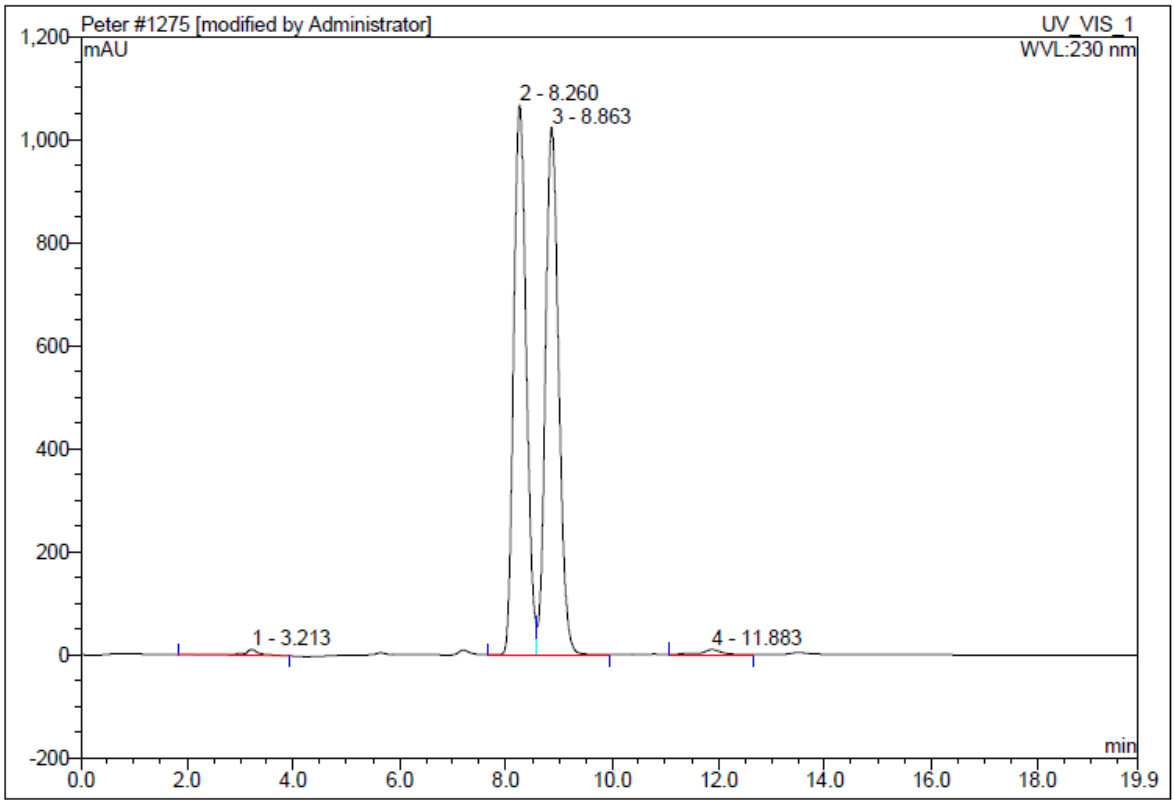

No.	Ret.Time min	Peak Name	Height mAU	Area mAU*min	Rel.Area %	Amount	Type
1	3.21	n.a.	11.380	4.554	0.76	n.a.	BMB*
2	8.26	n.a.	1066.324	292.751	49.14	n.a.	BM *
3	8.86	n.a.	1023.069	294.249	49.39	n.a.	MB*
4	11.88	n.a.	9.461	4.219	0.71	n.a.	BMB*
Total:			2110.234	595.772	100.00	0.000	

Figure 42: HPLC chromatogram of the racemic acetate **105a**

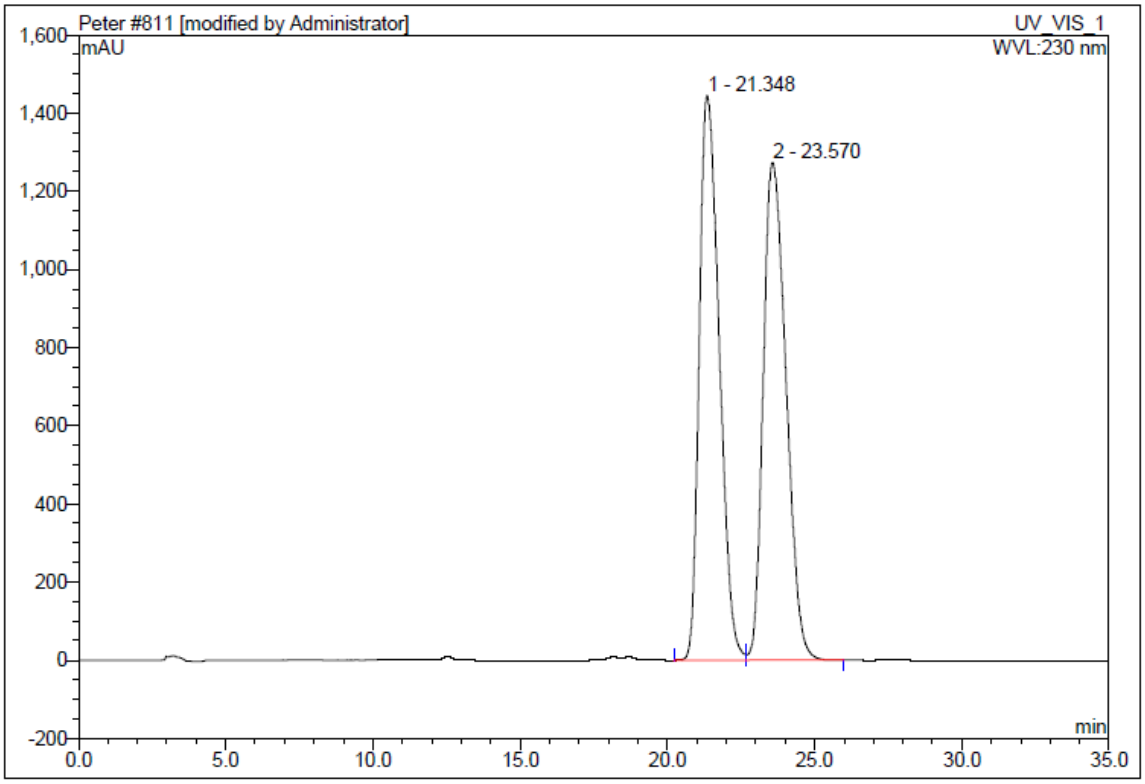

No.	Ret.Time min	Peak Name	Height mAU	Area mAU*min	Rel.Area %	Amount	Type
1	21.35	n.a.	1444.444	1134.991	49.82	n.a.	BM *
2	23.57	n.a.	1273.256	1143.243	50.18	n.a.	MB*
Total:			2717.701	2278.234	100.00	0.000	

Figure 43: HPLC chromatogram of the racemic **75a**

Table 24: Hydrolysis of **105a** using different enzymes affording **75a**

Entry	Enzyme name	Time (h), Temp (°C)	Conv (%)	ee_s (%)	ee_p (%)	E
1	Lipase AK " Amano III" AKK026094	96, 30	30	38	91	30
2	Lipase AK-D "Amano" III ILAKX02509K	60,30	26	32	90	27
3	Lipase AK-D "Amano" II ILAKXW250N	60,30	28	35	90	28
4	Lipase AK "Amano" Lot No. 59.001	60,30	39	60	93	50
5	Amano Lipase AK Lot no. 0351202	96,30	48	80	87	36
6	Lipase AK "Amano" 20 lot No. LAKAFF0151102R	24, 30	47	78	88	37
		34, 30	51	87	83	31
7	Lipase AK" AMANO" conc.	24, 30	46	78	92	55
8	Lipase AK " Amano II" ILAKKW1150	93, 30	40	55	84	21
9	Lipase AK "Amano" Lot No. LAKWO9504	46, 30	48	83	90	44
10	Lipase AK "AMANO" Lot no. LAKVO7510	62, 30	52	98	90	89
11	Lipase AK-I Lottlo, ilakyo452/02k	20,30	44	70	90	40
12	Esterase ESL-001-01 with cut stabilizer	0.17, 20	43	49	66	8
13	Esterase Cat no. ESL-001-01, 720268	0.17, 20	45	45	56	5
14	Esterase cat. No. ESL-001-01, 6Z0248	0.17, 20	42	45	63	7
23	Esterase Cat no. ESL-001-01, 6Y0240	0.17, 20	47	54	62	7
15	Lipozyme® CALB L LCN 02106	26, 35	29	37	93	40
		120, 35	30	39	90	29
16	Novozym 435 LC 200233	16, 35	21	24	90	22
17	Novozym 435 LC 20017	16, 35	28	34	91	28
18	Lipo Max Cxt 1.00	4, 30	45	75	94	72
19	Alcalase (Novozymes)	93, 30	10	4	32	2
20	Lipase from *Candida antarctica* type B	62, 30	52	89	82	30
21	Lipase from *pseudomonas fluorescens* cat. no 95608	24, 30	22	26	94	44
22	Amano Lipase from *Pseudomonas fluorescens*, Cat. no. 534730	34, 30	46	79	92	58
23	Lipase from *pseudomonas cepacia* cat. no 62309	19, 30	51	94	90	65
24	Lipase from *Rhizopus orgzae* cat. no 80612	15,30	2	1	34	2
25	Lipase from porcine pancrease cat. no. L3126	24, 30	49	34	35	3

From literature, it is well understood that irreversible enzymatic hydrolysis reactions are only practically viable if the enantiomeric ratio (E) is above 15.[137] Therefore, it is transparent from **Table 24** that a total of 19 enzymes yielded an enantiomeric ratio of above 15. These enzymes were lipase AK of different preparations (**entries 1-11**), Lipozyme® CALB L LCN 02106 (**entry 15**), Lipo Max Cxt 1.00 (**entry 18**), Novozym 435 LC (e**ntries 16-17**), Lipase

from *Candida antarctica* type B (**entry 20**), Lipase from *Pseudomonas fluorescens* (**entries 21-22**), and Lipase from *Pseudomonas cepacia* (**entry 23**). The excellent enzymes that showed good enantiomeric excess of the substrate (ee_s), and enantiomeric excess of the product (ee_p) were Lipase AK "AMANO" Lot no. LAKVO7510 (**entry 10**) and Lipase from *Pseudomonas cepacia* (**entry 23**). Unfortunately, these two excellent enzymes could not be used for further reactions as the quantity remaining after screening exercises was very small (less than a milligram).

The next assignment was to find out the absolute configuration of the resolved alcohol. This was not a straightforward task as a literature search was done to find out which method was suitable for the investigation.

3.2.7.4 Determination of the method to use for the stereochemical determination of the enantiopure alcohol

The absolute configuration of an enantiopure compound is fundamentally important as stereochemistry dictates the physical, chemical, biological, and pharmaceutical properties of a molecule. Absolute configuration sounds very simple theoretically but is complex, especially when using experimental means to determine the stereochemistry of unreported compounds.[157] There are several techniques which one can employ to determine the absolute configuration of a new compound.[158] In any of these techniques, instruments such as X-ray crystallography, chiroptical spectrophotometers, and nuclear magnetic resonance (NMR) play a critical role.[159] Unfortunately, use of X-ray diffraction (XRD) is limited to good quality monocrystals.[160] Furthermore, use of XRD requires a complex machine that needs special training and this method will not apply to samples that are in solid or liquid form. Chiroptical spectrophotometers use techniques such as optical rotatory dispersion (ORD), vibrational circular dichroism (VCD), electronic circular dichroism (ECD) and vibrational Raman optical activity (VROA).[161] The use of chiroptical spectrophotometers is also disadvantageous in so many ways. Nuclear magnetic resonance (NMR) remains the only simple, reliable and straight forward route of finding the stereochemistry of a new compound.

The use of NMR in defining stereochemistry depends heavily on the use of enantiomerically pure reagents that combine with the compound being investigated. The resultant compound will have a precise, predictable shift in the ^{1}H NMR spectrum.[159] The enantiomerically pure reagent can be chiral derivatizing agents (CDA) that form a covalent bond with the analyte

or chiral solvating agent (CSA) which associates with the analyte through non-covalent interaction. The association can be in the form of a hydrogen bond, ion-ion and dipole-dipole interaction. Apparently, the use of chiral solvating agents has not been applied often as compared to chiral derivatizing agents. This simply means the use of CSA might be having some challenges which are not being reported despite giving accurate results.

After analysing all the methods, one will be convinced to use NMR spectroscopy with the help of CDA in assigning the stereochemistry of a new compound as supported by detailed reviews.[162, 163] The use of NMR and CDA dates back to 1973, where Mosher and Dale used (*R*)-(+) and (*S*)-(-)-α-methoxy-α-(trifluoromethyl)phenylacetic acid (MTPA) to determine the absolute configuration of enantiopure secondary alcohols and amines.[164] This method, which is famously known as Mosher's protocol was later used to assign the absolute configuration of chiral carboxylic acids[165], tropane alkaloids[166], and chiral cyclic amines.[167] For one to use Mosher's protocol, you need stereochemically determined enantiopure Mosher's acid and enantiopure secondary alcohol or amine whose absolute configuration is unknown. The next subsequent step involves coupling your enantiopure secondary alcohol or amine with (*R*)-(+) and (*S*)-(-)-α-methoxy-α-(trifluoromethyl)phenylacetic acid (MTPA) affording Mosher's esters with stable conformation. The last step involves obtaining ^{1}H NMR spectra and using it to assign the stereochemistry.

For example when one has a secondary alcohol in which the stereogenic carbon [C(1′) is attached to two different groups L_1 and L_2 then reacting it with (*R*)-(+) and (*S*)-(-)-(MTPA) forms Mosher's esters with preferred *syn*-periplanar conformation (**Figure 44**).

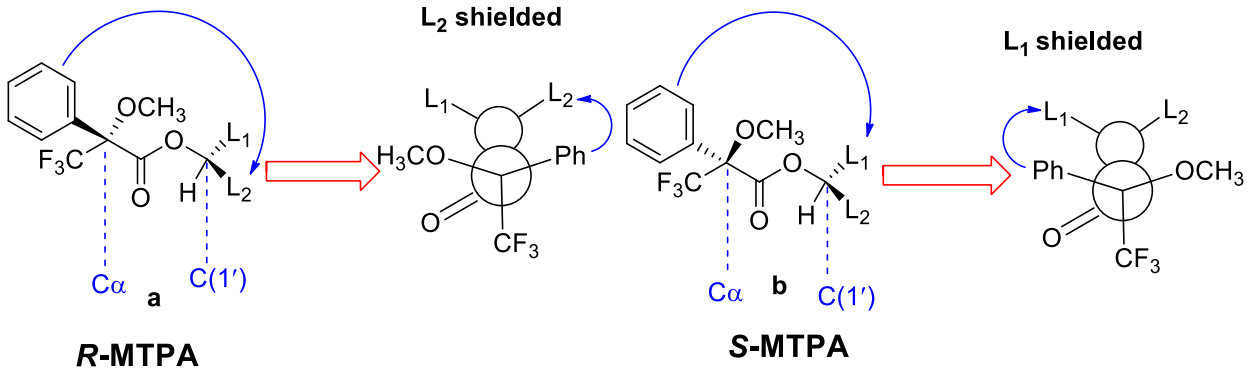

Figure 44: Shielding effect of *R* and *S* Mosher's Ester

The phenyl ring originating from *R*-Mosher's acid is positioned such that the diamagnetic effect of the ring shields the L_2 substituent group of the alcohol (**Figure 44 a**). The shielding will cause L_2 to appear upfield in the ^{1}H NMR spectrum of *R*-Mosher ester. This informs the investigator that the phenyl ring and L_2 are on the same side of the plane. The phenyl group originating from *S*-Mosher's group shields the L_1 substituent of the alcohol group. This causes L_1 to appear upfield on the ^{1}H NMR spectrum of *S*-Mosher ester; implying that L_1 and the phenyl ring are on the same side of the plane. The Δ*SR* values is calculated for the substituents L_1 (Δ*SR*L_1) and substituent L_2 (Δ*SR*L_2). The Δ*SR* is the difference between the chemical shift in the (*S*)-MTPA ester derivative [δ (*S*)] and in the (*R*)-MTPA derivative [δ (*R*)]. The comparison of the Mosher's ester spectra leads to Δ*SR*L_1< 0 and Δ*SR*L_2> 0 which is used to determine the absolute configuration of the alcohol. Therefore, we decided to make use of Mosher's protocol to determine the stereochemistry of the enantiopure isolated alcohol.

3.2.7.5 Stereochemical determination of the enantiopure alcohol 75a using Mosher's protocol

An enantiopure alcohol that is obtained after enzymatic reaction is required for this task to be accomplished. The use of the best performing enzymes in **Table 24** for large scale resolution of racemic **105a** was not possible as these enzymes were all used in the screening reactions. We therefore made use of Amano lipase from *P. fluorescens* of cat. no. 534730 that also displayed good enantiomeric ratio (E) during the screening exercise (**Table 24**, **entry 22**). The step of performing large scale reaction was done by adding 1.00g of racemic **105a** in acetone and adding the resultant solution to phosphate buffer at pH 7.00 containing 1.00 g Amano lipase from *P. fluorescens*. The reaction mixture was stirred at 30°C for 44 hours and this afforded a scalemic mixture of **105a** with an enantiomeric excess of 53% and an enantiopure **75a** as colourless oil in a yield of 46%. The yield calculations were based on expected maximum yield of 50% for complete hydrolysis of one acetate enantiomer. The specific optical rotation of the enantiopure **75a** was found to be +60.400 with an enantiomeric excess of 94% after a conversion of 36%. The HPLC chromatogram of the scalemic mixture **105a** and the enantiopure (+)-**75a** is shown in **Figures 45** and **46** respectively.

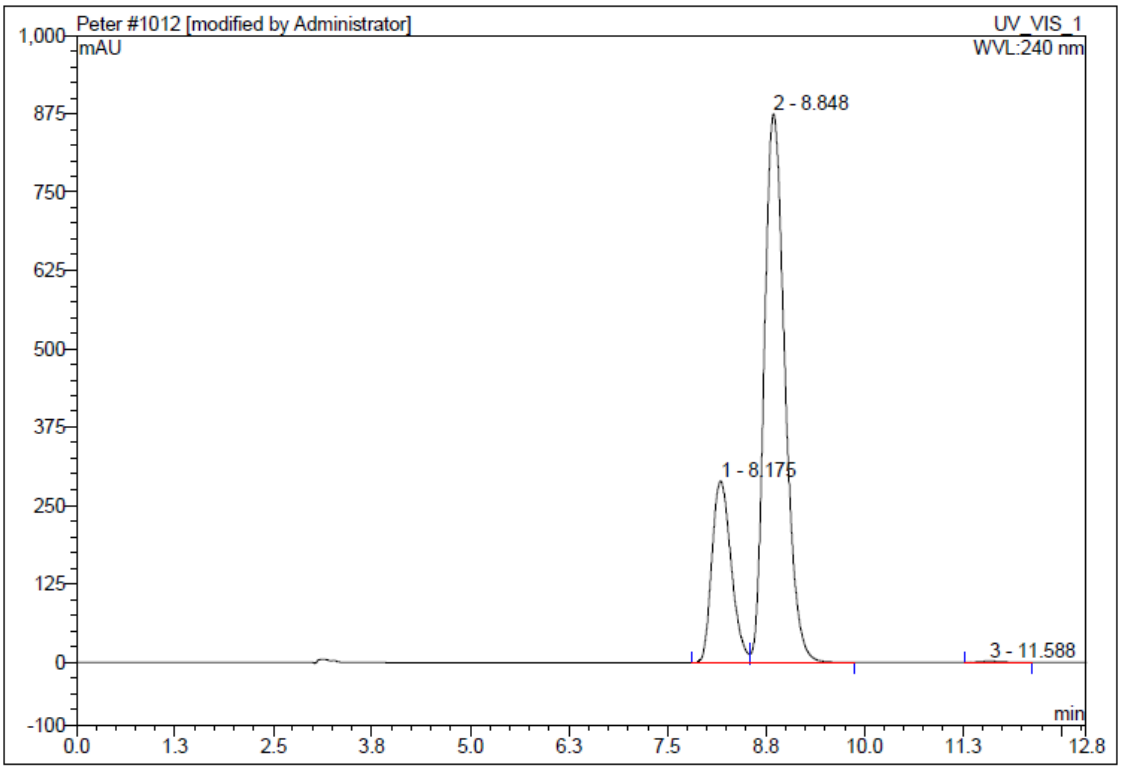

No.	Ret.Time min	Peak Name	Height mAU	Area mAU*min	Rel.Area %	Amount	Type
1	8.18	n.a.	288.884	81.899	23.63	n.a.	BM *
2	8.85	n.a.	874.375	264.177	76.22	n.a.	MB*
3	11.59	n.a.	1.673	0.536	0.15	n.a.	BMB
Total:			1164.933	346.612	100.00	0.000	

Figure 45: HPLC chromatogram of the isolated scalemic mixture **105a** after enzymatic activity

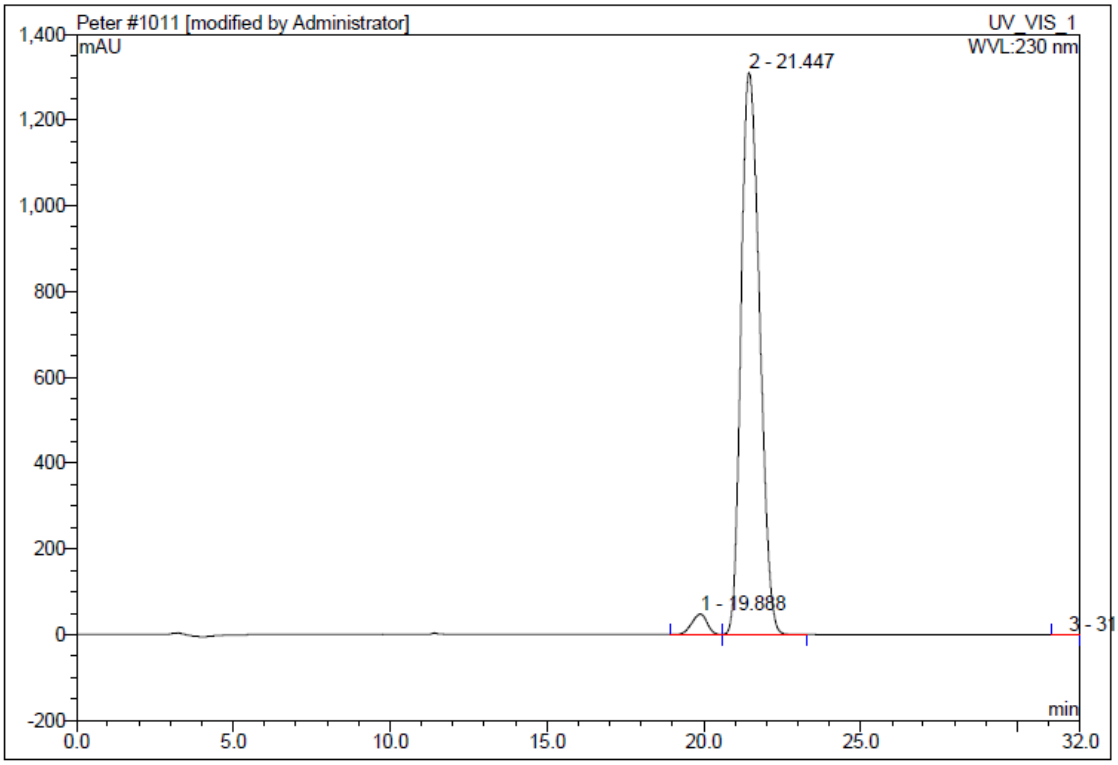

No.	Ret.Time min	Peak Name	Height mAU	Area mAU*min	Rel.Area %	Amount	Type
1	19.89	n.a.	47.825	27.562	2.96	n.a.	BM
2	21.45	n.a.	1309.866	902.190	97.02	n.a.	MB
3	31.63	n.a.	0.371	0.179	0.02	n.a.	BMB
Total:			1358.062	929.931	100.00	0.000	

Figure 46: HPLC chromatogram of the enantiopure alcohol (+)-**75a** after enzymatic hydrolysis

The next step was to determine the stereochemistry of the isolated enantiopure (+)-**75a**. This was the time to test the chosen Mosher's protocol to unambiguously assign the stereochemistry. The absolute configuration of the isolated enantiopure alcohol was deduced by taking two samples of (+)-**75a** and reacting each with (*R*)-(+) and (*S*)-(-)-α-methoxy-α-(trifluoromethyl)phenylacetic acid (MTPA) in the presence of a coupling reagent dicyclohexyl carbodiimide (DCC) and catalytic amount of DMAP at room temperature (**Scheme 69**). This led to Mosher's esters (*R*)-[(*S*)-2-Cyano-1-phenylallyl] 3,3,3-trifluoro-2-methoxy-2-phenylpropanoate **210** and (*S*)-[(*S*)-2-Cyano-1-phenylallyl] 3,3,3-trifluoro-2-methoxy-2-phenylpropanoate **211**. The two Mosher's esters were both isolated as colourless oils in a yield of 82% for **210** and 80% for **211**. The analysis of the two esters redrawn in the preferred stable conformation was used to determine the stereochemistry based on the shielding effect of protons.

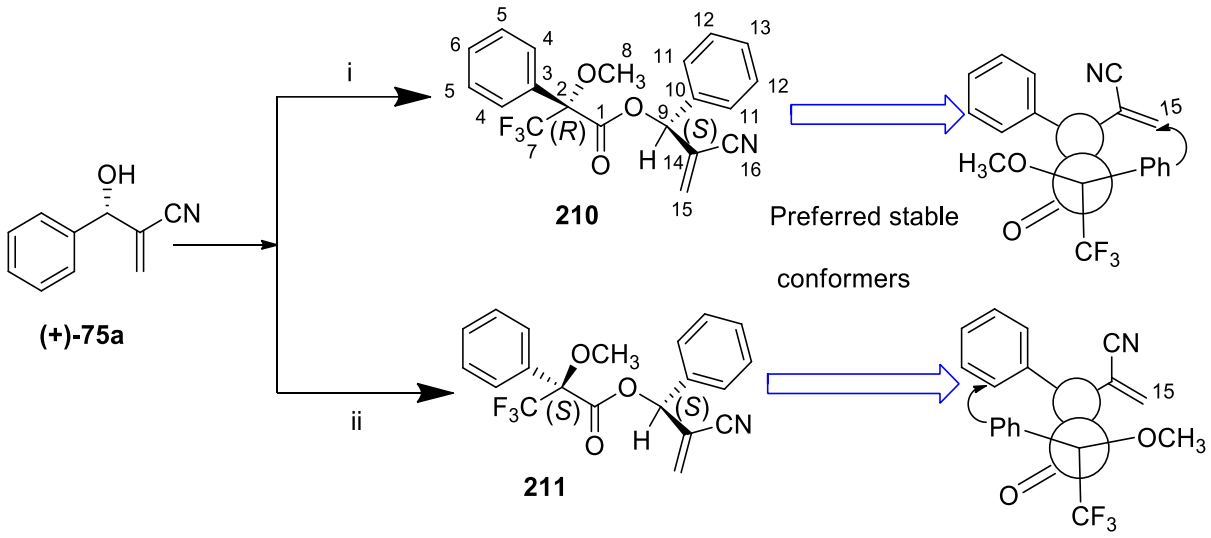

Scheme 69: Synthesis of Mosher's ester **210** and **211**. Reagents and conditions: (i) DCC, DMAP, (*R*)-(+)-MTPA in CH_2Cl_2 at room temperature. (ii) DCC, DMAP, (*S*)-(-)-MTPA in CH_2Cl_2 at room temperature.

The ^{1}H NMR spectrum of the ester **210** showed a total of five signals (**Figure 47**). The aromatic protons of the two phenyl rings appeared as a multiplet at δ 7.45 – 7.30. The second most deshielded multiplet at δ 6.56 - 6.52 was assigned to the stereogenic centre proton H-9. This was an indication that H-9 experienced a long range coupling with H-15a and H-15b. The appearance of two doublets at δ 6.06 and δ 5.93 were assigned to proton H-15a and H-15b respectively. This is because the two protons were attached to the same carbon as confirmed by their geminal coupling of 1.0 Hz and 1.4 Hz. The methoxy protons appeared as a multiplet at δ 3.49 – 3.46. The ^{1}H NMR spectrum of **211** had a total of six signals of which two multiplets appeared in the aromatic region (**Figure 48**). The first multiplet appeared at δ 7.46 – 7.30 integrating for nine aromatic protons and the second one appearing at δ 7.24 – 7.20 integrating for one aromatic proton. The stereogenic centre proton H-9 of **211** did not appear as a multiplet as observed in **210** but instead it appeared as a singlet at δ 6.49 suggecting there was no long range of H-9 with H-15a and H-15b. The geminal coupling between H-15a and H-15b was also observed in **211**. This was supported by the two doublets at δ 6.13 and δ 5.98 with a coupling constant of 1.2 and 1.5 Hz. The methoxy protons of **211** were observed as a multiplet at δ 3.60 – 3.57. From this discussion, it was clear that there was a difference in chemical shift between the proton signals of **210** and **211**.

These appreciable differences in the chemical shift, were used to determine the absolute configuration of the enantiopure alcohol (+)-**75a**.

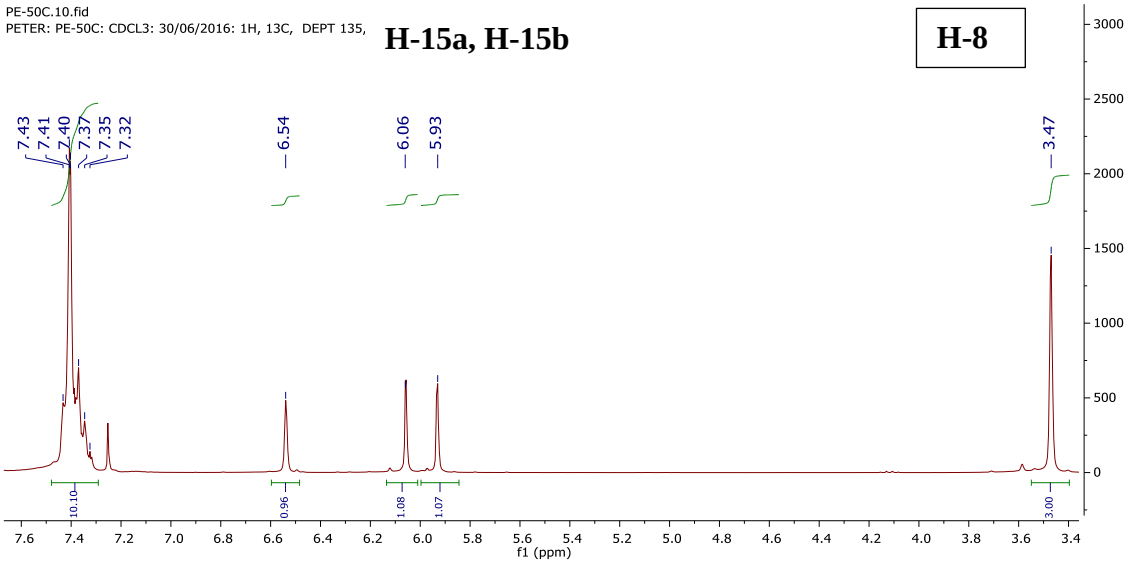

Figure 47: ^{1}H NMR spectrum of *R*-Mosher's ester **210**

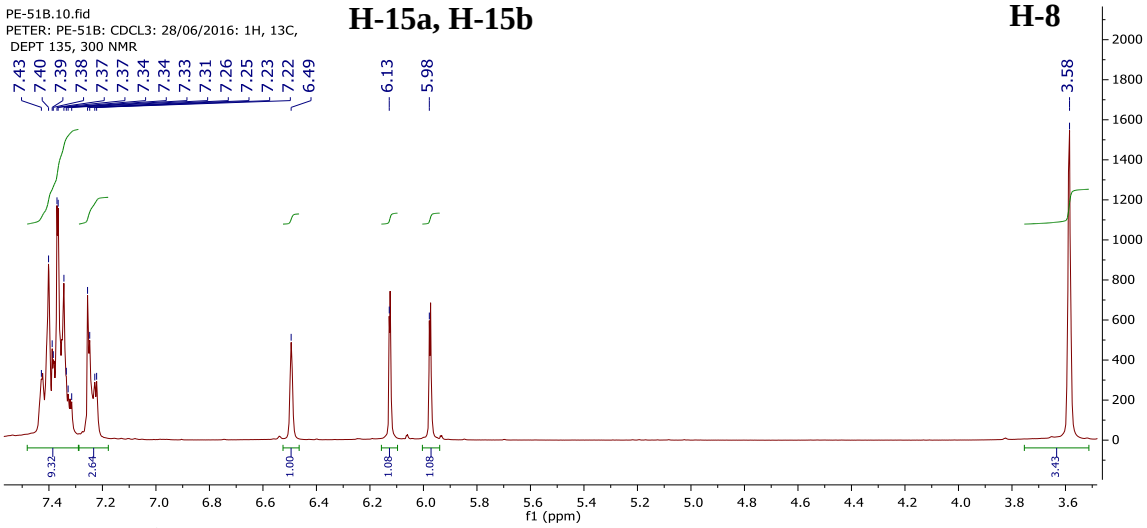

Figure 48: ^{1}H NMR spectrum of *S*-Mosher's ester **211**

By considering the ^{1}H NMR spectrum of Mosher's ester **210** as reference and comparing it with the ^{1}H NMR spectrum of **211**, then one will notice an appreciable chemical shift difference for the vinyl protons (H-15a and H-15b) and methoxy proton H-8. The vinyl protons H-15a and H-15b originating from (+)-**75a** are being shielded by the diamagnetic effect of the aromatic ring from *R*-Mosher's acid (ΔSR = 0.07, δ 6.13 – δ 6.03). This means that the phenyl ring and the vinyl protons are on the same side of the plane. It is also observed that the methoxy protons originating from *R*-Mosher's acid are being shielded by the

diamagnetic effect of the phenyl ring from the enantiopure alcohol (ΔSR = 0.11, δ 3.59 – δ 3.48). This simply means the phenyl ring of the alcohol and the methoxy protons emanating from Mosher's acid are on the same side of the plane. Less easy to see, is the fact that the aromatic protons in **211** are more shielded than those in **210**. All this information supports the stereochemistry of (+)-**75a** to be of *S*-configuration.

The ^{13}C NMR spectrum of **210** showed a total of 16 signals corresponding to 16 carbon atoms that are chemically non-equivalent. The most significant carbon signals which can be used as characteristic peaks were observed at δ 165.2 for C-1, 132.1 for C-15, 115.7 for C-16 and 75.9 for C-9. The precise assignment of C-9 and C-8 was confirmed by the DEPT 135 NMR spectrum. The C-F coupling was observed as expected with $^{1}J_{C\text{-}F}$ value of 289 Hz, $^{2}J_{C\text{-}F}$ value of 28Hz and $^{4}J_{C\text{-}F}$ value of 1Hz. The ^{13}C NMR spectrum of **211** was identical to **210** except that there was a slight difference in chemical shift of the carbon signals. For instance, the carbon signals for **210** appeared at δ132.1 for C-15, 115.7 for C-16 and 75.9 for C-9 while the same carbons signals for **211** appeared at δ 133.2, 116.0 and 76.3 respectively. This was expected as the two Mosher's esters are diastereomers.

The presence of peaks at 2230 cm^{-1} and 1753 cm^{-1} in the IR spectrum of both **210** and **211** confirmed the presence of nitrile and carbonyl functional groups, respectively. The molecular ion of **210** was confirmed by HRMS to be $[M+Na^{+}]$ 398.0985 which was consistent with the mass calculated for $C_{20}H_{16}F_3NO_3Na$ of 398.0980. The HRMS of **210** was the same as that of **211**.

It was convincing that Mosher's protocol chosen was successfully used to assign the absolute configuration of (+)-**75a**. In order to successfully conclude the protocol, and as required for peer-reviewed publication, the confirmation of the absolute configuration of the opposite enantiomer (-)-**75a**, obtained by hydrolysis of the unreacted acetate remaining after resolution was also important. Of course, it should have a stereochemistry that is opposite to the one established earlier.

In order to obtain enantiopure alcohol that was opposite to the alcohol (+)-**75a**, another hydrolysis reaction using Amano lipase from *P. fluorescens* of cat. no. 534730 was set. Similar reaction conditions were used except that the reaction time was increased to 14 days to maximize the enantiomeric excess of the acetate. This led to an enantiopure acetate **105a**

with an enantiomeric excess of 99% and a scalemic mixture of alcohol **75a** with an enantiomeric excess of 84% as shown in **Figures 49** and **Figure 50**. The enantiopure acetate was isolated as a colouress oil in a yield of 73% with a specific optical rotation of -27.8. The enantiopure acetate was hydrolysed by the promiscuous esterase of cat. no ESL-001-01, lot. No 6Y0240 for 30 hours. This step afforded an enantiopure alcohol **75a** in a yield of 99%, enantiomeric excess of 99% and a specific optical rotation of -23.000. The HPLC chromatogram of (-)-**75a** is shown in **Figure 50**.

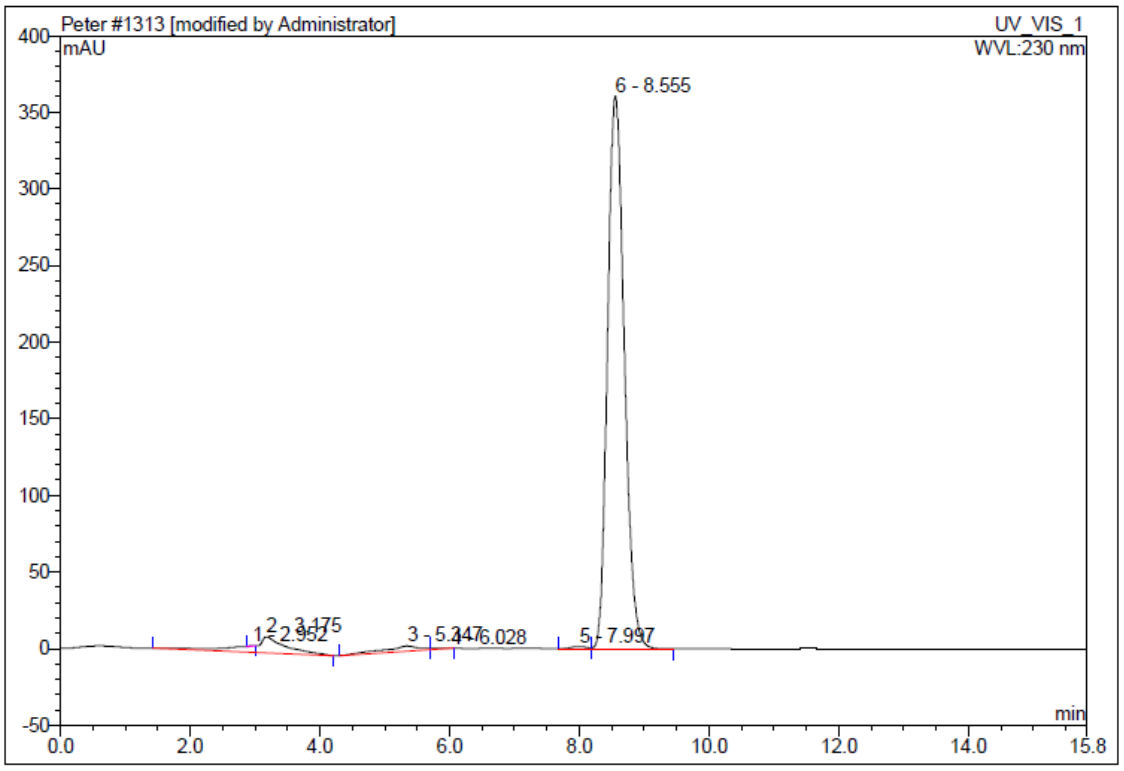

No.	Ret.Time min	Peak Name	Height mAU	Area mAU*min	Rel.Area %	Amount	Type
1	2.95	n.a.	0.383	0.031	0.03	n.a.	Ru
2	3.18	n.a.	10.575	7.285	6.17	n.a.	BMB
3	5.35	n.a.	3.431	2.226	1.89	n.a.	BM
4	6.03	n.a.	0.076	0.182	0.15	n.a.	MB
5	8.00	n.a.	1.307	0.343	0.29	n.a.	BM
6	8.56	n.a.	360.695	107.988	91.47	n.a.	MB
Total:			376.466	118.055	100.00	0.000	

Figure 49: HPLC chromatogram of the isolated enantiopure acetate (-)-**105a**

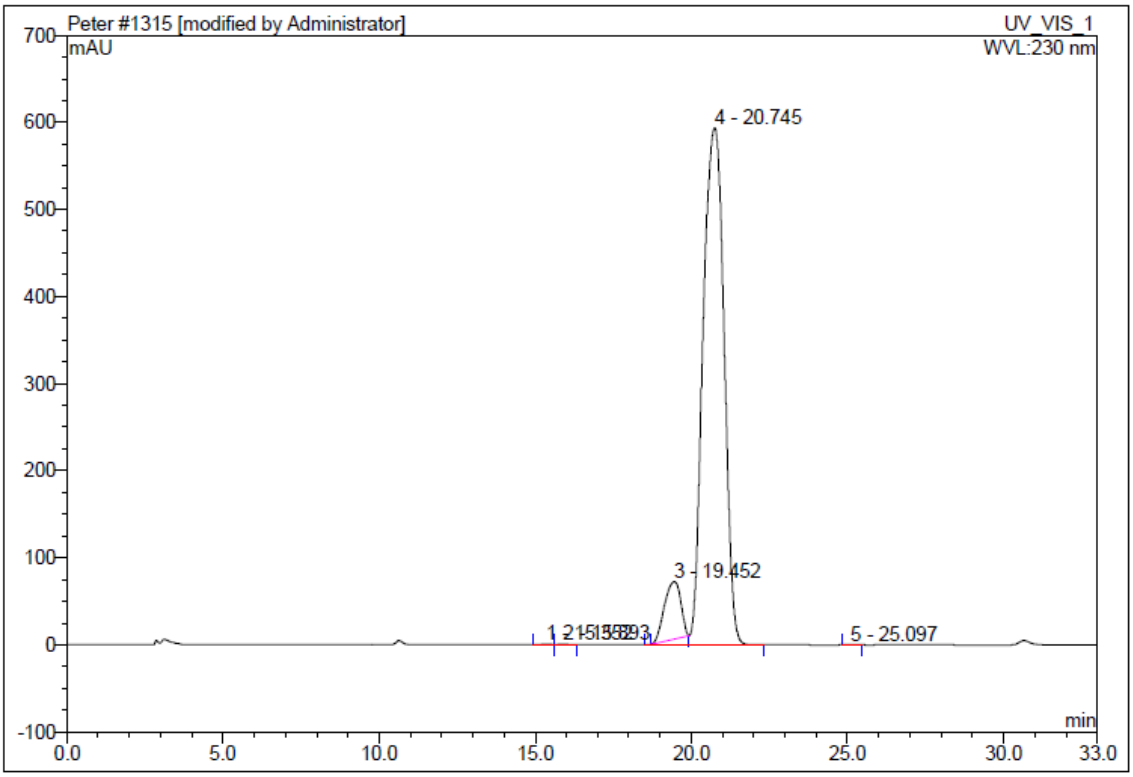

No.	Ret.Time min	Peak Name	Height mAU	Area mAU*min	Rel.Area %	Amount	Type
1	15.35	n.a.	1.045	0.360	0.07	n.a.	BM
2	15.89	n.a.	0.964	0.348	0.07	n.a.	MB
3	19.45	n.a.	65.872	40.180	7.90	n.a.	Ru
4	20.75	n.a.	593.747	467.471	91.95	n.a.	BMB
5	25.10	n.a.	0.087	0.032	0.01	n.a.	BMB
Total:			661.715	508.390	100.00	0.000	

Figure 50: HPLC chromatogram of the isolated scalemic alcohol **75a**

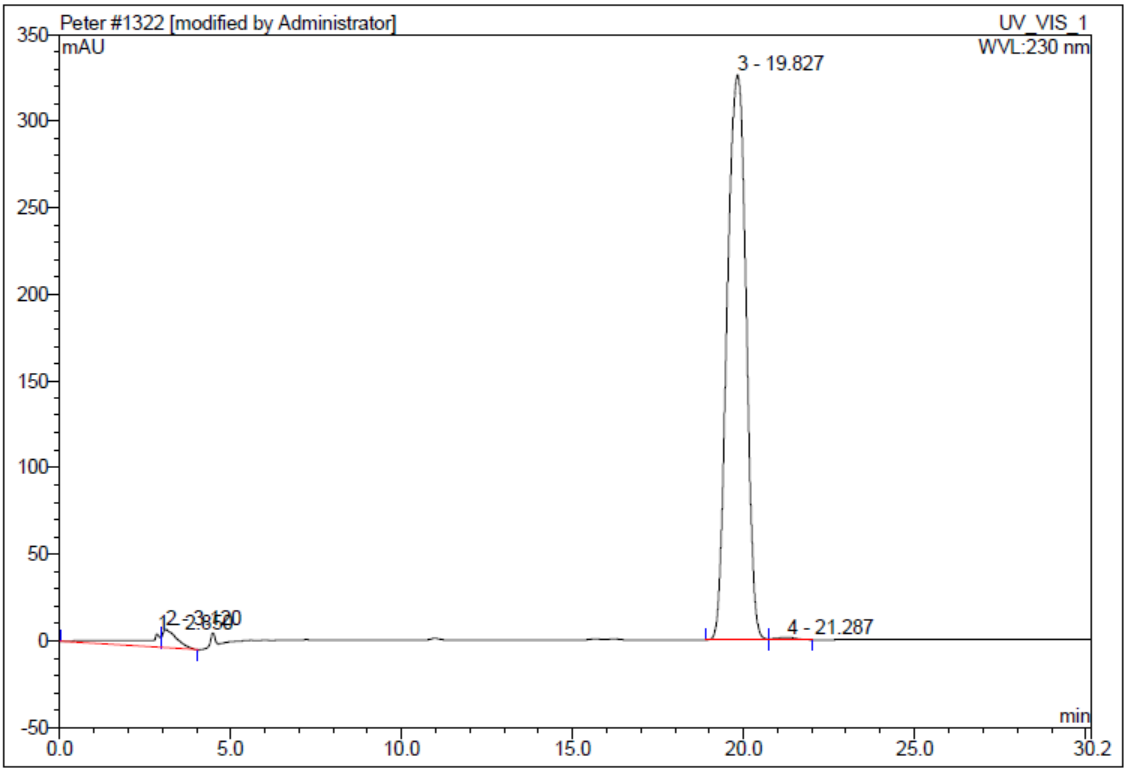

No.	Ret.Time min	Peak Name	Height mAU	Area mAU*min	Rel.Area %	Amount	Type
1	2.85	n.a.	7.601	6.427	2.92	n.a.	BM
2	3.12	n.a.	10.483	5.176	2.35	n.a.	MB
3	19.83	n.a.	325.977	207.923	94.33	n.a.	BM
4	21.29	n.a.	1.241	0.901	0.41	n.a.	MB
Total:			345.302	220.428	100.00	0.000	

Figure 51: HPLC chromatogram of enantiopure alcohol (-)-**75a**

By applying Mosher's protocol of coupling each sample of an enantiopure alcohol (-)-**75a** with (*R*)-(+) and (*S*)-(-)-α-methoxy-α-(trifluoromethyl)phenylacetic acid (MTPA) using dicyclohexyl carbodiimide (DCC) and a catalytic amount of DMAP resulted in Mosher's esters (*R*)-[(*R*)-2-Cyano-1-phenylallyl] 3,3,3-trifluoro-2-methoxy-2-phenylpropanoate **212** and (*S*)-[(*R*)-2-Cyano-1-phenylallyl] 3,3,3-trifluoro-2-methoxy-2-phenylpropanoate **213**. The Mosher's esters were isolated as colourless oils in a yield of 76% for **212** and a yield of 74% for **213**. The synthesis of the Mosher's esters is shown in **Scheme 70**.

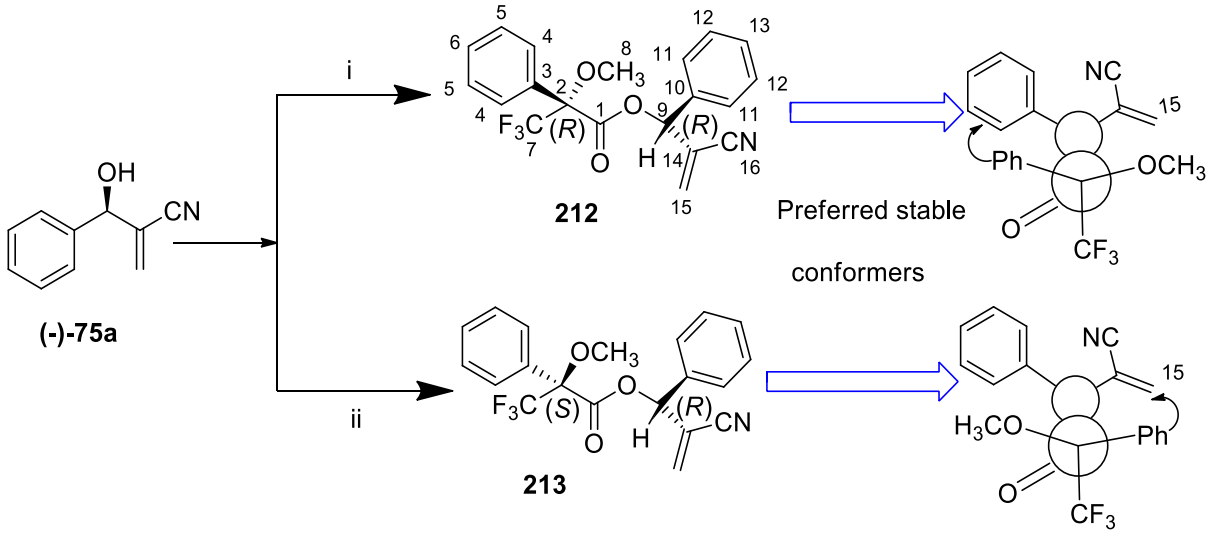

Scheme 70: Synthesis of Mosher's ester **212** and **213**. Reagents and conditions: (i) DCC, DMAP, (*R*)-(+)-MTPA in CH_2Cl_2 at room temperature. (ii) DCC, DMAP, (*S*)-(-)-MTPA in CH_2Cl_2 at room temperature.

The use of spectroscopic techniques was very useful for the confirmation of the structures of the Mosher's esters. The ^{1}H NMR spectrum of **212** showed six signals corresponding to six protons in different chemical environments. There were two multiplets at δ 7.46 – 7.30 and δ 7.24 – 7.20 integrating for nine protons and one proton respectively that were assigned to the aromatic protons. The presence of a singlet at δ 6.50 corresponded well with the stereogenic centre proton H-9. The presence of a singlet for H-9 suggested that there was no observed long range coupling between H-9 and H-15a and H-15b. The visible doublet at δ 6.13 with a geminal coupling value of 1.2 Hz was assigned to H-15a while the coupling partner H-15a appeared as a multiplet at δ 5.99 – 5.97. The methoxy protons appeared as a multiplet at δ 3.61 – 3.58. The ^{1}H NMR spectrum of **213** was the same as that of **212** except that some signals of **213** appeared upfield. In addition, there was one multiplet at δ 7.45 – 7.32 assigned to the ten aromatic protons and stereogenic centre proton H-9 appeared as a multiplet at δ 6.55 – 6.53. The presence of a visible geminal coupling of 1.1 Hz and 1.5 Hz clearly confirmed to us that indeed H-15a and H-15b were attached to the same carbon atom.

The significant difference in chemical shifts of proton signals was used for determining the stereochemistry of the enantiopure (-)-**75a** using the most stable conformer of Mosher's esters.

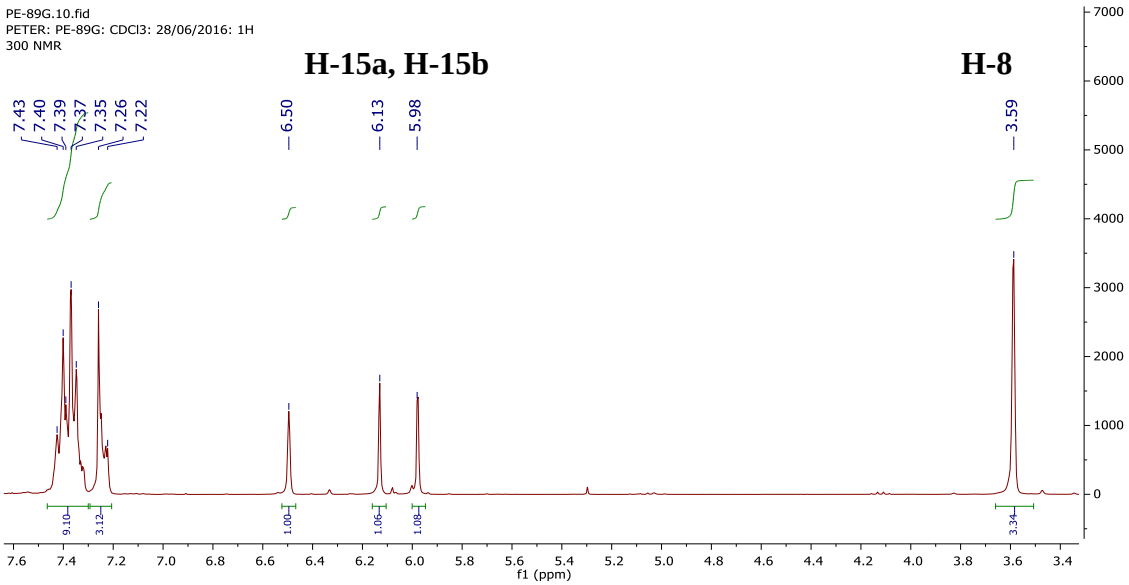

Figure 52: ^{1}H NMR spectrum of the *R*-Mosher's ester **212**

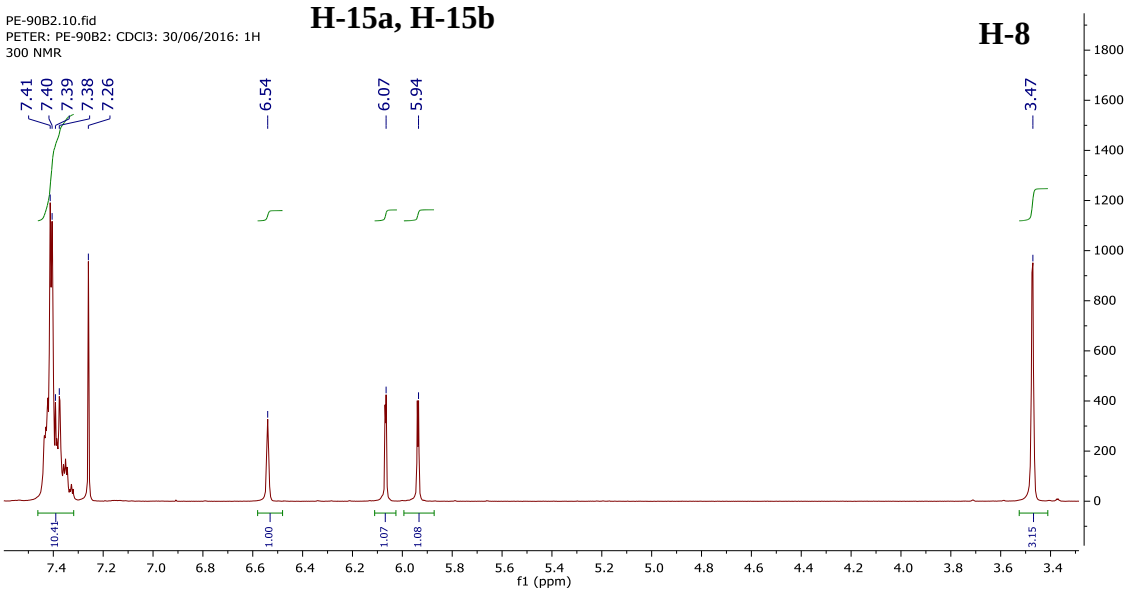

Figure 53: ^{1}H NMR spectrum of the *S*-Mosher's ester **213**

By examining the spectra in **Figures 52** and **53**, then one will notice that protons H-15a, H-15b and H-8 are being shielded or deshielded by the diamagnetic effect of the phenyl ring originating from either Mosher's acid or enantiopure alcohol depending on the reference spectrum chosen. It is visible that the vinyl protons of the alcohol are deshielded by the phenyl group from (*R*)-MTP acid (ΔSR = -0.06, δ 6.07 – δ 6.13). This means that the vinyl protons (H-15a, H-15b) and the phenyl ring of (*R*)-MTP acid are on opposite sides of the plane. This was a confirmation that for sure the stereochemistry of (-)-**75a** is of *R*-configuration.

The ^{13}C NMR spectra of both **212** and **213** showed a total of 16 signals corresponding to 16 carbon atoms that are in different chemical environments. Both spectra showed C-F coupling as expected with $^{1}J_{C\text{-}F}$ value of 289 Hz, $^{2}J_{C\text{-}F}$ value of 28Hz, and $^{4}J_{C\text{-}F}$ value of 1Hz. The other characteristic carbon signals of **212** were observed at δ 165.2 for C-1, 133.1 for C-15 and 116.0 for C-16 while the same carbon signals appeared at δ 165.2, 132.1 and 115.6 for **213**. The difference in the chemical shifts of carbon signals between the two Mosher's esters is a confirmation that truly the two compounds are diastereomers.

The presence of nitrile and carbonyl functional groups was confirmed by the appearance of signals at 2230 cm^{-1} and 1753 cm^{-1} respectively in the IR spectra for both **212** and **213**. The molecular ion of both **219** and **220** was confirmed by HRMS to be $[M+NH_4^+]$ 393.1412 and 393.1429 respectively which was consistent with the mass calculated for $C_{20}H_{20}F_3N_2O_3Na$ of 393.1421.

By analysing the ^{1}H and ^{13}C NMR spectra of the four Mosher's esters, then it is true that the spectrum of **210** is identical to the spectrum of **213** meaning that these two compounds are mirror images of each other. Conversely, the spectrum of **211** is the same as to the spectrum of **212** implying that these two compounds are also mirror images of each other.

The remaining enzymes that were tested hydrolysed the acetate of the opposite configuration, affording alcohol of *R*-configurations (**Scheme 71**). These enzymes are shown in **Table 25**.

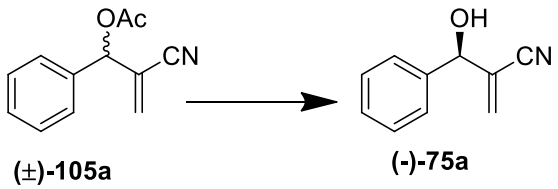

Scheme 71: Hydrolysis of **105a** using different lipases in phosphate buffer at pH-7.00 leading to the formation of (-)-**75a**

Table 25: Hydrolysis of **105a** using different enzymes affording (-)-**75a**

Entry	Enzyme name	Time (h), Temp (°C)	Conv (%)	ee_s (%)	ee_p (%)	E
1	XP-415	60, 30	54	55	48	5
2	Lipase AY AMANO IAYTO2510	96,30	37	16	28	2
3	Lipase F-AP15 LFW02523	20, 30	73	89	33	5
4	Lipase-L036P Batch no 14397 (Biocatalyst)	93, 30	78	88	25	4
5	Lipase AY "Amano" from *Candida rugosa* LAYA0750964	46, 30	71	22	9	1
6	Lipase AS Amano LAW035145 (from *Aspergillus niger*)	3, 30	75	90	30	5
7	Lipase from *Candida rugosa* cat. no. 62316	24, 30	67	19	9	1
8	Lipase from Wheat germ cat. no. 62306	18, 30	46	5	7	1
9	Lipase from *Rhozopus arrhizus* cat. no. 62305	24, 30	19	12	51	3

Unfortunately, none of the enzymes in **Table 25** had an acceptable enantiomeric ratio (E) of 15 and above, meaning that the practical use of any of these enzymes is not beneficial in any way. The lipases giving the best E values were lipase F-AP15 LFW02523, Lipase-L036P and Lipase AS Amano LAW035145 (**Table 25**, **entry 3**, **4** and **6**). These enzymes led to a reasonable enantiomeric excess of the substrate (ee_s) of above 88%. The HPLC chromatogram of Lipase F-AP15 LFW02523 (e**ntry 3**) is shown in **Figures 54** and **55**.

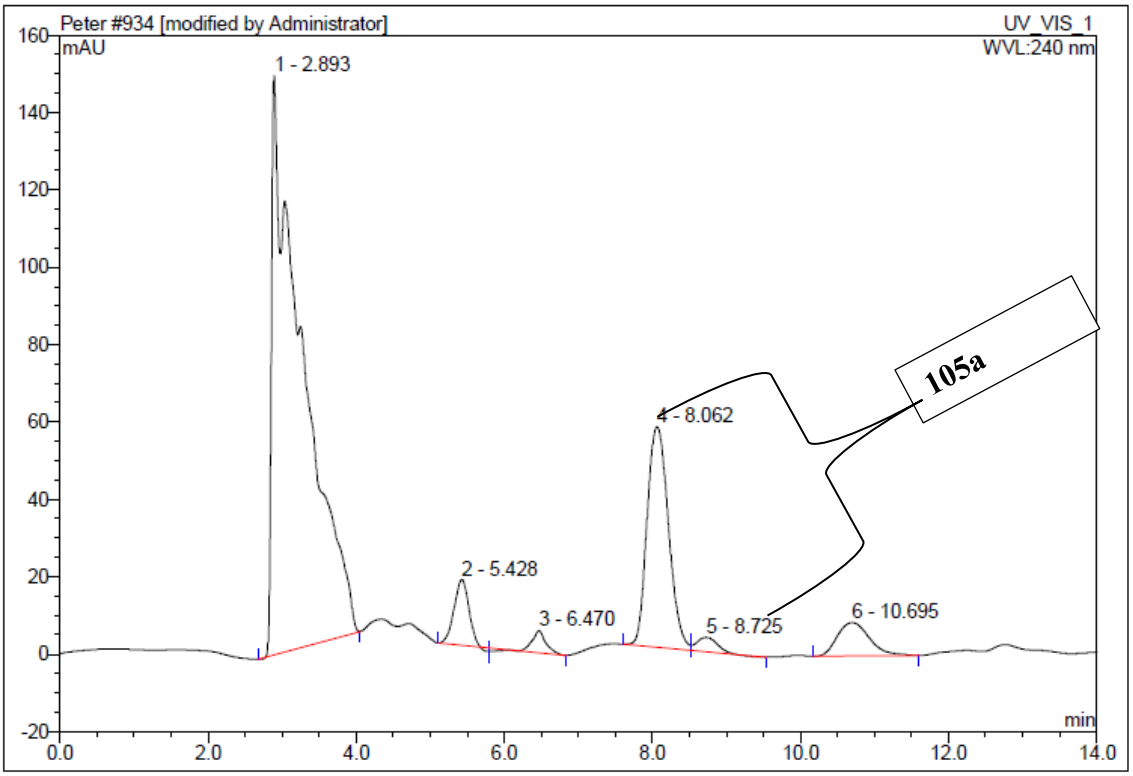

No.	Ret.Time min	Peak Name	Height mAU	Area mAU*min	Rel.Area %	Amount	Type
1	2.89	n.a.	149.630	70.871	70.58	n.a.	BMB*
2	5.43	n.a.	17.013	3.904	3.89	n.a.	BM *
3	6.47	n.a.	5.725	1.098	1.09	n.a.	MB*
4	8.06	n.a.	56.946	19.055	18.98	n.a.	BM *
5	8.73	n.a.	3.679	1.115	1.11	n.a.	MB*
6	10.70	n.a.	8.619	4.377	4.36	n.a.	BMB
Total:			241.611	100.419	100.00	0.000	

Figure 54: HPLC chromatogram of the acetate **105a** after enzymatic activity of Lipase F-AP15 LFW02523 after 20 hours at 30 °C

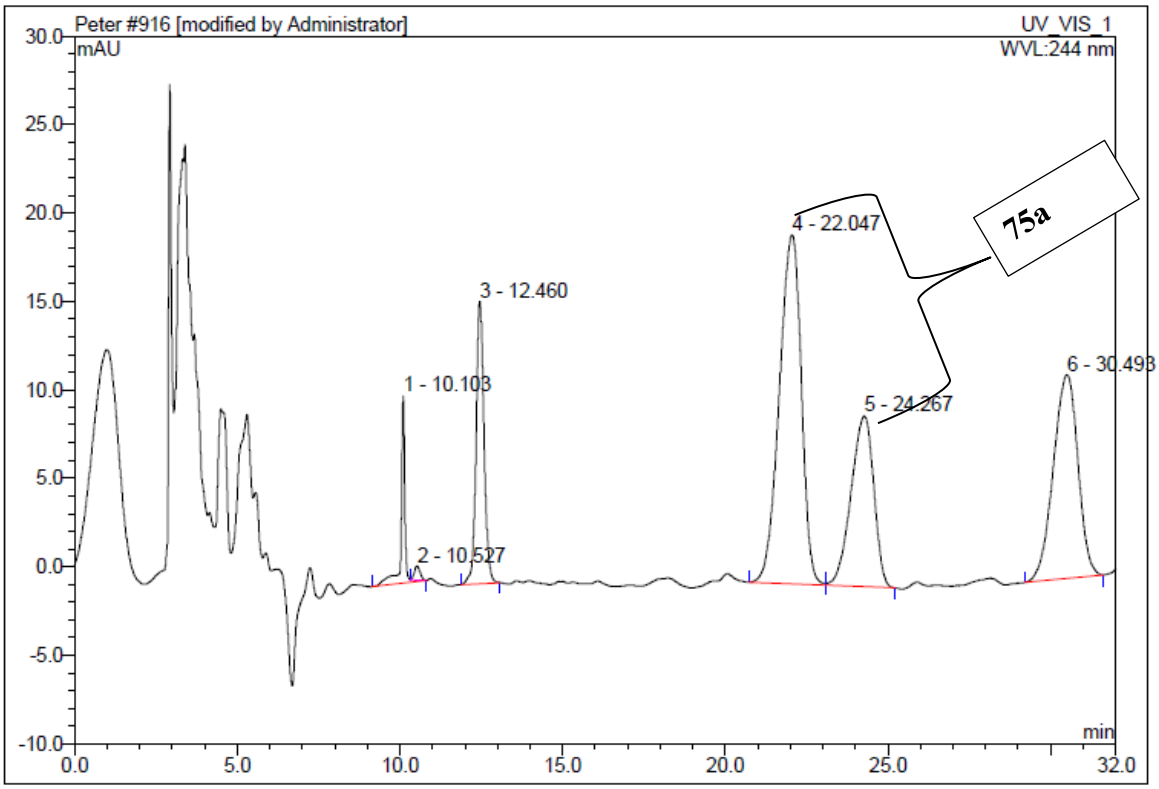

No.	Ret.Time min	Peak Name	Height mAU	Area mAU*min	Rel.Area %	Amount	Type
1	10.10	n.a.	10.587	1.393	3.53	n.a.	BMB*
2	10.53	n.a.	0.811	0.161	0.41	n.a.	Rd
3	12.46	n.a.	15.968	4.519	11.45	n.a.	BMB
4	22.05	n.a.	19.728	15.465	39.17	n.a.	BM *
5	24.27	n.a.	9.649	7.825	19.82	n.a.	MB*
6	30.49	n.a.	11.526	10.121	25.63	n.a.	BMB
Total:			68.269	39.484	100.00	0.000	

Figure 55: HPLC chromatogram of the alcohol **75a** after enzymatic activity of Lipase F-AP 15LFW02523 after 20 hours at 30 °C

3.2.7.6 Comparing enzymatic results arising from hydrolysis of the racemic acetate 105a with literature material

The outstanding enzymes that hydrolysed *S*-acetate of **105a** with reasonable enantiomeric ratio (E) were different preparations of lipase AK, Lipo Max Cxt 1.00, Lipozyme® CALB L LCN 02106, Novozym 435 LC, Lipase from *Candida antarctica* type B, Lipase from *P. fluorescens*, and Lipase from *P. cepacia* (**Table 24, page 121**).

By perusing literature, it is a fact that lipase AK "Amano" of different preparations stems from *P. fluorescens* while Lipo Max Cxt 1.00 originates from *P alcaligenes*.[168, 169] It is also

true that lipozyme® CALB L LCN 02106 and Novozym 435 LC are lipase from *Candida antarctica* type B with Novozym 435 being an immobilized form of CALB.[170] Therefore by comprehensively analysing lipases from *P. fluorescens*, *P. alcaligenes*, *P. cepacia*, and lipase from *C. antarctica* type B will enable one to draw some conclusions as to why they performed very well on racemic acetate **105a**.

As mentioned earlier, lipase F-AP15 LFW02523, Lipase-L036P and Lipase AS Amano LAW035145 can be used to hydrolyse the *R*- acetate of **105a.** It is well established from literature that lipase F-AP15 and lipase L036P originate from *Rhizopus oryzae* while lipase AS Amano emanates from *Aspergillus niger*.[171, 172] Consequently, the observed performance of this enzyme can only be explained by looking at chemical characteristics of lipases from *Rhizopus oryzae* and *Aspergillus niger*. The critical question that can be answered later after analysing the performance of all enzymes on different substrates is why enzymes in **Table 24** hydrolyse the *S*-acetate of **105a** while the enzymes in **Table 25** hydrolyse the *R*-acetate of **105a**.

The kinetic resolution of the racemic **105a** by both hydrolysis and esterification has been reported in literature. In the first report, Basavaiah used crude pig liver acetone powder (PLAP) to hydrolyse (±)-**105a** in a mixture of ether and phosphate buffer for 24 hours affording scalemic **75a** with a yield of 14% and enantiomeric excess (ee) of 60%.[173] The use of this enzyme is not the best as it gave very poor enantiomeric excess of 60% that lowers the chances of being used for synthetic application. The second report made use of *Pseudomonas cepacia* lipase in the presence of acyl donors to resolve racemic **75a**.[82] Unfortunately, the results were not attractive as a scalemic mixture of **105a** with an ee of 76% was obtained after 33 days. In addition, the low percentage conversion of 9% at ee of 76% was too discouraging. The third report which was aimed at synthesizing enantiopure MBH amides using *Rhodococcus erythropolis* SET1 also resulted to the formation of scalemic **75a** with a yield of 72.4% and disappointing ee of 18.7 after 5 days.[69] The last report describes resolution of (±)-**75a** using chemical means.[174] In this report the undetermined optical rotation of enantiopure alcohol **75a** was obtained in a yield of 13% with an ee of 93%. These four reports were incomplete as the major task of stereochemical determination was not done. All these limitations make this work on resolving (±)-**105a** outstanding because the stereochemically confirmed isolated enantiopure **75a** that has a lot of synthetic potential is being reported for the first time.

The use of racemic **75a** as a starting material for the synthesis 1-benzyl-5-[(4-chloro-phenyl)-methoxy-methyl]-3-(3,4-dichloro-phenyl)-4-imino-tetrahydro-pyrimidine **214** heterocyclic compound **215** and **216** has been explored.[175, 176] The report on the synthesis of **214**, **215** and **216** is sketchy as it would have been more appealing if the synthetic methodology would have used enantiopure **75a** and the stereoselectivity had been controlled throughout the reaction. This would have been very important, especially for compound **214** which has shown significant antibacterial activity. The situation is not different on a racemic **75a** that has been reported to display antipyroptotic activity.[177] The reported antipyroptotic activity can only make sense if the data for each enantiomer of **75a** is available. These three illustrations demonstrate how important our stereochemically determined enantiopure **75a** is for addressing the inconclusive reported reactions.

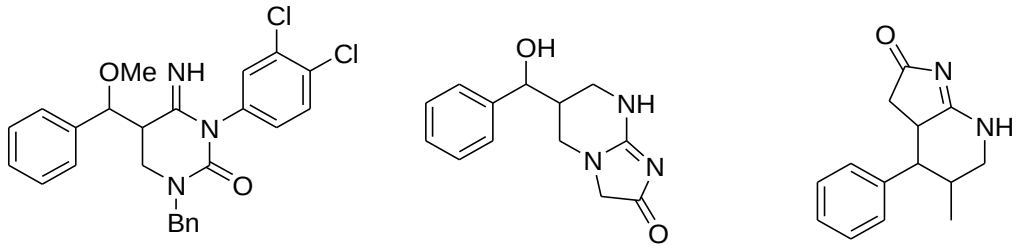

214 **215** **216**

Figure 56: Reported compounds that have been synthesized using racemic **75a**

After successfully resolving the racemic **105a**, and successfully employing Mosher's protocol, it was now time to challenge the enzymes by substituting the acetate group with other ester groups of varying chain lengths. To make the work easier, only enzymes that displayed activities on **75a** were chosen for investigating the resolution of esters. The synthesis of the esters has been described earlier. These esters are (±)-2-cyano-1-phenylallyl 2-chloroacetate **202**, (±)-2-cyano-1-phenylallyl butyrate **203** and (±)-2-cyano-1-phenylallyl 3-methylbutanoate **204** (**Scheme 61**).

3.2.7.7 Resolution of (±)-2-Cyano-1-phenylallyl 2-chloroacetate 202

The first compound which was screened using the earlier procedure was **202**. This racemic ester dissolved in acetone was added to an Eppendorf tube containing phosphate buffer at pH 7.00 (**Scheme 72**). The mixture was put on an orbital shaker at 30 °C for 15 hours and the results arising from this are shown in **Table 26**. For the reaction to be monitored accurately, both **202** and **75a** were resolved on a Lux-3µm chiral column using a mobile flow rate of 1 mL/min. The composition of the mobile phase used was hexane and IPA in the ratio of 96:4 (**Figures 57** and **58**).

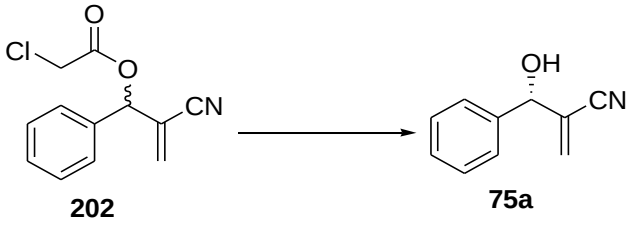

202 **75a**

Scheme 72: Hydrolysis of **202** using different lipases at pH-7.00 affording **75a** after 15 hours

Table 26: Hydrolysis of **202** using different lipases affording **75a** at 30 °C

Entry	Enzyme name	Conv (%)	ee_s (%)	ee_p (%)	E
1	Lipase AK-D "Amano" II ILAKX02509K	52	6	5	1
2	Lipase AK-D "Amano" II LAKXW250N	68	7	3	1
3	Lipase AK "Amano" 59.001	41	15	22	2
4	Lipase AK "Amano" 20.ILAKAFF0151102R	7	6	74	7
5	Lipase AK "Amano" II ILAKW1150	20	3	11	1
6	Lipase AK "Amano" II LAKW09504	13	7	49	3
7	Lipase AK "Amano" LAKY07570	15	13	73	7
8	Novozym 435 LC 200217	12	8	58	4
9	Amano lipase from *Pseudomonas fluorescens* cat. no. 534730	15	16	89	21

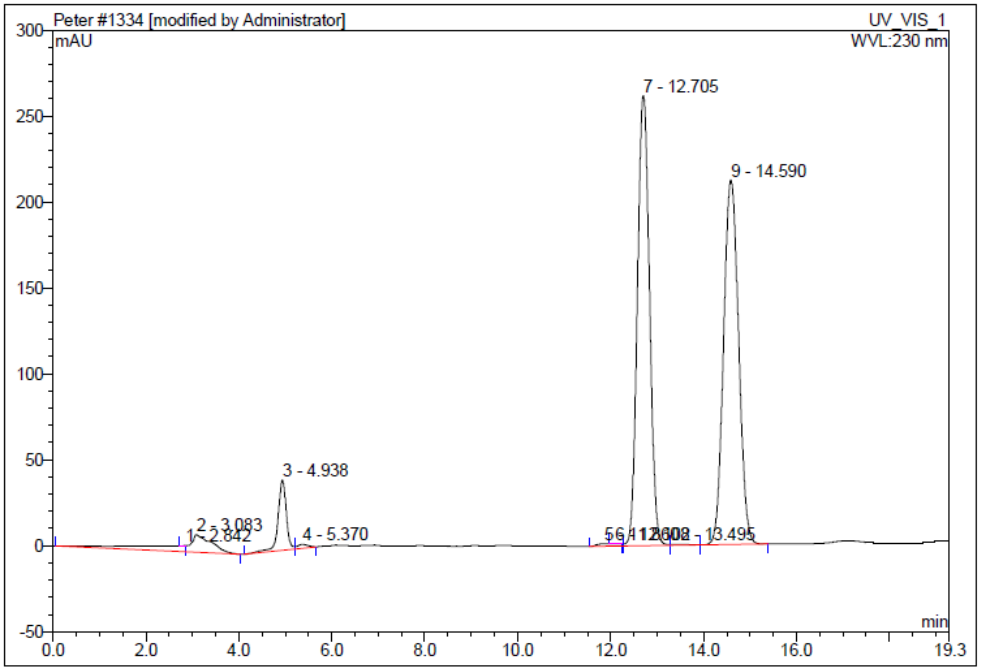

No.	Ret.Time min	Peak Name	Height mAU	Area mAU*min	Rel.Area %	Amount	Type
1	2.84	n.a.	0.039	0.005	0.00	n.a.	Ru
2	3.08	n.a.	10.220	9.735	5.45	n.a.	BMB
3	4.94	n.a.	40.847	8.427	4.72	n.a.	BM *
4	5.37	n.a.	2.205	0.594	0.33	n.a.	MB*
5	11.86	n.a.	1.502	0.822	0.46	n.a.	BM *
6	12.10	n.a.	0.222	0.037	0.02	n.a.	Rd
7	12.71	n.a.	261.806	78.932	44.22	n.a.	M *
8	13.50	n.a.	0.542	0.210	0.12	n.a.	M *
9	14.59	n.a.	212.020	79.736	44.67	n.a.	MB*
Total:			529.403	178.498	100.00	0.000	

Figure 57: HPLC chromatogram of the racemic ester **202**

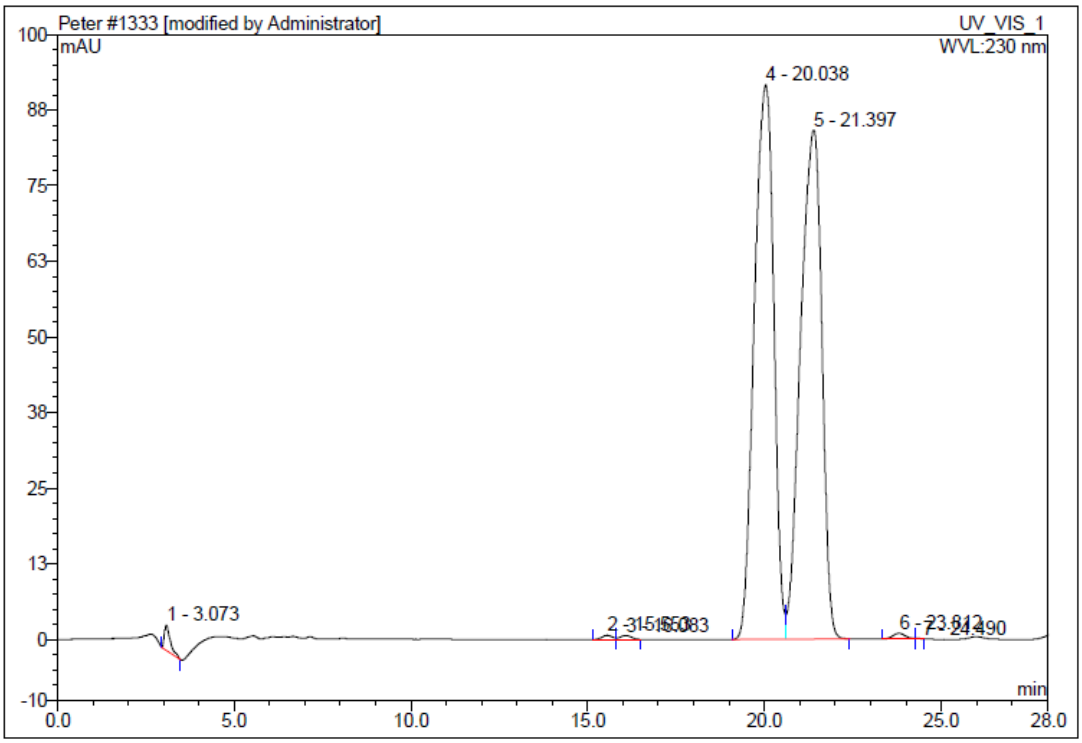

No.	Ret.Time min	Peak Name	Height mAU	Area mAU*min	Rel.Area %	Amount	Type
1	3.07	n.a.	4.134	0.817	0.69	n.a.	BMB
2	15.55	n.a.	0.688	0.228	0.19	n.a.	BM
3	16.08	n.a.	0.673	0.228	0.19	n.a.	MB
4	20.04	n.a.	91.608	58.453	49.23	n.a.	BM *
5	21.40	n.a.	84.091	58.619	49.37	n.a.	MB*
6	23.81	n.a.	0.943	0.387	0.33	n.a.	BM
7	24.49	n.a.	0.001	0.009	0.01	n.a.	MB
Total:			182.138	118.741	100.00	0.000	

Figure 58: HPLC chromatogram of racemic alcohol **75a**

Apart from Amano lipase from *Pseudomonas fluorescens* cat. no. 534730 which displayed an enantiomeric ratio (E) of 21 (**Table 26**, **Entry 9**), the rest of the enzymes performed poorly to an extent that their use on this substrate cannot be recommended. The average performing enzyme, Amano lipase from *P. fluorescens* had an ee_p of 89% but with very poor ee_s of 16% at a conversion of 15%. The obtained enantiomeric ratio (E) of 21 is not significant given that the conversion is very low. The presence of a halogen atom has been documented to improve enantioselectivity but it terribly lowered the enantioselectivity on this substrate.[178] All the enzymes in **Table 26** originate from *Candida antarctica* type B and *Pseudomonas fluorescens*. It was now time to find out the performance of similar enzymes if the butanoic ester derivative was used.

3.2.7.8 Resolution of (±)-2-Cyano-1-phenylallyl butyrate 203

This was the second compound to scrutinize using a similar procedure as described in section 3.7.7.7 with the difference of applying two different columns for the racemic **203** and **75a**. Separation conditions for the racemic **75a** had already been established and therefore the only task was to find the chromatographic conditions for separating the racemic **203**. The column that was able to separate **203** was chiral Lux 5µm cellulose-1. The mobile phase that composed of hexane and IPA in the ratio of 96:4 with a flow rate of 1 mL/min achieved this. The HPLC chromatogram of **203** is shown in **Figure 59**. The results arising from this inquiry are shown in **Table 27**.

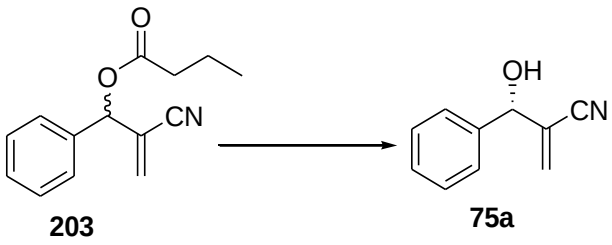

203 **75a**

Scheme 73: Hydrolysis of **203** using different lipases leading to the formation of **75a** in phosphate buffer at pH-7.00 after 15 hours

Table 27: Hydrolysis of **203** using different enzymes affording **75a**

Entry	Enzyme	Time (h)	Conv (%)	ee_s (%)	ee_p (%)	E
1	Lipase AK-D "Amano" II SLAKX02509K	120	3	2	89	18
2	Lipase AK-D "Amano" II LAKXW250N	96	14	14	86	15
3	Lipase AK "Amano" 59.001	96	32	42	90	29
4	Lipase AK "Amano" 20.ILAKAFF0151102R	96	11	10	88	17
5	Lipase AK "Amano" II ILAKW1150	120	34	44	86	21
6	Lipase AK "Amano" II LAKW09504	96	1	1	92	23
7	Lipase AK "Amano" LAKY07570	96	20	22	89	21
8	Novozym 435 LC 200217	96	25	33	98	180
9	Amano lipase from *Pseudomonas fluorescens* cat. no. 534730	96	2	2	88	16

The racemic **203** performed better as compared to **202** implying that the long chain butyl group seems to have interacted well with active sites of the enzymes investigated as compared to the chloro derivative. It is observed that the enzymes in **Table 27** gave an acceptable enantiomeric ratio of 15 and above. However, only four enzymes are observed to be very good as their conversions of 20% and above are reasonable. These are lipase AK "Amano" 59.001, lipases AK "Amano" II ILAKW1150, lipase AK "Amano" LAKY07570 and Novozym 435 LC 200217 (**Table 27**, **entry 3**, **5**, **7** and **8**). Although the enantiomeric excess of the substrates (ee_s) of these enzymes were not good, their enantiomeric excess of the product (ee_p) were better. The enzymes that showed significant hydrolytic activity can simply be grouped into two lipases; lipase from *Pseuodomonas fluorescens* and lipase from *C. antarctica* (CALB).

No reaction at all took place during the attempted resolution of (±)-2-cyano-1-phenylallyl 3-methylbutanoate **204** despite varying the temperature, reaction times and enzyme loading. This is not strange as enzymes are very specific with the substrate they are able to hydrolyse and this compound has a branched substituent, which is not always acceptable to enzymes.

After successfully working on the acetate and esters of acrylonitrile derivative, the next compounds for investigation were the acrylonitrile derivatives as discussed in the following sections.

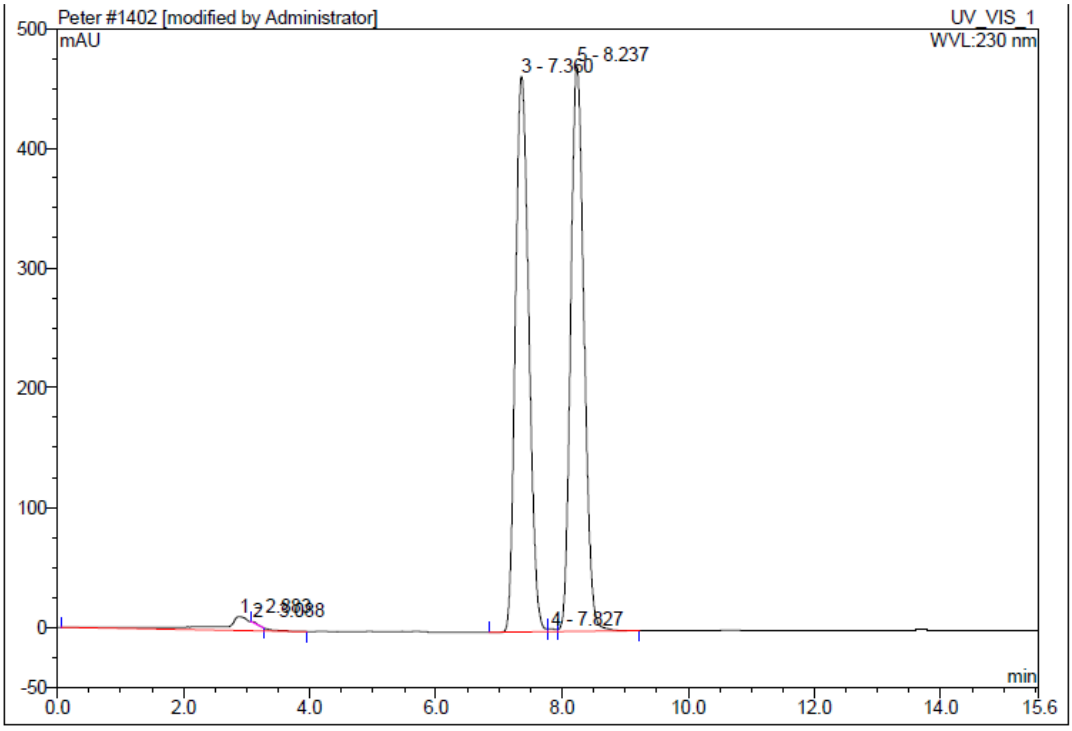

No.	Ret.Time min	Peak Name	Height mAU	Area mAU*min	Rel.Area %	Amount	Type
1	2.88	n.a.	11.615	8.034	3.37	n.a.	BMB
2	3.09	n.a.	0.794	0.102	0.04	n.a.	Rd
3	7.36	n.a.	463.766	114.549	47.99	n.a.	BM *
4	7.83	n.a.	2.249	0.297	0.12	n.a.	M *
5	8.24	n.a.	473.150	115.687	48.47	n.a.	MB*
Total:			951.574	238.669	100.00	0.000	

Figure 59: HPLC chromatogram of the racemic **203**

3.2.7.9 Resolution of (±)-(E)-4-cyano-1-phenylpenta-1,4-dien-3-yl acetate 200

The next compound to investigate was the acetate (±)-(*E*)-4-cyano-1-phenylpenta-1,4-dien-3-yl acetate **200**. We were curious to find out what the effect would be of increasing the length and rigidity between the phenyl ring and the acetate group. A similar procedure as previously described of dissolving **200** in acetone and introducing the solution to buffer containing the enzyme as shown in **Scheme 74** was used. A total of 101 enzymes were screened and monitored by HPLC using a C18-column. The enzymes consisted of lipases and esterases of different preparations. Those enzymes that showed activity were further investigated for enantioselectivity using chiral HPLC.

In order to investigate the enzymatic activities of different enzymes and their enantiomeric ratio (E) from the beginning of the reaction and after a certain period of reaction time, it was

necessary to establish the chromatographic conditions for separating the racemic acetate **200** and racemic alcohol (±)-(*E*)-3-hydroxy-2-methylene-5-phenyl-4-pentenenitrile **191**. Using the chiral Lux 5µm cellulose-1 column and applying a mobile flow rate of 1 mL/min consisting of hexane: IPA (90:10) led to the separation of **200** and **191** as shown in **Figure 60**.

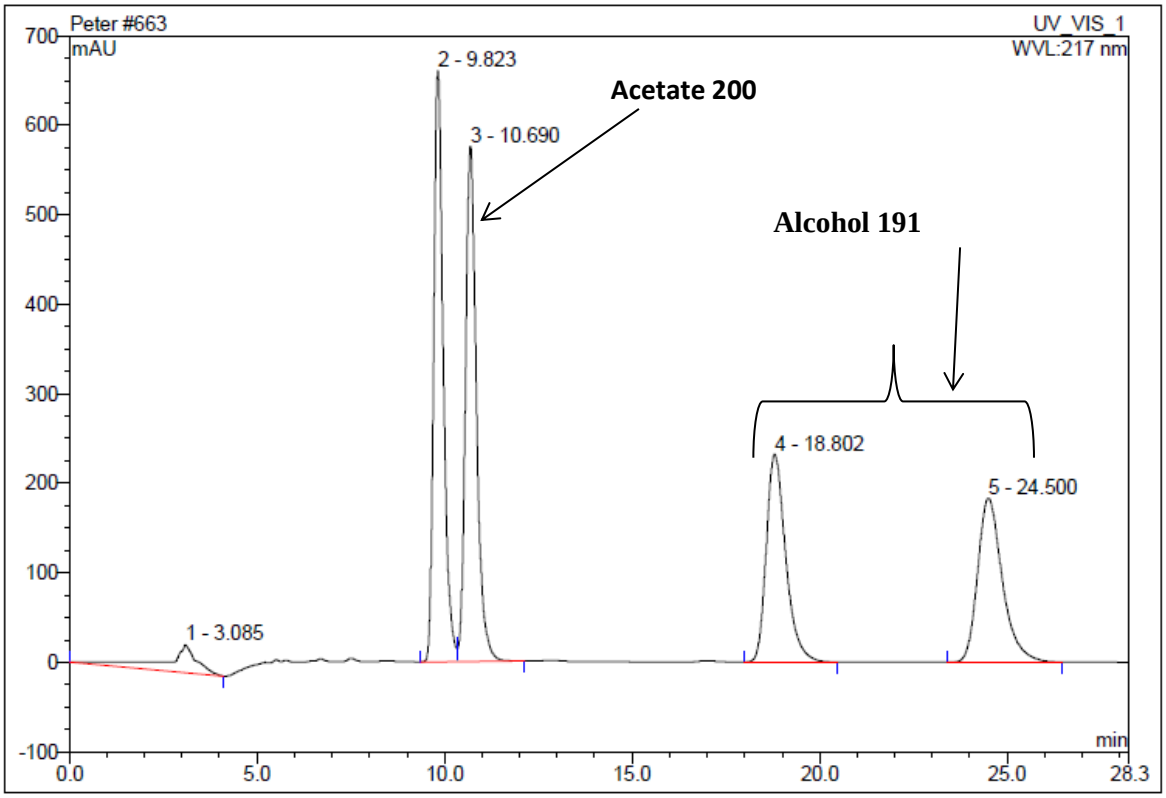

No.	Ret.Time min	Peak Name	Height mAU	Area mAU*min	Rel.Area %	Amount	Type
1	3.09	n.a.	30.880	31.437	4.49	n.a.	BMB
2	9.82	n.a.	659.694	195.468	27.91	n.a.	BM
3	10.69	n.a.	575.474	194.382	27.75	n.a.	MB
4	18.80	n.a.	231.925	139.190	19.87	n.a.	BMB
5	24.50	n.a.	183.015	139.896	19.97	n.a.	BMB
Total:			1680.987	700.372	100.00	0.000	

Figure 60: HPLC Chromatogram of the racemic acetate **200** and the racemic alcohol **191**

The results obtained by monitoring the reactions using chiral column chromatography are shown in **Table 28**.

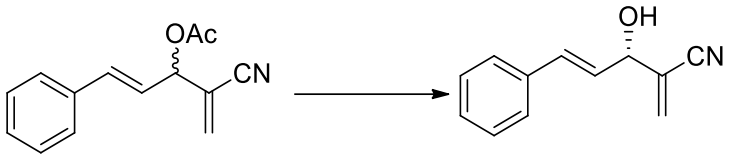

200 **(+)-191**

Scheme 74: Hydrolysis of **200** using different lipases and esterases in phosphate buffer at pH-7.00 at different temperatures

Table 28: Hydrolysis of **200** using different enzymes affording **191**

Entry	Enzyme name	Time (h), Temp (°C)	Conv (%)	ee_s (%)	ee_p (%)	E
1	Lipase AK "Amano" Lot No. lakwa09504	3, 20	46	72	85	27
2	Lipase AK "Amano" Lot No. 59.001	24,20	26	30	87	20
3	Lipase AK "Amano" Lot No. LAKVO7510	15, 20	26	30	85	16
4	Amano Lipase AK Lot no. 0351202	48, 20	39	61	96	100
5	Lipase AK " Amano II" ILAKKW1150	14, 25	34	48	93	46
6	Lipase AK " Amano III" AKK026094	14, 25	12	13	93	29
7	Lipase AK-D "Amano" III ILAKX02509K	21, 25	16	17	86	16
8	Lipase AK-D "Amano" II ILAKXW250N	21, 25	21	22	85	15
9	Lipase AK CJ Solut N (lot no E 54-001)	17, 20	2	2	85	13
		23.5, 20	17	18	85	15
10	Esterase Cat no. ESL-001-01, 720268	1, 20	58	60	43	5
11	Esterase Cat no. ESL-001-01, 6Y0240	1, 20	44	43	54	5
12	Esterase Cat no. ESL-001-01 with CUT stabilizer	1,20	62	68	42	5
13	Esterase Cat no. ESL-001-01, 6Z0248	0.5, 20	52	73	67	11
14	Lipase L036P batch no. 143971 (from Biocatalysis)	3, 20	16	14	72	7
15	Lipozyme® CALB L LCN 02106	3, 20	20	24	96	70
16	Lipozyme® CALB L (from Novozyme)	24, 20	18	22	96	67
17	Lipase *Candida antarctica* type B	3, 20	44	69	89	37
18	Novozym 435 LC200233	15, 20	10	11	95	41
19	Lipo Max Cxt 1.00	3, 20	24	29	93	36
20	Lipase sigma (EC-3.1.10) type II crude from porcine pancrease	21, 25	20	7	28	2
21	Lipase hog pancrease (62300. biochemika)	14, 25	16	11	58	4
22	Lipase from *Rhizopus neveus* (62310 biochemika)	35, 30	14	3	16	1
23	EST DM esterase ZA Biotech	17, 20	9	5	49	3
24	ESL CI esterase ZA Biotech	1.5, 20	17	10	47	3
25	Amano Lipase from *Pseudomonas fluorescens* cat. no. 534730	17, 20	35	24	45	3
		23.5, 20	34	17	33	2

Entry	Enzyme name	Time (h), Temp (°C)	Conv (%)	ee_s (%)	ee_p (%)	E
26	Lipase from *pseudomonas fluorescens* cat no. 95608	72, 30	51	96	93	100
27	Lipase from *pseudomonas cepacia* cat. no. 62309	5, 30	23	6	20	2

Table 28 shows that a total of fifteen enzymes afforded an acceptable overall enantiomeric ratio (E) of 15 and above. These enzymes were all lipase AK (**entries 1-9**) and Lipozyme® CALB L (**entries 15-16**) of different preparations, Lipo Max cxt (**entry 19**), lipase from *Candida antarctica* (**entry 17**), Novoym 435 LC200233 (**entry 18**), and lipase from *Pseudomonas fluorescens* (**entry 26**). Among these enzymes, eight enzymes gave an enantiomeric excess of product (ee_p) greater than 90% (**entries 4-6, 15-16, 18-19** and **entry 26**) while three gave an ee_p of more than 85% (**entry 2, 7, 17**). The rest of the tested enzymes performed poorly as their enantiomeric ratio (E) values were below 15 (**entry 9, entries 10-14, entrie 20-25** and **entry 27**).

Amano Lipase AK Lot no. 0351202 (**entry 4**) and lipase from *Pseudomonas fluorescens* (**entry 26**) showed good conversion and better enantioselectivity. Lipase from *P. fluorescens* (**entry 26**) performed excellently by affording an enantiomeric excess of the substrate (ee_s) of 96% and an enantiomeric excess of the product (ee_p) of 93% with an overall enantiomeric ratio (E) of 100 after 72 hours at 30 °C. From experience, it is rare to come across an enzyme that has a selectivity of this nature on an unnatural substrate, unless it is a bioengineered enzyme. The percentage of ee_s, conversion (conv) and ee_p were compared during hydrolysis using lipase from *P fluorescens* of cat no. 95608 at different times in hours and the results are shown in **Figure 61**.

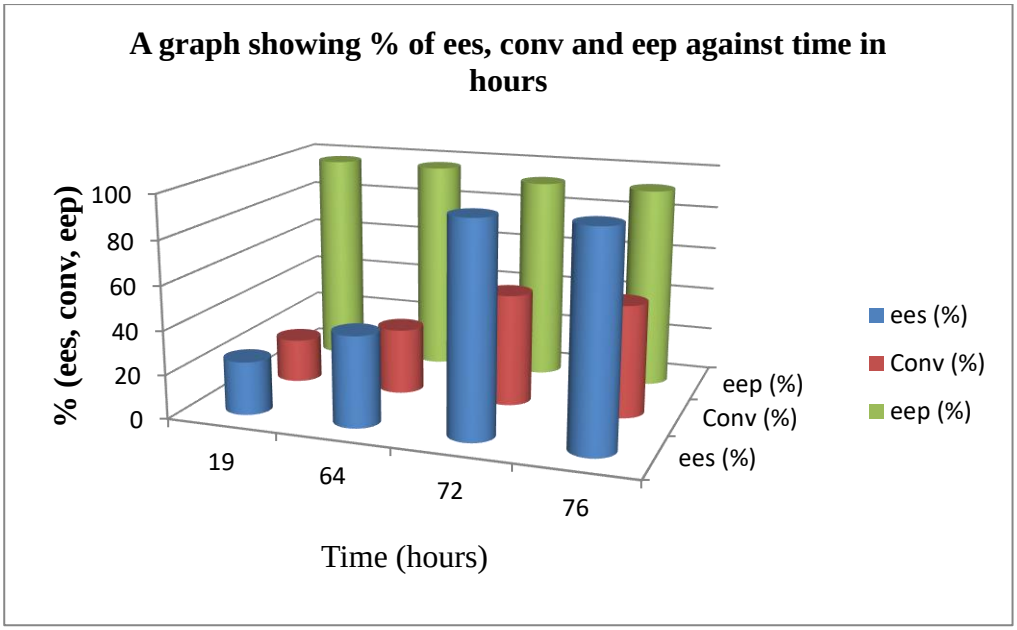

Figure 61: Comparing the percentage ee_s, conv and ee_p during the hydrolysis of **200** using lipase from *Pseudomonas fluorescens* cat. no. 95608

It is clear from the graph that the percentage ee_s and conversion is increasing steadily until it reaches maximum. Conversely, the percentage ee_p decreases steadily to a minimum value of 92%.

The percentage ee_p, conversion and ee_s was also compared and presented in **Figure 62**.

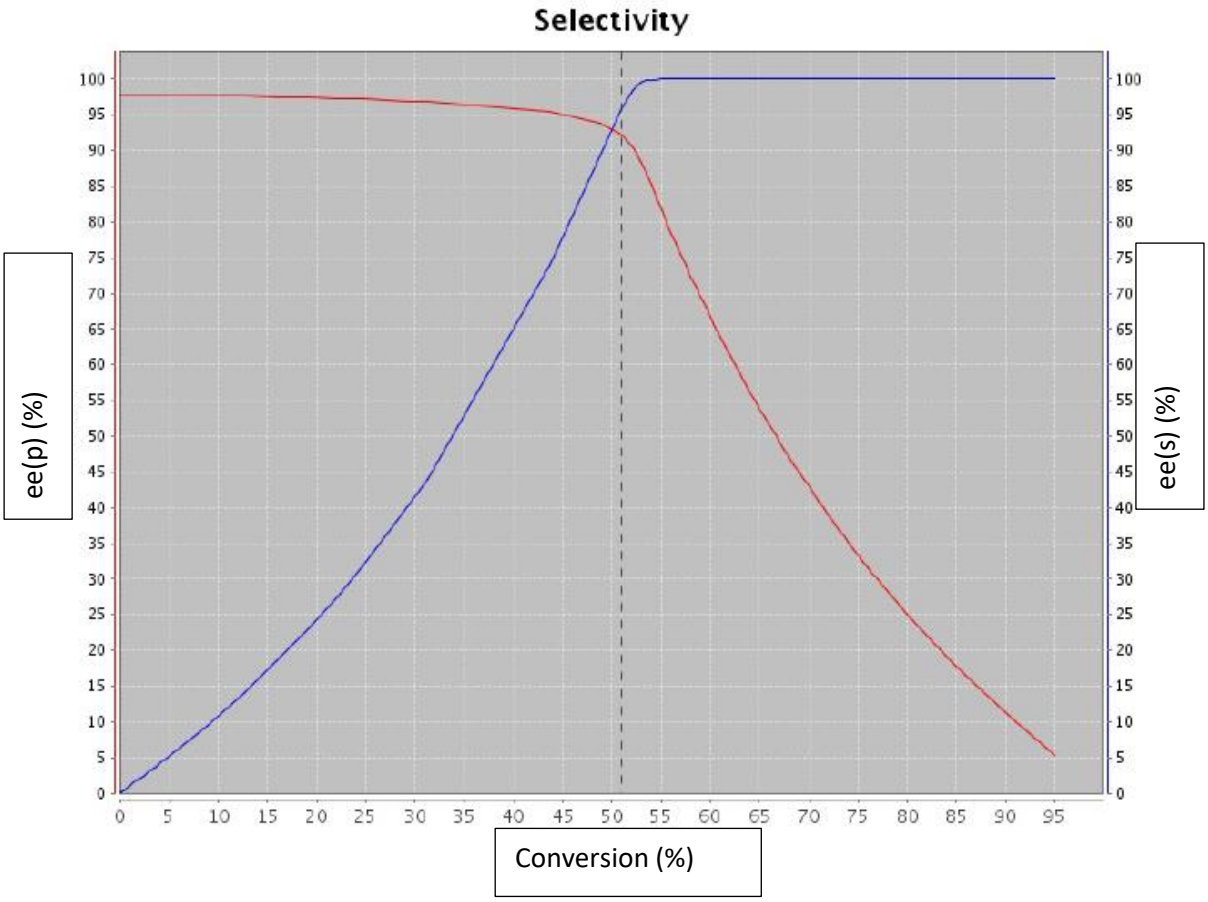

Figure 62: A comparison of enantiomeric ratio (E) values at different pecentages of ee_p and ee_s when lipase originating from *P. fluorescens* of cat. no. 95608 was used

It is clear from **Figure 62** that at a conversion percentage of 51, then the percentage ee_p and ee_s are 92 and 96 respectively (a point where the dotted line meets the red line and blue line). It is at this percentage conversion of 51 that an enantiomeric ratio of 95 is obtained. This simply means *P. fluorescens* of cat no. 95608 is selective on this substrate and either *S* or *R* alcohol can be obtained with high enantioselectivity. Unfortunately, this enzyme was completely used for screening reactions and therefore the same enzyme with a similar name was ordered so that extra reactions could be underaken.

Regrettably, *Pseudomonas fluorescens* cat. no. 534730 that was new from Sigma Aldrich was among the worst performing enzymes. This enzyme gave an enantiomeric ratio of 3 with poor ee_s and ee_p percentages below 45% (**Table 28, entry 25**). It was very hard to explain why a similar enzyme from the same microorganism was giving very poor results as compared to *P. fluorescens* of cat no. 95608 and Amano Lipase AK Lot no. 0351202. Therefore, it was a chance to analyse them and to establish if indeed the three enzymes were

similar. Use of polyacrylamide Gel electrophoresis (SDS-PAGE) afforded a chromatographic profile shown in **Figure 63**.

Fermentas protein marker prestained: Cat NO SM1811	Protein gel for **C** (Lipase from *P. fluorescens* cat. no 95608), **43** (Amano lipase AK Lot LAKA 0351200), and **102** (Amano lipase from *P. fluorescens* cat. no. 534730)
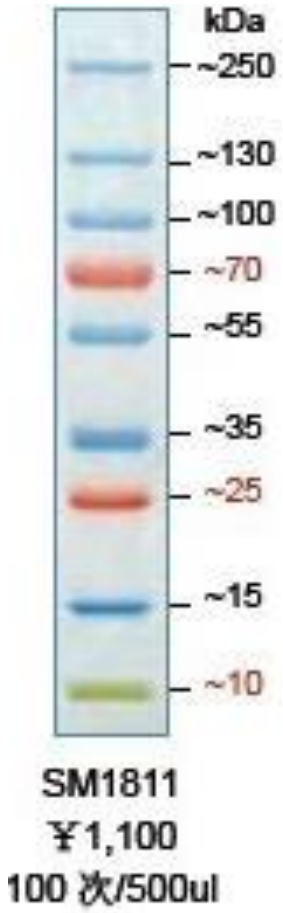	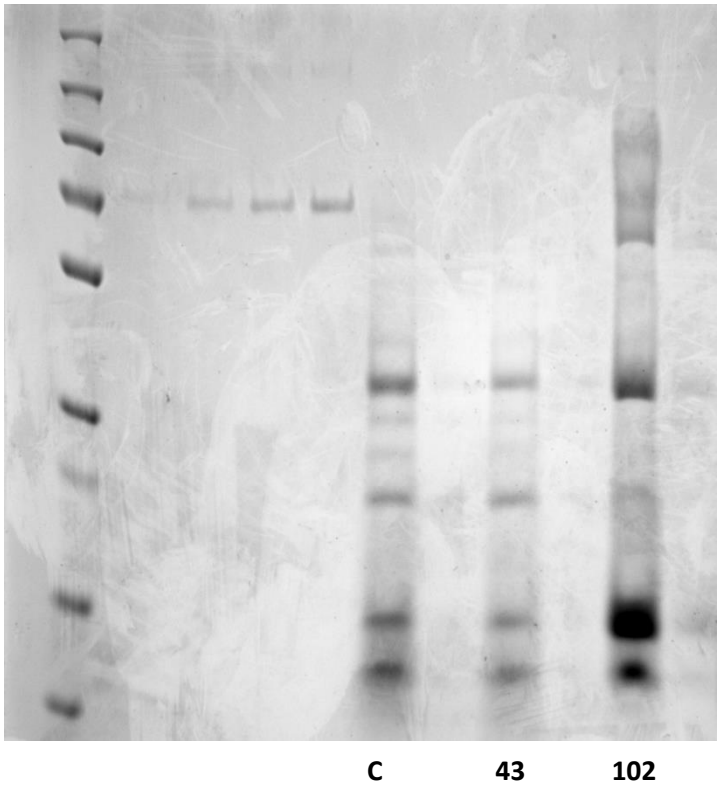

Figure 63: Chromatographic profile of the three lipases

By comparing the stained band of lipase C, 43 and 102, with prestained protein standard, then it was clear that the three lipases have proteins of 20, and 35 kDa (**Figure 63**). Lipase from *P. fluorescens* cat. no. 534730 (102) had other darker bands. Attempts to perform the amino acids sequencing of the bands was not successful due to financial constraints. It was sad that the Japanese company that produced similar enzyme had stopped their production. We needed to identify the next best performing enzymes in order to perform the next set of reactions. This next set of reactions included large scale synthesis of enantiopure **191** with

an aim of determining the stereochemistry and for subsequent nucleophilic addition reactions.

The next alternative enzymes for use were the Amano Lipase AK Lot no. 0351202 and Lipozyme® CALB L as their overall enantiomeric ratios (E) were above 60, with the same value of ee_p of 96% (**Table 28**, **entry 4**, **15-16**). This implied that using one of these enzymes would give an alcohol of high enantiomeric excess that could be used for stereochemical determination.

Amano Lipase AK Lot no. 0351202 was chosen for large scale as its overall E value was greater than the overall E value for Lipozyme® CALB L.

3.2.7.10 Stereochemical determination of the enantiopure alcohol 191

This process was achieved by obtaining an enantiopure alcohol and subjecting it to Mosher's double derivatization protocol as described from previous sections. The enantiopure alcohol was obtained by dissolving 600 mg of **200** in acetone and introducing it to a phosphate buffer at pH 7.00 containing 600 mg of Amano Lipase AK Lot no. 0351202. The reaction was stirred at 25 °C for 24 hours to obtain the maximum amount of alcohol of high enantioselectivity as guided by chiral HPLC chromatography. Thereafter, the reaction was immediately stopped and the product was extracted using ethyl acetate. Purification of the crude product by column chromatography afforded an enantiopure alcohol (+)-**191** as a colourless oil in a yield of 42% and a scalemic mixture of **200** in a yield of 33%. The ee_p of the enantiopure alcohol **191** was found to be 97% while the specific optical rotation was +50.4. The HPLC chromatogram of **200** is shown in **Figure 64** while the chromatogram of the enantiopure alcohol is shown in **Figure 65**.

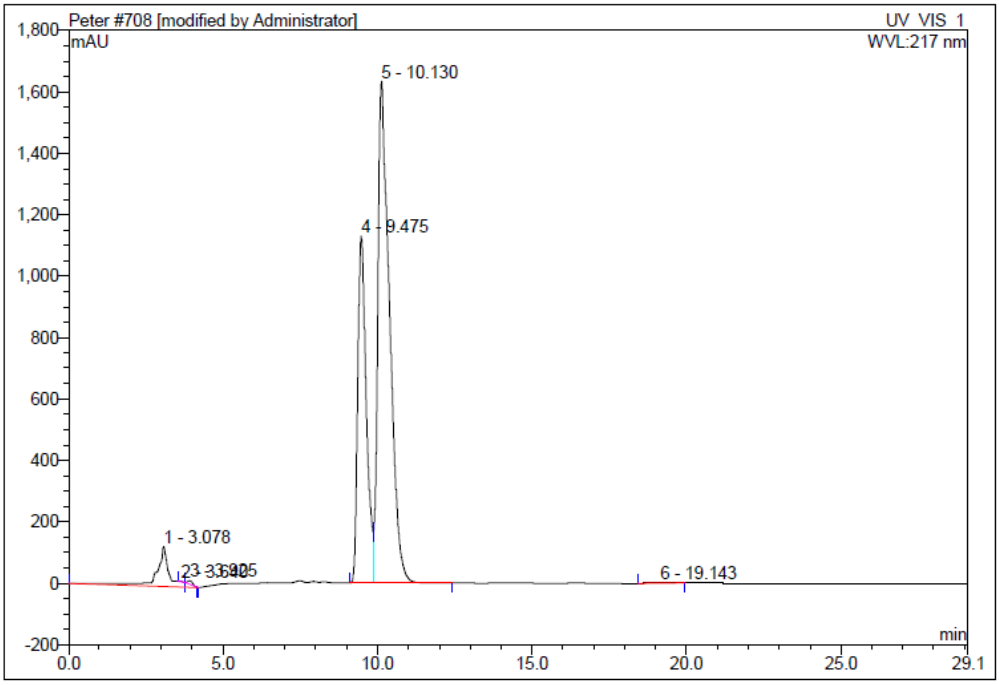

No.	Ret.Time min	Peak Name	Height mAU	Area mAU*min	Rel.Area %	Amount	Type
1	3.08	n.a.	129.716	63.266	5.50	n.a.	BMB
2	3.64	n.a.	2.525	0.302	0.03	n.a.	Rd
3	3.93	n.a.	11.963	2.325	0.20	n.a.	Rd
4	9.48	n.a.	1129.381	363.730	31.64	n.a.	BM *
5	10.13	n.a.	1633.626	718.773	62.53	n.a.	MB*
6	19.14	n.a.	1.517	1.063	0.09	n.a.	BMB
Total:			2908.730	1149.458	100.00	0.000	

Figure 64: HPLC chromatogram of isolated scalemic mixture **200**

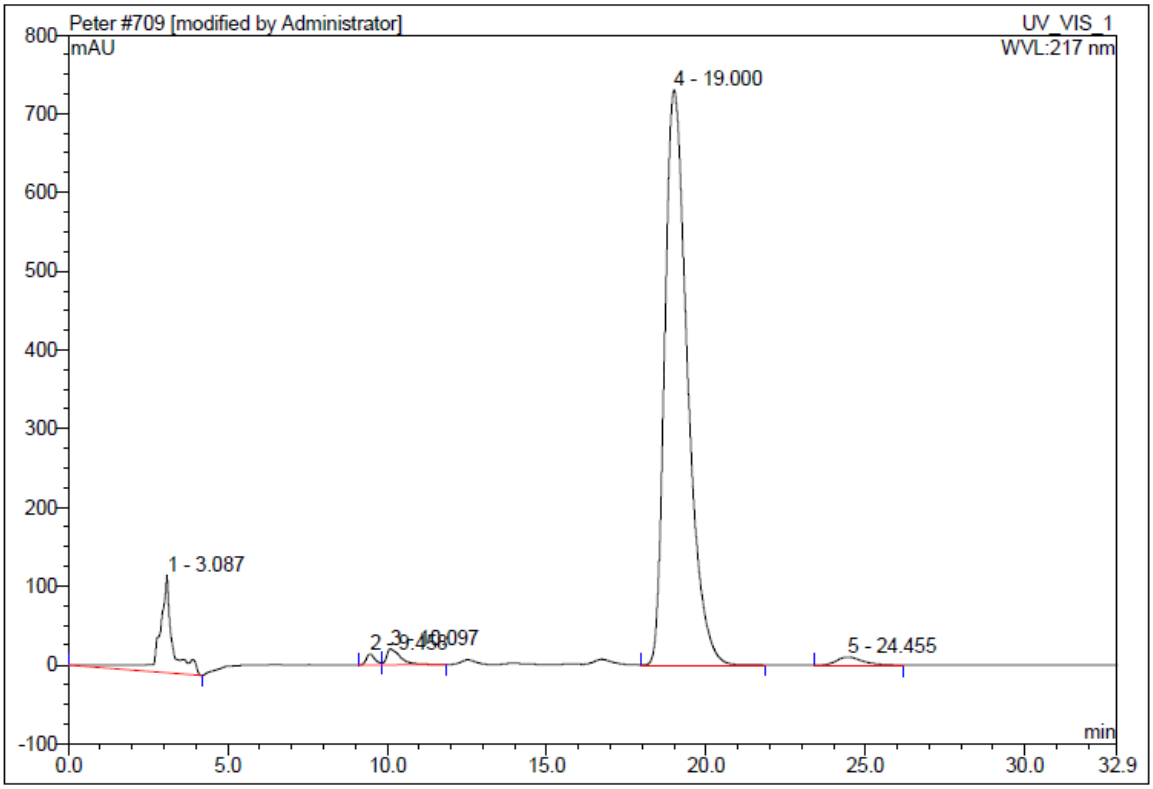

No.	Ret.Time min	Peak Name	Height mAU	Area mAU*min	Rel.Area %	Amount	Type
1	3.09	n.a.	123.621	63.429	9.21	n.a.	BMB*
2	9.46	n.a.	13.871	4.332	0.63	n.a.	BM *
3	10.10	n.a.	20.148	9.959	1.45	n.a.	MB*
4	19.00	n.a.	730.064	601.489	87.33	n.a.	BMB
5	24.46	n.a.	10.302	9.518	1.38	n.a.	BMB*
Total:			898.006	688.727	100.00	0.000	

Figure 65: HPLC Chromatogram of the enantiopure alcohol (+)-**191**

The stereochemistry of the isolated enantiopure alcohol was determined by reacting a sample of **191** with (*R*)-(+) and a sample with (*S*)-(-)-α-methoxy-α-(trifluoromethyl)phenylacetic acid (MTPA) in the presence of a coupling reagent dicyclohexyl carbodiimide (DCC) and a catalytic amount of DMAP at room temperature. This afforded two Mosher's esters (*R*)-[(*S*,*E*)-4-Cyano-1-phenylpenta-1,4-dien-3-yl] 3,3,3-trifluoro-2-methoxy-2-phenylpropan-oate **217** and (*S*)-[(*S*,*E*)-4-Cyano-1-phenylpenta-1,4-dien-3-yl] 3,3,3-trifluoro-2-methoxy-2-phenylpropan-oate **218** (**Scheme 75**) each giving a yield above 80%. The analysis of the two esters redrawn in their preferred conformations as determined by Mosher enabled us to determine the stereochemistry based on the shielding effect of protons.

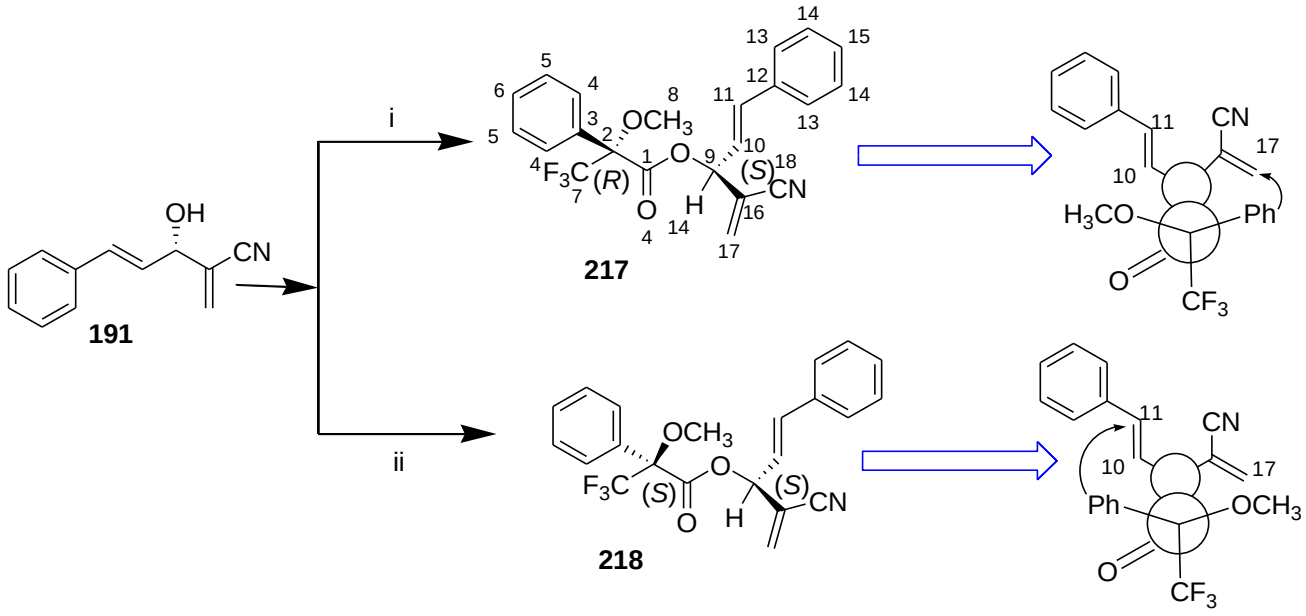

Scheme 75: Synthesis of Mosher's esters **217** and **218**. Reagents and conditions: (i) DCC, DMAP, (*R*)-(+)-MTPA in CH_2Cl_2 at room temperature. (ii) DCC, DMAP, (*S*)-(-)-MTPA in CH_2Cl_2 at room temperature.

The structures of the Mosher's esters were confirmed using spectroscopic techniques. The ^{1}H NMR spectra clearly indicated protons that were in seven different chemical environments as expected. The ^{1}H NMR spectrum of **217** showed the aromatic protons appearing as two multiplets at δ 7.54 – 7.50 and δ 7.45 – 7.30. The presence of a doublet at δ 6.85 with a *trans*-coupling constant of 15 Hz corresponded well with H-11. The overlapping multiplet at δ 6.23 – 6.13 was assigned to H-10 and H-9. The presence of H-17a and H-17b was evidenced by two doublets each appearing at δ 6.08 and 6.01 and having a geminal coupling constant of 1 Hz. The methoxy protons of **217** appeared as a multiplet at δ 3.57 – 3.55. The ^{1}H NMR spectrum of **218** was the same as the ^{1}H NMR spectrum of **217** except that there was a variation in chemical shifts of H-11, H-10 and H-17. This variation in chemical shifts was used to determine the absolute configuration of the isolated enantiopure alcohol as discussed below.

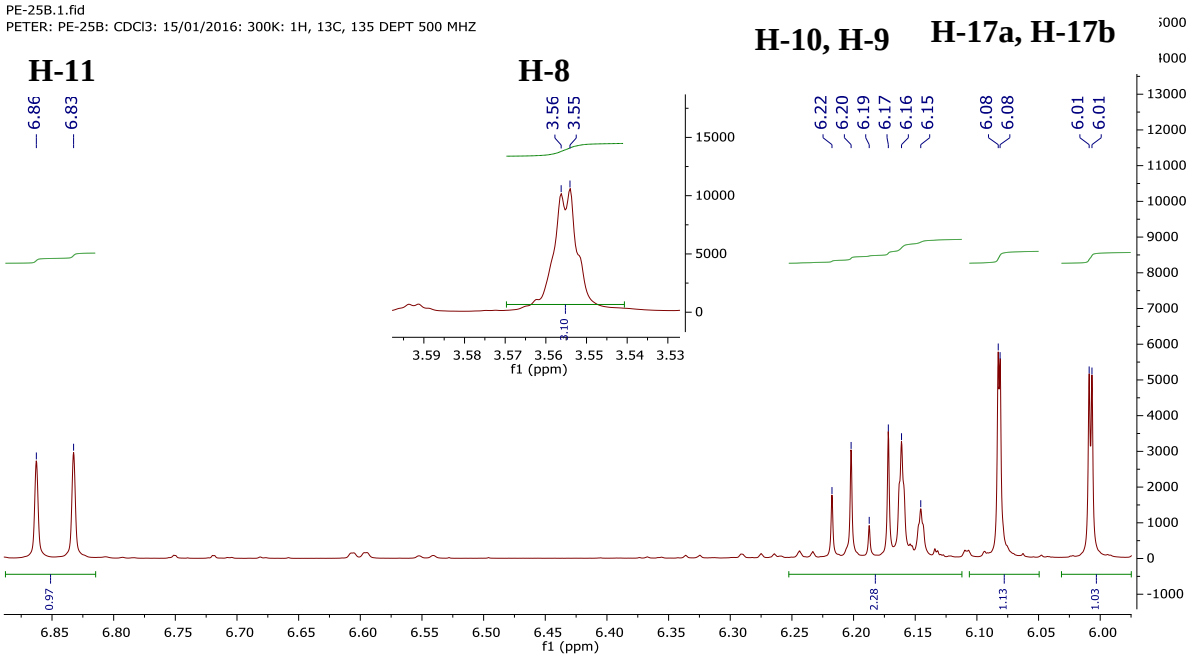

Figure 66: ^{1}H NMR spectrum of *R*-Mosher's ester **217**

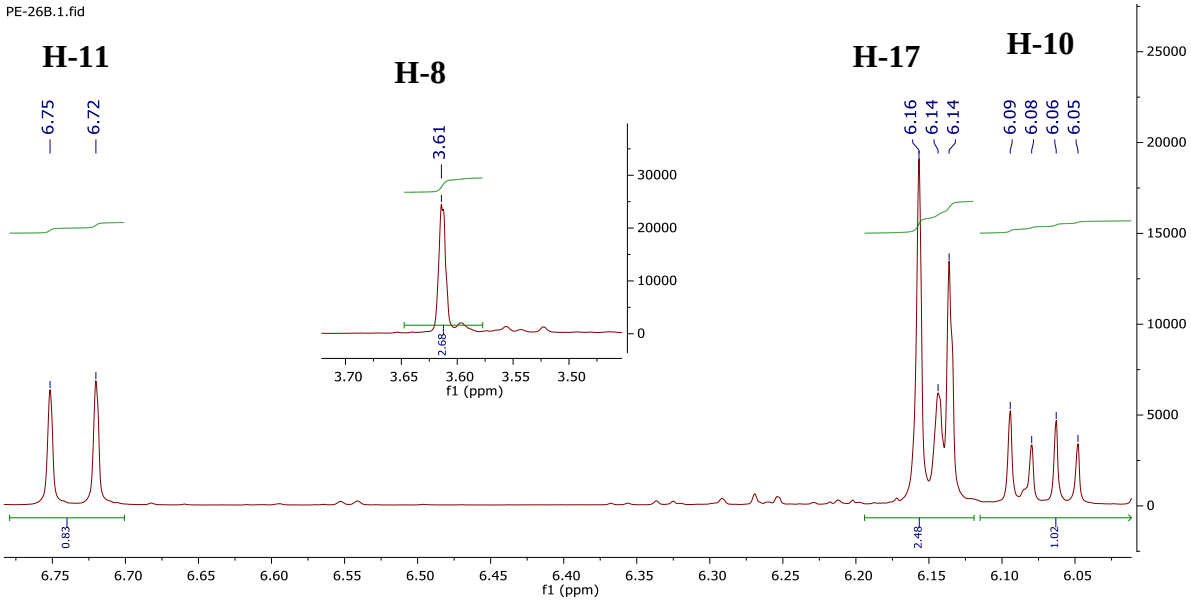

Figure 67: ^{1}H NMR spectrum of *S*-Mosher's ester **218**

By comparing the two ^{1}H NMR spectra in **Figure 66** and **67**, it is clear that the phenyl group of (*R*)-MTP acid is shielding the vinyl protons H-17a and H-17b (ΔSR = 0.08, δ 6.16 – δ 6.08) implying that the phenyl group originating from *R*-Mosher's acid and the vinyl protons H-17a and H-17b are on the same side of the plane (**Scheme 75**). The signals of the trans-cinnamaldehyde protons H-10 and H-11 are deshielded in the (*R*)-MTP acid derivative, indicating that the Mosher's group phenyl ring and these H-10 and H-11 protons are on opposite sides of the plane (ΔSR = -0.11, δ 6.75 – δ 6.86). All this

information confirms that the enantiopure alcohol **(+)-191** obtained had an ***S***-configuration.

The structures of the Mosher's esters were supported by the ^{13}C NMR spectra. Each of the two spectra had 18 signals corresponding to 18 carbon atoms that are in different chemical environment. The characteristic carbon signals were observed at δ 165.3 for C-1, 133.3 for C-17, 116.0 for C-18 and 75.3 for C-9. The presence of the fluorine atom was evidenced by its characteristic behaviour of coupling with carbon nuclei. This was revealed by the appearance of C-F coupling with $^{4}J_{C\text{-}F}$ value of 1 Hz, $^{1}J_{C\text{-}F}$ value of 289 Hz, $^{2}J_{C\text{-}F}$ value of 28 Hz, and $^{4}J_{C\text{-}F}$ value of 1 Hz for C-4, C-7, C-2 and C-8 respectively. The number of carbon signals in the ^{13}C NMR spectra of **217** and **218** were the same except that there was a slight difference in chemical shifts. For example, carbons C-11, C-2, C-9 and C-8 appeared at δ 137.5, 84.7, 75.2 and 55.6 respectively in the ^{13}C NMR spectrum of **217**. The same carbons appeared at δ 137.2, 84.8, 75.3 and 55.9 in the ^{13}C NMR spectrum of **218**. This observation supports the diastereomeric relationship between **217** and **218**.

The presence of peaks at 2219 cm^{-1} and 1752 cm^{-1} in the IR spectrum of **217** verified the presence of a nitrile and carbonyl functional group, respectively. Similar observation of peaks at 2224 cm^{-1} and 1753 cm^{-1} in the IR spectrum of **218** confirmed the presence of nitrile and carbonyl functional groups. The molecular ion of **217** was confirmed by HRMS to be $[M+Na^{+}]$ 424.1110 which was consistent with the mass calculated for $C_{22}H_{18}F_3NO_3Na$ of 424.1136. The HRMS data for **218** was similar to that of **217**.

Theoretically, if the resulting hydrolysed alcohol (+)-**191** is of *S*-configuration, then the un-hydrolysed acetate must be of *R*-configuration. The only way to confirm this unequivocally was to isolate the enantiopure acetate from a large scale reaction, hydrolyse it and determine its absolute configuration.

A similar procedure to that described previously using Lipozyme® CALB L LCN 02106 instead of Amano lipase AK lot. No 0351202 was used. This procedure involved dissolving **200** in acetone and introducing the solution to phosphate buffer containing Lipozyme® CALB L LCN 02106 at 25 °C. This afforded enantiopure acetate **200** as a colourless oil in a yield of 69% after 14 days. The enantiopure acetate **200** had an enantiomeric excess of 92% and a specific optical rotation of -58.8. The HPLC chromatogram of (-)-**200** is shown in **Figure 68**. The scalemic alcohol **191** isolated in this process had an ee of 81% and its HPLC chromatogram is shown in **Figure 69**.

The enantiopure acetate (-)-**200** was hydrolysed to the corresponding alcohol using the highly promiscuous esterase cat. no. ESL-001-01, 6Z0248. This afforded an enantiopure alcohol (-)-**191** as a colourless oil in a yield of 77% and ee of 92%. The HPLC chromatogram of (-)-**191** is shown in **Figure 70**.

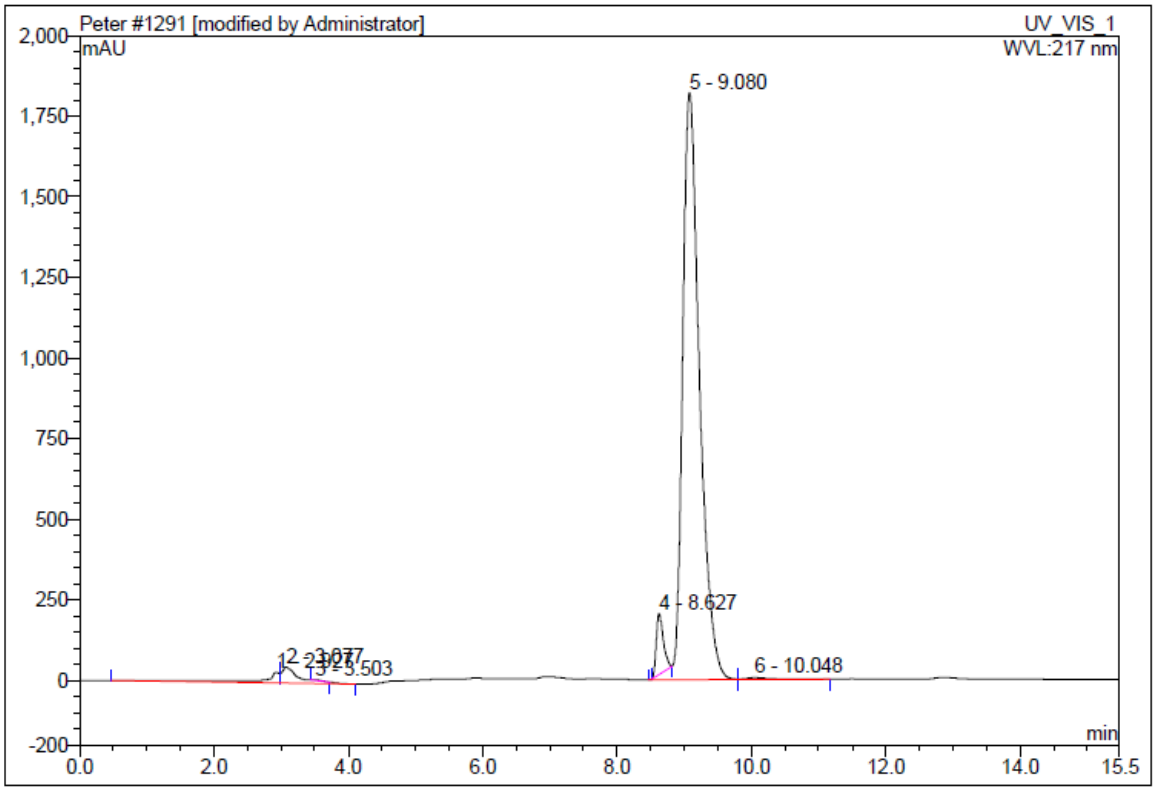

No.	Ret.Time min	Peak Name	Height mAU	Area mAU*min	Rel.Area %	Amount	Type
1	2.93	n.a.	33.420	13.737	2.32	n.a.	BM *
2	3.08	n.a.	50.601	15.813	2.67	n.a.	MB
3	3.50	n.a.	1.820	0.304	0.05	n.a.	Rd
4	8.63	n.a.	188.654	22.972	3.88	n.a.	Ru
5	9.08	n.a.	1819.953	536.243	90.61	n.a.	BM *
6	10.05	n.a.	6.337	2.721	0.46	n.a.	MB*
Total:			2100.785	591.791	100.00	0.000	

Figure 68: HPLC chromatogram of enantiopure acetate (-)-**200**

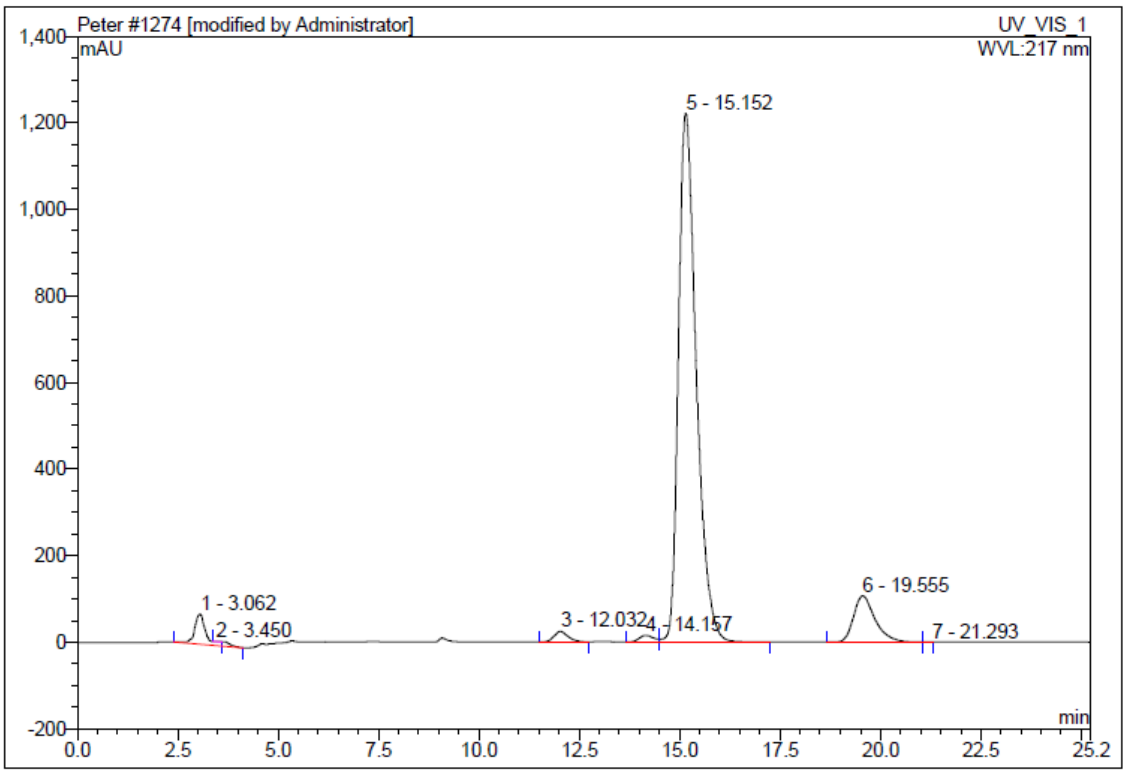

No.	Ret.Time min	Peak Name	Height mAU	Area mAU*min	Rel.Area %	Amount	Type
1	3.06	n.a.	69.713	24.828	3.37	n.a.	BMB*
2	3.45	n.a.	0.463	0.067	0.01	n.a.	Rd
3	12.03	n.a.	24.187	9.922	1.35	n.a.	BMB*
4	14.16	n.a.	15.114	6.435	0.87	n.a.	BM *
5	15.15	n.a.	1221.038	628.895	85.36	n.a.	MB*
6	19.56	n.a.	107.152	66.599	9.04	n.a.	BM
7	21.29	n.a.	0.001	0.006	0.00	n.a.	MB
Total:			1437.667	736.754	100.00	0.000	

Figure 69: HPLC chromatogram of scalemic alcohol **191**

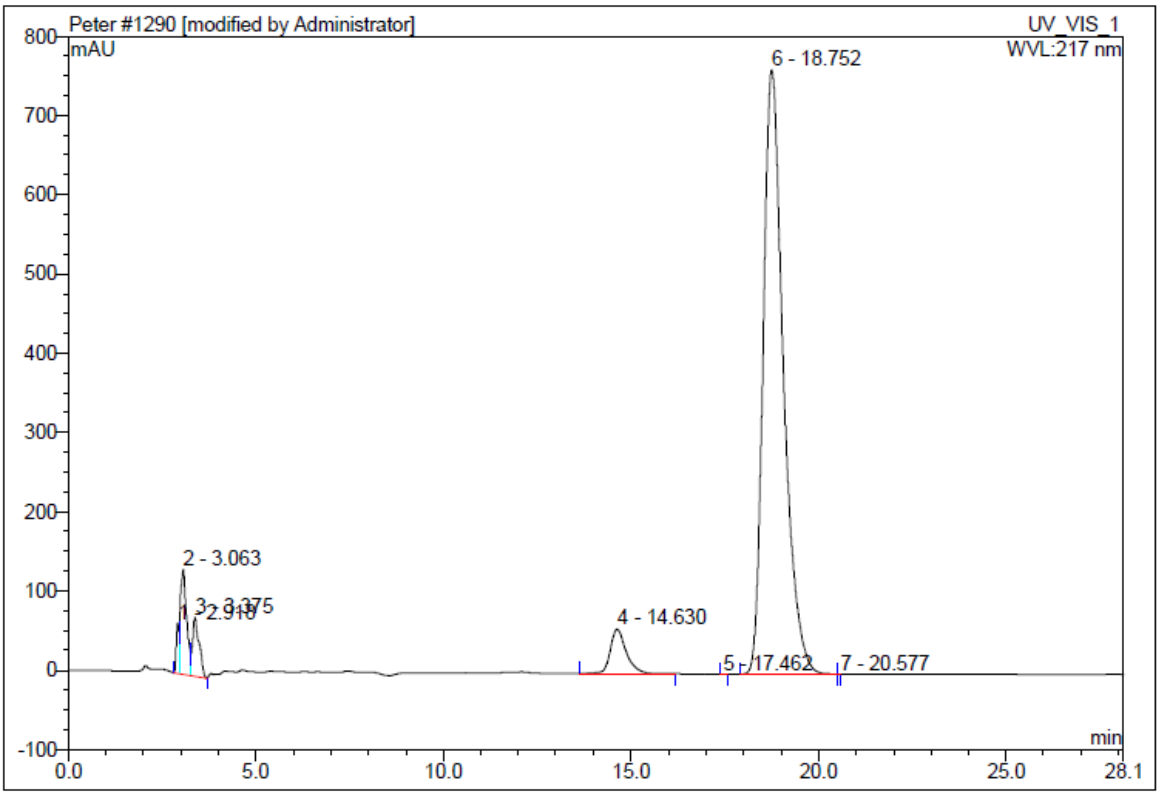

No.	Ret.Time min	Peak Name	Height mAU	Area mAU*min	Rel.Area %	Amount	Type
1	2.92	n.a.	63.999	4.883	0.89	n.a.	BM *
2	3.06	n.a.	132.065	25.952	4.75	n.a.	M
3	3.38	n.a.	74.264	14.851	2.72	n.a.	MB
4	14.63	n.a.	55.933	27.427	5.02	n.a.	BMB
5	17.46	n.a.	0.038	0.005	0.00	n.a.	BMB
6	18.75	n.a.	762.301	473.670	86.63	n.a.	BM
7	20.58	n.a.	0.000	0.001	0.00	n.a.	MB
Total:			1088.599	546.790	100.00	0.000	

Figure 70: HPLC chromatogram of enantiopure alcohol (-)-**191**

The obtained enantiopure alcohol (-)-**191** was now ready for use in Mosher's double derivatization protocol to determine the absolute stereochemistry. This was accomplished by dividing a sample of (-)- **191** in two portions and reacting each portion with (*R*)-(+) and (*S*)-(-)-α-methoxy-α-(trifluoromethyl)phenylacetic acid (MTPA) in the presence of dicyclohexyl carbodiimide (DCC) and a catalytic amount of DMAP at room temperature. This afforded Mosher's esters (*R*)-[(*R*,*E*)-4-cyano-1-phenylpenta-1,4-dien-3-yl] 3,3,3-trifluoro-2-methoxy-2-phenyl-propanoate **219** and (*S*)-[(*R*,*E*)-4-Cyano-1-phenylpenta-1,4-dien-3-yl] 3,3,3-trifluoro-2-methoxy-2-phenylpropan-oate **220** (**Scheme 76**) in yields of 73% and 71%, respectively. The most stable conformation of the two esters was used to

determine the stereochemistry basing on the shielding and deshielding of protons by the diamagnetic effects of the phenyl rings.

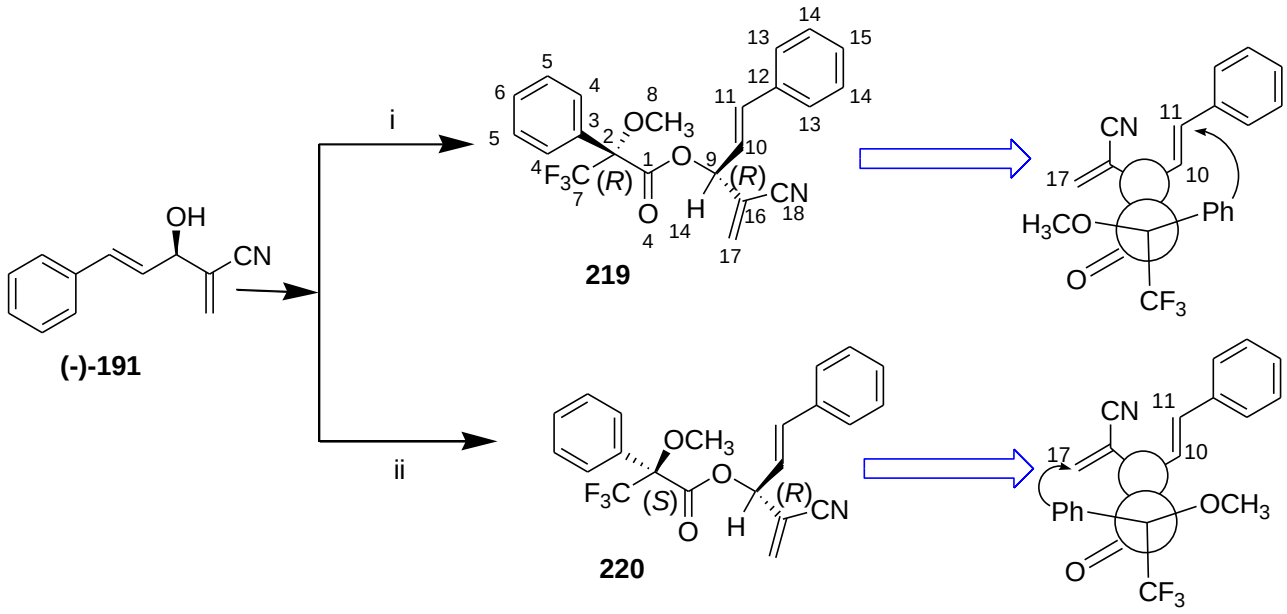

Scheme 76: Synthesis of the Mosher's esters **219** and **220**. Reagents and conditions: (i) DCC, DMAP, (*R*)-(+)-MTPA in CH_2Cl_2 at room temperature. (ii) DCC, DMAP, (*S*)-(-)-MTPA in CH_2Cl_2 at room temperature.

The structure of the Mosher's esters **219** was determined using spectroscopic techniques. The appearance of six signals on ^{1}H NMR spectrum of **219** confirmed the presence of six set of protons that were in different chemical environment. The aromatic protons appeared as two doublets; the first one appearing at δ 7.54 – 7.48 integrating for two protons while the second one appearing at δ 7.42 – 7.31 integrating for eight protons. The doublet at δ 6.74 with a *trans*-coupling constant of 15.6 Hz was assigned to H-11. The overlapping multiplet at δ 6.18 – 6.12 was assigned to H-9, 17a and H-17b. The last two multiplets at δ 6.12 – 6.00 and δ 3.63 -3.60 were assigned to H-10 and H-8 respectively. The ^{1}H NMR signals of **219** were identical to the ^{1}H NMR signals of **220**. The only difference that was visible between the ^{1}H NMR spectrum of **219** and **220** was the visible geminal coupling of 1Hz between H-17a and H-17b. In addition, the chemical shift of H-8, H-10 and H-11 between the two Mosher's esters was also different. The measurable differences in chemical shifts were used in determining the absolute configuration of the alcohol.

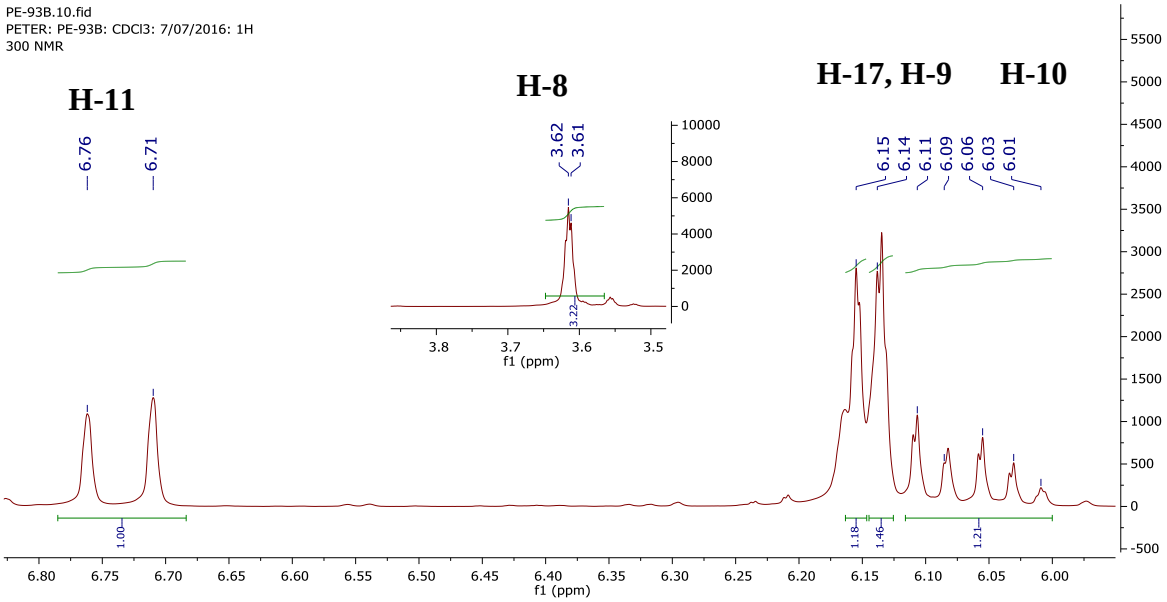

Figure 71: ^{1}H NMR spectrum of the *R*-Mosher's ester **219**

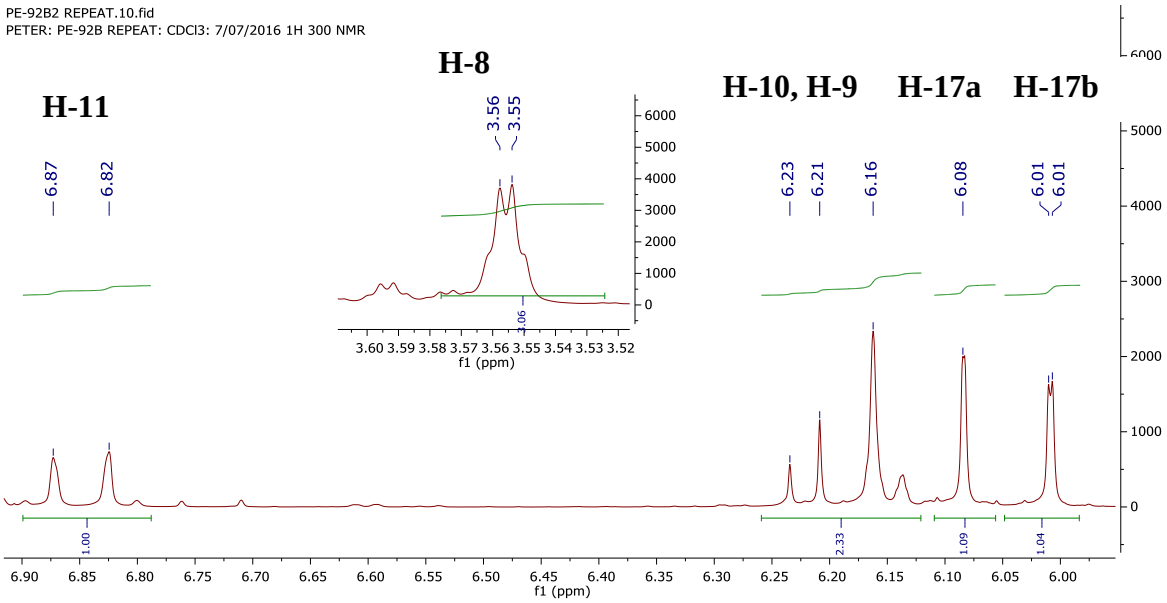

Figure 72: ^{1}H NMR spectrum of the *S*-Mosher's ester **220**

It is very clear from ^{1}H NMR spectra in **Figure 71** and **72** that H-8, H-11 and H-17 are shielded or deshielded by the diamagnetic effect of the phenyl ring either from the alcohol or from the Mosher's acid. By considering the ^{1}H NMR spectrum of **219** as a reference, then is clear that the phenyl group of (*R*)-MTP acid is shielding the *trans*-cinnamaldehyde protons H-10 and H-11 (ΔSR = 0.11, δ 6.87 – δ 6.76) confirming that the phenyl group originating from Mosher's acid is *syn*-periplanar to the protons H-10 and H-11 (**Scheme 76**). On the other hand, the deshielding of the vinyl protons H-17a and H-17b for the (*R*)-MTP acid derivative (ΔSR = -0.07, δ 6.08 – δ 6.15) indicates that the H-17 protons are

anti-periplanar to the phenyl ring emanating from (*R*)-MTP acid. It is therefore logical that the enantiopure alcohol **(-)-191** obtained has an *R*-configuration.

The expected 18 signals for both **219** and **220** were observed on the ^{13}C NMR spectra. The expected characteristic C-F coupling with $^{4}J_{C-F}$ value of 1 Hz, $^{1}J_{C-F}$ value of 289 Hz, $^{2}J_{C-F}$ value of 28 Hz, and $^{4}J_{C-F}$ value 1 Hertz for C-4, C-7, C-2 and C-8 respectively were observed for the two Mosher's esters. The other characteristics carbon signals for **219** were observed at δ 165.3 for C-1, 133.3 for C-17, 115.9 for C-18 and 75.3 for C-9. These same characteristic signals appeared at δ 165.3, 132.6, 115.7 and 75.2 for **220**. Apart from variation in chemical shift of these characteristic signals, there were other carbon signals that also differed slightly in chemical shifts. This variation in chemical shifts truly confirms that **219** and **220** are diastereomers.

The IR spectrum of the two Mosher's esters confirmed the presence of nitrile and carbonyl functional groups as expected. These characteristic peaks appeared at 2230 cm^{-1} and 1751 cm^{-1} for both esters in the IR spectrum. The HRMS ([$M+Na^{+}$]: 424.1110) data confirmed the formation of the two Mosher's esters.

By comparison, the ^{1}H and ^{13}C NMR spectrum of **217** is identical to the ^{1}H and^{13}C NMR spectra of **220** confirming these compounds are mirror images of each other. Similarly, ^{1}H and ^{13}C NMR spectra of **218** and **219** are identical, verifying that indeed the two compounds are mirror images of each other.

All the enzymes shown in **Table 28** hydrolysed **200** affording (+)-**191** of *S*-configuration. The other set of enzymes were able to hydrolyse **200** affording (-)-**191** with an *R*-configuration as shown in **Scheme 77**. These enzymes are presented in **Table 29**.

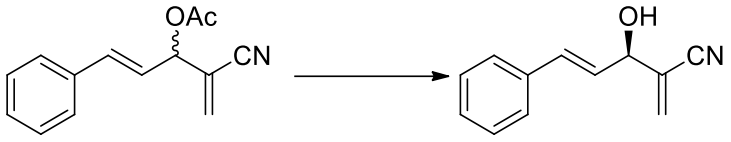

200 (-)-191

Scheme 77: Hydrolysis of **200** using different lipases in phosphate buffer at pH-7.00 leading to the formation of (-)-**191**

Table 29: Hydrolysis of **200** using different enzymes affording (-)-**191**

Entry	Enzyme name	Time (h), Temp (°C)	Conv (%)	ee_s (%)	ee_p (%)	E
1	Lipase A5 Amano A niger LAW035145	30, 20	57	77	21	2
2	Lipase F-AP 15 LFW02523	30, 20	64	83	47	7
3	XP-415	21, 25	15	14	79	10
4	Lipase AY amano IAYTO2510	21, 25	12	7	51	3
5	Lipase AH-D" Amano" II ILAHX01526K	14, 25	7	4	44	3
6	Lipopan FBG	24,30	27	31	90	27
		35,30	33	44	87	23
7	Alcalase (Novo industries)	35, 30	23	17	57	4
8	Alcalase (Novozymes)	24, 30	22	24	88	20
9	C. rugosa Lipase AY "Amano" LAYA0750964	35,30	34	22	43	3
10	Lipase from wheat germ cat. no. 62306	4, 30	59	30	21	2
11	Lipase from *Candida rugosa* cat. no. 62316	5, 30	4	2	54	3
12	Lipase from *Candida rugosa* 90860	72, 30	26	16	46	3

From **Table 29**, it is true that only three enzymes gave an overall enantiomeric ratio (E) above 15. These enzymes are Lipopan FBG (**entry 6**), and Alcalase of different preparations (**entries 7-8**). One of the chromatograms confirming that the hydrolysis of the *R*- acetate **200** took place is shown in **Figure 73**. For better understanding of these enzymes, then their sources become very important. Lipopan F BG is known to originate from *Fusarium oxysporum* produced by submerged fermentations of genetically modified *Aspergillus oryzae*,[179, 180] while Alcalase is produced by submerged fermentation of *Bacillus licheniforrmis*.[181] Alcalase is in fact classified as a protease, and proteases often display opposite enantioselectivity to lipases.

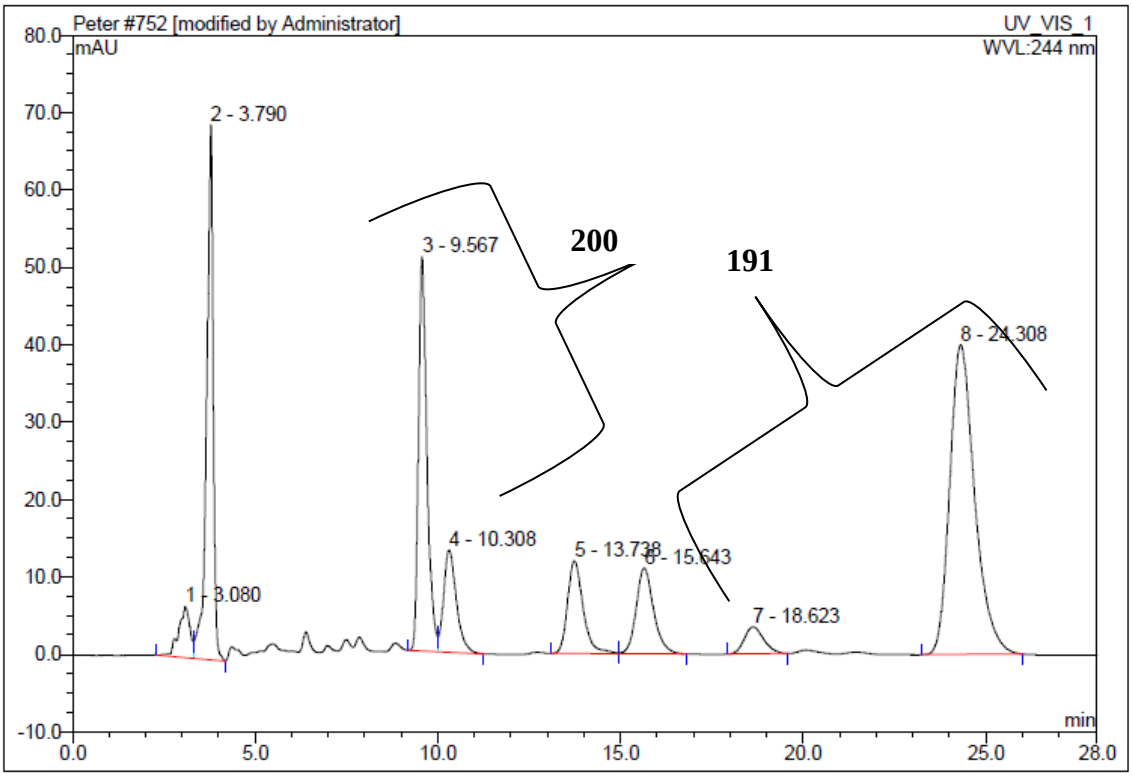

No.	Ret.Time min	Peak Name	Height mAU	Area mAU*min	Rel.Area %	Amount	Type
1	3.08	n.a.	6.607	2.321	2.84	n.a.	BM *
2	3.79	n.a.	69.076	14.563	17.80	n.a.	MB
3	9.57	n.a.	50.947	13.630	16.66	n.a.	BM *
4	10.31	n.a.	13.180	5.360	6.55	n.a.	MB*
5	13.74	n.a.	11.947	5.948	7.27	n.a.	BM *
6	15.64	n.a.	11.089	6.125	7.49	n.a.	MB*
7	18.62	n.a.	3.495	2.156	2.64	n.a.	BMB
8	24.31	n.a.	40.002	31.704	38.75	n.a.	BMB
Total:			206.343	81.807	100.00	0.000	

Figure 73: HPLC chromatogram when Lipopan FBG is used after 35 hours at 30 °C

3.2.7.11 Resolution of (±)-2-cyano-5-phenyl-pent-1-ene-yl acetate 201

The last compound to investigate was the racemic 2-cyano-5-phenyl-pent-1-ene-yl acetate **201**. This compound was used to find out what the effect would be of having a flexible linker between the phenyl ring and acrylonitrile group. A total of 101 enzymes comprising of different preparations of lipases and esterase were used for screening while monitoring the enzymatic activity by HPLC using a C-18-column. The enzymes with promising activity were further subjected to chiral HPLC for enantioselectivity investigation.

The enantioselectivity inquiry was only possible after establishing the chromatographic conditions for resolving the racemic acetate **201** and racemic alcohol (±)-3-hydroxy-2-methylene-5-phenylpentanenitrile **195**. The task of determining the chromatographic conditions was very challenging as compared to the previously discussed compounds. Separation of the racemic acetate **201** was done on a Lux 5µm Amylose-2 column with a mobile flow rate of 1 mL/min using hexane and IPA (96:4) as eluent (**Figure 74**). This method was developed after the failure of the original chromatographic conditions to resolve the racemic acetate peaks within a reasonable run time. The original method made use of a Chiralcel OJ at a flow rate of 1 mL/min using hexane and IPA (98:2) as eluent (**Figure 75**). The racemic alcohol **195** was separated on a Lux 3µm cellulose-2 column at a flow rate of 1 mL/min with a mobile phase composition of hexane: IPA (96:4). The HPLC chromatogram of the racemic **195** is shown in **Figure 76**.

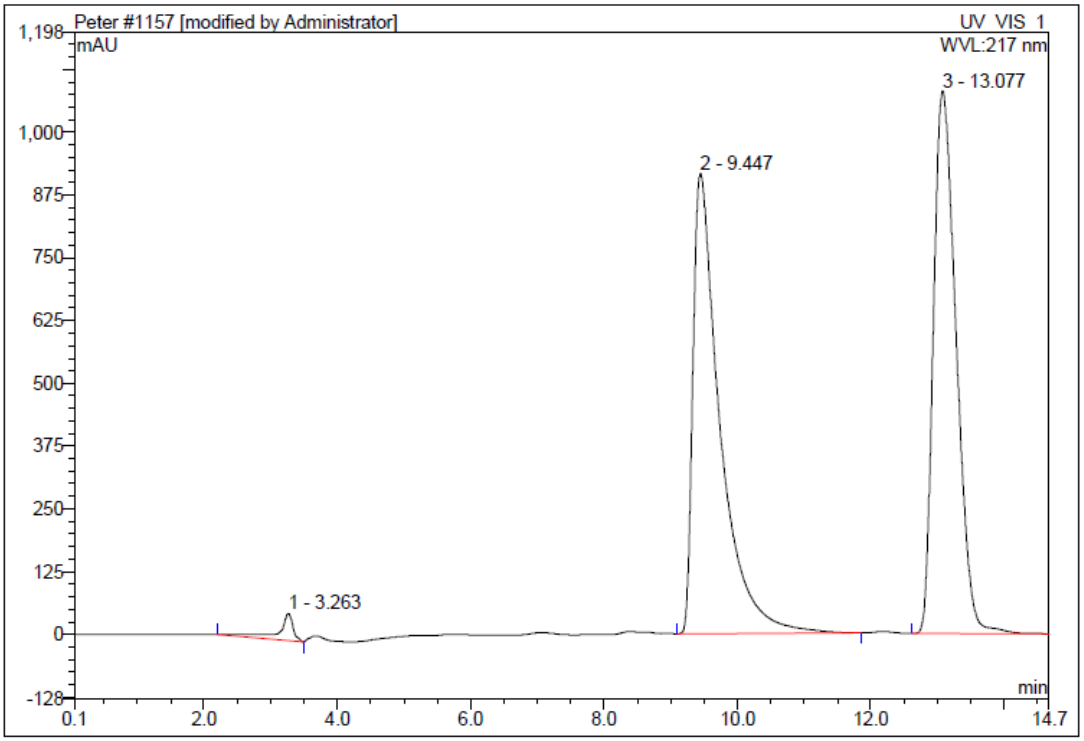

No.	Ret.Time min	Peak Name	Height mAU	Area mAU*min	Rel.Area %	Amount	Type
1	3.26	n.a.	54.555	14.121	1.62	n.a.	BMB
2	9.45	n.a.	916.146	430.086	49.43	n.a.	BMB*
3	13.08	n.a.	1080.586	425.919	48.95	n.a.	BMB*
Total:			2051.287	870.126	100.00	0.000	

Figure 74: HPLC Chromatogram of the racemic acetate **201**

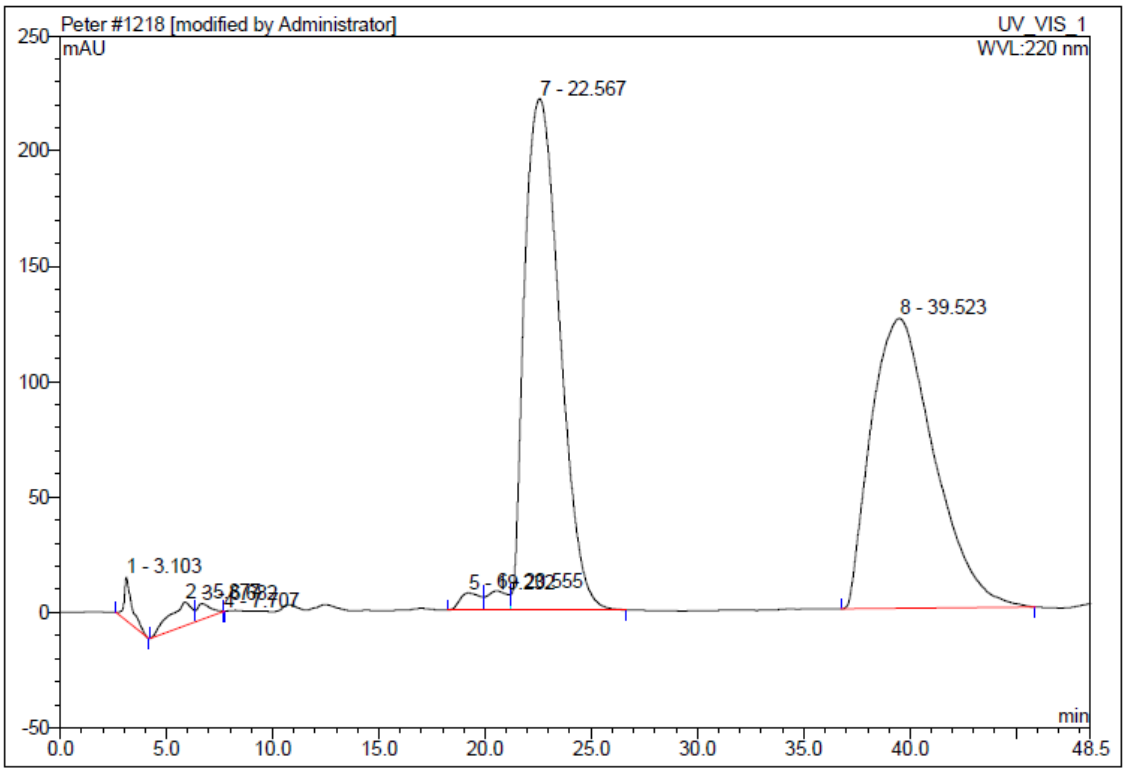

No.	Ret.Time min	Peak Name	Height mAU	Area mAU*min	Rel.Area %	Amount	Type
1	3.10	n.a.	18.708	8.300	0.92	n.a.	BMB
2	5.88	n.a.	10.072	12.805	1.42	n.a.	BM *
3	6.68	n.a.	6.709	4.968	0.55	n.a.	MB*
4	7.71	n.a.	0.000	0.000	0.00	n.a.	Rd
5	19.23	n.a.	7.468	8.221	0.91	n.a.	BM *
6	20.56	n.a.	8.336	8.954	0.99	n.a.	M *
7	22.57	n.a.	221.802	425.551	47.18	n.a.	MB*
8	39.52	n.a.	125.745	433.154	48.02	n.a.	BMB*
Total:			398.840	901.955	100.00	0.000	

Figure 75: HPLC chromatogram of the racemic acetate **201**

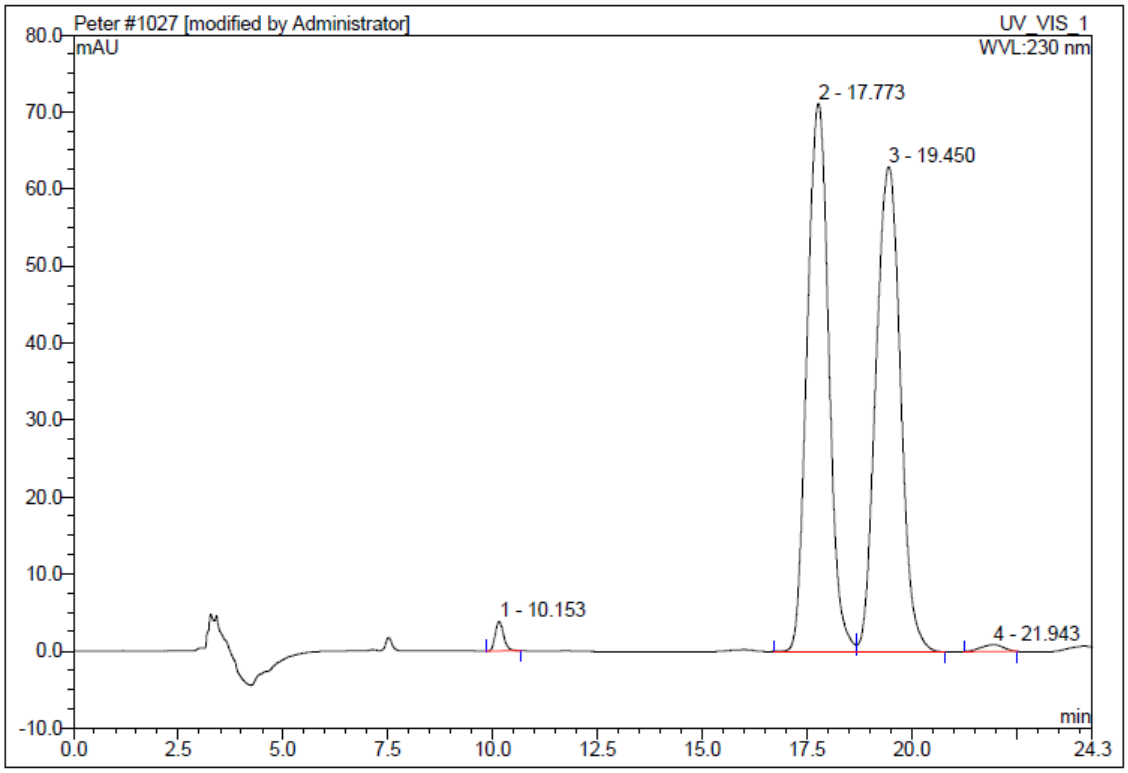

No.	Ret.Time min	Peak Name	Height mAU	Area mAU*min	Rel.Area %	Amount	Type
1	10.15	n.a.	3.829	0.901	1.04	n.a.	BMB*
2	17.77	n.a.	71.189	42.577	49.02	n.a.	BM
3	19.45	n.a.	62.963	42.831	49.31	n.a.	MB
4	21.94	n.a.	0.873	0.547	0.63	n.a.	BMB
Total:			138.855	86.855	100.00	0.000	

Figure 76: HPLC chromatogram of the racemic alcohol **195**

The reaction shown in **Scheme 78** was used to monitor the enzymatic activities of different lipases and the results where hydrolysis was achieved are summarised in **Table 30**.

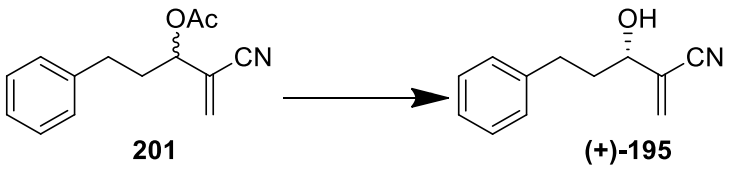

Scheme 78: Hydrolysis of **201** using different lipases and esterases in phosphate buffer at pH-7.00 at different temperatures

Table 30: Hydrolysis of **201** using different enzymes affording **195**

Entry	Enzyme name	Time (h), Temp (°C)	Conv (%)	ee_s (%)	ee_p (%)	E
1	Esterase with gut stabiliser	0.5, 35	19	1	4	1
2	Esterase cat. no. 6y0240	0.17, 25	34	8	15	1
3	Esterase cat. no. 6Z0248	0.17, 25	41	4	6	1
4	Lipase from *Candida antarctica* type B	20, 35	28	37	94	44
5	Lipozyme® CALB L435 LC 200217 (Novozym)	17, 35	17	20	96	54
6	Lipozyme® CALB L LCN 02106	43, 35	29	38	94	51
7	Lipozyme® CALB (Novozymes)	43, 35	29	38	90	29
8	Lipozyme® CALB L (Novozym)	43, 35	30	35	83	15

Five enzymes afforded an overall enantiomeric ratio (E) of 15 and above. These enzymes were lipase from *Candida antarctica* type B and Lipozyme® CALB of different preparations (**Table 30**, **entry 4**, **5-8**). These enzymes showed a significant enantiomeric ratio (E) and good enantioselectivity of the product (ee_p) of above 90%. Unfortunately, the enantioselectivity of the substrate (ee_s) of 30% and below was very low (**entry 1-3**).

Th next task was to determine the stereochemistry of the resulting alcohol. As was the case for the previous compound **200**, this information was significant given that this is the first-time resolution of racemic acetate **201** is being reported. This was achieved by dissolving 720 mg of racemic **201** in acetone and adding the solution in a phosphate buffer at pH 7.00 containing 720 mg of Lipozyme® CALB L LCN02106. This reaction step afforded a scalemic mixture **201** with an enantiomeric excess of 25% and an enantiopure alcohol (+)-**195** with an enantiomeric excess of 95% in a yield of 44%. The specific optical rotation of the isolated enantiopure alcohol was found to be +31.6. The HPLC chromatograms of the scalemic acetate and enantiopure alcohol are shown in **Figure 77** and **78** respectively.

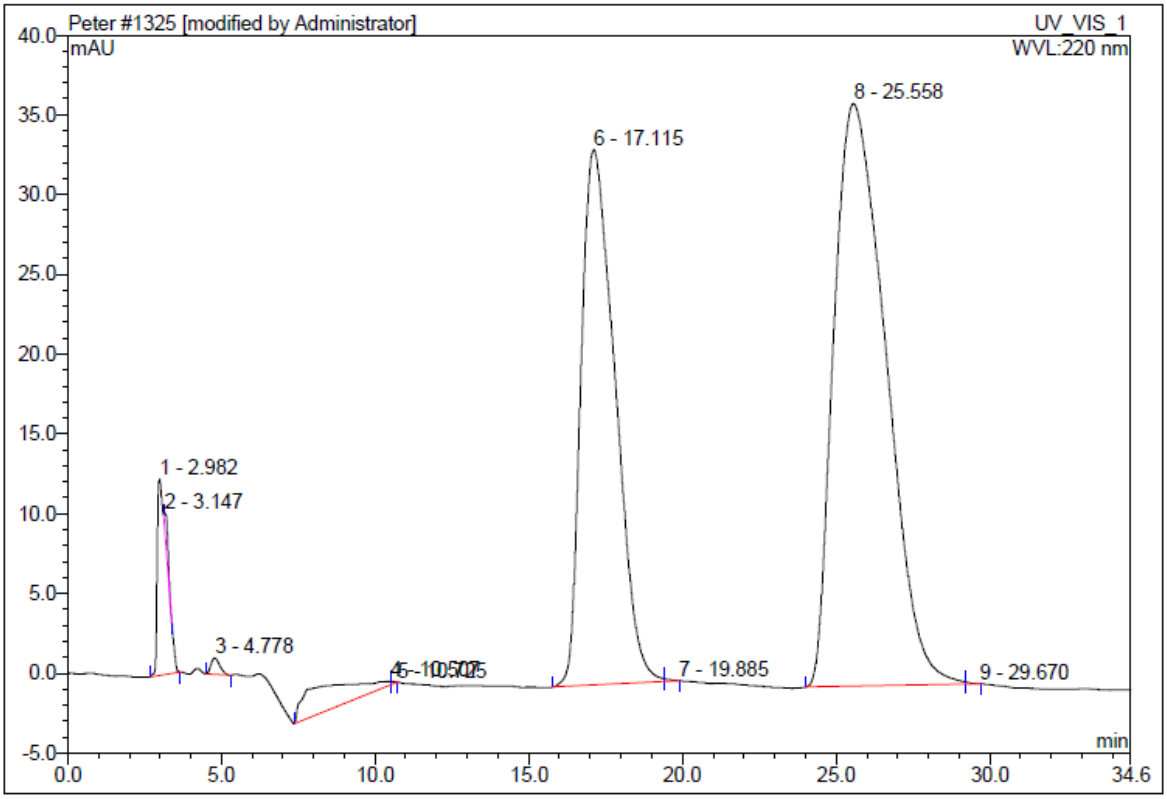

No.	Ret.Time min	Peak Name	Height mAU	Area mAU*min	Rel.Area %	Amount	Type
1	2.98	n.a.	12.295	4.497	3.67	n.a.	BMB*
2	3.15	n.a.	0.956	0.275	0.22	n.a.	Rd
3	4.78	n.a.	1.034	0.346	0.28	n.a.	BMB*
4	10.51	n.a.	0.212	3.395	2.77	n.a.	BM
5	10.73	n.a.	0.008	0.021	0.02	n.a.	MB
6	17.12	n.a.	33.556	42.819	34.91	n.a.	BM
7	19.89	n.a.	0.002	0.030	0.02	n.a.	MB
8	25.56	n.a.	36.512	71.256	58.09	n.a.	BM
9	29.67	n.a.	0.002	0.020	0.02	n.a.	MB
Total:			84.577	122.658	100.00	0.000	

Figure 77: HPLC chromatogram of the isolated scalemic acetate **201**

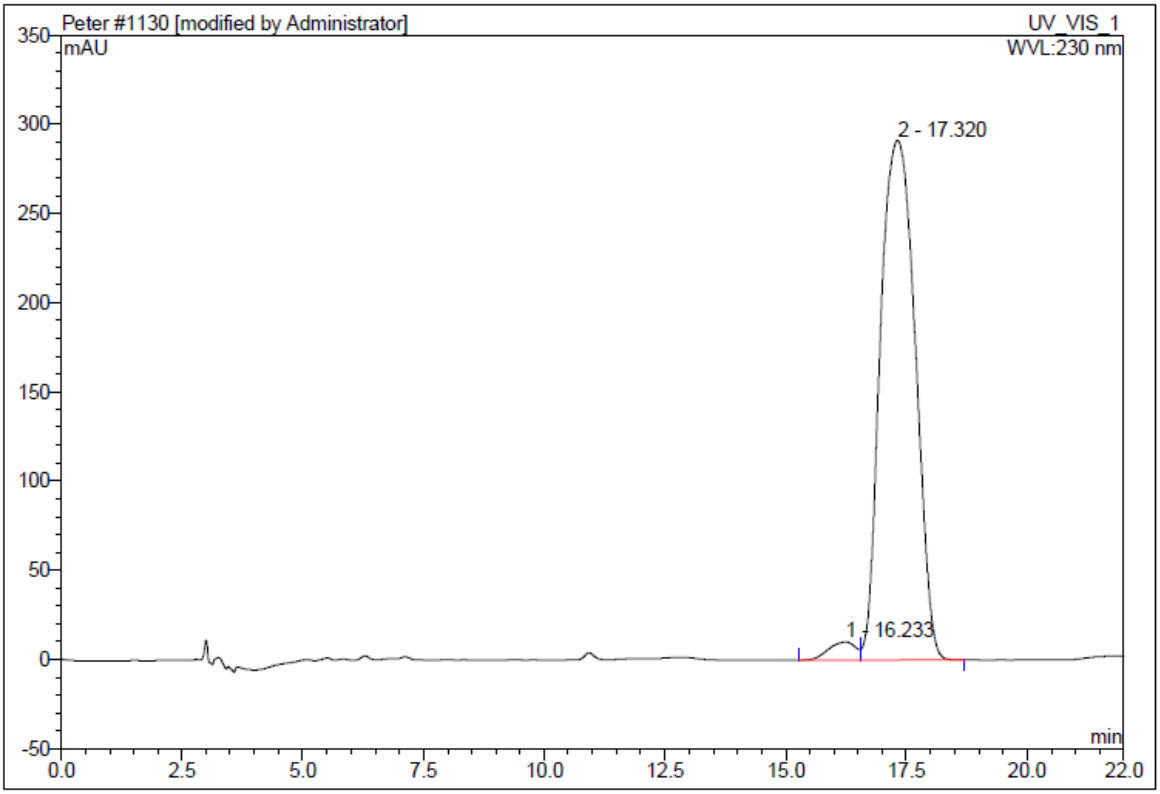

No.	Ret.Time min	Peak Name	Height mAU	Area mAU*min	Rel.Area %	Amount	Type
1	16.23	n.a.	10.166	6.572	2.63	n.a.	BM
2	17.32	n.a.	291.262	243.488	97.37	n.a.	MB
Total:			301.428	250.060	100.00	0.000	

Figure 78: HPLC chromatogram of the isolated enantiopure alcohol **(+)-195**

By reacting a sample of enantiopure alcohol (+)-**195** with (*R*)-(+) and a sample with (*S*)-(-)-α-methoxy-α-(trifluoromethyl)phenylacetic acid (MTPA) afforded Mosher's esters with stable conformation which guided us in determining the stereochemistry (**Scheme 79**). The Mosher's esters *R*)-[(*S*)-2-Cyano-5-phenylpent-1-en-3-yl] 3,3,3-trifluoro-2-methoxy-2-phenylpropanoate **221** and (*S*)-[(*S*)-2-Cyano-5-phenylpent-1-en-3-yl] 3,3,3-trifluoro-2-methoxy-2-phenylpropanoate **223** were isolated as colourless oils in a yields of 81% and 82% respectively.

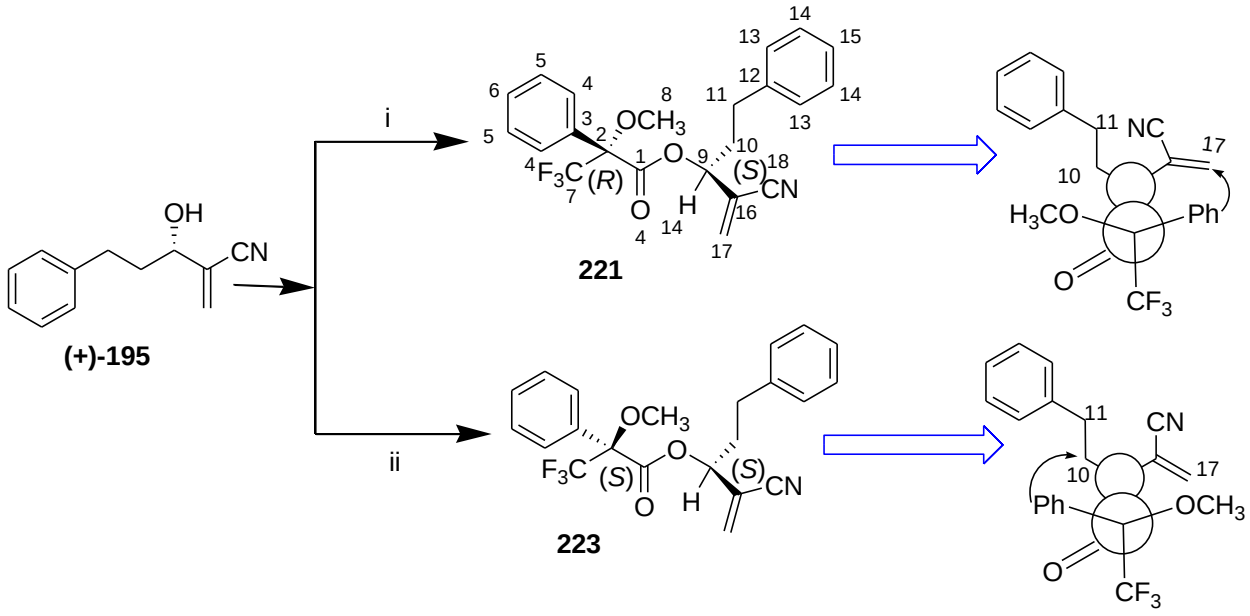

Scheme 79: Synthesis of Mosher's esters **221** and **223**. Reagents and conditions: (i) DCC, DMAP, (*R*)-(+)-MTPA in CH_2Cl_2 at room temperature. (ii) DCC, DMAP, (*S*)-(-)-MTPA in CH_2Cl_2 at room temperature.

The isolated Mosher's esters were fully characterised using spectroscopic techniques. The presence of the aromatic protons in the ^{1}H NMR spectrum of **221** was confirmed by the appearance of four multiplets at δ 7.56 – 7.48, δ 7.47 – 7.38, δ 7.34 – 7.18 and δ 7.16 – 7.10; integrating for two, three, three and two protons respectively. The singlet at δ 6.08 and a doublet at δ 5.96 with a geminal coupling constant of 1 Hz were assigned to H-17a and H-17b. The remaining protons appeared as four multiplets. The first one at δ 5.50 – 5.43 integrating for one proton was assigned to the stereogenic centre proton, H-9. The second multiplet that appeared at δ 3.58 - 3.53 was assigned to the methoxy protons. The last two multiplets which appeared at δ 2.71 – 2.61 and 2.32 – 2.05 were assigned to proton H-11 and H-10 respectively. The splitting pattern of **221** in the ^{1}H NMR spectrum was similar to the splitting pattern of **223** except that geminal coupling was clearer for **223** than for **221**. There was also a difference in chemical shifts for H-8, H-10 and H-17. The information on the differences in chemical shifts for proton H-8, H-10 and H-17 was used to determine the absolute configuration of our enantiopure alcohol (+)-**195** (**Figure 79** and **80**).

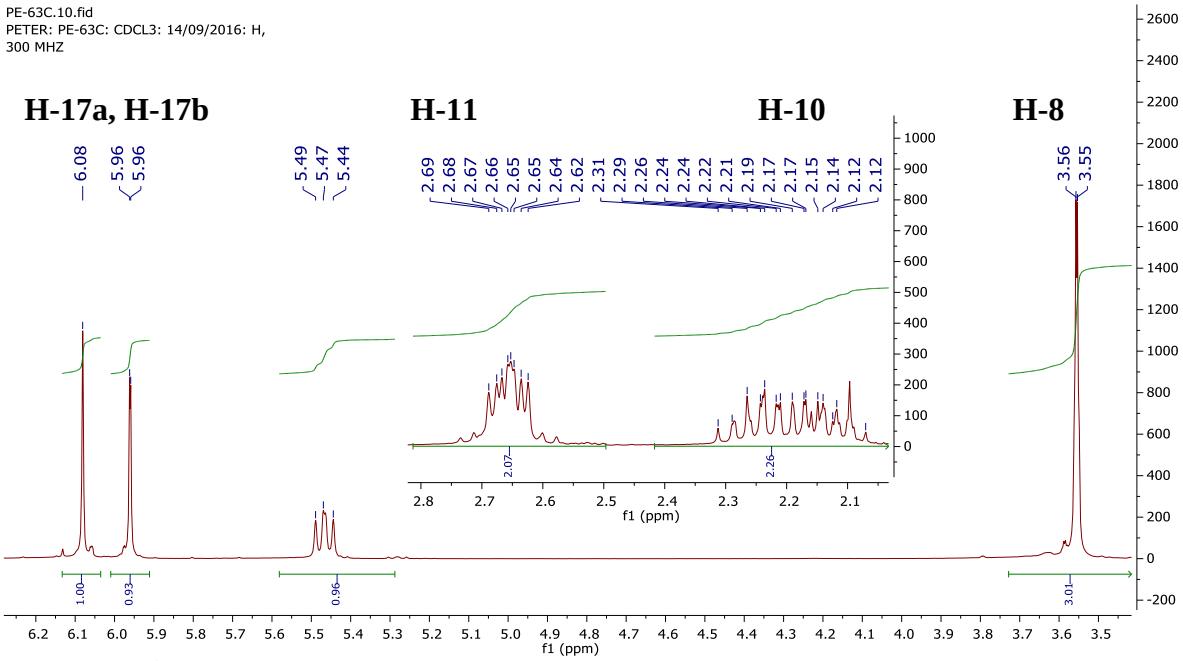

Figure 79: ^{1}H NMR spectrum of *R*-Mosher's ester **221**

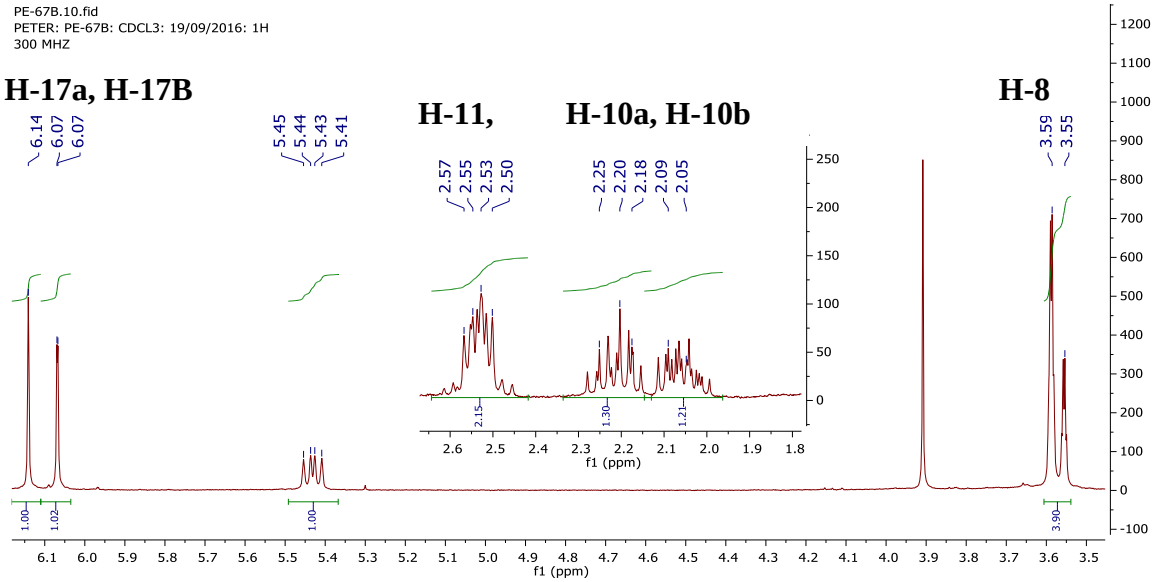

Figure 80: ^{1}H NMR spectrum of *S*-Mosher's ester **223**

The portion of the spectrum shown in **Figure 79** and **80** clearly shows a difference in chemical shift for H-17, H-8 and H-10. This shift is attributed to the diamagnetic effect of the phenyl ring of the alcohol or R-MTP acid. By examining the ^{1}H NMR of *R*-Mosher's ester as a reference spectrum, then it is true that the phenyl ring of (*R*)-MTP acid is shielding the vinyl protons H-17 (ΔSR = 0.06, δ 6.14 – δ 6.08) implying that the phenyl ring originating from the (*R*)-MTP acid and the vinyl protons H-17 are in a *syn*-periplanar arrangement (**Scheme 79**). The deshielding of the proton H-11 in the (*R*)-MTP acid derivative (ΔSR = -0.12, δ 2.54 – δ 2.66) confirms that indeed these two groups are in an

anti-periplanar arrangement. This information confirms to that the enantiopure alcohol **(+)-195** obtained has the *S*-configuration. It was impossible to confirm the stereochemistry of the alcohol with opposite stereochemistry because all of the enzymes capable of hydrolyzing **201** enantioselectively had been used either during the screening exercise or in the scaled-up reaction. In spite of not confirming the stereochemistry, it is with confident that the opposite alcohol is of *R*-configuration as confirmed from previous discussions.

^{13}C NMR spectroscopy was used to further confirm the structures of the Mosher's esters **221** and **223**. The ^{13}C NMR spectra for both esters had a total of 18 signals confirming the presence of 18 carbons that were chemically non-equivalent. Both spectra showed the expected C-F coupling as revealed by the appearance of carbon at δ 127.3 with $^{4}J_{C-F}$ value of 1 Hz for C-4, δ 123.2 with $^{1}J_{C-F}$ value of 289 Hz for C-7, δ 84.7 with $^{2}J_{C-F}$ value of 28 Hz for C-2 and δ 55.6 with $^{4}J_{C-F}$ value of 1 Hz for C-8. The characteristic carbon signals of **221** were observed at δ 165.7 for C-1, 134.0 for C-17, 115.5 for C-18 and 74.7 for C-9. The ^{13}C NMR spectra of **221** and **223** were similar except that there was a small difference in terms of chemical shift. These differences in chemical shifts supports the fact that the two compounds are diastereomers.

The presence of peaks at 2230 cm^{-1} and 1752 cm^{-1} in the IR spectrum of **221** confirmed the presence of the nitrile and carbonyl functional group, respectively. The similar observation of peaks at 2229 cm^{-1} and 1752 cm^{-1} in the IR spectrum of **223** confirmed the presence of nitrile and carbonyl functional group, respectively. The HRMS data [M+Na^{+}]: 426.1268 for both **221** and **223** confirmed that the coupling reaction between the alcohol and the Mosher's acid had taken place.

The remaining set of enzymes that showed hydrolysis of the acetate, gave rise to the opposite enantiomer as shown in **Scheme 80**. The results for these enzymes are shown in **Table 31**.

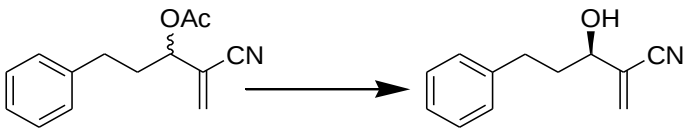

201 **195**

Scheme 80: Hydrolysis of **201** using different lipases and esterases in phosphate buffer at pH-7.00 at different temperatures

Table 31: Hydrolysis of **201** using different enzymes affording **195**

Entry	Enzyme name	Time (h), Temp (°C)	Conv (%)	ee_s (%)	ee_p (%)	E
1	XP-415	120, 35	30	10	24	2
2	Lipase hog pancrease (62300. Biochemika)	120, 35	24	13	41	3
3	Lipopan FBG (Novozymes)	120,35	13	8	57	4
4	Lipase F-AP15 LFW02523	42, 20	42	32	44	3
5	Lipase AK-D "Amano" ILAKX0250K	120, 35	52	3	3	1
6	Lipase AK-D "Amano" ILAKX0W250N	120, 35	21	7	28	2
7	Lipase AK " AMANO " no. 59.001	7, 30	20	14	56	4
8	Lipase LO36P batch no. 143971	7, 30	45	31	38	3
9	Lipase AK "Amano" LAKW09504	7, 30	24	9	30	2
10	Lipase AH-D " Amano" ILAHX015281C	120, 35	20	23	90	24
11	Lipase AY Amano IAYTO2510	7, 30	35	45	84	18
12	Lipase from *Candida rugosa* cat. no 62316	25, 25	26	31	86	18
13	Lipase from *Pseudomonas cepacia* cat. no 62309	25, 25	30	37	86	19
14	Lipo Max Cxt 1.00	3, 35	56	36	29	3
15	Lipase AK "Amano" Lot no. LAKV07510	20, 35	45	44	54	5
16	Amano lipase from *Pseuodomonas fluorescens* cat. no 534730	43, 35	62	74	45	6

The enzymes that hydrolysed the *R*-acetate of **201** generally performed poorly. Only four enzymes gave an overall enantiomeric ratio (E) above 15 with reasonable ee_p but very poor ee_s. These enzymes are all lipases from different microorganisms (**Table 31**, **entries 10-13**). The chromatogram of the alcohol arising from hydrolysis of the *R*-acetate of **201** is shown in **Figure 81**.

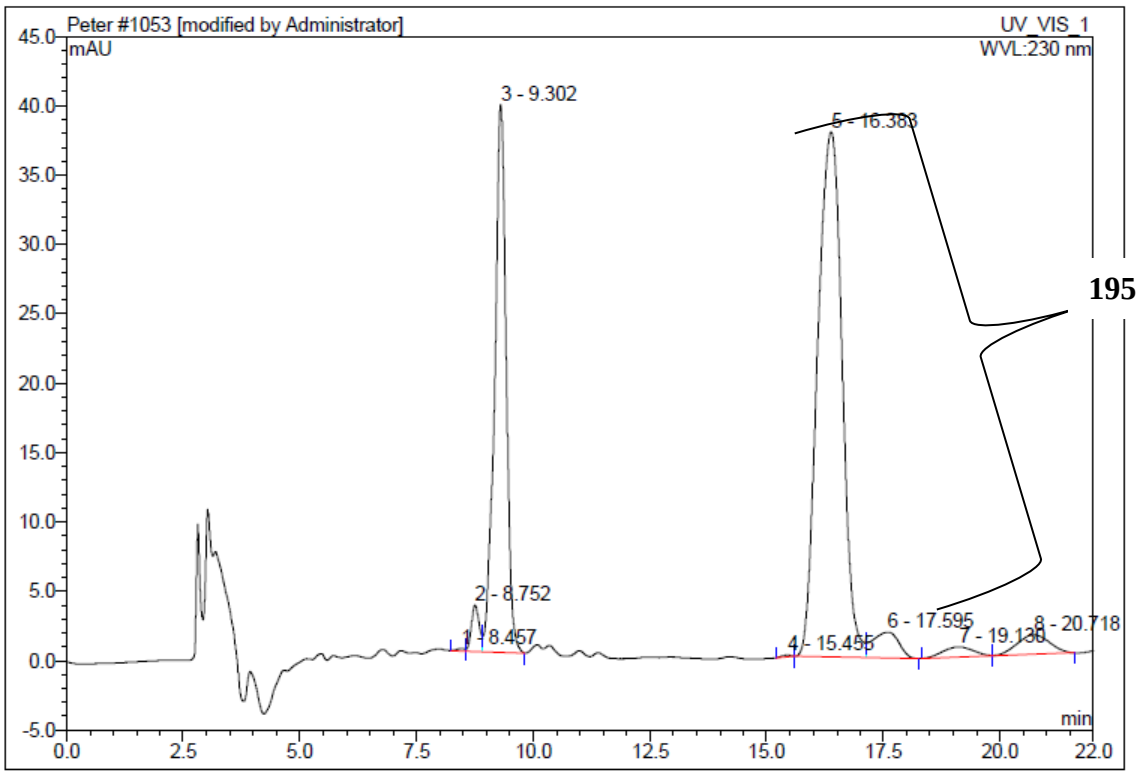

No.	Ret.Time min	Peak Name	Height mAU	Area mAU*min	Rel.Area %	Amount	Type
1	8.46	n.a.	0.177	0.033	0.09	n.a.	BM *
2	8.75	n.a.	3.345	0.654	1.73	n.a.	M
3	9.30	n.a.	39.467	11.294	29.83	n.a.	MB
4	15.46	n.a.	0.109	0.026	0.07	n.a.	BMb*
5	16.38	n.a.	37.820	22.924	60.54	n.a.	bM
6	17.60	n.a.	1.866	1.216	3.21	n.a.	MB
7	19.13	n.a.	0.742	0.572	1.51	n.a.	BM
8	20.72	n.a.	1.411	1.147	3.03	n.a.	MB
Total:			84.937	37.865	100.00	0.000	

Figure 81: HPLC chromatogram after enzymatic activity of Lipase AH-D "Amano" ILAHX015281C after 120 hours at 35 °C

3.2.7.12 Analysis of the results from resolution of acrylonitrile derivatives

Figure 82 shows all the substrates that were subjected to attempted enzymatic kinetic resolution. It can be concluded that the exercise of resolution led to the identification of some enzymes, specifically lipases that performed well on substrates **105a**, **200**, **201** and **203**. The enzymes tested on substrate **202** performed poorly and no enzymatic reaction was observed on substrate **204**. **Table 32** summarises the enzymes that showed good enantiomeric ratio (E) and their sources. It is good to note that by identifying the enzyme

sources by organism will help us analyse the observed performance as shown in the **Table 32**.

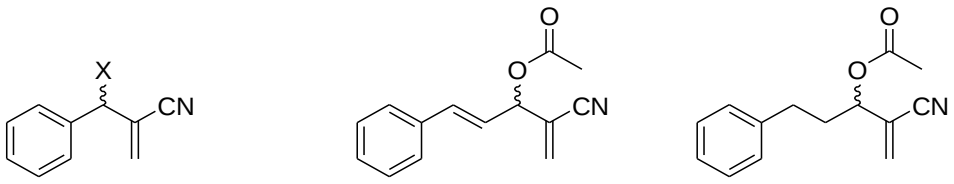

105a X = $OCOCH_3$

202 X = $OCOCH_2Cl$

203 X = $OCO(CH_2)_2CH_3$

204 X = $OCOCH_2CH(CH_3)_2$

200

201

Figure 82: The racemic MBH acetates resolved by hydrolysis

As far as we are aware, the enzymatic kinetic resolution of substrates **200** and **201** has not been reported previously and enantiopure alcohols **191** and **195** have not been obtained previously by other workers. Basavaiah used crude pig liver acetone powder for kinetic resolution of compound **105a**, but obtained a very poor ee of 60% and he did not determine absolute stereochemistry.[169] Bornsheuer *et al*.[78] could achieve only 9% conversion and 76% ee of (+)-product after 33 days when they attempted resolution of **105a** by *P. cepacia* lipase-catalysed transesterification. The method described in this thesis is therefore the first practical resolution method reported for obtaining MBH alcohols **75a**, **191** and **195** in enantiopure form.

Work described here, covering the successful enzymatic kinetic resolution of compounds **105a**, **200** and **201**, together with the determination of absolute stereochemistry for the alcohol and acetate products has been published as: W.P. Juma, V. Chhiba, D. Brady, M.L. Bode. Enzymatic kinetic resolution of Morita-Baylis-Hillman acetates. *Tetrahedron: Asymmetry*, 2017, **28**, 1169-1174.

Table 32: Comparing the enzymatic activity of different enzymes during the hydrolysis of MBH acetates

Compound	**Enzyme source**	**Enzymes that Hydrolysed *S*-acetate**	**ee_s (%)**	**Ee_p (%)**	**E**	**Enzyme source**	**Enzymes that hydrolysed *R*-acetate**	**ees (%)**	**ee_p (%)**	**E**
(±)-**105a**		A total of **25** enzymes showed activity					A total of **9** enzymes showed activity			
	P. fluorescens	Lipase AK "AMANO" Lot no. LAKVO7510	98	90	89	*R. oryzae*	Lipase F-AP15 LFW02523	89	33	5
	P. fluorescens	Amano Lipase from *P. fluorescens*, Cat. no. 534730	79	92	58	*R. oryzae*	Lipase-L036P Batch no 14397 (Biocatalyst)	88	25	4
	P alcaligenes	Lipo Max Cxt 1.00	75	94	72	*A. niger*	Lipase AS Amano LAW035145	90	30	5
	P. cepacia	Lipase from *P. cepacia* cat. no 62309	94	90	65	*C. rugosa*	Lipase from *C. rugosa* cat. no. 62316	19	9	1
	C. Antarctica type B	Lipozyme® CALB L LCN 02106	37	93	40					
	C. Antarctica type B	Novozym 435 LC 20017	34	91	28					
(±)-**202**		A total of **9** enzymes showed activity								
	P. fluorescens	Amano lipase from *P. fluorescens* cat. no. 534730	16	89	21					
(±)-**203**		A total of **9** enzymes showed activity								
	P. fluorescens	Lipase AK "Amano" 59.001	42	90	29					
	C. antarctica type B	Novozym 435 LC 200217	33	98	180					

Compound	**Enzyme source**	**Enzymes that Hydrolysed *S*-acetate**	**ee_s (%)**	**Ee_p (%)**	**E**	**Enzyme source**	**Enzymes that hydrolysed *R*-acetate**	**ees (%)**	**ee_p (%)**	**E**
(±)-**200**		A total of **27** enzymes showed activity					A total of **12** enzymes showed activity			
	P. fluorescens	Lipase from *P. fluorescens* cat no. 95608	96	93	100	*F. oxysporum*	Lipopan FBG	31	90	27
	P. fluorescens	Amano Lipase AK Lot no. 0351202	61	96	100	*B. licheniforrmis*	Alcalase (Novozymes)	24	88	20
	C. Antarctica type B	Lipozyme® CALB L LCN 02106	24	96	70					
	P alcaligenes	Lipo Max Cxt 1.00	29	93	36					
(±)-**201**		A total of **8** enzymes showed activity					A total of **16** enzymes showed activity			
	C. antarctica type B	Lipase from *C. antarctica* type B	37	94	44	*P. fluorescens*	Lipase AH-D " Amano" ILAHX015281C	23	90	24
	C. antarctica type B	Lipozyme® CALB L435 LC 200217	20	96	54	*C. rugosa*	Lipase AY Amano IAYTO2510	45	84	18
						P. cepacia	Lipase from *P. cepacia* cat. no 62309	37	96	19

Note. *P* for *Pseudomonas*, *C* for *Candida*, *R* for *Rhizopus*, *A* for *Aspergillus*, *F* for *Fusarium*, *B* for *Bacillus*

3.2.8 Enzymatic kinetic resolution of MBH ethyl esters

3.2.8.1 Background information

Enzymatic resolution by hydrolysis of an ethyl ester bond is a method that is famously known and applied to separate racemates.[182] The applied enzyme selectively hydrolyses one ethyl ester as it leaves the other one untouched, hence two different compounds are formed that can be separated easily. An example showing the resolution of 3-hydroxy-3-phenylpropanoate **224** by hydrolysing the ethyl ester bond to give **225** is shown in **Scheme 81** .[183]

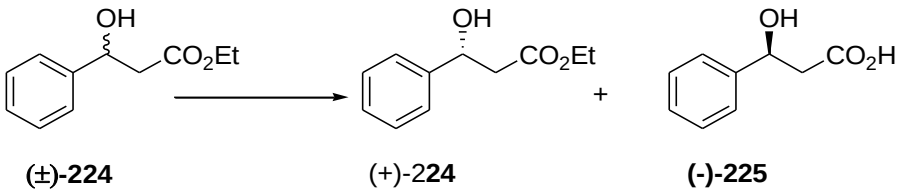

(±)-224 (+)-2**24** **(-)-225**

Scheme 81: Resolution of the racemic **224** using lipase PS-30 from *Pseudomonas sp*. (Amano) in phosphate buffer at pH 7.00

It was therefore important to find out what would be the results in the case where Morita-Baylis-Hillman ethyl esters are subjected to different enzymes. These sets of compounds that should be selectively hydrolysed to the corresponding carboxylic acids are the racemic ethyl 2-(hydroxy(phenyl)methyl)acrylate **196**, (*E*)-ethyl 3-hydroxy-2-methylene-5-phenylpent-4-enoate **102e** and (±)-ethyl 3-hydroxy-2-methylene-5-phenylpentanoate **197**. The resulting compounds that are supposed to be enantiopure after hydrolysis are the acids 2-(hydroxy(phenyl)methyl)acrylic acid **205**, (*E*)-3-hydroxy-2-methylene-5-phenylpent-4-enoic acid **103e** and -3-hydroxy-2-methylene-5-phenylpentanoic acid **206**. The synthesis of both the esters and their corresponding acids has already been described earlier. We were interested in these compounds so that we could fully compare the results with the earlier resolved compounds; and also relate our results to those found in literature. Furthermore, enantiopure adducts arising from this resolution have a lot of synthetic potential.

3.2.8.2 Resolution of the Morita-Baylis-Hillman ethyl esters

A similar procedure described before was applied for screening all the three ethyl esters. This procedure involved taking 7 mg of the ester, dissolving in acetone and adding to an Eppendorf containing 7 mg of the enzymes in a phosphate buffer at pH 7.00. The reaction mixture was placed on an orbital shaker and the temperature set at 30 °C. This optimum

temperature at which we could observe a new spot by TLC was obtained after trying various temperatures. Those reactions that showed a new spot by TLC were further subjected to HPLC using a C-18 column and finally to chiral HPLC analysis for enantioselectivity determination.

Each of the substrates was screened against 65 enzymes that comprised of lipases and esterases. The screening exercise began with the racemic ethyl 2-(hydroxy(phenyl)methyl)acrylate **196** expecting it to be hydrolysed to an enantiopure 2-(hydroxy(phenyl)methyl)acrylic acid **205.** Enantioselectivity monitoring of the reaction mixture was possible after determining the chromatographic separation of the enantiomers **196** and **205**. Using the chiral Lux® 5µm Amylose-2 column at a flow rate of 1 mL/min comprising of hexane, IPA and methanol (90:9:1) led to the separation of the ester **196** (**Figure 83**). The column used for separating the acid **205** was a Lux® 5µm Amylose-1 at a mobile flow rate of 1 mL/min with a mobile composition hexane and IPA and methanol (90:5:5). The reaction shown in **Scheme 82** afforded the results shown in **Table 33**.

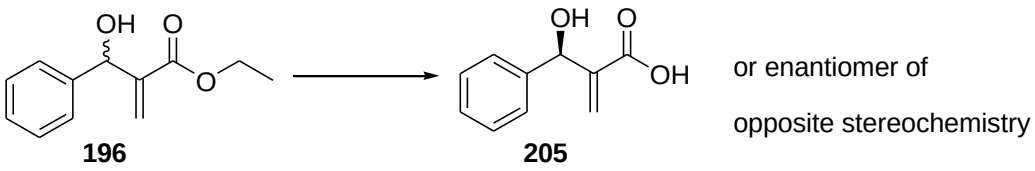

Scheme 82: Hydrolysis of **196** using different enzymes in phosphate buffer at pH 7.00 at 30 °C

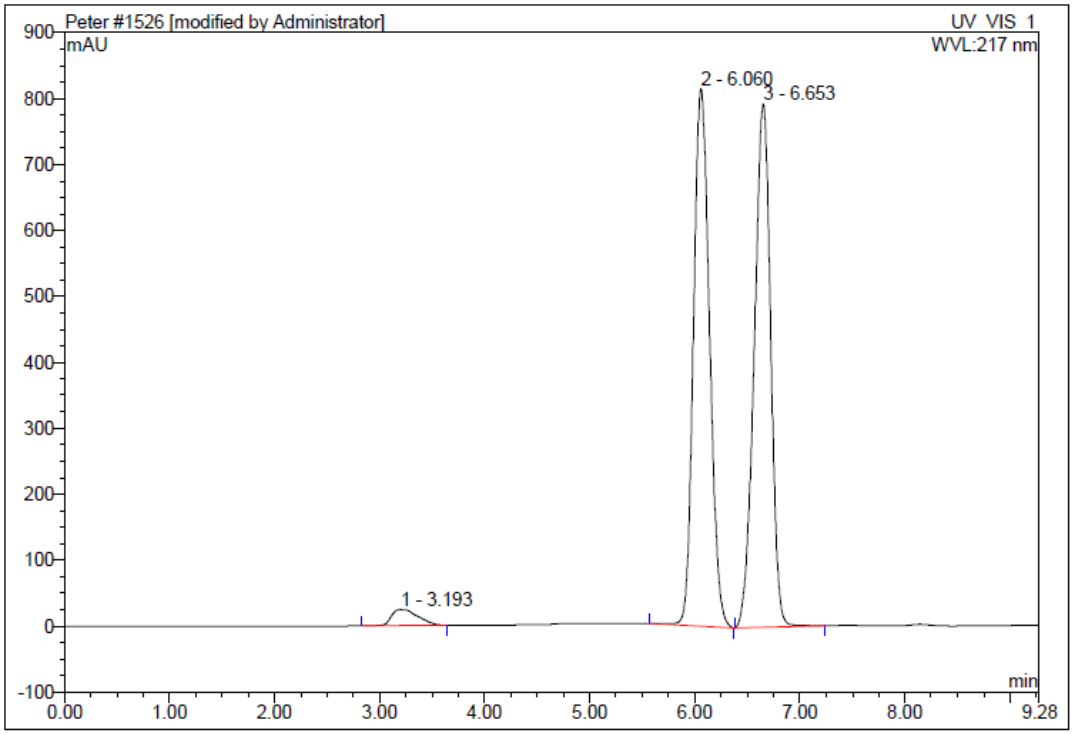

No.	Ret.Time min	Peak Name	Height mAU	Area mAU*min	Rel.Area %	Amount	Type
1	3.19	n.a.	24.187	7.010	2.37	n.a.	BMB*
2	6.06	n.a.	815.167	144.368	48.88	n.a.	BMB*
3	6.65	n.a.	793.402	143.979	48.75	n.a.	BMB*
Total:			1632.756	295.357	100.00	0.000	

Figure 83: HPLC chromatogram of the racemic ester **196**

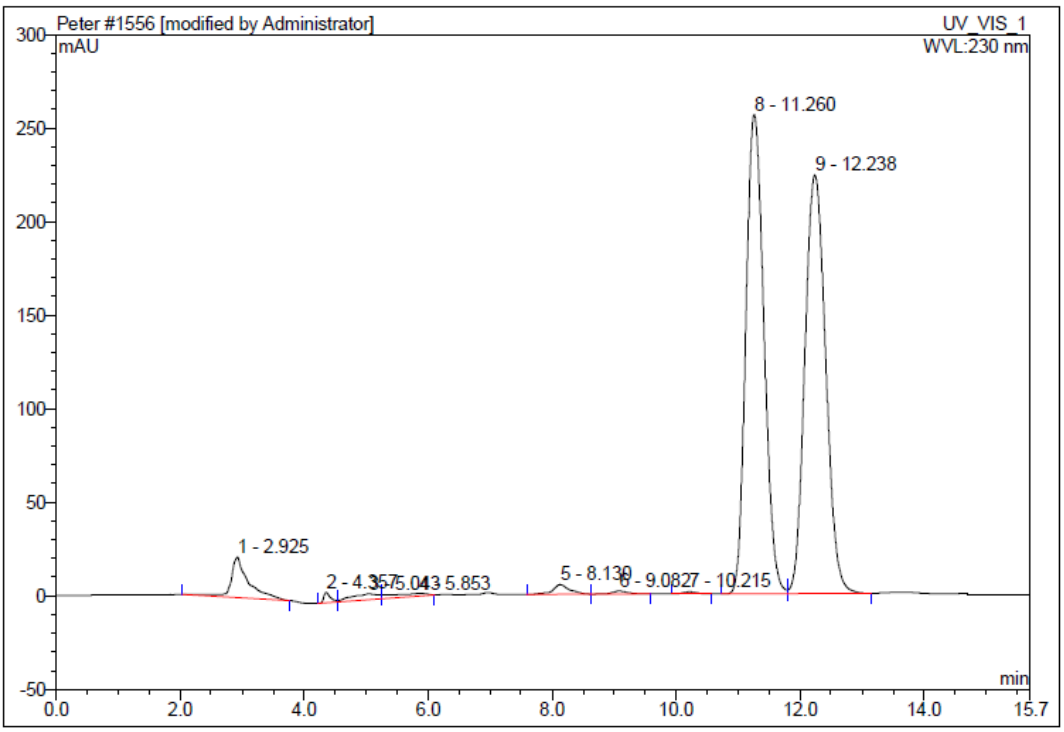

No.	Ret.Time min	Peak Name	Height mAU	Area mAU*min	Rel.Area %	Amount	Type
1	2.93	n.a.	21.728	7.211	3.86	n.a.	BMB*
2	4.36	n.a.	5.512	0.679	0.36	n.a.	BM *
3	5.04	n.a.	3.162	1.606	0.86	n.a.	M *
4	5.85	n.a.	1.499	1.205	0.65	n.a.	MB*
5	8.13	n.a.	5.202	1.643	0.88	n.a.	BM
6	9.08	n.a.	1.544	0.475	0.25	n.a.	MB
7	10.22	n.a.	1.227	0.325	0.17	n.a.	BMB
8	11.26	n.a.	256.040	86.442	46.30	n.a.	BM *
9	12.24	n.a.	223.710	87.112	46.66	n.a.	MB*
Total:			519.624	186.698	100.00	0.000	

Figure 84: HPLC chromatogram of the racemic acid **205**

Table 33: Hydrolysis of the ester **196** using different enzymes affording **205**

Entry	Enzyme name	Time (h)	Conv (%)	ee_s (%)	ee_p (%)	E
1	Lipase AK " Amano' 20 Lot No LAKWA09504	64	44	34	43	3
2	Lipase AK " Amano' 20 Lot No 59.001	64	21	14	54	4
3	Amano lipase from *Pseudomonas fluorescens* cat. no. 534730	46	20	14	56	4
4	Lipo Max Cxt 1.00	64	24	25	81	12
5	Lipase AK " Amano" Lot No. ILAKW 1150	64	9	5	50	3
6	Lipase AH-D " Amano" ILAHXO15281C	48	6	5	76	86
8	Lipase AK "Amano" Lot No. AKK026094	64	7	4	49	3
9	Amano lipase AK Lot. no. 0351202	64	30	19	44	3
10	Lipase from *pseudomonas fluorescens* Cat. no. 28602	67	6	4	58	4
11	Lipase B *candida antarctica*, recombinant *from aspergillus oryzae* Cat. no. 62288	67	37	1	2	1
12	Lipase from *pseudomonas cepacia* Cat. no. 62309	67	20	14	57	4

Unfortunately, none of the enzyme tested on these substrates gave an acceptable enantiomeric ratio of 15 and above. The best result was obtained for the lipase Lipo Max cxt 1.00 that gave an enantiomeric ratio of 12, which is below the recommended value for an effective process (**Table 33, entry 4**). The ee_p and ee_s at this enantiomeric ratio were calculated to be 81% and 25%, respectively at a conversion of 24%. Lipomax is a lipase originating from *Pseuodomonas alcaligenes*. The use of lipase AH-D " Amano" ILAHXO15281C gave an E value of 86 (**Table 25, entry 6**), which is not significant at the calculated conversion of 6%. Apparently, it seems the availability of literature material confirming the resolution of **196** either by hydrolysis or esterification is missing suggesting that this is the first report. The compound **205** has been reported during the hydrolysis of a nitrile functional group by hydratase/amidase *Rhodococcus sp.* AJ270.[66]

The other set of enzymes whose results were obtained using **Scheme 83** hydrolysed the opposite ethyl ester (**Table 34**). The enzyme that hydrolysed the opposite ethyl ester were the worst in terms of performance.

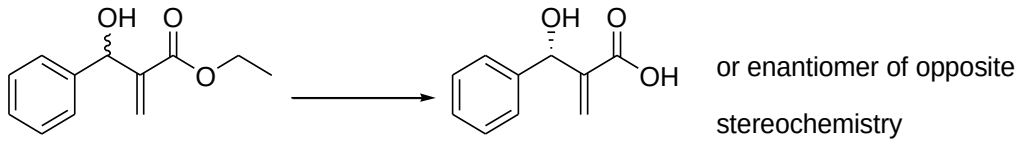

196 **205**

Scheme 83: Hydrolysis of **202** using different enzymes in phosphate buffere at pH 7.00 at 30 °

Table 34: Hydrolysis of the ester **196** using different enzymes affording **205**

Entry	Enzyme name	Time (h)	Conv (%)	ee_s (%)	ee_p (%)	E
1	Novozym 435 LC 200217	45	23	11	36	2
2	Novozym CALB	46	54	5	5	1
3	Esterase Cat no. ESL-001-01, with cut stabiliser	64	1	1	80	9
4	Esterase Cat no. ESL-001-01, 6Z0248	64	17	14	73	7
5	Lipozyme CALB LCN 02106	88	84	5	1	1
8	Lipase from *mucor miehei* Cat no. 62298	67	28	2	6	1

The synthesis of an adequate quantity of **205** for conversion to Mosher esters was not possible as all the enzymes had been used for the previous reactions.

The same procedure that was used for investigating **196** was applied to the resolution of **102e**. Separation of the acetate **102e** and the acid **103e** on two different chiral HPLC columns enabled us to monitor the reaction progress. The acetate separated on a Lux 5µm cellulose-1 column using a mobile flow composition of hexane and IPA (90:10) at a flow rate of 1 mL/min (**Figure 85**). The use of a Lux® 5µm Amylose-1 with a mobile flow composition of hexane, IPA and methanol (90:5:5) flowing at the rate of 1mL/min led to the resolution of the acid **103e (Figure 86)**. Using the reaction shown in **Scheme 84** afforded the results presented in **Table 35**.

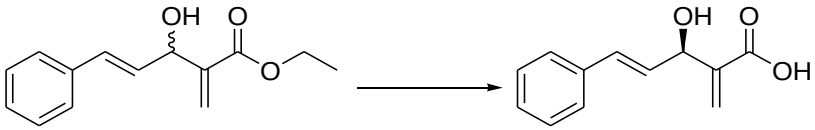

102e **103e**

or enantiomer of opposite stereochemistry

Scheme 84: Hydrolysis of **102e** using different enzymes in phosphate buffer at pH-7.00 at 30 °C

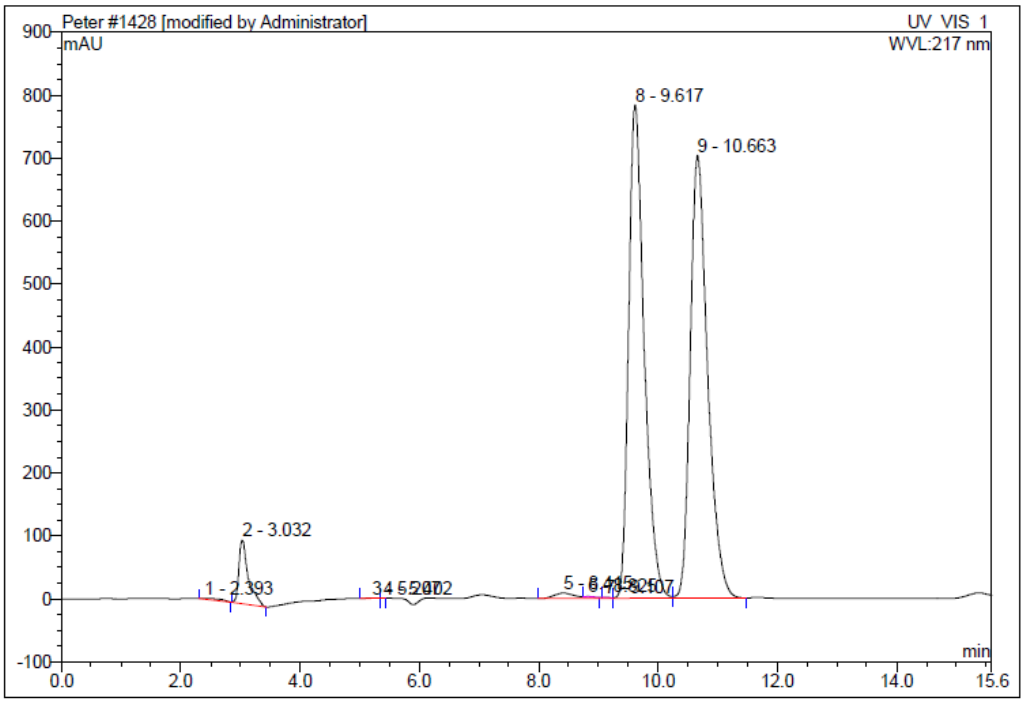

No.	Ret.Time min	Peak Name	Height mAU	Area mAU*min	Rel.Area %	Amount	Type
1	2.39	n.a.	0.986	0.920	0.18	n.a.	BMB*
2	3.03	n.a.	101.014	18.388	3.69	n.a.	BMB
3	5.21	n.a.	0.677	0.137	0.03	n.a.	BM *
4	5.40	n.a.	0.046	0.006	0.00	n.a.	MB*
5	8.42	n.a.	8.512	4.100	0.82	n.a.	BM *
6	8.83	n.a.	0.862	0.117	0.02	n.a.	Rd
7	9.11	n.a.	0.126	0.016	0.00	n.a.	Rd
8	9.62	n.a.	784.095	236.741	47.49	n.a.	M *
9	10.66	n.a.	703.531	238.052	47.76	n.a.	MB*
Total:			1599.849	498.477	100.00	0.000	

Figure 85: HPLC chromatogram of the racemic **102e**

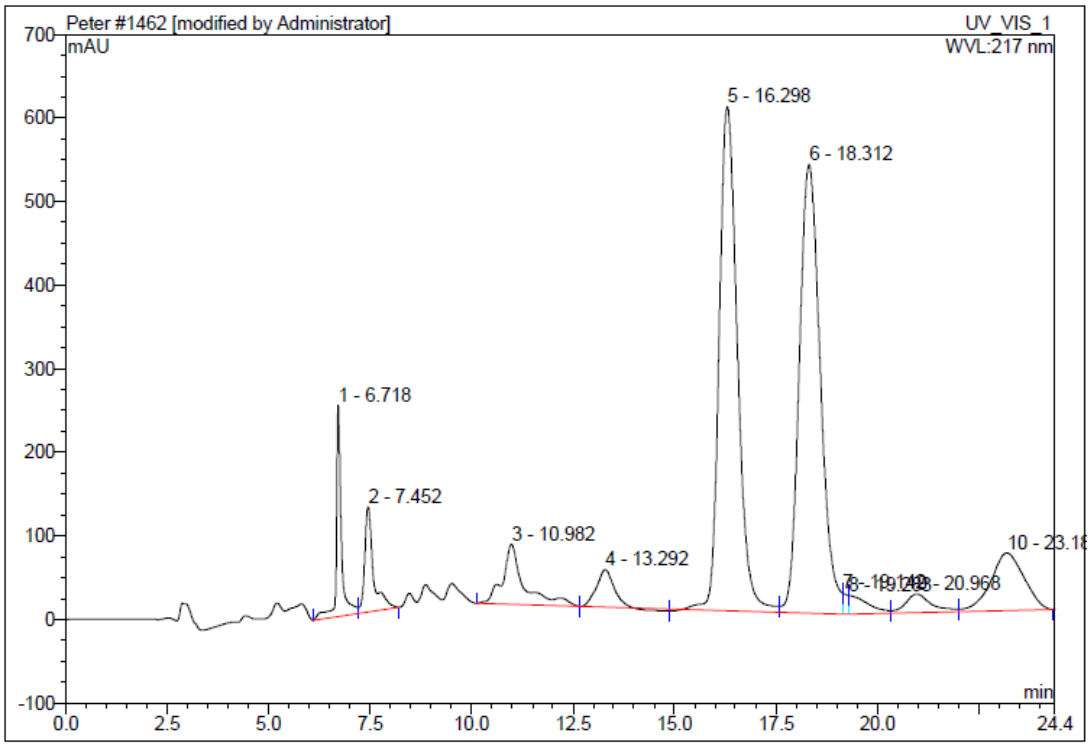

No.	Ret.Time min	Peak Name	Height mAU	Area mAU*min	Rel.Area %	Amount	Type
1	6.72	n.a.	252.915	36.218	4.18	n.a.	BM *
2	7.45	n.a.	125.854	31.783	3.67	n.a.	MB*
3	10.98	n.a.	71.807	43.793	5.06	n.a.	BM *
4	13.29	n.a.	44.752	21.000	2.43	n.a.	M *
5	16.30	n.a.	602.834	313.142	36.17	n.a.	M *
6	18.31	n.a.	536.424	322.027	37.20	n.a.	M *
7	19.14	n.a.	25.115	3.355	0.39	n.a.	M *
8	19.28	n.a.	22.698	12.396	1.43	n.a.	M *
9	20.97	n.a.	22.450	16.594	1.92	n.a.	M *
10	23.18	n.a.	68.809	65.428	7.56	n.a.	MB
Total:			1773.659	865.735	100.00	0.000	

Figure 86: HPLC chromatogram of the racemic acid **103e**

Table 35: Hydrolysis of the ester **102e** using different enzymes affording **103e**

Entry	Enzyme name	Time (d)	Conv (%)	ee_s (%)	ee_p (%)	E
1	lipase from porcine pancreas	23	16	0.2	30	2
2	Alcalase (Novozymes)	3.3	1	1	47	3
3	Esterase Cat no. ESL-001-01, with cut stabiliser	6.3	27	17	46	3
5	Esterase Cat no. ESL-001-01, 720268	6.3	28	31	80	12
6	Esterase Cat no. ESL-001-01, 6Y0240	6.3	36	20	36	3

Entry	Enzyme name	Time (d)	Conv (%)	ee_s (%)	ee_p (%)	E
7	Esterase Cat no. ESL-001-01, 6Z0248	8	44	46	58	6
8	Lipase from *Candida antarctica* type B	0.67	98	76	1	2
9	Novozym 435 LC200217	0.3	18	16	74	8
	Novozym 435 LC200217	0.8	41	49	72	10
10	Lipozyme CALB L LCN 02106	0.3	41	27	39	3
11	Novozym 435 LC 200233	0.3	25	25	78	10
12	Novozym CALB	0.3	30	20	45	3
13	Novozym CALB	0.3	31	20	43	3

It is visible from **Table 35** that all the enzymes performed poorly on this substrate with the best in in this group affording an enantiomeric ratio of 12 while the second best enzyme afforded an enantiomeric ratio of 10. These enzymes are esterase Cat no. ESL-001-01, 6Y0240 (**entry 5**) and Novozym 435 LC200217, which is an immobilised form of CALB (**entry 9**). The resolution of **102e** has been reported to be achieved using porcine liver esterase affording products with poor enantiomeric ratio (E) of 5.[81]

The second group of enzymes hydrolysed the opposite enantiomer of the acetate **102e**. Using the reaction shown in **Scheme 85** afforded results presented in **Table 36**.

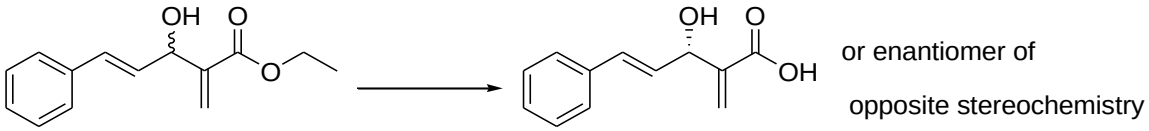

102e **103e**

Scheme 85: Hydrolysis of the ester **102e** using different enzymes in phosphate buffer at pH-7.00 at 30 °C

Table 36: Hydrolysis of the ester **102e** using different enzymes affording **103e**

Entry	Enzyme name	Time (d)	Conv (%)	ee_s (%)	ee_p (%)	E
1	lipase from *Pseudomonas cepacia*	23	25	31	93	38
2	Novozyme 388 LUN 00020	0.83	13	9	59	4
	Novozyme 388 LUN 00020	4.3	47	40	45	4
3	Lipase AY Amano IAYTO2510	3.3	59	88	61	12
4	*Candida rugosa* Lipase AY Amano	4.3	49	85	90	46
5	Lipase from *candida rugosa* Cat. no. 62316	0.67	49	80	82	25
6	Lipase from *candida rugosa* Cat. no. 62316	1	50	87	88	46
7	Lipase from *Candida rugosa* Cat. no. 90860	1	34	48	94	55

Table 36 clearly shows that a total of 6 enzymes afforded an enantiomeric ratio (E) of 15 and above. All the enzymes were lipases from *Pseudomonas cepacia*, lipase AY amano, different preparations of lipase from *Candida rugosa* (**entries 3-7**). The HPLC chromatograms of the enzymatic activity of lipase from *Candida rugosa* were very much encouraging as shown in the supporting data. It is good to note that Novozym 388 LUN 00020 is a lipase from *Rhizomocur miehei*.[184]The determination of the stereochemistry was not done because all the enzymes that gave reasonable results were used in performing the previous reactions.

The last ethyl ester to examine was ethyl 3-hydroxy-2-methylene-5-phenylpentanoate **197**. The screening exercise was possible after successfully separating **197** and its corresponding acid **206** on HPLC chiral column. The acetate separated on a Lux 5µm cellulose-1 column with a mobile flow rate of 1 mL/min using hexane and IPA (90:10) as eluent (**Figure 87**). The corresponding acid was able to resolve into two equal peaks on a Lux® 5µm Amylose-1 column with a mobile flow rate of 1 mL/min and composition of hexane and IPA (94:6) (**Figure 88**). The results arising from using the reaction shown in **Scheme 86** are shown in **Table 37**.

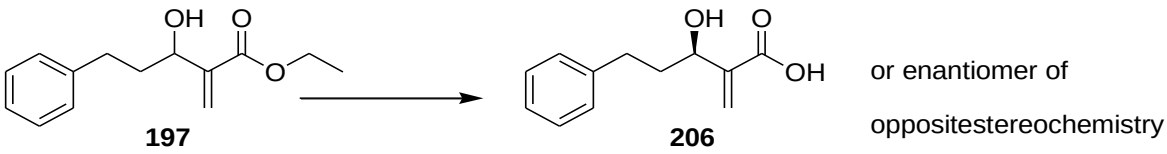

Scheme 86: Hydrolysis of **197** using different enzymes in phosphate buffer at pH 7.00 at 30 °C

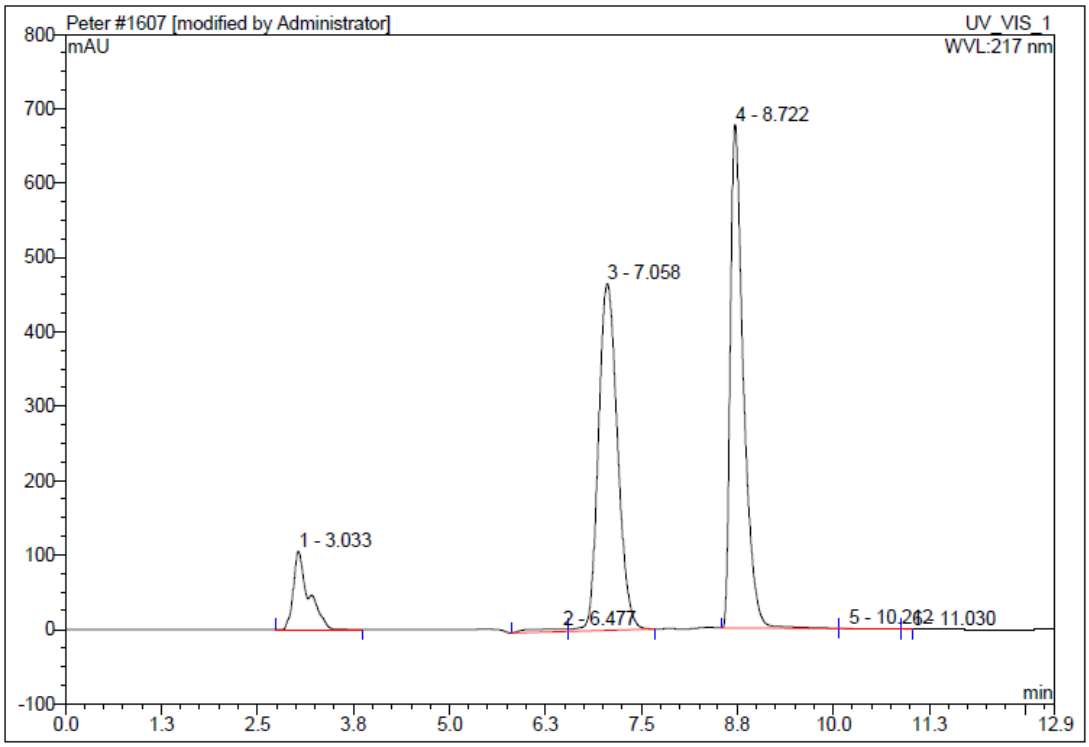

No.	Ret.Time min	Peak Name	Height mAU	Area mAU*min	Rel.Area %	Amount	Type
1	3.03	n.a.	105.127	24.356	8.22	n.a.	BMB*
2	6.48	n.a.	3.383	2.452	0.83	n.a.	BM *
3	7.06	n.a.	465.997	134.106	45.24	n.a.	MB*
4	8.72	n.a.	677.064	135.171	45.60	n.a.	BM *
5	10.21	n.a.	0.816	0.336	0.11	n.a.	M *
6	11.03	n.a.	0.000	0.002	0.00	n.a.	MB*
Total:			1252.388	296.424	100.00	0.000	

Figure 87: HPLC chromatogram of the racemic acetate **197**

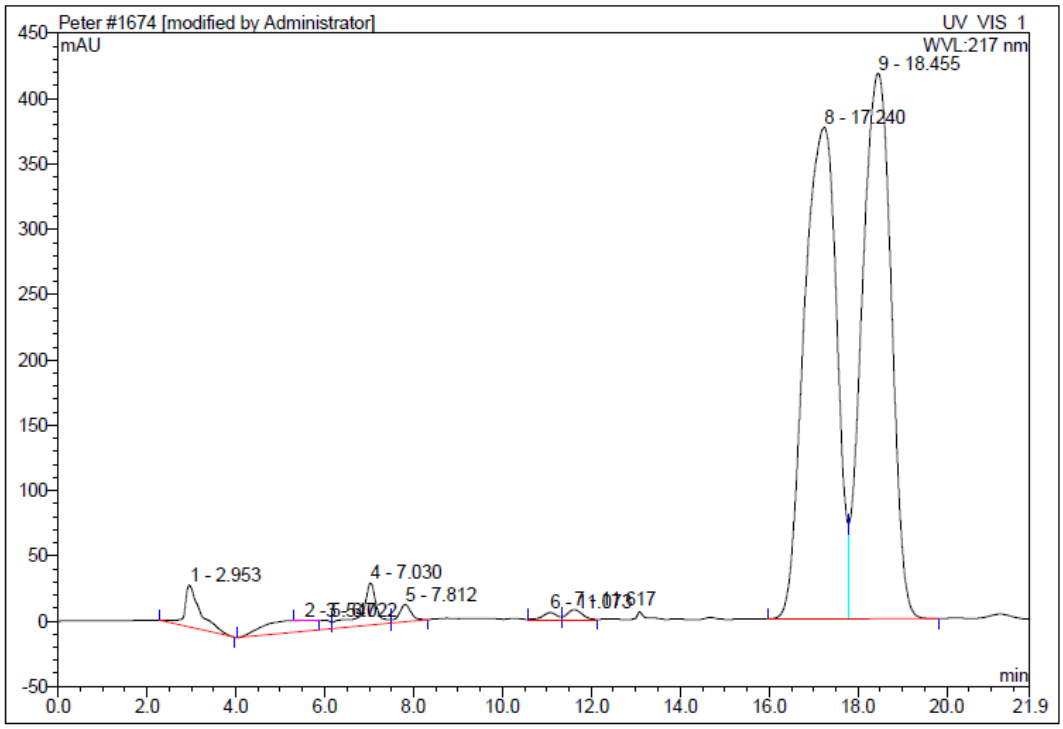

No.	Ret.Time min	Peak Name	Height mAU	Area mAU*min	Rel.Area %	Amount	Type
1	2.95	n.a.	32.074	13.530	1.98	n.a.	BMB*
2	5.55	n.a.	0.395	0.116	0.02	n.a.	Ru
3	6.02	n.a.	6.886	14.013	2.05	n.a.	BM *
4	7.03	n.a.	32.031	12.816	1.87	n.a.	M *
5	7.81	n.a.	12.914	3.997	0.58	n.a.	MB*
6	11.07	n.a.	5.263	1.855	0.27	n.a.	BM
7	11.62	n.a.	7.491	2.878	0.42	n.a.	MB
8	17.24	n.a.	376.262	317.751	46.39	n.a.	BM *
9	18.46	n.a.	417.472	318.064	46.43	n.a.	MB*
Total:			890.787	685.020	100.00	0.000	

Figure 88: HPLC chromatogram of the racemic acid **206**

Table 37: Hydrolysis of the ester **197** using different enzymes affording **206**

Entry	Enzyme name	Time (h)	Conv (%)	ees (%)	eep (%)	E
1	Novozym CALB	4.5	93	57	4	2
2	Novozym CALB	4.5	79	55	14	2
3	Novozym 435 LC200233	0.17	1	1	41	2
4	Novozyn CALB	4.5	79	57	16	2
5	Novozym 435 LC200217	0.17	5	1	23	2
6	Lipozyme CALB L LCN 02106	4.5	71	55	22	3

It is observed in **Table 37** that all the enzymes tested performed dismally to an extent that the use of these enzymes on this substrate cannot be recommended. The Novozym CALB recorded in the table are of different preparations. The other set of enzymes that gave very poor results hydrolysed the opposite enantiomer. The results are shown in **Table 38** and they were obtained using the reaction shown in **Scheme 87**.

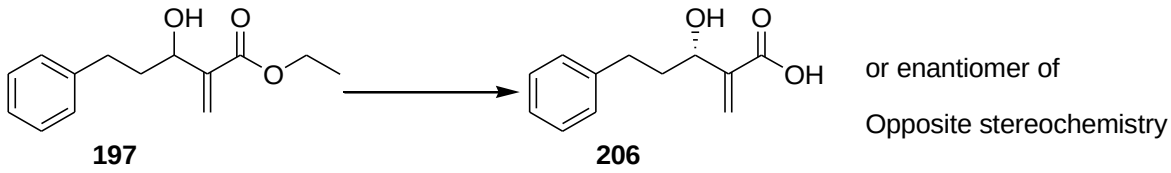

197 **206**

Scheme 87: Hydrolysis of **197** using different enzymes in phosphate buffer at pH 7.00 at 30 °C

Table 38: Hydrolysis of the ester **197** using different enzymes affording **206**

Entry	Enzyme name	Time (h)	Conv (%)	ee_s (%)	ee_p (%)	E
2	Esterase Cat no. ESL-001-01 with cut stabilizer	44	73	1	1	1
3	Lipase F-AP15	44	8	4	48	3
4	Lipase Sigma type II from porcine pancreas	44	14	7	46	3
5	Esterase Cat no. ESL-001-01, 6Z0248	44	12	4	27	1
6	Esterase Cat no. ESL-001-01, 6Y0240	44	19	5	21	2
7	Lipase from *candida rugosa* Cat no. 63316	50	46	48	56	6

The results in **Table 38** also indicate that the enzymes that hydrolysed the opposite enantiomer performed poorly. It is sad that only 13 enzymes showed activity (that was not selective) out of 65 enzymes tested. This suggests that only genetically engineered enzymes can improve enantioselectivity on this substrate. Unfortunately, it seems there are no reports on enzymatic resolution of **197**. It was not possible to determine the stereochemistry as all the enzymes had been used in the previous reactions.

3.2.8.3 Analysis of the results from enzymatic kinetic resolution of MBH esters

Enzymatic kinetic resolution by hydrolysis of the carboxylic esters of the MBH adducts proved to be less successful than that using the MBH acetates. This is perhaps not surprising, as the hydrolysis occurs closer to the stereogenic centre for the acetates than for the carboxylic ester derivatives, where the stereogenic centre is further away.

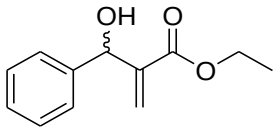

196

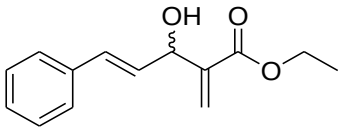

102e

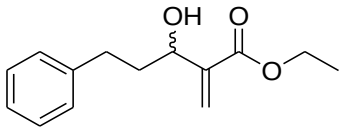

197

Figure 89: The racemic MBH ethyl esters tested for resolution by hydrolysing the ester bond

Table 39: Comparing the enzymatic activity of different enzymes during hydrolysis of the ester bond

Compound	**Enzyme source**	**Enzymes that Hydrolysed *S*-acetate**	**ee_s (%)**	**Eep (%)**	**E**	**Enzyme source**	**Enzymes that hydrolysed *R*-acetate**	**ees (%)**	**ee_p (%)**	**E**
(±)-**196**		A total **12** enzymes showed activity					A total of **8** enzymes showed activity			
	P. alcaligenes	Lipo Max Cxt 1.00	25	81	12		Esterase Cat no. ESL-001-01, 6Z0248	14	73	7
(±)-**102e**		A total of **7** enzymes showed activity					A total of **13** enzymes showed activity			
	C. rugosa	Lipase AY Amano	85	90	46		Esterase Cat no. ESL-001-01, 720268	31	80	12
	p. cepacia	lipase from *p. cepacia*	31	92	38	*C. antarctica* type B	Novozym 435 LC200217	49	72	10
(±)-**197**		A total of **6** enzymes showed activity					A total of **7** enzymes showed activity			
	C. antarctica type B	Lipozyme CALB L LCN 02106	55	22	3	*C. rugosa*	Lipase from *candida rugosa* Cat no. 63316	48	56	6

3.3 Nucleophilic addition of different nucleophiles on Morita-Baylis-Hillman adducts (MBHA)

3.3.1 Background information

It was a milestone after successfully resolving several MBH adducts including the nitrile, methyl and ethyl acrylate derivatives of *trans*-cinnamaldehyde as shown in the previous section. These sets of compounds were very important for the next series of reactions. These series of reactions to be investigated should overcome the challenge of racemisation that was encountered, as described in the first section of the results and discussion. The only option at hand was to think of chemical transformations that could make use of **191**, **193** and **102e** (**Figure 90**) as suggested in the first section of results and discussion. The new route should lead to similar compounds that had been previously intended to be synthesized (for example **171**) as shown in **Figure 90**.

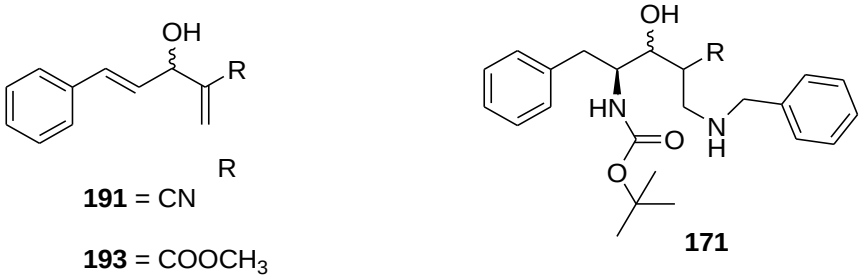

191 = CN

193 = $COOCH_3$

102e = $COOCH_2CH_3$

171

Figure 90: MBH adducts **191**, **193** and **102e** proposed to be the starting material for the synthesis of scaffold **171**

The first proposal was to use the synthetic route shown in **Scheme 88**. In this scheme, the first step involves protecting the hydroxyl group of the MBH adduct (**191**, **193** or **102e**) using *tert*-butyldimethylsilyl chloride (TBSCl) in the presence of imidazole as a base in dimethylformamide (DMF) or the use of *tert*-butyldimethylsilyl trifluoromethanesulfonate (TBSOTf) in the presence of triethylamine (TEA) in dry dichloromethane to give **226**. Protection of this nature is very important as it allows stereoselective nucleophilic addition to the α,β-unsaturated system[185] which is of great interest in this investigation.

The second step involves nucleophilic addition of benzylamine to the double bond of the protected MBHA (Michael addition) in either THF or methanol. It is expected that this step will be stereoselective because of the protected hydroxyl group of the MBH adduct. The next step will be epoxidation using *m*-CPBA to give **228**, followed by nucleophilic opening of the

epoxide using sodium azide affording **229**. It is assumed that this process could be regioselective because of the nature of the substrate. It is assumed that the bulk *tert*-butyl group would support this regioselective epoxide opening. Hydrogenation of benzyl alcohol **229** using a catalytic amount of palladium(II) chloride mixed with triethylsilane in ethanol would form compound **230**. This method of hydrogenation that has been applied to different scaffolds has been reported in literature.[186] The next step would involve the conversion of the azide group to an amine **231** using hydrogen in the presence of palladium on carbon as reported in literature.[187] The last step would be the removal of TBS by use of TBAF in THF at zero degrees to give **232**.

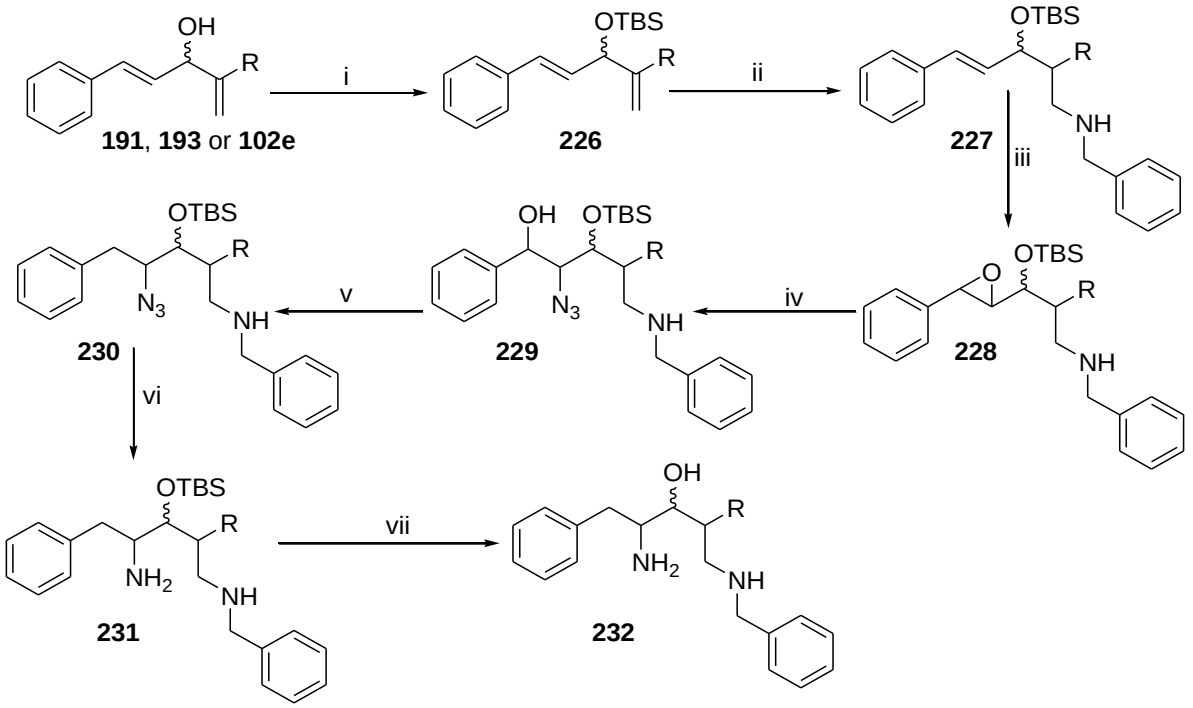

Scheme 88: Proposed synthetic route for the synthesis of the **232**, equivalent to deprotected scaffold **171**. *Reagent and conditions*: (i) TBSCl, imidazole in DMF at RT or TBSOTf, TEA in DCM at 0 °C; (ii) Benzylamine in THF or methanol at RT; (iii) *m*-CPBA, $NaHCO_3$ at 0 °C; (iv) NaN_3, MeoH: H_2O or DMF at 60 °C; (v) cat. $PdCl_2$, Et_3SiH in EtOH; (vi) H_2, Pd/C; (vii) TBAF in THF at 0 °C.

The second proposed method was to perform Sharpless asymmetric dihydroxylation on **227** using AD mix-α in *t*BuOH and water in the ratio of 1:1 to get a diol **233** as shown in **Scheme 89**. This procedure has been widely reported [188] to work on many substrates and therefore it was hoped that it would also work on these scaffolds. Hydrogenation of the benzyl alcohol

233 would lead to compound **234**. Tosylation of alcohol **234** will be achieved using tosyl chloride in triethylamine (TEA) at elevated temperatures. Nucleophilic substitution of the tosyl group by azide will generate scaffold **230**. Scaffold **230** will be subjected to hydrogenation in the presence of palladium and thereafter deprotection would be carried out to arrive at the intended scaffold **232**.

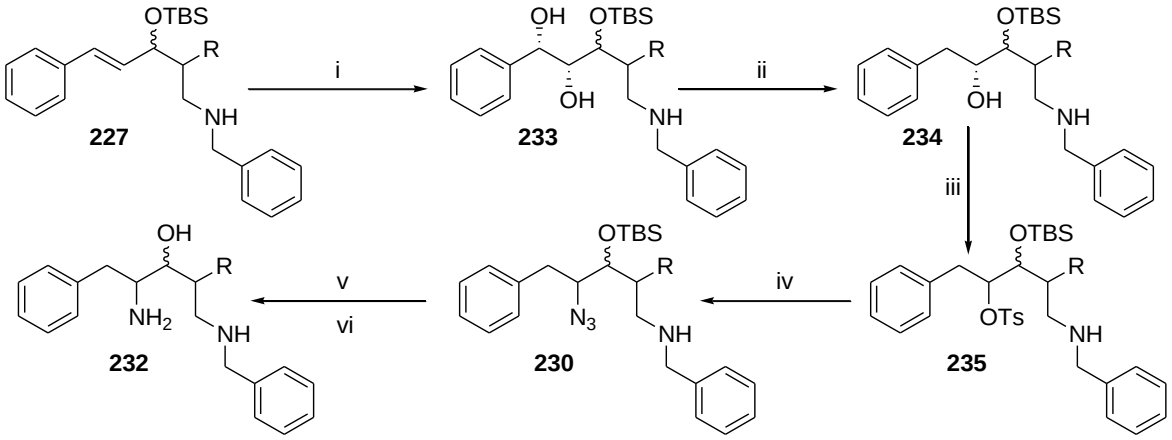

Scheme 89: Alternative proposed synthetic route for the synthesis of scaffold **232**. *Reagents and conditions*: (i) AD mix-α, ^{t}BuoH-H_2O (1:1) (ii) cat. $PdCl_2$, Et_3SiH in EtOH (iii) TsCl, TEA, DCM (iv) NaN_3, MeoH: H_2O (1:1) or DMF at 65° C (v)H_2**,** Pd (C); (vi) TBAF in THF at 0 °C.

It was convincing that synthetic principles had been used to logically propose the two schemes and therefore it was reasonable that either of the routes would be manageable. Knowing that the practical aspects in organic synthesis do not always match the expected theoretical outcome, other avenues would also be explored in case the above routes could not work.

It was clear that alcohol protection and nucleophilic addition using benzylamine (**Scheme 88 step i and ii**) were possible but there was a doubt if epoxidation (**Scheme 88 step iii**) could work. There was also uncertainty of the nucleophilic ring opening of the epoxide using sodium azide (**Scheme 88, step iv**). There use of Sharpless asymmetric dihydroxylation on the substrates was also based on probalities (**Scheme 89, step i**). As a result of this uncertainty, it was necessary to test epoxidation and Sharpless asymmetric dihydroxylation on known substrates first. This test would aid in explaining what might be observed when a similar

reaction is carried out on the desired substrates. Therefore, the first step was to carry out these reactions on model systems.

3.3.2 Epoxidation and nucleophilic ring opening of the epoxide on reported substrate

This section began by transforming commercially available *trans*-cinnamaldehyde to *trans*-cinnamyl alcohol **236** (**Scheme 90, step i**). This was achieved by using a mild reducing agent sodium borohydride in methanol at 0 °C. The formation of **236** was confirmed by ^{1}H NMR spectroscopy. This was confirmed by the appearance of a doublet at δ 4.28 integrating for two protons corresponding to H-1 and a singlet at δ 2.19 integrating for one proton corresponding to the hydroxyl group. In addition, there was a multiplet at δ 7.40 – 7.17 integrating for five protons corresponding to the aromatic protons. The *trans*-alkene protons were evident at δ 6.58 for H-3 and δ 6.33 for H-2 appearing as two doublets of triplets. Proton H-3 appeared as a doublet of triplets with a coupling constant of 15.9 and 1.8 Hz confirming that it was *trans* to H-2 and it was experiencing long range coupling with H-1. Proton H-2 also appeared as doublet of a triplets with a coupling constant of 15.9 and 5.7 Hz for H-2.

The structure was further confirmed by ^{13}C NMR spectroscopy. The carbonyl peak was replaced by the alcohol peak at δ 63.6. The rest of the carbon signals were similar to the signals of the starting material. The presence of the peak at 3295 cm^{-1} in the IR spectrum confirmed the presence of the hydroxyl group. The spectroscopic data obtained were in agreement with literature data. [187, 189]

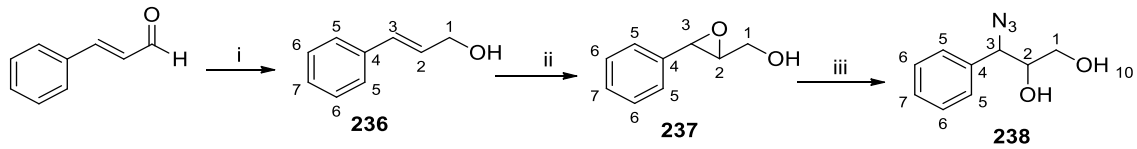

Scheme 90: Transformation of *trans*-cinnamaldehyde to azido diol via epoxidation. *Reagents and conditions*: (i) $NaBH_4$, methanol at 0 °C (ii) *m*-CPBA, $NaHCO_3$, CH_2Cl_2 at 0 °C (iii) NaN_3, NH_4Cl in MeOH: H_2O (1:1).

The second step was to form an epoxide using trans-cinnamyl alcohol as a starting material (**Scheme 90, step ii**). This was achieved by using *meta*-chlorobenzoic acid in dichloromethane at 0 °C. The formation of the racemic epoxide **237** was confirmed by the

presence of a multiplet at δ 4.05 – 3.95 integrating for one proton corresponding to H-3 in the ^{1}H NMR spectrum. The multiplet at δ 3.90 – 3.86 was assigned to H-2. The presence of H-3 and H-2, more shielded than the *trans*- protons of **236** confirmed that the reaction had taken place. The remaining protons had chemical shifts similar to the starting material. The ^{13}C NMR spectrum supported the formation of the epoxide. The appearance of carbon signals at δ 62.6 and 55.7 which are carbon atoms attached to oxygen confirmed that the double bond had been oxidised. The spectroscopic data obtained was in agreement with that reported in literature.[190]

The last step was to open the epoxide using sodium azide and ammonium chloride in methanol (**Scheme 90, step iii**). This reaction led to the formation of azido diol **238** that was confirmed by ^{1}H NMR spectroscopy. The assignment of ^{1}H and ^{13}C NMR signals was in agreement with reported assignment in literature.[187] In order to be certain that the azide had added to the epoxide on the side indicated, 2D- NMR experiments were conducted. The 2D experiments performed included COSY and HMBC. From the COSY spectrum, we observed that a doublet at δ 4.46 (H-3) coupled with a multiplet at δ 3.75 – 3.65 (H-2) which in turn coupled with a doublet of doublets at δ 3.54 (H-1). It was further observed from HMBC that an aromatic proton correlated with the carbon signal at δ 67.0 (C-3) while a doublet at δ 4.46 (H-3) correlated with the carbon signals at δ 136.1 (C-4), 128.6 (C-5), 74.0 (C-2) and 62.9 (C-1). ^{14}N NMR spectroscopy was further used to confirm where the azide group was attached as described in literature.[191] The two signals in the ^{15}N NMR spectrum correlated well with a doublet at δ 4.46 (H-3) indeed confirming the azide had been attached at the C-3 position.

3.3.3 Sharpless asymmetric dihydroxylation on reported substrate

Ethyl cinnamate was selected as a model substrate for performing Sharpless dihydroxylation. [192] Synthesis of ethyl cinnamate **239** involved addition of thionyl chloride and refluxing the mixture at 75 °C for 2 hours (**Scheme 91, step i**). The unreacted thionyl chloride was removed under reduced pressure and the resultant mixture was added to dry dichloromethane in which ethanol was added and stirred for 16 hours. The resultant mixture was purified by silica gel column chromatography, affording ethyl cinnamate **239** as a colourless oil. The formation of the ester was evident by the appearance of an IR peak at 1707 cm^{-1} in the spectrum confirming the presence of a C=O of an ester group. Additional signals were observed in the ^{1}H NMR

and ^{13}C NMR spectra. For example, there was a quartet at δ 4.26 and a triplet at δ 1.33, integrating for two and three protons, respectively, corresponding to H-8 and H-9. The carbon signals at δ 60.5 for C-8 and δ 14.3 for C-9 were also observed. This clearly indicated that the reaction had taken place. The spectroscopic data was in agreement with that found in literature.[193]

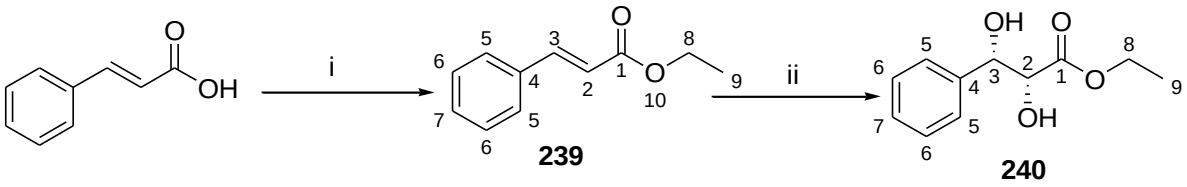

Scheme 91: Esterification and Sharpless asymmetric dihydroxylation. *Conditions and reagents*: (i) $SOCl_2$, CH_2Cl_2 and CH_3CH_2OH at RT (ii) AD mix-α, tBuoH-H_2O at RT.

The next step was to use a reported procedure for performing Sharpless asymmetric dihydroxylation (SAD).[194] The reaction was achieved using AD mix-α in a mixture of *tert*-butyl alcohol and water in a ratio of 1: 1. This led to a diol **240** whose structure was confirmed using ^{1}H and ^{13}C NMR spectroscopy. The disappearance of the alkene protons and the appearance of the stereogenic centre protons H-3 and H-4 and the two hydroxyl protons confirmed that the product had formed. The presence of a doublet of doublets at δ 4.99 with a coupling constant of 6.9 and 3.1 Hz integrating for one proton corresponded to H-3 while the other doublet of doublets at 4.35 with a coupling constant of 5.6 and 3.1 Hz corresponded well with H-2. The presence of a coupling constant of 3.1 Hz between the H-3 and H-2 confirmed that the two protons are on the same side of the bond as described by Karplus.[195, 196] The ^{13}C NMR spectrum also confirmed that the two alkene carbon signals had disappeared but instead were replaced by the carbon signals at δ 74.4 and 74.6 for C-3 and C-2 respectively. All the spectroscopic data obtained was similar to the spectroscopic data reported in literature.[197]

After successfully carrying out epoxidation and Sharpless asymmetric dihydroxylation reactions, these two reactions were now ready for testing on the intended substrate.

3.3.4 Nucleophilic addition of nitrogen nucleophiles on racemic MBH alcohols

It was time to investigate nucleophilic addition using nitrogen nucleophiles on the different MBH alcohols arising from *trans*-cinnamaldehyde. These reactions were very crucial for noting the difference in terms of selectivity when the alcohol is protected and when the alcohol of MBHA is unprotected. It is expected that when nucleophilic addition is performed using the reaction shown in **Scheme 92**, then four stereoisomers shown in **Figure 91** will be obtained. Among the four stereoisomers, compounds **a** and **c** are enantiomers and **b** and **d** are enantiomers. It is expected that NMR will be used for calculating the reaction diastereoselectivity, ie. *syn* versus *anti* selectivity.

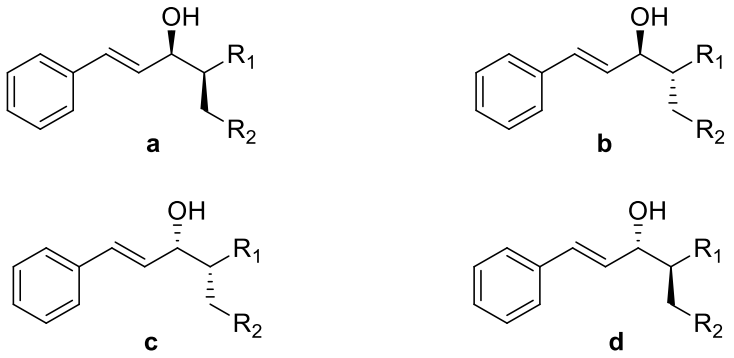

Figure 91: Expected stereoisomers after performing nucleophilic addition on MBHA racemates

It was time to embark on nucleophilic addition of nitrogen nucleophiles using the reaction shown in **Scheme 92**. This reaction led to several nucleophilic adducts that were isolated and characterised.

.

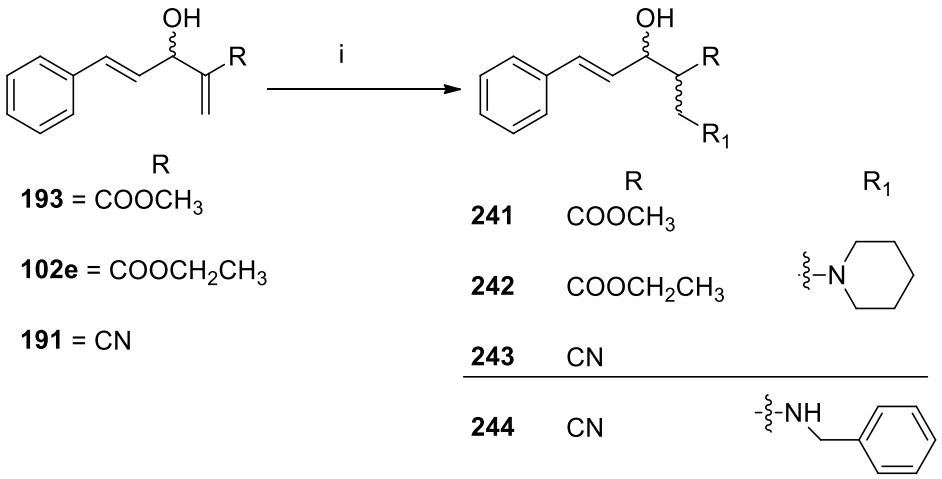

Scheme 92: Nucleophilic addition of nitrogen nucleophiles to MBHA. *Reagents and conditions*: (i) either piperidine /benzylamine in methanol or piperidine/benzylamine in THF at RT.

The investigation began by reacting piperidine with **(***E*)-methyl 3-hydroxy-2-methylene-5-phenylpent-4-enoate **193** in different solvents. The solvents tested for this reaction included ethanol, methanol, acetonitrile and THF. Among the solvents investigated, only THF led to a new product as indicated by TLC. The use of THF for 24 hours resulted in a crude product that was purified by column chromatography using 50% ethyl acetate in hexane. This step afforded (*E*)-methyl 3-hydroxy-5-phenyl-2-(piperidin-1-ylmethyl)pent-4-enoate **241** as a colourless oil that was a mixture of diastereomers in a yield of 74% and an R_f value of 0.54 in 50% ethyl acetate in hexane. The ratio of the major and minor diastereomers was found to be 1.2:1 from the integration of the proton peaks in ^{1}H NMR spectrum. It was possible to distinctively characterise each diastereomer using ^{1}H, ^{13}C and 2D-NMR techniques.

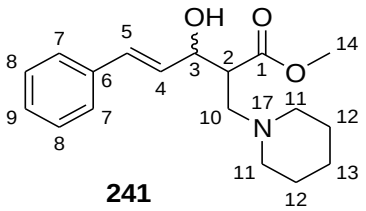

241

The first diastereomer whose protons appeared deshielded in the ^{1}H NMR spectrum was the minor diastereomer. The appearance of a new stereogenic centre proton H-2 and non-equivalent methylene protons H-10 supported the formation of the new product. The multiplet at δ 3.28 – 3.20 integrating for one proton was assigned to H-2 while a triplet at δ 2.91 and a multiplet at 2.76 – 2.52 each integrating for one proton were assigned to H-10a and H-10b respectively. The most upfield protons that were poorly resolved in the ^{1}H NMR spectrum

were assigned to the piperidinyl ring. The multiplets at δ 2.76 – 2.52 and δ 1.70 – 1.53 each integrating for four protons were assigned H-11 and H-12 respectively. The last upfield multiplet at δ 1.51 – 1.37 integrating for two protons was assigned H-13. The characteristic stereogenic centre H-3 was observed as a multiplet at δ 4.86 – 4.80 while the methoxy protons H-14 appeared as a singlet at δ 3.67. The presence of a doublet at δ 6.75 with a *trans*-coupling constant of 15.8 Hz was assigned proton H-5, while the coupling neighbour H-4 was seen at δ 6.25 as a doublet of doublets with a coupling constant of 15.8 and 4.3 Hz. This coupling information confirmed that H-4 is coupling with H-3 and *trans*-coupling with H-5. The phenyl protons were the most downfield protons and they appeared as a multiplet at δ 7.43 – 7.19 with an integration value of five. The ^{1}H NMR spectrum is shown in **Figure 92**.

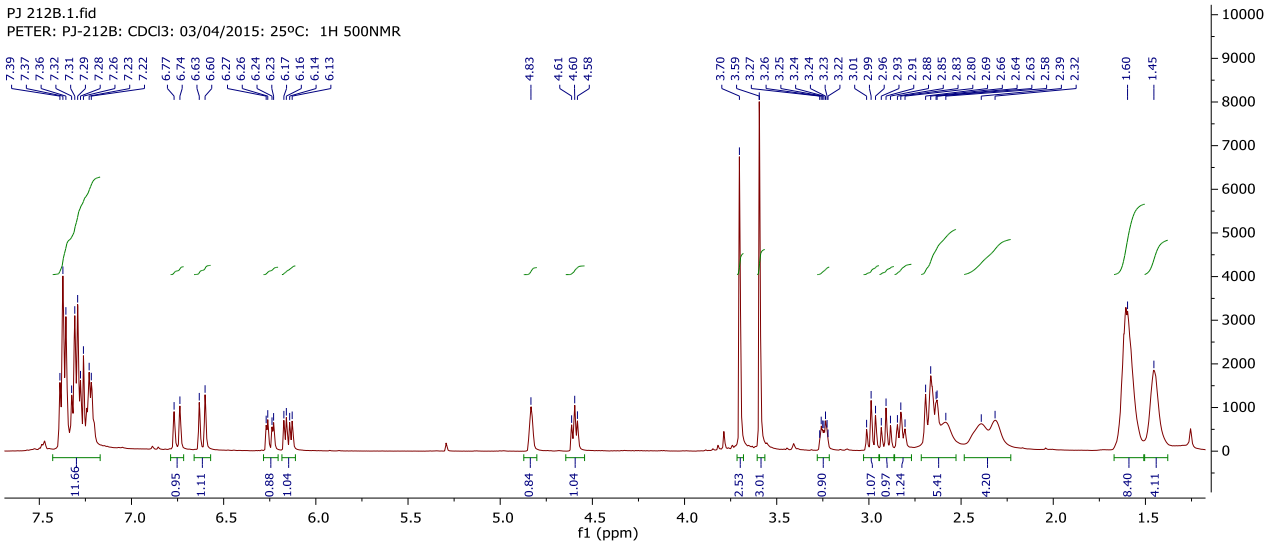

Figure 92: ^{1}H NMR spectrum of the minor and major diastereomers of compound **241**

The assignment of H-5, H-4, H-3 and H-10 was supported by ^{1}H-^{1}H 2D-COSY spectrum. The spectrum confirmed that H-5 was coupling with H-4 which in turn coupled with H-3. In addition, H-3 coupled with H-2 which in turn coupled with H-10. There was also observed coupling correlation between H-12 and H-13.

The formation of **241** was supported by the presence of 14 carbon signals in the ^{13}C NMR spectrum. The characteristic carbon signals at δ 45.6 and 56.8 were assigned to C-2 and C-10 while the piperidinyl ring carbon signals were observed at δ 54.8, 26.0 and 24.0 for C-11, C-12 and C-13 respectively. The stereogenic centre carbon C-3 was observed at δ 73.2 while the

methoxy carbon C-14 was observed at 51.9 ppm. The rest of the peaks were assigned to the phenyl ring carbon atms and the vinyl carbon atoms C-5 and C-4.

The assignment of C-2, C-5, C-4, C-3, C-10, C-11, C-12 and C-13 was confirmed by ^{1}H-^{1}H 2D-HSQC spectrum. The ^{13}C DEPT 135 experiment was also very useful for supporting the assignment. The disappearance of two signals from the DEPT 135 spectrum led to the accurate assignment of quarternary carbons C-1 and C-6. The appearance of a positive carbon signal in the DEPT 135 spectrum led to the identification of CH and CH_3 carbons. The signals that appeared downfield were assigned to the aromatic carbons C-7, C-8, C-9 and alkene carbons C-5 and C-4. The oxygenated CH and CH_3 signals were assigned to C-3 and C-14 while the saturated CH signal was assigned to C14. The presence of negative carbon signals in the DEPT 135 spectrum led to the possible assignment of C-10, C-11, C-12 and C-13.

The cross-peaks in the heteronuclear Multiple Bond Coherence (HMBC) spectrum between H-5 and C-7; H-4 and C-6/C-2; H-10 and C-11/C-3; H-3 and C-10 were used to unambiguously assign these protons and carbons. All the the 2D correlations that were similar for the minor and major diastereomers are shown in **Table 40**.

Table 40: 2D NMR data of the minor and major diastereomer **241**

COSY		**HSQC**		**HMBC**	
H-5	H-4	H-5	C-5	H-5	C-3, C-7, C-6
H-4	H-3	H-4	C-4	H-4	C-2, C-3, C-6
H-3	H-2	H-3	C-3	H-3	C-2, C-5, C-10
H-2	H-10	H-10	C-10	H-10a	C-1
H-12	H-13	H-14	C-14	H-14	C-1
		H-2	C-2	H-2	C-1, C-3, C-4, C-10,
		H-11	C-11	H-10b	C-1, C-2, C-3, C-11
		H-12	C-12	H-13	C-11
		H-13	C-13		

The second diastereomer to be characterised was the major diastereomer. This was represented by a larger integration value in the ^{1}H NMR spectrum. The proton peak patterns

were similar to the minor diastereomer with only a slight difference in the chemical shifts of proton and carbon signals (**Table 41**).

The table confirms that the multiplicities of the protons were the same with the only difference that the minor diastereomer protons appeardownfield as compared to the protons of the major diastereomer. On the other hand, the chemical shift of carbon signals of the minor diastereomer were upfield as compared to the chemical shifts of carbon signals of the major diastereomer. The only exception was the uniqueness of C-6 and C-14 (**bolded in Table 41**). The chemical shifts of these carbons were downfield for the minor and upfield for the major diastereomer. The other observation noted was the large difference in δ value between C-2 and C-3 of the major and minor diastereomer. These differences are expected to be greatest at the stereogenic centres.

Table 41: Comparison of characteristic ^{1}H and ^{13}C NMR peaks of the minor and major diastereomer of **241**

Proton and carbon number	**Minor diastereomer**	**Major diastereomer**
H-5	6.75 (1H, d, *J* = 15.8 Hz)	6.62 (1H, d, *J* = 15.7 Hz)
C-5	131.0	131.2
H-4	6.25 (1H, dd, *J* = 15.8, 4.3 Hz)	6.15 (1H, dd, *J* = 15.8, 6.2 Hz)
C-4	129.5	129.6
H-3	4.86 – 4.80 (1H, m)	4.62 – 4.54 (1H, m)
C-3	**73.2**	**76.3**
H-14	3.67 (3H, s)	3.60 (3H, s)
C-14	**51.9**	**51.7**
H-2	3.28 – 3.20 (1H, m)	2.87 – 2.79 (1H, m)
C-2	45.6	48.1
C-1, **C-6**, C-7, C-10	172.15, **137.0**, 126.5, 45.6	172.18, **136.9**, 127.6, 48.1

The IR spectrum of **241** included hydroxyl (3220 cm^{-1}) and carbonyl (1731 cm^{-1}) absorption bands. The molecular formula of **241** was established as $C_{18}H_{26}NO_3$ on the basis of molecular ion peak at *m/z* 304.1922 [$M+H^+$] (calculated for $C_{18}H_{26}NO_3$: 304.1907) in the HRMS.

The next step was to investigate the reaction between piperidine and (*E*)-ethyl 3-hydroxy-2-methylene-5-phenylpent-4-enoate **102e**. The same reaction conditions that were used for preparation of **241** also worked for the synthesis of **242**. Performing the reaction in THF afforded **242**, a mixture of diastereomers, as a colourless oil in 54% yield with R_f value of 0.56 in 30% ethyl acetate in hexane. The ratio of the major and minor diastereomers was found to be 2:1.

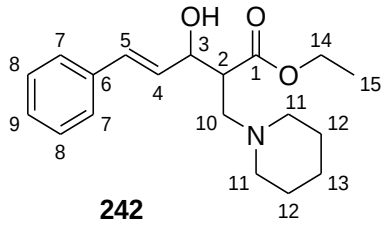

242

The IR spectrum exhibited intense hydroxyl and carbonyl bands at 3220 cm^{-1} and 1731 cm^{-1} respectively. The mass spectrum corresponded well with the expected mass of the product (calculated for $C_{19}H_{28}NO_3$: 318.2064, found: $[M+H^+]$: 318.2080). ^1H and ^{13}C NMR spectra of **242** was almost identical to that of **241**. The only difference observed was existence of the ethoxy group in **242** instead of methoxy group as observed in **241**. The signals appearing as mutliplet at δ 4.20 – 4.12 integrating for two protons was assigned to H-14 while the triplet at δ 1.26 was assigned to H-15 of the minor diastereomer. The same pattern was observed for the major diastereomer only that the protons were shielded. The appearance of H-14 as a multiplet is probably due to compound **242** adopting multiple conformational forms. These data were supported by the appearance of a signal for oxygenated carbon appearing at δ 60.7 for C-14 and a signal for a methyl carbon observed at δ 14.5 in the ^{13}C NMR spectrum of the minor diastereomer. Similar upfield carbon signals were observed for the major diastereomer.

In addition to the ^1H and ^{13}C NMR data being identical, COSY, DEPT, HMQC and HMBC data of **242** was similar to **241**. All the 2D NMR correlation information used to fully assign the major and minor diastereomers of **242** are shown in **Table 42**.

Table 42: 2D NMR data for the minor and major diastereomer **242**

COSY		HSQC		HMBC	
H-5	H-4	H-5	C-5	H-5	C-3, C-4, C-6, C-7
H-4	H-3	H-4	C-4	H-4	C-2, C-3, C-6
H-2	H-2	H-3	C-3	H-3	C-1, C-2, C-5, C-10,
H-2	H-10a	H-14	C-14	H-14	C-1, C-15
H-10a	H-10b	H-2	C-2	H-2	C-3, C-10
H-14	H-15	H-10	C-10	H-15	C-14
		H-11	C-11	H-10a	C-2, C-3, C-11
				H-13	C-11

The chemical shift pattern of key proton and carbon signals of the major and minor diastereomers of **242** was also the same as that observed for **241**. The comparison of the key characteristic signals for the major and minor diastereomers are shown in **Table 43**.

Table 43: Comparison of characteristics ^{1}H and ^{13}C NMR peaks of the minor and major diastereomer **242**

Proton and carbon number	**Minor diastereomer**	**Major diastereomer**
H-5	6.75 (1H, d, *J* = 15.7 Hz)	6.61 (1H, d, *J* = 15.8 Hz)
C-5	130.9	131.2
H-4	6.30 – 6.22 (1H, m,	6.17 (1H, dd, *J* = 15.7, 6.2 Hz)
C-4	129.5	129.6
H-3	4.86 – 4.80 (1H, m)	4.59 (1H, t, *J* = 7.4 Hz)
C-3	**73.2**	**76.5**
H-14	4.20 – 4.12(2H, m)	4.10 – 4.00(2H, m)
C-14	**60.7**	**60.6**
H-2	3.27 – 3.17 (1H, m)	2.80 (1H, t, *J* = 10.3 Hz)
C-2	45.7	48.1
H-15	1.26 (3H, t, *J* = 6.4 Hz)	1.14 (3H, t, *J* = 6.8 Hz)
C-15	14.3	14.2
C-1, **C-6**, C-7, C-10	172.73, **137.0**, 126.5, 56.8	171.68, **136.9**, 126.6, 48.1

The final investigation was the use of (*E*)-3-hydroxy-2-methylene-5-phenyl-4-pentenenitrile **191** for performing two nucleophilic reactions. The first reaction involved reacting (*E*)-3-hydroxy-2-methylene-5-phenyl-4-pentenenitrile **191** with piperidine in different solvents. The solvents tested for this reaction were methanol, ethanol, acetonitrile and THF. Only the use of methanol for 20 hours led to a new spot. Purification of the crude product by column chromatography using 50% ethyl acetate in hexane afforded **243** as a mixture of diastereomers that was as a colourless oil in a yield of 76%. The R_f value of **243** was found to be 0.46 in 50% ethyl acetate while the ratio between the major and minor diastereomer was 2:1.

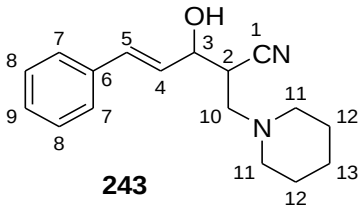

243

The ^{1}H NMR spectrum of the major diastereomer showed key characteristic signals as evidenced by one stereogenic centre proton at δ 3.09 – 3.00 (1H, m, H-2), one diastereotopic proton at δ 2.95 – 2.77 (1H, m, H-10a), one diastereotopic proton at δ 2.71 – 2.67 (1H, m, H-10b), 4 saturated methylene proton at δ 2.60 – 2.33 (4H, m, H-11), 1.66 – 1.48 (4H, m, H-12) and one saturated methylene proton at δ 1.47 – 1.33 (2H, m, H-13). The resolution of the piperidinyl protons in the ^{1}H NMR spectrum was poor, such that it was impossible to differentiate the axial and equatorial coupling protons. The other characteristic signal was the stereogenic centre proton that appeared at δ 4.69 – 4.61 (1H, m, H-3). The cross-peak correlation on the COSY spectrum led to the identification of coupling protons H-5 and H-4, H-4 and H-3, H-3 and H-2, H-2 and H-10, H-11 and H-12 and finally H-12 and H-13. The characteristic proton signals were also supported by their corresponding carbon signals in ^{13}C NMR spectrum. These carbon signals appeared at δ 34.4 for C-2, 59.8 for C-10 and 72.2 for C-3. The piperidinyl ring carbon signals appeared at δ 54.8, 25.9 and 23.7 for C-11, C-12 and C-13, respectively. The other characteristic signal in the ^{13}C NMR spectrum was the ntrile group that appeared at δ 118.9.

The use of the HSQC spectrum led to the identifications of all the carbons carrying protons that appeared in the aromatic region (C-7 and C-8), alkene region (C-5 and C-4), oxygenated/nitrogenated region (C-3, C-10 and C-11) and saturated region (C-2, C-12 and C-

13). Using the DEPT 135 spectrum, the aromatic and alkene carbons were identified, oxygenated C-3, saturated C-2 as positive signals. The same DEPT experiment was used to identify C-10, C-11, C-12 and C-13 as they appeared as negative signals. The disappearance of the quaternary carbons ofrom the DEPT spectrum confirmed the chemical shifts of C-6 and C-1.

Having all the pieces of information, it was then easier to use the HMBC spectrum to unambiguously assign the proton and carbon signals. Using the cross-peaks led to accurate assignment of signals for H-5 and C-7; H-4, C-2 and C-6; H-3, C-5 and C-10; H-10, C-1 and C-11. The summarized data used for 2D assignment is shown in **Table 44**. All the spectroscopic data of the major and minor diastereomer were similar.

Table 44: 2D NMR data of the major and major diastereomer **243**

COSY		**HSQC**		**HMBC**	
H-5	H-4	H-5	C-5	H-5	C-3, C-6, C-7
H-4	H-3	H-4	C-4	H-4	C-2, C-3, C-6
H-3	H-2	H-3	72.2	H-3	C-1, C-2, C-5, C-10
H-2	H-10a	H-2	C-2	H-2	C-3, C-10
H-2	H-10b	H-10	C-10	H-10	C-1, C-3, C-11
H-10a	H-10b				
H -11	H-12	H-11	C-11		
H-12	H-13	H-12	C-12		
		H-13	C-13	H-13	C-11

The chemical shifts and the multiplicities of ^{1}H and ^{13}C NMR spectroscopic characteristic signals of the major and minor diastereomers were compared and the results are summarized in **Table 45**. The only major observation from the table is that the protons of the major diastereomer are downfield as compared to the protons of the minor diastereomer. This observation is opposite to what was observed for **241** and **242**. The chemical shifts of specific characteristic carbon signals appeared as shielded while others were deshielded.

Table 45: Comparison of the characteristic ^{1}H and ^{13}C NMR peaks of the major and minor diastereomer of **243**

Proton and carbon number	**Minor diastereomer**	**Major diastereomer**
H-5	6.77 (1H, d, *J* = 15.6 Hz)	6.79 (1H, d, *J* = 15.9 Hz)
C-5	132.4	132.2
H-4	6.27 (1H, ddd, *J* = 15.9, 6.0, 0.9 Hz)	6.34 (1H, ddd, *J* = 15.9, 6.0, 0.9 Hz)
C-4	128.0 or 127.9	127.9 or 127.7
H-3	4.56 (1H, t, *J* = 6.0 Hz)	4.69 – 4.61 (1H, m)
C-3	74.3	72.2
H-2	2.94 – 2.76 (1H, m)	3.09 – 3.00 (1H, m)
C-2	34.6	34.4

The IR spectrum identified the characteristic functional groups of **243**. The presence of IR stretches at 3400 cm^{-1} and 2242 cm^{-1} in the IR spectrum confirmed the presence of OH and C≡N functional groups. The molecular ion of **243** was confirmed by HRMS to be $[M+H^{+}]$ 271.1825 which was consistent with the mass calculated for $C_{17}H_{23}N_2O$ of 271.1805.

A comparison of the chemical shifts of the stereogenic centre carbon atoms of the major and minor diastereomers of **241**, **242** and **243** is as shown in **Table 46**. It was observed that the carbon signals for C-2 and C-3 of the minor diastereomers **241** and **242** appeared upfield while the same signals for the major diastereomer appeared downfield. There was no significant difference in chemical shift for the C-2 signal of the minor and major diastereomer of **243** but a significant difference was observed for the C-3 signal. It is not clear if this reversal in order of the stereogenic centre signals at C-3 could be an indication that the major diastereomer is of opposite configuration (*syn* versus *anti*) for the esters as for the nitrile derivative.

The observation in **Table 46** can only be explained if further studies using computational techniques are explored.

Table 46: Comparison of chemical shifts of diastereomeric compounds

Compound number	**Minor diastereomer**		**Major diastereomer**	
	C-2	**C-3**	**C-2**	**C-3**
241	45.6	73.2	48.1	76.3
242	45.7	73.2	48.1	76.5
243	34.6	74.4	34.4	72.2

The ^{1}H NMR spectra of **241**, **242** and **187** did not show the signal of the hydroxyl group although the IR and Mass spectra clearly confirmed its presence.

The last nucleophilic reaction in this series involved reacting (*E*)-3-hydroxy-2-methylene-5-phenyl-4-pentenenitrile **191** with benzylamine in methanol which resulted in a new spot in 48 hours. Purification of the crude product by column chromatography using 40% ethyl acetate in hexane afforded a mixture of diastereomers **244** as a colourless oil in a yield of 65%. The R_f value for **244** was found to be 0.5 in 80% ethyl acetate in hexane while the ratio between the major and minor diastereomer was found to be 2:1. The spectroscopic data for the major and minor diastereomer were very similar.

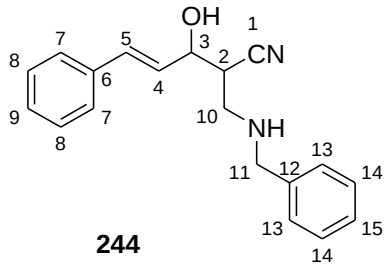

244

The ^{1}H NMR spectrum of the major diastereomer exhibited 9 signals representing including the characteristic signal for H-2 that appeared as a multiplet at δ 2.94 – 2.88, H-10a and H-10b that appeared as two doublets of doublets. The first doublet of doublets signal appeared at δ 3.21 with vicinal and geminal coupling of 12.4 and 5.7 Hz and was assigned to H-10a. The second doublet of doublets signal that was assigned to H-10b appeared at δ 3.00 with vicinal and geminal coupling constants of 12.3 and 4.2 Hz. The other characteristic signals for H-11 appeared as a multiplet at δ 3.91 – 3.76 while the stereogenic centre proton signal H-3 also appeared as a multiplet at δ 4.64 – 4.57. The appearance of a multiplet signal at δ 7.47 – 7.16 integrating for ten protons was a confirmation of two phenyl rings in the product.

The presence of a broad singlet at δ 3.61 with an integration value of two represented the presence of the hydroxyl and amine groups.

The ^{13}C NMR spectrum showed a total of 15 signals with the characteristic signal for C-2 appearing at δ 38.1 and C-10 appearing at δ 48.6. The stereogenic centre carbon C-3 appeared at δ 72.8 and the benzylic carbon C-11 was observed at δ 53.6. The use of the HSQC spectrum led to the identification of the alkene CHs C-5 and C-4, oxygenated C-3, nitrogenated C-10 and C-11 and saturated C-2. In conjunction with the cross-peaks in the COSY spectrum this led to the identification of H-5/H-4, H-4/H-3, H-3/H-2 and H-2 and H-10

The use a DEPT 135 spectrum identified the quaternary carbons C-6 and C-12, oxygenated stereogenic carbon C-3 and stereogenic carbon C-2. This was on the basis that quaternary carbons disappeared from the DEPT spectrum while the CHs appeared as positive signals in the designated region. The negative signals that appeared in the region of the nitrogenated carbon signals were assigned to C-10 and C-11. HMBC correlations were used to assign H-11 with C-10/C-12/C-13; H-3 with C-1/C-5/C-10 and H-4 with C-6/C-2. All the correlations for the major and minor diastereomer that were used for assignments are shown in **Table 47**.

Table 47: 2D NMR data of the major and minor diastereomer of **244**

COSY		**HSQC**		**HMBC**	
H-5	H-4	H-5	C-5	H-5	C-3, C-6, C-7
H-4	H-3	H-4	C-4	H-4	C-2, C-3, C-6
H-3	H-2	H-3	C-3	H-3	C-1, C-2, C-4, C-5, C-10
H-2	H-10a	H-11	C-11	H-11	C-10, C-12, C-13
H-10a	H-10b	H-10	C-10		
		H-2	C-2		

The IR spectrum confirmed the presence of the hydroxyl functional group peak at 3030 cm^{-1} and the nitrile functional group peak at 2237 cm^{-1}. The mass spectrum corresponded well with the expected mass of **250** (calculated for $C_{19}H_{21}N_2O$: 293.1648, found: $[M+H^+]$ 293.1652).

Unlike the previous diastereomers **241**, **243** and **242** which showed a significant difference in chemical shifts of proton and carbon signals of characteristics peaks, **244** only showed a slight difference in terms of chemical shifts. The use of compound **198**, derived from methyl vinyl ketone, for nucleophilic reaction investigations was not successful as the TLC showed many spots, confirming the earlier observation that **198** is unstable.

3.3.5 Synthesis of silylated MBHA

After successfully performing nucleophilic addition reactions on Morita-Baylis-Hillman alcohols, the next step was to synthesize several silylated MBH adducts to be used for the stereoselective nucleophilic addition investigation. The synthesis of silylated compounds was achieved by reacting MBH alcohols with *tert*-butyldimethylsilyl trifluoromethanesulfonate in the presence of triethylamine in dichloromethane for at least 1 hour (**Scheme 93**). This led to three protected Morita-Baylis-Hillman adducts **226a-c**, whose structures were confirmed using spectroscopic techniques.

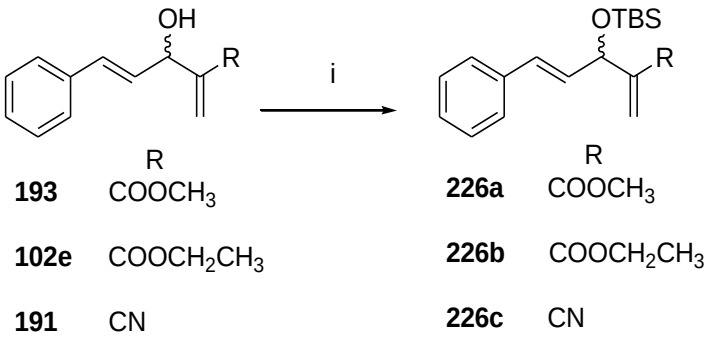

Scheme 93: Silylation of MBH alcohol. *Reagents and conditions*: (i) TBSOTf, TEA in DCM at 0 °C.

All the silylated compounds were isolated as colourless oils. The first compound (*E*)-methyl 3-((tert-butyldimethylsilyl)oxy)-2-methylene-5-phenylpent-4-enoate **226a** with R_f value of 0.60 in 10% ethyl acetate / hexane was isolated in a yield of 94%. This was followed by (*E*)-ethyl 3-((*tert*-butyldimethylsilyl)oxy)-2-methylene-5-phenylpent-4-enoate **226b** and (*E*)-3-((*tert*-butyldimethylsilyl)oxy)-2-methylene-5-phenylpent-4-enenitrile **226c** that were obtained in 89 and 90% yield, respectively. The R_f values of **226b** and **226c** in 10% ethyl

acetate in hexane were 0.74 and 0.70 respectively. All the silylated compounds were characterised using spectroscopic techniques.

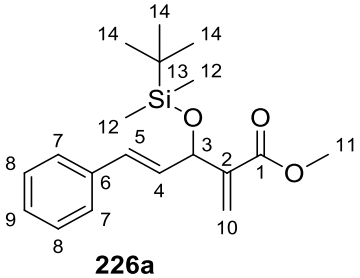

226a

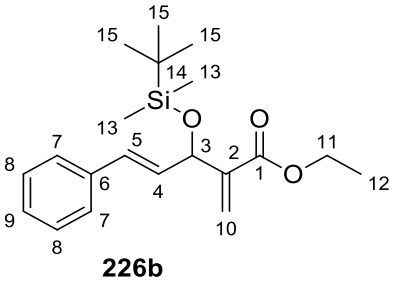

226b

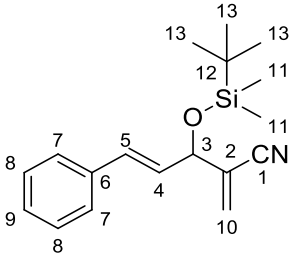

226c

The formation of **226a, 226b and 226c** was confirmed by ^{1}H and ^{13}C NMR spectroscopy. The disappearance of the hydroxyl group signal and the appearance of the silyl ether signal observed in the ^{1}H NMR spectrum in all the compounds clearly confirmed the formation of the product. This was evidenced by the presence of the most shielded protons of the methyl group attached to the silicon atom. Signals for the methoxy and ethoxy groups were observed in the ^{1}H NMR spectra. The methoxy proton H-11 in **226a** was observed as a singlet at δ 3.74 while the ethoxy protons H-11, H-12 in **226b** appeared as a multiplet at δ 4.31 – 4.10 and a singlet at δ 1.29 respectively. The multiplet for H-11 suggest that **226b** may existin different conformations.

A comparison of the characteristic peaks from ^{1}H NMR spectroscopy of the three silylated compounds is tabulated in **Table 48**. Most of the characteristic peaks show a similar pattern in terms of chemical shift and multiplicity. The *trans* coupled protons H-5 and H-4 were evidenced by the coupling constant 15.8 Hz. Almost all the signals of proton H-10 in all the silylated compound appeared as a multiplet confirming that H-10 was experiencing geminal and long range coupling with the stereogenic centre proton H-3. It was one of the protons H-10 in **226a** that appeared as a triplet suggesting it was being split by its neighbour H-10 and H-3 at the same time. H-3 was observed as a multiplet as it experienced ^{3}J coupling with H-4 and allylic long range coupling with H-10. The three methyl groups in all the compounds appeared asthe most shielded singlet.

Table 48: Comparison of characteristic ^{1}H NMR peaks of the silylated compounds

Proton number	**226a**	**226b**	**226c**
H-5	6.63 (1H, d, *J* = 15.8 Hz)	6.63 (1H, d, *J* = 15.8 Hz)	6.67 (1H, d, *J* = 15.8 Hz)
H-4	6.18 (1H, dd, *J* = 15.8, 6.1 Hz)	6.18 (1H, dd, *J* = 15.8, 6.2 Hz)	6.12 (1H, dd, *J* = 15.8, 6.6 Hz)
H-10	6.26 – 6.24 (1H, m, H-10a) 6.03 (t, J = 1.6 Hz, H-10b)	6.26 – 6.24 (1H, m, 10-Ha) 6.04 – 6.00 (m, H-10b)	6.06 – 6.03 (1H, m, H-10a) 5.96 – 5.93 (m, H-10b)
H-3	6.26 – 6.24 (1H, m)	5.27 – 5.22 (1H, m)	4.88 – 4.82 (1H, m)
H-12, H-13 and H-11	0.10 (3H, s, H-12a) 0.09 (3H, s, H-12b)	0.12 – 0.07 (3H, m, H-13)	0.14 – 0.08 (3H, m, H-11)
H-14, H-15 and H-13	0.94 (9H, s, H-14)	0.94 (9H, s, H-15)	0.94 (9H, s, H-13)

The chemical shift of the characteristic ^{13}C NMR peaks were also analysed and are presented in **Table 49**. It is evident from the table that the chemical shifts of these characteristic signals are almost the same. The only observed difference was the chemical shift of C-10 and C-3 in **226c** which was deshielded as compared to **226a** and **226b**. This suggests that the presence of a nitrile group has some electronic effect or anisotropic effect on the affected carbons. This suggestion can only be confirmed by computational techniques.

Table 49: Comparison of ^{13}C NMR peaks of the silylated compounds

Carbon number	**226a**	**226b**	**226c**
C-5 and C-4	130.7, 127.5	130.8, 127.5	132.3, 128.2
C-1 and C-10	166.4, 124.2	165.9, 123.9	117.2, 128.7
C-3	71.2	71.3	73.7
C-12 for **245a,** C-13 for **245b** C-11 for **245c**	-4.6, -5.0	-4.6, -5.0	-4.5, -4.9
C-14 for **245a,** C-15 for **245b** C-13 for **245c**	25.7	25.9	25.8

The characteristic carbonyl functional group for **226a** and **226b** appeared at 1715 cm^{-1} in the IR spectrum. The C≡N stretching vibrations of the nitrile group was observed at 2226 cm^{-1} in the IR spectrum. The spectroscopic data of **226a** was similar to that reported in literature.[198] The HRMS data corresponded well with the expected masses (calculated for $C_{20}H_{31}O_3Si$: 347.1868, found: $[M+H^+]$ 347.1898) for **226b** (calculated for $C_{18}H_{25}NOSiNa$: 322.1598, found: $[M+Na^+]$ 322.1598) for **226c**.

The next set of reactions involved Michael addition to the silylated compounds for diastereoselective investigations.

3.3.6 Nucleophilic addition of nitrogen nucleophile to silylated MBH adducts

The silylated compound **226a**, **226b** and **226c** were ready to be subjected to nucleophilic addition reactions. This was investigated according to the reaction shown in **Scheme 94** in order to prepare compounds **227c,** and **245 - 247**.

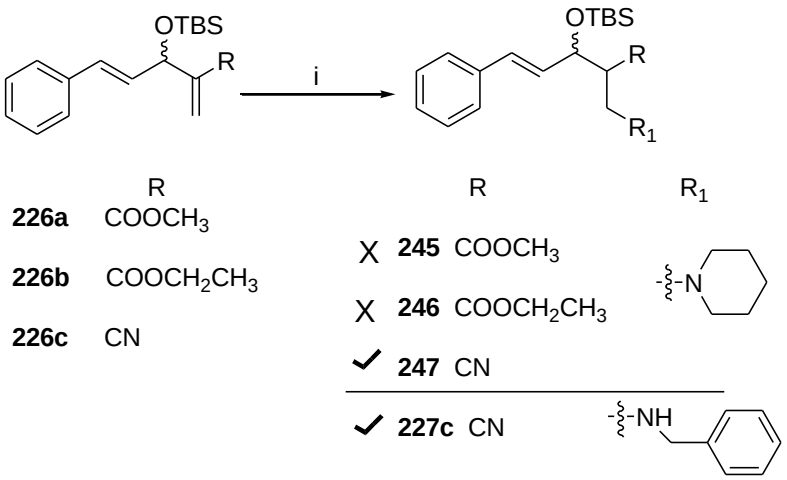

Scheme 94: Nucleophilic addition of nitrogen nucleophiles to silylated MBHA. *Reagent and conditions* (i) either piperidine/benzylamine in methanol or piperidine/benzylamine in THF

The first compound to be investigated was **226a**. The reaction was done in THF using piperidine as a nitrogen nucleophile for 20 hours affording a crystalline structure **248** in a yield of 69% (**Scheme 95**). Unfortunately, the product obtained did not have the most shielded proton signals at $\delta < 0.12$ and carbon signals $\delta < -4.6$ as expected from the starting materials. The only way to account for this observation is that an allylic substitution reaction took place

instead of nucleophilic addition. It was necessary to use all the spectroscopic techniques available to identify the isolated crystalline solid with R_f value of 0.53 in ethyl acetate hexane and a melting point (M.P) range of 91 – 92 °C.

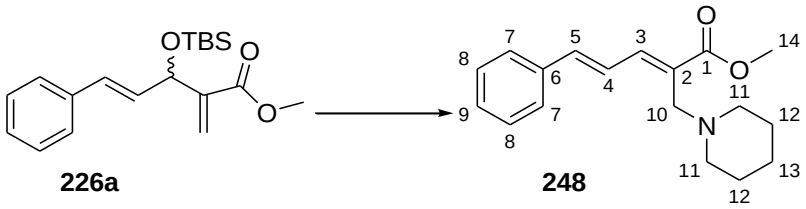

Scheme 95: Nucleophilic addition of piperidine on silylated MBH methyl esters giving allylic substitution product. *Reagents and conditions*: Piperidine in THF at RT

The ^{1}H NMR spectrum of the unexpected compound showed three multiplets. The first multiplet appeared at δ 7.52 -7.43 for Ar-2H and H-3, the second mutliplet appearing at δ 7.37 – 7.32 for Ar-2H and H-4 and the third appearing at δ 7.32 – 7.25 for one aromatic proton. The *trans* coupled proton H-5 appeared at δ 6.85 as a doublet with a coupling constant of 15.3 Hz. The methoxy and the methylene appeared as singlets at δ 3.77 and δ 3.40 respectively. The multiplet at δ 2.52 – 2.38 was assigned to the protons H-11 while its immediate multiplet at δ 1.59 – 1.51 was assigned to protons H-12. The last multiplet was assigned to H-13. The ^{13}C NMR spectrum showed the deshielded carbon signal at δ 168.7 that was assigned to C-1 followed by a carbon signal at δ 142.0 that was assigned to C-3. The characteristic C-10 signal was observed at δ 54.2 and the piperidinyl carbon signals were observed at δ 54.4 for C-11, 51.9 for C-14, 26.0 for C-12 and 24.3 for C-13.

The assignment of deshielded protons was supported by the fact that H-3 coupled with H-4 and H-4 coupled with H-5 as confirmed by the cross-peaks that were at δ > 6.74 in the COSY spectrum. The remaining cross-peaks which could not be used to accurately assign axial and equatorial protons of the piperidinyl ring protons only confirmed that H-11 was coupling with H-12. The use of COSY spectrum supported the assignment of H-5, H-4 and H-3. The HSQC spectrum identified carbon signals for carbon atoms carrying protons; of importance is the fact H-11, H-12 and H-13 were attached to C-11, C-12 and C-13 repectively. This suggested that the axial and equatorial protons of the piperidinyl ring could not be differentiated as they appeared as a multiplet. It was difficult to precisely assign the aromatic carbons, C-4 and C-3 using the HSQC spectrum. Using the DEPT spectrum led to the accurate assignment of quaternary carbons C-6, C-2 and C-1. The DEPT spectrum was also used to accurately assign

the positive CH_3 and negative CH_2 signals. This experiment could not be used to accurately assign the alkene and aromatic CH signals. The use of HMBC spectroscopy was useful in identifying the CH protons. The correlations in the HMBC experiment identified H-10 as correlating with C-2 and C-3; and H-5 with C-3 and C-4. All the two 2D correlations tabulated in **Table 50** were used for assigning all the signals. All NMRspectra for compound **248** are attached in **Appendix II**.

Table 50: 2D correlations for crystalline structure **248**

COSY		**HSQC**		**HMBC**	
H-3	H-4	H-5	C-5	H-3	C-1
H-4	H-5	H-14	C-14	H-4	C-3, C-6,
H-11	H-12	H-10	C-10	H-5	C-3, C-4,
H-12	H-13	H-11	C-11	H-14	C-1
		H-12	C-12	H-10	C-1, C-2, C-3, C-11
		H-13	C-13	H-12	C-11, C-13
				H-11	C-12, C-13
				H-13	C-11

The IR characteristic peak at 1701 cm^{-1} confirmed the presence of the carbonyl group in the unexpected product. The mass spectrum corresponded well with the expected mass of the crystalline product; HRMS *m/z* calculated for $C_{18}H_{24}NO_2$: 266.1807, found $[M+H^+]$ 286.1820. Using all the spectroscopic data, compound **248** was identified as (2*E*,4*E*)-methyl 5-phenyl-2-(piperidin-1-ylmethyl)penta-2,4-dienoate.

All the information used corresponded well with the X-ray crystal structure data acquired for the product. The X-ray crystal structure is shown in **Figure 93**.

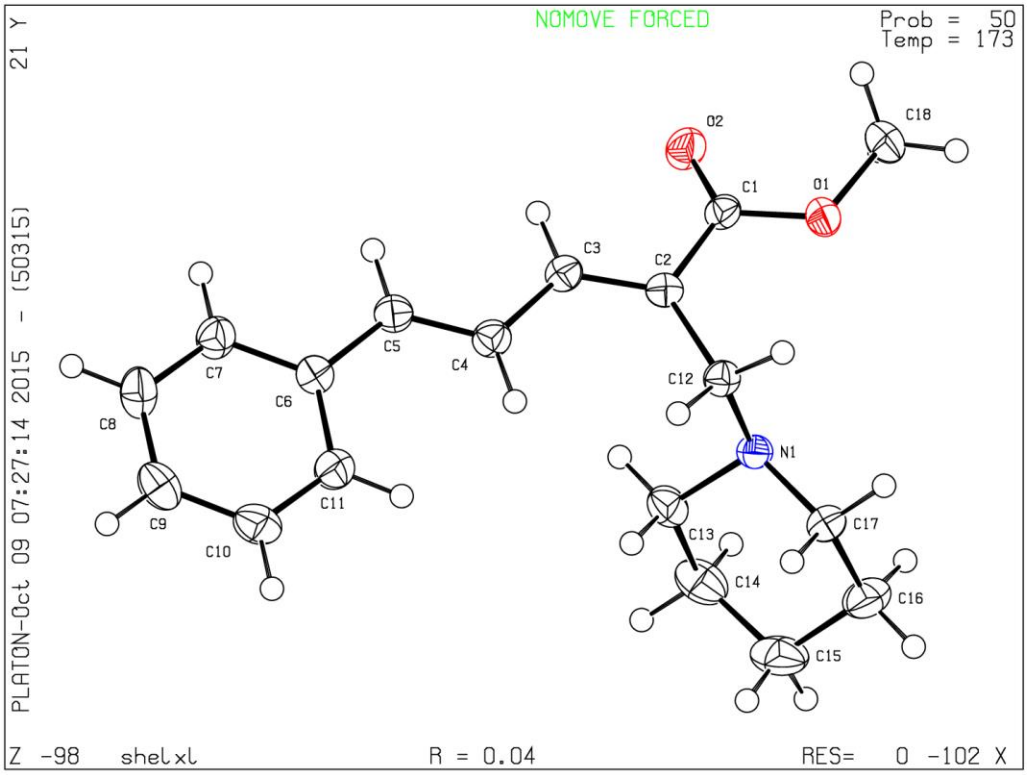

Figure 93: ORTEP diagram of **248** crystal structure

The observation of allylic substitution taking place instead of nucleophilic addition was a surprise as it was not expected that the silyl group would be a good leaving group in the presence of the electron withdrawing methyl ester group. An allylic substitution product has been reported when benzylamine was reacted with a tetrahydropyranyl (THP) MBH adduct.[199] In addition, nucleophilic allylic substitution reactions have also been widely reported on MBH acetates as the synthetic route towards molecules with various biological activities.[103, 200] For example the synthesis of ureides for antibacterial evaluation was achieved via nucleophilic allylic substitutions of nucleophiles on MBH acetates.[175] In another example, synthesis of β^2-amino acid derivatives documented to be useful synthetic intermediates was obtained by performing nucleophilic allylic substitution on MBH acetates.[95] The next question was to investigate if a substitution reaction would also occur on silylated MBH adducts of the ethyl acetate derivative **226b**.

This investigation was achieved by reacting **226b** with piperidine as a nitrogen nucleophile in THF at room temperature for 24 hours (**Scheme 96**). This led to unexpected product that was a colourless oil in a yield of 54%. The absence of the most shielded protons signals at $\delta < 0.12$

and carbons siganls δ < 4.6 in both the ^{1}H and ^{13}C NMR spectrasuggested that nucleophilic allylic substitution had taken place instead of nucleophilic addition because the silyl group was absent.

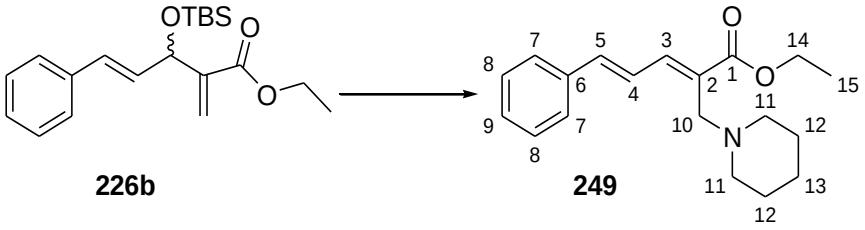

Scheme 96: Nucleophilic addition of piperidine on silylated ethyl esters giving allylic substitution product: *Reagents and conditions*: Piperidine in THF at RT

The ^{1}H NMR spectrum of **249** was almost identical to that of **249** except that the spectrum of **249** showed the addition ethoxy protons. This was evidenced by the presence of H-14 which appeared as a quartet at δ 4.24 and H-15 which appeared as a triplet at δ 1.32 with equal coupling constants of 7.1 Hz. The additional signals were also observed in the ^{13}C NMR spectrum at δ 60.6 for C-14 and δ 14.3 for C-15. The confirmation of the assignment of thequaternary, CH_2 and CH_3 signals that had similar chemical shifts to that of **248** was done using a DEPT 135 experiment. For example, quaternary carbons C-6, C-2 and C-3 were confirmed by the disappearance of their signals in the DEPT 135 experiment.

The IR characteristic peak at 1710 cm^{-1} confirmed the presence of the ester group in the unexpected product. The mass spectrum corresponded well with the expected mass of the allylic substitution product; HRMS *m/z* calculated for $C_{19}H_{26}NO_2$: 300.1598, found: $[M+H^+]$ 300.1968. Compound **249** was successfully identified as (2*E*,4*E*)-ethyl 5-phenyl-2-(piperidin-1-ylmethyl)penta-2,4-dienoate.

The last nucleophilic reactions were done on acrylonitrile derivative **226c**. A similar procedure of adding piperidine to a solution containing **226c** in methanol (**Scheme 97**) was used. This reaction was successful and afforded compound **247**. Using different nucleophiles afforded **227c**, **250** and **251** that were characterised using spectroscopic techniques.

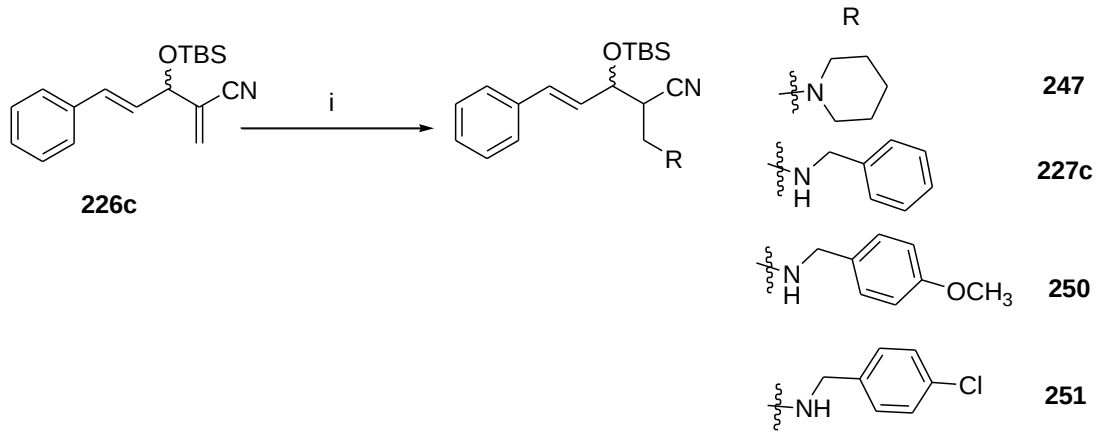

Scheme 97: Nucleophilic addition of nitrogen nucleophiles to silylated MBHA. *Reagents and conditions*: Piperidine or benzylamine or 4-methoxybenzylamine or 4-chlorobenzylamine in methanol at RT.

The nucleophilic addition of piperidine to racemic **226c** in methanol led to a racemic **247** as a colourless oil in a yield of 70% after 24 hours. The structure of the compound was confirmed using spectroscopic techniques.

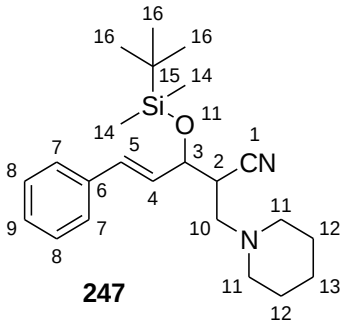

247

There were a total of 12 signals in the ^{1}H NMR spectrum which confirmed the presence of protons in 12 different chemical environments. Four of these signals confirmed the addition of the piperidine ring. The appearance of the stereogenic centre proton H-2, diastereotopic protons H-10 and piperidinyl proton signals supported the formation of the product. The stereogenic centre proton H-2 appeared as a multiplet at δ 3.00 – 2.4 while the diastereotopic protons H-10 were assigned to a multiplet at δ 2.59 – 2.54. The multiplets that appeared at δ 2.49 – 2.33, δ 1.61 – 1.53 and δ 1.47 – 1.37 were assigned to the piperidinyl protons H-11, H-12 and H-13. The remaining 8 signals were similar to the signals of the starting material in terms of chemical shift and multiplicity. The appearance of new proton signals in the ^{1}H NMR

spectrum was supported by the ^{13}C NMR spectroscopic data. The presence of carbon signals at δ 56.8, 54.6, 38.68, 25.95 and 24.15 supported the presence of C-10, C-11, C-2, C-12 and C-13 respectively. The rest of the carbon signals that represented the remaining parts of the compound were not different from the starting material. The duplication of carbon signals was a clear indication that **247** was a mixture of diastereomers.

The presence of a stretch at 2243 cm^{-1} in the IR spectrum confirmed the presence of the nitrile functional group. The molecular ion of **253** was confirmed by HRMS to be [M+H^+] 385.2689 which was consistent with the mass calculated for $C_{23}H_{37}N_2OSi$, found: 385.2675. Similar conditions were applied for reacting benzylamine derivatives to generate three additional compounds. These additional adducts generated were compound **227c**, **250**, and **251**.

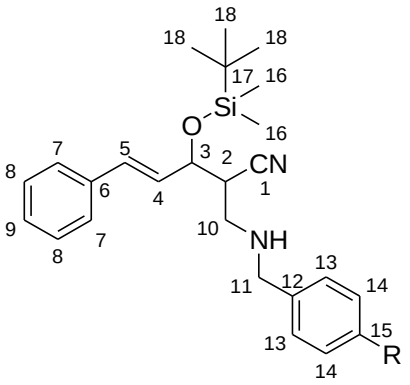

227c R = H

250 R = OCH_3

251 R = Cl

The reaction times varied from 14 hours to 30 hours. The presence of 4-methoxy benzylamine reduced the reaction time to 14 hours while the use of 4-chlorobenzylamine increased the reaction time to 30 hours relative to unsubstituted benzylamine that took 18 hours. All the compounds that were isolated in yields range of 72 – 76% were characterized using spectroscopic techniques.

The presence of 11 signals in the ^1H NMR spectrum of **227c** confirmed protons that were in 11 different chemical environments. The signals of the two phenyl ring protons appeared as three multiplets at δ 7.37 – 7.32, δ 7.32 – 7.27 and δ 7.26 – 7.21 integrating for two, six and one proton respectively. The characteristic signals for H-11, H-2, H-10 and NH were also present in the ^1H NMR spectrum. The singlet at δ 3.78 was assigned to H-11, while the multiplet at δ 2.94 – 2.83 was assigned to H-2 and H-10. The NH peak appeared as a broad

singlet at δ 1.56. The chemical shift and multiplicity of the remaining protons was the same as for **226c**.

The ^{13}C NMR spectrum showed a total of 18 signals, 7 being significant as they confirmed the formation of the product. The new carbon signals appeared at δ 53.48 for C-11, 47.0 for C-10 and 41.0 for C-2. It was very difficult to precisely assign the carbon signals from the phenyl ring originating from benzylamine. The remaining carbon signals were similar to the carbon signals of the starting material. The use of a DEPT 135 experiment and 2D NMR spectra led to the precise assignment of some signals (**Table 51**). For instance, the HSQC spectrum was used to assign the protonated carbons except C-8, C-9, C-14 and C-15. The correlation of H-11 with carbon signals for C-12 and C-13 led to the precise assignment of these three carbons. The use of a DEPT 135 spectrum led to the precise identification of CH_2 attached to a nitrogen for C-10 and C-11, saturated CH for C-2 and carbon attached to oxygen C-3.

Table 51: 2D NMR data for **227c**

COSY		**HSQC**		**HMBC**	
H-5	H4	H-5	C-5	H-5	C-3, C-6, C-7
H-4	H3	H-4	C-4	H-4	C-3, C-6
H-3	H2	H-3	C-3	H-3	C-2, C-10, C-5
H-2	H-10	H-10	C-10	H-2	C-3, C-4, C-10
		H-11	C-11	H-11	C-10, C12, C13
		H-2	C-2	H-10	C-1, C-2, C-3, C-11
		H-18	C-18		
		H-16	C-16		

The duplication of carbon signals confirmed the existence of **227c** as a diastereomeric mixture. The IR stretch at 2242 cm^{-1} confirmed the presence of nitrile group. The ^{1}H and ^{13}C NMR of spectra for **227c**, **250** and **251** were very similar in terms of chemical shifts and the splitting pattern of the protons (**Table 52**). The only slight difference which was expected was the present of a methoxy signal for **250**. There were also *ortho*-coupled signals for H-14 in the spectra of **250** and **251**. A similar observation of carbon signal duplication for **250** and

251 suggested the existence of diastereomeric mixtures. The precise assignment of all the protons and carbon signals of **250** and **251** was achieved using a DEPT 135 experiment and 2D NMR data.

Table 52: Characteristics proton and carbon signals of the silylated compounds

Proton and carbon number	**227c**	**250**	**251**
H-3	4.53 – 4.48 (1H, m)	4.56 – 4.46 (1H, m)	4.55 – 4.45 (1H, m)
C-3	72.1	72.1	72.2
H-11	3.78 (2H, s)	3.76 (2H, s)	3.77 (2H, s)
C-11	53.48	52.9	52.8
H-2, H-10	2,94 – 2.83 (3H, m)	2.98 – 2.84 (3H, m)	2.93 – 2.85 (3H, m)
C-2 and C-10	41.0 and 47.0	41.1 and 46.5	41.1 and 46.6
NH	1.56 (1H, br s)	1.55 (1H, s)	1.58 (1H, s)

The IR data for **250** and **251** confirmed the presence of a nitrile functional group which appeared at 2952 cm^{-1}. The molecular ion of **250** was confirmed by HRMS to be $[M+H^+]$ 437.2633 which was consistent with the mass calculated for $C_{26}H_{37}N_2O_2Si$ of 437.2619. The mass spectrum of **251** corresponded well with the expected mass of the product (calculated for $C_{25}H_{34}ClN_2O$: 441.2123, found $[M+H^+]$ 441.2129).

The nucleophilic addition occurred in a stereoselective manner for each of the four compounds prepared (**Scheme 97**). The ratio between major and minor diastereomer was between 4 and 5 to 1. This shows much greater selectivity than those compounds without the bulky silyl group. The selectivity observed is because one side of the plane of the double bond is blocked by the bulky silyl group and therefore as the addition of the nucleophile takes place on one side of the plane, the incoming proton is also added to the side that is less blocked promoting the *syn*- addition product as the major diastereomer (see NMR evidence for *syn*-product later). Adducts that lacked the bulky protecting group did not experience diastereoselectivity as the addition of the nucleophile and the proton took place on both sides of the plane thus promoting the formation of *anti*- and *syn*- product almost equally.

It was also observed that the silylated methyl and ethyl esters underwent allylic substitution reactions while the silylated cyanoacrylate successfully underwent nucleophilic addition under the reaction conditions used. There is a possibility that the use of methanol as a solvent on silylated cyanoacrylate led to an intermediate that was stabilized by hydrogen bonding and thus promoted nucleophilic addition. It was observed that the use THF as a solvent on methyl and ethyl esters promoted allylic substitution because of lack of hydrogen bond interactions. The use of other nucleophiles like thiols, or alcohols for nucleophilic addition was not successful in spite of varying several conditions.

It was now time to deprotect one of the products and confirm the outcome in terms of stereoselectivity. Compound **227c** was picked as a representative for deprotection. Deprotection of **227c** using TBAF in toluene at 0 °C for 20 minutes led to the formation of **244** as white solid in a yield of 80%. The ratio of the major diastereomer **244A** to the minor diastereomer **244B** was found to be 4:1. From the ^{1}H NMR data, it appeared that the major and minor diastereomers existed in a chair conformation, most likely promoted by hydrogen bonding between the OH and the NH group, as shown below.

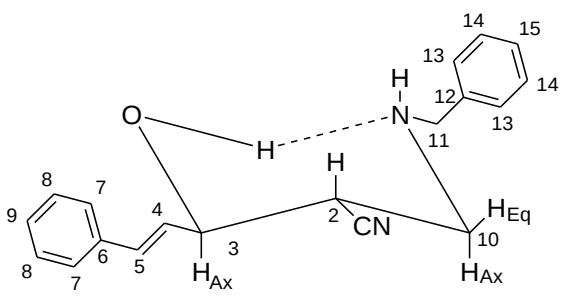

Major diastereomer-244A

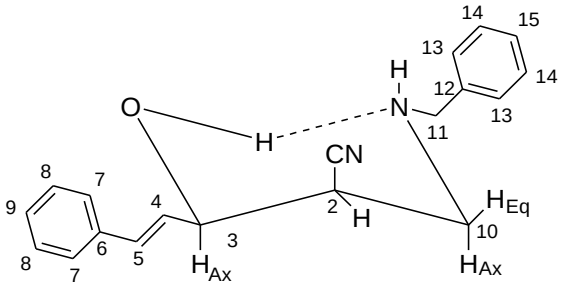

Minor diastereomer-244B

It is proposed that the positioning of the two phenyl groups will be in the equatorial position as this would give the most stable conformation. This means that the nitrile group at the stereogenic centre (carbon 2) can be in either the equatorial or the axial position, depending on which diastereomer is being considered. ^{1}H NMR data was used to distinguish the two diastereomers and propose that the *syn*-diastereomer was the major diastereomer (**244A**) while the *anti*-diastereomer was the minor diastereomer (**244B**). **Table 53** shows the coupling constants that were used to propose the structures of the major and minor diastereomers. The coupling protons were identified using a COSY spectrum that is attached in **Appendix II**. Even though the major and minor diastereomers were not physically separated, most of their

signals in the ^{1}H NMR spectrum were found well apart from each other, so that coupling constants for each diastereomer could be calculated. The NMR data matched that previously obtained for compound **244**.

In order to make the assignment, the general coupling constants found for six-membered rings were used as follows: ^{3}J coupling axial-axial = 7-12 Hz; ^{3}J coupling equatorial-equatorial = 2-5 Hz; ^{3}J coupling axial – equatorial = 2-5 Hz; and ^{2}J coupling axial – equatorial = 12-13 Hz. From Table 60, it is clear that the major diasteromer is the *syn*-diastereomer. The obtained coupling values are in agreement with already established coupling values for chair conformers.[201] Using the obtained coupling constant to calculate the ratio $(J_{trans}/2)/(J_{cis}/2)$ as proposed by Lambert led to 1.10 which suggested that a flattened chair conformer existed.[202]

Table 53: Coupling constant data for identifying major and minor diastereomers **244A and 244B**

Major diastereomer **244A**			Minor diastereomer **244B**		
Coupling partners		*J* (Hz)	Coupling partners		*J* (Hz)
H-2 ax. (ddd)	H-10 eq.	4.7	**H-2 eq. (ddd)**	H-10 eq.	5.7
	H-10 ax.	6.90		H-10 ax.	4.4
	H-3 ax.	6.88		H-3 ax.	3.3
H-10 eq. (dd)	H-10 ax.	12.5	**H-10 eq. (dd)**	H-10 ax.	12.5
	H-2 ax.	4.7		H-2 eq.	5.8
H-10 ax. (dd)	H-10 eq.	12.5	**H-10 ax. (dd)**	H-10 eq.	12.5
	H-2 ax.	7.1		H-2 eq.	4.4
H-4 (dd)	H-5	15.8	**H-4 (dd)**	H-5	16.0
	H-3 ax.	6.0		H-3 ax.	6.0
H-3 ax. (ddd)	H-4	6.3	**H-3 ax.**	Not clear	
	H-2 ax.	6.3			
	H-5	1.3			

The next reaction was to use *m*-CPBA for the epoxidation of silyl derivative **227c**. This reaction was not successful as the starting material was recovered. The reason for the unsuccessful reaction might be the presence of the bulky silyl group that prevents the

interaction of the peroxy group with the double bond. To establish if this was the reason, unprotected **244** was used to perform epoxidation. Unfortunately, only the sterting material was recovered. For some reason, this particular cinnamyl double bond was not reactive to epoxidation. This suggests that more versatile methods of carrying out epoxidation should be employed.

The other method of functionalising the double bond of **227c** and **244** is by using AD mix-α in a mixture of *tert*-butyl alcohol and water**.** These reactions which employed Sharpless dihydroxylations were also fruitless as only the starting material was recovered. The repeat of Sharpless dihydroxylation on **244** by refluxing at 80°C for 50 hours did not lead to any new product and the starting material was recovered. A repeat of these reaction conditions of refluxing at 80°C on **227c** led to an elimination reaction that afforded **252**. This is because the AD-mix-α contains a base that abstracted proton H-2 leading to **252**.

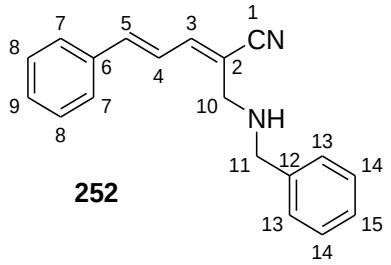

252

The structure of **252** was confirmed by ^{1}H and ^{13}C NMR spectroscopy. The most deshielded signal appeared at δ 7.50 as a doublet of doublets with coupling constants of 7.9 and 1.5 Hz that was assigned to proton H-7. Proton H-7 is observed as a doublet of doublets because it is coupling with neighbouring protons H-8 and long range coupling with H-5. The remaining aromatic protons appeared as a multiplet at δ 7.42 – 7.28 while the multiplet at δ 7.22 – 7.14 was assigned to H-5. The multiplet at δ 6.93 – 6.81 with an integration value of two was assigned H-4 and H-3. The three singlets at δ 3.82, 3.59 and 1.64 were assigned to H-11, H-10 and NH respectively. The ^{13}C NMR spectra showed a total of 15 signals as expected. The characteristic nitrile signal was observed at δ117.7 as expected while saturated carbon signals that appeared at δ 52.3 and 51.0 were assigned to C-11 and C-10. The presence of IR stretches at 3062 cm^{-1} and 2207 cm^{-1} in the IR spectrum confirmed the presence of NH and CN functional groups on **252**. The molecular ion peak of $[M+H^{+}]$ was found to be 275.1545 which was consistent with the calculated formula of $C_{19}H_{19}N_2$ for 275.1543.

Considering that nucleophilic addition reactions to silylated derivatives gave considerable selectivity, we decided to proceed with the use of an enantiopure MBH adduct for investigating Michael addition under these conditions. Using an enantiopure product we hoped would lead to a diastereoselective Michael addition reaction, giving rise to a significantly enantio-enriched final product.

3.3.6 Diastereoselective nucleophilic addition of benzylamine on enantiopure MBHA

Reactions shown in **Scheme 98** were used to accomplish Michael addition on an enantiopure (*S,E*)-3-hydroxy-2-methylene-5-phenylpent-4-enenitrile **191**.

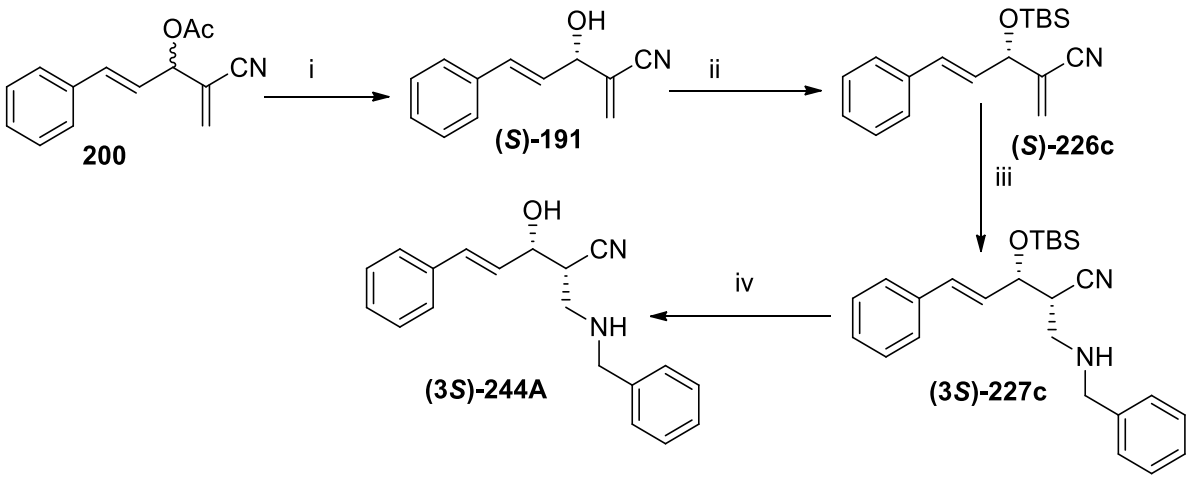

Scheme 98: Diastereoselective nucleophilic addition of benzylamine on an enantiopure MBHA. *Reagents and conditions*. (i) Novozym 435, Phosphate buffer at pH 7.00 (ii) TBSOTf, TEA in DCM at 0 °C (iii) Benzylamine in methanol at RT (iv) TBAF in THF at 0 °C.

The first step involved resolving **200** using Novozym 435 in phosphate buffer, using the method previously described. This step afforded enantiopure (*S,E*)-3-hydroxy-2-methylene-5-phenylpent-4-enenitrile **191** as a colourless oil with a yield of 60%, and an enantiomeric excess (ee) of 97%. The specific optical rotation was found to be +50.4 in methanol. The other unimportant fraction after enzymatic reaction was a scalemic mixture. The chromatogram of the enantiopure alcohol **191** is shown in **Figure 93**.

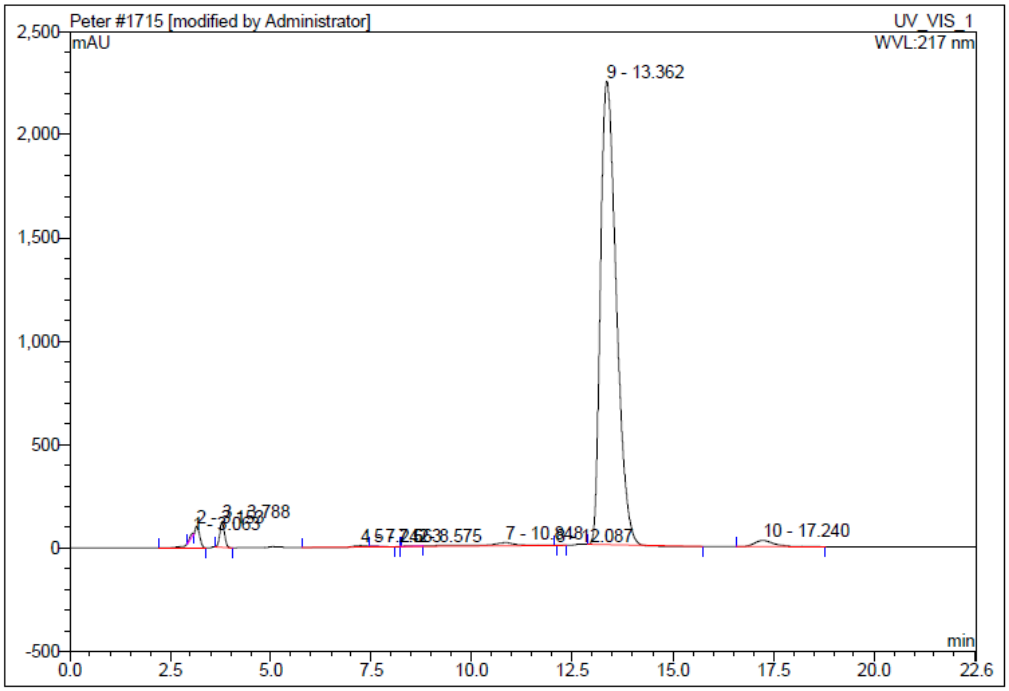

No.	Ret.Time min	Peak Name	Height mAU	Area mAU*min	Rel.Area %	Amount	Type
1	3.06	n.a.	11.880	1.498	0.14	n.a.	Ru
2	3.15	n.a.	106.599	25.086	2.27	n.a.	BMB*
3	3.79	n.a.	121.590	16.586	1.50	n.a.	BMB*
4	7.24	n.a.	7.847	4.809	0.43	n.a.	BM *
5	7.56	n.a.	1.460	0.503	0.05	n.a.	Rd
6	8.58	n.a.	3.142	1.373	0.12	n.a.	Ru
7	10.85	n.a.	15.833	19.842	1.79	n.a.	MB*
8	12.09	n.a.	0.017	0.001	0.00	n.a.	Rd
9	13.36	n.a.	2244.143	1020.424	92.21	n.a.	BMB*
10	17.24	n.a.	29.751	16.468	1.49	n.a.	BMB
Total:			2542.261	1106.588	100.00	0.000	

Figure 94: HPLC chromatogram of enantiopure **191**

The next task was to perform silylation on the enantiopure alcohol. It was envisioned that the bulky silyl group would promote diastereoselective Michael addition of the nitrogen nucleophile, as previously observed. The silylation process was achieved using *tert*-butyldimethylsilyl trifluoromethanesulfonate in the presence of triethylamine in dichloromethane. This afforded (*S*)-**226c** as a colourless oil, whose structure was confirmed by spectroscopic techniques. Spectroscopic data matched that for the previously isolated silylated racemic **226c**.

The next step was to carry out the nucleophilic addition reaction on the protected enantiopure adduct using benzylamine. This reaction led to (3*S*)-**227c** that was characterized using

spectroscopic data. All data agreed with that previously obtained for the racemic **227c**. As previously observed, the diastereoselectivity for this nucleophilic addition reaction was 4:1.

The next step was to deprotect (3*S*)-**227c** using TBAF that led to a white solid (3*S*)-**244** in 80% yield. The NMR data was compared with that for racemic **244**, and the data corresponded, as expected.

We were delighted to have achieved the successful diastereoselective nucleophilic addition reaction on our enantiopure compound, giving rise to a significantly enantio-enriched final product. Although the nucleophilic addition reaction was not completely diastereoselective, we believe that we have demonstrated the success of our approach to enantiopure MBH derivatives.

3.3.7 Conclusions

The second approach, which involved enzymatic kinetic resolution of racemic MBH acetates by hydrolysis proved to be very successful, with both the acetates and the corresponding alcohols being obtained in excellent enantiomeric excess (ee). This method allowed for the isolation of enantiopure MBH products that could be used in the next step: a diastereoselective Michael addition reaction with a nitrogen nucleophile. The Michael addition reactions on cyanoacrylate alcohols protected with a bulky silyl group proceeded with significant diastereoselectivity of between 4 and 5 to 1. Conducting this reaction on an enantiopure cyanoacrylate adduct, allowed a significantly enantio-enriched final product to be obtained.

CHAPTER FOUR

4 CONCLUSION AND RECOMMENDATIONS

A. The Morita- Baylis-Hillman reaction has been used to synthesise adducts **181 - 185** and **187** starting from phenylalaninal in poor yields with longreaction times. The use of these adducts for further reactions was not possible because of the racemisation of the stereogenic centre of phenylalaninal. It is recommended that alternative routes that do not lead to racemisation need to be investigated.

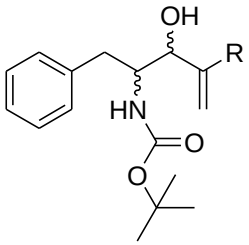

R

181, 182 = CN

183, 194 = $COOCH_3$

185 = $COOCH_2CH_3$

187 = $COCH_3$

B. Enzymatic kinetic resolution of racemic MBH acetates afforded enantiopure adducts **75a**, **191** and **195** with high enantiomeric excess (ee) ranges of 94 – 97%. Lipases from *Pseudomonas fluorescens* and *Candida antarctica* were the best performing enzymes in the hydrolysis of MBH acetates. The resolution of MBH esters also led to enantiopure acids **205** and **103e** with average ee ranges of 81 - 94%. Lipase from *Candida rugosa* and Lipo max Cxt were the best performing enzymes on esters. It is recommended that more substrates with synthetic significance should be resolved.

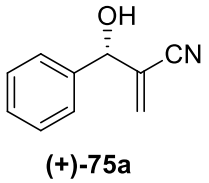

(+)-75a

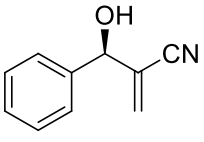

(-)-75a

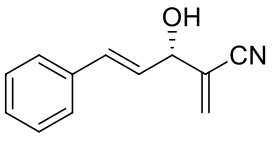

(+)-191

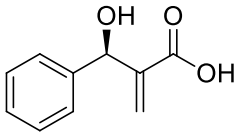

205

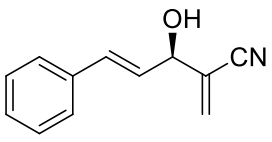

(-)-191

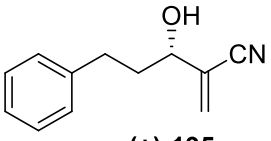

(+)-195

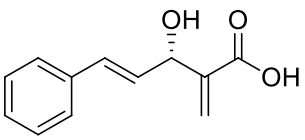

103e

C. The investigation of diastereoselective Michael addition reactions with a nitrogen nucleophile on cyanoacrylate alcohols protected with a bulky silyl group proceeded with significant diastereoselectivity of between 4 and 5 to 1. The use of this reaction on an enantiopure cyanoacrylate adduct afforded significantly enantio-enriched final product **227c**. The use of other enantiopure MBHA in Michael addition reactions and further functionalisation should be investigated. The diastereoselectivity of the Michael addition reaction needs to be improved, however, if an enantiopure final product is to be obtained. Future work should also focus on trying to improve Michael addition on enantiopure MBHA having different protecting groups.

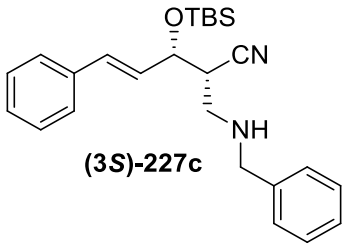

(3*S*)-227c

CHAPTER FIVE

5 EXPERIMENTAL PROCEDURES

5.1 Purification of solvents and reagents

All reagents and solvents were obtained from Sigma-Aldrich (South Africa) and MerK KGAA (South Africa). All the solvents used for chromatographic separation were distilled before use while solvents used for reactions were dried and distilled under nitrogen before use. When dry solvents were required, toluene was distilled from sodium wire whereas tetrahydrofuran and diethyl ether were distilled from sodium wire using benzophenone as an indicator. Acetonitrile, dichloromethane and dimethylformamide were distilled from calcium hydride. HPLC analytical reagents were used without purification.

5.2 Sources of enzymes used in this work

The enzymes used were purchased from Sigma-Aldrich, Enzymes SA or Amano, or were gifts from Novozymes. Esterases and nitrile hydratase were preparations by the Council for Scientific and Industrial Research (CSIR), Pretoria. Small scale enzymatic reactions were performed on an Esco provocell ^{TM} microplate shaker at varying temperatures.

5.3 Chromatography

Reactions were monitored using TLC (thin layer chromatography) on aluminium-backed Merck silica gel 60 F_{254} plates. Separation of compounds by column chromatography was performed on normal silica gel (particle size 063-0.200 mm) or flash silica gel (particle size 0.040-0.063) purchased from Merck.

5.4 Spectroscopy and physical data

^{1}H NMR and ^{13}C NMR spectra were recorded on either a Bruker AVANCE 300 MHz, Bruker AVANCE 400 MHz or on a Bruker AVANCE III 500 MHz spectrometer. Spectra were recorded in deuterated chloroform, unless otherwise stated. The chemical shift values for all spectra obtained are reported in parts per million and referenced against the internal standard, TMS, which occurs at zero parts per million. Coupling constants are given in Hertz. High resolution mass spectra were recorded on a Waters Synapt G1 or G2 mass spectrometer using an ESI positive source and a cone voltage of 15 V. Infra-red spectra were

recorded using a Bruker Tensor 27 single channel infrared spectrometer. The optical rotations of the enantiopure compounds were recorded on a Jasco P-2000 polarimeter. The melting point of all the compounds are uncorrected and were performed using open capillary tubes on a Stuart SMP 10 melting point apparatus.

The intensity data of X-ray crystallography were collected on a Bruker Apex II CCD area detector diffractometer with graphite monochromated Mo Kα radiation (50 kV, 30 mA). The data was collected using APEX data collection software. The method of data collection entailed ϾϴϽ-scans of width 0.5° and 512X512 data frames whereas the program SAINT+ was used for data reduction and the program XPREP was used for face indexed absorption corrections. A direct method using SHELXTL was used to solve the structure. SHELXTL, PLATON and ORTEP-3 programs were used to generate diagrams and publication data.

5.5High Performance Liquid Chromatography

High performance liquid chromatography (HPLC) was done on a Dionex HPLC Ultimate 3000 instrument equipped with a photodiode array detector using CHROMELEON version 6.80 software. Analysis of chiral compounds was done on Lux 3µ cellulose-2, Lux 5µ cellulose-1, Chiralpak AD-H, Lux 5µM Amylose-2, Chiralcel OJ, Lux 5µ Amylose-1, and Lux 5µ Amylose-2 columns. Luna 5µ C18(2) 100A was used for preliminary investigation of enzymatic activities on Morita-Baylis-Hillman alcohols and acetates.

The mobile phase used for chiral chromatography consisted of either a mixture of isopropyl alcohol (IPA) and hexane or a mixture of isopropyl alcohol (IPA), hexane and methanol. The mobile phase for C18 reverse phase column chromatography consisted of acetonitrile and water. Detection of the eluted analytes was achieved using a TSP variable wavelength UV detector at 215 nm. All calculations were based on peak area.

5.6Reagents used for the synthesis of the compounds

All the reagents used for the synthesis of all the compounds were commercially available and therefore, they have not been numbered in the experimental procedure. The only compounds that have been numbered are the synthetic intermediates.

5.7 Synthetic experimental procedures

5.7.1 Use of α-amino acid derived aldehydes in the Morita-Baylis-Hillman reaction

5.7.1.1 Synthesis of (S)-tert-butyl (1-(methoxy(methyl)amino)-1-oxo-3-phenylpropan-2-yl)carbamate (178)[118]

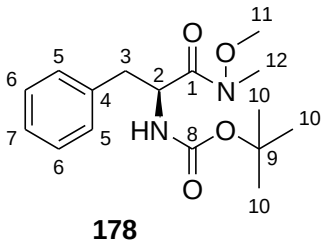

178

To dry dichloromethane (50 mL), was added *N*-Boc-L-phenylalanine **177** (10.0g, 0.038 mol) followed by portionwise addition of 1, 1-carbonyldiimidazole (7.3 g, 0.045 mol). Effervescence was observed indicating that there was a release of carbon dioxide. The reaction was left open to the environment and stirring was continued for one hour. *N*,*O*-dimethylhydroxylamine hydrochloride (4.41g, 0.045 mol) was immediately added and stirring continued for an addition 15 hours. The crude product was diluted with water (30 mL) followed by extraction using dichloromethane (5 x 40 mL). The organic layer was dried over magnesium sulphate, concentrated under reduced pressure and purified by column chromatography using 20% ethyl acetate in hexane. This afforded **178** as a viscous colourless oil (11.23g, 97%). R_f = 0.63 (30% ethyl acetate/hexane). IR (neat, cm^{-1}) 3289 (NH), 2970 (=C-H), 1698 (C=O), 1650 (C=O), 1496 (C=C), 1253 (C-N); ^{1}H NMR (300 MHz, Chloroform-*d*) δ 7.32 – 7.13 (5H, m, Ar-H), 5.20 (1H, d, *J* = 7.2 Hz, NH), 5.08 – 4.81 (1H, m, H-2), 3.65 (3H, s, H-11), 3.16 (3H, s, H-12), 3.11 – 2.98 (1H, m, H-3a), 2.87 (1H, dd, *J* = 13.0, 7.0 Hz, H-3b), 1.39 (9H, s, H-10); ^{13}C NMR (75 MHz, $CDCl_3$) δ 172.4 (C-1), 155.2 (C-8), 136.7 (C-4), 129.5 (C-5 or C-6), 128.3 (C-5 or C-6), 126.7 (C-7), 79.6 (C-9), 61.5 (C-11), 51.6 (C-2), 38.9 (C-3), 32.1 (C-12), 28.3 (C-10).

5.7.1.2 Synthesis of (R)-tert-butyl (1-(methoxy(methyl)amino)-1-oxo-3-phenylpropan-2-yl)carbamate (180)[118]

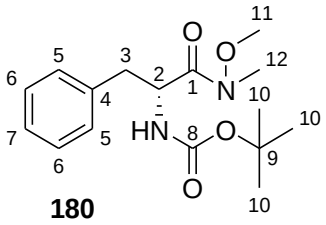

180

The same procedure as the one used for the synthesis of **178** was used except that *N*-Boc-D-phenylalanine **179** was used. This afforded **180** as a colourless oil (2.79 g, 95%). R_f = 0.63 (30% ethyl acetate/hexane). IR (neat, cm^{-1}) 3289 (NH), 2974 (=C-H), 1699 (C=O), 1657 (C=O), 1497 (C=C), 1255 (C-N); ^{1}H NMR (300 MHz, Chloroform-*d*) δ 7.33 – 7.12 (5H, m, Ar-H), 5.20 (1H, d, *J* = 7.4 Hz, NH), 5.06 – 4.86 (1H, m, H-2), 3.65 (3H, s, H-11), 3.16 (3H, s, H-12), 3.05 (1H, dd, *J* = 13.5, 6.1 Hz, H-3a), 2.87 (1H, dd, J = 13.2, 7.2 Hz, H-3b), 1.39 (9H, s, H-10). ^{13}C NMR (75 MHz, $CDCl_3$) δ 172.4 (C-1), 155.2 (C-8), 136.7 (C-4), 129.5 (C-5 or C-6), 128.3 (C-5 or C-6), 126.8 (C-7), 79.7 (C-9), 61.5 (C-11), 51.7 (C-2), 38.9 (C-3), 32.0 (C-12), 28.2 (C-10).

5.7.1.3 Synthesis of (S)-tert-butyl (1-oxo-3-phenylpropan-2-yl)carbamate (173)[203]

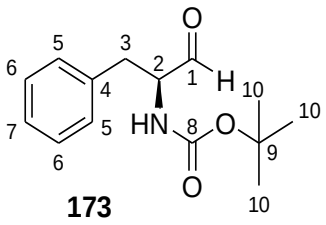

173

N-Boc-L-phenylalanine Weinreb amide **178** (5.53 g, 0.018 mol) was added to a two- necked flamed dried round bottom flask containing dry THF (110 mL). The mixture was stirred and cooled to 0°C followed by portionwise addition of $LiAlH_4$ (1.37 g, 0.036 mol). The reaction continued with stirring under nitrogen for four hours, after which $KHSO_4$ (2.49, 0.022 mol) was added portionwise as stirring continued for 15 minutes. The reaction mixture was transferred to a separating funnel, and ethyl acetate (40 mL) was added, followed by 1M HCL (30 mL). The organic layer was further washed with a saturated solution of $NaHCO_3$ (30 mL) followed by brine (30 mL). It was dried over magnesium sulphate and concentrated under reduced pressure. This yielded **173** as a white solid (4.41g, 92%). R_f = 0.40 (30% ethyl

acetate/hexane). MP: 84 – 85 °C; $[\alpha]_D$= -45.500 (c = 0.5, MeOH). IR (neat, cm^{-1}) 3365(NH), 2978 (=C-H), 1687(2 x C=O), 1454 (C=C), 1248 (C-N); ^{1}H NMR (300 MHz, Chloroform-*d*) δ 9.62 (1H, s, H-1), 7.35 – 7.23 (3H, m, Ar-H), 7.20 – 7.14 (2H, m, Ar-H), 5.17 – 5.01 (1H, m, NH), 4.48 – 4.35 (1H, m, H-2), 3.11 (2H, d, *J* = 6.5 Hz, H-3), 1.43 (9H, s, H-10); ^{13}C NMR (75 MHz, $CDCl_3$) δ 199.2 (C-1), 155.4 (C-8), 135.8 (C-4), 129.3 (C-5 or C-6), 128.8 (C-5 or C-6), 127.1 (C-7), 80.2 (C-9), 60.8 (C-2), 35.5 (C-3), 28.3 (C-10).

5.7.1.4 Synthesis of (R)-tert-butyl (1-oxo-3-phenylpropan-2-yl)carbamate (174)[203]

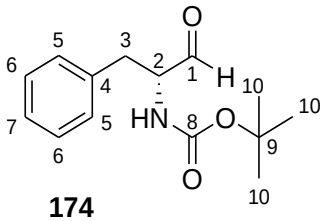

174

The same procedure as the one used for the synthesis of **173** was used except that (R)-*tert*-butyl (1-(methoxy(methyl)amino)-1-oxo-3-phenylpropan-2-yl)carbamate **180** was used. This afforded **174** as a white solid (4.41g, 92%). R_f = 0.40 (30% ethyl acetate/hexane). MP: 84 - 85°C; $[\alpha]_D$= +43.400 (c = 0.5, MeOH). IR (neat, cm^{-1}) 3367 (NH), 2981 (=C-H), 1728 (C=O), 1687 (C=O), 1453 (C=C), 1250 (C-N). ^{1}H NMR (300 MHz, Chloroform-*d*) δ 9.62 (1H, s, H-1), 7.36 – 7.23 (3H, m, Ar-H), 7.19 – 7.14 (2H, m, Ar-H), 5.13 – 5.00 (1H, s, NH), 4.50 – 4.33 (1H, m, H-2), 3.11 (2H, d, *J* = 6.4 Hz, H-3), 1.43 (9H, s, H-10); ^{13}C NMR (75 MHz, $CDCl_3$) δ 199.4 (C-1), 155.4 (C-8), 135.8 (C-4), 129.3 (C-5 or C-6), 128.7 (C-5 or C-6), 127.1 (C-7), 80.2 (C-9), 60.8 (C-2), 35.4 (C-3), 28.3 (C-10).

5.7.1.5 Synthesis of tert-butyl ((2S)-4-cyano-3-hydroxy-1-phenylpent-4-en-2-yl)carbamate (181a and 181b)

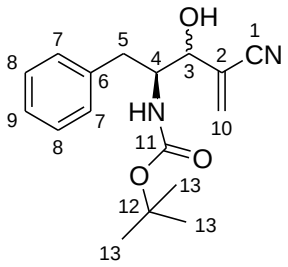

181a and 181b

To a solution of (*S*)-*tert*-butyl (1-oxo-3-phenylpropan-2-yl)carbamate **173** (113 mg, 2.07 mmol) and acrylonitrile (410 µL, 6.21 mmol) was added DABCO (230 mg, 2.07 mmol). The reaction mixture was stirred at room temperature for 12 d. This was followed by diluting the reaction mixture with water (20 mL) and extracting the crude product with ethyl acetate (3 x 30 mL). The crude organic layer was dried over $MgSO_4$, concentrated under reduced pressure and purified by column chromatography using 20% ethyl acetate in hexane as eluent. This afforded two products, **181a** as a white solid (90 mg, 14%) and **181b** as a colourless oil (200 mg, 32%).

White solid 181a: R_f = 0.40 (40% ethyl acetate/hexane); IR (neat, cm^{-1}) 3651 (NH), 3376 (OH), 3029 (=C-H), 2225 (C≡N), 1698 (C=O), 1454 (C=C), 1248 (C-N); ^{1}H NMR (300 MHz, Chloroform-*d*) δ 7.34 – 7.15 (5H, m, Ar-H), 6.13 – 6.05 (1H, m, H-10a), 6.03 – 5.98 (1H, m, H-10b), 5.12 (1H, d, *J* = 8.6 Hz, NH), 5.00 (1H, d, *J* = 6.5 Hz, H-3), 4.46 – 4.16 (1H, m, OH), 4.18 – 3.78 (1H, m, H-4), 3.05 – 2.75 (2H, m, H-5), 1.42 – 1.30 (9H, s, H-13); ^{13}C NMR (75 MHz, $CDCl_3$) δ 156.7 (C-11), 137.8 (C-6), 130.9 (C-10), 129.2 (C-7 or C-8), 128.6 (C-7 or C-8), 126.7 (C-9), 124.9 (C-2), 117.3 (C-1), 80.3 (C-12), 72.0 (C-3), 55.9 (C-4), 37.3 (C-5), 28.2 (C-13). HRMS *m/z* calcd for $C_{17}H_{22}N_2O_3Na$ [M+Na^+]: 325.1523, found: 325.1524.

Reverse phase C18 HPLC column: Luna 5µm C18 (2) 100A (250 x 4.60 mm); mobile phase, acetonitrile: water (40:60); flow rat = 1 mL/min; t_R = 14.90 min, t_R = 17.94 min. It was contaminated with diastereomer **181b**.

Colourless oil 181b: R_f = 0.40 (40% ethyl acetate/hexane); IR (neat, cm^{-1}) 3440 (NH), 3373 (OH), 3031 (=C-H), 2225 (C≡N), 1679 (C=O), 1453 (C=C), 1250 (C-N) ;^{1}H NMR (300 MHz, Chloroform-*d*) δ 7.36 – 7.16 (5H, m, Ar-H), 6.12 (2H, brs, H-10), 5.07 – 4.94 (1H, m, NH), 4.88 – 4.74 (1H, m, H-3), 4.39 (1H, s, OH), 4.12 – 3.94 (1H, m, H-4), 2.95 – 2.80 (2H, m, H-5), 1.43 – 1.34 (9H, m, H-13); ^{13}C NMR (75 MHz, $CDCl_3$) δ 157.3 (C-11), 137.1 (C-6), 132.3

(C-10), 129.2 (C-7 or C-8), 128.7 (C-7 or C-8),126.9 (C-9), 123.5 (C-2), 117.5 (C-1), 80.8 (C-12), 74.5 (C-3), 57.0 (C-4), 35.5 (C-5), 28.2 (C-13). HRMS *m/z* calcd for $C_{17}H_{22}N_2O_3Na$ [M+Na^+]: 325.1523, found: 325.1528.

Reverse phase C18 HPLC column: Luna 5µm C18 (2) 100A (250 x 4.60 mm); mobile phase, acetonitrile: water (40:60); flow rate = 1 mL/min; t_R = 14.90 min, t_R = 17.94 min. It was contaminated with **181a**.

5.7.1.6 Synthesis of tert-butyl ((2R)-4-cyano-3-hydroxy-1-phenylpent-4-en-2-yl)carbamate (182a and 182b)

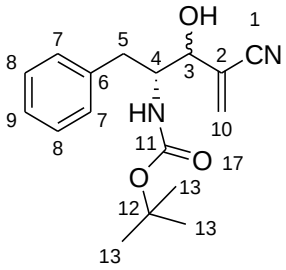

182a and 182b

A similar procedure that was used for the synthesis of **181a** and **181b** was also used to synthesise **182a** and **182b**. Compound **182a** was isolated as a colourless oil (128 mg, 13%). R_f = 0.40 (40% ethyl acetate/hexane); IR (neat, cm^{-1}) 3372 (NH), 3358 (OH), 3029 (=C-H), 2224 (C≡N), 1680 (C=O), 1453 (C=C), 1249 (C-N); ^{1}H NMR (300 MHz, Chloroform-*d*) δ 7.35 – 7.18 (5H, m, Ar-H), 6.13 – 6.07 (1H, m, H-10a), 6.05 – 5.99 (1H, m, H-10b), 5.06 (1H, d, *J* = 8.0 Hz, NH), 4.97 (1H, d, *J* = 6.1 Hz, H-3), 4.26 (1H, s, OH), 3.97 – 3.74 (1H, m, H-4), 3.10 – 2.81 (2H, m, H-5), 1.44 – 1.31 (9H, m, H-13); ^{13}C NMR (75 MHz, $CDCl_3$) δ 156.9 (C-11), 137.7 (C-6), 130.9 (C-10) 129.2 (C-7 or C-8), 128.6 (C-7 or C-8), 126.7 (C-9), 124.8 (C-2), 117.3 (C-1), 80.4 (C-12), 72.3 (C-3), 56.2 (C-4), 37.0 (C-5), 28.2 (C-13). HRMS *m/z* calcd for $C_{17}H_{22}N_2O_3Na$ [M+Na^+]: 325.1523, found: 325.1528.

Reverse phase C18 HPLC column: Luna 5µm C18 (2) 100A (250 x 4.60 mm); mobile phase, acetonitrile: water (40:60); flow rate = 1 mL/min; t_R = 15.01 min, t_R = 18.02 min.

Colourless oil 182b (170 mg, 18%). R_f = 0.40 (40% ethyl acetate/hexane); IR (neat, cm^{-1}) 3370 (NH), 3356 (OH), 3029 (=C-H), 2224 (C≡N), 1680 (C=O), 1453 (C=C), 1249 (C-N);

^{1}H NMR (300 MHz, Chloroform-*d*) δ 7.38 – 7.15 (5H, m, Ar-H), 6.13 (2H, brs, H-10), 5.05 – 4.90 (1H, m, NH), 4.85 – 4.70 (1H, m, H-3), 4.40 (1H, brs, OH), 4.13 – 3.93 (1H, m, H-4), 2.95 – 2.80 (2H, m, H-5), 1.46 – 1.30 (9H, m, H-13); ^{13}C NMR (75 MHz, $CDCl_3$) δ 157.5 (C-11), 137.0 (C-6), 132.3 (C-10), 129.2 (C-7 or C-8), 128.8 (C-7 or C-8), 126.9 (C-9),123.4 (C-2), 117.5 (C-1), 80.9 (C-12), 74.6 (C-3), 57.2 (C-4), 35.4 (C-5), 28.3 (C-13). HRMS *m/z* calcd for $C_{17}H_{22}N_2O_3Na$ [M+Na$^+$]: 325.1523, found: 325.1529.

Reverse phase C18 HPLC column: Luna 5μm C18 (2) 100A (250 x 4.60 mm); mobile phase, acetonitrile: water (40:60); flow rate = 1 mL/min; t_R = 15.01 min, t_R = 18.02 min.

5.7.1.7 Synthesis of (4S)-methyl 4-((tert-butoxycarbonyl)amino)-3-hydroxy-2-methylene-5-phenylpentanoate (183)[123]

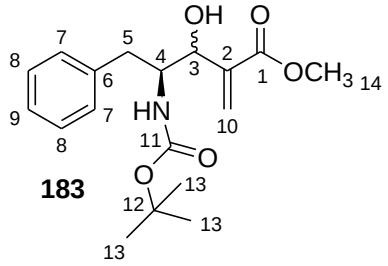

183

To a solution of (*S*)-*tert*-butyl (1-oxo-3-phenylpropan-2-yl)carbamate **173** (56 mg, 0.22 mmol) and methy acrylate (200 μL, 2.38 mmol) was added DABCO (300 mg, 0.223 mmol). The reaction mixture was stirred at room temperature for 10 d. This was followed by diluting the reaction mixture with water (20 mL) and extracting the crude product with ethyl acetate (4 x 30 mL). The crude organic layer was dried over $MgSO_4$, concentrated under reduced pressure and purified by column chromatography using 30% ethyl acetate in hexane as eluent. This afforded **183** as a colourless oil which was a mixture of diastereomers with a diastereomeric ratio of 1:4 (23 mg, 31%). R_f = 0.45 (40% ethyl acetate/hexane); IR (neat, cm^{-1}) 3385 (NH and OH), 2974 (=C-H), 1697 (C=O), 1690 (C=O), 1442 (C=C), 1251 (C-N);^{1}H NMR (300 MHz, Chloroform-*d*) δ 7.34 – 7.15 (5H, m, Ar-H), 6.32 (1H, s, H-10a), 5.95 – 5.88 (1H, m, H-10b), 4.83 (1H, d, *J* = 8.7 Hz, NH), 4.52 (1H, d, *J* = 5.7 Hz, H-3), 4.11 – 3.92 (1H, m, H-4), 3.81 – 3.69 (3H, m, H-14), 3.62 (d, *J* = 5.8 Hz, OH), 3.14 – 2.80 (2H, m, H-5), 1.43 – 1.24 (9H, m, H-13); major diastereomer ^{13}C NMR (75 MHz, $CDCl_3$) δ 166.6 (C-1), 156.3 (C-11), 140.6 (C-2), 138.4 (C-6), 129.3 (C-7 or C-8), 128.4 (C-7 or C-8), 126.4 (C-9), 125.9 (C-10), 79.55 (C-12), 70.8 (C-3), 54.9 (C-4), 51.8 (C-14), 38.3 (C-5), 28.2 (C-13); minor diastereomer ^{13}C NMR (75 MHz, $CDCl_3$) δ 138.0 (C-6), 129.5 (C-7 or C-8), 128.4,

126.3 (C-9), 79.64 (C-12), 74.45 (C-3), 55.6 (C-4), 52.0 (C-14), 28.2. HRMS *m/z* calcd for $C_{18}H_{25}NO_5Na$ [M+Na^+]: 358.1625, found: 358.1640.

Reverse phase C18 HPLC column: Luna 5µm C18 (2) 100A (250 x 4.60 mm); mobile phase, acetonitrile: water (40:60); flow rate = 1 mL/min; t_R = 17.90 min, t_R = 20.03 min.

5.7.1.8 Synthesis of (4R)-methyl 4-((tert-butoxycarbonyl)amino)-3-hydroxy-2-methylene-5-phenylpentanoate (184)[123]

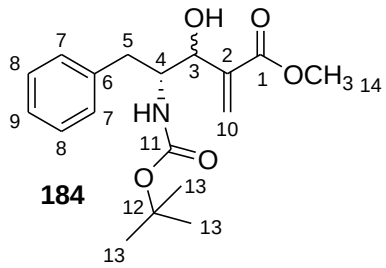

184

The same procedure used for the synthesis of **183** was used for the synthesis of **184**. This led to compound **184** as a colourless oil which was a mixture of diastereomers with a diastereomeric ratio of 1:3 (212.6 mg, 32%). R_f = 0.45 (40% ethyl acetate/hexane); IR (neat, cm^{-1}) 3376 (NH and OH), 2977 (=C-H), 1700 (C=O), 1685 (C=O), 1454 (C=C), 1259 (C-N). ^{1}H NMR (300 MHz, Chloroform-*d*) δ 7.32 – 7.14 (5H, m, Ar-H), 6.34 – 6.24 (1H, m, H-10a), 5.92 (1H, s, H-10b), 5.12 – 4.93 (1H, m, NH), 4.54 – 4.43 (1H, m, H-3), 4.12 – 3.95 (2H, m, H-4 and OH), 3.78 – 3.64 (3H, m, H-14), 3.08 – 2.83 (2H, (m, H-5), 1.42 – 1.19 (9H, m, H-13); major diastereomer ^{13}C NMR (75 MHz, $CDCl_3$) δ 166.5 (C-1), 156.3 (C-11), 140.7 (C-2), 138.5 (C-6), 129.3 (C-7 or C-8), 128.4 (C-7 or C-8), 126.30 (C-9), 125.8 (C-10), 79.4 (C-12), 70.2 (C-3), 54.6 (C-4), 51.8 (C-14), 38.2 (C-5), 28.2 (C-13); minor diastereomer ^{13}C NMR (75 MHz, $CDCl_3$) δ 166.0 (C-1), 155.9 (C-11), 139.6 (C-2), 138.1 (C-6), 129.5 (C-7 or C-8), 126.25 (C-9), 79.5 (C-12), 73.9 (C-3) 55.6 (C-4) 52.0 (C-14). HRMS *m/z* calcd for $C_{18}H_{25}NO_5Na$ [M+Na^+]: 358.1625, found: 358.1640.

Reverse phase C18 HPLC column: Luna 5µm C18 (2) 100A (250 x 4.60 mm); mobile phase, acetonitrile: water (40:60); flow rate = 1 mL/min; t_R = 18.84 min, t_R = 20.96 min.

Chiral HPLC: Chiralcel OJ; mobile phase, hexane: IPA (96:4); flow rate 1 mL/min; t_R = 4.41 min, t_R = 12.95 min. t_R = 16.46 min, t_R = 19.16 min.

5.7.1.9 Synthesis of (4S)-ethyl 4-((tert-butoxycarbonyl)amino)-3-hydroxy-2-methylene-5-phenylpentanoate (185)

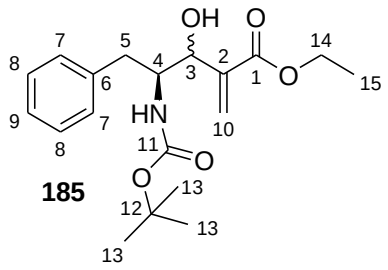

To a solution of (*S*)-*tert*-butyl (1-oxo-3-phenylpropan-2-yl)carbamate **173** (260 mg, 1.04 mmol) and ethyl acrylate (1.21 mL, 11.024 mmol) was added DABCO (116 mg, 1.04 mmol). The reaction mixture was stirred at room temperature for 12 d. This was followed by diluting the reaction mixture with water (25 mL) and extracting the crude product with ethyl acetate (4 x 30 mL). The crude organic layer was dried over $MgSO_4$, concentrated under reduced pressure and purified by column chromatography using 30% ethyl acetate in hexane as eluent. This afforded **185** as a colourless oil as a mixture of diastereomers with a diastereomeric ratio of 1:2 (100 mg, 28%). R_f = 0.50 (40% ethyl acetate/hexane); IR (neat, cm^{-1}) 3328 (NH and OH), 2978 (=C-H), 1690 (C=O), 1687 (C=O), 1454 (C=C), 1251 (C-N);^{1}H NMR (300 MHz, Chloroform-*d*) δ 7.34 – 7.14 (5H, m, Ar-H), 6.32 (1H, s, H-10a), 5.92 – 5.86 (1H, m, H-10b), 4.88 (1H, d, *J* = 9.3 Hz, NH), 4.55 – 4.49 (1H, m, H-3), 4.31 – 4.11 (2H, m, H-14), 4.10 – 3.99 (1H, m, H-4), 3.75 – 3.60 (1H, s, OH), 3.14 – 2.82 (2H, m, H-5), 1.50 – 1.17 (12H, m, H-13 and H-15); major diastereomer ^{13}C NMR (75 MHz, $CDCl_3$) δ 166.1 (C-1), 156.3 (C-11), 140.8 (C-2), 138.5 (C-6), 129.3 (C-7 or C-8), 128.42 (C-7 or C-8), 126.4 (C-9), 125.6 (C-10), 79.4 (C-12), 70.6 (C-3), 60.8 (C-14), 54.9 (C-4), 38.2 (C-5), 28.3 (C-13), 14.1 (C-15); minor diastereomer ^{13}C NMR (75 MHz, $CDCl_3$) δ 166.6 (C-1), 155.7 (C-11), 139.7 (C-2), 138.1 (C-6), 129.5 (C-7 or C-8), 128.37 (C-7 or C-8), 126.3 (C-9), 125.6 (C-10), 79.6 (C-12), 74.4 (C-3), 61.0 (C-14), 55.9 (C-4), 38.2 (C-5), 28.3 (C-13), 14.1 (C-15). HRMS *m/z* calcd for $C_{19}H_{28}NO_2$ [$M+H^+$]: 350.1922, found: 350.1955.

Reverse phase C18 HPLC column: Luna 5µ C18 (2) 100A (250 x 4.60 mm); mobile phase, acetonitrile: water (40:60); flow rate = 1 mL/min; t_R = 120.20 min, t_R = 128.77 min.

5.7.1.10 Synthesis of tert-butyl ((2S)-3-hydroxy-4-methylene-5-oxo-1-phenylhexan-2-yl)carbamate (187)

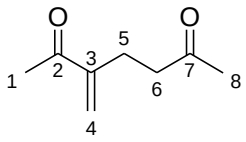

186

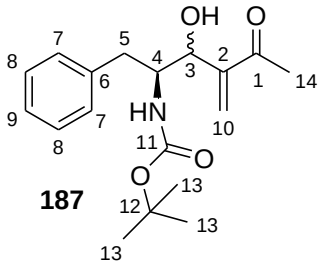

187

To a solution of (*S*)-*tert*-butyl (1-oxo-3-phenylpropan-2-yl)carbamate **173** (661 mg, 0.276 mmol) and methy vinyl ketone (120 µL, 1.401 mmol) in dichloromethane (1 mL) was added DABCO (300 mg, 0.267 mmol). The reaction mixture was stirred at room temperature for 12 d. Dichloromethane was removed under reduced pressure, followed by diluting the reaction mixture with water (20 mL) and extracting the crude product with ethyl acetate (3 x 30 mL). The crude organic layer was dried over $MgSO_4$, concentrated under reduced pressure and purified by column chromatography using 20% ethyl acetate in hexane as eluent. This afforded two products, 3-methyleneheptane-2,6-dione **186** (400 mg, 47%) as a colourless oil and **187** (300 mg, 35%) as a colourless oil. A repeat of this reaction afforded a crystalline compound that matched **187** (670 mg, 52%) with a M.P: 89 – 90 ºC.

Colourless oil 186: R_f = 0.60 (20% ethyl acetate/hexane); IR (neat, cm^{-1}) 1675 (C=O), 1671 (C=O), 145 (C=C) ; ^{1}H NMR (300 MHz, Chloroform-*d*) δ 6.04 (1H, s, H-4a), 5.84 (1H, s, H-4b), 2.64 – 2.49 (4H, m, H-5 and H-6), 2.34 (3H, s, H-1), 2.13 (3H, s, H-8); ^{13}C NMR (75 MHz, $CDCl_3$) δ 207.8 (C-7), 199.5 (C-2), 147.7 (C-3), 126.2 (C-4), 42.4 (C-6), 29.8 (C-8), 25.8 (C-1), 25.3 (C-5).

Colourless oil 187: R_f = 0.50 (40% ethyl acetate/hexane); IR (neat, cm^{-1}) 3334 (NH and OH), 3026 (=C-H), 1671 (C=O), 1664 (C=O), 1453 (C=C) 1250 (C-N); ^{1}H NMR (300 MHz, Chloroform-*d*) δ 7.34 – 7.15 (5H, m, Ar-H), 6.12 (1H, s, H-10a), 6.08 (1H, s, H-10b), 4.78 (1H, d, *J* = 8.9 Hz, NH), 4.59 (1H, d, *J* = 5.1 Hz, H-3), 4.02 – 3.89 (1H, m, H-4), 3.57 – 3.49 (1H, m, H-5), 3.06 – 2.80 (2H, m, H-5 and OH), 2.32 (3H, s, H-14), 1.40 – 1.32 (9H, m, H-13); ^{13}C NMR (75 MHz, $CDCl_3$) δ 200.2 (C-1), 156.3 (C-11), 148.7 (C-2), 138.4 (C-6), 129.3 (C-7 or C-8), 128.4 (C-7 or C-8), 126.4 (C-9), 125.6 (C-10), 79.4 (C-12), 70.6 (C-3), 54.7 (C-4), 38.1 (C-5), 28.3 (C-13), 26.3 (C-14). HRMS *m/z* calcd for $C_{18}H_{25}NO_4Na$ [M+Na^+]: 342.1676, found: 342.1676.

Reverse phase C18 HPLC column: Luna 5µm C18 (2) 100A (250 x 4.60 mm); mobile phase, acetonitrile: water (40:60); flow rate = 1 mL/min; t_R = 16.91 min, t_R = 18.41 min.

White crystalline 187: Rf= 0.50 (40% ethyl acetate/hexane): M.P: 89 – 90 ºC, IR (neat, cm-1) 3335 (NH and OH), 3024 (=C-H), 1672 (C=O), 1665 (C=O), 1450 (C=C), 1250 (C-N); ^{1}H NMR (300 MHz, Chloroform-*d*) δ 7.34 – 7.15 (5H, m, Ar-H), 6.11 (1H, s, H-10a), 6.07 (1H, s, H-10b), 4.81 (1H, d, *J* = 9.3 Hz, NH), 4.61 – 4.56 (1H, m, H-3), 4.01 – 3.89 (1H, m, H-4), 3.64 – 3.57 (1H, m, H-5), 3.06 – 2.86 (2H, m, H-5 and OH), 2.31 (3H, s, H-14), 1.40 – 1.32 (9H, m, H-13);^{13}C NMR (75 MHz, $CDCl_3$) δ 200.2 (C-1), 156.3 (C-11), 148.7 (C-2), 138.4 (C-6), 129.3 (C-7 or C-8), 128.4 (C-7 or C-8), 126.4 (C-10), 125.6 (C-9), 79.3 (C-12), 70.4 (C-3), 54.6 (C-4), 38.1 (C-5), 28.2 (C-13), 26.3 (C-14).

5.8 Enzymatic kinetic resolution

5.8.1 Preparation of Morita-Baylis-Hillman adducts

5.8.1.1 Synthesis of (±)-methyl 2-(hydroxy(phenyl)methyl)acrylate (101a)[204, 205]

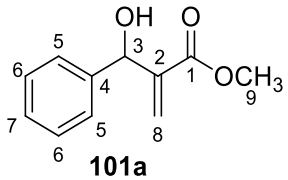

101a

To a solution of benzaldehyde (12.54 g, 0.118 mol) with methy acrylate (112 mL, 1.250 mol) was added DABCO (13.24 g, 0.118 mol). The reaction mixture was stirred at 0 °C until the reaction was complete (3 d). The completed reaction mixture was diluted with water (20 mL), followed by extraction of the crude product with ethyl acetate (4 x 30 mL). The organic layer was dried over $MgSO_4$, concentrated under reduced pressure, and purified by column chromatography using 40% ethyl acetate in hexane. This resulted in compound **101a** as a colourless oil (16.99 g, 74%). R_f = 0.70 (40% ethyl acetate/hexane); IR (neat, cm^{-1}) 3338 (OH), 2950 (=C-H), 1708 (C=O), 1456 (C=C); ^{1}H NMR (300 MHz, Chloroform-*d*) δ 7.29 – 7.23 (2H, m, Ar-H), 7.22 – 7.08 (3H, m, Ar-H) 6.20 (1H, s, H-8a), 5.85 (1H, s, H-8b), 5.45 (1H, d, *J* = 4.8 Hz, H-3), 4.23 (1H, d, *J* = 5.0 Hz, OH), 3.41 (3H, s, H-9); ^{13}C NMR (75 MHz,

$CDCl_3$) δ 166.5 (C-1), 142.7 (C-4), 141.8 (C-2), 128.3 (C-5 or C-6), 127.6 (C-7), 126.9 (C-5 or C-6), 125.1 (C-8), 72.3 (C-3), 51.6 (C-9).

Chiral HPLC: Lux 5μm cellulose-1 (250 x 4.60 mm); mobile phase, hexane: IPA (90:10); flow rate = 1 mL/min; t_R = 16.99 min, t_R = 19.01 min.

5.8.1.2 Synthesis of (±)-methyl 2-(hydroxy(4-nitrophenyl)methyl)acrylate **(192)**[143, 206]

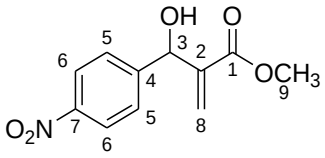

192

To a solution of 4-nitrobenzaldehyde (7.00 g, 0.046 mol) and methyl acrylate (42 mL, 0.460 mol) was added DABCO (6.00 g, 0.046 mol). The reaction mixture was stirred at room temperature until the reactants were consumed (4 h) as indicated by TLC. This was followed by diluting the reaction mixture with water (30 mL) and extracting the crude product with ethyl acetate (3 x 30 mL). The crude organic layer was dried over $MgSO_4$, concentrated under reduced pressure, and purified by column chromatography using 40% ethyl acetate in hexane as eluent. This afforded the desired product **192** as a colourless oil (9.17 g, 84%). R_f = 0.44 (40% ethyl acetate/hexane); IR (neat, cm^{-1}) 3508 (OH), 3105 (=C-H), 1695 (C=O), 1443 (C=C); ^{1}H NMR (300 MHz, Chloroform-*d*) δ 8.20 (2H, d, *J* = 8.6 Hz, H-6), 7.57 (2H, d, *J* = 8.9 Hz, H-5), 6.40 (1H, s, H-8a), 5.88 (1H, s, H-8b), 5.63 (1H, d, *J* = 6.2 Hz, H-3), 3.75 (3H, s, H-9), 3.35 (1H, d, *J* = 6.2 Hz, OH);^{13}C NMR (75 MHz, $CDCl_3$) δ 166.4 (C-1), 148.6 (C-7), 147.5 (C-4), 141.0 (C-2), 127.4 (C-6), 127.2 (C-8), 123.6 (C-5), 72.8 (C-3), 52.2 (C-9).

Lux 5μ cellulose-1 (250 x 4.60 mm), mobile phase, hexane: IPA (92:8); flow rate = 1 mL/min; t_R = 14.73 min, t_R = 16.46 min.

5.8.1.3 Synthesis of (±)-(E)-methyl 3-hydroxy-2-methylene-5-phenylpent-4-enoate (193)[207]

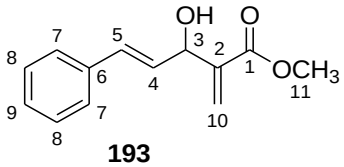

193

To a solution of *trans*-cinnamaldehyde (10.50 g, 0.008 mol) with methyl acrylate (21 mL, 0.238 mol) was added DABCO (17.81 g, 0.159 mol) and phenol (7 mL, 0.079 mol). The reaction mixture was stirred at 25 °C for 48 h. The completed reaction mixture was diluted with water (20 mL), followed by extraction of the crude product with ethyl acetate (4 x 30 mL). The organic layer was dried over $MgSO_4$, concentrated under reduced pressure, and purified by column chromatography using 20% ethyl acetate in hexane. This resulted in **193** as a viscous oil (12.47 g, 72%). R_f = 0.63 (40% ethyl acetate/hexane); IR (neat, cm^{-1}) 3256 (OH), 2956 (=C-H), 1715 (C=O), 1434 (C=C); ^{1}H NMR (500 MHz, Chloroform-*d*) δ 7.37 (2H, d, *J* = 7.6 Hz, H-7), 7.29 (2H, t, *J* = 7.5 Hz, H-8), 7.22 (1H, t, *J* = 7.2 Hz, H-9), 6.65 (1H, d, *J* = 15 Hz, H-5), 6.32-6.24 (2H, m, H-4 and H-10a), 5.91 (1H, s, H-10b), 5.15 – 5.10 (1H, m, H-3), 3.77 (3H, s, H-11), 3.16 (1H, d, *J* = 5.8 Hz, OH); ^{13}C NMR (126 MHz, $CDCl_3$) δ 166.7 (C-1), 141.3 (C-6), 136.5 (C-2), 131.4 (C-5), 129.3 (C-9), 128.5 (C-7 or C-8), 127.8 (C-4), 127.0 (C-7 or C-8), 125.8 (C-10), 71.9 (C-3), 52.0 (C-11).

5.8.1.4 Synthesis of (±)-methyl 3-hydroxy-2-methylene-5-phenylpentanoate (194)[208]

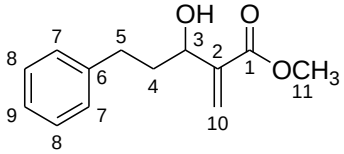

194

A similar procedure used to synthesize **101a** was used except that hydrocinnamaldehyde was used and the reaction took 8 d. This afforded **194** as a colourless oil (10.70 g, 64%). R_f = 0.64 (40% ethyl acetate/hexane); IR (neat, cm^{-1}) 3434 (OH), 2951 (=C-H), 1711 (C=O), 1495 (C=C); ^{1}H NMR (300 MHz, Chloroform-*d*) δ 7.30 – 7.22 (2H, m, Ar-H), 7.21 – 7.12 (3H, m, Ar-H), 6.22 (1H, s, H-10a), 5.80 (1H, s, H-10b), 4.47 – 4.37 (1H, m, H-3), 3.73 (3H, s, H-1), 2.95 (1H, d, *J* = 6.5 Hz, OH), 2.86 – 2.61 (2H, m, H-5), 2.03 – 1.82 (2H, m, H-4); ^{13}C NMR

(75 MHz, $CDCl_3$) δ 167.0 (C-1), 142.3 (C-6), 141.6 (C-2), 128.5 (C-9), 128.4 (C-7 or C-8), 125.9 (C-7 or C-8), 125.2 (C-10), 70.8 (C-3), 51.9 (C-11), 37.7 (C-4), 32.0 (C-5).

5.8.1.5 Synthesis of (±)-2-[(hydroxyphenyl)methyl]acrylonitrile (75a)[209-211]

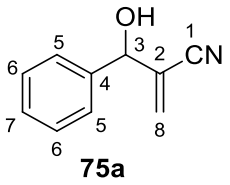

75a

To a solution of benzaldehyde (10.45 g, 0.098 mol) and acrylonitrile (40 mL, 0.608 mol) was added DABCO (10.90 g, 0.098 mol) and the reaction was stirred at 0 °C until the reaction was complete (19 h) as indicated by TLC. This was followed by diluting the reaction mixture with water (50 mL) and extracting the crude product with ethyl acetate (4 x 50 mL). The crude organic layer was dried over $MgSO_4$, concentrated under reduced pressure, and purified by column chromatography using 40% ethyl acetate in hexane as eluent. This afforded the desired product **75a** as a colourless oil (14.81 g, 95%). R_f = 0.56 (40% ethyl acetate/hexane); IR (neat, cm^{-1}) 3421 (OH), 3032 (=C-H), 2229 (C≡N), 1453 (C=C); ^1H NMR (300 MHz, $CDCl_3$) δ 7.41 – 7.34 (5H, m, Ar-H), 6.09 (1H, d, *J* = 1.5 Hz, H-8a), 6.01 (1H, d, *J* = 1.2 Hz, H-8b), 5.28 – 5.26 (1H, m, H-3), 2.69 (1H, br s, OH); ^{13}C NMR (75 MHz, $CDCl_3$): δ 139.2 (C-4), 130.3 (C-8), 128.7 (C-5 or C-6), 128.6 (C-7), 126.5 (C-5 or C-6), 126.0 (C-2), 117.0 (C-1), 73.7 (C-3).

Chiral HPLC: Lux 3 μm cellulose-2 (250 x 4.6 mm); mobile phase, hexane: IPA (96:4); flow rate = 1 mL/min); t_R = 21.35 min, t_R = 23.57 min.

5.8.1.6 Synthesis of (±)-(E)-3-hydroxy-2-methylene-5-phenyl-4-pentenenitrile (191)[209]

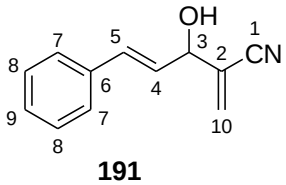

191

To a solution of *trans*-cinnamaldehyde (10.50 g, 0.008 mol) and acrylonitrile (16 mL, 0.239 mol) was added DABCO (17.83 g, 0.159 mol) and phenol (8 mL, 0.079 mol). The reaction mixture was stirred at 25°C until all the reactants were consumed (24 h) as determined by

TLC. The reaction mixture was diluted with water (50 mL), followed by extraction of the crude product with ethyl acetate (4 x 50 mL). The organic layer was dried over $MgSO_4$, concentrated under reduced pressure, and purified by column chromatography using 20% ethyl acetate in hexane. This resulted in **191** as a colourless oil (11.50 g, 80%). R_f = 0.52 (40% ethyl acetate/hexane); IR (neat, cm^{-1}) 3421 (OH), 3028 (=C-H), 2228 (C≡N), 1449 (C=C); ^1H NMR (300 MHz, $CDCl_3$) δ 7.43 – 7.23 (5H, m, Ar-H), 6.73 (1H, d, *J* = 15.8 Hz, H-5), 6.19 (1H, dd, *J* = 15.9, 6.9 Hz, H-4), 6.11 – 6.07 (1H, m, H-10a), 6.04 – 5.99 (1H, m, H-10b), 4.90 (1H, d, *J* = 6.7 Hz, H-3), 2.52 (1H, br s, OH); ^{13}C NMR (75 MHz, $CDCl_3$): δ 135.6 (C-6), 133.8 (C-5), 130.1 (C-10), 128.7 (C-7 or C-8), 128.5 (C-9), 126.9 (C-7 or C-8), 126.6 (C-4), 125.5 (C-2), 117.0 (C-1), 72.9 (C-3).

Chiral HPLC: Lux 5 μm cellulose-1 (250 x 4.60 mm); mobile phase, hexane: IPA (90:10); flow rate = 1 mL/min; t_R = 18.80 min, t_R = 24.50 min.

5.8.1.7 Synthesis of (±)-3-hydroxy-2-methylene-5-phenylpentanenitrile (195)[145]

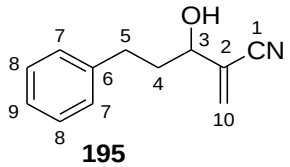

195

The same procedure for the synthesis of **75a** was used except that hydrocinnamaldehyde was used instead of benzaldehyde. It took 6 d for the reaction to take place; and this afforded **195** as a colourless oil (9.00 g, 65%). R_f = 0.60 (40% ethyl acetate/hexane); IR (neat, cm^{-1}) 3420 (OH), 3027 (=C-H), 2227 (C≡N), 1454 (C=C); ^1H NMR (300 MHz, $CDCl_3$) δ 7.30 – 7.22 (2H, m, Ar-H), 7.20 – 7.13 (3H, m, Ar-H), 5.95 – 5.89 (2H, m, H-10a and H-10b), 4.21 – 4.12 (1H, m, H-3), 3.21 (1H, d, *J* = 4.4 Hz, OH), 2.79 – 2.59 (2H, m, H-5), 2.06 – 1.85 (2H, m, H-4); ^{13}C NMR (75 MHz, $CDCl_3$) δ 140.8 (C-6), 130.4 (C-10), 128.5 (C-7 or C-8), 128.4 (C-7 or C-8), 126.6 (C-2), 126.1 (C-9), 117.1 (C-1), 71.3 (C-3), 37.0 (C-4), 31.2 (C-5).

Chiral HPLC: Lux 3 μm cellulose-2 (250 x 4.6 mm); mobile phase, hexane: IPA (96:4); flow rate= 1 mL/min; t_R= 17.77 min, t_R= 19.45 min.

5.8.1.8 Synthesis of (±)-ethyl 2-(hydroxy(phenyl)methyl)acrylate (196)[212, 213]

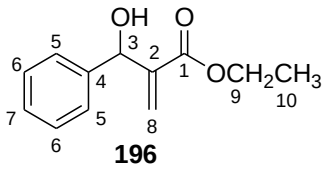

To a solution of benzaldehyde (5 mL, 0.049 mol) in ethyl acrylate (16 mL, 0.147 mol) was added DABCO (11.00g, 0.098 mol). The reaction mixture was stirred at room temperature until the reaction was complete (6 d). The completed reaction mixture was diluted with water (20 mL), followed by extraction of the crude product with ethyl acetate (4 x 30 mL). The organic layer was dried over $MgSO_4$, concentrated under reduced pressure, and purified by column chromatography using 10% ethyl acetate in hexane. This resulted in **196** as a colourless oil (7.80 g, 77 %). R_f = 0.59 (30% ethyl acetate/hexane); IR (neat, cm^{-1}) 3432 (OH), 2981 (=C-H), 1702 (C=O), 1453 (C=C); ^{1}H NMR (300 MHz, Chloroform-*d*) δ 7.35 - 7.18 (5H, m, Ar-H), 6.28 (1H, s, H-8a), 5.82 (1H, s, H-8b), 5.48 (1H, d, *J* = 5.2 Hz, H-3), 4.07 (2H, q, *J* = 6.5 Hz, H-9), 3.68 – 3.48 (1H, m, OH), 1.16 (3H, t, *J* = 7.1 Hz, H-10); ^{13}C NMR (75 MHz, $CDCl_3$) δ 166.2 (C-1), 142.5 (C-4), 141.6 (C-2), 128.3 (C-5 or C-6), 127.7 (C-5 or C-6), 126.7 (C-7), 125.4 (C-8), 72.8 (C-3), 60.81 (C-9), 14.0 (C-10).

Chiral HPLC: Lux 5µ Amylose-2 (250 x 4.60 mm); mobile phase, hexane: IPA: Methanol (90:9:1); flow rate = 1 mL/min; t_R = 6.06 min, t_R = 6.65 min.

5.8.1.9 Synthesis of (±)-(E)-ethyl 3-hydroxy-2-methylene-5-phenylpent-4-enoate (102e)[147]

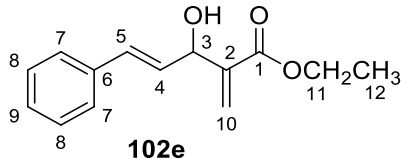

To a solution of *trans*-cinnamaldehyde (10.50 g, 0.008 mol) in ethyl acrylate (25 mL, 0.239 mol) was added DABCO (17.81 g, 0.159 moles) and phenol (7 mL, 0.079 moles). The reaction mixture was stirred at 25 °C until the reaction was complete (48 hours). The reaction mixture was diluted with water (20 mL), followed by extraction of the crude product with ethyl acetate (4 x 30 mL). The organic layer was dried over $MgSO_4$, concentrated under reduced pressure,

and purified by column chromatography using 10% ethyl acetate in hexane. This resulted in **102e** as a colourless oil (14.50 g, 79%). R_f = 0.61 (40% ethyl acetate/hexane); IR (neat, cm^{-1}) 3422 (OH), 3026 (=C-H), 1701 (C=O), 1434 (C=C); ^{1}H NMR (300 MHz, Chloroform-*d*) δ 7.42 – 7.18 (5H, m, Ar-H), 6.66 (1H, d, *J* = 16.0 Hz, H-5), 6.34 – 6.24 (2H, m, H-4 and H-10a), 5.90 (1H, s, H-10b), 5.17 – 5.09 (1H, m, H-3), 4.24 (2H, q, *J* = 7.1 Hz, H-11), 3.09 (1H, d, *J* = 5.2 Hz, OH), 1.31 (3H, t, *J* = 7.1 Hz, H-12); ^{13}C NMR (75 MHz, $CDCl_3$) δ 166.4 (C-1), 141.6 (C-6), 136.5 (C-2) 131.41 (C-5), 129.4 (C-9), 128.6 (C-7 or C-8), 127.8 (C-4), 126.6 (C-7 or C-8), 125.6 (C-10), 72.12 (C-3), 61.0 (C-11), 14.2 (C-12).

Chiral HPLC: Lux 5μ cellulose-1; size of 250 x 4.60 mm; mobile phase, hexane: IPA (90:10); flow rate = 1 mL/min; t_R = 9.62 min, t_R = 10.66 min.

5.8.1.10 Synthesis of (±)-ethyl 3-hydroxy-2-methylene-5-phenylpentanoate (197)[214]

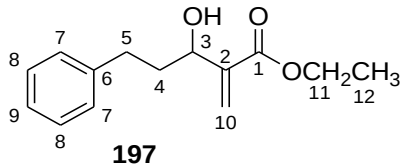

197

A similar procedure used to synthesize **196** was used except that hydrocinnamaldehyde was used. This afforded **197** as a colourless oil (7.42 g, 77 %). R_f = 0.54 (30% ethyl acetate/hexane); IR (neat, cm^{-1}) 3398 (OH), 2981 (=C-H), 1701 (C=O), 1495 (C=C); ^{1}H NMR (300 MHz, Chloroform-*d*) δ 7.30 – 7.10 (5H, m, Ar-H), 6.25 – 6.19 (1H, m, H-10a), 5.84 – 5.75 (1H, m, H-10b), 4.50 – 4.38 (1H, m, H-3), 4.17 (2H, q, *J* = 7.1 Hz, H-11), 3.32 – 3.18 (1H, m, OH), 2.90 – 2.58 (2H, m, H-5), 2.06 – 1.80 (2H, m, H-4), 1.24 (3H, t, *J* = 7.1 Hz, H-12); ^{13}C NMR (75 MHz, $CDCl_3$) δ 166.5 (C-1), 143.0 (C-6), 141.8 (C-2), 128.4 (C-9), 128.3 (C-7 or C-8), 125.8 (C-7 or C-8), 124.7 (C-10), 70.5 (C-3), 60.8 (C-11), 37.9 (C-4), 32.0 (C-5), 14.1 (C-12).

Chiral HPLC: Lux 5u cellulose-1 (250 x 4.60 mm); mobile phase, hexane: IPA (90:10); flow rate = 1 mL/min; t_R = 7.06 min, t_R = 8.72 min.

5.8.1.11 Synthesis of (±)-(E)-4-hydroxy-3-methylene-6-phenylhex-5-en-2-one (198)[149]

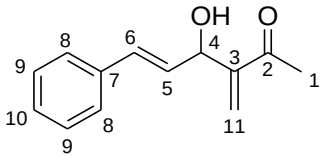

198

Methyl vinyl ketone (8 mL, 0.318 moles) was added to a solution containing *trans*-cinnamaldehyde (10.50 g, 0.079 mol) and DMAP (970.00 mg, 0.794 mmol). The reaction mixture was stirred at room temperature for 9 days. The reaction mixture was diluted with water (30 mL), followed by extraction of the crude product with ethyl acetate (6 x 50 mL). The organic layer was dried over $MgSO_4$, concentrated under reduced pressure, and purified by column chromatography using 20% ethyl acetate in hexane. This afforded **198** as a viscous oil (4.90 g, 31%). R_f = 0.52 (40% ethyl acetate/hexane); IR (neat, cm^{-1}) 3471 (OH), 2922 (=C-H), 1709 (C=O), 1448 (C=C); ^{1}H NMR (300 MHz, Chloroform-*d*) δ 7.38 – 7.16 (5H, m, Ar-H), 6.63 (1H, d, *J* = 16.0 Hz, H-6), 6.24 (1H,dd, *J* = 15.9, 6.2 Hz, H-5), 6.13 – 6.08 (2H, m, H-11a and H-11b), 5.22 - 5.12 (1H, m, H-4), 3.56 - 3.36 (1H, m, OH), 2.32 (3H, s, H-1); ^{13}C NMR (75 MHz, $CDCl_3$) δ 200.2 (C-2), 149.3 (C-7), 136.6 (C-3), 130.9 (C-11), 129.7 (C-3), 128.6 (C-8 or C-9), 127.7 (C-10), 126.6 (C-8 or C-9), 126.2 (C-5), 71.2 (C-4), 26.4 (C-1).

5.8.2 Preparation of Morita-Baylis-Hillman acetates

5.8.2.1 General procedure for the synthesis of acetates (105a, 199 and 201)

To a stirred solution of Morita-Baylis-Hillman alcohol (1 equiv) in dichloromethane (25 mL), was added Et_3N (2 equiv), Ac_2O (2 equiv), and DMAP (0.01 equiv). The reaction mixture was stirred for 30 minutes at 25 °C. Thereafter, aqueous saturated solution of $NaHCO_3$ (20 mL) was added to the reaction mixture, followed by extraction of the crude product with ethyl acetate (4 x 30 mL). This resulted to an organic layer that was dried over $MgSO_4$, concentrated under reduced pressure and purified by column chromatography using ethyl acetate in hexane.

5.8.2.2 Preparation of (E)-methyl 2-(acetoxymethyl)-3-(4-nitrophenyl)acrylate (207)

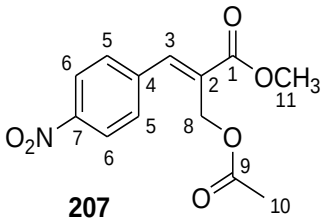

207

The reaction mixture was stirred for two hours and this led to unexpected product. The isolated product was a colourless oil (E)-methyl 2-(acetoxymethyl)-3-(4-nitrophenyl)acrylate **207** (117.38 mg, 96%). R_f = 0.60 (40% ethyl acetate/hexane). IR (neat, cm^{-1}) 3120 (=C-H), 1739 (C=O), 1715 (C=O), 1476 (C=C); ^{1}H NMR (300 MHz, Chloroform-*d*) δ 8.28 (2H, d, *J* = 8.8 Hz, H-5), 7.97 (1H, s, H-3), 7.55 (2H, d, *J* = 8.4 Hz, H-6), 4.91 (2H, s, H-8), 3.88 (3H, s, H-11), 2.10 (3H, s, H-10); ^{13}C NMR (75 MHz, $CDCl_3$) δ 170.4 (C-9), 166.5 (C-1), 148.1 (C-7), 142.3 (C-3), 140.6 (C-4), 130.18 (C-2), 130.1 (C-6), 123.9 (C-5), 58.7 (C-8), 52.6 (C-11), 20.9 (C-10). HRMS *m/z* calcd for $C_{13}H_{13}NO_6Na$ [M+Na^+]: 302.0635, found: 302.0629.

5.8.2.3 Preparation of (±)-methyl 2-(acetoxy(4-nitrophenyl)methyl)acrylate (199)[95]

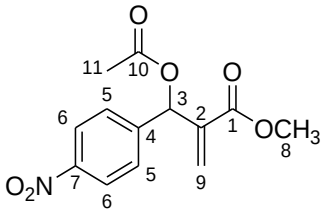

199

The general procedure described in section 5.8.2.1 was applied. This afforded **199** as a yellow solid (3.88g, 99%). M.P: 88 – 89 °C. R_f= 0.50 (40% ethyl acetate/hexane). IR (neat, cm^{-1}) 2963 (=C-H), 1736 (C=O), 1713 (C=O), 1492 (C=C); ^{1}H NMR (300 MHz, Chloroform-*d*) δ 8.20 (2H, d, *J* = 8.8 Hz, H-6), 7.57 (2H, d, *J* = 8.7 Hz, H-5), 6.72 (1H, s, H-9a), 6.47 (1H, s, H-9b), 5.98 (1H, s, H-3), 3.72 (3H, s, H-8), 2.14 (3H, s, H-11); ^{3}C NMR (75 MHz, $CDCl_3$) δ 169.1 (C-10), 164.9 (C-1), 147.8 (C-7), 145.1 (C-4), 138.7 (C-2), 128.5 (C-6), 126.2, (C-9) 123.7 (C-5), 72.2 (C-3), 52.2 (C-8), 21.0 (C-11).

5.8.2.4 Preparation of (±)-2-cyano-phenyl acetate (105a)[215, 216]

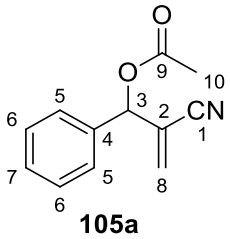

105a

The general procedure described was applied. This afforded (±)-2-Cyano-phenyl acetate **105a** isolated as a colourless oil (3.56 g, 89%). R_f = 0.61 (30% ethyl acetate/hexane). IR (neat, cm^{-1}) 3035 (=C-H), 2229 (C≡N), 1745 (C=O), 1454 (C=C); ^{1}H NMR (300 MHz, $CDCl_3$): δ 7.41 – 7.32 (5H, m, Ar-H), 6.33 – 6.31 (1H, m, H-3), 6.03 – 6.00 (1H, m, H-8a), 5.98 – 5.96 (1H, m, H-8b), 2.13 (3H, s, H-10); ^{13}C NMR (75 MHz, $CDCl_3$) δ 169.2 (C-9), 135.7 (C-4), 132.0 (C-8), 129.2 (C-7), 128.9 (C-5 or C-6), 126.9 (C-5 or C-6), 123.2 (C-2), 116.2 (C-1), 74.3 (C-3), 20.8 (C-10). HRMS *m/z* calcd for $C_{12}H_{11}NO_2Na$ [M+Na^+]: 224.0687, found: 224.0681. Chiral HPLC: Chiralpak AD-H (250 x 4.6 mm); mobile phase, hexane: IPA (96:4); flow rate = 1 mL/min; t_R = 8.26 min, t_R = 8.86 min.

5.8.2.5 Synthesis of (±)-(E)-4-cyano-1-phenylpenta-1,4-dien-3-yl acetate (200)

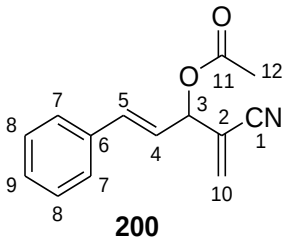

200

Et_3N (12 mL, 0.087 moles) and AcCl (4 mL, 0.087 moles) were added to a solution of **191** (2.02 g, 0.011 moles) in dry THF at 0 °C. The reaction was stirred until all the reactants were consumed (20 minutes). This was followed by the removal of THF under reduced pressure. Water (30 mL) was added to the viscous crude product followed by extraction of the crude product with ethyl acetate (4 x 30 mL). The organic layer was washed with H_2O (20 mL), brine (20 mL), and dried over Na_2SO_4. The crude extract was concentrated and purified by column chromatography using 20% ethyl acetate in hexane. The purification process afforded **200** as a colourless oil (2.01 g, 82%). R_f = 0.68 (40% EtOAc/hexane); IR (neat, cm^{-1}) 3028 (=C-H), 2228 (C≡N), 1741 (C=O), 1496 (C=C); ^{1}H NMR (300 MHz, $CDCl_3$) δ 7.43 – 7.24

(5H, m, Ar-H), 6.76 (1H, d, *J* = 15.9 Hz, H-5), 6.17 (1H, dd, *J* = 15.9, 7.3 Hz, H-4), 6.08 – 6.04 (2H, m, H-10a and H-10b), 5.96 – 5.91 (1H, m, H-3), 2.14 (3H, s, H-12); ^{13}C NMR (75 MHz, $CDCl_3$) δ 169.3 (C-11), 135.7 (C-5), 135.3 (C-6), 132.2 (C-10), 128.8 (C-9), 128.7 (C-7 or C-8), 126.9 (C-7 or C-8), 122.5 (C-4), 122.3 (C-2), 116.2 (C-1), 73.4 (C-3), 21.0 (C-12). HRMS *m/z* calcd for $C_{14}H_{13}NO_2Na$ [M+Na$^+$]: 250.0844, found: 250.0824.

Chiral HPLC: Lux 5 μm cellulose-1 (250 x 4.60 mm); mobile phase, hexane: IPA (90:10); flow rate =1 mL/min; t_R = 9.82 min, t_R = 10.69 min.

5.8.2.6 Preparation of (±)-2-cyano-5-phenylpent-1-en-3-yl acetate (201)[148]

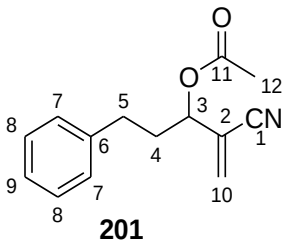

201

The general procedure described in section 5.8.2.1 was applied. This afforded **201** as a colourless oil (4.80 g, 91%). R_f = 0.54 (20% ethyl acetate/hexane); IR (neat, cm^{-1}) 2937 (=C-H), 2227 (C≡N), 1742 (C=O), 1454 (C=C), ^{1}H NMR (300 MHz, $CDCl_3$) δ 7.31 – 7.12 (5H, m, Ar-H), 6.01 – 5.99 (1H, m, H-10a), 5.94 – 5.92 (1H, m, H-10b), 5.30 – 5.21 (1H, m, H-3), 2.65 (2H, t, *J* = 7.8 Hz, H-5), 2.23 – 1.96 (2H, m, H-4) overlapping 2.06 (3H, s, H-12); ^{13}C NMR (75 MHz, $CDCl_3$) δ 169.7 (C-11), 140.1 (C-6), 132.9 (C-10), 128.6 (C-7 or C-8), 128.3 (C-7 or C-8), 126.3, (C-9) 122.5 (C-2), 116.1 (C-1), 72.6 (C-3), 34.4 (C-4), 31.1 (C-5), 20.8 (C-12). HRMS *m/z* calcd for $C_{14}H_{15}NO_2Na$ [M+Na$^+$]: 252.1000, found: 252.0985.

Chiral HPLC: Lux 5 μm amylose-2 (250 x 4.6 mm); mobile phase, hexane: IPA (96:4); flow rate = 1 mL/min, t_R = 9.45 min, t_R =13.08 min.

5.8.3 General method for the synthesis of Morita-Baylis-Hillman nitrile containing esters

To solution of alcohol (1 equiv) in dichloromethane (50 mL) was added acid (2.5 equiv), DCC (0.87 equiv) and DMAP (0.13 equiv). The reaction mixture was stirred for 2 h. Water (40 mL) was added and the organic material was extracted with dichloromethane (4 x 30 mL). The organic layer was separated, dried over $MgSO_4$, concentrated under reduced pressure and

purified by column chromatography using 10% ethyl acetate in hexane. This procedure was used to synthesize **202**, **203** and **204**.

5.8.3.1 Preparation of (±)-2-cyano-1-phenylallyl 2-chloroacetate (202)

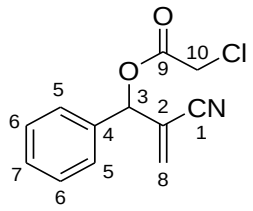

202

(±)-2-Cyano-1-phenylallyl 2-chloroacetate **202** was isolated as a colourless oil (1.21g, 41%). R_f = 0.70 (40% ethyl acetate/hexane). IR (neat cm^{-1}): 2950 (=C-H), 2230 (C≡N), 1747 (C=O), 1454 (C=C); ^{1}H NMR (300 MHz, Chloroform-*d*) δ 7.43 -7.37 (5H, m, Ar-H), 6.38 – 6.36 (1H, m, H-3), 6.09 (1H, d, *J* = 0.9 Hz, H-8a), 6.05 (1H, d, *J* = 1.3 Hz, H-8b), 4.15 (2H, d, *J* = 2.2 Hz, H-10); ^{13}C NMR (75 MHz, $CDCl_3$) δ 165.8 (C-9), 134.8 (C-4), 132.7 (C-8), 129.6 (C-7), 129.1 (C-5 or C-6), 127.0 (C-5 or C-6), 122.4 (C-2), 115.9 (C-1), 75.8 (C-3), 40.7 (C-10). HRMS *m/z* calcd for $C_{12}H_{10}ClNO_2Na$ [M+Na^+]: 258.0292, found: 258.0282.

Chiral HPLC: Lux 3 μm cellulose-2 (250 x 4.6 mm); mobile phase, hexane: IPA (96:4); flow rate = 1 mL/min); t_R = 12.71 min, t_R= 14.59 min.

5.8.3.2 Preparation of (±)-2-cyano-1-phenylallyl butyrate (203)

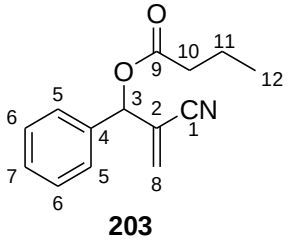

203

(±)-2-Cyano-1-phenylallyl butyrate **203** was isolated as a colourless oil (1.39g, 48%). R_f = 0.59 (20% ethyl acetate/hexane). IR (neat cm^{-1}): 2967 (=C-H), 2229 (C≡N), 1744 (C=O), 1455 (C=C); ^{1}H NMR (300 MHz, Chloroform-*d*) δ 7.44 - 7.33 (5H, m, Ar-H), 6.35 – 6.33 (1H, s, H-3), 6.07 (1H, d, *J*= 0.6 Hz, H-8a), 5.99 (1H, d, *J* = 1.3 Hz, H-8b), 2.41 (2H, td, *J* =

7.4, 1.9 Hz, H-10), 1.70 (2H, h, *J* = 7.4 Hz, H-11), 0.95 (3H, t, *J* = 7.4 Hz, H-12); ^{13}C NMR (75 MHz, $CDCl_3$) δ 171.2 (C-9), 135.8 (C-4), 131.9 (C-8), 129.2 (C-7), 129.0 (C-5 or C-6), 127.0 (C-6 or C-7), 123.4 (C-2), 116.2 (C-1), 74.1 (C-3), 36.1 (C-10), 18.3 (C-11), 13.6 (C-12). HRMS *m/z* calcd for $C_{14}H_{16}NO_2$ [M+H$^+$]: 230.1176, found: 230.1112.

Chiral HPLC: Lux 5μM Amylose-2 (250 x 4.6 mm); mobile phase, hexane: IPA (96:4); flow rate = 1 mL/min; t_R = 7.36 min, t_R = 8.24 min.

5.8.3.3 Preparation of (±)-2-cyano-1-phenylallyl 3-methylbutanoate (204)[151]

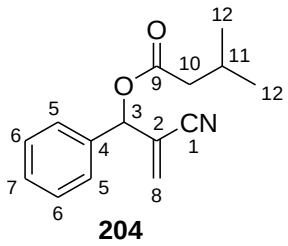

204

(±)-2-Cyano-1-phenylallyl 3-methylbutanoate **204** was isolated as a colourless oil (2.20 g, 72%). R_f = 0.63 (20% ethyl acetate/hexane). IR (neat cm^{-1}): 2935 (=C-H), 2214 (C≡N), 1704 (C=O), 1466 (C=C); ^{1}H NMR (300 MHz, Chloroform-*d*) δ 7.42 - 7.35 (5H, s, Ar-H), 6.36 – 6.33 (1H, m, H-3), 6.07 – 6.05 (1H, m, H-8a), 6.00 - 5.98 (1H, s, H-8b), 2.40 – 2.24 (2H, m, H-10), 2.15 (1H, hept, *J* = 6.9 Hz, H-11), 0.96 (6H, d, *J* = 6.6 Hz, H-12); ^{13}C NMR (75 MHz, $CDCl_3$) δ 171.3 (C-9), 135.8 (C-4), 131.9 (C-8), 129.2 (C-7), 128.9 (C-5 or C-6), 126.9 (C-5 or C-6), 123.4 (C-2), 116.2 (C-1), 74.1 (C-3), 43.2 (C-10), 25.7 (C-11), 22.4 (C-12). HRMS *m/z* calcd for $C_{15}H_{17}NO_2Na$ [M+Na$^+$]: 266.1151, found: 266.1144.

5.8.4 Synthesis of Morita Baylis Hillman acids

5.8.4.1 General method for the synthesis of Morita-Baylis-Hillman acids

Potassium hydroxide (1.2 equiv) in water (10 mL) was added to methyl ester (1 equiv) in ethanol (2 mL). The mixture was refluxed at 70 °C until all the starting material was consumed as indicated by TLC (1 h). Ethanol was removed under reduced pressure and any unreacted ester was extracted using ethyl acetate (20 mL). The resulting aqueous layer was acidified, and extraction using ethyl acetate (4 x 20 mL) afforded the corresponding acid.

5.8.4.2 Preparation of (±)-2-(hydroxy(phenyl)methyl)acrylic acid (205)[217]

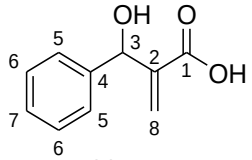

205

Compound **205** was obtained as a white solid (0.95 g, 91%). M.P: 81 – 82 °C. R_f = 0.50 (40% ethyl acetate/hexane); IR (neat, cm^{-1}) 3556 (OH), 2973 (=C-H), 1681 (C=O), 1454 (C=C); ^{1}H NMR (300 MHz, Chloroform-*d*) δ 7.35 – 7.21 (5H, m, Ar-H), 6.82 (2H, br s, 2 x OH), 6.43 (1H, s, H-8a), 5.89 (1H, s, H-8b), 5.52 (1H, s, H-3); ^{13}C NMR (75 MHz, $CDCl_3$) δ 171.0 (C-1), 141.4 (C-4), 140.9 (C-2), 128.5 (C-5 or C-6), 128.4 (C-8), 128.0 (C-7), 126.7 (C-6 or C-5), 72.8 (C-3).

Chiral HPLC: Lux 5µ Amylose-1 (250 x 4.60 mm); mobile phase, Hexane: IPA: Methanol (90:5:5); flow rate = 1 mL/min; t_R = 11.26 min, t_R = 11.25 min.

5.8.4.3 Preparation of (±)-(E)-3-hydroxy-2-methylene-5-phenylpent-4-enoic acid (103e)

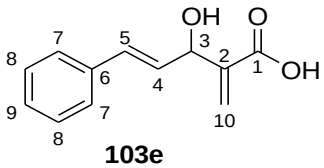

103e

Compound **103e** was obtained as a viscous oil (0.89 g, 95%). R_f = 0.58 (40% ethyl acetate/hexane); IR (neat, cm^{-1}) 3368 (OH), 2973 (=C-H), 1685 (C=O), 1449 (C=C); ^{1}H NMR (300 MHz, Chloroform-*d*) δ 7.93 (2H, br s, 2 x OH), 7.38 – 7.14 (5H, m, Ar-H), 6.62 (IH, d, *J* = 15.9 Hz, H-5), 6.39 (1H, s, H-10a), 6.25 (1H, dd, *J* = 15.9, 6.4 Hz, H-4), 5.97 (1H, s, H-10b), 5.14 (1H, d, *J* = 6.3 Hz, H-3); ^{13}C NMR (75 MHz, $CDCl_3$) δ 170.8 (C-1), 140.8 (C-6), 136.4 (C-2), 131.9 (C-5), 128.8 (C-9), 128.6 (C-7 or C-8), 128.1 (C-10), 128.0 (C-4), 126.7 (C-7 or C-8), 71.6 (C-3).

Chiral HPLC: Lux 5µ Amylose-1 (250 x 4.60 mm); mobile phase, Hexane: IPA: Methanol (90:5:5); flow rate = 1 mL/min; t_R = 16.30 min, t_R = 18.31 min.

5.8.4.4 Preparation of-(±)-3-hydroxy-2-methylene-5-phenylpentanoic acid (206)[218]

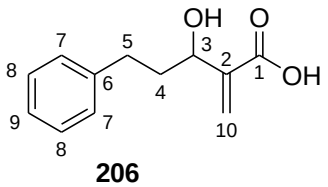

206

Compound **206** was obtained as a white solid (0.95 g, 82%). M.P: 70 – 72 °C. R_f = 0.54 (40% ethyl acetate/hexane); IR (neat, cm^{-1}) 3341 (OH), 2925 (=C-H), 1692 (C=O), 1454 (C=C); ^{1}H NMR (300 MHz, Chloroform-*d*) δ 8.01-6.67 (7H, m, Ar-H and 2 x OH), 6.40 (1H, s, H-10a), 5.92 (1H, s, H-10b), 4.45 (1H, t, *J* = 6.3 Hz, H-3), 2.88 – 2.62 (2H, m, H-4), 2.08 – 1.92 (2H, m, H-5);^{13}C NMR (75 MHz, $CDCl_3$) δ 171.0 (C-1), 141.7 (C-6), 141.4 (C-2), 128.5 (C-7 or C-8), 128.4 (C-7 or C-8), 127.5 (C-10), 125.9 (C-9), 70.7 (C-3), 37.5 (C-4), 32.0 (C-5).
Chiral HPLC: Lux 5 μm cellulose-1 (250 x 4.60 mm); mobile phase, hexane: IPA (96:4); flow rate = 1 mL/min; t_R = 17.24 min, t_R = 18.46 min.

5.9Enzymatic kenetic resolution reactions

5.9.1 Method development for enzymatic resolutions

5.9.1.1 Bio-catalytic transformation of benzyl alcohol to benzyl acetate (208)[219]

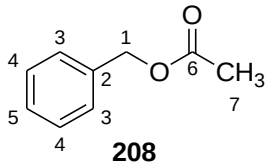

208

This was a test reaction to determine whether the lipases available were still active. To a solution of benzyl alcohol (0.50 g, 4.620 mmol) in acetonitrile (10 mL) was added vinyl acetate (1.21 g, 0.014 moles) and Lipase AH-D amino (0.50 g). The mixture was stirred at 35 °C until the reaction was complete (23 h) as indicated by TLC. This was followed by the removal of acetonitrile under reduced pressure. To the crude mixture, was added aqueous saturated solution of $NaHCO_3$ (20 mL) and the organic compound was extracted with ethyl acetate (3 x 20 mL). The resulting organic layer was dried over $MgSO_4$, concentrated under reduced pressure and purified by column chromatography using 10% ethyl acetate in hexane. This afforded **208** as a colourless oil (0.66 g, 95%). R_f = 0.61 (20% ethyl acetate/hexane). IR (neat, cm^{-1}) 3002 (=C-H), 1745 (C=O), 1480 (C=C); ^{1}H NMR (300 MHz, Chloroform-*d*) δ

7.44 – 7.13 (5H, m, Ar-H), 5.06 (2H, s, H-1), 2.03 (3H, s, H-7); ^{13}C NMR (75 MHz, $CDCl_3$) δ 170.6 (C-6), 136.1 (C-2), 128.5 (C-3), 128.2 (C-4), 128.2 (C-5), 66.2 (C-5), 20.8 (C-7).
A Similar reaction was done on all the enzymes in the biocatalysis store with monitoring being done using TLC by co-spotting the reaction mixture with fully characterized **208**. A total of 101 enzymes were identified to be active.

5.9.1.2 Synthesis of 4-chlorophenyl acetate (209)[220]

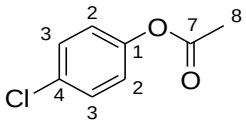

209

To a stirred solution of 4-chlorophenol (1.00 g, 7.78 mmol) in dichloromethane (20 mL), was added Et_3N (2 mL, 15.560 mmol), Ac_2O (2 mL, 15.56 mmol), and DMAP (9.51 mg, 0.078 mmol). The reaction mixture was stirred for 1 h at 25 °C. To the reaction mixture, was added aqueous saturated solution of $NaHCO_3$ (10 mL) followed by extraction of the crude product with ethyl acetate (3 x 25 mL). The resulting organic layer was dried over $MgSO_4$, concentrated under reduced pressure and purified by column chromatography using 10% ethyl acetate in hexane. This afforded **209** as a colourless oil (1.25 g, 96%). R_f = 0.60 (40% ethyl acetate/hexane). IR (neat, cm^{-1}) 2981 (=C-H), 1760 (C=O), 1486 (C=C); ^{1}H NMR (300 MHz, Chloroform-*d*) δ 7.31 (2H, d, *J* = 8.6 Hz, H-2), 7.01 (2H, d, *J* = 8.7 Hz, H-3), 2.25 (3H, s, H-8); ^{13}C NMR (75 MHz, $CDCl_3$) δ 169.1 (C-7), 149.2 (C-1), 131.1 (C-4), 129.4 (C-2), 123.0 (C-3), 21.0 (C-8).

5.9.2 Enzymatic hydrolysis of Morita-Baylis-Hillman (MBH) acetates and esters

5.9.2.1 Screening procedure for small scale enzymatic hydrolysis of MBH acetates and esters

To phosphate buffer (950 μL) at pH 7.00 containing enzyme (7.0 mg) in an Eppendorf tube was added MBH acetate or esters (7.0 mg) dissolved in acetone (50 μL). The Eppendorf tube containing the reaction mixture was put on an orbital shaker at the specified temperature and monitored using TLC. This was followed by the removal of acetone under reduced pressure. Water was added to the crude mixture and the crude product was extracted with ethyl acetate (5 mL). The resulting organic layer was dried over $MgSO_4$, and concentrated under reduced pressure in readiness for chiral HPLC analysis.

5.9.2.2 Enzymatic hydrolysis of (±)-2-cyano-1-phenylallyl acetate (**105a**)

5.9.2.3 Isolation of (+)-75a

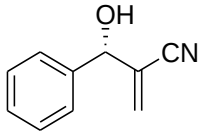

(+)-75a, ee_p = 94%

To a mixture containing Amano lipase from *P. fluorescens* (534730) (1.00 g) in phosphate buffer (47.5 mL) at pH 7.00 was added Compound **105a** (1.00 g) dissolved in acetone (2.5 mL). The resulting mixture was stirred for 44 h at 30 °C and the product was extracted using ethyl acetate (4 x 40 mL). Purification by column chromatography using 10% ethyl acetate in hexane afforded (+)-**75a** as a colourless oil [180 mg, 46%, ee = 94%; $[\alpha]_D$ = +68.4 (c. 0.5, MeOH)] and scalemic (-)-**105a** (404 mg, ee = 53%).

5.9.2.4 Isolation of (-)-105a

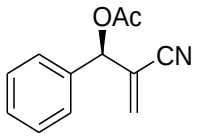

(-)-105a, ee_p = 99%

Compound **105a** (1.50 g) was reacted under the conditions described in section **5.9.2.3** for 14 d, after which column chromatography using 10% ethyl acetate in hexane afforded (-)-**105a** as a colourless oil [544 mg, 73%, ee = 99%; $[\alpha]_D$ = -27.8 (c. 0.5, MeOH)] and (+)-**75a** (655 mg, ee = 84%).

5.9.2.5 Isolation of (-)-75a

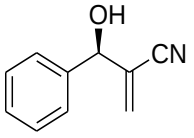

(-)-75a, ee_p = 99%

To a mixture containing esterase cat. no. ESL-001-01 Lot no. 6Y0240 (327 mg) in phosphate buffer (47.5 mL) at pH 7.00 was added (-)-**105a** (327 mg) dissolved in acetone (1.5 mL). The resulting mixture was stirred for 30 h at room temperature. The product was extracted using ethyl acetate (4 x 40 mL) and Purification by column chromatography using 10% ethyl acetate in hexane afforded (-)-**75a** as a colourless oil [255 mg, 99%, ee = 99%; $[\alpha]_D$ = -23.0 (c. 0.5, MeOH)]

5.9.2.6 Enzymatic hydrolysis of (±)-(E)-4-cyano-1-phenylpenta-1,4-dien-3-yl acetate (**200**)

5.9.2.7 Isolation of (+)-191

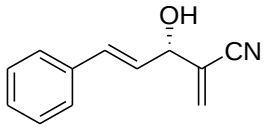

(+)-191; ee_p = 97%

To a mixture containing Amano AK lipase (lot 0351202) (0.60 g) in phosphate buffer (47.5 mL) at pH 7.00 was added **200** (0.60 g) dissolved in acetone (2.5 mL). The resulting mixture was stirred for 24 h at 25 °C. The product was extracted using ethyl acetate (4 x 40 mL) and purification by column chromatography using 20% ethyl acetate in hexane afforded (+)-**191** as a colourless oil [100 mg, 42%, ee = 97%; $[\alpha]_D$ = +50.4 (c. 0.5, MeOH)] and scalemic (-)-**200** (336 mg, ee = 33%).

5.9.2.8 Isolation of (-)-200

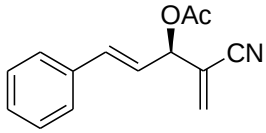

(-)-200; ee_p = 92%

Compound **200** (1.17 g) was reacted under the conditions descried in **5.9.2.7** except that the enzyme used was Lipozyme® CALB L (Novozymes). After 14 days, column chromatography using 20% ethyl acetate in hexane resulted in (-)-**200** as a colourless oil [330 mg, 69%, ee = 92%; $[\alpha]_D$ = -58.8 (c. 0.5, MeOH)] and (+)-**191** (465 mg, ee = 81%).

5.9.2.9 Isolation of (-)-191

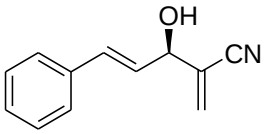

(-)-191; ee_p = 92%

To a mixture containing esterase cat.no. ESL-001-01 lot. No. 6Y0240 (300 mg) in phosphate buffer (38.5 mL) at pH 7.00 was added (-)-**200** (300 mg) dissolved in acetone (1.5 mL). The resulting mixture was stirred for 50 h at room temperature. The product was extracted using ethyl acetate (4 x 20 mL) and purified by column chromatography using 20% ethyl acetate in hexane to afford (-)-**191** as a colourless oil [230 mg, 77%, ee = 92%; $[\alpha]_D$ = -5.8 (c. 0.5, MeOH)]

5.9.2.10 Enzymatic hydrolysis of (±)-2-cyano-5-phenyl-pent-1-ene-yl acetate (201)

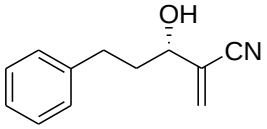

(+)-195; ee_p = 95%

To a mixture containing Lipozyme® CALB L (Novozymes) (0.72 g) in phosphate buffer (47.5 mL) at pH 7.00 was added **201** (0.72g) dissolved in acetone (2.5 mL). The resulting mixture was stirred for 64 h at 35 °C. The product was extracted using ethyl acetate (4 x.40 mL) and purification by column chromatography using 20% ethyl acetate in hexane afforded (+)-**195** as a colourless oil [130 mg, 44%, ee = 95%; $[\alpha]_D$ = +31.6 (c. 0.5, MeOH)] and scalemic (-)-**201** (440 mg, ee = 25%).

5.9.3 Determination of the absolute configuration of the enantiopure alcohols

5.9.3.1 General method for the preparation of Mosher derivatives

DCC (2 equiv) and DMAP (0.39 equiv) were added to a 25 mL round bottom flask containing (+)- or (-)-Alcohol (1 equiv), and either (*R*)-MTPA or (*S*)-MTPA (3.2 equiv) dissolved in dichloromethane (3 mL). The reaction mixture was stirred for 30 minutes and thereafter it was

transferred to separating funnel. Water (3 mL) was added to the reaction mixture in the separating funnel and shaken. The organic layer was separated and dried over Na_2SO_4, dried and subjected to flash column chromatography on silica gel using ethyl acetate in hexane as eluent. This led to the following compounds.

5.9.3.2 Preparation of (R)-[(S)-2-cyano-1-phenylallyl] 3,3,3-trifluoro-2-methoxy-2-phenylpropanoate (210)

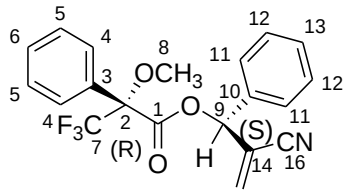

210

(*R*)-[(*S*)-2-Cyano-1-phenylallyl] 3,3,3-trifluoro-2-methoxy-2-phenylpropanoate (**210**) was isolated as a colourless oil (133 mg, 82%). R_f = 0.64 (30% ethyl acetate/hexane); IR (neat, cm^{-1}) 2951 (=C-H), 2230 (C≡N), 1753 (C=O), 1452 (C=C); ^{1}H NMR (300 MHz, $CDCl_3$) δ 7.45 – 7.30 (10H, m, Ar-H), 6.56 – 6.52 (1H, m, H-9), 6.06 (1H, d, *J* = 1.0 Hz, H-15a), 5.93 (1H, d, *J* = 1.4 Hz, H-15b), 3.49 – 3.46 (3H, m, H-8); ^{13}C NMR (75 MHz, $CDCl_3$) δ 165.2 (C-1), 134.3 (C-10), 132.1 (C-15), 131.7 (C-3), 129.8 (C-6 or C-13), 129.1 (C-6 or C-13), 128.5 (C-11 or C-12), 127.4 (C-11 and C-12), 127.3 (q, $J_{C\text{-}F}$ = 1 Hz, C-4), 123.2 (q, $J_{C\text{-}F}$ = 289 Hz, C-7), 122.0 (C-14), 115.7 (C-16), 84.7 (q, $J_{C\text{-}F}$ = 28 Hz, C-2), 75.9 (C-9), 55.6 (q, $J_{C\text{-}F}$ = 1 Hz, C-8). HRMS *m/z* calcd for $C_{20}H_{16}F_3NO_3Na$ [M+Na^+]: 398.0980, found: 398.0969.

5.9.3.3 Preparation (*S*)-[(*S*)-2-cyano-1-phenylallyl] 3,3,3-trifluoro-2-methoxy-2-phenylpropanoate (211)

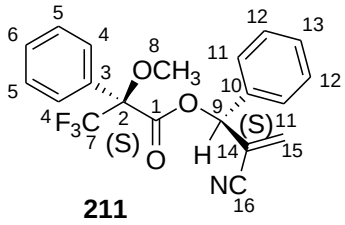

211

(*S*)-[(*S*)-2-Cyano-1-phenylallyl] 3,3,3-trifluoro-2-methoxy-2-phenylpropanoate (**211)** (230 mg, 80%) was isolated as a colourless oil. R_f = 0.64 (30% ethyl acetate/hexane); IR (neat, cm^{-1}) 2952 (=C-H), 2230 (C≡N), 1753 (C=O), 1453 (C=C); ^{1}H NMR (300 MHz, $CDCl_3$) δ 7.46 – 7.30 (9H, m, Ar-H), 7.24 – 7.20 (1H, m, Ar-H), 6.49 (1H, s, H-9), 6.13 (1H, d, *J* = 1.2 Hz, H-15a), 5.98 (1H, d, *J* = 1.5 Hz, H-15b), 3.60 – 3.57 (3H, m, H-8); ^{13}C NMR (100 MHz, $CDCl_3$) δ 165.2 (C-1), 134.1 (C-10), 133.2 (C-15), 131.5 (C-3), 129.8 (C-6 or C-13), 129.6 (C-6 or C-13), 129.0 (C-5 or C-12), 128.5 (C-11 or C-12), 127.2 (q, J_{C-F} = 1 Hz, C-4), 127.1 (C-11, or C-12), 123.1 (q, J_{C-F} = 289 Hz, C-7), 122.2 (C-14), 116.0 (C-16), 84.7 (q, J_{C-F} = 28 Hz, C-2), 76.3 (C-9), 55.9 (q, J_{C-F} = 1 Hz, C-8). HRMS *m/z* calcd for $C_{20}H_{16}F_3NO_3Na$ [M+Na^+]: 398.0980, found: 398.0985.

5.9.3.4 Preparation of (R)-[(R)-2-cyano-1-phenylallyl] 3,3,3-trifluoro-2-methoxy-2-phenylpropanoate (212)

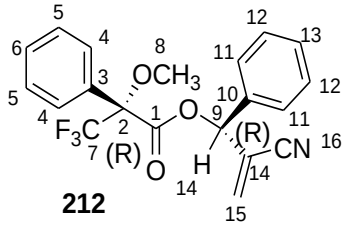

212

(*R*)-[(*R*)-2-Cyano-1-phenylallyl] 3,3,3-trifluoro-2-methoxy-2-phenylpropanoate (**212**) was isolated as a colourless oil (130 mg, 76%). R_f = 0.64 (30% ethyl acetate/hexane). IR (neat, cm^{-1}) 2951 (=C-H), 2230 (C≡N), 1753 (C=O), 1452 (C=C); ^{1}H NMR (300 MHz, $CDCl_3$) δ 7.46 – 7.30 (9H, m, Ar-H), 7.24 – 7.20 (1H, m, Ar-H), 6.50 (1H, s, H-9), 6.13 (1H, d, *J* = 1.2 Hz, H-15a), 5.99 – 5.97 (1H, m, H-15b), 3.61 – 3.58 (3H, m, H-8); ^{13}C NMR (126 MHz,

$CDCl_3$) δ 165.2 (C-1), 134.1 (C-10), 133.1 (C-15), 131.6 (C-3), 129.8 (C-6 or C-13), 129.6 (C-6 or C-13), 129.0 (C-5 or C-12), 128.5 (C-11 or C-12), 127.3 (q, $J_{C\text{-}F}$ = 1 Hz, C-4), 127.2 (C-11 or C-12), 123.2 (C-14), (q, $J_{C\text{-}F}$ = 289 Hz, C-7), 122.3, 116.0 (C-16), 84.8 (q, $J_{C\text{-}F}$ = 28 Hz, C-2), 76.4 (C-9), 55.8 (q, $J_{C\text{-}F}$ = 1 Hz, C-8). HRMS *m/z* calcd for $C_{20}H_{20}F_3N_2O_3$ [M+NH_4^+]: 393.1421, found 393.1412.

5.9.3.5 Preparation of (*S*)-[(*R*)-2-cyano-1-phenylallyl] 3,3,3-trifluoro-2-methoxy-2-phenylpropanoate (213)

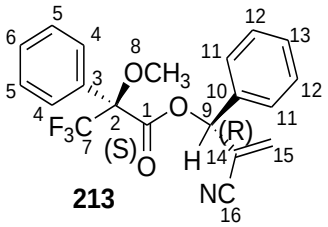

213

(*S*)-[(*R*)-2-Cyano-1-phenylallyl] 3,3,3-trifluoro-2-methoxy-2-phenylpropanoate (**213**) was isolated as a colourless oil (155 mg, 74%). R_f = 0.64 (30% ethyl acetate/hexane). IR (neat, cm^{-1}) 2951 (=C-H), 2230 (C≡N), 1753 (C=O), 1452 (C=C); ^{1}H NMR (300 MHz, CDCl3) δ 7.45 – 7.32 (10H, m, Ar-H), 6.55 – 6.53 (1H, m, H-9), 6.07 (1H, d, *J* = 1.1 Hz, H-15a), 5.94 (1H, d, *J* = 1.5 Hz, H-15b), 3.48 – 3.46 (3H, m, H-8); ^{13}C NMR (126 MHz, $CDCl_3$) δ 165.2 (C-1), 134.3 (C-10), 132.1 (C-15), 131.7 (C-3), 129.9 (C-6 or C-13), 129.9 (C-6 or C-13), 129.1 (C-5 or C-12), 128.5 (C-11 or C-12), 127.4 (C-11 or C-12), 127.3 (q, $J_{C\text{-}F}$ = 1 Hz, C-4), 123.2 (q, $J_{C\text{-}F}$ = 289 Hz, C-7), 122.0 (C-14), 115.7 (C-16), 84.6 (q, $J_{C\text{-}F}$ = 28 Hz, C-2), 75.9 (C-9), 55.6 (q, $J_{C\text{-}F}$ = 1 Hz, C-8). HRMS *m/z* calcd for $C_{20}H_{20}F_3N_2O_3$ [M+NH_4^+]: 393.1421, found 393.1429.

5.9.3.6 Preparation of (*R*)-[(*S*,*E*)-4-cyano-1-phenylpenta-1,4-dien-3-yl] 3,3,3-trifluoro-2-methoxy-2-phenylpropan-oate (217)

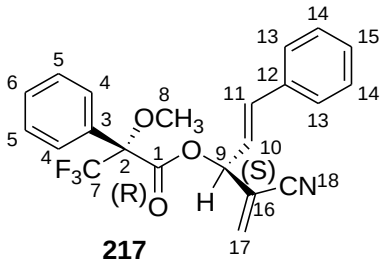

217

(*R*)-[(*S*,*E*)-4-Cyano-1-phenylpenta-1,4-dien-3-yl] 3,3,3-trifluoro-2-methoxy-2-phenylpropan-oate (**217**) was isolated as a colourless oil (58 mg, 84%). R_f = 0.75 (40% ethyl acetate/hexane); IR (neat, cm^{-1}) 2950 (=C-H), 2219 (C≡N), 1752 (C=O), 1452 (C=C); ^{1}H NMR (500 MHz, $CDCl_3$) δ 7.54 – 7.50 (2H, m, Ar-H), 7.45 – 7.30 (8H, m, Ar-H), 6.85 (1H, d, *J* = 15.1 Hz, H-11), 6.23 – 6.13 (2H, m, H-10 and H-9), 6.08 (1H, d, *J* = 1 Hz, H-17a), 6.01 (1H, d, *J* = 1 Hz, H-17b), 3.57 – 3.55 (3H, m, H-8); ^{13}C NMR (126 MHz, $CDCl_3$) δ 165.3 (C-1), 137.5 (C-11), 134.9 (C-12), 132.7 (C-17), 131.7 (C-3), 129.9 (C-6 or C-15), 129.2 (C-6 or C-15), 128.8 (C-5 or C-14), 128.6 (C-13 or C-14), 127.3 (q, $J_{C\text{-}F}$ =1 Hz, C-4), 127.1 (C-13 or C-14), 123.2 (q, $J_{C\text{-}F}$ = 289 Hz, C-7), 121.2 (C-10), 121.0 (C-16), 115.7 (C-18), 84.7 (q, $J_{C\text{-}F}$ = 28 Hz, C-2), 75.2 (C-9), 55.6 (q, $J_{C\text{-}F}$ = 1 Hz, C-8). HRMS *m/z* calcd for $C_{22}H_{18}F_3NO_3Na$ [M+Na^+]: 424.1136, found: 424.1145.

5.9.3.7 Preparation of (*S*)-[(*S*,*E*)-4-cyano-1-phenylpenta-1,4-dien-3-yl] 3,3,3-trifluoro-2-methoxy-2-phenylpropanoate (218)

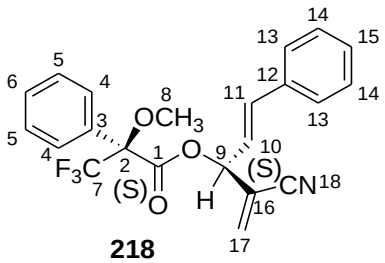

218

(*S*)-[(*S*,*E*)-4-Cyano-1-phenylpenta-1,4-dien-3-yl] 3,3,3-trifluoro-2-methoxy-2-phenylpropan-oate (**218**) was isolated as a colourless oil (80 mg, 82%). R_f = 0.75 (40% ethyl

acetate/hexane); IR (neat, cm^{-1}) 2951 (=C-H), 2224 (C≡N), 1753 (C=O), 1452 (C=C); ^{1}H NMR ($CDCl_3$, 500 MHz) δ 7.53 – 7.49 (2H, m, Ar-H), 7.44 – 7.29 (8H, m, Ar-H), 6.74 (1H, d, *J* = 15.7 Hz, H-11), 6.16 (1H, br s, H-9), 6.15 – 6.13 (2H, m, H-17a and H-17b), 6.07 (1H, dd, *J* = 15.8, 7.4 Hz, H-10), 3.62 – 3.61 (3H, m, H-8); ^{13}C NMR (126 MHz, $CDCl_3$) δ 165.3 (C-1), 137.2 (C-11), 134.9 (C-12), 133.3 (C-17), 131.7 (C-3), 129.8 (C-6 or C-15), 129.1 (C-6 or C-15), 128.8 (C-5 or C-14), 128.5 (C-13 or C-14), 127.3 (q, $J_{C\text{-}F}$ = 1 Hz, C-4), 127.0 (C-13 or C-14), 123.2 (q, $J_{C\text{-}F}$ = 289 Hz, C-7), 121.3 (C-16), 120.70 (C-16), 116.0 (C-18), 84.8 (q, $J_{C\text{-}F}$ = 28 Hz, C-2), 75.3 (C-9), 55.9 (q, $J_{F\text{-}C}$ = 1 Hz, C-8). HRMS *m/z* calcd for $C_{22}H_{18}F_3NO_3Na$ [M+Na^+]: 424.1136, found: 424.1135.

5.9.3.8 Preparation of (*R*)-[(*R*,*E*)-4-cyano-1-phenylpenta-1,4-dien-3-yl] 3,3,3-trifluoro-2-methoxy-2-phenylpropanoate (219)

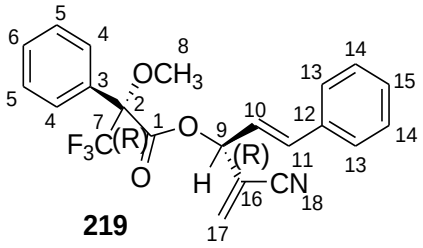

219

(*R*)-[(*R*,*E*)-4-cyano-1-phenylpenta-1,4-dien-3-yl] 3,3,3-trifluoro-2-methoxy-2-phenylpropanoate (**219**) was isolated as a colourless oil (131 mg, 73%). R_f = 0.75 (40% ethyl acetate/hexane). IR (neat, cm^{-1}) 2951 (=C-H), 2230 C≡N), 1751 (C=O), 1450 (C=C); ^{1}H NMR (300 MHz, $CDCl_3$) δ 7.54 – 7.48 (2H, m, Ar-H), 7.42 – 7.31 (8H, m, Ar-H), 6.74 (1H, d, *J* = 15.6 Hz, H-11), 6.18 – 6.12 (3H, m, H-9, H-17a and H-17b), 6.12 - 6.00 (1H, m, H-10), 3.63 – 3.60 (3H, m, H-8); ^{13}C NMR (126 MHz, $CDCl_3$) δ 165.3 (C-1), 137.2 (C-11), 134.9 (C-12), 133.3 (C-17), 131.8 (C-3), 129.8 (C-6 or C-16), 129.1 (C-6 0r C-15), 128.8 (C-5 or C-14), 128.5 (C-13 or C-14), 127.3 (q, $J_{C\text{-}F}$ = 1 Hz, C-4), 127.0 (C-13 or C-14), 123.2 (q, $J_{C\text{-}F}$ = 289 Hz, C-7), 121.3 (C-16), 120.8 (C-10), 115.9 (C-18), 84.8 (q, $J_{C\text{-}F}$ = 28 Hz, C-2), 75.3 (C-9), 55.8 (q, $J_{C\text{-}F}$ = 1 Hz, C-8). HRMS *m/z* calcd for $C_{22}H_{18}F_3NO_3Na$ [M+Na^+]: 424.1136, found 424.1110.

5.9.3.9 Preparation of (*S*)-[(*R*,*E*)-4-cyano-1-phenylpenta-1,4-dien-3-yl] 3,3,3-trifluoro-2-methoxy-2-phenylpropan-oate (220)

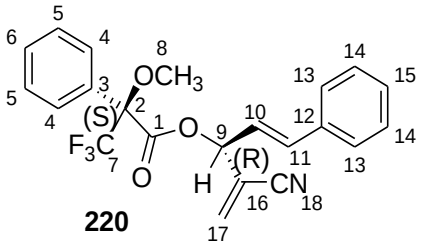

220

(*S*)-[(*R*,*E*)-4-Cyano-1-phenylpenta-1,4-dien-3-yl] 3,3,3-trifluoro-2-methoxy-2-phenylpropan-oate (**220**) was isolated as a colourless oil (122 mg, 71%). R_f = 0.75 (40% ethyl acetate/hexane). IR (neat, cm^{-1}) 2950 (=C-H), 2229 (C≡N), 1751 (C=O), 1451 (C=C); ^{1}H NMR (300 MHz, $CDCl_3$) δ 7.56 – 7.48 (2H, m, Ar-H), 7.46 – 7.31 (8H, m, Ar-H), 6.85 (1H, d, *J* = 14.5 Hz, H-11), 6.25 – 6.12 (2H, m, H-10 and H-9), 6.08 (1H, d, *J* = 1 Hz, H-17a), 6.01 (1H, d, *J* = 1 Hz, H-17b), 3.57 – 3.54 (3H, m, H-8); ^{13}C NMR (126 MHz, $CDCl_3$) δ 165.3 (C-1), 137.5 (C-11), 134.9 (C-12), 132.6 (C-17), 131.7 (C-3), 129.9 (C-6 or C-15), 129.2 (C-6 or C-15), 128.8 (C-5 or C-14), 128.6 (C-13 or C-14), 127.3 (q, $J_{C\text{-}F}$ = 1 Hz, C-4), 127.0 (C-13 or C-14), 123.2 (q, $J_{C\text{-}F}$ = 289 Hz, C-7), 121.2 (C-16), 121.0 (C-10), 115.7 (C-18), 84.7 (q, $J_{C\text{-}F}$ = 28 Hz, C-2), 75.2 (C-9), 55.6 (q, $J_{C\text{-}F}$ = 1 Hz, C-8). HRMS *m/z* calcd for $C_{22}H_{18}F_3NO_3Na$ [M+Na^+]: 424.1136, found 424.1155.

5.9.3.10 Preparation of (*R*)-[(*S*)-2-cyano-5-phenylpent-1-en-3-yl] 3,3,3-trifluoro-2-methoxy-2-phenylpropanoate (221)

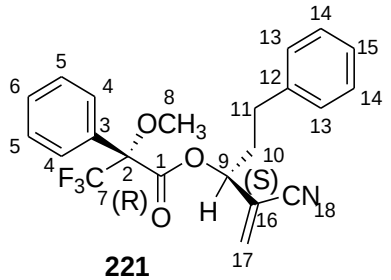

221

(*R*)-[(*S*)-2-Cyano-5-phenylpent-1-en-3-yl] 3,3,3-trifluoro-2-methoxy-2-phenylpropanoate (**221**) was isolated as a colourless oil (192 mg, 81 %). R_f = 0.59 (20% ethyl acetate/hexane); IR (neat, cm^{-1}) 3030 (=C-H), 2230 (C≡N), 1752 (C=O), 1452 (C=C); ^{1}H NMR (300 MHz, $CDCl_3$) δ 7.56 – 7.48 (2H, m, Ar-H), 7.47 – 7.38 (3H, m, Ar-H), 7.34 – 7.18 (3H, m, Ar-H), 7.16 – 7.10 (2H, m, Ar-H), 6.08 (1H, s, H-17a), 5.96 (1H, d, *J* = 1 Hz, H-17a), 5.50 – 5.43

(1H, m, H-9), 3.58 – 3.53 (3H, m, H-8), 2.71 – 2.61 (2H, m, H-11), 2.32 – 2.05 (2H, m, H-10); ^{13}C NMR (100 MHz, $CDCl_3$) δ 165.7 (C-1), 139.5 (C-12), 134.0 (C-17), 131.4 (C-3), 129.9 (C-6 or C-15), 128.7 (C-5), 128.6 (C-5 or C-14), 128.3 (C-14 or C-13), 127.3 (q, $J_{C\text{-}FC}$ = 1 Hz, C-4), 126.6 (C-6 or C-15), 123.2 (q, $J_{C\text{-}F}$ = 289 Hz, C-7), 121.3 (C-16), 115.5 (C-18), 84.7 (q, $J_{C\text{-}F}$ = 28 Hz, C-2), 74.7 (C-9), 55.6 (q, $J_{C\text{-}FC}$ = 1Hz, C-8), 34.4 (C-10), 30.9 (C-11). HRMS *m/z* calcd for $C_{22}H_{20}F_3NO_3Na$ [M+Na^+]: 426.1293, found: 426.1268.

5.9.3.11 Preparation of (*S*)-[(*S*)-2-cyano-5-phenylpent-1-en-3-yl] 3,3,3-trifluoro-2-methoxy-2-phenylpropanoate (223)

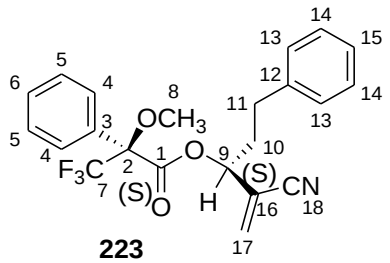

223

(*S*)-[(*S*)-2-Cyano-5-phenylpent-1-en-3-yl] 3,3,3-trifluoro-2-methoxy-2-phenylpropanoate (**223**) was isolated as a colourless oil (56 mg, 82%). R_f = 0.59 (20% ethyl acetate /hexane); IR (neat, cm^{-1}) 3030 (=C-H), 2229, 1752, 1453 (C=C); ^{1}H NMR (300 MHz, $CDCl_3$) δ 7.58 – 7.48 (2H, m, Ar-H), 7.46 – 7.38 (3H, m, Ar-H), 7.32 – 7.18 (3H, m, Ar-H,), 7.08 – 7.02 (2H, m, Ar-H,), 6.14 (1H, s, H-17a), 6.07 (1H, d, *J* = 1 Hz, H-17b), 5.43 (1H, dd, *J* = 8.4, 5.2 Hz, H-9), 3.60 – 3.54 (3H, m, H-8), 2.60 – 2.47 (2H, m, H-11), 2.30 – 2.15 (1H, m, H-10a), 2.11 – 1.97 (1H, m, H-10b); ^{13}C NMR (126 MHz, $CDCl_3$) δ 165.9 (C-1), 139.6 (C-12), 134.6 (C-17), 131.7 (C-3), 129.9 (C-6 or C-15), 128.7 (C-5 or C-14), 128.6 (C-14 or C-13), 128.3 (C-13 or C-14), 127.2 (q, $J_{C\text{-}F}$ = 1 Hz, C-4), 126.5 (C-6 or C-15), 123.2 (q, $J_{C\text{-}F}$ = 290 Hz, C-7), 121.5 (C-16), 115.7 (C-18), 84.6 (q, $J_{C\text{-}F}$ = 28 Hz, C-2), 74.9 (C-9), 55.7 (q, $J_{C\text{-}F}$ = 1 Hz, C-8), 34.3 (C-10), 30.6 (C-11). HRMS *m/z* calcd for $C_{22}H_{20}F_3NO_3Na$ [M+Na^+]: 426.1293, found: 426.1285.

5.9.4 Epoxidation and dihydroxylation reactions

5.9.4.1 Epoxidation reaction and nucleophilic ring opening of the epoxide on reported substrate

5.9.4.2 Synthesis of (E)-3-phenylprop-2-en-1-ol (236)[221]

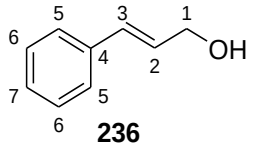

236

Sodium borohydride (4.5 g, 0.119 moles) was added to a solution of *trans*-cinnamaldehyde **(**10.5 g, 0.079 moles) in methanol (100 mL) at 0 °C. The resulting mixture was stirred until all the starting material was consumed as indicated by TLC (1 h). Methanol was removed under reduced presure, and the crude product was diluted with water (30 mL), followed by extraction using ethyl acetate (5 x 40 mL). The organic layer was dried over magnesium sulphate, concentrated under reduced pressure and purified by column chromatograpy using 20% ethyl acetate in hexane. This afforded **236** as a colourless oil (9.2 g, 86%).

R_f = 0.63 (40% ethyl acetate/hexane). IR (neat, cm^{-1}) 3295 (OH), 3026 (=C-H), 1447 (C=C); ^{1}H NMR (300 MHz, Chloroform-*d*) δ 7.40 – 7.17 (5H, m, Ar-H), 6.58 (1H, dt, *J* = 15.9, 1.8 Hz, H-3), 6.33 (1H, dt, *J* = 15.9, 5.7 Hz, H-2), 4.28 (2H, d, *J* = 5.4 Hz, H-1), 2.19 (1H, s, OH); ^{13}C NMR (75 MHz, $CDCl_3$) δ 136.7 (C-4), 131.0 (C-3), 128.6 (C-5 or C-6), 128.5 (C-7), 127.6 (C-2), 126.5 (C-5 or C-6), 63.6 (C-1).

5.9.4.3 Synthesis of (3-phenyloxiran-2-yl)methanol (237)[222]

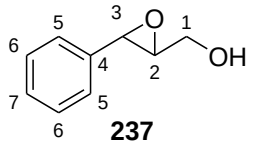

237

To a solution of **236** (0.48 g, 3.58 mmol) in dichloromethane (50 mL) at 0 °C, was added $NaHCO_3$ (1.8 g, 21.49 mmol) and *m*-CPBA (1.24 g, 7.16 mmol). The mixture was stirred until all the starting material was consumed as indicated by TLC (22 h). The resulting reaction mixture was diluted with 10% aqueous sodium sulphate (30 mL), followed by extraction using dichloromethane (4 x 30 mL). The organic layer was dried over sodium sulphate, concentrated under reduced pressure and purified by column chromatography using 20% ethyl acetate in

hexane. This afforded **237** as a colourless oil (0.48 g, 89%). R_f = 0.57 (50% ethyl acetate/hexane). IR (neat, cm^{-1}) 3371 (OH), 3000 (=C-H), 1453 (C=C), 1026 (C-O); ^{1}H NMR (300 MHz, Chloroform-*d*) δ 7.38 – 7.19 (5H, m, Ar-H), 4.05 – 3.95 (H, m, H-3), 3.92 - 386 (1H, m, H-2), 3.83 – 3.68 (1H, m, H-1a), 3.23 – 3.18 (1H, m, H-1b), 3.11 (1H, brs, OH); ^{13}C NMR (75 MHz, $CDCl_3$) δ 136.7 (C-4), 128.5 (C-5 or C-6), 128.3 (C-7), 125.7 (C-5 or C-6), 62.6 (C-2), 61.4 (C-1), 55.7 (C-3).

5.9.4.4 Synthesis of 2-azido-1-phenylpropane-1,3-diol (238)[223]

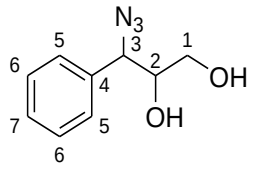

238

Epoxide **237** (0.40 g, 2.65 mmol), NaN_3 (345 mg, 5.3 mmol) and NH_4Cl (281 mg, 5.3 mmol) were all added to a solvent mixture containing methanol (15 mL) and water (1.8 mL) and refluxed for 18 h. This was followed by the removal of methanol under reduced pressure and diluting the crude product with water (20 mL). Extraction using ethyl acetate (3 x 20 mL) afforded an organic product **238** as a colourless oil. IR (neat, cm^{-1}) 3372 (OH), 3001 (=C-H), 1453 (C=C), 1026 (C-O); ^{1}H NMR (500 MHz, Chloroform-*d*) δ 7.39 – 7.19 (5H, m, Ar-H), 4.46 (1H, d, *J* = 7.0 Hz, H-3), 3.95 – 3.75 (2H, m, 2-OH), 3.75 – 3.65 (1H, m, H-2), 3.54 (1H, dd, *J* = 11.5, 2.2 Hz, H-1a), 3.47 (1H, dd, *J* = 11.5, 3.0 Hz, H-1b); ^{13}C NMR (75 MHz, $CDCl_3$) δ 136.1 (C-4), 128.6 (C-5), 128.7 (C-7), 127.8 (C-6), 74.0 (C-2), 67.0 (C-3), 62.9 (C-1).

5.9.4.5 Sharpless asymmetric dihydroxylation on reported substrates

5.9.4.6 Synthesis of ethyl cinnamate (239)[224]

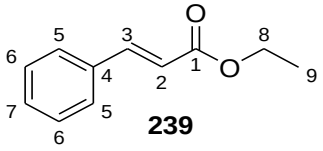

239

Cinnamic acid (2.15 g, 0.0145 moles) and thionyl chloride (13 mL) were mixed together and refluxed at 75 °C for 2 h. Unreacted thionyl chloride was removed under reduced pressure. The reacted crude product was dissolved in dry dichloromethane (30 mL), followed by

addition of ethanol (9 mL) at 0 °C. The resultant mixture was stirred for 16 h at room temperature. The solvent of the reaction mixture was removed in *vacuo* and the crude product was purified by silica gel column chromatography using 10% ethyl acetate in hexane. This afforded **239** as a colourless oil (2.5 g, 98%). R_f = 0.63 (20% ethyl acetate/hexane). IR (neat, cm^{-1}) 3028 (=C-H), 1707 (C=O), 1449 (C=C); ^{1}H NMR (300 MHz, Chloroform-*d*) δ 7.69 (1H, d, *J* = 16.0 Hz, H-3), 7.55 – 7.48 (2H, m, Ar-H), 7.40 – 7.34 (3H, m, Ar-H), 6.44 (1H, d, *J* = 16.0 Hz, H-2), 4.26 (2H, q, *J* = 7.1 Hz, H-8), 1.33 (3H, t, *J* = 7.1 Hz, H-9); ^{13}C NMR (75 MHz, $CDCl_3$) δ 167.0 (C-1), 144.6 (C-3), 134.5 (C-4), 130.2 (C-7), 128.9 (C-5 or C-6), 128.0 (C-5 or C-6), 118.3 (C-2), 60.5 (C-8), 14.3 (C-9).

5.9.4.7 Synthesis of (2R,3S)-ethyl 2,3-dihydroxy-3-phenylpropanoate (240)[197]

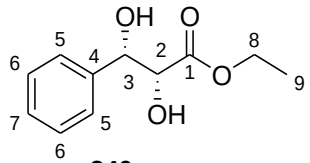

240

Ethyl cinnamate **239** (1.0 g, 568 mmol) was added to a solution of AD mix-α (8 g) in *tert*-butyl alcohol (50 mL) and water (50 mL) at room temperature. The reaction mixture was stirred for 20 h at room temperature. The reaction mixture was cooled to 0 °C and solid sodium sulfite (8.0 g) was added. The mixture was stirred for an addition 45 minutes. Thereafter; the compound of interest was extracted using ethyl acetate (3 x 100 mL), dried over anhydrous magnesium sulphate and concentrated under reduced pressure. Separation by silica gel column chromatography using 40% ethyl acetate in hexane afforded a white solid **240** (1.0 g, 84 %). R_f = 0.57 (50% ethyl acetate/hexane). IR (neat, cm^{-1}) 3448 (OH), 3023, 1694 (C=O), 1021, 886; ^{1}H NMR (300 MHz, Chloroform-*d*) δ 7.44 – 7.27 (5H, m, Ar-H), 4.99 (1H, dd, *J* = 6.9, 3.1 Hz, H-3), 4.35 (1H, dd, *J* = 5.6, 3.1 Hz, H-2), 4.24 (2H, q, *J* = 7.1 Hz, H-8), 3.17 (1H, d, *J* = 5.8 Hz, OH), 2.82 (1H, d, *J* = 7.1 Hz, OH), 1.26 (3H, t, *J* = 7.1 Hz, H-9); ^{13}C NMR (75 MHz, $CDCl_3$) δ 172.7 (C-1), 140.0 (C-4), 128.4 (C-5 or C-6), 128.1 (C-7), 126.3 (C-5 or C-6), 74.7 (C-3), 74.6 (C-2), 62.2 (C-8), 14.1 (C-9). HRMS *m/z* calcd for $C_{11}H_{14}O_4Na$ [M+Na^+]: 233.0784, found: 233.0787.

5.9.5 Nucleophilic addition of nitrogen nucleophile on Morita-Baylis-Hillman-adducts (MBHA)

5.9.5.1 Synthesis of (*E*)-methyl 3-hydroxy-5-phenyl-2-(piperidin-1-ylmethyl)pent-4-enoate (241)

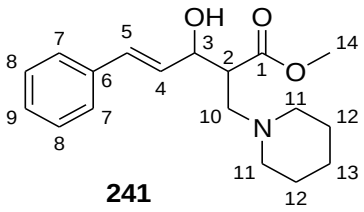

241

A mixture of piperidine (60 μL, 0.62 mmol) and **(**E)-methyl 3-hydroxy-2-methylene-5-phenylpent-4-enoate **193** (67.2 mg, 0.31 mmol) in THF (4 mL) was stirred at room temperature for 24 h in a stoppered flask. The solvent was removed *in vacuo* and the crude product was purified by column chromatography using 50% ethyl acetate in hexane. This afforded **241** as a colourless oil that was a mixture of diastereomers (68.4 mg, 73%). R_f = 0.54 (50% ethyl acetate/hexane). IR (neat, cm^{-1}) 3220 (OH), 2935 (=C-H), 1731 (C=O), 1435 (C=C), 1114 (C-N). The ratio of the major and minor diastereomer is 1.2:1. **Minor diastereomer**, ^{1}H NMR (500 MHz, Chloroform-*d*) δ 7.43 – 7.19 (5H, m, Ar-H), 6.75 (1H, d, *J* = 15.8 Hz, H-5), 6.25 (1H, dd, *J* = 15.8, 4.3 Hz, H-4), 4.86 – 4.80 (1H, m, H-3), 3.67 (3H, s, H-14), 3.28 – 3.20 (1H, m, H-2), 2.91 (1H, t, *J* = 10.0 Hz, H-10a), 2.76 – 2.52 (1H, m, H-10a), 2.76 – 2.52 (4H, H-11), 1.70 – 1.53 (4H, H-12), 1.51 – 1.37 (2H, H-13); ^{13}C NMR (126 MHz, $CDCl_3$) δ 172.15 (C-1), 137.0 (C-6), 131.0 (C-5), 129.5 (C-4), 128.52 (C-8), 127.5 (C-9), 126.5 (C-7), 73.2 (C-3), 56.8 (C-10), 54.8 (C-11), 51.9 (C-14), 45.6 (C-2), 26.0 (C-12), 24.0 (C-13); **major diastereomer**, ^{1}H NMR (500 MHz, Chloroform-*d*) δ 7.43 – 7.19 (5H, m, Ar-H), 6.62 (1H, d, *J* = 15.7 Hz, H-5), 6.15 (1H, dd, *J* = 15.8, 6.2 Hz, H-4), 4.62 – 4.54 (1H, m, H-3), 3.60 (3H, s, H-14), 2.99 (1H, t, *J* = 12.0 Hz, H-10a), 2.87 – 2.79 (1H, m, H-2), 2.76 – 2.52 (1H, m, H-10b), 2.45 – 2.23 (4H, m, H-11), 1.70 – 1.53 (4H, H-12), 1.51 – 1.37 (2H, H-13); ^{13}C NMR (126 MHz, $CDCl_3$) δ 172.18 (C-1), 136.9 (C-6), 131.2 (C-5), 129.6 (C-4), 128.46 (C-8), 127.6 (C-9), 126.6 (C-7), 76.3 (C-3), 61.1 (C-10), 54.7 (C-11), 51.7 (C-14), 48.1 (C-2), 25.9 (C-12), 23.9 (C-13). HRMS *m/z* calcd for $C_{18}H_{26}NO_3$ [M+H^+]: 304.1907, found: 304.1922.

5.9.5.2 Synthesis of (*E*)-ethyl 3-hydroxy-5-phenyl-2-(piperidin-1-ylmethyl)pent-4-enoate (242)

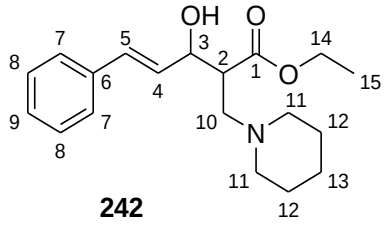

242

A mixture of piperidine (250 µL, 2.52 mmol) and (*E*)-ethyl 3-hydroxy-2-methylene-5-phenylpent-4-enoate **102e** (291.4 mg, 1.26 mmol) in THF (5 mL) was stirred at room temperature for 20 h in a stoppered flask. The solvent was removed *in vacuo* and the crude product was purified by column chromatography using 30% ethyl acetate in hexane. This afforded **248** as a colourless oil, mixture of diastereomers (217 mg, 54%). R_f = 0.56 (40% ethyl acetate/hexane). IR (neat, cm^{-1}) 3284 (OH), 2853 (=C-H), 1726 (C=O), 1444 (C=C), 1114 (C-N). The ratio of the major and minor diastereomer is 2:1**. Minor diastereomer**, ^{1}H NMR (500 MHz, Chloroform-*d*) δ 7.41 – 7.17 (5H, m, Ar-H), 6.75 (1H, d, *J* = 15.7 Hz, H-5), 6.30 – 6.22 (1H, m, H-4), 4.86 – 4.80 (1H, m, H-3), 4.20 -4.12 (2H, m, H-14), 3.27 – 3.17 (1H, m, H-2), 2.90 (1H, t, *J* = 12.3 Hz, H-10a), 2.72 – 2.15 (1H, m, H-10b), 2.65 – 2.51 and 2.50 – 2.25 (4H, m, H-11**),** 1.69 – 1.52 (4H, m, H-12), 1.51 – 1.37 (2H, m, H-13), 1.26 (3H, t, *J* = 6.4 Hz, H-15); ^{13}C NMR (126 MHz, $CDCl_3$) δ 171.73 (C-1), 137.0 (C-6), 130.9 (C-5), 129.5 (C-4), 128.5 (C-8), 127.4 (C-9), 126.5 (C-7), 73.2 (C-3), 60.7 (C-14), 56.8 (C-10), 54.7 (C-11), 45.7 (C-2), 26.0 (C-12), 24.00 (C-13), 14.3 (C-15); **major diastereomer**, ^{1}H NMR (500 MHz, Chloroform-*d*) δ 7.41 – 7.17 (5H, m, Ar-H), 6.61 (1H, d, *J* = 15.8 Hz, H-5), 6.17 (1H, dd, *J* = 15.7, 6.2 Hz, H-4), 4.59 (1H, t, *J* = 7.4 Hz, H-3), 4.10 – 4.00 (2H, m, H-14), 2.99 (1H, t, *J* = 12.0 Hz, H-10a), 2.80 (1H, t, *J* = 10.3 Hz, H-2), 2.72 – 2.65 (1H, m, H-10b), 2.65 – 2.51 and 2.50 – 2.25 (4H, m, H-11), 1.69 – 1.52 (4H, m, H-12), 1.51 – 1.37 (2H, m, H-13), 1.14 (3H, t, *J* = 6.8 Hz, H-15); ^{13}C NMR (126 MHz, $CDCl_3$) 171.68 (C-1), 136.9 (C-6), 131.2 (C-5), 129.6 (C-4), 128.4 (C-8), 127.5 (C-9), 126.6 (C-7), 76.5 (C-3), 61.1 (C-10), 60.6 (C-14), 54.8 (C-11), 48.1 (C-2), 25.9 (C-12), 23.95 (C-13), 14.2 (C-15). HRMS *m/z* calcd for $C_{19}H_{28}NO_3$ [$M+H^+$]: 318.2064, found: 318.2080.

5.9.5.3 Synthesis of (*E*)-3-hydroxy-5-phenyl-2-(piperidin-1-ylmethyl)pent-4-enenitrile (243)

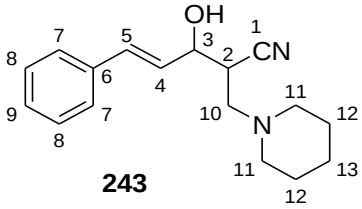

243

A mixture of piperidine (380 µL, 3.90 mmol) and (*E*)-3-hydroxy-2-methylene-5-phenyl-4-pentenenitrile **191** (480.5 mg, 2.60 mmol) in methanol (5 mL) was stirred at room temperature for 20 h in a stoppered flask. The solvent was removed *in vacuo* and the crude product was purified by column chromatography using 50% ethyl acetate in hexane. This afforded **243** as a colourless oil that was a mixture of diastereomer (536 mg, 76%). R_f = 0.46 (50% ethyl acetate/hexane). IR (neat, cm^{-1}) 3400 (OH), 2935 (=C-H), 2242 (C≡N), 1469 (C=C), 1118 (C-N), 860. The ratio of the major diastereomer to the minor diastereomer is 2:1. **Major diastereomer**, ^{1}H NMR (300 MHz, Chloroform-*d*) δ 7.44 – 7.19 (5H, m, Ar-H), 6.79 (1H, d, *J* = 15.9 Hz, H-5), 6.34 (1H, ddd, *J* = 15.9, 5.1, 0.9 Hz, H-4), 4.69 – 4.61 (1H, m, H-3), 3.09 – 3.00 (1H, m, H-2), 2.95 – 2.77 (1H, m, H-10a), 2.71 – 2.67 (1H, m, H-10b), 2.60 – 2.33 (4H, m, H-11), 1.66 – 1.48 (4H, m, H-12), 1.47 – 1.33 (2H, m, H-13); ^{13}C NMR (75 MHz, $CDCl_3$) δ 136.23 (C-6), 132.2 (C-5), 128.6 (C-7), 127.9 (C-4 or C-9), 127.7 (C-4 or C-9), 126.6 (C-8), 118.9 (C-1), 72.2 (C-3), 59.8 (C-10), 54.8 (C-11), 34.4 (C-2), 25.9 (C-12), 23.7 (C-13); **Minor diastereomer**, ^{1}H NMR (300 MHz, Chloroform-*d*) δ 7.44 – 7.19 (5H, m, Ar-H), 6.77 (1H, d, J = 15.6 Hz, H-5), 6.27 (1H, ddd, *J* = 15.9, 6.0, 0.9 Hz, H-4), 4.56 (1H, t, J = 6.0 Hz, H-3), 2.94 – 2.76 (1H, m, H-2), 2.60 – 2.32 (6H, m, H-10a, H-10b and H-11, 1.66 – 1.48 (4H, m, H-12), 1.47 – 1.33 (2H, m, H-13); ^{13}C NMR (75 MHz, $CDCl_3$) δ 136.21 (C-6), 132.4 (C-5), 128.5 (C-7), 128.0 (C-4 or C-9), 127.9 (C-4 or C-9), 126.7 (C-8), 118.7 (C-1), 74.3 (C-3), 59.7 (C-10), 54.5 (C-11), 34.6 (C-2), 25.7 (C-12), 24.0 (C-13). HRMS *m/z* calcd for $C_{17}H_{23}N_2O$ [M+H$^+$]: 271.1805, found: 271.1825.

5.9.5.4 Synthesis of (*E*)-2-((benzylamino)methyl)-3-hydroxy-5-phenylpent-4-enenitrile (244)

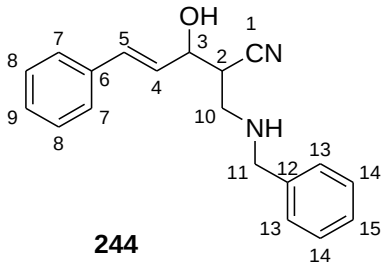

244

A mixture of benzylamine (67.5 µL, 0.62 mmol) and (*E*)-3-hydroxy-2-methylene-5-phenyl-4-pentenenitrile **191** (481 mg, 2.60 mmol) in methanol (2 mL) was stirred at room temperature for 48 h in a stoppered flask. The solvent was removed *in vacuo* and the crude product was purified by column chromatography using 40% ethyl acetate in hexane. This afforded **244** as a colourless oil (100 mg, 65%). R_f = 0.5 (80% ethyl acetate/hexane). IR (neat, cm^{-1}) 3301 (N-H), 3038 (OH), 2911(=C-H), 2237 (C≡N), 1451 (C=C). The ratio of the major to the minor diastereomer was 2:1. **Major diastereomer**, ^{1}H NMR (300 MHz, Chloroform-*d*) δ 7.47 – 7.16 (10H, m, Ar-H), 6.73 (1H, d, *J* = 15.8 Hz, H-5), 6.24 (1H, dd, *J* = 15.6, 6.0 Hz, H-4), 4.64 – 4.57 (1H, m, H-3), 3.91 – 3.76 (2H, m, H-11), 3.61 (2H, br s, OH, NH), 3.21 (1H, dd, J = 12.4, 5.7 Hz, H-10a), 3.00 (1H, dd, J = 12.3, 4.2 Hz, H-10b), 2.94 – 2.88 (1H, m, H-2); ^{13}C NMR (75 MHz, $CDCl_3$) δ 138.39 (C-12), 136.0 (C-6), 132.6 (C-5), 128.7 (C-8 or C-14), 128.6 (C-8 or C-14), 128.2 (C-13), 128.1 (C-9 or C-15), 127.6 (C-4), 127.5 (C-9 or C-15), 126.7 (C-7), 118.5 (C-1), 72.8 (C-3), 53.6 (C-11), 48.6 (C-10), 38.1 (C-2); **Minor diastereomer**, ^{1}H NMR (300 MHz, Chloroform-*d*) δ 7.47 – 7.16 (10H, m, Ar-H), 6.72(1H, d, *J* = 15.8 Hz, H-5), 6.18 (1H, dd, *J* = 15.3, 6.0 Hz, H-4), 4.64 – 4.57 (1H, m, H-3), 3.91 – 3.76 (2H, m, H-11), 3.61 (2H, br s, OH, NH), 3.14 (1H, dd, *J* = 12.5, 4.8 Hz, H-10a), 3.05 (1H, dd, *J* = 12.3, 7.2 Hz, H-10b), 2.86 – 2.78 (1H, m, H-2); ^{13}C NMR (75 MHz, $CDCl_3$) δ 138.36 (C-12), 136.0 (C-6), 132.8 (C-5), 128.7 (C-8 or C-14), 128.6 (C-8 or C-14), 128.3 (C-13), 128.1 (C-9 or C-15), 127.7 (C-4), 127.5 (C-9 or C-15), 126.7 (C-7), 119.0 (C-1), 73.2 (C-3), 53.5 (C-11), 48.2 (C-10), 37.6 (C-2). HRMS *m/z* calcd for $C_{19}H_{21}N_2O$ $[M+H^+]$: 293.1648, found: 293.1652.

5.9.6 Synthesis of silylated ethers from MBH alcohols

5.9.6.1 General procedure for the synthesis of silylated ethers from MBH alcohols

Tert-butyldimethylsilyl trifluoromethanesulfonate (1 equiv) was added dropwise to a stirring solution containing Morita-Baylis-Hillman alcohol (1 equiv) and triethylamine (2 equiv) in dichloromethane (42 mL) at 0 °C. The resulting mixture was stirred at room temperature until all the starting material was consumed as indicated by TLC (1 h). The reacted mixture was diluted with water (30 mL), followed by extraction using dichloromethane (4 x 50 mL). The organic layer was dried over magnesium sulphate, concentrated under reduced pressure and purified by column chromatography using 5% ethyl acetate in hexane.

5.9.6.2 Preparation of (±) (*E*)-methyl 3-((*tert*-butyldimethylsilyl)oxy)-2-methylene-5-phenylpent-4-enoate (226a)

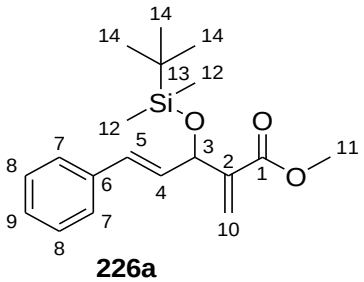

226a

(±) (*E*)-methyl 3-((*tert*-butyldimethylsilyl)oxy)-2-methylene-5-phenylpent-4-enoate **226a** was isolated as a colourless oil (2.0 g, 94%). R_f = 0.60 (10% ethyl acetate/hexane). IR (neat, cm^{-1}) , 2951 (=C-H), 1715 (C=O), 1470 (C=C), 861 (Si-O); ^{1}H NMR (500 MHz, Chloroform-*d*) δ 7.37 – 7.34 (2H, m, H-7), 7.30 – 7.25 (2H, m, H-8), 7.22 – 7.17 (1H, m, H-9), 6.63 (1H, d, *J* = 15.8 Hz, H-5), 6.26 – 6.24 (1H, m, H-10a), 6.18 (1H, dd, *J* = 15.8, 6.1 Hz, H-4), 6.03 (1H, t, *J* = 1.6 Hz, H-10b), 6.26 – 6.24 (1H, m, H-3), 3.74 (3H, s, H-11), 0.94 (9H, s, H-14), 0.10 (3H, s, H-12a), 0.09 (3H, s, H-12b); ^{13}C NMR (75 MHz, $CDCl_3$) δ 166.4 (C-1), 142.8 (C-6), 137.0 (C-2), 130.7 (C-5), 129.8 (C-9), 128.5 (C-7 or C-8), 127.5 (C-4), 126.6 (C-7 or C-8), 124.2 (C-10), 71.2 (C-3), 51.7 (C-11), 25.7 (C-14), 18.1 (C-13), -4.6 (C-12a), -5.0 (C-12b).

5.9.6.3 Preparation of (±) (*E*)-ethyl 3-((*tert*-butyldimethylsilyl)oxy)-2-methylene-5-phenylpent-4-enoate (226b)

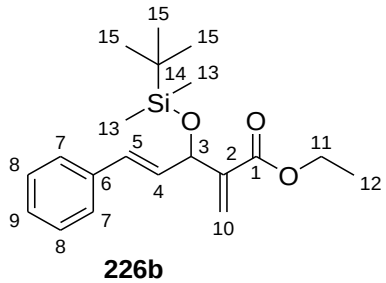

226b

(±) (*E*)-ethyl 3-((*tert*-butyldimethylsilyl)oxy)-2-methylene-5-phenylpent-4-enoate **226b** was isolated as a colourless oil (2.5 g, 89%). R_f = 0.74 (10% ethyl acetate/hexane). IR (neat, cm^{-1}) , 2929 (=C-H), 1715 (C=O), 1471 (C=C), 833 (Si-O); ^{1}H NMR (300 MHz, Chloroform-*d*) δ 7.38 – 7.15 (5H, m, Ar-H), 6.63 (1H, d, *J* = 15.8 Hz, H-5), 6.26 – 6.24 (1H, m, H-10a), 6.18 (1H, dd, *J* = 15.8, 6.2 Hz, H-4), 6.04 – 6.00 (1H, m, H-10b), 5.27 – 5.22 (1H, m, H-3), 4.31 – 4.10 (2H, m, H-11), 1.29 (3H, t, *J* = 7.1 Hz, H-12), 0.94 (9H, s, H-15), 0.12 – 0.07 (6H, m, H-13); ^{13}C NMR (75 MHz, $CDCl_3$) δ 165.9 (C-1), 143.1 (C-6), 137.0 (C-2), 130.8 (C-5), 129.8 (C-9), 128.5 (C-7 or C-8), 127.5 (C-4), 126.5 (C-7 or C-8), 123.9 (C-10), 71.3 (C-3), 60.6 (C-11), 25.9 (C-15), 18.3 (C-14), 14.2 (C-12), -4.6 (C-13a), -5.0 (C-13b). HRMS *m/z* calcd for $C_{20}H_{31}O_3Si$ $[M+H^+]$: 347.1868, found: 347.1898.

5.9.6.4 Preparation of (±) (*E*)-3-((*tert*-butyldimethylsilyl)oxy)-2-methylene-5-phenylpent-4-enenitrile (226c)

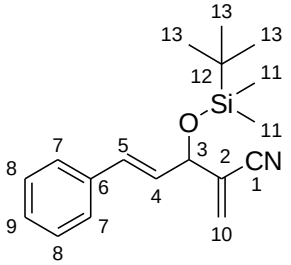

226c

(±) (*E*)-3-((*tert*-butyldimethylsilyl)oxy)-2-methylene-5-phenylpent-4-enenitrile **226c** was isolated as colourless oil (2.02 g, 90%). R_f = 0.70 (10% ethyl acetate/hexane). IR (neat, cm^{-1}) , 3028 (=C-H), 2226 (C≡N), 1463 (C=C), 829 (Si-O); ^{1}H NMR (300 MHz, Chloroform-*d*) δ

7.42 – 7.20 (5H, m, Ar-H), 6.67 (1H, d, *J* = 15.8 Hz, H-5), 6.12 (1H, dd, *J* = 15.8, 6.6 Hz, H-4), 6.06 – 6.03 (1H, m, H-10a), 5.96 – 5.93 (1H, m, H-10b), 4.88 – 4.82 (1H, m, H-3), 0.94 (9H, s, H-13), 0.14 – 0.08 (6H, m, H-11b); ^{13}C NMR (75 MHz, $CDCl_3$) δ 136.0 (C-6), 132.3 (C-5), 128.7 (C-10), 128.7 (C-7 or C-8), 128.2 (C-4) , 127.9 (C-9), 126.8 (C-7 or C-8), 126.6 (C-2), 117.2 (C-1), 73.7 (C-3), 25.8 (C-13), 18.3 (C-12), -4.5 (C-11a), -4.9 (C-11b). HRMS *m/z* calcd for $C_{18}H_{25}NOSiNa$ [M+Na$^+$]: 322.1598, found: 322.1598.

5.9.7 Nucleophilic addition of nitrogen nucleophile on silylated MBH adducts

5.9.7.1 Synthesis of (2*E*,4*E*)-methyl 5-phenyl-2-(piperidin-1-ylmethyl)penta-2,4-dienoate (248)

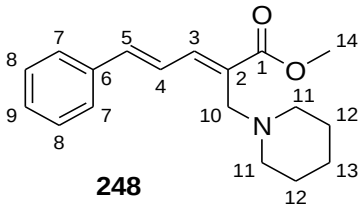

248

A mixture of piperidine (612 μL, 6.20 mmol) and (*E*)-methyl 3-((tert-butyldimethylsilyl)oxy)-2-methylene-5-phenylpent-4-enoate **226a** (1.04 g, 3.1 mmol) in THF (30 mL) was stirred at room temperature for 20 hours in a stoppered flask. The solvent of the reacted mixture was removed *in vacuo* and the crude product was purified by column chromatography using 30% ethyl acetate in hexane. This afforded **248** as white crystals form (0.61g, 69%). M.P: 91-92°C. R_f = 0.53 (30% ethyl acetate/hexane). IR (neat, cm^{-1}) 2939 (=C-H), 1701 (C=O), 1435 (C=C), 1202 (C-N); ^{1}H NMR (500 MHz, Chloroform-*d*) δ 7.52 – 7.43 (3H, m, Ar-2H and H-3), 7.37 – 7.32 (3H, m, Ar-2H and H-4), 7.32 – 7.25 (1H, m, Ar-H), 6.85 (1H, d, *J* = 15.3 Hz, H-5), 3.77 (3H, s, H-14), 3.40 (2H, s, H-10), 2.52 – 2.38 (4H, m, H-11), 1.59 – 1.51 (4H, m, H-12), 1.44 – 1.36 (2H, m, H-13); ^{13}C NMR (126 MHz, $CDCl_3$) δ 168.7 (C-1), 142.0 (C-3), 140.2 (C-5), 136.5 (C-6), 128.9 (C-9), 128.8 (C-8), 127.9 (C-2), 127.2 (C-7), 124.2 (C-4), 54.4 (C-11), 54.2 (C-10), 51.9 (C-14), 26.0 (C-12), 24.3 (C-13). HRMS *m/z* calcd for $C_{18}H_{24}NO_2$ [M+H$^+$]: 266.1807, found: 286.1820.

5.9.7.2 Synthesis of (2*E*,4*E*)-ethyl 5-phenyl-2-(piperidin-1-ylmethyl)penta-2,4-dienoate (249)

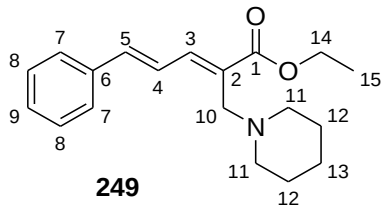

249

A mixture of piperidine (200 μL, 1.76 mmol) and (*E*)-ethyl 3-((tert-butyldimethylsilyl)oxy)-2-methylene-5-phenylpent-4-enoate **226b** (304 mg, 0.879 mmol) in THF (4 mL) was stirred at room temperature for 24 hours in a stoppered flask. The solvent of the reacted mixture was removed *in vacuo* and the crude product was purified by column chromatography using 20% ethyl acetate in hexane. This afforded **249** as a colourless oil (217 mg, 54%). R_f = 0.56 (30% ethyl acetate/hexane). IR (neat, cm^{-1}) 2970 (=C-H), 1710 (C=O), 1451 (C=C), 1201 (C-N); ^{1}H NMR (500 MHz, Chloroform-*d*) δ 7.50 – 7.44 (3H, m, Ar-2H, H-3), 7.38 – 7.32 (3H, m, Ar-2H, H-4), 7.32 – 7.26 (2H, m, Ar-2H), 6.86 (1H, d, *J* = 15.4 Hz, H-5), 4.24 (2H, q, *J* = 7.1 Hz, H-14), 3.39 (2H, s, H-10), 2.47 – 2.38 (4H, m, H-11), 1.58 – 1.51 (4H, m, H-12), 1.44 – 1.37 (2H, m, H-13), 1.32 (3H, t, *J* = 7.1 Hz, H-15); ^{13}C NMR (126 MHz, $CDCl_3$) δ 168.3 (C-1), 141.4 (C-3), 139.8 (C-5), 136.6 (C-6), 128.8 (C-7 or C-8), 128.4 (C-2), 127.2 (C-7 or C-8), 124.3 (C-9), 60.6 (C-14), 54.4 (C-11), 54.2 (C-10), 26.1 (C-12), 24.3 (C-13), 14.3 (C-15). HRMS *m/z* calcd for $C_{19}H_{26}NO_2$ [M+H$^+$]: 300.1958, found: 300.1968.

5.9.7.3 Synthesis of (*E*)-3-((*tert*-butyldimethylsilyl)oxy)-5-phenyl-2-(piperidin-1-ylmethyl)pent-4-enenitrile (247)

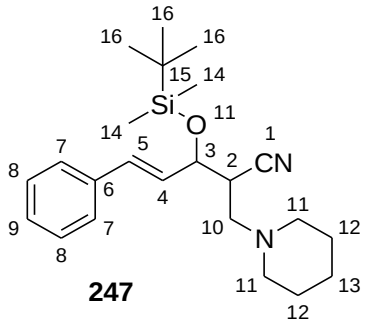

247

A mixture of piperidine (220 µL, 2.25 mmol) and **(***E*)-3-((*tert*-butyldimethylsilyl)oxy)-2-methylene-5-phenylpent-4-enenitrile **226c** (336.7 mg, 1.12 mmol) in methanol (5 mL) was stirred at room temperature for 24 h in a stoppered flask. The solvent was removed *in vacuo* and the crude product was purified by column chromatography using 20% ethyl acetate in hexane. This afforded **247** as a colourless oil (302 mg, 70%). R_f = 0.56 (30% ethyl acetate/hexane). IR (neat, cm^{-1}) 2932 (=C-H), 2243 (C≡N), 1452 (C=C), 1250 (C-N), 832 (Si-O); ^{1}H NMR (500 MHz, Chloroform-*d*) δ 7.42 – 7.37 (2H, m, Ar-H), 7.36 – 7.30 (2H, m, Ar-H), 7.29 – 7.23 (1H, m, Ar-H), 6.60 (1H, d, *J* = 15.9 Hz, H-5), 6.22 (1H, dd, *J* = 16.0, 7.3 Hz, H-4), 4.58 – 4.50 (1H, m, H-3), 3.00 – 2.94 (1H, m, H-2), 2.59 – 2.54 (2H, m, H-10), 2.49 – 2.33 (4H, m, H-11), 1.61 – 1.53 (4H, m, H-12), 1.47 – 1.37 (2H, m, H-13), 0.93 (9H, s, H-16), 0.12 (3H, s, H-14a), 0.07 (3H, s, H-14b); **Major diastereomer** ^{13}C NMR (126 MHz, $CDCl_3$) δ 136.10 (C-6), 132.9 (C-5), 128.6 (C-7 or C-8), 128.1 (C-9), 127.9 (C-4), 126.69 (C-7 or C-8), 120.2 (C-1), 72.3 (C-3), 56.8 (C-10), 54.60 (C-11), 38.68 (C-2), 25.95 (C-12), 25.8 (C-16), 24.15 (C-13) , 18.11 (C-15), -4.1 (C-14a), -4.92 (C-14b); **minor diastereomer** ^{13}C NMR (126 MHz, $CDCl_3$) δ 136.06 (C-6), 132.1 (C-5), 129.2 (C-7 or C-8), 128.1 (C-9), 127.9 (C-4), 126.65 (C-7 or C-8), 119.8 (C-1), 71.5 (C-3), 57.0 (C-10), 54.57 (C-11), 38.73 (C-2), 25.97 (C-12), 25.8 (C-16), 24.18 (C-13), 18.14 (C-15) , -4.0 (C-14a), -4.99 (C-14b. HRMS *m/z* calcd for $C_{23}H_{37}N_2OSi$ [M+H^+]: 385.2675, found: 385.2689.

5.9.7.4 Synthesis of (*E*)-2-((benzylamino)methyl)-3-((*tert*-butyldimethylsilyl)oxy)-5-phenylpent-4-enenitrile (227c)

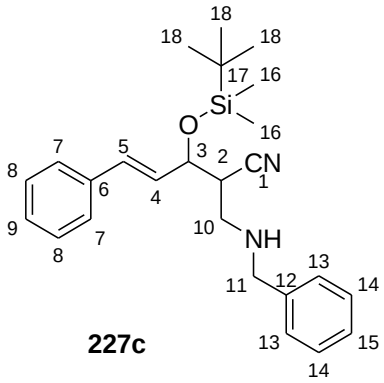

227c

A mixture of benzylamine (2 mL, 18.60 mmol) and **(***E*)-3-((*tert*-butyldimethylsilyl)oxy)-2-methylene-5-phenylpent-4-enenitrile **226c** (1.59 g, 5.3 mmol) in methanol (30 mL) was stirred at room temperature for 18 h in a stoppered flask. The solvent was removed *in vacuo*

and the crude product was purified by column chromatography using 10% ethyl acetate in hexane. This afforded **227c** as a colourless oil (1.58 g, 73%). R_f = 0.56 (30% ethyl acetate/hexane). IR (neat, cm^{-1}) 3026 (N-H), 2952 (=C-H), 2242 (C≡N), 1494 (C=C), 1451 (C=C), 833 (Si-O); ^{1}H NMR (500 MHz, $CDCl_3$) δ 7.37 - 7.32 (2H, m, Ar-H), 7.32 - 7.27 (6H, m, Ar- H), 7.26 - 7.21 (2H, m, Ar-H), 6.57 (1H, d, *J* = 15.9 Hz, H-5), 6.15 (1H, dd, *J* = 15.9, 7.2 Hz, H-4), 4.53 – 4.48 (1H, m, H-3), 3.78 (2H, s, H-11), 2.94 - 2.83 (3H, m, H-2, H-10a and H-10b), 1.56 (1H, br s, NH), 0.90 (9H, s, H-18), 0.10 (3H, s, H-16a), 0.06 (3H, s, H-16b); **Major diastereomer**, ^{13}C NMR (126 MHz, $CDCl_3$) δ 139.58(C-12), 135.9 (C-6), 132.7 (C-5), 132.4 (C-5), 128.6 (C-8 or C-14), 128.4 (C-7 or C-13), 128.12 (C-4), 128.08 (C-9 or C-15), 128.05 (C-8 or C-14), 127.1 (C-9 or C-15), 126.7 (C-7 or C-13), 119.7 (C-1), 72.1 (C-3), 53.48 (C-11), 47.0 (C-10), 41.0 (C-2), 25.7 (C-18), 18.0 (C-17), -4.3 (C-16a), -5.0 (C-16b**); minor diastereomer**, ^{13}C NMR (126 MHz, $CDCl_3$) δ 139.61 (C-12), 135.9 (C-6), 132.4 (C-5), 128.6 (C-8 or C-14), 128.4 (C-7 or C-13), 128.12 (C-4), 128.08 (C-9 or C-15), 128.05 (C-8 or C-14), 127.1 (C-9 or C-15), 126.6 (C-7 or C-13), 119.5 (C-1), 71.6 (C-3), 53.46 (C-11), 46.6 (C-10), 41.2 (C-2), 25.7 (C-18), 18.1 (C-17), -4.1 (C-16a), 15.0 (C-16b). HRMS *m/z* calcd for $C_{25}H_{35}N_2OSi$ [$M+H^+$]: 407.2513, found: 407.2523.

5.9.7.5 Synthesis of (*E*)-3-((*tert*-butyldimethylsilyl)oxy)-2-(((4-methoxybenzyl)amino)methyl)-5-phenylpent-4-enenitrile (250)

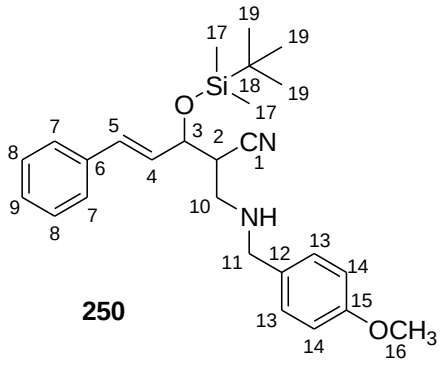

250

A mixture of 4-methoxybenzylamine (550 μL, 4.21 mmol) and **(***E*)-3-((*tert*-butyldimethylsilyl)oxy)-2-methylene-5-phenylpent-4-enenitrile **226c** (360 mg, 1.20 mmol) in methanol (8 mL) was stirred in a stoppered flask for 14 h. The solvent was removed *in vacuo* and the crude product was purified by column chromatography using 10% ethyl acetate in hexane. This afforded **250** as a colourless oil (401 mg, 76%). R_f = 0.63 (40% ethyl acetate/hexane). IR (neat, cm^{-1}) 3026 (N-H), 2952 (=C-H), 2242 (C≡N), 1451 (C=C), 833 (Si-

O); ^{1}H NMR (300 MHz, Chloroform-*d*) δ 7.40 – 7.16 (7H, m, Ar-H), 6.84 (2H, d, *J* = 8.5 Hz, H-14), 6.57 (1H, d, *J* = 15.9 Hz, H-5), 6.15 (1H, dd, *J* = 15.9, 7.2 Hz, H-4), 4.56 - 4.46 (1H, m, H-3), 3.76 (3H, s, H-16), 3.73 (2H, s, H-11), 2.98 – 2.84 (3H, m, H-2, H-10a and H-10b), 1.55 (1H, br s, NH), 0.96 – 0.86 (9H, m, H-19), 0.10 (3H, s, H-17a), 0.05 (3H, s, H-17b); **major diastereomer** ^{13}C NMR (75 MHz, $CDCl_3$) δ 158.8 (C-15), 135.9 (C-6), 132.8 (C-5), 131.7 (C-12), 129.3 (C-13), 128.6 (C-8), 128.2 (C-4), 128.1 (C-9), 126.7 (C-7),, 119.7 (C-1), 113.8 (C-14), 72.1 (C-3), 55.2 (C-16), 52.9 (11), 46.5 (C-10), 41.1 (C-2), 25.7 (C-19), 18.06 (C-18), -4.12 (C-17a), -5.0 (C-17b); **minor diastereomer** ^{13}C NMR (75 MHz, $CDCl_3$) δ 158.8 (C-15), 135.9 (C-6), 132.5 (C-5), 131.7 (C-12), 129.3 (C-13), 128.6 (C-8), 128.2 (C-4), 128.1 (C-9), 126.6 (C-7), 119.5 (C-1), 113.8 (C-14), 71.7 (C-3), 55.2 (C-16), 52.9 (11), 47.0 (C-10), 41.2 (C-2) 25.7 (C-19), 18.09 (C-18), -4.07(C-17a), -5.0 (C-17b). HRMS *m/z* calcd for $C_{26}H_{37}N_2O_2Si$ [M+H$^+$]: 437.2619, found: 437.2633.

5.9.7.6 Synthesis of (*E*)-3-((*tert*-butyldimethylsilyl)oxy)-2-(((4-chlorobenzyl)amino)methyl)-5-phenylpent-4-enenitrile (251)

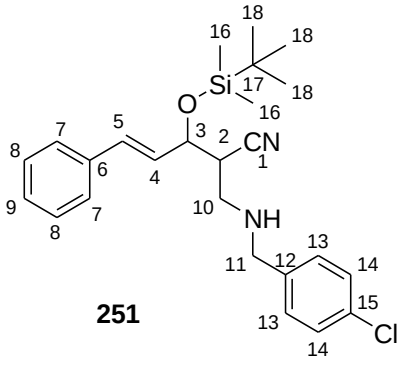

251

A mixture of 4-chlorobenzylamine (412 μL, 3.39 mmol, 3.5 equivalents) and **(***E*)-3-((*tert*-butyldimethylsilyl)oxy)-2-methylene-5-phenylpent-4-enenitrile **226c** (295 mg, 0.97 mmol) in methanol (8 mL) was stirred in a stoppered flask for 30 h. The solvent was removed *in vacuo* and the crude product was purified by column chromatography using 10% ethyl acetate in hexane. This afforded **251** as a colourless oil (1 g, 72%). R_f = 0.59 (40% ethyl acetate/hexane). IR (neat, cm^{-1}) 3025 (N-H), 2952 (=C-H), 2243 (C≡N), 1449 (C=C), 833 (Si-O), ^{1}H NMR (300 MHz, Chloroform-*d*) δ 7.40 – 7.20 (9H, m, Ar-H), 6.58 (1H, d, *J* = 15.9 Hz, H-5), 6.15 (1H, dd, *J* = 15.9, 7.1 Hz, H-4), 4.55 - 4.45 (1H, m, H-3), 3.77 (2H, s, H-11), 2.93 – 2.85 (3H, m, H-2, H-10a and H-10b), 1.58 (1H, br s, NH), 0.90 – 0.77 (9H, m, H-18), 0.10 (3H, s, H-16a), 0.05 (3H, s, H-16b); **major diastereomer** ^{13}C NMR (75 MHz, $CDCl_3$) δ 138.1 (C-12),

135.9 (C-6), 132.9 (C-5), 132.6 (C-15), 129.4 (C-13), 128.7 (C-8 or C-14), 128.6 (C-8 or C-14), 128.2 (C-9), 128.1 (C-4), 126.7 (C-7), 119.6 (C-1), 72.2 (C-3), 52.8 (C-11), 46.6 (C-10), 41.1 (C-2), 25.7 (C-18), 18.05 (C-17), -4.1 (C-16a), -5.0 (C-16b); **minor diastereomer** ^{13}C NMR (75 MHz, $CDCl_3$) 138.1 (C-12), 135.9 (C-6), 132.9 (C-5), 132.6 (C-15), 129.4 (C-13), 128.7 (C-8 or C-14), 128.6 (C-8 or C-14), 128.2 (C-9) , 128.1 (C-4), 126.6 (C-7), 119.4 (C-1), 71.8 (C-3), 52.9 (C-11), 47.0 (C-10), 41.3 (C-2), 25.7 (C-18), 18.01 (C-17), 4.1 (C-16a), -5.0 (C-16b). HRMS *m/z* calcd for $C_{25}H_{34}ClN_2O$ [M+H$^+$]: 441.2123, found: 441.2129.

5.9.7.7 Synthesis of (*E*)-2-((benzylamino)methyl)-3-hydroxy-5-phenylpent-4-enenitrile (244)

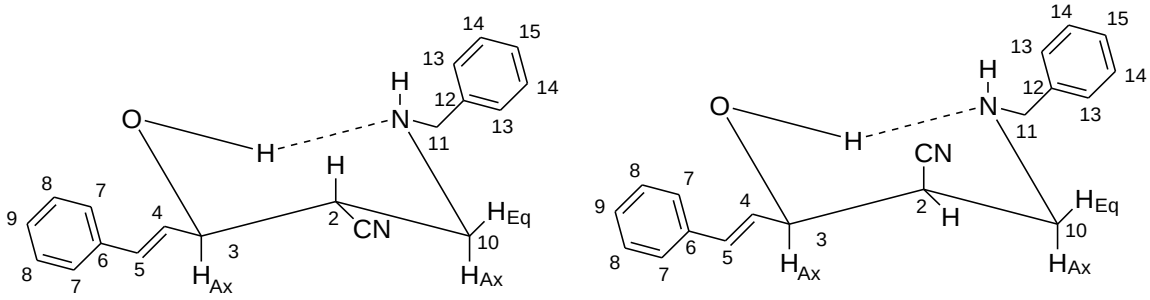

Major diastereomer-244A **Minor diastereomer-244B**

To a solution of (*E*)-2-((benzylamino)methyl)-3-((*tert*-butyldimethylsilyl)oxy)-5-phenylpent-4-enenitrile **226c (**312.6 mg, 0.77 mmol) in THF (20 mL) at 0 °C was added a solution of TBAF (267 μL, 0.92 mmol) in toluene. The mixture was warmed to room temperature after stirring for 20 minutes. The solvent was removed under vacuum and the crude product was purified by column chromatography using 40% ethyl acetate in hexane. This afforded racemic **244** as a white solid (180 mg, 80%) with a M.P of 85 -86 ºC. The ratio between the major and minor diastereomer was found to be 4: 1. The two diastereomers were in the form of chair conformation due to hydrogen bonding between NH and OH. R_f = 0.63 (50% ethyl acetate/hexane). IR (neat, cm^{-1}) 3301 (OH), 3027 (N-H), 2911 (=C-H), 2237 (C≡N), 1451 (C=C); **major diastereomer**, ^{1}H NMR (500 MHz, Chloroform-*d*) δ 7.40 – 7.22 (10H, m, Ar-H), 6.73 (1H, dd, *J* = 16.0, 1.0 Hz, H-5), 6.19 (1H, dd, *J* = 15.8, 6.0 Hz, H-4), 4.61 (1H, ddd, *J* = 6.33, 6.31, 1.34 Hz, H-3), 3.80 (2H, s, H-11), 3.14 (1H, dd, *J* = 12.5, 4.7 Hz, H-10$_{eq}$), 3.06 (1H, dd, *J* = 12.5, 7.1 Hz, H-10$_{ax}$), 2.82 (1H, ddd, *J* = 6.90, 6.88, 4.70 Hz, H-2); ^{13}C NMR (126 MHz, $CDCl_3$) δ 138.38 (C-12), 136.00 (C-6), 132.8 (C-5), 128.7 (C-8 or C-14), 128.6 (C-13), 128.3 (C-8 or C-14), 128.12 (C-9 or C-15), 127.8 (C-9 or C-15), 127.6 (C-4), 126.8

(C-7), 119.0 (C-1), 73.2 (C-3), 53.5 (C-11), 48.2 (C-10), 37.6 (C-2); **minor diastereomer**, ^{1}H NMR (500 MHz, Chloroform-*d*) δ 7.40 – 7.22 (10H, m, Ar-H), 6.74 (1H, dd, *J* = 15.5, 1.0 Hz, H-5), 6.24 (1H, dd, *J* = 16.0, 6.0 Hz, H-4), 4.61 – 4.53 (1H, m, H-3), 3.82 (2H, s, H-11), 3.21 (1H, dd, *J* = 12.5, 5.8 Hz, H-10$_{eq}$), 3.01 (1H, dd, *J* = 12.5, 4.4 Hz, H-10$_{ax}$), 2.91 (1H, ddd, *J* = 5.7, 4.4, 3.3 Hz, H-2); ^{13}C NMR (126 MHz, $CDCl_3$) δ 138.41 (C-12), 136.04 (C-6), 132.6 (C-5), 128.7 (C-8 or C-14), 128.6 (C-13), 128.2 (C-8 or C-14), 128.10 (C-9 or C-15), 127.8 (C-9 or C-15), 127.5 (C-4), 126.8 (C-7), 118.5 (C-1), 72.9 (C-3), 53.7 (C-11), 48.7 (C-10), 38.2 (C-2). HRMS *m/z* calcd for $C_{19}H_{21}N_2O$ [M+H$^+$]: 293.1648, found: 293.1645.

5.9.7.8 Synthesis of (2*E*,4*E*)-2-((benzylamino)methyl)-5-phenylpenta-2,4-dienenitrile (252)

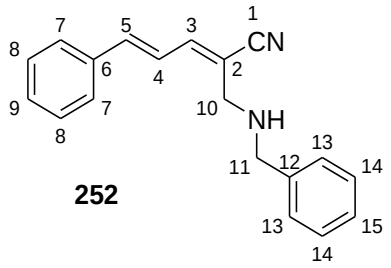

252

(*E*)-2-((benzylamino)methyl)-3-((tert-butyldimethylsilyl)oxy)-5-phenylpent-4-enenitrile **227c** (71.4 mg) was added to a stirring solution of AD mix-α (571.2 mg) in *tert*-butyl alcohol (5 mL) and water (5 mL). The mixture was stirred at room temperature for 20 h without the formation of new spots on TLC analysis. Thereafter, it was immediately refluxed at 80 °C for an additional 50 h. The resultant reaction mixture was cooled to 0 °C and solid sodium sulfite (571.2 mg) was added. The mixture was stirred for 30 minutes and ethyl acetate (50 mL) was added. The organic layer was separated, washed with water, dried over anhydrous sodium sulphate and concentrated under vacuum. Separation of the crude on silica gel column chromatography using 20% ethyl acetate in hexane afforded **252** as a colourless oil (6 mg, 13%). R_f = 0.63 (4% ethyl acetate/hexane). IR (neat, cm^{-1}) 3062 (NH), 2207 (C≡N), 1449 (C=C); ^{1}H NMR (300 MHz, Chloroform-*d*) δ 7.50 (2H, dd, *J* = 7.9, 1.5 Hz, H-7), 7.42 – 7.28 (8H, m, H-13, H-14, H-15, H-8 and H-9), 7.22 – 7.14 (1H, m, H-5), 6.93 – 6.81 (2H, m, H-4 and H-3), 3.82 (2H, s, H-11), 3.49 (2H, s, H-10), 1.64 (1H, s, NH); ^{13}C NMR (126 MHz, $CDCl_3$) δ 144.8 (C-3), 140.1 (C-5), 139.4 (C-12), 135.6 (C-6), 128.2 (C-13 or C-14), 128.9 (C-7 or C-8), 128.5 (C-7 or C-8), 127.4 (C-9 or C-15), 127.4 (C-13 or C-14),127.2 (C-9 or C-

15), 124.1 (C-4), 117.7 (C-1), 112.2 (C-2), 52.3 (C-11), 51.0 (C-10). HRMS *m/z* calcd for $C_{19}H_{19}N_2$ [M+H$^+$]: 275.1543, found: 275.1545.

5.9.8 Stereoselective nucleophilic addition of nitrogen nucleophile on an enantiopure Morita-Baylis-Hillman adduct

5.9.8.1 Isolation of (S,E)-3-hydroxy-2-methylene-5-phenylpent-4-enenitrile (*S*) -191

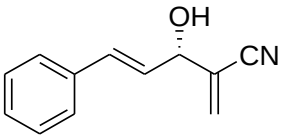

(S)-191 ee_P = 97%

To a mixture containing Novozym 435 (1.0g) in phosphate buffer (130 mL) at pH 7.00 was added **200** (1.0 g) dissolved in acetone (5 mL). The resulting mixture was stirred for 48 h at 25 °C. The product was isolated using ethyl acetate (4 x 40 mL) and purification by column chromatography using 20% ethyl acetate in hexane afforded (+)-**191** as a colourless oil [300 mg, 60%, ee = 97%; $[\alpha]_D$ = +50.4 (c. 0.5, MeOH)] and scalemic (-)-**200** (440 mg).

5.9.8.2 Synthesis of (S,E)-3-((*tert*-butyldimethylsilyl)oxy)-2-methylene-5-phenylpent-4-enenitrile (226c)

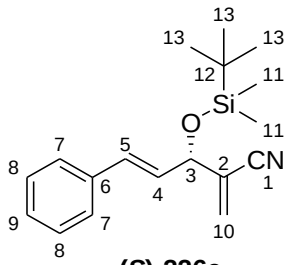

(*S*)-226c

Triethylamine (2.0 mL, 14.30 mmol) and *tert*-butyldimethylsilyl triflate (475 µL, 2.0 mmol) were added to a solution containing (*S,E*)-3-hydroxy-2-methylene-5-phenylpent-4-enenitrile (*S*)-**191** (295 mg, 2 mmol) in dichloromethane (20 mL). The resulting mixture was stirred at room temperature until all the starting material was consumed as indicated by TLC (1 h). The reacted mixture was diluted with water (20 mL), followed by extraction using dichloromethane (4 x 20 mL). The organic layer was dried over magnesium sulphate,

concentrated under reduced pressure and purified by column chromatography using 5% ethyl acetate in hexane. This afforded a silylated ether (*S*)-**226c** as colourless oil (586 g, 91%). R_f = 0.70 (10% ethyl acetate/hexane). IR (neat, cm^{-1}) , 3028 (=C-H), 2226 (C≡N), 1463 (C=C), 829 (Si-O); ^{1}H NMR (300 MHz, Chloroform-*d*) δ 7.50 – 7.15 (5H, m, Ar-H), 6.69 (1H, d, *J* = 15.8 Hz, H-5), 6.18 – 6.06 (1H, m, H-4), 6.06 – 6.00 (1H, m, H-10a), 5.96 – 5.90 (1H, m, H-10b), 4.89 – 4.81 (1H, m, H-3), 1.04 – 0.90 (9H, m, H-13), 0.20 – 0.07 (6H, m, H-11); ^{13}C NMR (75 MHz, $CDCl_3$) δ 136.0 (C-6), 132.3 (C-5), 128.6 (C-10), 128.6 (C-7 or C-8), 128.1 (C-4), 127.9 (C-9), 126.7 (C-7 or C-8), 126.6 (C-2) 117.1 (C-1), 73.6 (C-3), 25.7 (C-13), 18.2 (C-12), -4.6 (C-11a), -5.0 (C-11b). HRMS *m/z* calcd for $C_{18}H_{25}NOSiNa$ [M+Na^+]: 322.1598, found: 322.1598.

5.9.8.3 Synthesis of (3S,E)-2-((benzylamino)methyl)-3-((*tert*-butyldimethylsilyl)oxy)-5-phenylpent-4-enenitrile (3*S*)-227c

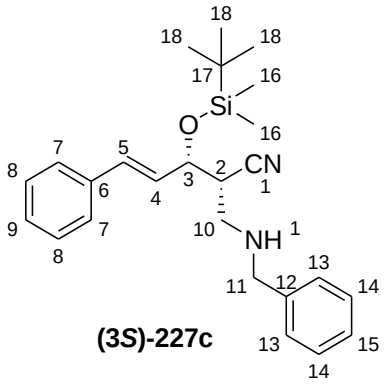

(3*S*)-227c

A mixture of benzylamine (529.0 µL, 5.4 mmol) and (S,E)-3-((*tert*-butyldimethylsilyl)oxy)-2-methylene-5-phenylpent-4-enenitrile (*S*)-**226c** (500 mg, 1.5 mmol) in methanol (30 mL) was stirred at room temperature for 18 hours in a stoppered flask. The solvent of the reacted mixture was removed *in vacuo* and the crude product was purified by column chromatography using 10 % ethyl acetate in hexane. This afforded *syn*-(3*S*)-**227c** as a colourless oil (442.4 mg, 70%). R_f = 0.56 (30% ethyl acetate/hexane). IR (neat, cm^{-1}) 3061 (N-H), 3027 (=C-H), 2242 (C≡N), 1494 (C=C), 1451 (C=C), 833 (Si-O); ^{1}H NMR (500 MHz, Chloroform-*d*) δ 7.39 – 7.23 (10H, m, Ar-H), 6.59 (1H, d, *J* = 15.8 Hz, H-5), 6.16 (1H, dd, *J* = 15.8, 7.0 Hz, H-4), 4.56 – 4.47 (1H, m, H-3), 3.82 (2H, s, H-11), 2.99 – 2.87 (3H, m, H-2, H-10a and H-10b), 1.58 (2H, s, NH), 0.90 (9H, s, H-18), 0.10 (3H, s, H-16a), 0.05 (3H, s, H-16b); ^{13}C NMR (126

MHz, $CDCl_3$) δ 139.6 (C-12), 136.0 (C-6), 132.9 (C-5), 128.7 (C-4), 128.5 (C-13), 128.23 (C-8 or C-14), 128.17 (C-8 or C-14), 128.1 (C-9 or C-15), 127.2 (C-9 or C-15), 126.7 (C-7), 119.7 (C-1), 72.2 (C-3), 53.6 (C-11), 46.8 (C-10), 41.2 (C-2), 25.8 (C-18), 18.1 (C-17), -4.1 (C-16a), -4.9 (C-16b). HRMS *m/z* calcd for $C_{25}H_{35}N_2OSi$ [$M+H^+$]: 407.2513, found: 407.2523

5.9.8.4 Synthesis of (3S,E)-2-((benzylamino)methyl)-3-hydroxy-5-phenylpent-4-enenitrile (*S*)-244A

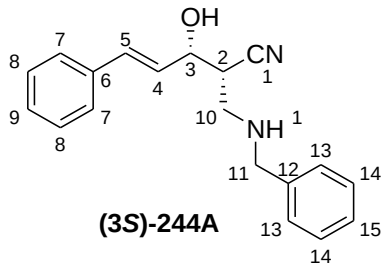

To a solution of (3S,E)-2-((benzylamino)methyl)-3-((*tert*-butyldimethylsilyl)oxy)-5-phenylpent-4-enenitrile (*S*)-**227c (**312.6 mg, 0.77 mmol) in THF (20 mL) at 0 °C was added a solution of TBAF (267 µL, 0.92 mmol) in toluene. The mixture was warmed to room temperature after stirring for 20 minutes. The solvent of the reacted mixture was removed under vacuum and the crude product was purified by column chromatography using 40% ethyl acetate in hexane. This afforded *syn*-(3*S*)-**244A** as a white solid (180 mg, 80%) with a M.P of 85 – 86 ºC. R_f = 0.63 (50% ethyl acetate/hexane). IR (neat, cm^{-1}) 3305 (OH), 3060 (N-H), 3026 (=C-H), 2242 (C≡N), 1450 (C=C); The ratio of the major and minor diastereomer is 4:1. ^{1}H NMR (300 MHz, Chloroform-*d*) δ 7.42 – 7.20 (10H, m, Ar-H), 6.73 (1H, d, *J* = 15.8 Hz, H-5), 6.19 (1H, dd, *J* = 15.8, 6.0 Hz, H-4), 4.62 (1H, t, *J* = 6.2 Hz, H-3), 3.81 (2H, s, H-11), 3.52 (2H, br s, OH and NH), 3.15 (1H, dd, *J* = 12.5, 4.7 Hz, H-10a), 3.06 (1H, dd, *J* = 12.5, 7.0 Hz), 2.82 (1H, ddd, *J* = 6.74, 6.72,4.9 Hz, H-2); **major diastereomer**, ^{13}C NMR (75 MHz, $CDCl_3$) δ 138.3 (C-12), 136.97 (C-6), 132.8 (C-5), 128.7 (C-8 or C-14), 128.6 (C-8 or C-14), 128.3 (C-13), 128.1 (C-9 or C-15), 127.72 (C-4), 127.6 (C-9 or C-15), 126.7 (C-7), 119.0 (C-1), 73.3 (C-3), 53.5 (C-11), 48.2 (C-10), 37.50 (C-2); **minor diastereomer**, ^{13}C NMR (75 MHz, $CDCl_3$) δ 138.3 (C-12), 136.01 (C-6), 132.6 (C-5), 128.7 (C-8 or C-14), 128.6 (C-8 or C-14), 128.3 (C-13), 128.1 (C-9 or C-15), 127.72 (C-4), 127.6 (C-9 or C-15), 126.7

(C-7), 119.0 (C-1), 72.9 (C-3), 53.7 (C-11), 48.7 (C-10), 38.1 (C-2). HRMS *m/z* calcd for $C_{19}H_{21}N_2O$ [$M+H^+$]: 293.1648, found: 293.1645.

CHAPTER SIX

6 REFERENCES

1. Bharadwaj, K. C., *ChemistrySelect* **2017,** *2*, 5384-5389.
2. Declerck, V.; Martinez, J.; Lamaty, F., *Chemical Reviews* **2009,** *109*, 1-48.
3. Morita, K.-i.; Suzuki, Z.; Hirose, H., *Bulletin of the Chemical Society of Japan* **1968,** *41*, 2815-2815.
4. Baylis, A.; Hillman, M. In *German Patent 2155113, 1972*, Chem. Abstr, 1972; p 34174q.
5. Li, Y.-Q.; Wang, H.-J.; Huang, Z.-Z., *The Journal of Organic Chemistry* **2016,** 81, 4429-4433.
6. Gowrisankar, S.; Lee, H. S.; Kim, S. H.; Lee, K. Y.; Kim, J. N., *Tetrahedron* **2009,** *65*, 8769-8780.
7. Basavaiah, D.; Rao, P. D.; Hyma, R. S., *Tetrahedron* **1996,** *52*, 8001-8062.
8. Basavaiah, D.; Rao, A. J.; Satyanarayana, T., *Chemical Reviews* **2003,** *103*, 811-892.
9. Basavaiah, D.; Reddy, B. S.; Badsara, S. S., *Chemical Reviews* **2010,** *110*, 5447-5674.
10. Lee, K.-Y.; Gowrisankar, S.; Kim, J.-N., *Bulletin of the Korean Chemical Society* **2005,** *26*, 1481-1490.
11. Sousa, S. C.; Junior, C. G.; Silva, F. P.; Andrade, N. G.; Barbosa, T. P.; Vasconcellos, M. L., *Journal of the Brazilian Chemical Society* **2011,** *22*, 1634-1643.
12. Coelho, F.; Almeida, W. P.; Veronese, D.; Mateus, C. R.; Lopes, E. C. S.; Rossi, R. C.; Silveira, G. P.; Pavam, C. H., *Tetrahedron* **2002,** *58*, 7437-7447.
13. Hayashi, Y.; Okado, K.; Ashimine, I.; Shoji, M., *Tetrahedron Letters* **2002,** *43*, 8683-8686.
14. Oishi, T.; Oguri, H.; Hirama, M., *Tetrahedron: Asymmetry* **1995,** *6*, 1241-1244.
15. De Souza, R. O.; Pereira, V. L.; Esteves, P. M.; Vasconcellos, M. L., *Tetrahedron Letters* **2008,** *49*, 5902-5905.
16. Ghosh, S.; Dey, R.; Chattopadhyay, K.; Ranu, B. C., *Tetrahedron Letters* **2009,** *50*, 4892-4895.
17. Gong, H.; Cai, C.-q.; Yang, N.-f.; Yang, L.-w.; Zhang, J., *Journal of Molecular Catalysis A: Chemical* **2006,** *249*, 236-239.
18. Rosa, J. N.; Afonso, C. A.; Santos, A. G., *Tetrahedron* **2001,** *57*, 4189-4193.
19. Hill, J. S.; Isaacs, N. S., *Journal of Physical Organic Chemistry* **1990,** *3*, 285-288.
20. Bode, M. L.; Kaye, P. T., *Tetrahedron Letters* **1991,** *32*, 5611-5614.
21. Denmark, S. E.; Beutner, G. L., *Angewandte Chemie International Edition* **2008,** *47*, 1560-1638.
22. Marko, I. E.; Giles, P. R.; Hindley, N. J., *Tetrahedron* **1997,** *53*, 1015-1024.
23. Isenegger, P. G.; Bächle, F.; Pfaltz, A., *Chemistry-A European Journal* **2016,** *22*, 17595-17599.
24. Perlmutter, P.; Puniani, E.; Westman, G., *Tetrahedron Letters* **1996,** *37*, 1715-1718.
25. Khan, A. A.; Emslie, N. D.; Drewes, S. E.; Field, J. S.; Ramesar, N., *Chemische Berichte* **1993,** *126*, 1477-1480.
26. Aggarwal, V. K.; Fulford, S. Y.; Lloyd-Jones, G. C., *Angewandte Chemie* **2005,** *117*, 1734-1736.
27. Cai, J.; Zhou, Z.; Zhao, G.; Tang, C., *Organic Letters* **2002,** *4*, 4723-4725.
28. Price, K. E.; Broadwater, S. J.; Jung, H. M.; McQuade, D. T., *Organic Letters* **2005,** *7*, 147-150.

29. Price, K. E.; Broadwater, S. J.; Walker, B. J.; McQuade, D. T., *The Journal of Organic Chemistry* **2005,** *70*, 3980-3987.
30. Robiette, R.; Aggarwal, V. K.; Harvey, J. N., *Journal of the American Chemical Society* **2007,** *129*, 15513-15525.
31. Plata, R. E.; Singleton, D. A., *Journal of the American Chemical Society* **2015,** *137*, 3811-3826.
32. Cantillo, D.; Kappe, C. O., *The Journal of Organic Chemistry* **2010,** *75*, 8615-8626.
33. Santos, L. S.; Pavam, C. H.; Almeida, W. P.; Coelho, F.; Eberlin, M. N., *Angewandte Chemie International Edition* **2004,** *43*, 4330-4333.
34. Carrasco-Sanchez, V.; Simirgiotis, M. J.; Santos, L. S., *Molecules* **2009,** *14*, 3989-4021.
35. Mansilla, J.; Saá, J. M., *Molecules* **2010,** *15*, 709-734.
36. Shairgojray, B. A.; Dar, A. A.; Bhat, B. A., *Tetrahedron Letters* **2013,** *54*, 2391-2394.
37. Yu, C.; Hu, L., *The Journal of Organic Chemistry* **2002,** *67*, 219-223.
38. Basavaiah, D.; Rao, K. V.; Reddy, R. J., *Chemical Society Reviews* **2007,** *36*, 1581-1588.
39. S Santos, M.; Coelho, F.; G Lima-Junior, C.; LAA Vasconcellos, M., *Current Organic Synthesis* **2015,** *12*, 830-852.
40. Manickum, T.; Roos, G., *Synthetic Communications* **1991,** *21*, 2269-2274.
41. Manickum, T.; Roos, G. H., *South African Journal of Chemistry* **1994,** *47*, 1-1.
42. Bjelic, S.; Nivón, L. G.; Çelebi-Ölçüm, N.; Kiss, G.; Rosewall, C. F.; Lovick, H. M.; Ingalls, E. L.; Gallaher, J. L.; Seetharaman, J.; Lew, S., *ACS Chemical Biology* **2013,** *8*, 749-757.
43. Kapoor, M.; Majumder, A. B.; Gupta, M. N., *Catalysis Letters* **2015,** *145*, 527-532.
44. Reetz, M. T.; Mondiere, R.; Carballeira, J. D., *Tetrahedron Letters* **2007,** *48*, 1679-1681.
45. Xue, J.-W.; Song, J.; Manion, I. C.; He, Y.-H.; Guan, Z., *Journal of Molecular Catalysis B: Enzymatic* **2016,** *124*, 62-69.
46. Tian, X.; Zhang, S.; Zheng, L., *Enzyme and Microbial Technology* **2016,** *84*, 32-40.
47. Jiang, L.; Yu, H.-w., *Biotechnology Letters* **2014,** *36*, 99-103.
48. Straathof, A.; Jongejan, J., *Enzyme and Microbial Technology* **1997,** *21*, 559-571.
49. Gawley, R. E., *The Journal of Organic Chemistry* **2006,** *71*, 2411-2416.
50. Masson, G.; Housseman, C.; Zhu, J., *Angewandte Chemie International Edition* **2007,** *46*, 4614-4628.
51. France, S.; Guerin, D. J.; Miller, S. J.; Lectka, T., *Chemical Reviews* **2003,** *103*, 2985-3012.
52. Barrett, A. G.; Dozzo, P.; White, A. J.; Williams, D. J., *Tetrahedron* **2002,** *58*, 7303-7313.
53. Chauhan, P.; Chimni, S. S., *Asian Journal of Organic Chemistry* **2013,** *2*, 586-592.
54. Yang, K.-S.; Lee, W.-D.; Pan, J.-F.; Chen, K., *The Journal of Organic Chemistry* **2003,** *68*, 915-919.
55. Pihko, P. M., *Angewandte Chemie International Edition* **2004,** *43*, 2062-2064.
56. Connon, S. J., *Chemistry–A European Journal* **2006,** *12*, 5418-5427.
57. Sohtome, Y.; Tanatani, A.; Hashimoto, Y.; Nagasawa, K., *Tetrahedron Letters* **2004,** *45*, 5589-5592.
58. Pellissier, H., *Tetrahedron* **2017,** *73*, 2831-2861.
59. Rossetti, A.; Sacchetti, A.; Bonfanti, M.; Roda, G.; Rainoldi, G.; Silvani, A., *Tetrahedron* **2017,** *73*, 4584-4590.
60. Velankar, H.; Clarke, K. G.; du Preez, R.; Cowan, D. A.; Burton, S. G., *Trends in Biotechnology* **2010,** *28*, 561-569.

61. Grogan, G., *Annual Reports Section" B"(Organic Chemistry)* **2012,** *108*, 202-227.
62. Utaka, M.; Onoue, S.; Takeda, A., *Chemistry Letters* **1987,** *16*, 971-972.
63. Walton, A. Z.; Conerly, W. C.; Pompeu, Y.; Sullivan, B.; Stewart, J. D., *ACS Catalysis* **2011,** *1*, 989-993.
64. Chaves, M. R.; Moran, P. J.; Rodrigues, J. A. R., *Journal of Molecular Catalysis B: Enzymatic* **2013,** *98*, 73-77.
65. Ramteke, P. W.; Maurice, N. G.; Joseph, B.; Wadher, B. J., *Biotechnology and Applied Biochemistry* **2013,** *60*, 459-481.
66. Wang, M.-X.; Wu, Y., *Organic & Biomolecular Chemistry* **2003,** *1*, 535-540.
67. Zhao, S. M.; Wang, M. X., *Chinese Journal of Chemistry* **2002,** *20*, 1291-1299.
68. Wang, M.-X., *Topics in Catalysis* **2005,** *35*, 117-130.
69. Coady, T. M.; Coffey, L. V.; O'Reilly, C.; Lennon, C. M., *European Journal of Organic Chemistry* **2015,** *2015*, 1108-1116.
70. Jiang, S.; Zhang, L.; Cui, D.; Yao, Z.; Gao, B.; Lin, J.; Wei, D., *Scientific Reports* **2016,** *6*, 34750.
71. Huang, W.; Jia, J.; Cummings, J.; Nelson, M.; Schneider, G.; Lindqvist, Y., *Structure* **1997,** *5*, 691-699.
72. Kobayashi, M.; Goda, M.; Shimizu, S., *FEBS Letters* **1998,** *439*, 325-328.
73. Lopes, D. B.; Fraga, L. P.; Fleuri, L. F.; Macedo, G. A., *Food Science and Technology* **2011,** *31*, 603-613.
74. Ferrer, M.; Bargiela, R.; Martínez-Martínez, M.; Mir, J.; Koch, R.; Golyshina, O. V.; Golyshin, P. N., *Biocatalysis and Biotransformation* **2015,** *33*, 235-249.
75. Montella, I. R.; Schama, R.; Valle, D., *Memorias do Instituto Oswaldo Cruz* **2012,** *107*, 437-449.
76. Reis, P.; Holmberg, K.; Watzke, H.; Leser, M.; Miller, R., *Advances in Colloid and Interface Science* **2009,** *147*, 237-250.
77. Burgess, K.; Jennings, L. D., *Journal of the American Chemical Society* **1990,** *112*, 7434-7436.
78. Burgess, K.; Jennings, L. D., *The Journal of Organic Chemistry* **1990,** *55*, 1138-1139.
79. Hayashi, N.; Yanagihara, K.; Tsuboi, S., *Tetrahedron: Asymmetry* **1998,** *9*, 3825-3830.
80. Basavaiah, D.; Rao, P. D., *Synthetic Communications* **1994,** *24*, 917-923.
81. Bhuniya, D.; Narayanan, S.; Lamba, T. S.; Krishna Reddy, K., *Synthetic Communications* **2003,** *33*, 3717-3726.
82. Bornscheuer, U.; Schapöhler, S.; Scheper, T.; Schügerl, K., *Tetrahedron: Asymmetry* **1991,** *2*, 1011-1014.
83. Strub, D. J.; Garboś, A.; Lochyński, S., Arkivoc: *Online Journal of Organic Chemistry* **2017,** part ii, 313-323.
84. Xavier, F. J.; Neto, J. S.; Néris, P. L.; Oliveira, M. R.; Vale, J. A.; Vasconcellos, M. L., *Journal of Molecular Catalysis B: Enzymatic* **2014,** *108*, 7-12.
85. Huerta, F. F.; Minidis, A. B.; Bäckvall, J.-E., *Chemical Society Reviews* **2001,** *30*, 321-331.
86. Pamies, O.; Bäckvall, J.-E., *Chemical Reviews* **2003,** *103*, 3247-3262.
87. Xia, B.; Xu, J.; Xiang, Z.; Cen, Y.; Hu, Y.; Lin, X.; Wu, Q., *ACS Catalysis* **2017,** *7*, 4542-4549.
88. Talma, M.; Mucha, A., Arkivoc: *Online Journal of Organic Chemistry* **2017,** part ii, 324-344.
89. Du, Y.; Han, X.; Lu, X., *Tetrahedron Letters* **2004,** *45* (25), 4967-4971.
90. Yang, L.; Xu, L.; Yu, C., *Phosphorus, Sulfur, and Silicon* **2009,** *184* (8), 2049-2057.

91. Kim, S. H.; Kim, S. H.; Lee, H. S.; Kim, J. N., *Bulletin of the Korean Chemical Society* **2013,** *34*, 133-138.
92. Elleuch, H.; Ayadi, M.; Bouajila, J.; Rezgui, F., *The Journal of Organic Chemistry* **2016,** *81*, 1757-1761.
93. Amarante, G. W.; Coelho, F., *Tetrahedron* **2010,** *66*, 6749-6753.
94. Bhowmik, S.; Batra, S., *Current Organic Chemistry* **2014,** *18*, 3078-3119.
95. Guo, Y.; Shao, G.; Li, L.; Wu, W.; Li, R.; Li, J.; Song, J.; Qiu, L.; Prashad, M.; Kwong, F. Y., *Advanced Synthesis & Catalysis* **2010,** *352*, 1539-1553.
96. Srihari, P.; Dutta, P.; Rao, R. S.; Yadav, J.; Chandrasekhar, S.; Thombare, P.; Mohapatra, J.; Chatterjee, A.; Jain, M. R., *Bioorganic & Medicinal Chemistry Letters* **2009,** *19*, 5569-5572.
97. Lee, K. Y.; Lee, C. G.; Kim, T. H.; Kim, J. N., *Bulletin-Korean Chemical Society* **2004,** *25*, 33-34.
98. Pathak, R.; Singh, V.; Nag, S. N.; Kanojiya, S.; Batra, S., *Synthesis* **2006,** *2006*, 813-816.
99. Singh, V.; Pathak, R.; Batra, S., *Catalysis Communications* **2007,** *8*, 2048-2052.
100. Yadav, J.; Reddy, B. S.; Singh, A. P.; Majumder, N., *Tetrahedron Letters* **2010,** *51*, 2291-2294.
101. Kim, J. M.; Kim, S. H.; Kim, J. N., *Bulletin-Korean Chemical Society* **2007,** *28*, 2505.
102. Lu, X.; Petersen, J. L.; Wang, K. K., *Organic Letters* **2003,** *5*, 3277-3280.
103. Lee, C. G.; Lee, K. Y.; GowriSankar, S.; Kim, J. N., *Tetrahedron Letters* **2004,** *45*, 7409-7413.
104. Pathak, R.; Roy, A. K.; Batra, S., *Synlett* **2005,** *2005*, 0848-0850.
105. Batra, S.; Roy, A. K.; Patra, A.; Bhaduri, A.; Surin, W.; Raghavan, S.; Sharma, P.; Kapoor, K.; Dikshit, M., *Bioorganic & Medicinal Chemistry* **2004,** *12*, 2059-2077.
106. Idahosa, K. C.; Lee, Y.-C.; Nyoni, D.; Kaye, P. T.; Caira, M. R., *Tetrahedron Letters* **2011,** *52*, 2972-2976.
107. Hernández-Ibinarriaga, I.; Miranda, L. D., *Journal of the Mexican Chemical Society* **2009,** *53*, 55-58.
108. Kamimura, A.; Morita, R.; Matsuura, K.; Omata, Y.; Shirai, M., *Tetrahedron Letters* **2002,** *43*, 6189-6191.
109. Fear, G.; Komarnytsky, S.; Raskin, I., *Pharmacology & Therapeutics* **2007,** *113*, 354-368.
110. Brik, A.; Wong, C.-H., *Organic & Biomolecular Chemistry* **2003,** *1*, 5-14.
111. Ghosh, A. K.; Osswald, H. L.; Prato, G., *Journal of Medicinal Chemistry* **2016,** *59*, 5172-5208.
112. Ghosh, A. K.; Bilcer, G.; Schiltz, G., *Synthesis* **2001,** *2001*, 2203-2229.
113. Izawa, K.; Onishi, T., *Chemical Reviews* **2006,** *106*, 2811-2827.
114. Motwani, H. V.; De Rosa, M.; Odell, L. R.; Hallberg, A.; Larhed, M., *European Journal of Medicinal Chemistry* **2015,** *90*, 462-490.
115. Leung, D.; Abbenante, G.; Fairlie, D. P., *Journal of Medicinal Chemistry* **2000,** *43*, 305-341.
116. De Luca, L.; Giacomelli, G.; Taddei, M., *The Journal of Organic Chemistry* **2001,** *66*, 2534-2537.
117. Zimuwandeyi, M.; Kola, F.; Lemmerer, A.; Brady, D.; Rousseau, A. L.; Bode, M. L., *Tetrahedron* **2018,** *74*, 2925-2941.
118. Mentzel, M.; Hoffmann, H., *Journal für Praktische Chemie/Chemiker-Zeitung* **1997,** *339*, 517-524.
119. Hisler, K.; Tripoli, R.; Murphy, J. A., *Tetrahedron Letters* **2006,** *47*, 6293-6295.
120. Haghshenas, P.; Gravel, M., *Organic Letters* **2016,** *18*, 4518-4521.

121. Romo, D.; Meyer, S. D.; Johnson, D. D.; Schreiber, S. L., *Journal of the American Chemical Society* **1993,** *115*, 7906-7907.
122. Idahosa, K. C.; Molefe, D. M.; Pakade, V. E.; Brown, M. E.; Kaye, P. T., *South African Journal of Chemistry* **2011,** *64*, 144-150.
123. Coelho, F.; Diaz, G.; Abella, C. A.; Almeida, W. P., *Synlett* **2006,** *2006*, 0435-0439.
124. Diaz, G.; de Freitas, M. A.; Ricci-Silva, M. E.; Diaz, M. A., *Molecules* **2014,** *19*, 7429-7439.
125. Nakano, A.; Takahashi, K.; Ishihara, J.; Hatakeyama, S., *Organic Letters* **2006,** *8*, 5357-5360.
126. Ader, U.; Andersch, P.; Berger, M.; Goergens, U.; Seemayer, R.; Schneider, M., *Pure and Applied Chemistry* **1992,** *64*, 1165-1170.
127. Milner, S. E.; Maguire, A. R., Arkivoc: *Online Journal of Organic Chemistry* **2012,** part i**,** 321-382.
128. Borowiecki, P.; Justyniak, I.; Ochal, Z., *Tetrahedron: Asymmetry* **2017,** *28*, 1717-1732.
129. Franssen, M. C.; Jongejan, H.; Kooijman, H.; Spek, A. L.; Bell, R. P.; Wijnberg, J. B.; de Groot, A., *Tetrahedron: Asymmetry* **1999,** *10*, 2729-2738.
130. Kapoor, M.; Gupta, M. N., *Process Biochemistry* **2012,** *47*, 555-569.
131. Deasy, R. E.; Brossat, M.; Moody, T. S.; Maguire, A. R., *Tetrahedron: Asymmetry* **2011,** *22*, 47-61.
132. Kovács, B.; Megyesi, R.; Forró, E.; Fülöp, F., *Tetrahedron: Asymmetry* **2017,** *28*, 1829-1833.
133. Allen, J. V.; Williams, J. M., *Tetrahedron Letters* **1996,** *37*, 1859-1862.
134. Adam, W.; Groer, P.; Saha-Möller, C. R., *Tetrahedron: Asymmetry* **1997,** *8*, 833-836.
135. Cao, Y.; Wu, S.; Li, J.; Wu, B.; He, B., *Journal of Molecular Catalysis B: Enzymatic* **2014,** *99*, 108-113.
136. Chen, C. S.; Fujimoto, Y.; Girdaukas, G.; Sih, C. J., *Journal of the American Chemical Society* **1982,** *104*, 7294-7299.
137. Faber, K.; Kroutil, W., 2012 (Available online - http://biocatalysis.uni-graz.at/enantio/DataFiles/Selectivity-Help.pdf).
138. Kim, K. H.; Lee, H. S.; Kim, Y. M.; Kim, J. N., *Bulletin of the Korean Chemical Society* **2011,** *32*, 1087-1090.
139. Sá, M. M.; Meier, L.; Fernandes, L.; Pergher, S. B., *Catalysis Communications* **2007,** *8*, 1625-1629.
140. Caumul, P.; Hailes, H. C., *Tetrahedron Letters* **2005,** *46*, 8125-8127.
141. Gong, J.-J.; Yuan, K.; Wu, X.-Y., *Tetrahedron: Asymmetry* **2009,** *20*, 2117-2120.
142. Latorre, A.; Sáez, J. A.; Rodríguez, S.; González, F. V., *Tetrahedron* **2014,** *70*, 97-102.
143. Zhao, S.-H.; Bie, H.-Y.; Chen, Z.-B., *Organic Preparations and Procedures International* **2005,** *37*, 231-237.
144. Lim, C. H.; Kim, S. H.; Kim, K. H.; Kim, J. N., *Tetrahedron Letters* **2013,** *54*, 2476-2479.
145. Chandrasekhar, S.; Narsihmulu, C.; Saritha, B.; Sultana, S. S., *Tetrahedron Letters* **2004,** *45*, 5865-5867.
146. Nag, S.; Yadav, G.; Maulik, P.; Batra, S., *Synthesis* **2007,** *2007*, 911-917.
147. Pawar, B.; Padalkar, V.; Phatangare, K.; Nirmalkar, S.; Chaskar, A., *Catalysis Science & Technology* **2011,** *1*, 1641-1644.
148. Kalyva, M.; Zografos, A. L.; Kapourani, E.; Giambazolias, E.; Devel, L.; Papakyriakou, A.; Dive, V.; Lazarou, Y. G.; Georgiadis, D., *Chemistry-A European Journal* **2015,** *21*, 3278-3289.

149. Shi, M.; Li, C.-Q.; Jiang, J.-K., *Tetrahedron* **2003,** *59*, 1181-1189.
150. Shanmugam, P.; Singh, P. R., *Synlett* **2001,** *2001*, 1314-1316.
151. Sousa, B. A.; Dos Santos, A. A., *European Journal of Organic Chemistry* **2012,** *2012*, 3431-3436.
152. Martínez, I.; Andrews, A. E.; Emch, J. D.; Ndakala, A. J.; Wang, J.; Howell, A. R., *Organic Letters* **2003,** *5*, 399-402.
153. Richter, H.; Jung, G., *Molecular Diversity* **1997,** *3*, 191-194.
154. Garlapati, V. K.; Banerjee, R., *Enzyme Research* **2013,** *2013, 1-6*.
155. Melo, A. D.; Silva, F. F.; dos Santos, J.; Fernández-Lafuente, R.; Lemos, T. L.; Dias Filho, F. A., *Molecules* **2017,** *22*, 2165.
156. Zhang, A.; Gao, R.; Diao, N.; Xie, G.; Gao, G.; Cao, S., *Journal of Molecular Catalysis B: Enzymatic* **2009,** *56*, 78-84.
157. Archelas, A.; Furstoss, R., *The Journal of Organic Chemistry* **1999,** *64*, 6112-6114.
158. Wagner, A. J.; Rychnovsky, S. D., *The Journal of Organic Chemistry* **2013,** *78*, 4594-4598.
159. Mishra, S. K.; Suryaprakash, N., *Tetrahedron: Asymmetry* **2017,** *28*, 1220-1232.
160. Flack, H.; Bernardinelli, G., *Chirality: The Pharmacological, Biological, and Chemical Consequences of Molecular Asymmetry* **2008,** *20*, 681-690.
161. Li, Q.-M.; Ren, J.; Zhou, B.-D.; Bai, B.; Liu, X.-C.; Wen, M.-L.; Zhu, H.-J., *Tetrahedron* **2013,** *69*, 3067-3074.
162. Seco, J. M.; Quinoá, E.; Riguera, R., *Chemical Reviews* **2004,** *104*, 17-118.
163. Seco, J.; Quiñoá, E.; Riguera, R., *Chemical Reviews* **2012,** *112*, 4603-4641.
164. Dale, J. A.; Mosher, H. S., *Journal of the American Chemical Society* **1973,** *95*, 512-519.
165. Tyrrell, E.; Tsang, M. W.; Skinner, G. A.; Fawcett, J., *Tetrahedron* **1996,** *52*, 9841-9852.
166. Humam, M.; Shoul, T.; Jeannerat, D.; Muñoz, O.; Christen, P., *Molecules* **2011,** *16*, 7199-7209.
167. Hoye, T. R.; Renner, M. K., *The Journal of Organic Chemistry* **1996,** *61*, 8489-8495.
168. Gupta, R.; Gupta, N.; Rathi, P., *Applied Microbiology and Biotechnology* **2004,** *64*, 763-781.
169. Jiang, L.; Yu, H., *Chemical Research in Chinese Universities* **2014,** *30*, 396-399.
170. Mittersteiner, M.; Machado, T. M.; Jesus, P. C. d.; Brondani, P. B.; Scharf, D. R.; Wendhausen Jr, R., *Journal of the Brazilian Chemical Society* **2017,** *28*, 1185-1192.
171. Kaieda, M.; Samukawa, T.; Matsumoto, T.; Ban, K.; Kondo, A.; Shimada, Y.; Noda, H.; Nomoto, F.; Ohtsuka, K.; Izumoto, E., *Journal of Bioscience and Bioengineering* **1999,** *88*, 627-631.
172. Souza, L. T.; Mendes, A. A.; Castro, H. F. d., *BioMed Research International* **2016,** *2016*.
173. Basavaiah, D., *Arkivoc* **2001,** *8*, 70-82.
174. Ó Dálaigh, C.; Connon, S. J., *The Journal of Organic Chemistry* **2007,** *72*, 7066-7069.
175. Nag, S.; Pathak, R.; Kumar, M.; Shukla, P.; Batra, S., *Bioorganic & Medicinal Chemistry Letters* **2006,** *16*, 3824-3828.
176. Pathak, R.; Batra, S., *Tetrahedron* **2007,** *63*, 9448-9455.
177. Cocco, M.; Garella, D.; Di Stilo, A.; Borretto, E.; Stevanato, L.; Giorgis, M.; Marini, E.; Fantozzi, R.; Miglio, G.; Bertinaria, M., *Journal of Medicinal Chemistry* **2014,** *57*, 10366-10382.
178. Pan, S.-H.; Kawamoto, T.; Fukui, T.; Sonomoto, K.; Tanaka, A., *Applied Microbiology and Biotechnology* **1990,** *34*, 47-51.

179. Andronic, D.; Bulancea, M.; Dabija, A.; Miron, A., *Journal of Agroalimentary Processes and Technologies* **2007,** *13*, 381-386.
180. Šinkūnienė, D.; Bendikienė, V.; Juodka, B., *Romanian Biotechnological Letters* **2011,** *16*, 5891-5901.
181. Silva, C. M.; da Fonseca, R. d. S.; Prentice, C., *International Food Research Journal* **2014,** *21*, 1757-1761.
182. Gérard, D.; Guéroult, M.; Casas-Godoy, L.; Condoret, J.-S.; André, I.; Marty, A.; Duquesne, S., *Tetrahedron: Asymmetry* **2017,** *28*, 433-441.
183. Ribeiro, C. M.; Passaroto, E. N.; Brenelli, E., *Journal of the Brazilian Chemical Society* **2001,** *12*, 742-746.
184. Martínez-Martínez, M.; Alcaide, M.; Tchigvintsev, A.; Reva, O.; Polaina, J.; Bargiela, R.; Guazzaroni, M.-E.; Chicote, Á.; Canet, A.; Valero, F., *Applied and Environmental Microbiology* **2013**, *79*, 3553-3562.
185. Trazzi, G.; André, M. F.; Coelho, F., *Journal of the Brazilian Chemical Society* **2010,** *21*, 2327-2339.
186. Mirza-Aghayan, M.; Boukherroub, R.; Rahimifard, M., *Tetrahedron Letters* **2009,** *50*, 5930-5932.
187. Venkatesan, K.; Srinivasan, K., *Arkivoc* **2008,** *16*, 302-310.
188. Chandrasekhar, S.; Reddy, N. R.; Rao, Y. S., *Tetrahedron* **2006,** *62*, 12098-12107.
189. Takale, B. S.; Wang, S.; Zhang, X.; Feng, X.; Yu, X.; Jin, T.; Bao, M.; Yamamoto, Y., *Chemical Communications* **2014,** *50*, 14401-14404.
190. Yamada, K.; Igarashi, Y.; Betsuyaku, T.; Kitamura, M.; Hirata, K.; Hioki, K.; Kunishima, M., *Organic Letters* **2018,** *20*, 2015-2019.
191. Chachibaia, T.; Martin Pastor, M., *Journal of Carbon Research* **2017,** *3*, 13.
192. Rao, A. R.; Chakraborty, T.; Reddy, K. L.; Rao, A. S., *Tetrahedron Letters* **1994,** *35*, 5043-5046.
193. Zhou, K.; Chen, D.; Li, B.; Zhang, B.; Miao, F.; Zhou, L., *Plos One* **2017,** *12*, e0176189.
194. Heravi, M. M.; Zadsirjan, V.; Esfandyari, M.; Lashaki, T. B., *Tetrahedron: Asymmetry* **2017,** *28*, 987-1043.
195. Lopez-Herrera, F. J.; Pino-González, M. S.; Planas-Ruiz, F., *Tetrahedron: Asymmetry* **1990,** *1*, 465-475.
196. Callant, D.; Coussens, B.; Maten, T. v.; de Vries, J. G.; de Vries, N. K., *Tetrahedron, Asymmetry* **1992,** *3*, 401-414.
197. Jagdale, A. R.; Reddy, R. S.; Sudalai, A., *Organic Letters* **2009,** *11*, 803-806.
198. Švenda, J.; Myers, A. G., *Organic Letters* **2009,** *11*, 2437-2440.
199. Kundu, M. K.; Bhat, S. V., *Synthetic communications* **1999,** *29*, 93-101.
200. Lee, H. S.; Kim, S. J.; Kim, J. N., *Bulletin-Korean Chemical Society* **2006,** *27*, 1063.
201. Jebaraj, J. W.; Gopalakrishnan, M.; Baskar, G. *Asian Journal of Chemistry*, **2008,** *20*, 5282-5288.
202. Lambert, J. B. *Journal of the American Chemical Society*, **1967,** *89*, 1836-1840.
203. Fehrentz, J.-A.; Castro, B., *Synthesis* **1983,** *1983*, 676-678.
204. Mi, X.; Luo, S.; Cheng, J.-P., *The Journal of Organic Chemistry* **2005,** *70*, 2338-2341.
205. Gomes, R. C.; Barcelos, R. C.; Rodrigues, M. T.; Santos, H.; Coelho, F., *ChemistrySelect* **2017,** *2*, 926-930.
206. Yu, C.; Liu, B.; Hu, L., *The Journal of Organic Chemistry* **2001,** *66*, 5413-5418.
207. Garrido, N. M.; Sánchez, M. R.; Díez, D.; Sanz, F.; Urones, J. G., *Tetrahedron: Asymmetry* **2011,** *22*, 872-880.

208. Jiang, S.-S.; Xu, Q.-C.; Zhu, M.-Y.; Yu, X.; Deng, W.-P., *The Journal of Organic Chemistry* **2015,** *80*, 3159-3169.
209. Jeong, Y.; Ryu, J.-S., *The Journal of Organic Chemistry* **2010,** *75*, 4183-4191.
210. Junior, C. G.; Silva, F. P.; Oliveira, R. G. d.; Subrinho, F. L.; Andrade, N. G. d.; Vasconcellos, M. L., *Journal of the Brazilian Chemical Society* **2011,** *22*, 2220-2224.
211. Aggarwal, V. K.; Emme, I.; Fulford, S. Y., *The Journal of Organic Chemistry* **2003,** *68*, 692-700.
212. Krishna, P. R.; Manjuvani, A.; Kannan, V.; Sharma, G., *Tetrahedron Letters* **2004,** *45*, 1183-1185.
213. Kim, H. S.; Kim, T. Y.; Lee, K. Y.; Chung, Y. M.; Lee, H. J.; Kim, J. N., *Tetrahedron Letters* **2000,** *41*, 2613-2616.
214. Schmidt, Y.; Breit, B., *Chemistry-A European Journal* **2011,** *17*, 11789-11796.
215. Pakala, K., *Journal of the Chemical Society, Chemical Communications* **1992,** 13, 955-957.
216. Basavaiah, D.; Lingaiah, B.; Reddy, G. C.; Sahu, B. C., *European Journal of Organic Chemistry* **2016,** *2016*, 2398-2403.
217. Kim, H.-S.; Lee, S.-J.; Yoon, C. M., *Bulletin of the Korean Chemical Society* **2013,** *34*, 325-327.
218. Bosanac, T.; Wilcox, C. S., *Chemical Communications* **2001,** 17, 1618-1619.
219. De Souza, E. C.; Romero-Ortega, M.; Olivo, H. F., *Tetrahedron Letters* **2018,** *59*, 287-290.
220. Basumatary, G.; Bez, G., *Tetrahedron Letters* **2017,** *58*, 4312-4315.
221. Hao, C.-H.; Guo, X.-N.; Pan, Y.-T.; Chen, S.; Jiao, Z.-F.; Yang, H.; Guo, X.-Y., *Journal of the American Chemical Society* **2016,** *138*, 9361-9364.
222. Gao, Y.; Klunder, J. M.; Hanson, R. M.; Masamune, H.; Ko, S. Y.; Sharpless, K. B., *Journal of the American Chemical Society* **1987,** *109*, 5765-5780.
223. Prasad, P.; Reddi, R.; Sudalai, A., *Chemical Communications* **2015,** *51*, 10276-10279.
224. Nicolaou, K. e. C.; Dethe, D. H.; Leung, G. Y.; Zou, B.; Chen, D. Y. K., *Chemistry–An Asian Journal* **2008,** *3*, 413-429.

APPENDIX II- NMR SPECTRA AND HPLC CHROMATOGRAMS

APPENDIX I- CRYSTALLOGRAPHIC DATA

X-ray crystallographic data of (2*E*,4*E*)-methyl 5-phenyl-2-(piperidin-1-ylmethyl)penta-2,4-dienoate (**248**)

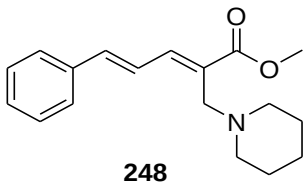

248

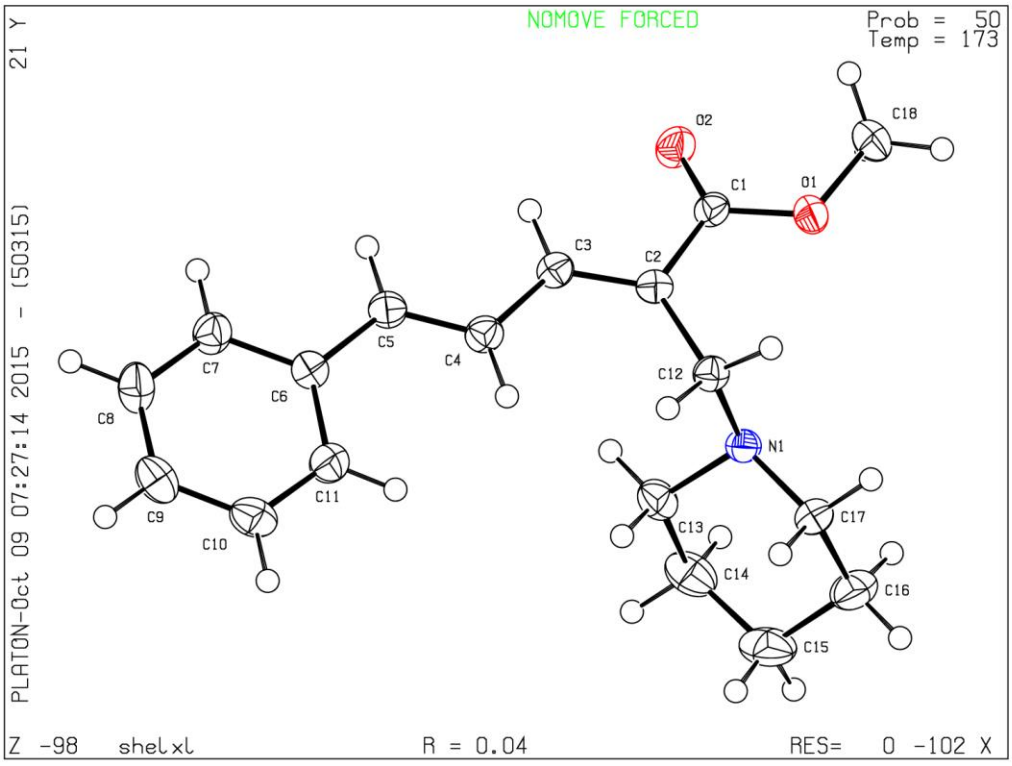

Table 1. Crystal data and structure refinement for 15m_cdk1_pj1250b_0s.

Identification code	shelxl	
Empirical formula	C18 H23 N O2	
Formula weight	285.37	
Temperature	173(2) K	
Wavelength	0.71073 Å	
Crystal system	?	
Space group	?	
Unit cell dimensions	a = 9.0439(2) Å	α= 110.7280(10)°.
	b = 9.5854(2) Å	β= 97.4960(10)°.
	c = 10.9341(2) Å	γ = 110.5620(10)°.
Volume	794.13(3) $Å^3$	
Z	2	
Density (calculated)	1.193 Mg/m^3	
Absorption coefficient	0.077 mm^{-1}	
F(000)	308	
Crystal size	0.48 x 0.33 x 0.29 mm^3	
Theta range for data collection	2.08 to 28.00°.	
Index ranges	-11<=h<=11, -12<=k<=12, -14<=l<=14	
Reflections collected	12868	
Independent reflections	3832 [R(int) = 0.0390]	
Completeness to theta = 28.00°	99.8 %	
Max. and min. transmission	0.9780 and 0.9640	
Refinement method	Full-matrix least-squares on F^2	
Data / restraints / parameters	3832 / 0 / 191	
Goodness-of-fit on F^2	1.084	
Final R indices [I>2sigma(I)]	R1 = 0.0409, wR2 = 0.1024	
R indices (all data)	R1 = 0.0558, wR2 = 0.1105	
Largest diff. peak and hole	0.183 and -0.290 $e.Å^{-3}$	

Table 2. Atomic coordinates (x 10^4) and equivalent isotropic displacement parameters ($Å^2$x 10^3) for 15m_cdk1_pj1250b_0s. U(eq) is defined as one third of the trace of the orthogonalized U^{ij} tensor.

	x	y	z	U(eq)
C(1)	4730(1)	2519(1)	7018(1)	24(1)
C(2)	4032(1)	2837(1)	5888(1)	23(1)
C(3)	3936(1)	1850(1)	4616(1)	25(1)
C(4)	3294(1)	1906(1)	3363(1)	26(1)
C(5)	3318(1)	924(1)	2145(1)	26(1)
C(6)	2691(1)	889(1)	823(1)	25(1)
C(7)	2801(1)	-222(1)	-355(1)	31(1)
C(8)	2222(2)	-306(2)	-1630(1)	37(1)
C(9)	1515(2)	720(2)	-1748(1)	37(1)
C(10)	1388(2)	1827(2)	-592(1)	37(1)
C(11)	1975(1)	1920(1)	680(1)	32(1)
C(12)	3550(1)	4252(1)	6250(1)	24(1)
C(13)	591(1)	2636(1)	5505(1)	31(1)
C(14)	-980(2)	2256(2)	5939(1)	41(1)
C(15)	-1222(2)	3810(2)	6614(1)	46(1)
C(16)	315(2)	5136(2)	7770(1)	41(1)
C(17)	1824(1)	5419(1)	7257(1)	29(1)
C(18)	5974(2)	3628(2)	9391(1)	35(1)
N(1)	2034(1)	3899(1)	6667(1)	23(1)
O(1)	5241(1)	3817(1)	8242(1)	29(1)
O(2)	4875(1)	1270(1)	6876(1)	33(1)

Table 3. Bond lengths [Å] and angles [°] for 15m_cdk1_pj1250b_0s.

C(1)-O(2)	1.2078(12)
C(1)-O(1)	1.3451(12)
C(1)-C(2)	1.4883(13)
C(2)-C(3)	1.3476(14)
C(2)-C(12)	1.5054(13)
C(3)-C(4)	1.4438(14)
C(3)-H(3)	0.9500
C(4)-C(5)	1.3391(14)
C(4)-H(4)	0.9500
C(5)-C(6)	1.4665(14)
C(5)-H(5)	0.9500
C(6)-C(7)	1.3929(14)
C(6)-C(11)	1.3975(15)
C(7)-C(8)	1.3872(15)
C(7)-H(7)	0.9500
C(8)-C(9)	1.3795(17)
C(8)-H(8)	0.9500
C(9)-C(10)	1.3821(17)
C(9)-H(9)	0.9500
C(10)-C(11)	1.3818(15)
C(10)-H(10)	0.9500
C(11)-H(11)	0.9500
C(12)-N(1)	1.4658(12)
C(12)-H(12A)	0.9900
C(12)-H(12B)	0.9900
C(13)-N(1)	1.4663(14)
C(13)-C(14)	1.5201(16)
C(13)-H(13A)	0.9900
C(13)-H(13B)	0.9900
C(14)-C(15)	1.5176(19)
C(14)-H(14A)	0.9900
C(14)-H(14B)	0.9900
C(15)-C(16)	1.5192(19)
C(15)-H(15A)	0.9900
C(15)-H(15B)	0.9900
C(16)-C(17)	1.5155(15)

C(16)-H(16A)	0.9900
C(16)-H(16B)	0.9900
C(17)-N(1)	1.4617(13)
C(17)-H(17A)	0.9900
C(17)-H(17B)	0.9900
C(18)-O(1)	1.4431(12)
C(18)-H(18A)	0.9800
C(18)-H(18B)	0.9800
C(18)-H(18C)	0.9800

O(2)-C(1)-O(1)	122.72(9)
O(2)-C(1)-C(2)	125.12(9)
O(1)-C(1)-C(2)	112.14(8)
C(3)-C(2)-C(1)	116.41(9)
C(3)-C(2)-C(12)	125.34(9)
C(1)-C(2)-C(12)	118.22(8)
C(2)-C(3)-C(4)	126.64(9)
C(2)-C(3)-H(3)	116.7
C(4)-C(3)-H(3)	116.7
C(5)-C(4)-C(3)	122.60(9)
C(5)-C(4)-H(4)	118.7
C(3)-C(4)-H(4)	118.7
C(4)-C(5)-C(6)	126.42(9)
C(4)-C(5)-H(5)	116.8
C(6)-C(5)-H(5)	116.8
C(7)-C(6)-C(11)	117.82(9)
C(7)-C(6)-C(5)	119.11(9)
C(11)-C(6)-C(5)	123.07(9)
C(8)-C(7)-C(6)	121.30(10)
C(8)-C(7)-H(7)	119.4
C(6)-C(7)-H(7)	119.4
C(9)-C(8)-C(7)	119.92(10)
C(9)-C(8)-H(8)	120.0
C(7)-C(8)-H(8)	120.0
C(8)-C(9)-C(10)	119.65(10)
C(8)-C(9)-H(9)	120.2
C(10)-C(9)-H(9)	120.2
C(11)-C(10)-C(9)	120.51(10)

C(11)-C(10)-H(10)	119.7
C(9)-C(10)-H(10)	119.7
C(10)-C(11)-C(6)	120.79(10)
C(10)-C(11)-H(11)	119.6
C(6)-C(11)-H(11)	119.6
N(1)-C(12)-C(2)	112.54(8)
N(1)-C(12)-H(12A)	109.1
C(2)-C(12)-H(12A)	109.1
N(1)-C(12)-H(12B)	109.1
C(2)-C(12)-H(12B)	109.1
H(12A)-C(12)-H(12B)	107.8
N(1)-C(13)-C(14)	111.23(9)
N(1)-C(13)-H(13A)	109.4
C(14)-C(13)-H(13A)	109.4
N(1)-C(13)-H(13B)	109.4
C(14)-C(13)-H(13B)	109.4
H(13A)-C(13)-H(13B)	108.0
C(15)-C(14)-C(13)	111.07(10)
C(15)-C(14)-H(14A)	109.4
C(13)-C(14)-H(14A)	109.4
C(15)-C(14)-H(14B)	109.4
C(13)-C(14)-H(14B)	109.4
H(14A)-C(14)-H(14B)	108.0
C(14)-C(15)-C(16)	110.23(10)
C(14)-C(15)-H(15A)	109.6
C(16)-C(15)-H(15A)	109.6
C(14)-C(15)-H(15B)	109.6
C(16)-C(15)-H(15B)	109.6
H(15A)-C(15)-H(15B)	108.1
C(17)-C(16)-C(15)	110.32(10)
C(17)-C(16)-H(16A)	109.6
C(15)-C(16)-H(16A)	109.6
C(17)-C(16)-H(16B)	109.6
C(15)-C(16)-H(16B)	109.6
H(16A)-C(16)-H(16B)	108.1
N(1)-C(17)-C(16)	111.40(9)
N(1)-C(17)-H(17A)	109.3
C(16)-C(17)-H(17A)	109.3

N(1)-C(17)-H(17B)	109.3
C(16)-C(17)-H(17B)	109.3
H(17A)-C(17)-H(17B)	108.0
O(1)-C(18)-H(18A)	109.5
O(1)-C(18)-H(18B)	109.5
H(18A)-C(18)-H(18B)	109.5
O(1)-C(18)-H(18C)	109.5
H(18A)-C(18)-H(18C)	109.5
H(18B)-C(18)-H(18C)	109.5
C(17)-N(1)-C(12)	109.36(8)
C(17)-N(1)-C(13)	110.18(8)
C(12)-N(1)-C(13)	111.17(8)
C(1)-O(1)-C(18)	115.75(8)

Table 4. Anisotropic displacement parameters ($Å^2$x 10^3)for 15m_cdk1_pj1250b_0s. The anisotropic displacement factor exponent takes the form: $-2\pi^2[h^2a^{*2}U^{11} + ... + 2 h k a^* b^* U^{12}]$

	U^{11}	U^{22}	U^{33}	U^{23}	U^{13}	U^{12}
C(1)	23(1)	25(1)	24(1)	10(1)	9(1)	12(1)
C(2)	21(1)	23(1)	26(1)	12(1)	7(1)	10(1)
C(3)	26(1)	24(1)	26(1)	11(1)	9(1)	12(1)
C(4)	29(1)	26(1)	28(1)	13(1)	9(1)	14(1)
C(5)	30(1)	26(1)	27(1)	13(1)	7(1)	14(1)
C(6)	26(1)	24(1)	26(1)	12(1)	7(1)	10(1)
C(7)	39(1)	27(1)	29(1)	12(1)	10(1)	16(1)
C(8)	48(1)	34(1)	24(1)	10(1)	10(1)	16(1)
C(9)	38(1)	39(1)	29(1)	18(1)	4(1)	12(1)
C(10)	37(1)	40(1)	39(1)	22(1)	6(1)	20(1)
C(11)	37(1)	34(1)	29(1)	13(1)	10(1)	20(1)
C(12)	24(1)	21(1)	26(1)	10(1)	7(1)	9(1)
C(13)	26(1)	29(1)	30(1)	10(1)	2(1)	8(1)
C(14)	23(1)	46(1)	46(1)	23(1)	4(1)	5(1)
C(15)	28(1)	69(1)	55(1)	35(1)	17(1)	26(1)
C(16)	39(1)	51(1)	44(1)	20(1)	19(1)	29(1)
C(17)	31(1)	28(1)	30(1)	10(1)	8(1)	17(1)
C(18)	38(1)	41(1)	25(1)	13(1)	3(1)	19(1)
N(1)	21(1)	23(1)	24(1)	9(1)	6(1)	10(1)
O(1)	34(1)	29(1)	22(1)	8(1)	3(1)	16(1)
O(2)	47(1)	32(1)	29(1)	15(1)	12(1)	25(1)

Table 5. Hydrogen coordinates (x 10^4) and isotropic displacement parameters ($Å^2$x 10^3) for 15m_cdk1_pj1250b_0s.

	x	y	z	U(eq)
H(3)	4331	1034	4536	30
H(4)	2836	2669	3403	31
H(5)	3787	177	2137	32
H(7)	3282	-936	-284	37
H(8)	2313	-1069	-2421	44
H(9)	1118	667	-2619	44
H(10)	894	2528	-672	44
H(11)	1890	2695	1467	39
H(12A)	4460	5244	7004	28
H(12B)	3391	4499	5450	28
H(13A)	749	1614	5114	38
H(13B)	484	3027	4788	38
H(14A)	-1938	1446	5127	49
H(14B)	-921	1757	6585	49
H(15A)	-2180	3556	6978	56
H(15B)	-1452	4217	5929	56
H(16A)	189	6178	8142	49
H(16B)	457	4793	8514	49
H(17A)	1712	5836	6558	34
H(17B)	2817	6269	8025	34
H(18A)	5157	2711	9489	53
H(18B)	6339	4648	10225	53
H(18C)	6924	3396	9241	53

Table 6. Torsion angles [°] for 15m_cdk1_pj1250b_0s.

O(2)-C(1)-C(2)-C(3)	-16.91(15)
O(1)-C(1)-C(2)-C(3)	161.22(9)
O(2)-C(1)-C(2)-C(12)	165.17(10)
O(1)-C(1)-C(2)-C(12)	-16.70(13)
C(1)-C(2)-C(3)-C(4)	179.33(10)
C(12)-C(2)-C(3)-C(4)	-2.92(17)
C(2)-C(3)-C(4)-C(5)	176.73(10)
C(3)-C(4)-C(5)-C(6)	179.73(10)
C(4)-C(5)-C(6)-C(7)	-179.55(11)
C(4)-C(5)-C(6)-C(11)	0.23(18)
C(11)-C(6)-C(7)-C(8)	0.05(17)
C(5)-C(6)-C(7)-C(8)	179.84(10)
C(6)-C(7)-C(8)-C(9)	-0.25(18)
C(7)-C(8)-C(9)-C(10)	-0.01(18)
C(8)-C(9)-C(10)-C(11)	0.47(18)
C(9)-C(10)-C(11)-C(6)	-0.68(18)
C(7)-C(6)-C(11)-C(10)	0.42(17)
C(5)-C(6)-C(11)-C(10)	-179.37(11)
C(3)-C(2)-C(12)-N(1)	108.80(11)
C(1)-C(2)-C(12)-N(1)	-73.49(11)
N(1)-C(13)-C(14)-C(15)	56.07(13)
C(13)-C(14)-C(15)-C(16)	-53.03(13)
C(14)-C(15)-C(16)-C(17)	53.62(13)
C(15)-C(16)-C(17)-N(1)	-57.84(12)
C(16)-C(17)-N(1)-C(12)	-177.18(8)
C(16)-C(17)-N(1)-C(13)	60.34(11)
C(2)-C(12)-N(1)-C(17)	168.78(8)
C(2)-C(12)-N(1)-C(13)	-69.33(10)
C(14)-C(13)-N(1)-C(17)	-59.16(11)
C(14)-C(13)-N(1)-C(12)	179.43(8)
O(2)-C(1)-O(1)-C(18)	-0.30(14)
C(2)-C(1)-O(1)-C(18)	-178.48(8)

APPENDIX II- NMR SPECTRA OF SELECTED COMPOUNDS

^{1}H NMR spectrum of (±) 2-[(Hydroxyphenyl) methyl] acrylonitrile (**75a**)

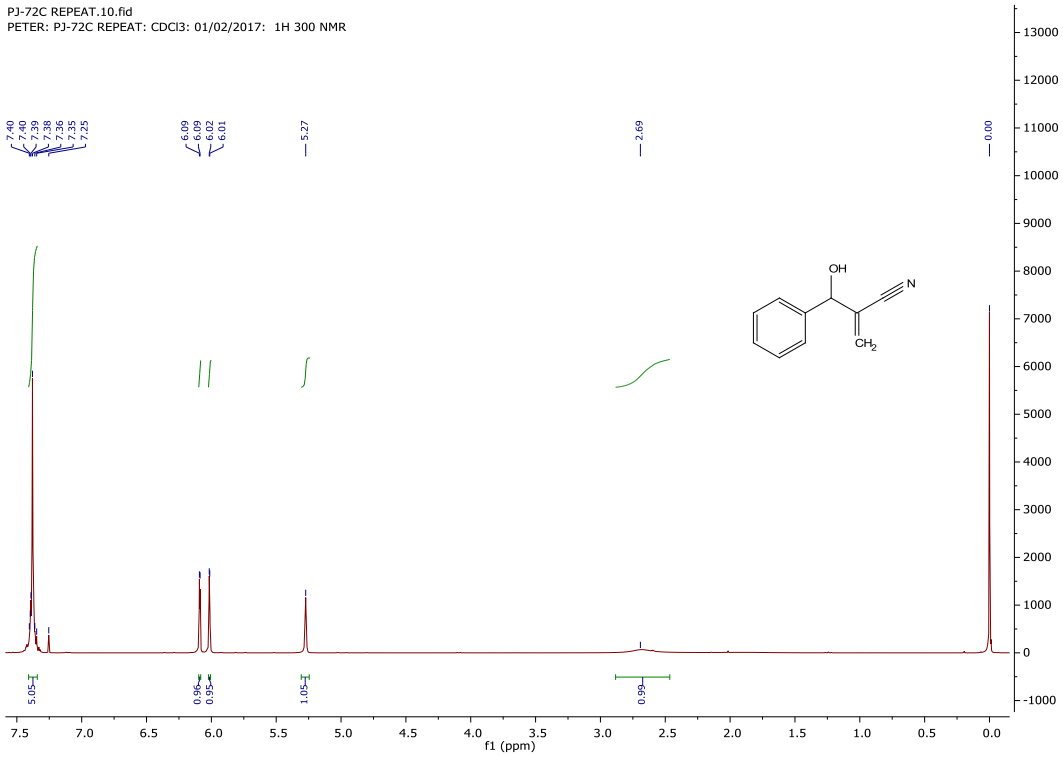

^{13}C NMR spectrum of (±) 2-[(Hydroxyphenyl) methyl] acrylonitrile (**75a)**

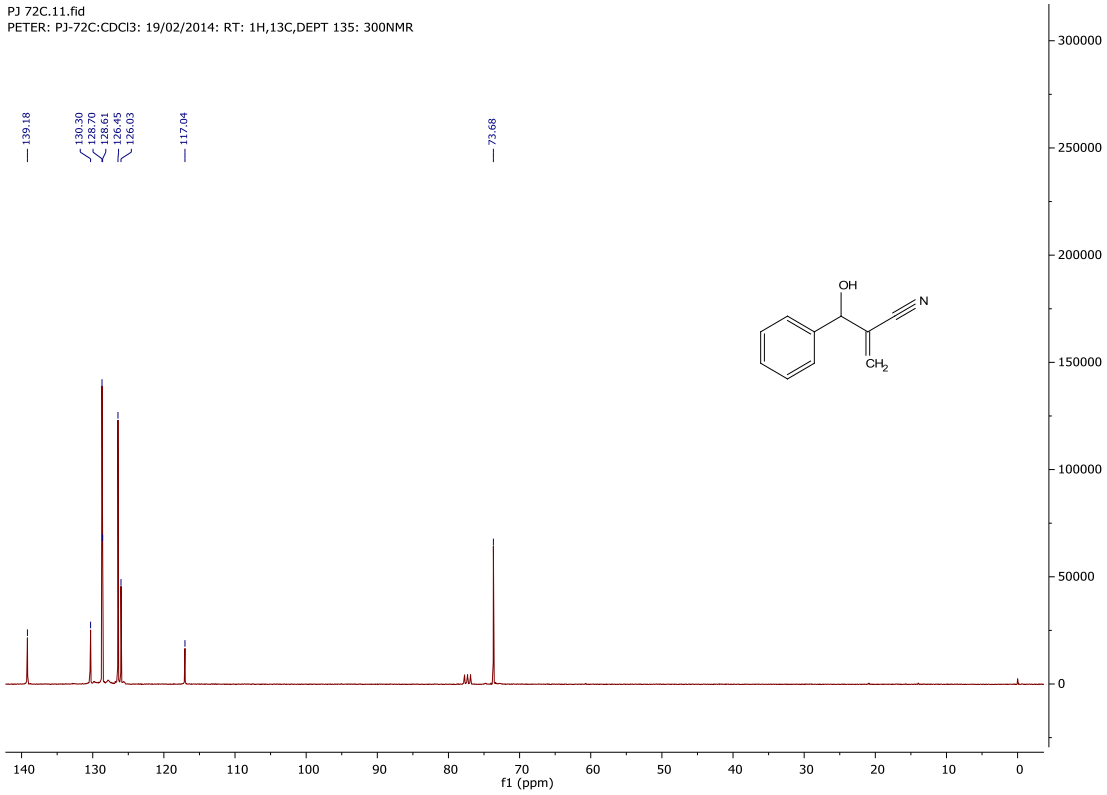

^{1}H NMR spectrum of (±) 3-Hydroxy-2-methylene-5-phenyl-4-pentenenitrile (**191**)

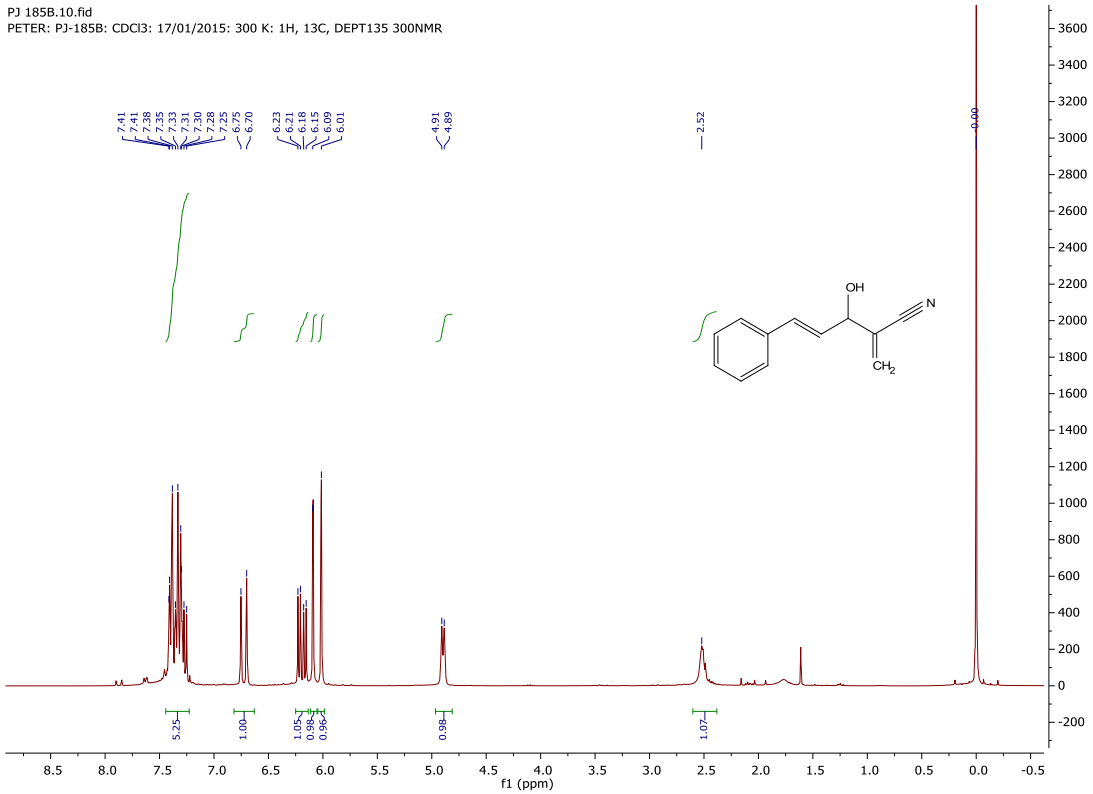

^{13}C NMR spectrum of (±) 3-Hydroxy-2-methylene-5-phenyl-4-pentenenitrile (**191**)

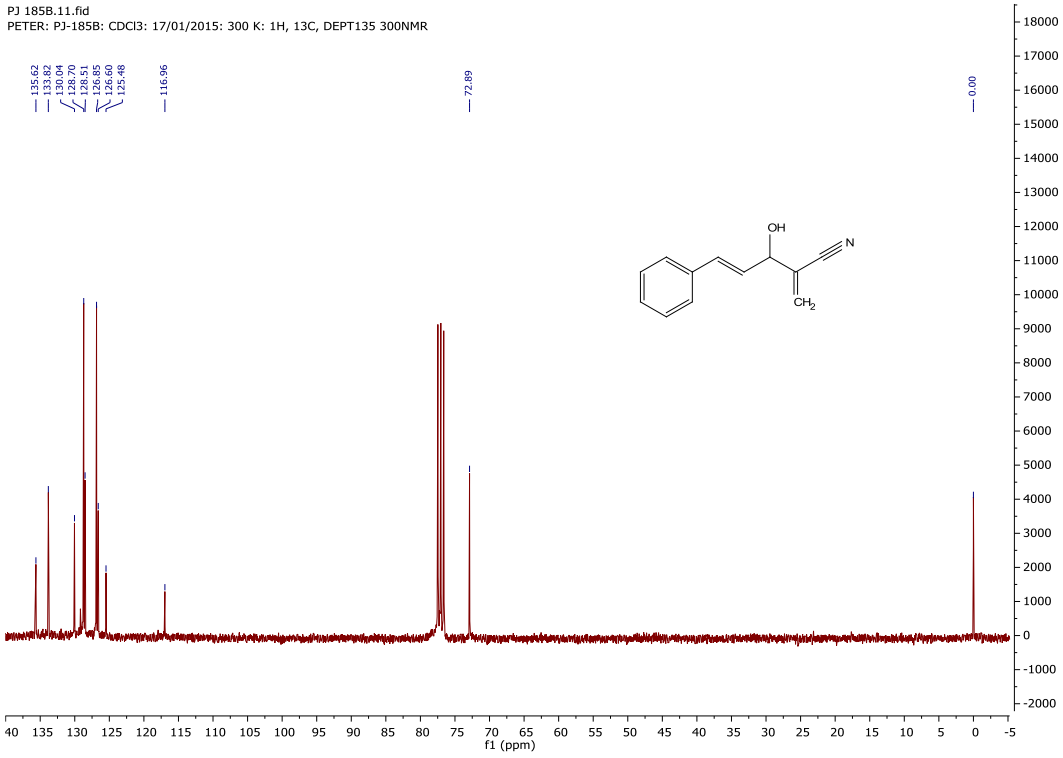

^{1}H NMR spectrum of (±) 3-hydroxy-2-methylene-5-phenylpentanenitrile (**195**)

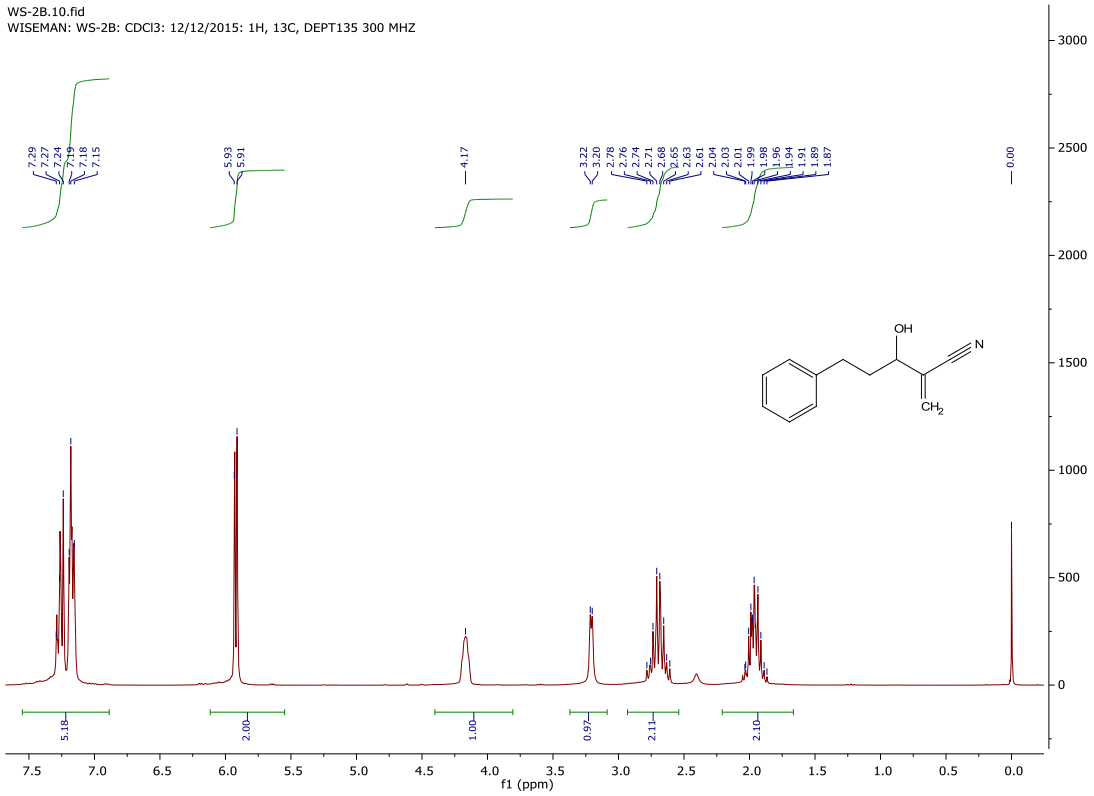

^{13}C NMR spectrum of (±) 3-hydroxy-2-methylene-5-phenylpentanenitrile (**195**)

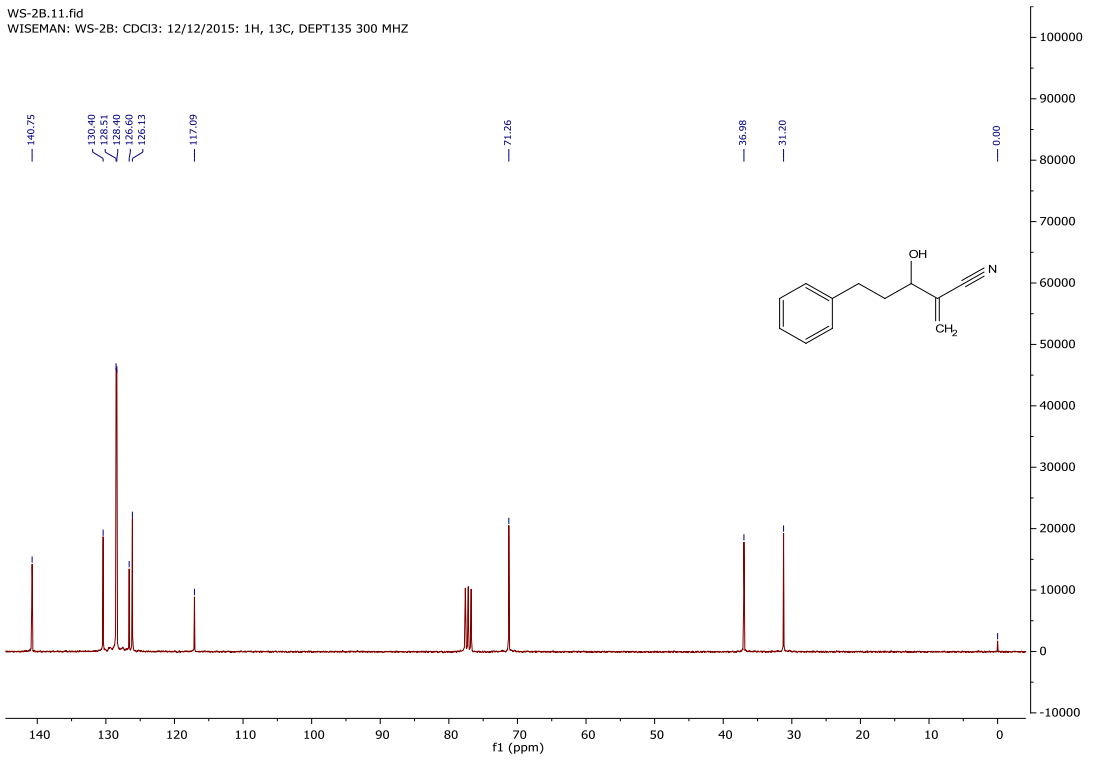

^{1}H NMR spectrum of (±) 2-cyano-1-phenylallyl acetate (**105a**)

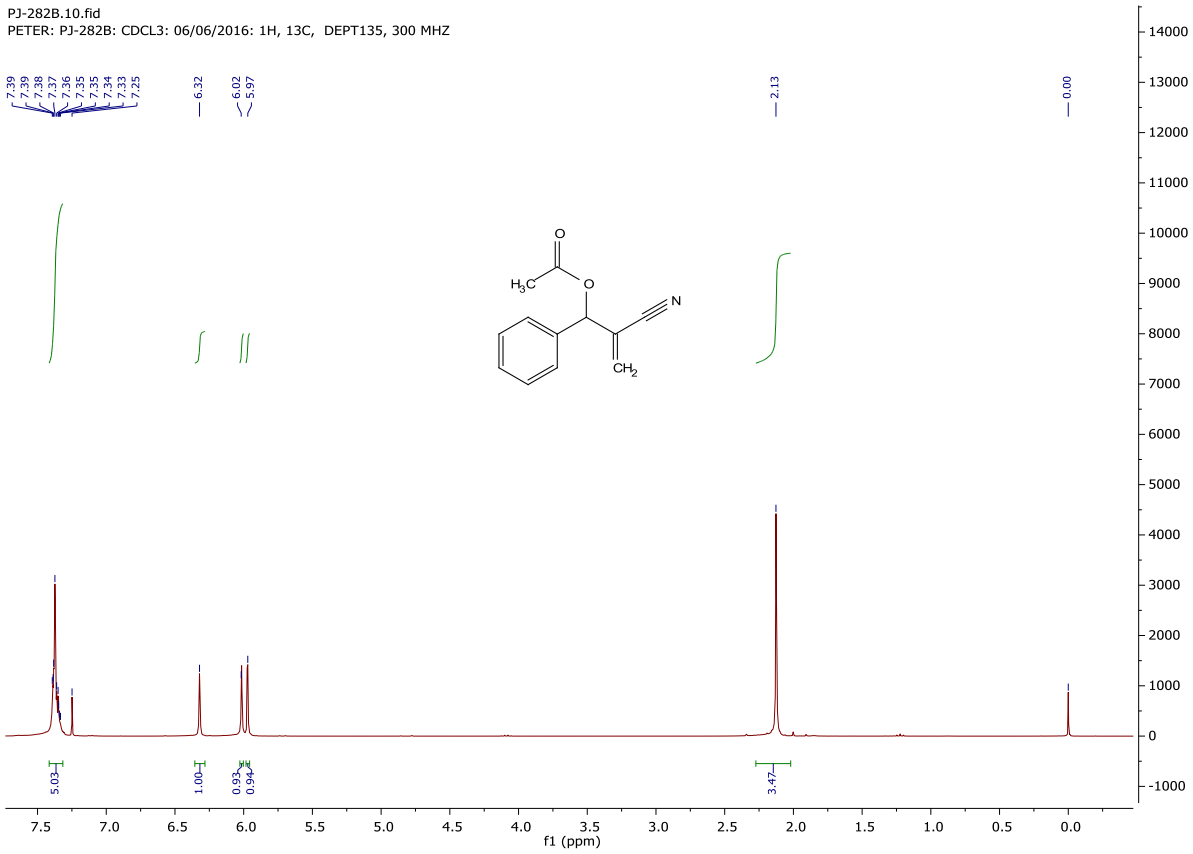

^{13}C NMR spectrum of (±) 2-cyano-1-phenylallyl acetate (**105a**)

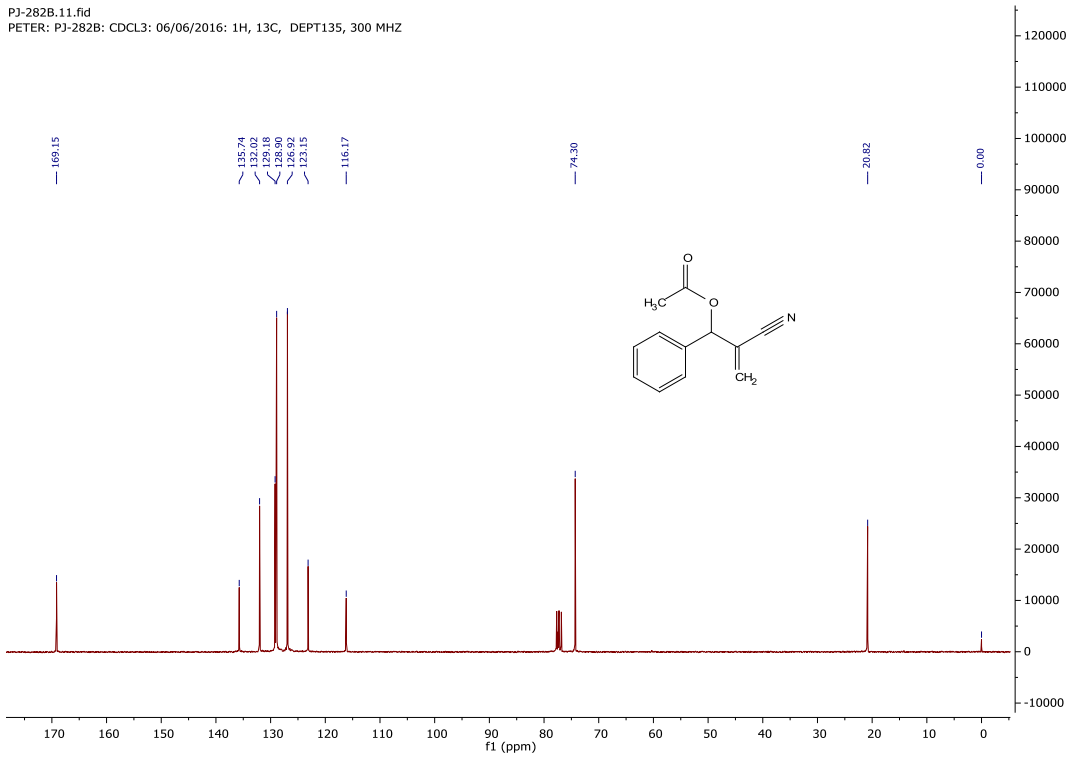

^{1}H NMR spectrum of (±) (E)-4-cyano-1-phenylpenta-1,4-dien-3-yl acetate (**200**)

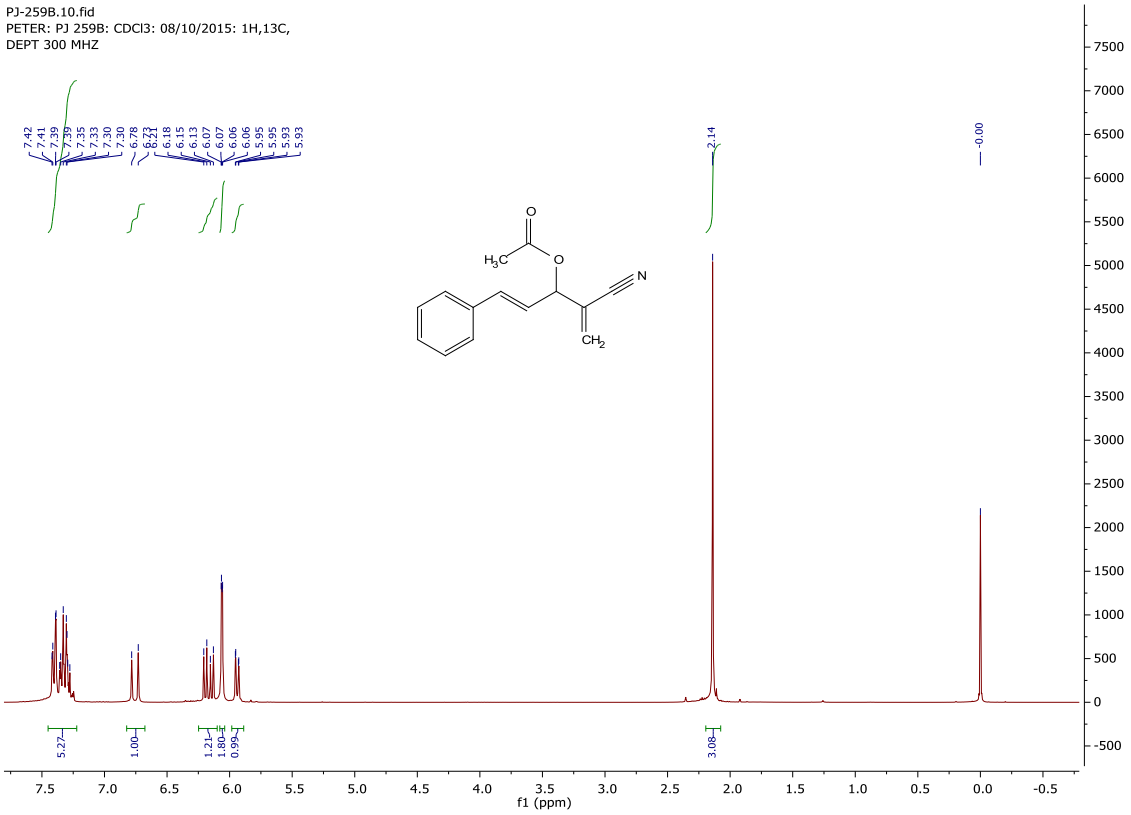

^{13}C NMR spectrum of (±) (E)-4-cyano-1-phenylpenta-1,4-dien-3-yl acetate (**200**)

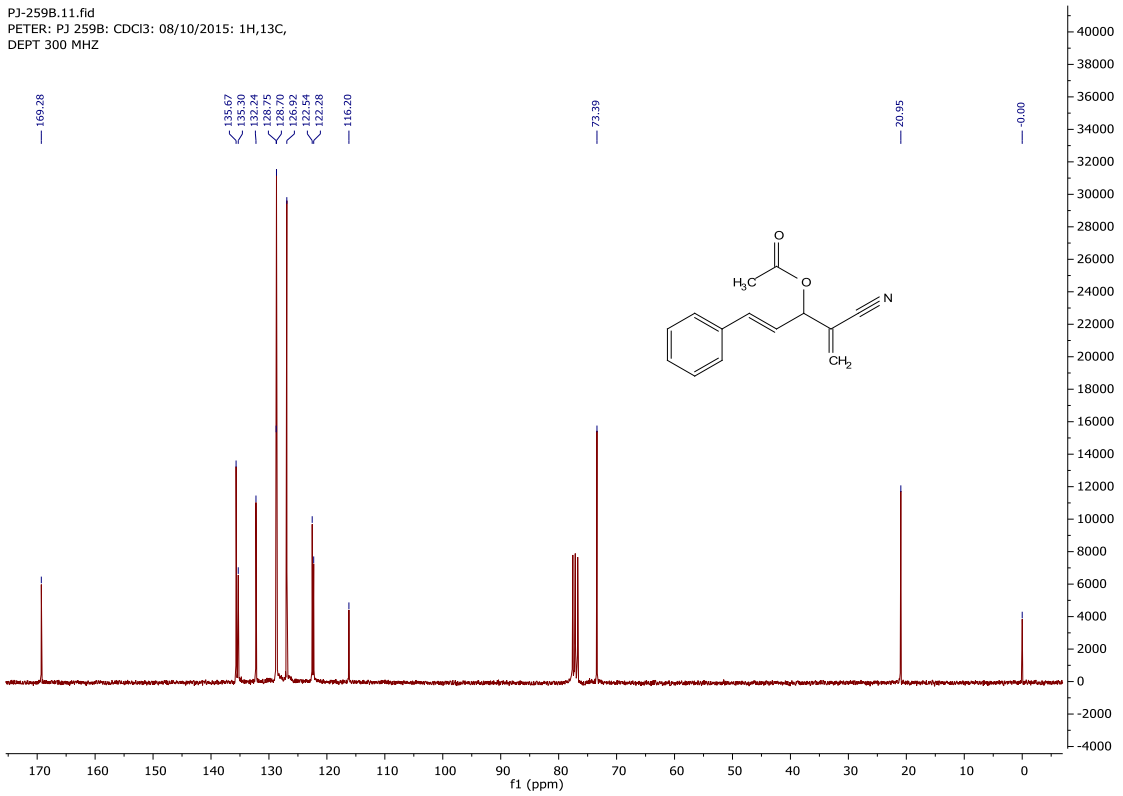

^{1}H NMR spectrum of (±) 2-cyano-5-phenyl-pent-1-ene-yl acetate (**201**)

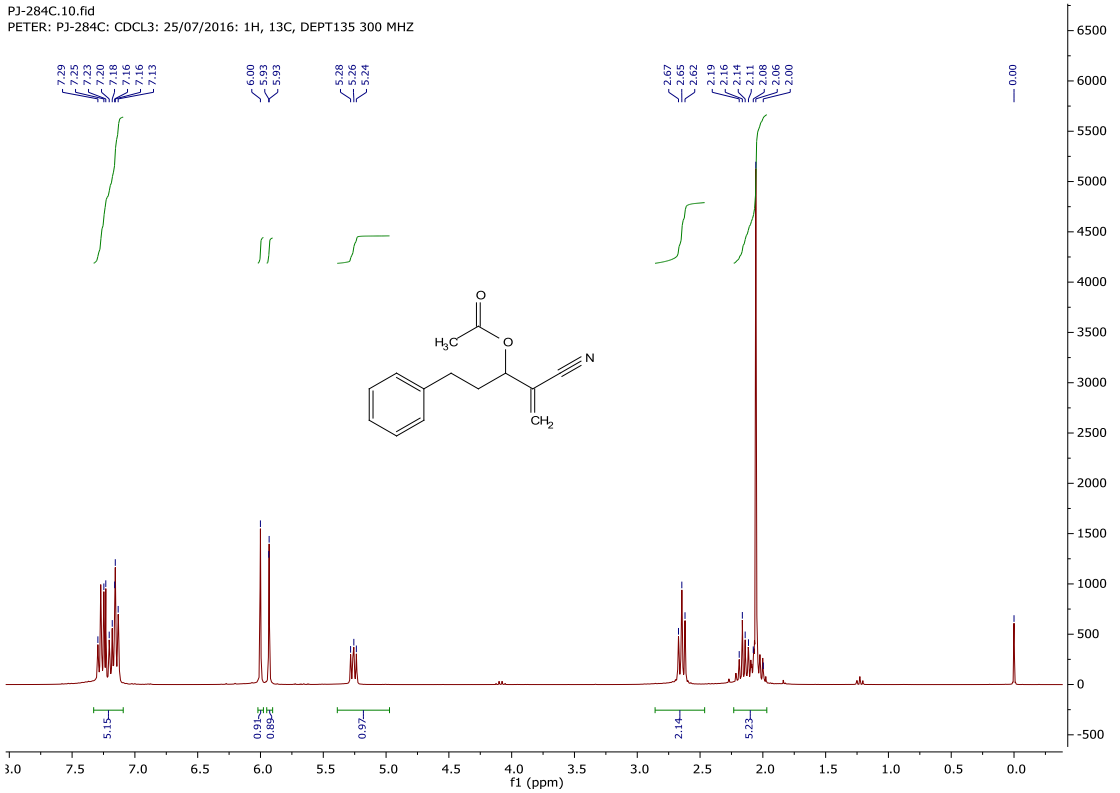

^{13}C NMR spectrum of (±) 2-cyano-5-phenyl-pent-1-ene-yl acetate (**201**)

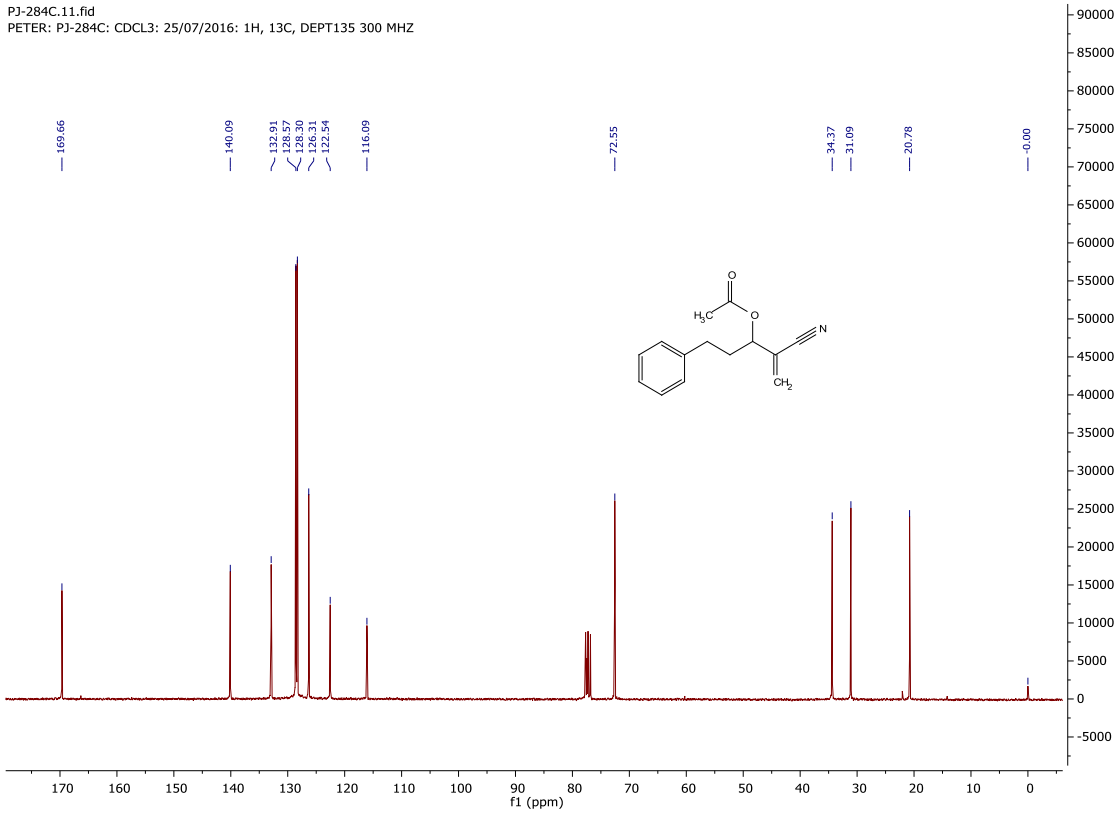

^{1}H NMR spectrum (±) (*E*)-3-((*tert*-butyldimethylsilyl)oxy)-2-methylene-5-phenylpent-4-enenitrile **(226c)**

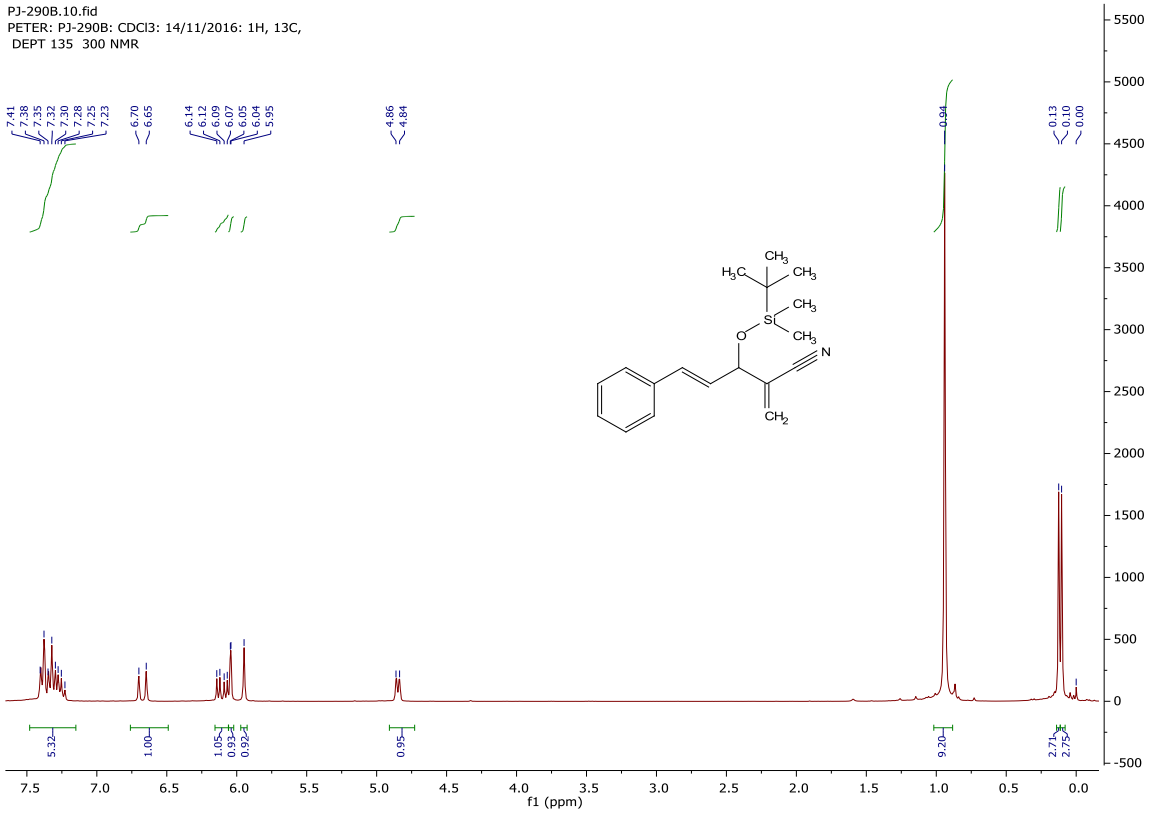

^{13}C NMR spectrum (±) (*E*)-3-((*tert*-butyldimethylsilyl)oxy)-2-methylene-5-phenylpent-4-enenitrile (**226c)**

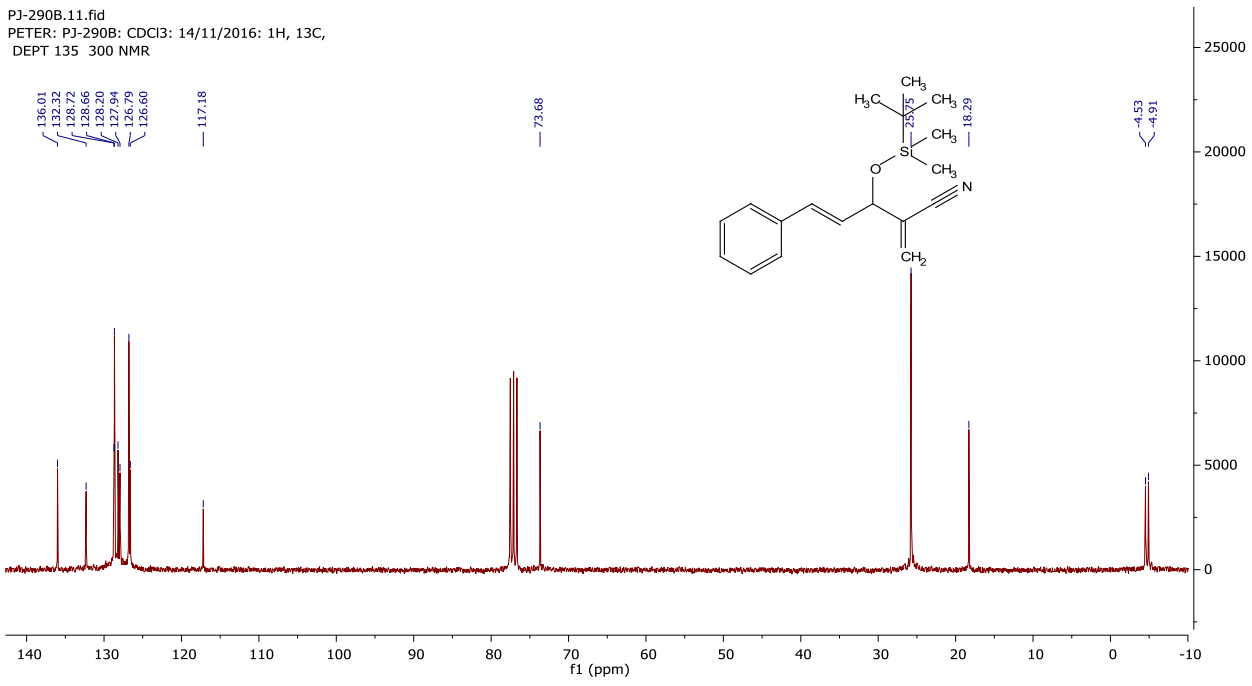

^{1}H NMR spectrum of (2*E*,4*E*)-methyl 5-phenyl-2-(piperidin-1-ylmethyl)penta-2,4-dienoate (**248**)

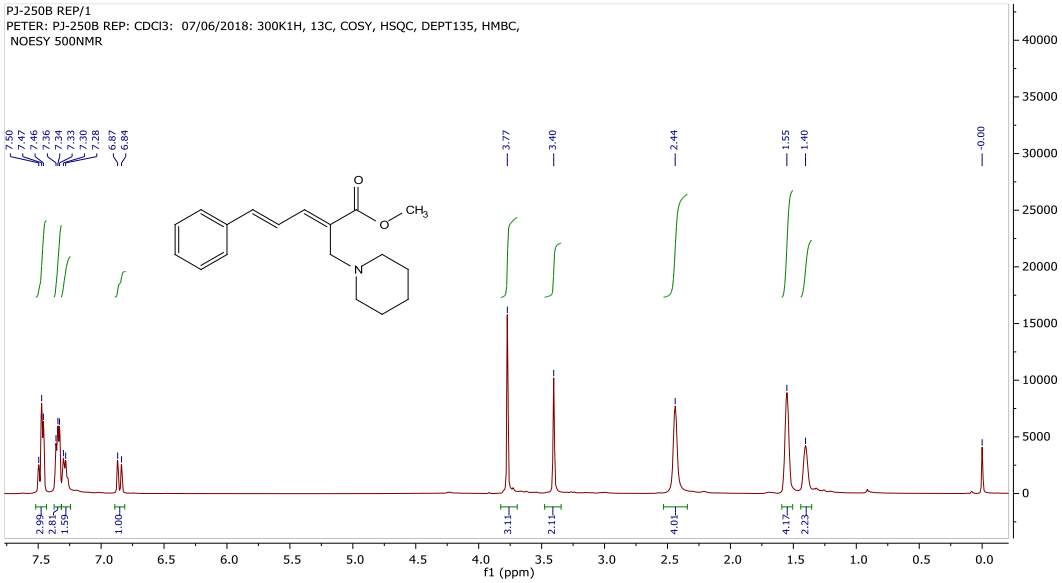

^{13}C NMR spectrum of (2*E*,4*E*)-methyl 5-phenyl-2-(piperidin-1-ylmethyl)penta-2,4-dienoate (**248**)

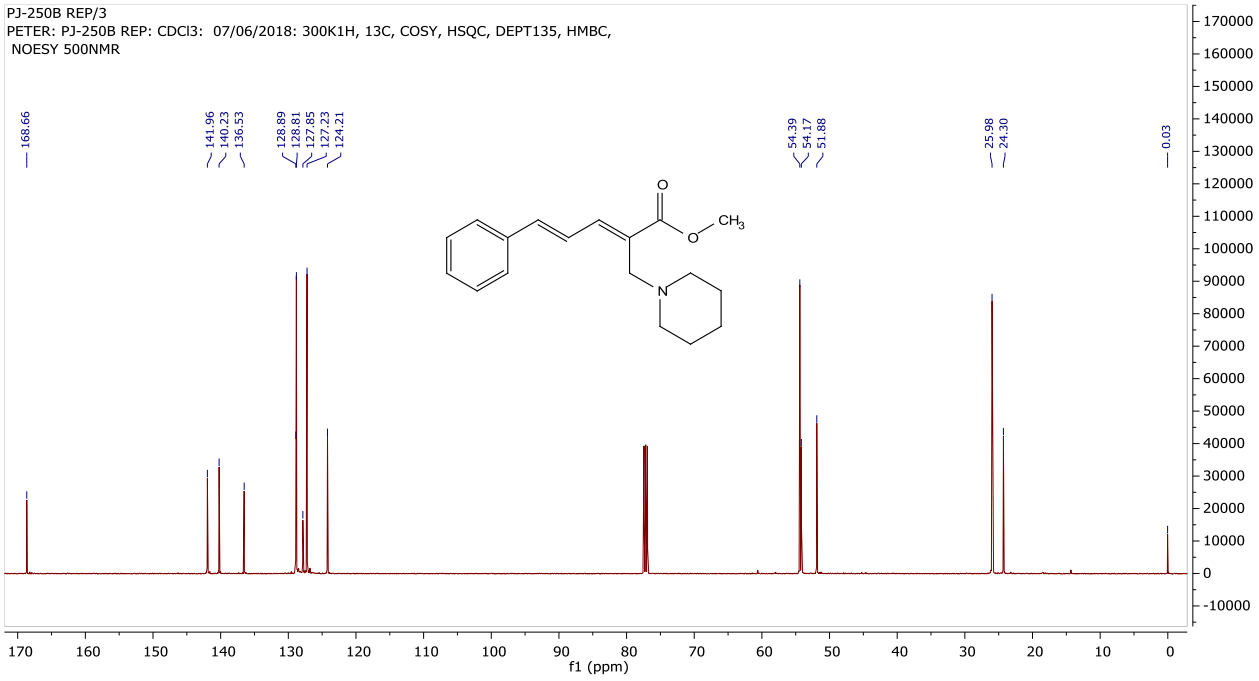

COSY NMR spectrum of (2*E*,4*E*)-methyl 5-phenyl-2-(piperidin-1-ylmethyl)penta-2,4-dienoate (**248)**

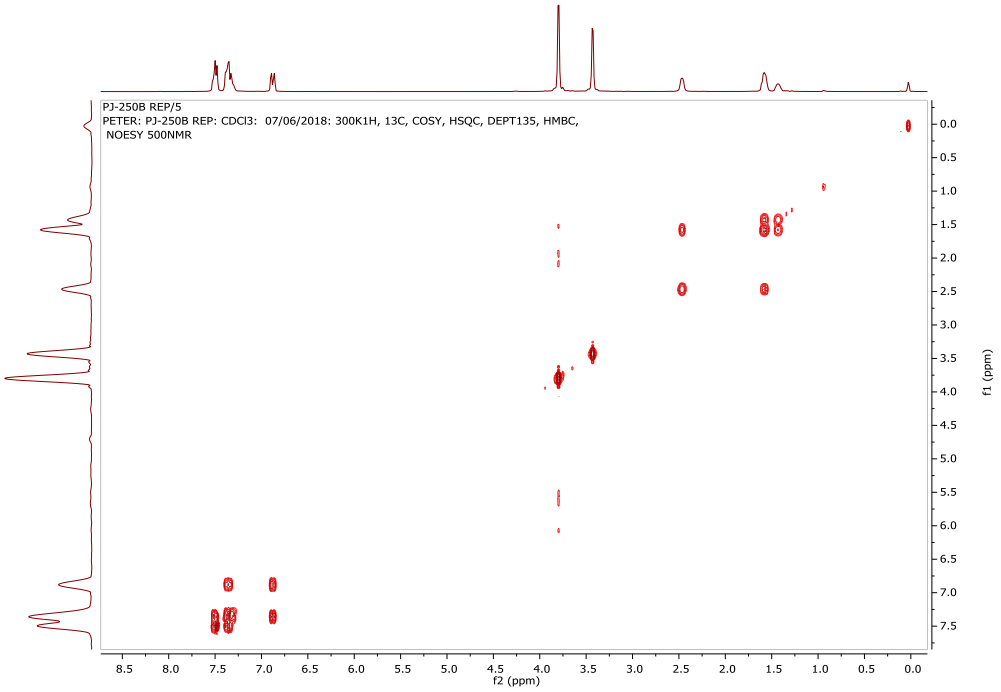

HMQC NMR spectrum of (2*E*,4*E*)-methyl 5-phenyl-2-(piperidin-1-ylmethyl)penta-2,4-dienoate (**248)**

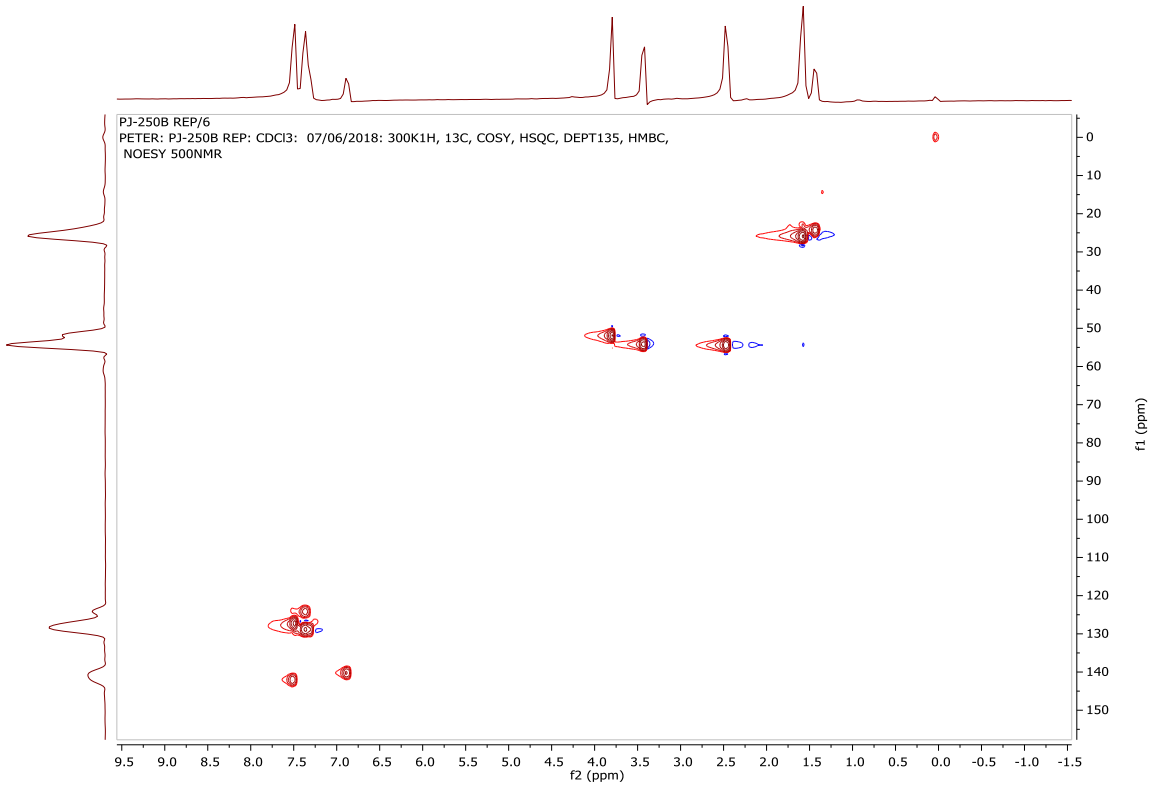

HMBC NMR spectrum of (2*E*,4*E*)-methyl 5-phenyl-2-(piperidin-1-ylmethyl)penta-2,4-dienoate (**248)**

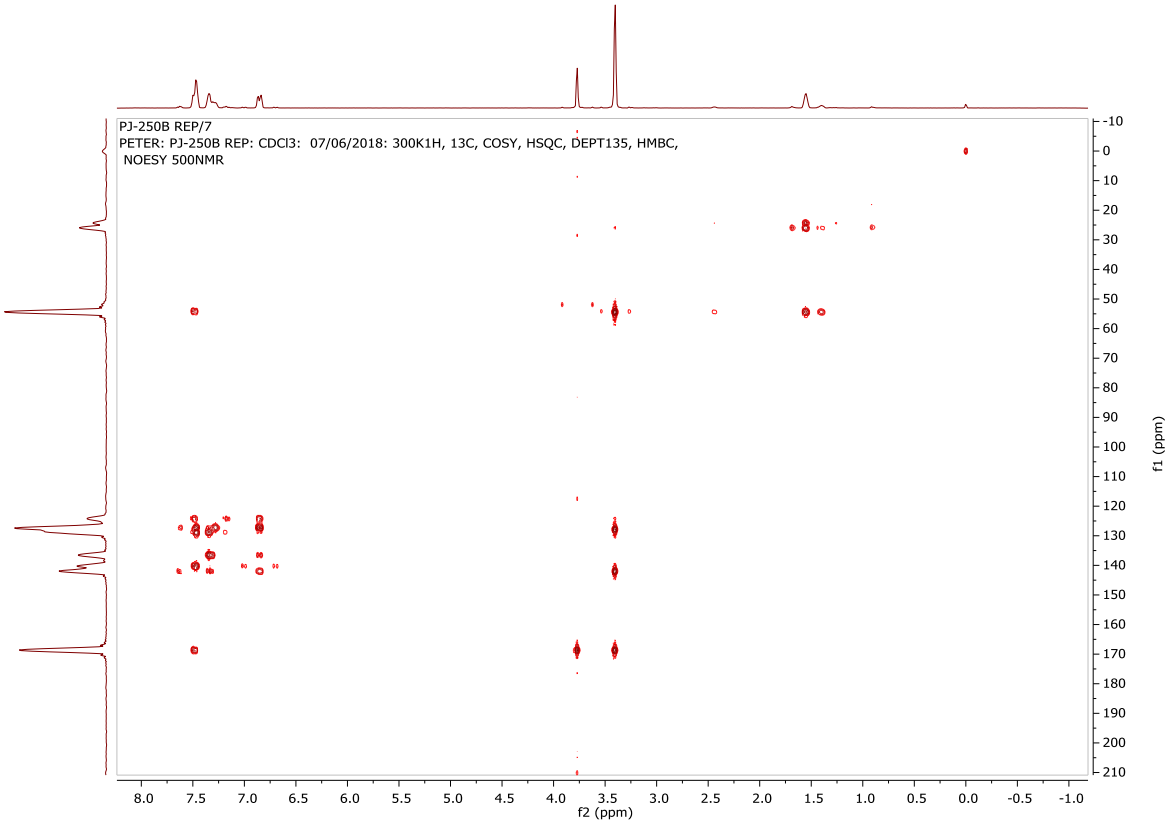

^{1}H NMR spectrum (*E*)-2-((benzylamino)methyl)-3-((*tert*-butyldimethylsilyl)oxy)-5-phenylpent-4-enenitrile (**227c**)

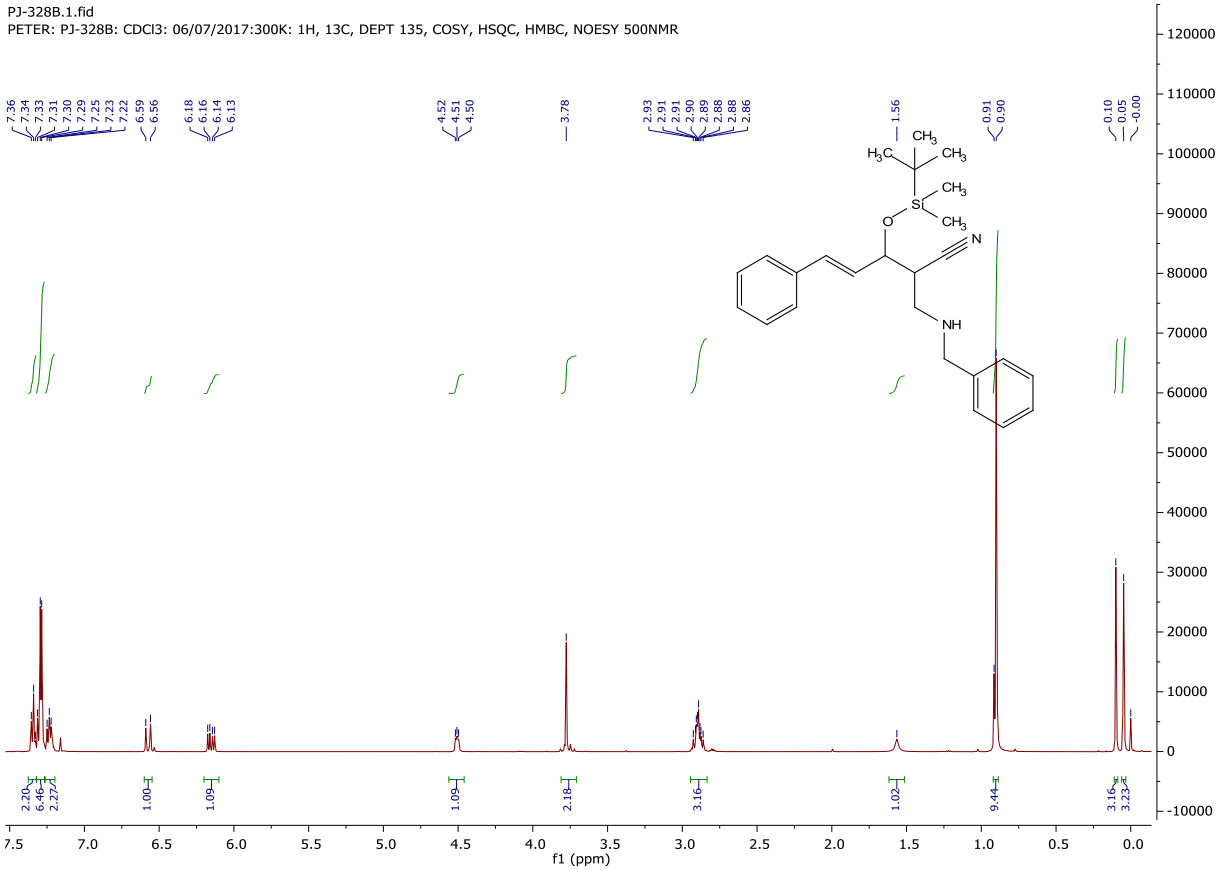

^{13}C NMR spectrum (*E*)-2-((benzylamino)methyl)-3-((*tert*-butyldimethylsilyl)oxy)-5-phenylpent-4-enenitrile (**227c**)

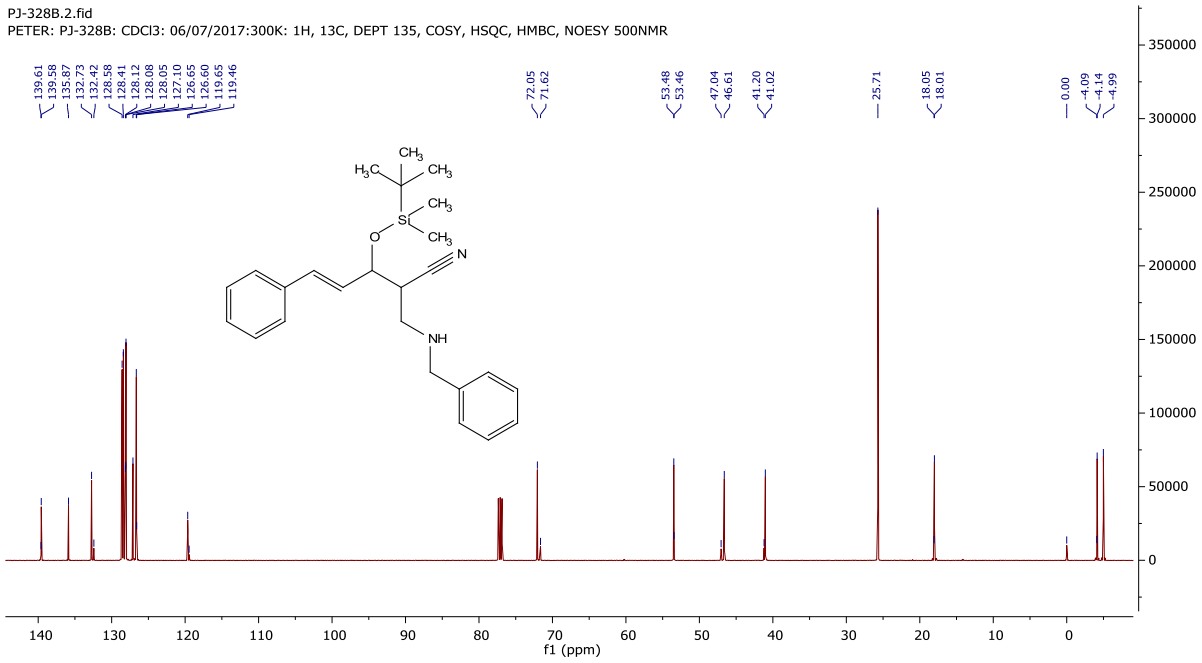

^{1}H NMR spectrum (*E*)-2-((benzylamino)methyl)-3-hydroxy-5-phenylpent-4-enenitrile (**244**)

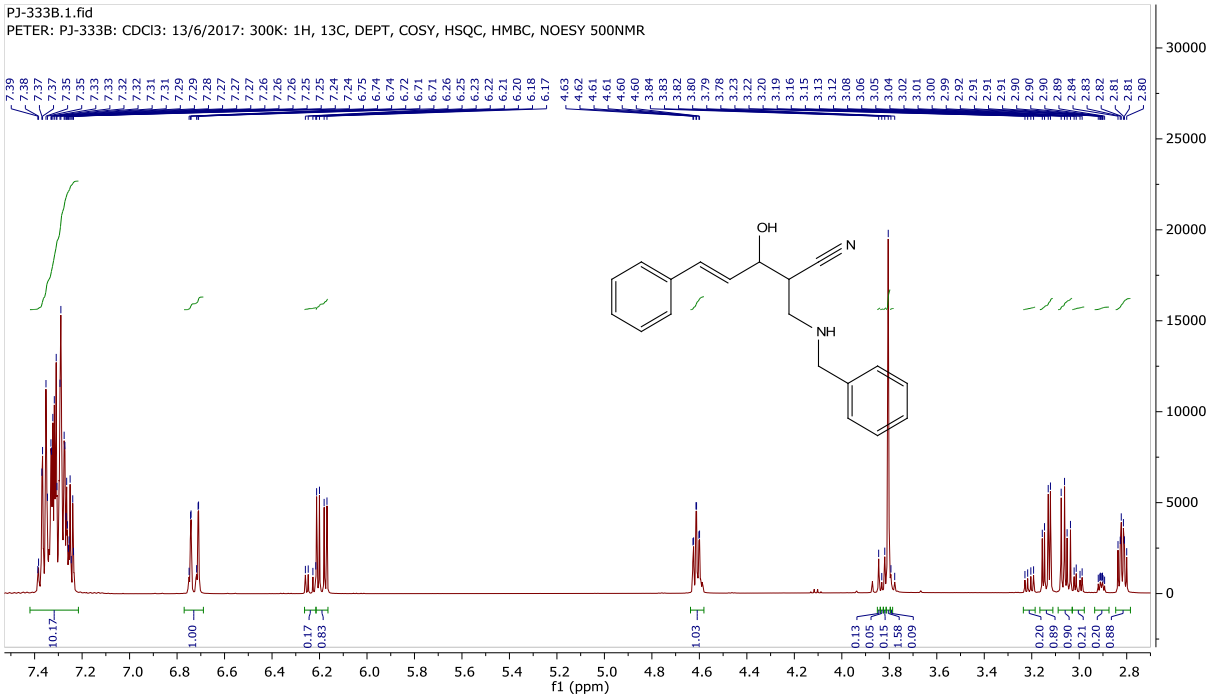

Expanded ^{1}H NMR spectrum of (*E*)-2-((benzylamino)methyl)-3-hydroxy-5-phenylpent-4-enenitrile (**244**)

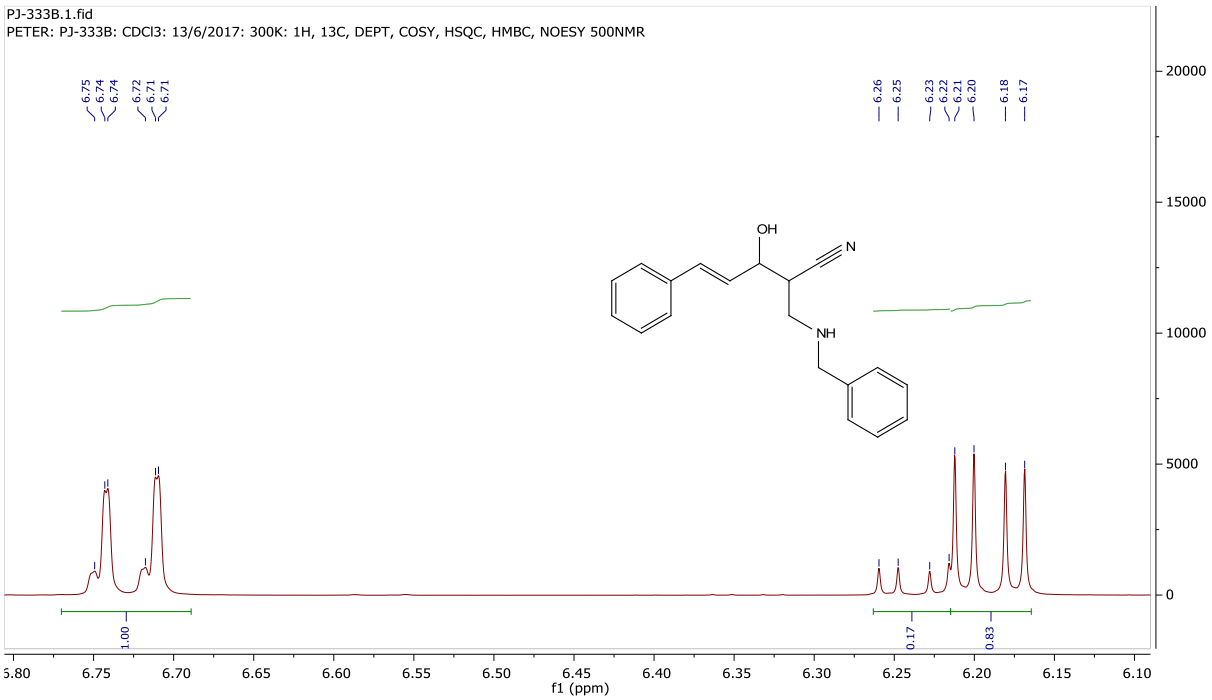

Expanded ^{1}H NMR spectrum of (*E*)-2-((benzylamino)methyl)-3-hydroxy-5-phenylpent-4-enenitrile (**244**)

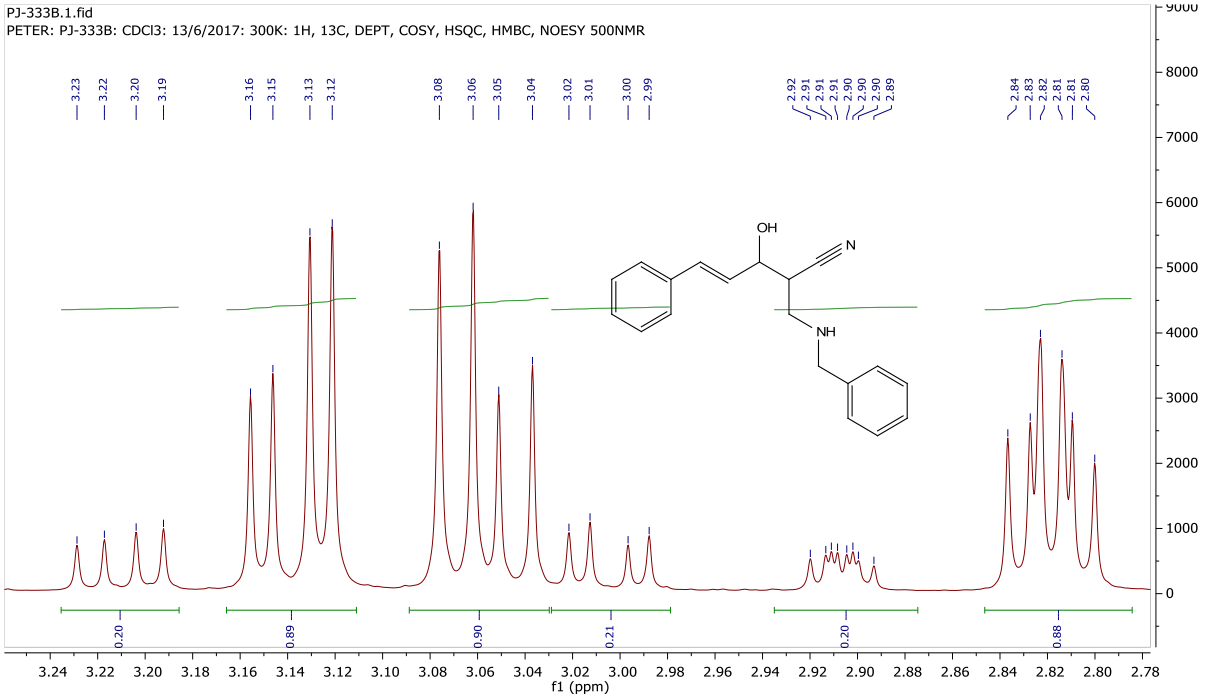

COSY NMR spectrum of (*E*)-2-((benzylamino)methyl)-3-hydroxy-5-phenylpent-4-enenitrile (**244**)

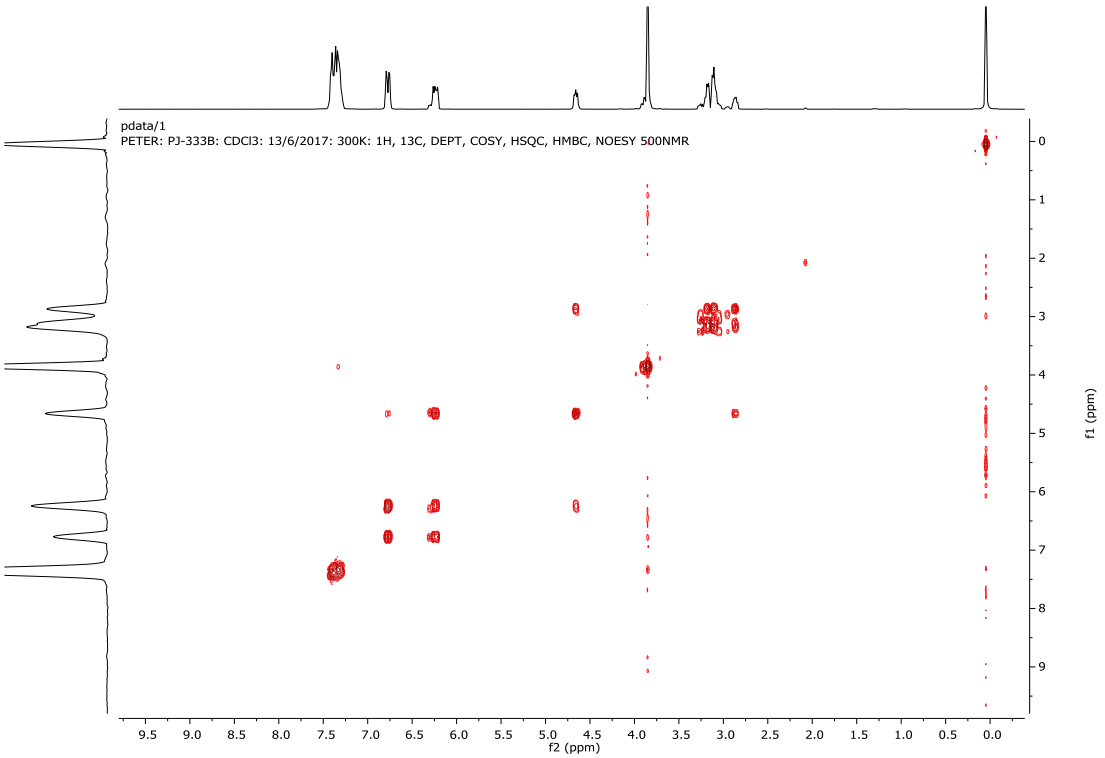

Expanded COSY NMR spectrum of (*E*)-2-((benzylamino)methyl)-3-hydroxy-5-phenylpent-4-enenitrile (**244**)

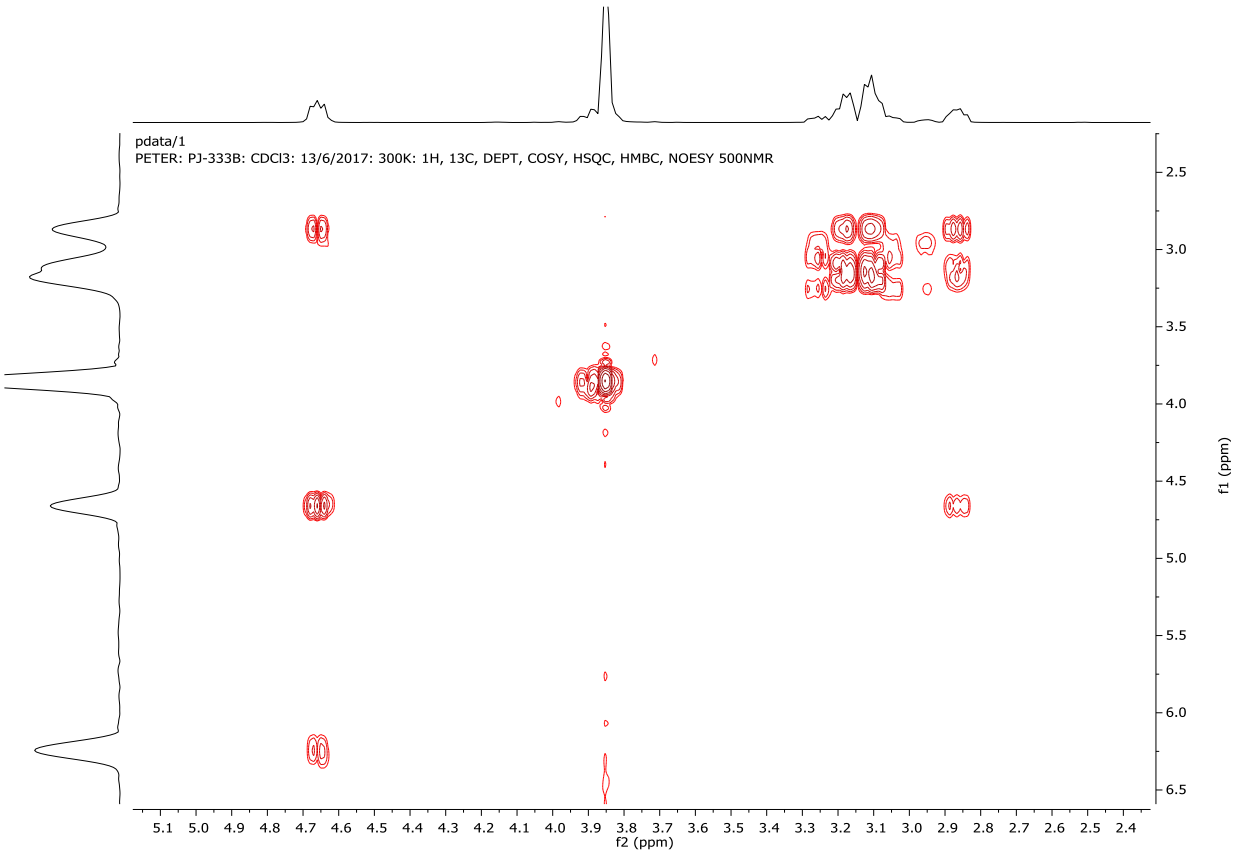

^{13}C NMR spectrum of (*E*)-2-((benzylamino)methyl)-3-hydroxy-5-phenylpent-4-enenitrile (**244**)

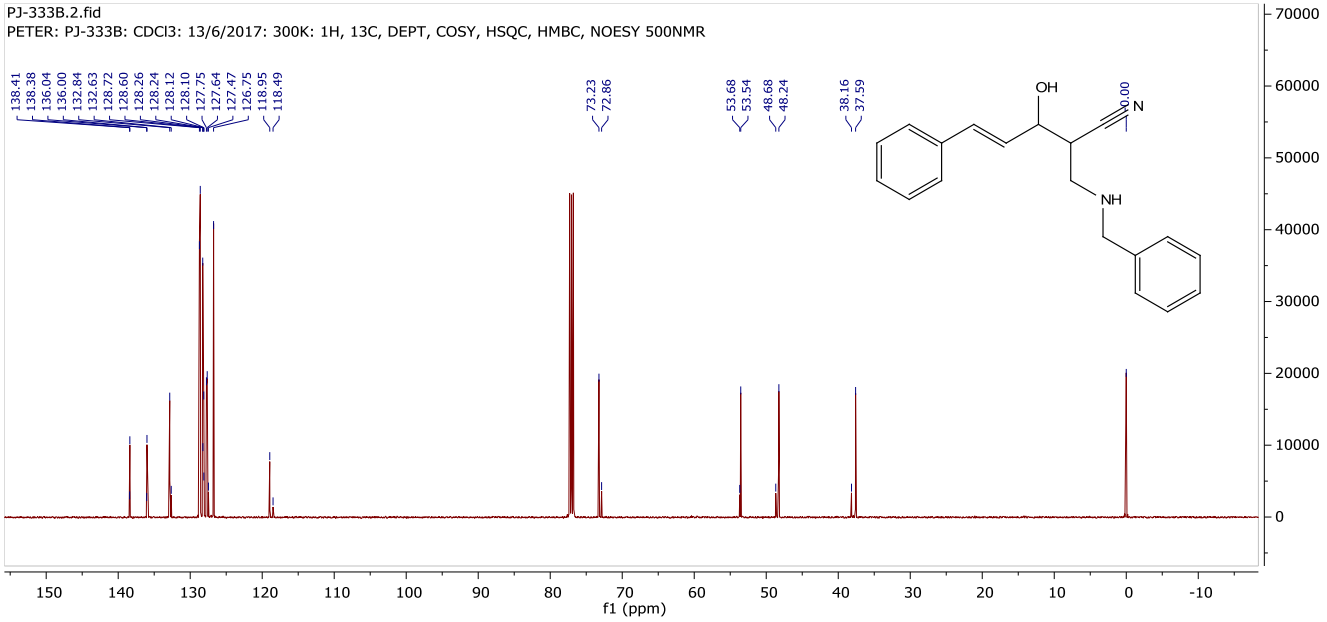

DEPT 135 NMR spectrum of of (*E*)-2-((benzylamino)methyl)-3-hydroxy-5-phenylpent-4-enenitrile (**244**)